ЖУРНАЛ
ЭКСПЕРИМЕНТАЛЬНОЙ И ТЕОРЕТИЧЕСКОЙ
ФИЗИКИ
АКАДЕМИЯ НАУК СССР

SOVIET PHYSICS

JETP

VOLUME 1 NUMBER 2

A Translation

of the

Journal of Experimental and Theoretical Physics

of the

Academy of Sciences of the USSR

SEPTEMBER, 1955

Published by the

AMERICAN INSTITUTE OF PHYSICS
INCORPORATED

SOVIET PHYSICS
JETP

A translation of the Journal of Experimental and Theoretical Physics of the USSR.

A publication of the
AMERICAN INSTITUTE OF PHYSICS

SOVIET PHYSICS is a bi-monthly journal published by the American Institute of Physics for the purpose of making available in English reports of current Soviet research in physics as contained in the Journal of Experimental and Theoretical Physics of the Academy of Sciences of the USSR. All issues of the Soviet journal after January 1, 1955, will be translated. The page size of SOVIET PHYSICS will be 7⅞" x 10½", the same as other Institute journals.

Transliteration of the names of Russian authors follows the system employed by the Library of Congress.

This translating and publishing project was undertaken by the Institute in the conviction that dissemination of the results of researches everywhere in the world is invaluable to the advancement of science. The National Science Foundation of the United States encouraged the project initially and is supporting it in large part by a grant.

One volume is published annually. Volume 1 (1955) will contain three issues. Subsequent volumes, beginning with January 1956, will contain six issues.

Subscription Prices:

Per year (6 issues)
United States and Canada.....$30.00
Elsewhere 32.00

1st Volume (3 issues)
United States and Canada.....$15.00
Elsewhere 16.00

Back Numbers
Single copies .....$ 6.00

Subscriptions should be addressed to the American Institute of Physics, 57 East 55 Street, New York 22, New York.

SOVIET PHYSICS
JETP

A translation of the Journal of Experimental and Theoretical Physics of the USSR.

VOL. 1, NO. 2, PP. 197-408 SEPTEMBER, 1955

The Kinetics of the Destruction of Superconductivity by a Magnetic Field *

A. A. GALKIN AND P. A. BEZUGLYI
Physico-technical Institute of the Academy of Sciences of the Ukrainian SSR
(Submitted to JETP editor March 23, 1954)
J. Exper. Theoret. Phys. USSR 28, 463-470 (April, 1955)

The kinetics of destruction of superconductivity of a cylindrical tin specimen has been studied in audio-frequency alternating magnetic fields and the experimental data compared with theory. A region of values of "supercriticality" has been found, in which the phase transition in the specimen takes place by boundary movement. The times for establishment of a nucleus of normal and superconducting phase are estimated.

A number of experimental studies[1,2] have been made on the kinetics of distribution of superconductivity by a magnetic field. However, it is difficult on the basis of the published data to make a comparison of the experiments with the theory developed by Lifshitz[3,4,**]. It therefore seemed desirable to carry out experiments, the data of which could allow a more detailed comparison of experiment with theory. For this purpose the method of a transformer with a superconducting core[6] was used in a somewhat modified form.

DESCRIPTION OF THE APPARATUS

The secondary coil of the transformer was wound on a glass capillary containing a monocrystalline specimen of tin of initial purity 99.99%. The surface of the glass free from the winding was then dissolved in hydrofluoric acid. Since the winding occupied only 20% of the total surface of the specimen the latter was in good thermal contact with the liquid helium during the measurements. This circumstance and the high thermal conductivity of the specimen ensured that the processes of destruction and restoration of superconductivity were isothermal.

Later the transformer with its superconducting core was improved by putting the secondary winding directly on the solenoid, and the specimen, completely free from glass, was placed along the axis of the transformer. The transfer of the secondary winding from the specimen to the solenoid not only improved the isothermal character of the processes of destruction and restoration of superconductivity, but eliminated systematic errors in determining the "supercriticality" of the alternating field applied to the specimen. These errors arose from the screening action of eddy currents induced in the secondary coil, which led to a dependence of the constant of the solenoid on the frequency of the alternating current flowing in it.

The primary of the transformer, i.e., the solenoid

* This work was presented at the Session of the Academy of Sciences of the Ukrainian SSR on April 18, 1952

** In the investigation[5] which agreed with theory, questions of the kinetics of destruction of superconductivity by alternating magnetic fields and also questions of the limits of applicability of the theory are not discussed.

[1] N. E. Alekseevskii, Doklady Akad. Nauk SSSR 60, 37 (1948)

[2] T. E. Faber, Nature 164, 277 (1949)

[3] I. M. Lifshitz, J. Exper. Theoret. Phys. USSR 20, 834 (1950)

[4] I. M. Lifshitz, Doklady Akad. Nauk SSSR 90, 363 (1953)

[5] T. E. Faber, Proc. Roy. Soc. A 219, 75 (1953)

[6] A.A. Galkin, B. G. Lazarev and P. A. Bezuglyi, J. Exper. Theoret. Phys. USSR 20, 1145 (1950)

1 (see Fig. 1) was fed by the 50 watt audio-

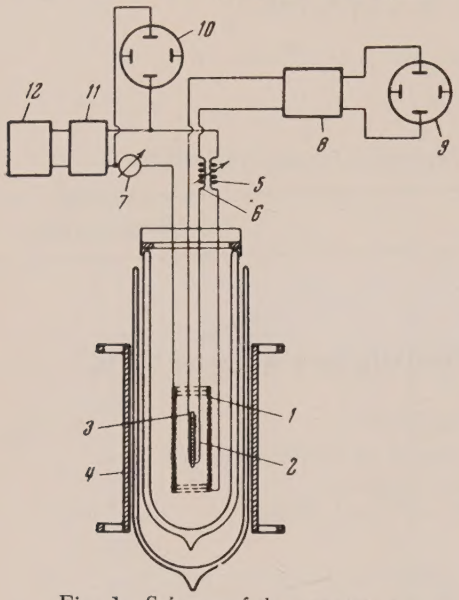

Fig. 1. Scheme of the apparatus.

frequency generator *12* and fields of amplitude up to 200 oersteds could be obtained. The impulses emf produced in the secondary at the instants of destruction and restoration of superconductivity of the tin core *3* were registered by the oscillograph *9*. At medium and extreme audio-frequencies these impulses were considerably distorted by the sinusoidal curve of emf arising from that part of the secondary cross-section not filled with the superconductor. To eliminate this background, a compensating transformer was added to the circuit. The compensation was achieved by varying the coupling between the coils *5* and *6* of the compensating transformer when the core was superconducting. For those frequencies for which compensation of both amplitude and phase could be achieved, the background was reduced practically to zero; in other cases it was considerably reduced.

The sinusoidal form of the current in *1* during the experiment was checked by a special oscillograph *10;* a sinusoidal form was required since the presence of harmonics made good compensation of the background impossible.

The generator, the power amplifier *11* and the wide-band amplifier *8* were supplied by batteries in order to eliminate 50 cycle/sec modulation and to make easier the synchronization of the linear time base of the oscillograph *9*. The current in the primary was measured by an ordinary AC meter. The frequency characteristic of this meter was taken several times and it was established that the meter sensitivity was practically independent of frequency. The calibration of the meter was made in the following way. At a temperature below T_c, a field of the form $H = H_{const} + H_0 \sin \omega t$ was applied with $H_{const} + H_0 < H_c$. Then, keeping H_0 constant, the steady field H_{const} was increased until impulses of emf were just obtained in the secondary corresponding to transitions from superconducting to normal state and vice-versa. The beginning of impulses then corresponds to $H_{const} + H_0 = H_c$ and, since H_c is known as a function of T, the true value of H_0 can be deduced from that of H_{const} (given by the reading of a precision DC meter): the value of I_0, the current amplitude, follows from H_0, and the corrections to the readings of the AC meter could be established. In this way the meter was calibrated over its entire scale and at all frequencies.

RESULTS OF MEASUREMENTS

For frequencies between 10^2 and 2×10^4 cycles/sec at various temperatures and various "supercriticalities" [defined as $u = (H - H_c)/H_c$] of the magnetic field, oscillograms were taken of the emf $E(t)$ in the secondary. A series of such oscillograms obtained at 200 cycles/sec and 3.621° K, in order of ascending u, is shown in Fig. 2 *a - f*. From these it follows that for $u < 0.5$ the "rule of areas" applies, i.e., the area $S = \int_{t_1}^{t_2} E(t)\,dt$ under the impulse for destruction of superconductivity is equal to $S_2 = \int_{t_3}^{t_4} E(t)\,dt$, the area corresponding to restoration of superconductivity. Moreover, either area S increases linearly with the maximum value of u (Fig. 3).

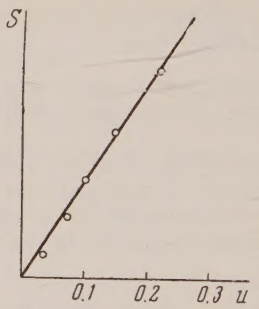

Fig. 3. Dependence of $S = \int E\,dt$ on "supercriticality" u for $\nu = 200$ cycles/sec

For larger values of u (Fig. 4 *a - c*) the oscillograms differ markedly in form from those for smaller u. In these, sharp jumps of emf can be seen in the transitions from the superconducting to the

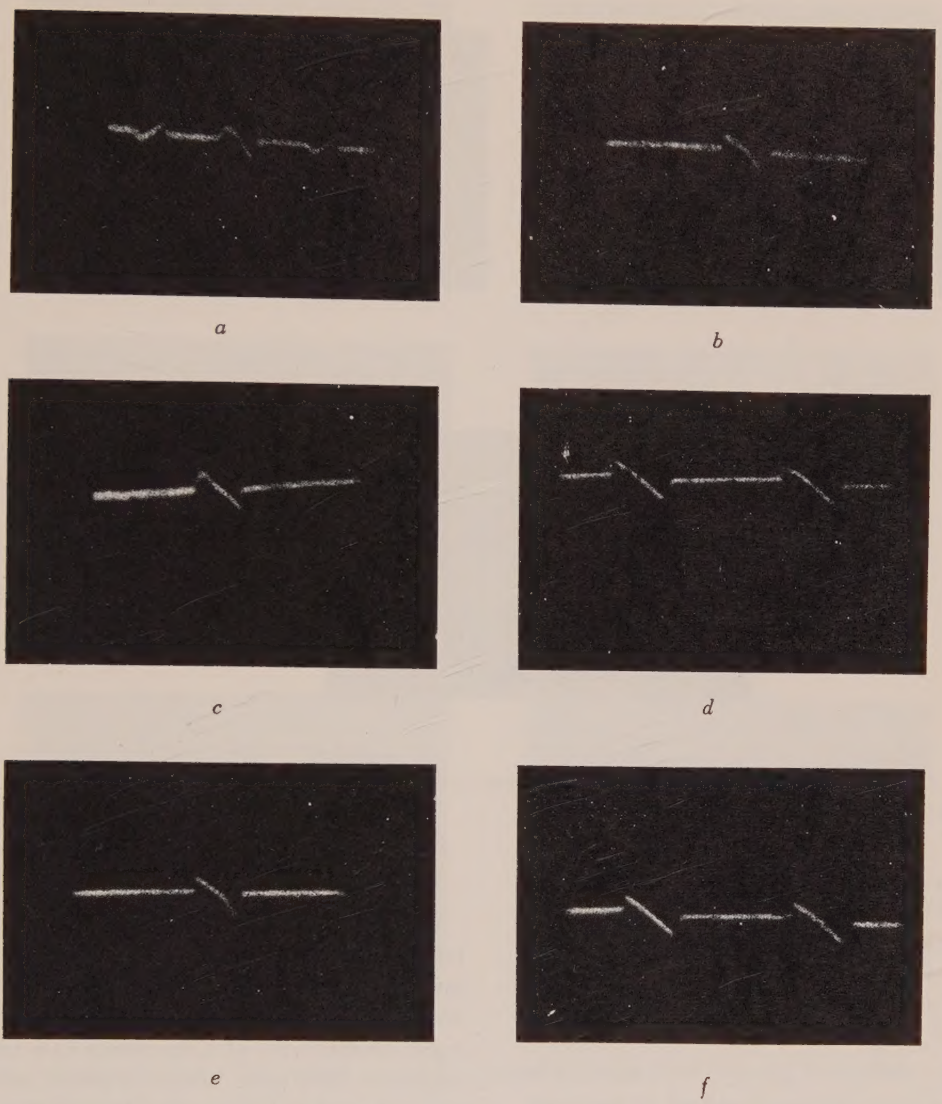

Fig. 2. Oscillograms of $E(t)$ for $\nu = 200$ cycles/sec, $T = 3.621°$ K and $H_0 = 16.1$ oersteds; H_{const} (in oersteds): $a = 0$, $b = 0.96$, $c = 1.18$, $d = 1.65$, $e = 3.76$, $f = 4.55$

normal state and vice-versa. The impression is that the transition from one state to the other takes place almost without expulsion of the field. In other words, the effects of destruction take place in a very thin surface layer with "freezing-in" of the field inside the specimen.

Figure 5 a-f shows the oscillograms obtained at 4000 cycles/sec and $T = 3.621°$ K. The amplitude of the alternating magnetic field was held constant throughout at about H_c, and the constant field was increased from zero to H_c. Figure 5 f is for the normal state alone, i.e., for $H_{const} > H_c$. From Fig. 5 a-e the symmetry of the areas $\int E(t)\,dt$ for the processes of destruction and restoration of superconductivity is again established; the "supercriticality" increases with H_{const}, and the area $\int E(t)\,dt$ increases linearly at the same time (Fig. 6).

It is characteristic that for small H_{const} there is some asymmetry of the oscillograms as between the first and second half periods: the impulses corresponding to destruction and restoration of superconductivity in the first half period are not equal to the corresponding impulses in the second half period. It turned out that this effect is connected with the presence of the earth's magnetic field, for

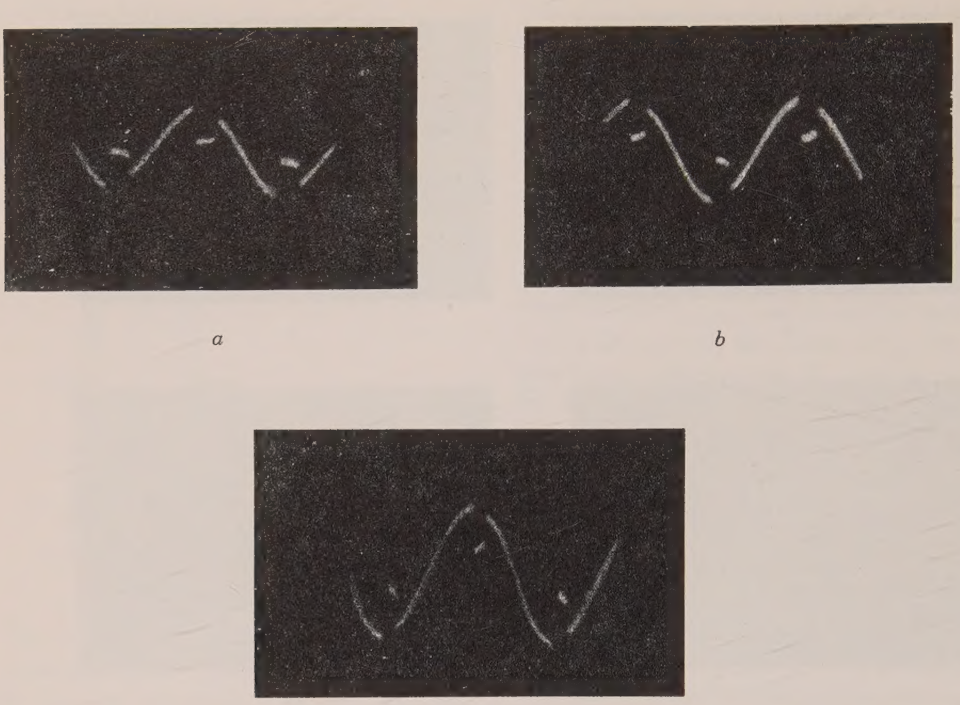

a *b*

c

Fig. 4. Oscillograms of $E(t)$ for $\nu = 200$ cycles/sec, $T = 3.621°$ K, H_0 in oersteds : $a = 24.6$, $b = 34.2$, $c = 45.7$

when the latter was compensated by Helmholtz coils, the oscillograms became quite symmetrical. Owing to technical difficulties we did not compensate the earth's field during photography of the oscillograms. From Lifshitz's theory it follows that for values of $H_{const} > H_c$ and for frequencies satisfying the condition $\delta_{skin} < r$, no transition to superconductivity should be observed at instants when $|H_{const} + H(t)| < H_c$. To check this prediction, the following experiment was carried out. The specimen was placed in a field $H_{const} > H_c$ and an alternating field was superimposed, whose amplitude and frequency could be varied. It turned out that for any of the frequencies applied, transitions to the superconducting state did take place, which could be observed by irregularities in the changes of emf in the secondary coil of the transformer. However, for each frequency, a minimum amplitude $H_{0\ min}$ of the alternating field was found, below which no transition took place. As illustrated in Fig. 7, the value of $H_{0\ min} - H_{const}$ increases with frequency.

DISCUSSION OF RESULTS

Lifshitz's theory is valid if there is a large difference between the time of formation of nuclei of the normal and superconducting phases. In this case the processes of destruction and restoration of superconductivity of a specimen in a longitudinal magnetic field take place by radial movement of a phase boundary. From the theory it is easy to obtain quantities which permit a quantitative comparison of the theory with experiment. Thus, Lifshitz showed that the dependence of Φ, the flux embraced by the contour of the specimen, on the maximum "supercriticality" u, should be $\Phi = \propto u^{3/4}$. Experiment gives $\Phi \propto u$. It should be noticed that a departure from the law $\Phi = \propto u^{3/4}$ is given also by the other, independent, measurements[2] in which it was found that the speed of movement of a phase boundary varied with the "supercriticality" rather more strongly than linearly. Thus comparison of the experimental data with theory leads to the conclusion that the dependence of the depth of destruction on "supercriticality" must be stronger than predicted by the theory. A similar discrepancy was

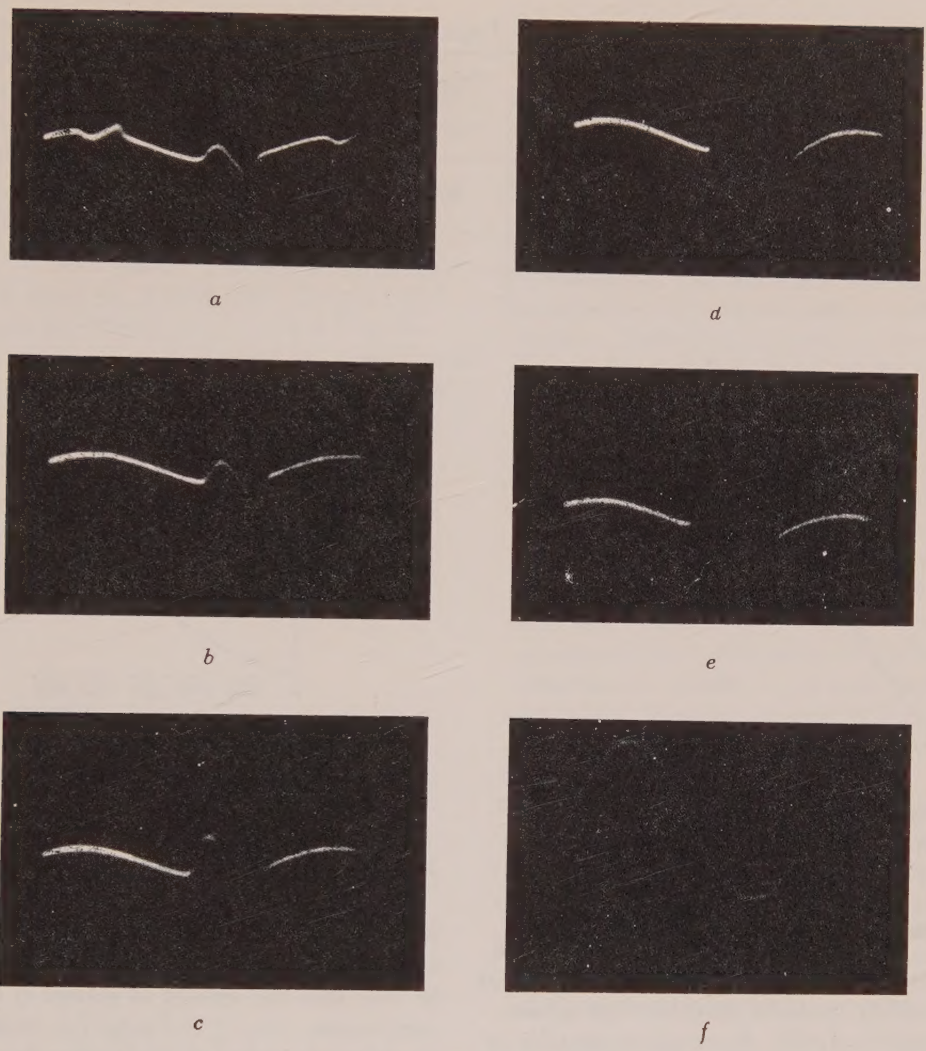

Fig. 5. Oscillograms of $E(t)$ for $\nu = 4000$ cycles/sec, $T = 3.621^\circ$ K and $H_0 \sim H_c$; H_{const} in oersteds: $a = 0$, $b = 0.7$, $c = 1.18$, $d = 1.95$, $e = 2.71$, f = for the specimen in the normal state.

established in experiments on the decay of currents induced in a ring[6].

Since there is some discrepancy between theory and experiment, let us look more closely into the comparison between the experimental results and theory, turning to the numerical values of the various quantities; in particular, the numerical values of the speeds of displacement of the phase boundary.

Consider the flux Φ_1, entering the specimen in destruction of superconductivity and the mean flux Φ_2 penetrating the same contour in the normal state during a quarter period; these fluxes are easily determined from the oscillograms. On the other hand, for small values of u, Φ_1 and Φ_2 are given by $\Phi_1 = 2\pi r d H_к$;

$$\Phi_2 = 2\pi r \frac{4}{T} \int_0^{T/4} \int_0^{\infty} H_0 \sin \omega t \, dt \, e^{-x/\delta} dx = 4r\delta H_0.$$

Here d is the maximum depth of destruction of superconductivity and δ the skin depth of penetration of the alternating field in the specimen. Since in our case $H_0 \approx H_c$, we have $d/\delta = (2/\pi)\Phi_1/\Phi_2$.

In table I we compare the values of d/δ obtained from experiment with those based on Lifshitz's theory.

After all the measurements on the specimen had

TABLE I

d/δ	Value of "supercriticality" u			
	0.22 ∓ 0.01	0.23 ∓ 0.01	0.27 ∓ 0.01	0.33 ∓ 0.01
Theor.	0.44	0.48	0.49	0.60
Exper.	0.38 ± 0.04	0.45 ± 0.05	0.48 ± 0.05	0.69 ± 0.07

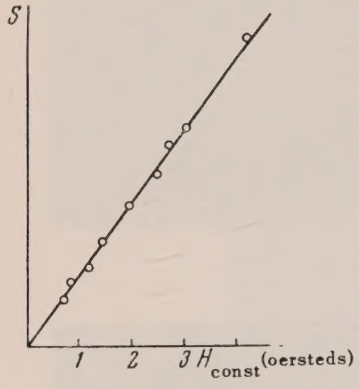

Fig. 6. Dependence of $S = \int E\,dt$ on "supercriticality" u for $\nu = 4000$ cycles/sec.

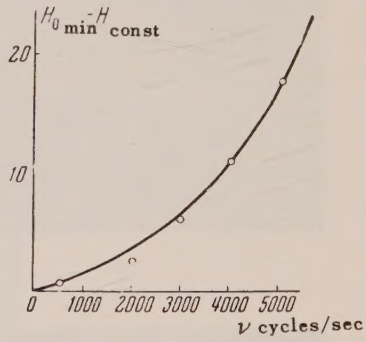

Fig. 7. Dependence of the difference $H_{0\,\min} - H_{\text{const}}$ (arbitrary units) on the frequency

been made, its DC electrical conductivity was determined ($\sigma = 1.2 \times 10^{20}$ cgs units) and from the values of $E(t)$ and σ, the speeds of displacement of the phase boundary could be calculated as a function of "supercriticality". It turned out that for increase of u the discrepancy between calculated and experimentally observed velocities increased, which agrees with the discrepancies found for the maximum depth of destruction. At the same time the theoretical law $v \propto \omega^{1/2}$ is confirmed for $u < 0.6$ at frequencies from 100 to 4000 cycles/sec (tin) and 50 to 500 cycles/sec (mercury). It should be noted that if the mercury oscillograms[6] are analyzed for the same u as for tin, it is found that $v_{Hg} > v_{Sn}$, the ratio being $v_{Hg} / v_{Sn} = 4.85$, which is just equal to $(\sigma_{Sn} / \sigma_{Hg})^{1/2}$. Thus from the data from the two metals we find that v is proportional to $\sigma^{-1/2}$, which together with the relation $v \propto \omega^{1/2}$ gives $v \propto (\omega/\sigma)^{1/2}$.

The exceptional sharpness of the oscillograms and the absence of additional spreading at places corresponding to transitions from one state to another, for all frequencies up to 1.5×10^4 cycles/sec, deserves special mention.

We shall now attempt to estimate an upper limit to the time τ_n for the formation of a nucleus of normal phase, based on the fact that this time must be less than the amount of spread of the line on the oscillogram, i.e., $\tau_n < T\,(\Delta t/T)$, where $\Delta t/T$ is the relative spread of the line on the oscillogram. Since $\Delta t/T \approx 1/60$, it follows that $\tau_n < 10^{-6}$ sec. Of course, this value must be related to the particular value of "supercriticality", since with increase of the latter the time of formation of a nucleus must decrease. Assuming that $u = 0.5$, we find that the "supercriticality" at the transition itself is $u_{s \to n} = 0.5/10 = 5 \times 10^{-2}$.

To explain the sharpness of the oscillograms we might have assumed that $\tau_n > 10^{-2}$ sec. However, the specimen surface would then always be covered with a thin layer of normal material, created at the moment of switching on the alternating field. Such a layer would lead to two consequences which were not experimentally observed: 1) to the existence of irregularities in the oscillograms at the instant of switching on the field, with impossibility of synchronizing the individual acts of destruction, 2) to a strong frequency dependence of velocity of

boundary displacement: $v \propto \omega^n$ where $n > 1$.

If we assume that the time of creation of a nucleus of normal phase is less than 10^{-6} sec, the time of destruction of such a nucleus may be considerably greater. Indeed, from oscillograph experiments on the transition curve [7] it was established that if AC flows through a specimen, then for temperatures below T_c it is possible to observe the continuance of the normal state even in those parts of the period where $I(t) < I_c$ (see Fig. 8). This means that in a quarter period the normal state cannot be destroyed, and consequently that $\tau' > 10^{-4}$ sec. Thus we can say that the times of creation τ_n and destruction τ_n' of a normal nucleus are different.

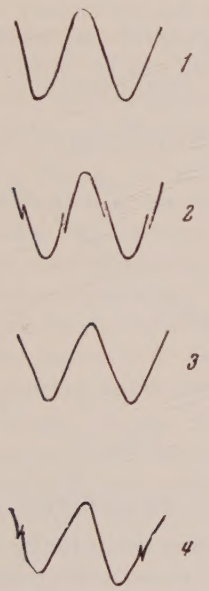

Fig. 8. Oscillograms of $E(t)$ observed on passing a sinusoidal alternating current through the specimen, for temperatures: $1 = 3.725°$ K, $2 = 3.711°$ K, $3 = 3.709°$ K, $4 = 3.7085°$ K. Curves without breaks correspond to the specimen remaining only in the normal state for the whole time.

Consider now a second possibility of explaining the sharpness of the oscillograms. We can suppose that there always exist on the surface of the specimen nuclei of normal phase, located at places of greatest curvature. For instance, in the case of monocrystals the surface has a step-like structure, so that on account of the demagnetizing factor these steps may be in the intermediate state [8]. This means that part of the volume of the monocrystal will provide nuclei of normal phase from which a practically inertialess boundary displacement can originate.

Here, however, we encounter the following kind of difficulty. For stability of a nucleus it is necessary that it should have a certain minimum volume. According to estimates in the work [9], $V_{min} = 4 \times 32^3 \pi^4 \alpha^3 / 27 H_c^6$, where α is the surface tension between normal and superconducting phases. For our case, $V_{min} = 10^{-6}$ cm^3 which agrees well with data obtained by Alekseevskii [10].

As already indicated, only that part of the surface of the specimen can go over into the normal state, in which the intermediate state is realized, i.e., in the regions of step-like structure. Assuming that this structure is oriented to have the largest demagnetizing coefficient, it is possible to estimate the volume V_1 of each little step, and this turns out to be 10^{-8} to 10^{-9} cm^3. Since $V_1 \ll V_{min}$, the formation of a stable nucleus of the new phase is impossible.

Experimentally, the question of the possibility of formation of nuclei at surface irregularities can be decided by investigations with specimens treated in various ways. For an etched surface the conditions for formation of nuclei should be most favorable; for a polished surface least favorable. If the time of formation of a normal nucleus $\tau_n > 10^{-6}$ sec, polishing of the specimen should lead, for certain frequencies, to smearing of the oscillograms. However, measurements on tin specimens in glass envelopes and etched specimens do not give appreciably different results. We are therefore inclined to conclude that $\tau_n < 10^{-6}$ sec.

As already mentioned, the theory gives the correct frequency dependence of velocity of boundary displacement for small "supercriticality", but starting with a maximum "supercriticality" $u > 0.6$ an appreciable departure of the experimental data

[7] A. A. Galkin and B. G. Lazarev, J. Exper. Theoret. Phys. USSR 18, 833 (1948)

[8] N. E. Alekseevskii, J. Exper. Theoret. Phys. USSR 16, 870 (1946)

[9] P. Bulashevich, J. Exper. Theoret. Phys. USSR 8, 1267 (1938)

[10] N. E. Alekseevskii, Dissertation, Institute for Physical Problems, Academy of Sciences of the USSR, Moscow, 1948

from the theoretical prediction sets in*. This appears particularly clearly with thin specimens, for which the departure sets in for even smaller values of u.

From the oscillograms taken for $u > 0.6$ it follows that the specimen is in the normal state for the greater part of the time. Indeed, if on an oscillogram taken in these conditions, one taken entirely in the normal state is superposed, they coincide with each other over practically the whole period. The transitions from state to state last only a short time and are not accompanied by large emf's. On the narrow portions of the oscillogram corresponding to the transition from the normal to the superconducting state, the emf diminishes to a value corresponding to the superconducting state. This characteristic of the oscillogram can be explained in the following way: if the field at the surface becomes less than critical (while remaining critical inside), then conditions arise for formation of superconducting nuclei at the surface, which grow over the whole surface and lock in the magnetic field in the interior. Consequently, destruction and restoration of superconductivity takes place in a thickness d, appreciably less than the skin depth δ_{skin}. Thus, the mechanism of destruction considered by Lifshitz is apparently not applicable in this case.

By investigating the process of destruction of superconductivity by an alternating magnetic field, it should in principle be possible to establish a regime, starting from which the mechanism of boundary displacement is replaced by the nucleation mechanism, and in this way to estimate the time of formation of a superconducting nucleus. However, since measurements of the dependence of $\int E(t)\,dt$ on "supercriticality" do not give a reliable determination of the exact moment of the beginning of the transition from one mechanism to the other, the time of formation of a superconducting nucleus should, in our opinion, be estimated from the following considerations.

For $H_{const} > H_c$, an unlimited progressive movement of the boundary inside the superconductor sets in. The presence of an alternating component $H(t)$ superimposes an oscillation of the boundary on its steady motion. In the case of a cylindrical specimen, for fields greater than H_c, it will be completely in the normal state. At certain instants the field at the surface will be less than critical, and conditions are suitable for the transition to the superconducting state.

Investigations carried out along these lines showed that the value of the field H_0, for which a transition to superconductivity begins to set in, is related to the frequency by the relation

$$u' = (H_к - H_0)/H_к = \alpha\omega^2 \quad \text{or} \quad u'T^2 = \text{const}.$$

From Fig 9 the time necessary for formation of a superconducting nucleus in the case of sudden removal of the field can be found. The duration of formation of a superconducting nucleus in these conditions turns out to be $\tau_s = 1.5 \times 10^{-4}$ sec.

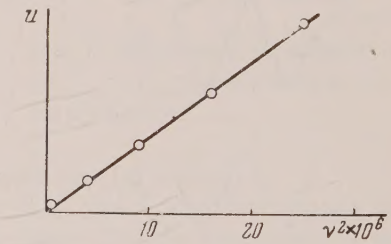

Fig. 9.

CONCLUSIONS

1. It is shown that the velocity of displacement of the boundary between normal and superconducting phases, follows the law $v \propto (\omega/\sigma)^{1/2}$ in agreement with theory.

2. The depth of destruction of superconductivity by an alternating magnetic field depends linearly on "supercriticality", which disagrees with the theoretical prediction ($d \propto u^{3/4}$).

3. Some discrepancies between the theoretical and experimental values of the velocity of boundary movement may be explained by the linear dependence of the depth of destruction on "supercriticality".

4. It is experimentally established that the times of τ_n, τ_s of formation of a nucleus of the superconducting and normal phase are different. In agreement with the assumption of Lifshitz's theory, it is found that $\tau_s \approx 1.5 \times 10^{-4}$ sec, $\tau_n < 10^{-6}$ sec.

5. The asymmetry of the processes of growth and

* It should be noted that the region of "supercriticality" for which Lifshitz's theory might be expected to hold, is limited not only from above, but also from below. Its lower limit is $\Delta H/H_c$ where ΔH is the breadth of the field interval over which the transition from one state to the other occurs. It seems to us that a number of the results of a recent investigation [see T. E. Faber, Proc. Roy. Soc. A 219, 75 (1953)] can be explained by supposing that in this investigation "supercriticalities" were used for which $u < \Delta H/H_c$.

collapse of nuclei of the normal phase is experimentally demonstrated.

In conclusion we express our deep gratitude to Professor B. G. Lazarev and Professor I. M. Lifshitz for their interest in this work and discussion of the results obtained, and also to A. I. Berdovskii for help in the measurements.

Translated by D. Shoenberg
82

SOVIET PHYSICS - JETP VOLUME 1, NUMBER 2 SEPTEMBER, 1955

The Velocity Distribution of Electrons in the Presence of a Varying Electric Field and a Constant Magnetic Field

V. M. FAIN
Gorki State University

(Submitted to JETP editor March 9, 1954)
J. Exper. Theoret. Phys. USSR 28, 422-430 (April, 1955)

The function of the velocity distribution of electrons in the presence of a varying electric field and a constant magnetic field is found. Two cases are examined: 1) an electric field depending harmonically on time; 2) an amplitude-modulated electric field.

1. INTRODUCTION

THE problem of finding the function for the velocity distribution in the case of elastic collisions of electrons with the atoms of a gas has been analyzed by several authors[1-5]. The basic work on this question appears to be that of Davydov[1]. In this work the function of the distribution of electrons in the presence of constant electric and magnetic fields was obtained. Margenau[3] analyzed the action in a varying electric field. The influence of a constant magnetic field in the presence of a varying electric field was examined by Jancel and Kahan[5]. However, they did not take into account the action of the components of the electric field parallel to the direction of the magnetic field.

In the works mentioned, the influence of the collision of electrons with each other was not considered. Meanwhile, as was shown by Cahn[6], the influence of inter-electronic collisions must be accounted for in the case of a constant electric field if the concentration of electrons is great.

In Part 2 we will give an analysis of the distribution function of the electrons according to velocity in the presence of an electric field, harmonically dependent on time, and a constant magnetic field.

In Part 3 we shall analyze the action in an amplitude-modulated electric field.

2. THE DISTRIBUTION OF ELECTRONS IN THE PRESENCE OF A HARMONIC ELECTRIC FIELD AND A CONSTANT MAGNETIC FIELD

Assuming that a gas is uniformly distributed in space, the kinetic equation takes the following form:

$$\frac{\partial f}{\partial t} + \mathbf{a}\,\nabla_v f = \frac{\delta}{\delta t} f, \tag{1}$$

where $f(\mathbf{v}, t)$ is a function of the velocity distribution of the electrons, $\mathbf{a}$ is the acceleration communicated by the field of electrons, $\partial f/\partial t$ denotes the rate of the change of the distribution due to the presence of the field, $(\delta/\delta t)f$ stands for the collision of electrons with gas atoms (the effects of the collision of electrons with each other are not considered)*, ∇_v is the gradient in the velocity domain. In our case

$$\mathbf{a} = \frac{e}{m}\mathbf{E}_0\Theta + \frac{e}{mc}[\mathbf{vH}] \equiv \vec{\Gamma}\Theta + \frac{e}{mc}[\mathbf{vH}], \tag{2}$$

[1] B. I. Davydov, J. Exper. Theoret. Phys. USSR 7, 1069 (1937)

[2] L. D. Landau, J. Exper. Theoret. Phys. USSR 7, 203 (1937)

[3] H. Margenau, Phys. Rev. 73, 297 (1948)

[4] Y. L. Klimontovich, J. Exper. Theoret. Phys. USSR 21, 1284 (1951)

[5] R. Jancel and T. Kahan, Comptes rend. 236, 788 (1953)

[6] J. Cahn, Phys. Rev. 75, 346 (1949)

* The effect of inter-electronic collisions is not essential when the concentration of electrons is not very great and the field frequencies are high[6,8].

where $\mathbf{E}_0$ represents the amplitude of the electric field, Θ is equal to cos ωt, and $\mathbf{H}$ denotes the magnetic field intensity.

To solve Eq. (1) we try to find a series of Legendre polynomials. By limiting ourselves to the first two terms, we set down this equation:

$$f(\mathbf{v}, t) = f_0(v, t) + \mathbf{v}\mathbf{f}'(v, t). \tag{3}$$

we break up $\mathbf{f}$ along three mutually perpendicular directions:

$$\mathbf{f}' = \vec{\Gamma}_\perp \varphi + [\mathbf{H}\vec{\Gamma}]\psi + \vec{\Gamma}_\parallel \xi, \tag{4}$$

where $\vec{\Gamma}_\perp$ and $\vec{\Gamma}_\parallel$ denote the components of $\vec{\Gamma}$, respectively perpendicular and parallel to the magnetic field $\mathbf{H}$. In the case of elastic collisions[1]:

$$\frac{\delta}{\delta t} f_0 = \frac{1}{v^2}\frac{m}{M}\frac{\partial}{\partial v}\left(\frac{v^4 f_0}{l}\right) + \frac{kT}{Mv^2}\frac{\partial}{\partial v}\left(\frac{v^3}{l}\frac{\partial f_0}{\partial v}\right), \tag{5}$$

$$\frac{\delta}{\delta t}\mathbf{v}\mathbf{f}' = -\mathbf{v}\frac{v}{l}\mathbf{f}', \tag{5'}$$

where l is the length of the free path of the electrons, M is the mass of the gas atoms. Let us substitute Eqs. (2) - (5) in Eq. (1). By comparing the terms of even powers of $\mathbf{v}$ in the result thus obtained, and averaging in all directions, we find

$$\frac{1}{3v^2}\frac{\partial}{\partial v}\{v^3(\Gamma_\perp^2 \varphi + \Gamma_\parallel^2 \xi)\Theta\} + \frac{\partial f_0}{\partial t} = \frac{1}{v^2}\frac{m}{M}\frac{\partial}{\partial v}\left(\frac{v^4}{l} f_0\right) + \frac{kT}{Mv^2}\frac{\partial}{\partial v}\left(\frac{v^3}{l}\frac{\partial f_0}{\partial v}\right), \tag{6}$$

while comparing terms of the first power $\mathbf{v}$ and taking projections in the chosen directions, we obtain

$$\frac{\partial \varphi}{\partial t} + \frac{1}{v}\frac{\partial f_0}{\partial v}\Theta - \frac{e}{mc}H^2\psi = -\frac{v}{l}\varphi, \tag{7}$$

$$\frac{\partial \xi}{\partial t} + \frac{1}{v}\frac{\partial f_0}{\partial v}\Theta = -\frac{v}{l}\xi, \tag{8}$$

$$\frac{\partial \psi}{\partial t} + \frac{e}{mc}\varphi = -\frac{v}{l}\psi. \tag{9}$$

It is easy to verify that the system of equations (6) - (9) is equivalent to that obtained by Davydov[1]. We shall look for the solution of equations (6) - (9) in the form of the sum of harmonics of the frequencies which are multiples of ω:

$$f_0 = \frac{F_0}{2} + \sum_k F_k \cos k\omega t + G_k \sin k\omega t = \sum_k \Phi_k e^{ik\omega t}, \tag{10}$$

where

$$\Phi_0 = \frac{F_0}{2}, \quad \Phi_k = \frac{1}{2}(F_k - iG_k) = \Phi_{-k}^*.$$

Analogously,

$$\varphi = \sum_k \varphi_k e^{ik\omega t}, \quad \psi = \sum_k \psi_k e^{ik\omega t}, \quad \xi = \sum_k \xi_k e^{ik\omega t}, \tag{11}$$

where

$$\varphi_k = \frac{1}{2}(f_k - ig_k) = \varphi_{-k}^*, \quad \psi_k = \frac{1}{2}(q_k - ir_k) = \psi_{-k}^*, \quad \xi_k = \frac{1}{2}(h_k - ip_k) = \xi_{-k}^*.$$

Substituting Eqs. (10) and (11) in Eqs. (6) - (9) and comparing the terms containing $e^{ik\omega t}$ we find

$$ik\omega\Phi_k + \frac{1}{6v^2}\frac{\partial}{\partial v}\{v^3[\Gamma_\perp^2(\varphi_{k-1} + \varphi_{k+1}) + \Gamma_\parallel^2(\xi_{k-1} + \xi_{k+1})]\} = \frac{\delta \Phi_k}{\delta t}; \tag{12}$$

$$ik\omega\varphi_k + \frac{1}{2v}\left(\frac{\partial \Phi_{k-1}}{\partial v} + \frac{\partial \Phi_{k+1}}{\partial v}\right) - \frac{e}{mc}H^2\psi_k = -\frac{v}{l}\varphi_k, \tag{13}$$

$$ik\omega\xi_k + \frac{1}{2v}\left(\frac{\partial \Phi_{k-1}}{\partial v} + \frac{\partial \Phi_{k+1}}{\partial v}\right) = -\frac{v}{l}\xi_k, \tag{14}$$

$$ik\omega\psi_k + \frac{e}{mc}\varphi_k = -\frac{v}{l}\psi_k. \tag{15}$$

From Eqs. (13) - (15) we find expressions for ϕ_k, ξ_k and ψ_k:

$$\varphi_k = -\frac{1}{2v}\left(\frac{\partial \Phi_{k-1}}{\partial v} + \frac{\partial \Phi_{k+1}}{\partial v}\right)\frac{ik\omega + \nu}{(ik\omega + \nu)^2 + \omega_H^2}, \tag{16}$$

$$\psi_k = -\frac{e}{mc}\frac{1}{ik\omega + \nu}\varphi_k,$$

$$\xi_k = -\frac{1}{2v}\left(\frac{\partial \Phi_{k-1}}{\partial v} + \frac{\partial \Phi_{k+1}}{\partial v}\right)\frac{1}{ik\omega + \nu},$$

where $\nu = v/l$; $\omega_H = |e/mc\ H|$.

In this manner we have obtained an infinite system of linear differential equations with an infinite number of unknown functions. We can solve this system in certain special cases.

It is evident that a varying electric field does

not create a constant one consisting of an asymmetrical part of the distribution function; that is, $\phi_0 = \psi_0 = \xi_0 = 0$. From Eq. (13) it then follows that $\Phi_1 = 0$, which in turn leads to the equality $\phi_2 = \psi_2 = \xi_2 = 0$. It is easily shown for the general case that

$$\Phi_1 = \Phi_3 = \ldots = \Phi_{2k+1} = 0, \qquad (17)$$

$$\varphi_{2k} = \psi_{2k} = \xi_{2k} = 0.$$

The system of equations (12) - (15) can be solved by the method of successive approximations. For a first approximation, we will neglect all harmonics except Φ_0, ϕ_1, ξ_1, ψ_1. From Eqs. (11) and (16) we will then find

$$f_1 = -\frac{\partial \Phi_0}{\partial v}\frac{1}{A}, \qquad h_1 = -\frac{l}{\omega^2 l^2 + v^2}\frac{\partial \Phi_0}{\partial v}, \qquad (18)$$

$$q_1 = \frac{e}{mc}\frac{1}{\omega^2 + \nu^2}(\omega g_1 - \nu f_1),$$

$$g_1 = B\frac{\partial \Phi_0}{\partial v}, \qquad p_1 = -\frac{\omega}{\omega^2 + \nu^2}\frac{1}{v}\frac{\partial \Phi_0}{\partial v},$$

$$r_1 = -\frac{e}{mc}\frac{1}{\omega^2 + \nu^2}(\omega f_1 + \nu g_1),$$

where

$$A = \frac{l^2\omega^2(1-z)^2 + v^2(1+z)^2}{l(1+z)}, \qquad z = \frac{\omega_H^2}{\omega^2 + \nu^2},$$

$$B = \frac{\omega}{v}\frac{(z-1)l^2}{\omega^2 l^2 (1-z)^2 + v^2(1+z)^2}.$$

Having integrated Eq. (12), taking $k = 0$, we obtain

$$\Phi_0 = C\exp \qquad (19)$$

$$\left\{-\int_0 \frac{mv\,dv}{kT + \left[\Gamma_\perp^2 Ml/6A\right] + \left[\Gamma_\parallel^2 Ml^2/6(\omega^2 l^2 + v^2)\right]}\right\}.$$

The constant C can be determined from the condition of normalization:

$$4\pi\int \Phi_0 v^2\,dv = 1. \qquad (20)$$

In this manner the distribution function to the first approximation takes on the form

$$f(\mathbf{v}, t) = \Phi_0 + v\left[\vec{\Gamma}_\perp(f_1\cos\omega t + g_1\sin\omega t)\right. \qquad (21)$$

$$+ [\mathbf{H}\vec{\Gamma}](q_1\cos\omega t + r_1\sin\omega t)$$

$$\left. + \vec{\Gamma}_\parallel(h_1\cos\omega t + p_1\sin\omega t)\right].$$

To obtain a second approximation, it is necessary to substitute the solution thus found in the original set of equations (12) - (15). We then find

$$i2\omega\Phi_2 + \frac{1}{6v^2}\frac{\partial}{\partial v}\{v^3[\Gamma_\perp^2\varphi_1 + \Gamma_\parallel^2\xi_1]\} = \frac{\delta\Phi_2}{\delta t} \qquad (22)$$

From these, separating the real and imaginary parts, we have

$$2\omega G_2 + \frac{1}{6v^2}\frac{\partial}{\partial v}\{v^3[\Gamma_\perp^2 f_1 + \Gamma_\parallel^2 h_1]\} = \frac{\delta F_2}{\delta t}; \qquad (23)$$

$$2\omega F_2 - \frac{1}{6v^2}\frac{\partial}{\partial v}\{v^3[\Gamma_\perp^2 g_1 + \Gamma_\parallel^2 p_1]\} = -\frac{\delta G_2}{\delta t} \qquad (24)$$

It will be shown below that under the conditions of Eq. (28) the right-hand sides of these equations are small. Assuming that the right-hand sides of Eqs. (23) and (24) are small, we shall immediately obtain an approximate expression for G_2 and F_2 which satisfy the condition of normalization at 0. These expressions can be substituted on the right-hand sides of Eqs. (23) and (24) in order to obtain a second approximation for G_2 and F_2, and so on. The solutions obtained in this manner converge well. To a first approximation, G_2 has the form

$$G_2 = \frac{1}{12\omega v^2}\frac{\partial}{\partial v}\left\{v^3\left[\frac{\Gamma_\perp^2}{A} + \frac{\Gamma_\parallel^2 l}{\omega^2 l^2 + v^2}\right]\frac{\partial \Phi_0}{\partial v}\right\}, \qquad (25)$$

and F_2, to a second approximation, has the form

$$F_2 = \frac{1}{12\omega v^2}\frac{\partial}{\partial v}\left\{v^3\left[B\Gamma_\perp^2\right.\right. \qquad (26)$$

$$\left.\left. - \frac{\omega}{v}\frac{1}{\omega^2 + \nu^2}\Gamma_\parallel^2\right]\frac{\partial \Phi_0}{\partial v}\right\} - \frac{1}{2\omega}\frac{\delta G_2}{\delta t},$$

where the operator $\delta/\delta t$ is determined by Eq. (5).

Now it is necessary to explain the stipulation that G_2 and F_2 be small in comparison with Φ_0 [in the same manner as the condition of smallness of the right-hand sides of Eqs. (23) and (24)], because this condition is necessary for the applicability of the method of successive approximations which we have used to determine the functions Φ_0, ϕ_1, ξ_1, ψ_1. We observe that the function of the distribution of electrons is, in effect, different from 0 only in the domain of the velocity v of the order of the average velocity $v_{av} = v_{av}(T, E, H)$. Therefore, attention is given to examining only the velocity region, in which v is appreciable.

From Eqs. (23) - (26), it can be easily shown that

$$G_2 \sim \frac{\delta\nu}{\omega}\Phi_0, \qquad F_2 \sim \left[\delta + \left(\frac{\delta\nu}{\omega}\right)^2\right]\Phi_0, \quad (27)$$
$$\frac{\delta F_2}{\delta t} \sim \delta\nu F_2, \qquad \frac{\delta G_2}{\delta t} \sim \delta\nu G_2,$$

where $v \sim v_{av}$ under the conditions

$$\delta\nu(v_{av}) \ll \omega \quad (28)$$

G_2 and F_2 will be small compared to Φ_0 and can be neglected; and the right-hand sides of Eqs. (23) and (24) will be small compared to the terms on the left-hand sides. It can be seen that the corrections to the following approximations to the functions Φ_0, F_2 and G_2, as well as the functions F_4, G_4, etc., are of a low order compared to $\delta\nu/\omega$. In this manner, Eq. (28) is demonstrated to be the condition for the applicability of the method of successive approximations. We note that these conditions place certain restrictions on the field intensity, because v_{av} is field-dependent.

Let us estimate the order of v_{av} in the case when the magnetic field $\mathbf{H} = 0$ and the influence of the molecular temperature on the function of the electron distribution can be neglected in comparison with the influence of the electric field $\mathbf{E}$. Furthermore, let the length of the free path be l = const. It is evident that v_{av} is of the order of magnitude of the v's for which the exponent in Eq. (19) is of the order of unity. Such an estimate gives the following information about v_{av}:

$$v_{av}^2 \sim \sqrt{\left(\frac{\omega^2 l^2}{2}\right)^2 + \frac{\Gamma_\parallel^2 l^2}{3\delta}} - \frac{\omega^2 l^2}{2} \quad (29)$$

Hence, Eq. (28) takes on the form

$$\frac{\delta^2}{l^2}\left(\sqrt{\left(\frac{\omega^2 l^2}{2}\right)^2 + \frac{\Gamma_\parallel^2 l^2}{3\delta}} - \frac{\omega^2 l^2}{2}\right) \ll \omega^2. \quad (30)$$

This stipulation is well satisfied for $\omega = 10^7$ sec^{-1}, $E \leq 10^{-1}$ V/cm or for $\omega = 10^6$ sec^{-1}, $E \leq 10^{-2}$ V/cm ($l = 1$ cm).

If we set $H = 0$ in Eqs. (19) - (21), then the distribution thus found agrees with that of Margenau[3] who disregarded the influence of the magnetic field. The formula arrived at in reference 5 erroneously omits the term $\Gamma_\parallel^2 Ml^2/6(\omega^2 l^2 + v^2)$ in Eq. (19) and the terms with $\Gamma_\parallel$ in Eq. (21).

In the quasi-stationary case ($\omega \ll \delta\nu$; see reference 9) the distribution function agrees with that in a constant electric field (it is necessary only to replace the constant electric field E_0 by $E_0 \cos \omega t$). The distribution function in a constant field cannot be found simply by substitution of $\omega = 0$ in Eqs. (18) and (19) as was done by Jancel and Kahan[5], since Eqs. (18) and (19) were derived from Eq. (28)*.

In the constant field ($\delta f/\delta t = 0$; $\Theta = 1$) Eqs. (6) - (9) take on the form

$$\frac{1}{3v^2}\frac{\partial}{\partial v}\{v^3(\Gamma_\perp^2\varphi + \Gamma_\parallel^2\xi)\} \quad (6')$$
$$= \frac{1}{v^2}\frac{m}{M}\frac{\partial}{\partial v}\left(\frac{v^4}{l}f_0\right) + \frac{kT}{Mv^2}\frac{\partial}{\partial v}\left(\frac{v^3}{l}\frac{\partial f_0}{\partial v}\right),$$

$$\frac{1}{v}\frac{\partial f_0}{\partial v} - \frac{e}{mc}H^2\psi = -\frac{v}{l}\varphi, \quad (7')$$

$$\frac{1}{v}\frac{\partial f_0}{\partial v} = -\frac{v}{l}\xi, \quad (8')$$

$$\frac{e}{mc}\varphi = -\frac{v}{l}\psi. \quad (9')$$

whence

$$\varphi = -\frac{1}{v}\frac{\partial f_0}{\partial v}\frac{\nu}{\omega_H^2 + \nu^2}, \quad (31)$$

$$\psi = -\frac{e}{mc\nu}\varphi, \qquad \xi = -\frac{1}{v\nu}\frac{\partial f_0}{\partial v},$$

$$f_0 = C\exp\left\{-\int_0^v \frac{mv\,dv}{kT + \left(\Gamma_\perp^2 Ml/3A'\right) + \left(\Gamma_\parallel^2 Ml^2/3v^2\right)}\right\},$$

$$A' = \frac{v^2}{l}(1 + z'), \qquad z' = \frac{\omega_H^2}{\nu^2}.$$

It can easily be seen that the distribution function coincides with that of Davydov[1].

Until now, we have not attempted to form a picture of the dependence of l on velocity. In a number of works[4,6,9], two very simple possibilities are considered: l = const and l = const $\times$ v;

---

* Jancel and Kahan[5] contend that with $\omega = 0$, the distribution obtained by them agrees with that obtained by Chapman and Cowling[7] for a constant field. This is not so.

[7] S. Chapman and T. Cowling, *The Mathematical Theory of Non-Uniform Gases*, Cambridge, 1952, p. 355

[8] V. L. Ginzburg, J. Exper. Theoret. Phys. USSR 21, 943 (1951)

[9] Y. L. Al'pert, V. L. Ginzburg and E. L. Feinberg, *Wave Propagation*, Gostekizdat, 1953

in the second case, the frequency of collision remains constant, $\nu = v/l$. To satisfy the condition

$$\left(\frac{1-z}{1+z}\right)^2 \frac{\omega^2}{\nu^2} \gg 1,$$

Eq. (19) turns into a Maxwellian distribution [independent of the form of the dependence $l(v)$]:

$$\Phi_0 = \left(\frac{m}{2\pi k T_{\text{eff}}}\right)^{3/2} \exp\left\{-\frac{mv^2}{2kT_{\text{eff}}}\right\}, \quad (19')$$

where

$$T_{\text{eff}} = T\left[1 + \frac{M}{6kT}\left(\frac{\Gamma_\perp^2 (1+z)}{\omega^2 (1-z)^2} + \frac{\Gamma_\parallel^2}{\omega^2}\right)\right],$$

$$z = \frac{\omega_H^2}{\omega^2}.$$

When the number of collisions is constant, then Eq. (19) again turns into a Maxwellian distribution, with an effective temperature

$$T_{\text{eff}} = T\left[1 + \frac{\Gamma_\perp^2 M (1+z)}{6kT(\omega^2(1-z)^2 + \nu^2(1+z)^2)} + \frac{\Gamma_\parallel^2 M}{6kT(\omega^2+\nu^2)}\right]. \quad (32)$$

Let us propose, as was done by Klimontovich [4], that $\nu = v_{\text{av}}/\tilde{l}$, where $\tilde{l}$ is independent of velocity, field and temperature, and v_{av} is some average velocity expressed by means of the effective temperature; e.g., in the following manner*

$$v_{\text{av}}^2 = kT_{\text{eff}}/m. \quad (33)$$

Then, the effective temperature is determined by Eqs. (32) and (33). In this case, Eq. (31) coincides with that obtained by Klimontovich [4] if we set $\Gamma_\parallel^2 = 0$ ($\mathbf{E} \perp \mathbf{H}$) ** in (31).

3. THE ELECTRON DISTRIBUTION IN THE PRESENCE OF A MODULATED ELECTRIC FIELD AND A CONSTANT MAGNETIC FIELD

At times it is necessary to know the function of the electron distribution in the presence of an amplitude-modulated electromagnetic wave (e.g., in the examination of ionospheric cross-modulation). Two cases must be distinguished here.

In the first case, when the modulation frequency* is

$$\Omega \ll \delta\nu, \quad (34)$$

it is only necessary to substitute in all formulas in the preceding part, $\vec{\Gamma}$ for $\vec{\Gamma}(1 + \mu \cos \Omega t)$, since Eq. (34) proves to be quasi-stationary.

In the second case, when

$$\Omega \gg \delta\nu, \quad (35)$$

it is necessary to carry out the integration of the system of Eqs. (6) - (9) where we must assume

$$\Theta = \cos \omega t (1 + \mu \cos \Omega t).$$

We shall seek a distribution function of the form

$$f(\mathbf{v}, t) = \sum_{n,k} \Phi_{n,k} e^{i\omega_{n,k} t} + \mathbf{v} \sum_{n,k} (\vec{\Gamma}_\perp \varphi_{n,k} + [\mathbf{H}\vec{\Gamma}]\psi_{n,k} + \vec{\Gamma}_\parallel \xi_{n,k}) e^{i\omega_{n,k} t}, \quad (36)$$

where

$$\omega_{n,k} = n\omega + k\Omega, \quad \Phi_{n,k} = \Phi^*_{-n,-k},$$

$$\varphi_{n,k} = \varphi^*_{-n,-k},$$

$$\psi_{n,k} = \psi^*_{-n,-k}, \quad \xi_{n,k} = \xi^*_{-n,-k}.$$

Having substituted Eq. (36) in Eqs. (6) - (9) and having taken into consideration that

$$\Theta = \cos \omega t (1 + \mu \cos \Omega t) \equiv \frac{1}{2} e^{i\omega_{1,0} t} + \frac{1}{2} e^{-i\omega_{1,0} t} + \frac{\mu}{4}(e^{i\omega_{1,-1} t} + e^{-i\omega_{1,-1} t} + e^{i\omega_{1,1} t} + e^{-i\omega_{1,1} t}),$$

we obtain the following equations for the determination of $\Phi_{n,k}$, $\psi_{n,k}$, $\phi_{n,k}$, $\xi_{n,k}$:

$$i\omega_{n,k}\Phi_{n,k} + \frac{1}{6v^2}\frac{\partial}{\partial v}\left\{v^3\left[\Gamma_\perp^2\left(\varphi_{n-1,k} + \varphi_{n+1,k} + \frac{\mu}{2}\varphi_{n-1,k-1} + \frac{\mu}{2}\varphi_{n+1,k-1} + \frac{\mu}{2}\varphi_{n-1,k+1} + \frac{\mu}{2}\varphi_{n+1,k+1}\right) + \Gamma_\parallel^2\left(\xi_{n-1,k} + \xi_{n+1,k} + \frac{\mu}{2}\xi_{n-1,k-1} + \frac{\mu}{2}\xi_{n+1,k-1} + \frac{\mu}{2}\xi_{n-1,k+1} + \frac{\mu}{2}\xi_{n+1,k+1}\right)\right]\right\} = \frac{\delta\Phi_{n,k}}{\delta t}; \quad (37)$$

* We observe that it is not essential which average velocity we substitute in the relation $\nu = v_{\text{av}}/\tilde{l}$ since this is reflected only in the magnitude of $\tilde{l}$.

** Equation (25) of Klimontovich [4] is incorrect, inasmuch as an applied magnetic field would change the plasma temperature even for the case when $E = 0$.

* Equation (35) and other analogous relations have the same connotation as in Part 2; that is, they must be satisfied in the domain of velocities of the order of v_{cp}.

$$\varphi_{n,k} = -\frac{1}{2v}\frac{i\omega_{n,k}+\nu}{(i\omega_{n,k}+\nu)^2+\omega_H^2}L_{n,k}; \quad (38)$$

$$\psi_{n,k} = -\frac{e}{mc}\frac{1}{i\omega_{n,k}+\nu}\varphi_{n,k}; \quad (39)$$

$$\xi_{n,k} = -\frac{1}{2v}\frac{1}{i\omega_{n,k}+\nu}L_{n,k}, \quad (40)$$

where

$$L_{n,k} = \frac{\partial\Phi_{n-1,k}}{\partial v} + \frac{\partial\Phi_{n+1,k}}{\partial v} + \frac{\mu}{2}\left(\frac{\partial\Phi_{n-1,k-1}}{\partial v} + \frac{\partial\Phi_{n+1,k+1}}{\partial v} + \frac{\partial\Phi_{n-1,k+1}}{\partial v} + \frac{\partial\Phi_{n+1,k-1}}{\partial v}\right).$$

We shall attempt to obtain the solution of Eqs. (37) - (40) by the method of successive approximations: furthermore, we shall assume that the relation

$$\omega \gg \Omega. \quad (41)$$

is satisfied.

To the first approximation, we neglect in $L_{n,k}$ all $\Phi_{n,k}$'s except $\Phi_{0,0}$. Then from Eqs. (38) - (40) we find [utilizing Eq. (41)]:

$$\varphi_{1,0} = -\frac{1}{2}\frac{\partial\Phi_{0,0}}{\partial v}\left(\frac{1}{A}+iB\right), \quad (42)$$

$$\varphi_{1,1} = \varphi_{1,-1} = \frac{\mu}{2}\varphi_{1,0},$$

$$\xi_{1,0} = -\frac{1}{2v}\frac{\partial\Phi_{0,0}}{\partial v}\frac{\nu-i\omega}{\omega^2+\nu^2},$$

$$\xi_{1,-1} = \xi_{1,1} = \frac{\mu}{2}\xi_{1,0},$$

$$\psi_{n,k} = -\frac{e}{mc}\frac{\nu-i\omega}{\omega^2+\nu^2}\varphi_{n,k},$$

where A and B have the same connotation as in the preceding parts. Integrating Eq. (37) and setting $n = 0$ and $k = 0$, we find

$$\Phi_{0,0} = C\exp\left\{-\int_0^v \frac{mvdv}{kT + [\Gamma_\perp^2 Ml(1+\mu^2/2)\,6A] + [\Gamma_\parallel^2 Ml^2(1+\mu^2/2)/6(\omega^2l^2+v^2)]}\right\}. \quad (43)$$

To obtain $\Phi_{0,1}$, $\Phi_{0,2}$, $\Phi_{2,0}$, $\Phi_{2,\pm1}$, $\Phi_{2,\pm2}$ to a first approximation, we write the following equations:

$$i\omega_{0,1}\Phi_{0,1} + \frac{1}{6v^2}\frac{\partial}{\partial v}\left\{v^3\left[\Gamma_\perp^2\left(\varphi_{-1,1}+\varphi_{1,1}+\frac{\mu}{2}\varphi_{1,0}+\frac{\mu}{2}\varphi_{-1,0}\right)\Gamma_\parallel^2\left(\xi_{-1,1}+\xi_{1,1}+\frac{\mu}{2}\xi_{1,0}+\frac{\mu}{2}\xi_{-1,0}\right)\right]\right\} = \frac{\delta\Phi_{0,1}}{\delta t}; \quad (44)$$

$$i\omega_{0,2}\Phi_{0,2} + \frac{1}{6v^2}\frac{\partial}{\partial v}\left\{v^3\left[\Gamma_\perp^2\left(\frac{\mu}{2}\varphi_{1,1}+\frac{\mu}{2}\varphi_{-1,1}\right) + \Gamma_\parallel^2\left(\frac{\mu}{2}\xi_{1,1}+\frac{\mu}{2}\xi_{-1,1}\right)\right]\right\} = \frac{\delta\Phi_{0,2}}{\delta t}; \quad (45)$$

$$i\omega_{2,0}\Phi_{2,0} + \frac{1}{6v^2}\frac{\partial}{\partial v}\left\{v^3\left[\Gamma_\perp^2\left(\varphi_{1,0}+\frac{\mu}{2}\varphi_{1,-1}+\frac{\mu}{2}\varphi_{1,1}\right) + \Gamma_\parallel^2\left(\xi_{1,0}+\frac{\mu}{2}\xi_{1,-1}+\frac{\mu}{2}\xi_{1,1}\right)\right]\right\} = \frac{\delta\Phi_{0,2}}{\delta t}; \quad (46)$$

$$i\omega_{2,\pm1}\Phi_{2,\pm1} + \frac{1}{6v^2}\frac{\partial}{\partial v}\left\{v^3\left[\Gamma_\perp^2\left(\varphi_{1,\pm1}+\frac{\mu}{2}\varphi_{1,0}\right) + \Gamma_\parallel^2\left(\xi_{1,\pm1}+\frac{\mu}{2}\xi_{1,0}\right)\right]\right\} = \frac{\delta\Phi_{2,\pm1}}{\delta t}; \quad (47)$$

$$i\omega_{2,\pm2}\Phi_{2,\pm2} + \frac{1}{6v^2}\frac{\partial}{\partial v}\left\{v^3\left[\Gamma_\perp^2\frac{\mu}{2}\varphi_{1,\pm1} + \Gamma_\parallel^2\frac{\mu}{2}\xi_{1,\pm1}\right]\right\} = \frac{\delta\Phi_{2,\pm2}}{\delta t}.$$

To find the coefficients for $\cos\omega_{n,k}t$ and $\sin\omega_{n,k}t$ in the distribution function, it is necessary to make a transformation from the complex form to the real form and to take into consideration a relationship analogous to that of Eq. (10) and Eq. (11). Then, with accuracy to terms of the order of $(\delta\nu/\Omega)\Phi_{0,0}$ we find

$$\Omega G_{0,1} + \frac{1}{6v^2}\frac{\partial}{\partial v}\{v^3[\Gamma_\perp^2(f_{1,-1}+f_{1,1}+\mu f_{1,0}) + \Gamma_\parallel^2(h_{1,-1}+h_{1,1}+\mu h_{1,0})]\} = 0; \quad (48)$$

$$\Omega F_{0,1} = 0; \quad (49)$$

$$2\Omega G_{0,2} + \frac{1}{6v^2}\frac{\partial}{\partial v}\left\{\frac{\mu}{2}v^3[\Gamma_\perp^2(f_{1,-1}+f_{1,1}) + \Gamma_\parallel^2(h_{1,-1}+h_{1,1})]\right\} = 0, \quad (50)$$

$$2\Omega F_{0,2} = 0. \tag{51}$$

Hence

$$G_{0,1} = \frac{1}{\Omega}\frac{1}{3v^2}\frac{\partial}{\partial v}\left\{\left(\frac{\Gamma_\perp^2}{A} + \frac{\Gamma_\parallel^2 l}{\omega^2 l^2 + v^2}\right)\mu v^3 \frac{\partial \Phi_{0,0}}{\partial v}\right\}, \tag{52}$$

$$G_{0,2} = \frac{\mu}{8} G_{0,1}, \quad F_{0,1} = F_{0,2} = 0.$$

Analogously, the functions $F_{2,0}$, $G_{2,0}$, etc., are found to a first approximation. These functions are small by comparison with $\Phi_{0,0}$, $G_{0,1}$ and $G_{0,2}$ on the strength of the condition (41). In the case where there is no magnetic field ($\mathbf{H} = 0$) the first term of the transformation (52) of degree $\Gamma_\parallel^2$ coincides with the solution achieved in reference 9 (page 355) for a weak electric field.

The first non-vanishing approximation for the functions $F_{0,1}$, $F_{0,2}$, $F_{0,3}$ and $F_{0,4}$, which will be of the order of $(\delta\nu/\Omega)^2 \Phi_{0,0}$, can be found by substituting in Eqs. (37) - (40) the functions obtained for $\Phi_{0,0}$, $G_{0,1}$ and $G_{0,2}$, and neglecting the remaining $\Phi_{n,k}$'s. Following are the formulas obtained in this manner:

$$F_{0,1} = -\frac{1}{6v^2\Omega}\frac{\partial}{\partial v}\left\{v^3\left(\frac{\Gamma_\perp^2}{A} + \frac{\Gamma_\parallel^2 l}{\omega^2 l^2 + v^2}\right)\left(1 + \frac{3\mu^2}{8}\right)\frac{\partial G_{0,1}}{\partial v}\right\} - \frac{1}{\Omega}\frac{\delta G_{0,1}}{\delta t}, \tag{53}$$

$$F_{0,2} = -\frac{1}{12v^2\Omega}\frac{\partial}{\partial v}\left\{v^3\left(\frac{\Gamma_\perp^2}{A} + \frac{\Gamma_\parallel^2 l}{\omega^2 l^2 + v^2}\right)\mu\left(\frac{9}{8} + \frac{\mu^2}{16}\right)\frac{\partial G_{0,1}}{\partial v}\right\} - \frac{\mu}{16\Omega}\frac{\delta G_{0,1}}{\delta t}, \tag{54}$$

$$F_{0,3} = -\frac{1}{18v^2\Omega}\frac{\partial}{\partial v}\left\{v^3\left(\frac{\Gamma_\perp^2}{A} + \frac{\Gamma_\parallel^2 l}{\omega^2 l^2 + v^2}\right)\frac{3\mu^2}{8}\frac{\partial G_{0,1}}{\partial v}\right\}, \tag{55}$$

$$F_{0,4} = \frac{\mu}{16} F_{0,3}. \tag{56}$$

Here the operator $\delta/\delta t$ is determined by Eq. (5). We shall also write the functions of $G_{0,3}$ and $G_{0,4}$ which, for the first non-vanishing approximation, are of the order of $(\delta\nu/\Omega)^3 \Phi_{0,0}$

$$G_{0,3} = \frac{1}{3\Omega}\frac{1}{6v^2}\frac{\partial}{\partial v}\left\{v^3\left(\frac{\Gamma_\perp^2}{A} + \frac{\Gamma_\parallel^2 l}{\omega^2 l^2 + v^2}\right)\left(\frac{\mu^2}{4}\frac{\partial F_{0,1}}{\partial v} + \mu\frac{\partial F_{0,2}}{\partial v} + \left(1 + \frac{\mu^2}{2}\right)\frac{\partial F_{0,3}}{\partial v} + \frac{\mu^2}{4}\frac{\partial F_{0,4}}{\partial v}\right)\right\} + \frac{1}{3\Omega}\frac{\delta F_{0,3}}{\delta t}, \tag{57}$$

$$\frac{\Gamma_\parallel^2 l}{\omega^2 l^2 + v^2}\left[\left(1 + \frac{\mu^2}{2}\right)\frac{\partial F_{0,4}}{\partial v} + \mu\frac{\partial F_{0,3}}{\partial v} + \Gamma_\parallel^2\frac{\mu}{2}\xi_{1,\pm 1}\right] = \frac{\delta \Phi_{2,\pm 2}}{\delta t} \cdot \left\{\frac{\mu^2}{4}\frac{\partial F_{0,2}}{\partial v}\right\} + \frac{1}{4\Omega}\frac{\delta F_{0,4}}{\delta t}. \tag{58}$$

The functions $\phi_{n,k}$, $\psi_{n,k}$, $\xi_{n,k}$ can easily be found from Eqs. (38) - (40) by substituting in them the functions obtained for $\Phi_{n,k}$. The functions $F_{0,1}$, $G_{0,1}$, $F_{0,2}$, $G_{0,2}$, etc., are normalized at 0, as seen from the corresponding formulas. Consequently, it is necessary to normalize only the function $\Phi_{0,0}$.

In conclusion, I express deep gratitude to S. A. Zhevakin for the direction and constant interest in the work, and also to V. L. Ginzburg, who looked over the manuscript and gave me many valuable suggestions.

Translated by F. A. Rojak
76

Certain Properties of a Spark Counter for Counting α-Particles

E. Andreeschchev and B. M. Isaev

(Submitted to JETP editor February 16, 1954)
J. Exper. Theoret. Phys. USSR 28, 335-342 (March, 1955)

It is shown that at the expense of a continuous corona discharge a spark counter possesses self-stabilizing characteristics. Investigations were made on the counting characteristics in relation to their dependence on various electrode spacings and on the humidity. It is shown that the efficiency of the counting increases with increasing humidity.

1. INTRODUCTION

In recent years there has appeared a series of investigations[1-5] devoted to the analysis of a new type of spark counter. The idea of using a spark discharge for counting ionizing radiations is not new. In 1935, Greinacher proposed a spark counter in which a small sphere or wire of diameter 0.5-1.5 mm served as the anode and a metallic plate served as the cathode. The anode was separated from the cathode by a distance of 0.5 mm[6].

A spark discharge appears in Greinacher's counter when it is operated in air at atmospheric pressure in the presence of ionizing radiations. The duration of the discharge is limited by a quenching circuit and is approximately 0.01 sec long. The faults of this type of counter are the following: the large slope and the small length of the counting characteristic, the unstable operation, the indeterminate operating volume and also the small resolving power. It is necessary to point out that a discharge in this particular counter is caused not only by α, but also by β- and γ-particles. These counters acquired no practical use because of these faults.

In reference 7 it was shown that all these faults could be corrected if a flat metallic plate were used as the cathode, and a thin (diameter 0.1 mm) metallic wire was used as the anode. The wire was stretched parallel to the plane of the cathode and was located a distance of 1 - 1.5 mm from it. A counter of this type is generally operated in air at atmospheric pressure and, most important of all, a discharge in it is caused only by particles of large specific ionization. Because of the simple construction of such counters and the easy recording of the pulses (the magnitude of a pulse is very large and may reach a value of several thousand volts), such counters have, in individual cases, several advantages over other methods for counting α-particles, slow neutrons and fission fragments of uranium [4,5].

An important characteristic of spark counters is the ability to count these forms of radiation in the presence of practically an unlimited background of β- and γ- radiations. Such counters are very directional.

In Fig. 1, the schematic shows a section of the spark counter in two directions. Here A is the anode in the form of a wire, and K is the flat cathode. The arrow points in the direction of flight of the α-particles; the α-particles are counted only in that case in which the angle ϕ is not larger than 5 - 6°. The related angle, ψ, may attain the considerably larger value of 40 - 50°. Within these limits, the intense ionization of the α-particles

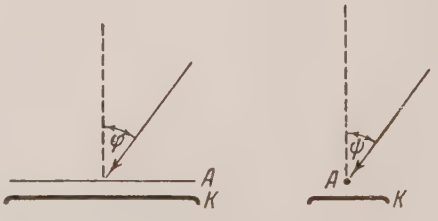

Fig. 1. A section of the spark counter. A -- anode, B -- cathode.

[1] R. D. Connor, Proc. Phys. Soc. (London) **64**, 30 (1951)

[2] M. Ronald and B. Payne, J. Sci. Instr. **26**, 321 (1949)

[3] R. D. Connor, J. Sci. Instr. **29**, 12 (1952)

[4] P. Savel, Compt. rend. **235**, 156 (1952)

[5] P. Savel, Compt. rend. **234**, 2596 (1952)

[6] H. Greinacher, Z. Phys. **16**, 165 (1935)

[7] W. V. Chang and S. Rosenblum, Phys. Rev. **67**, 222 (1945)

causes the appearance of a spark discharge. The pulse is counted by an electronic circuit.

Present work is devoted to the investigation of the properties of the spark counter, in particular, to the dependence of the counting characteristics on the inter-electrode spacing, the humidity, the temperature, etc.

2. EQUIPMENT

A tungsten filament of diameter 0.1 mm, fastened to the plexiglass frame, served as the anode of the counter; a carefully polished plate of silver or brass served as the cathode. It was possible to change the distance between the cathode and the anode by means of a micrometer screw. As a source of α-particles, a preparation consisting of a mixture of radium, and mesothorium was deposited in a thin layer on a plexiglass disc 30 mm in diameter. For testing the dependence of the counting efficiency as a function of the angle ψ, the source was attached to a special holder and was set at various angles. (The axis of rotation of the preparation coincided with the direction of the wire. See Fig. 2.) Radiations from the surface in these cases were limited by a slit diaphragm, 5 mm wide and 30 mm long, placed 3 cm from the wire.

Since the sensitive region of the counter is limited to a region approximately 0.5 mm[1] wide, the only α-particles recorded are those which lie within the angle shown as a shaded region in Fig. 2. This produces a naturally collimated beam of α-particles.

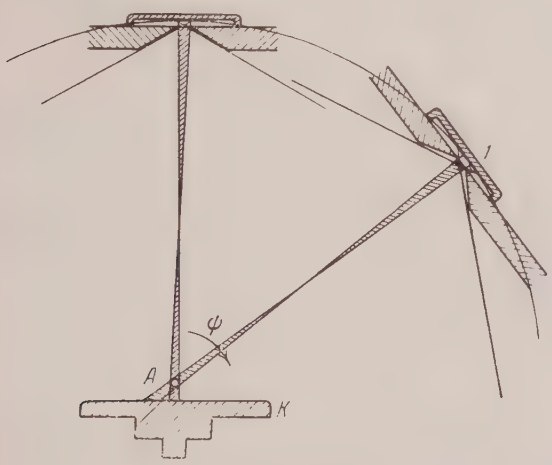

Fig. 2. A -- tungsten wire, K -- cathode, 1 -- source.

The pulses were counted by a scaling circuit, PS - 64. A rectifier supplied the high voltage for the wire (anode). The pulses arising from the discharge appeared across a voltage divider consisting of two series resistors, R_1 and R_2 ($R_1 = 5\,M\Omega$, $R_2 = 5\,k\Omega$), shunted by condensers C_1 and C_2. Pulses appearing across R_2 were fed to an amplifier which is in cascade with this scaler. This apparatus is mounted very close to the anode of the counter. For measuring the large corona currents, a microammeter was placed in series with the circuit*.

For measuring the dependence of the efficiency of the counter on temperature and humidity, the equipment was placed in a specially hermetically-sealed box (for decreasing the effect of ozone, produced by the discharge, the hermetically sealed volume was made equal to 1 m[3]).

3. EXPERIMENTAL RESULTS

In Fig. 3 (curve *1*) a count-rate characteristic of a spark counter is shown. (The distance l between the wire and the plate was 1.5 mm; the diameter of the wire was 0.1 mm; the source was undiaphragmed.) The count-rate per minute, N, is plotted on the ordinate axis, and the full voltage V_B, of the high voltage supply is plotted on the abscissa. Also shown in this Figure is the corona current, I, (Curve *2*) as read on the microammeter**. As is seen from the Figure, the value of the corona current in the working range of the characteristic reaches large values (several hundred microamperes). Noting that, in the circuit of the counter, the value of the quenching resistance is several megohms, it follows that the potential difference between the anode and the cathode will be significantly smaller than the full voltage V_B. The spark counter under consideration we may consider as a corona stabilizer. The degree of stability in the cathode, as shown by Veksler[8], is determined by the ratio of the internal resistance of the dis-

[8] B. I. Veksler, A. V. Groshev and N. A. Dobrotin, *Experimental Methods of Nuclear Physics*, Moscow, 1940

* The values of R_1, R_2, C_1 and C_2 are to a large degree arbitrarily chosen. Because of the short duration of the pulse (approximately 10^{-8} sec), clearly, the condensers play the basic role in the divider circuit.

** It is necessary to state that we did not observe a peak at the beginning of the counting characteristic as is described in a series of papers [e.g., see reference 1, R. D. Connor, Proc. Phys. Soc. (London) **64**, 30 (1951) and reference 2, M. Ronald and B. Payne, J. Sci. Instr. **26**, 321 (1949)]. Possibly the absence of the peak is explained by the fact that this characteristic disappears on using an uncollimated beam of α-particles.

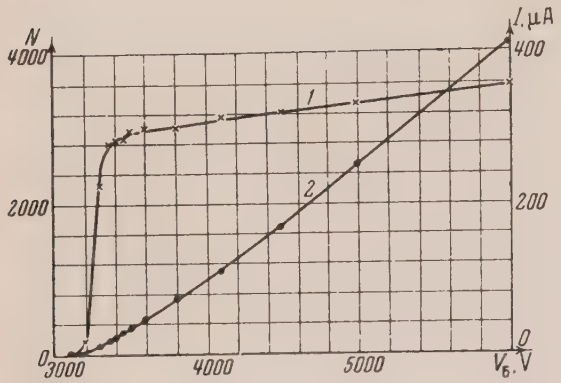

Fig. 3. *1* -- a typical counting characteristic of a spark counter; *2* -- the value of the corona current.

charge space and the external resistance, $R_1 + R_2$. Obviously, the true voltage in the counter will be

$$V_{A-K} = V_B - RI, \qquad (1)$$

where R is the value of the quenching resistance ($R \approx R_1 + R_2$) and I is the value of the corona current.

The count and corona characteristics of the spark counter which are shown in Fig. 4 were constructed from the basic data of Fig. 3. The abscissa depicts the voltage during the discharge interval, V_{A-K}. It is understandable that the slope and length of the counting characteristic will depend on the value of the quenching resistance $R = R_1 + R_2$, since, by changing the value R, the degree of stability of the voltage V_{A-K} will change.

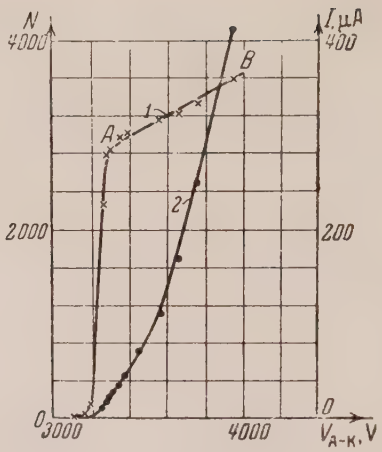

Fig. 4. *1* -- counting characteristic, and *2* -- corona characteristic of the spark counter, computed from the data in Fig. 3.

For illustration purposes, Fig. 5 shows the family of counting (curves *1* - *6*) and corona (curves *1′* - *6′*) characteristics for various values of resistance, R (R was varied from 2.5 to 150 MΩ).

Determining V_{A-K} from Eq. (1), all these curves can be combined into one counting and one corona characteristic, shown in Fig. 6. This Figure clearly shows the change in slope and magnitude of the counting rate with increasing values of quenching resistance. Increasing R increases the degree of stability, and even with significantly larger V_B, the voltage V_{A-K} on the counter still only corresponds to the initial rise of the counting

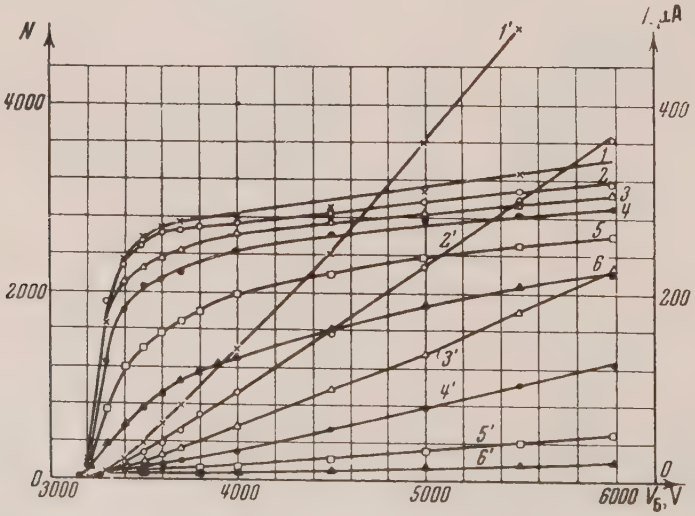

Fig. 5. *1* - *6* counting and *1′* - *6′* corona characteristics for various resistors: *1* = 2.5; *2* = 5; *3* = 10; *4* = 20; *5* = 50; and *6* = 150 MΩ.

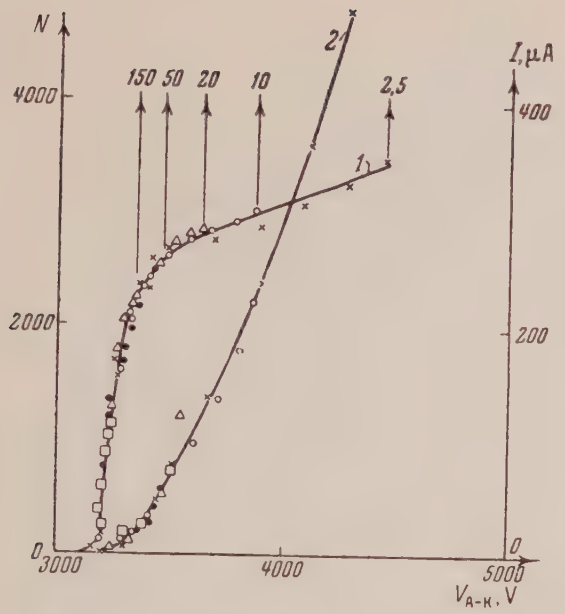

Fig. 6. *1* -- counting and *2* -- corona characteristics for various resistors: × = 2.5; ○ = 10; △ = 20; = 50; = 150 MΩ, computed from the data of Fig. 5.

characteristic in Fig. 6.

In Fig. 6 the arrows show the limiting value of V_{A-K} for various resistances and a voltage V_{A-K} = 6000 V. With the resistance R = 150 MΩ all of the counting characteristic lies in the steep region of the curve. This causes the large slope of the counting characteristic in Fig. 5, and correspondingly, the small efficiency.

As was mentioned previously, the sensitive region of the counter, through which the α-particle should pass in order to initiate a spark discharge, has a very small volume and extends with a corresponding drop in efficiency at a distance of 0.5 mm around the center of the wire. It is obvious that the sensitive region around the wire is determined by the geometry of the electric field. The force field should be somewhat extended in the direction of the cathode. For determining the form of the sensitive region the equigradient planes of the system were computed. The curves in Fig. 7 were obtained for a wire to plate distance of 1.5 mm and for the potentials V_{A-K} = 3300 V and V_{A-K} = 4000 V (curves *1* and *2*). These particular potentials correspond to the points A and B on the counting characteristic shown in Fig. 4, and are equal to a value of E/p = 20 V/cm-mm of Hg. At present it is difficult to know precisely the dimensions of the sensitive volume. It is possible to hypothesize that the sensitive volume is

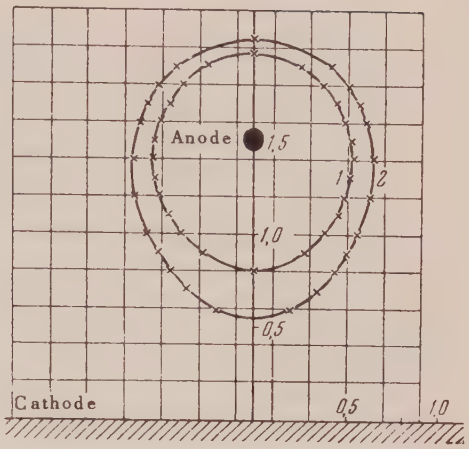

Fig. 7. Equigradient planes of the wire-plate system for E/p = 20 V/cm-mm of Hg.

positioned within the region bounded by the curve for E/p = 20 V/cm-mm of Hg, outside of which the negative ions begin to decay and the value of the Townsend ionization coefficient becomes largely equal to zero[9]. From the Figure it is seen that by increasing the potential of the wire, the sensitive volume expands. This leads to an increase in the number of counted particles and seems to affect the magnitude of the slope of the counting characteristic.

From these considerations, one must expect that the slope of the counting characteristic will change, depending on the angle at which the α-particles enter into the sensitive volume. To examine this hypothesis the number of counted particles was determined as a function of the angle ψ. The results of these measurements are shown in Fig. 8, where curve A is for V_{A-K} = 3600 V and curve B is for V_{A-K} = 4200 V. While ψ = 0 the number of counted particles increases, for example, by 5%, while at angles ψ = 30-60° the relative sensitivity increases 35 - 60%.

Two counting characteristics (linear part) for ψ = 0 and ψ = 40° are shown in Fig. 9.

It is obvious that the form of the counting characteristic already shows the existing dependence of the counter characteristics on the spacing of the anode relative to the cathode. Figure 10 illustrates a family of counting (*1* - *4*) and corona (*1′* - *4′*) characteristics for a wire-to-plane spacing of 1 to 5 mm and R = 5 MΩ. Now noting the decrease of effective counting rate with an increase of the distance, it is obvious that the connection

[9] N. A. Kaptsov, *Electrical Phenomena in Gases and Vacuum*, Moscow, 1950

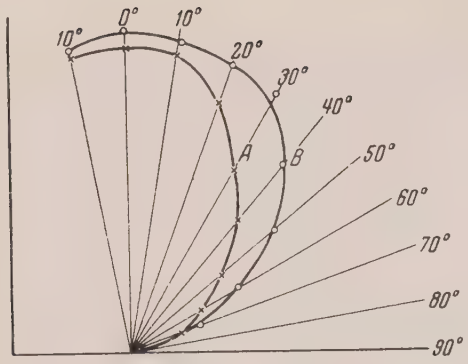

Fig. 8. The number of counted particles as a function of the angle ψ for the two values of voltage: A = 3600 V, B = 4200 V.

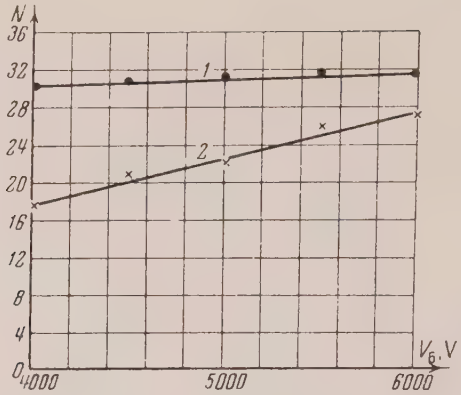

Fig. 9. *1* -- $\psi = 0°$, *2* -- $\psi = 40°$.

is due to the decreased probability of starting a streamer in a region of small field gradient. It is necessary to note that beginning with a distance of 3 mm the appearance of a visible spark is not generally observed at the start of the characteristic curve.

It should be noted that the substitution for the wire-plate system of electrodes, of a wire-cylinder or half cylinder system, improves the quality of the counting of the apparatus. By this change the efficiency of counting is increased at the expense of the geometry of the electric field. This is shown in Fig. 11. For comparison, the variation in counting sensitivity as a function of the impinging α-particles for a wire and plate system (curve *2*) and a wire and semicylinder system (curve *2'*), for a semicylinder of radius 1.5 mm, are shown. The counting efficiency at $\psi = 0$ we set equal to unity. As seen in Fig. 11, for the wire-semicylinder case, the counting sensitivity remains constant to the 60° angle. At larger angles the decrease in sensitivity can be explained as caused by the decrease of the electric field due to the edge effect.

The final important characteristic of this counter is the constant stability of the apparatus with changes in temperature and moisture. Experiments indicate that the sensitivity of the counter is strongly dependent on the amount of water vapor. As illustrated in Fig. 12, three counting characteristics (for a wire-plate structure) are shown for various water vapor pressures: 22 mm of Hg (curve *1*), 12 mm of Hg (curve *2*), and 5.6 mm of Hg (curve *3*). The corona characteristics are also shown in this Figure. As seen from the

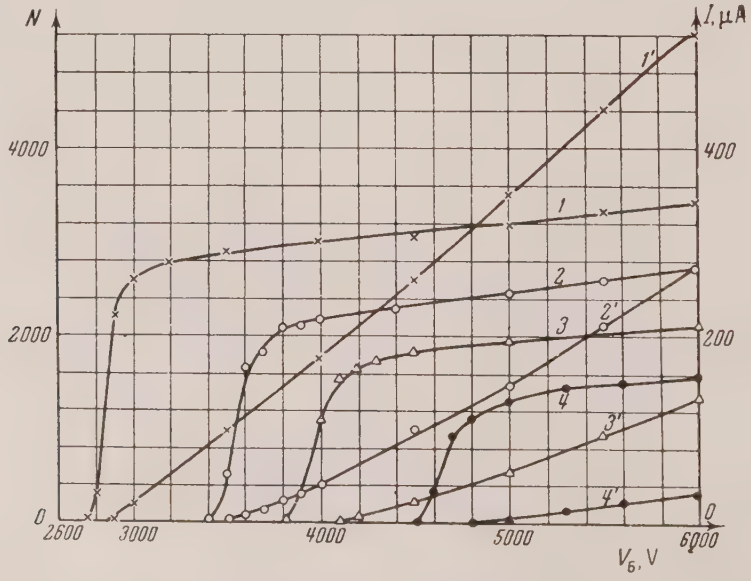

Fig. 10. *1* - *4* counting and *1'* - *4'* corona characteristics for various wire-to-plate spacings: *1* = 1; *2* = 2; *3* = 3; *4* = 5 mm.

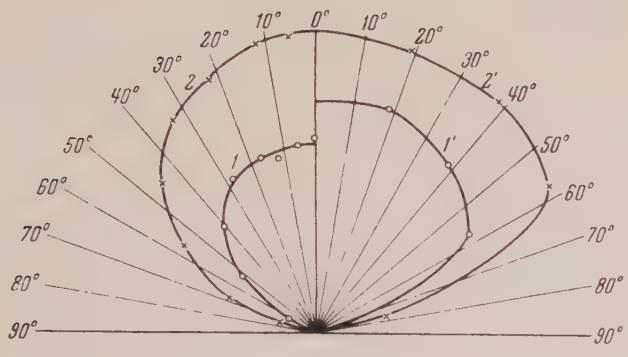

Fig. 11. The change in the sensitivity of the counter with the angle of the impinging α-particle; *2* -- for a wire-plate system, *2′* -- for a wire-semicylinder system.

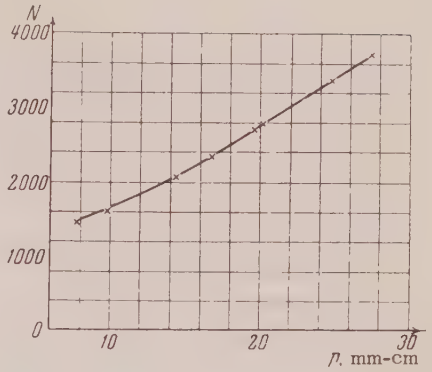

Fig. 13. The dependence of the count-rate on the water vapor pressure.

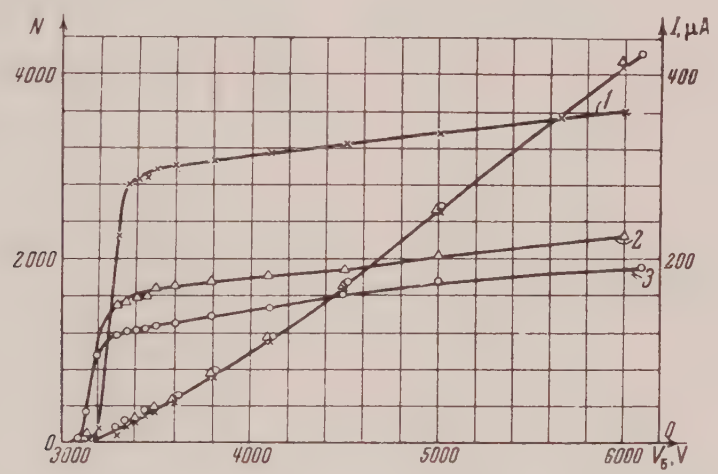

Fig. 12. *1*, *2*, *3* -- counting and corona characteristics (wire-plate system) for various water vapor pressures: *1* – 22; *2* – 12; *3* – 5.6 mm of Hg, $T = 23.5°$ C, a spacing $A - K = 1.5$ mm.

Figure, there is a rapid fall in efficiency of counting on decreasing the humidity (the value of the corona current at the same time remains constant).

In Fig. 13, the curve of the dependence of the counting rate (at constant voltage, $V_B = 4000$ V, on the counter and the spacing, $L = 1.5$ mm) on the water vapor pressure is shown. The observed dependence of the efficiency of counting on the moisture is a deficiency of the spark counter, and, in carrying out a number of measurements, periodic checks on the stability of the apparatus must be made. It is necessary, therefore, to state that in the practical case, the dependence of the counting rate on a change in humidity is rarely observed. Also, it is not difficult to control the stability of the apparatus.

The character of the angular dependence of the sensitivity of the counter does not change with changing humidity. This is seen from the companion curves *2* and *1*, and *2′* and *1′* of Fig. 11, for vapor pressures of 23.7 mm of Hg (curve *2*), 3.7 mm of Hg (curve *1* for wire-plate electrodes), 22.3 mm of Hg (curve *2′*), 6.0 mm of Hg (curve *1′* for wire-semicylinder electrodes).

The increase in the efficiency of the spark counter by increasing the humidity, apparently, is linked with the formation of heavy negative ions. Increasing the humidity increases the probability of forming heavy negative ions and as a result of this, diffusion is decreased. This fact may bring about the development of spark apparatus operating under more favorable conditions and consequently counting α-particles with greater efficiency.

Translated by I. B. Berlman
57

Density of States of Conduction Electrons in Ferromagnetic Materials

A. V. SOKOLOV AND S. M. TSIPIS
Institute of the Physics of Metals, Ural Branch, Academy of Sciences USSR

(Submitted to JETP editor March 12, 1954)
J. Exper. Theoret. Phys. USSR **28**, 321-325 (March, 1955)

The topic of state density of conduction electrons in ferromagnetic metals is considered in the limits of the model of interacting external and internal electrons of the ferromagnetic material.

KNOWLEDGE of the density of levels of valence electrons in metals is very important for the study of soft emission and absorption x-ray spectra of metals. On the other hand, from the study of the fine structure of the edge of the absorption band one can hope to get detailed information concerning the higher energy levels of the electrons in the metals.

Theoretical studies of this subject were formerly made on the basis of the single electron zonal theory of metals, which neglects the electron interaction. However, in the case of ferromagnetic metals, the electrons of which represent a united and a strongly interacting quantum system, study of this problem in the limits of the one electron model is without meaning, since ferromagnetism itself depends on interaction among the electrons.

For the generalization of the calculation of the density of states[1] in the case of ferromagnetic materials let us use a model of exchange interaction of external *s*-electrons and internal *d*-electrons as suggested by Vonsovskii[2,3]. This model has enabled us to understand the nature, and give the quantitative explanation, of "anomalies" of electrical, optical, galvanomagnetic and thermomagnetic properties of ferromagnetic metals [4-11]. According to this model we will consider the system of *s*-electrons in ferromagnetic metals as a mixture of two electron "gases" with two corresponding possible spin orientations. The energy of *s*-electrons in the approximation of effective mass is equal to

$$E = \alpha - \alpha' \mathbf{y}\vec{\sigma} + (\beta + \beta' \mathbf{y}\vec{\sigma})\mathbf{k}^2, \tag{1}$$

where α, α', β and β' are the parameters depending on the exchange integrals of the *s* and *d*-electrons and the translation integrals of the *s*-electron, y is the average relative atomic magnetic moment of the *d*-electron, $\vec{\sigma}$ is the spin vector of the *s*-electron and k is the quasimomentum of the electron. It is seen from Eq. (1) that the effective mass is equal to

$$m_{\pm} = \hbar^2/2a^2(\beta \pm \beta' y), \tag{2}$$

where the positive sign corresponds to right hand, and the negative to left hand, spin orientations, and a is the lattice constant.

According to the zonal theory of metals the expression for the density of states is as follows [1]:

$$n(E) = \pm 2 \frac{m^2}{8\pi^3\hbar^4 |g|} \times \int_{-E_g}^{E - V_{000} - E_g} \frac{\Gamma d\Gamma}{\sqrt{\Gamma^2 - |V_g|^2}}, \tag{3}$$

where E is the energy of the electron in the metal, $E_g = (\hbar^2/2m)\pi^2 g^2$ is the kinetic energy of an electron, which is moving in a direction perpendicular to the reflecting lattice and undergoing Bragg

[1] A. Wilson, *Quantum Theory of Metals*, 1941, pp. 42-44

[2] S. V. Vonsovskii, J. Exper. Theoret. Phys. USSR **16**, 981 (1946)

[3] S. V. Vonsovskii and E. A. Turov, J. Exper. Theoret. Phys. USSR **24**, 419 (1953)

[4] S. V. Vonsovskii, J. Exper. Theoret. Phys. USSR **18**, 219 (1948)

[5] S. V. Vonsovskii, Izv. Akad. Nauk SSSR, Ser. Fiz. **11**, 463 (1947)

[6] S. V. Vonsovskii and A. V. Sokolov, J. Exper. Theoret. Phys. USSR **19**, 615,703 (1949)

[7] S. V. Vonsovskii and A. V. Sokolov, Doklady Akad. Nauk SSSR **76**, 197 (1951)

[8] A. V. Sokolov and A. Z. Veksler, Doklady Akad. Nauk SSSR **81**, 27 (1951)

[9] A. V. Sokolov and A. Z. Veksler, J. Exper. Theoret. Phys. USSR **25**, 215 (1953)

[10] S. V. Vonsovskii and K. P. Rodionov, Doklady Akad. Nauk SSSR **75**, 643 (1950)

[11] S. V. Vonsovskii, L. Ja. Kobelev and K. P. Rodionov, Izv. Akad. Nauk SSSR, Ser. Fiz. **16**, 569 (1952)

reflection, V_{000} and V_g are the Fourier coefficients in the expansion of the lattice potential, g is the vector of the inverse lattice and

$$\Gamma = E - V_{000} - E_g - (\hbar^2/2m)(\varkappa_2^2 + \varkappa_3^2);$$

$\varkappa_2$ and $\varkappa_3$ are the components of the quasimomentum of the electron parallel to the zone boundary, and the component $\varkappa_1' = -\pi|g| + \varkappa_1$ is directed parallel to g. The positive sign in Eq. (3) should be taken for the states of the upper band and the negative for the states of the lower band.

In the case of ferromagnetic metals Eq.(1) is replaced by the expressions

$$n_+(E) = \pm\frac{m_+^2}{8\pi^3\hbar^4|g|}\int\frac{\Gamma_+ d\Gamma_+}{\sqrt{\Gamma_+^2 - |V_g|^2}}, \quad (4)$$

$$n_-(E) = \pm\frac{m_-^2}{8\pi^2\hbar^4|g|}\int\frac{\Gamma_- d\Gamma_-}{\sqrt{\Gamma_-^2 - |V_g|^2}}.$$

Note that the limits of integration in Eq. (4) are different from the limits of integration in Eq. (3). Here

$$\Gamma_\pm = \pm\sqrt{|V_g|^2 + \left(1 \pm \frac{\beta'}{\beta}y\right)^2\left(\frac{\pi\hbar^2 g\varkappa_1}{m}\right)^2}, \quad (5)$$

where $n_+(E)$ is the density of states corresponding to the right hand spin orientation, and $n_-(E)$ to the left hand spin orientation. Thus it is natural to consider as justified the relation

$$n(E, y) = n_+(E, y) + n_-(E, y). \quad (6)$$

By restricting ourselves to a temperature range "close" to the Curie point ($y \ll 1$), one can expand $\Gamma_\pm$ in a power series in y and retain only the terms up to second order. Then we get

$$\Gamma_\pm d\Gamma_\pm = \Gamma d\Gamma\left(1 \pm \frac{\beta'}{\beta}y\right)^2, \quad (7)$$

$$\sqrt{\Gamma_\pm^2 - |V_g|^2} = \left(1 \pm \frac{\beta'}{\beta}y\right)\sqrt{\Gamma^2 - |V_g|^2}. \quad (8)$$

From this it follows that the integrand of Eqs. (4) can be represented as follows:

$$\frac{\Gamma_\pm d\Gamma_\pm}{\sqrt{\Gamma_\pm^2 - |V_g|^2}} = \left(1 \pm \frac{\beta'}{\beta}y\right)\frac{\Gamma d\Gamma}{\sqrt{\Gamma^2 - |V_g|^2}}. \quad (9)$$

Further, we have the obvious relation

$$m_\pm^2 X_\pm = \frac{m_1\Gamma d\Gamma}{\sqrt{\Gamma^2 - |V_g|^2}}\frac{1}{(1 \pm (\beta'/\beta)y)}, \quad (10)$$

where $X_\pm$ is equal to Eq. (9) and $m_1 = \hbar^2/2a^2\beta$ Taking into account Eqs. (4)-(10) we will get for the densities of states of the electrons, n_+ and n_-, the expression

$$n_\pm(E, y) = \pm\frac{m_1^2}{8\pi^3\hbar^4|g|}\frac{1}{(1 \pm (\beta'/\beta)y)}\int\frac{\Gamma d\Gamma}{\sqrt{\Gamma^2 - |V_g|^2}} \quad (11)$$

and, finally, for the total density of states of conduction electrons in ferromagnetic materials the relation:

$$n(E, y) = n_+(E, y) + n_-(E, y) \quad (12)$$
$$\approx \pm\frac{m_1^2}{4\pi^3\hbar^4|g|}(1 + A^2y^2)\int\frac{\Gamma d\Gamma}{\sqrt{\Gamma^2 - |V_g|^2}},$$

where $A = \beta'/\beta$ is not greater than unity. The limits of integration in Eq. (12) are the same as in Eq. (3)

Consider three different energy intervals:

I) $E < V_{000} + E_g - |V_g|$.

All states satisfying this inequality are in the lower band so that the negative sign is used:

$$n(E, y) = (1 + A^2y^2)\frac{m_1^2}{4\pi^3\hbar^4|g|}[(E^2 - |V_g|^2)^{1/2} \quad (13)$$
$$- \{(V_{000} + E_g - E)^2 - |V_g|^2\}^{1/2}].$$

II) $V_{000} + E_g - |V_g| < E < V_{000} + E_g + |V_g|$.

These states are also located in the lower band; however, for the upper limit of Γ here one should use $|V_g|$; then we get:

$$n(E, y) = (1 + A^2y^2)\frac{m_1^2}{4\pi^3\hbar^4|g|}(E_g^2 - |V_g|^2)^{1/2}. \quad (14)$$

III) $V_{000} + E_g + |V_g| < E$.

The states for which Γ is less than $|V_g|$ are in the lower band; the states for which Γ is greater than $|V_g|$ are in the upper band:

$$n(E, y) = (1 + A^2y^2)\frac{m_1^2}{4\pi^3\hbar^4|g|} \quad (15)$$

$$\times\left[-\int_{-E_g}^{-|V_g|} + \int_{|V_g|}^{E - V_{000} - E_g}\right]\frac{\Gamma d\Gamma}{(\Gamma^2 - |V_g|^2)^{1/2}}$$

$$= (1 + A^2y^2)\frac{m_1^2}{4\pi^3\hbar^4|g|}[(E_g^2 - |V_g|^2)^{1/2}$$

$$+ \{(E - E_g - V_{000})^2 - |V_g|^2\}^{1/2}].$$

The functions $n(E,\gamma)$ and $n(E,O)$ are plotted in the Figure [$n(E,O)$ is $n(E,\gamma)$ at $\gamma = 0$].

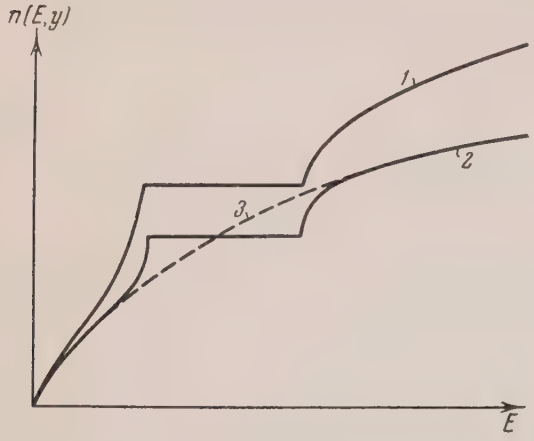

1-curve of $n(E,\gamma)$
2-curve of $n(E,O)$
3-n for free electrons

Notice that the deviation of the curves for $n(E,\gamma)$ and $n(E,O)$ from that for free electrons (shown by the dotted line) depends on only two planes, g and -g, while at least six planes should be considered. Hence these deviations should be multiplied by the number of pairs of equivalent planes which bound the lower band.

From Eqs. (12)-(15) and from the Figure one can see that the curve $n(E,\gamma)$ lies above the curve $n(E,O)$. From this it follows that if one were to take into account several equivalent planes, the jump in the density of states $n(E,\gamma)$ of the conduction electrons of the ferromagnetic material close to the Curie temperature would be greater than in the case of no magnetization. At $\gamma = 0$, Eq. (13) is the same as Eq. (3) for the density of states in ordinary metals. It is not hard to see that Eq. (13) can easily be put in the form:

$$n(E,\gamma) = n(E,0)(1 + A^2\gamma^2). \qquad (16)$$

Notice from this expression that the density of states of conduction electrons of ferromagnetic materials is a quadratic function of spontaneous magnetization. The spontaneous magnetization is a function of temperature, as a consequence of which the density value of electron states in the ferromagnetic material, which depends on γ, must show anomalous temperature dependence. Since the intensities of x-ray spectral lines (as well as the corresponding transition probabilities) are proportional to the densities of the electron states, these intensities for ferromagnetic metals will also show anomalous temperature dependences.

An increase of magnetization, as Eqs. (12)-(16) show, increases the density of states of the conduction electrons in a ferromagnetic material. This permits us to conclude that the band of s-electron levels of a ferromagnetic material becomes narrower. This conclusion is in agreement with the fact that in a ferromagnetic material to a first approximation the spins of the d-electron system are strongly bound among each other, the orbital moments cancel each other and a phenomenon analogous to the Paschen-Bach effect takes place. In other words, under the influence of a strong internal "magnetic field", caused by the exchange interaction of the s and d-electrons a simplification of the picture of levels of the s-electron system (narrowing of the band) occurs rather than a complication.

From Eq. (16) one can easily get an expression for the ferromagnetic "anomaly" of the density of electron states in ferromagnetic materials:

$$\frac{n(E,\gamma) - n(E,0)}{n(E,0)} = A^2\gamma^2. \qquad (17)$$

The value of the ferromagnetic "anomaly" of the density of electron states in ferromagnetic material is proportional to the square of the spontaneous magnetization γ. It is very desirable to check experimentally the theoretical conclusions represented by Eq. (17).

Hence, by using the exchange model of external and internal electrons of ferromagnetic materials, we have suceeded in showing that the density of electron states in ferromagnetic materials must depend on the spontaneous magnetization. Near the temperature of ferromagnetic transition this dependence is of a simple quadratic nature [Eq. (16)]. In addition the ferromagnetic "anomaly" of the density of electron states in ferromagnetic metals was obtained.

In conclusion, let us point out that the calculations described above are not claimed to provide a quantitative description of densities of states of conduction electrons in ferromagnetic metals, since they were carried out using a simplified model of ferromagnetic materials. Nevertheless, apparently, there is no reason to doubt that qualitative conclusions about the dependence of the density of states of conduction electrons on spontaneous magnetization must be correct.

Translated by G. Filipovich
54

Resistance of Metals at High Current Densities

V. V. Bondarenko, I. F. Kvartskhava,
A. A. Pliutto, and A. A. Chernov

(Submitted to JETP editor Feb. 16, 1954)
J. Exper. Theoret. Phys. USSR 28, 191-198 (1955)

Results are given of an investigation of the dependence of resistance of a few metals on current density. Comparison is made of experimental curves, presenting the dependence of resistance for copper, silver, platinum and other metals on the amount of energy introduced, with curves and calculations from tabulated data. For these metals, Ohm's law is maintained up to current densities of about 10^7 A/cm^2.

1. INTRODUCTION

IN the study of phenomena of electrically exploded metal wires, we were led to the investigation of the dependence of resistance of a few metals on current density. Many works [1-7] are devoted to this question, the authors of which have striven to obtain the highest possible current densities, with the aim of testing Ohm's law.

On the basis of classical electron theory of metals, it was pointed out[5,6] that deviations of measurements from Ohm's law could become effective with current densities of 10^{10} to 10^{11} A/cm^2, or gradients of the field of 10^6 V/cm and higher. Such current densities are not realizable with contemporary experimental means. However, the further devolepment of theory, as is well known, led to a reduction of the effective range of current density by a few orders of magnitude so that an opportunity for experimental verification of the theory was presented.

The available data in the literature on measurements of copper, silver, gold, tungsten, etc., show that up to a current density about 10^6 A/cm^2, deviations from Ohm's law are not noted. An exception must be made for the works of references 1 and 3, in which deviations from Ohm's law were given for current densities in a few units of 10^6 A/cm^2 for gold[3], platinum and tungsten[1]. Ignateva and Kalashnikov[1] indicated an increase in the resistance of platinum and tungsten in a few instances. As it was pointed out by Borovik[2] and Barlow[4], and as is also evident from the presentation given below, these results are incorrect.

Measurements at much higher current densities, as far as we know, have not yet been made. The method which we employed in investigations of electrical explosion of wires permits the obtaining of current densities up to 10^7 A/cm^2 and higher. By means of this method, the dependence of resistance of copper, silver, gold, platinum, aluminum, tungsten and iron on the current density was investigated.

2. METHOD OF MEASUREMENT

For investigation of the dependence of resistance of metals on the current density, use was made of a scheme customarily employed in experimental researches on electrical explosion of wires, i. e., discharge of a condenser through the wire being investigated. In these cases, when the energy of the condenser is large enough to evaporate the wire completely, evaporation follows in a very short time, and the gas is emitted with great speed producing the impression of explosion of the wire. This phenomenon is called electrical explosion of a wire.

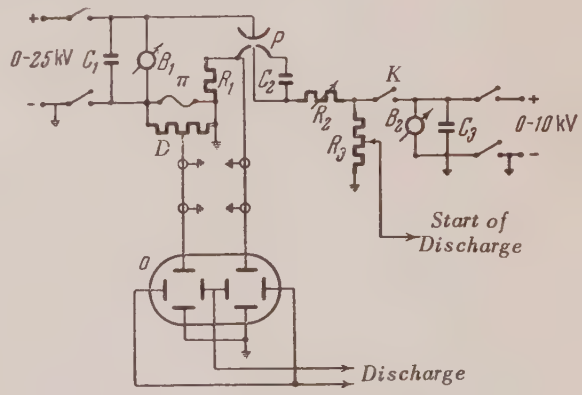

Fig. 1. Schematic diagram of the apparatus

The principal measuring scheme is shown in Fig. 1, where C_1 is the condenser for the explosion circuit, B_1 an electrostatic voltmeter, P a discharge gap with an initiating electrode, π the wire,

[1] L. A. Ignateva and S. G. Kalashnikov, J. Exper. Theoret. Phys. USSR 22, 385 (1952)

[2] E. S. Borovik, Doklady Akad. Nauk SSSR 91, 771 (1953)

[3] P. W. Bridgman, Phys. Rev. 19, 131 (1922)

[4] H. M. Barlow, Phil. Mag. 9, 1041 (1930)

[5] J. J. Thompson, *Corpuscular Theory of Matter*, 1908

[6] H. Margenau, Z. Phys. 56, 259 (1929)

[7] H. R. Traubenberg, Phys. Z. 18, 75 (1917)

D the voltage divider and R_1 a so-called current resistor whose character and construction will be discussed later. On the right of the diagram is shown the circuit for initiating the discharge of the gap P; in this circuit C_2 and C_3 are condensers, R_2 is a variable resistor, B_2 an electrostatic voltmeter and R_3 a resistor which has been set at a point at which the voltage serves to start up the sweep of the oscilloscope. The circuit of the initiator is brought into action by the switch K. In the lower part of Fig. 1 are shown the deflection plates of a twin beam oscilloscope with connecting cables. The parameters of the explosion circuit are: capacitance 8 to 10 microfarads, inductance 1 to 4 microhenries and voltage up to 10 KV.

The apparatus is activated in the following way. The capacitor C_1 is charged up by a rectifier to a variety of potentials, close to the breakdown potential of the discharge gap P. Further charging up to capacitor C_3 and closing of the key K brings the initiating circuit into action, which is connected through the resistance R_3 to the starting circuit of the common sweep of the twin beams of the oscilloscope used for simultaneous portrayal of the wire current and voltage. The sweep of the beams starts a few microseconds earlier than the initiated discharge P, so that the oscilloscope trace will be in the middle region of the sweep. On closing the key K, initiating the gap, a spark arises which almost instantaneously ignites the gap P, and the capacitor C_1 discharges through the wire. In this way, a voltage drop occurs in the "current" resistor R_1 proportional to the current through the wire. This voltage feeds one pair of the deflection plates of the oscilloscope through a coaxial cable. The voltage across the wire, after division in a voltage divider, feeds the other pair of deflection plates* by means of a second coaxial cable. The oscillogram was photographed by a "Kiev" photoapparatus with a "Jupiter 3" object lens on a sensitive photofilm RF[1]. The maximum speed of the sweep in our experiment was about 25 Km/sec.

Calibration of the sweep of the oscillograph is accomplished by using a standard signal generator. For checking the uniformity and linearity of the sweep, both beams have a single sequence of signals simultaneously applied to them. An oscillogram of these signals showed that the speeds of the beam sweeps coincide with sufficient accuracy, and that the sweep is sufficiently linear, with the exception of small regions at the beginning and at the end of the sweep.

The voltage calibration for the oscillograph film is obtained by an exact measurement of a constant voltage applied to the divider**. The current calibration reduces to a determination of the voltage sensitivity of the deflection plate, and then the current is calculated by exact measurement of the important resistor R_1. The sweep showed that, even for the most powerful pulses, the value of R_1 is unchanged. The inductance of the circuit is obtained by the well known method utilizing oscillograms of free damped oscillations of of the circuit.

Typical oscillograms, showing the current and voltage on exploding wires, are shown in Fig. 2. Oscillogram *a* is for copper wire, length 6 cm, diameter 0.05 mm and a 3.5 microsecond sweep, and *b* is for a platinum wire, length 6 cm, diameter 0.1 mm and an 8 microsecond sweep. The upper curve shows the current in KA and the lower shows the voltage in KV. The capacity of the explosion circuit is 8.4 microfarads, the initial voltage is 5 KV and the inductance of the circuit is about 1 microhenry.

As is evident from these oscillograms, the explosion circuit is switched on at a certain time after the start up of the sweep. In the case of copper, the current grows from zero to some maximum and then it quickly falls to zero. This current break takes place without regard to the fact that the larger part of the initial voltage still remains on the condenser. In the case of platinum, the curve of current does not suddenly fall towards zero, but remains a plateau, along which the current and voltage are nearly constant. For platinum, a current break takes place after this step. Generally the current break is followed by a second pulse of current, associated with evaporation of the wire and gaseous discharge in vapors. This second pulse leads to full discharge of the condenser. The first pulse is of interest to us, because the wire is not yet evaporated.

The voltage curve at the beginning of the oscillogram shows the initial small inductive fall of potential. The potential rises with further rise of current. At the maximum of current the voltage continues to increase, and at the wire there occurs an excess voltage which, depending on the rate of change of current, can be several times larger than the initial voltage. After the break, the voltage remains constant.

* For an oscillogram of the voltage on the wire, the voltage divider is applied to balanced capacitors. A test for the absence of distortion was made by putting on the divider a steep front voltage pulse (about 10^{-8} sec), in which case the pulse front did not undergo noticeable distortion. For a criterion of accuracy, the oscillogram is also used to satisfy the law of conservation of energy in the circuit, within the limits of accuracy of the measurements.

** On discharging condenser C_1 (Fig. 1) through a high power resistor divider D (about 1000 ohms) the oscilloscope voltage remains constant for a few microseconds with a high degree of accuracy.

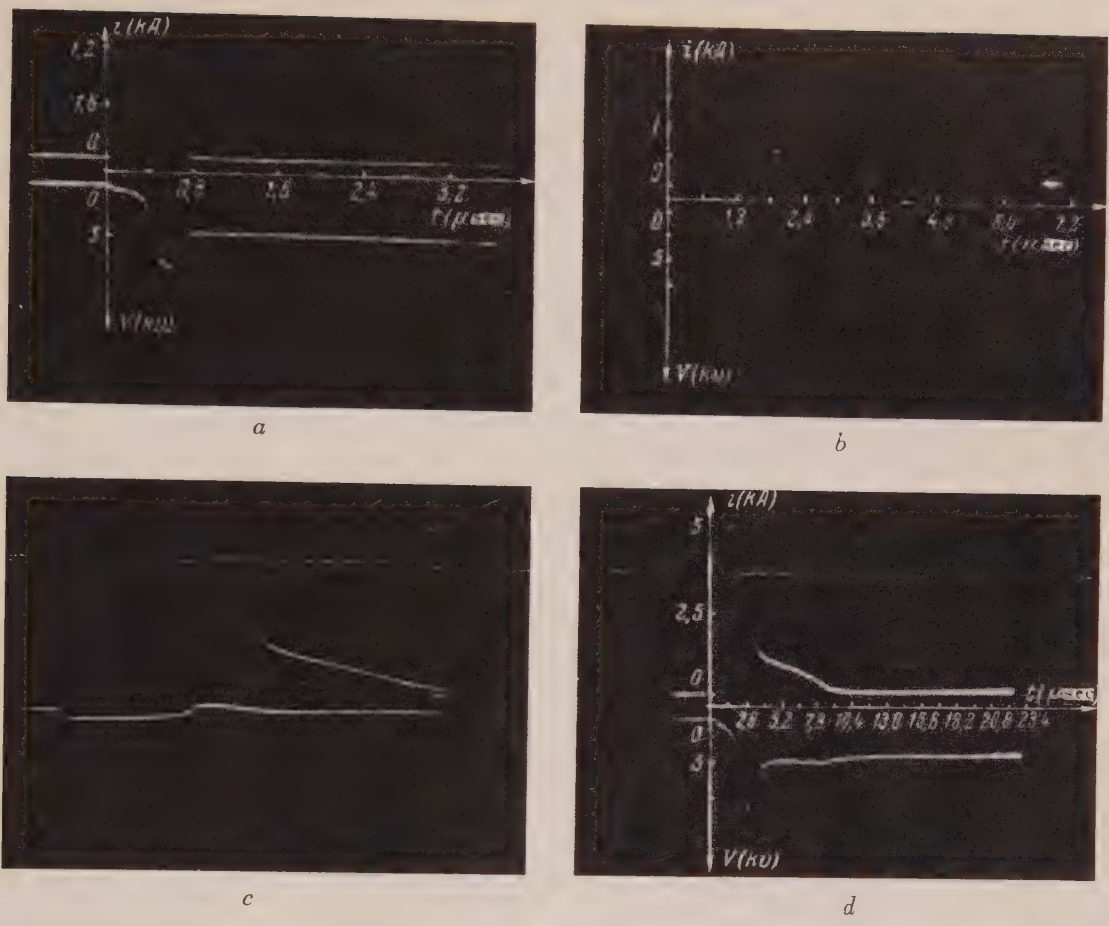

Fig. 2. Examples of oscillograms of current KA and voltage KV for electrical explosion of wires.

Oscillograms for silver, gold and aluminum wires are similar to the oscillogram for copper, that is, the characteristic of the plateau is absent. Oscillograms for iron, tungsten and molybdenum wires are similar to the oscillogram for platinum and clearly show a plateau.

The inductive fall of voltage is caused by the inductance of the wire itself and the contacts of the clamp. This can not be successfully avoided and we were obliged to introduce a suitable correction in the following way. After each explosion of the wire a correction oscillogram is taken in which the explosion is repeated with the very same kind of wire. Now the voltage divider is connected in another part of the condenser circuit possessing nearly the same inductance as that of the wire, but having negligible ohmic resistance†. Under these conditions the oscillogram of the voltage gives the amount of the induced voltage. Because the reproduction of the pulse of current and voltage was good, these oscillograms were satisfactory for use in correcting the curve of voltage along each impulse. In Fig. 2, oscillogram *c* gives a typical example of a correction oscillogram.

The oscillograms of current show no inductive effect. This situation was due to the special construction of the "current" resistor R_1 . It was made out of a graphite tube with good metallic contacts at the terminals. For connecting into the circuit (Fig. 1), one end is grounded, but the voltage at the other end is taken off through a small coaxial conductor stretched along the axis of the graphite tube. In this way, this resistor acts as if it were a continuation of a coaxial cable without distortion. The absence of inductive distortion of the current was verified by taking an oscillogram under the condition that when the graphite tube was substituted by a copper tube it gave the same freedom from distortion.

In spite of the measures undertaken to prevent distortion, we still found it necessary to find a criterion which would demonstrate the correction of the oscillograms. Such a criterion is the law of

† Equality of inductance is determined by calculation and is checked by the coinciding inductive fall of voltage at the beginning of the oscillogram.

conservation of energy in regard to the circuit in the explosion process of the wire. At each moment of time t, there exists the equality

$$\int_0^t i(t)\,V(t)\,dt + \frac{Li^2(t)}{2} = \frac{C_1}{2}(V_0^2 - V_t^2), \qquad (1)$$

where $i(t)$ is the current and $V(t)$ is the voltage across the wire at the moment t, L is the inductance of the circuit, C_1 is the capacity, V_0 is the initial voltage and V_t is the voltage of the condenser at the moment t. Thus the amount of energy given out by the condenser in the explosion process at the moment t, $C_1 (V_0^2 - V_t^2)/2$, should be equal to the the sum of the energy discharging up to that moment in the wire in the form of Joulean heat, $\int_0^t i(t)\,V(t)\,dt$ and the energy of the magnetic field $Li^2(t)/2$. We neglect the electromagnetic radiation of the circuit and assume that the discharge of heat proceeds only from the wire. The resistance of the wire being tens, and at the end of the pulse, hundreds, of times greater than that of the remaining part of the circuit, permits a simple calculation to show that this hypothesis is equitable. Thus Eq. (1) should accurately represent an energy balance for the explosion of the wire. Upon examination of the oscillograms, one can apply Eq. (1) at the end of the pulse, when $i(t)$ is zero and $V(t)$ is constant. Then the equation is simplified, and takes the form

$$\int_0^t i(t)\,V(t)\,dt = \frac{C_1}{2}(V_0^2 - V_t^2). \qquad (2)$$

If the oscillograms satisfy this equality with sufficient precision, one can assume that they describe the explosion process correctly. Repeated examination showed that our oscillograms satisfy this condition with precision within a few percent. On the basis of such oscillograms, the energy W put into the wire is calculated at a moment t by the formula

$$W = \int_0^t i(t)\,V(t)\,dt. \qquad (3)$$

Further, by means of tables of the specific heat $C_p(T)$, the wire temperature T is calculated by the formula

$$W = M\int_{T_0}^{T} C_p(T)\,dt, \qquad (4)$$

where M is the mass of the wire and T_0 is its initial temperature. Finally, knowing the values $i(t)$, $V(t)$ and $T(t)$, it was possible to calculate the resistance of the wire $R(W)$ as a function of the energy introduced.

In the following, the curve of dependence of R on the energy introduced is shown for different wires, using this method.

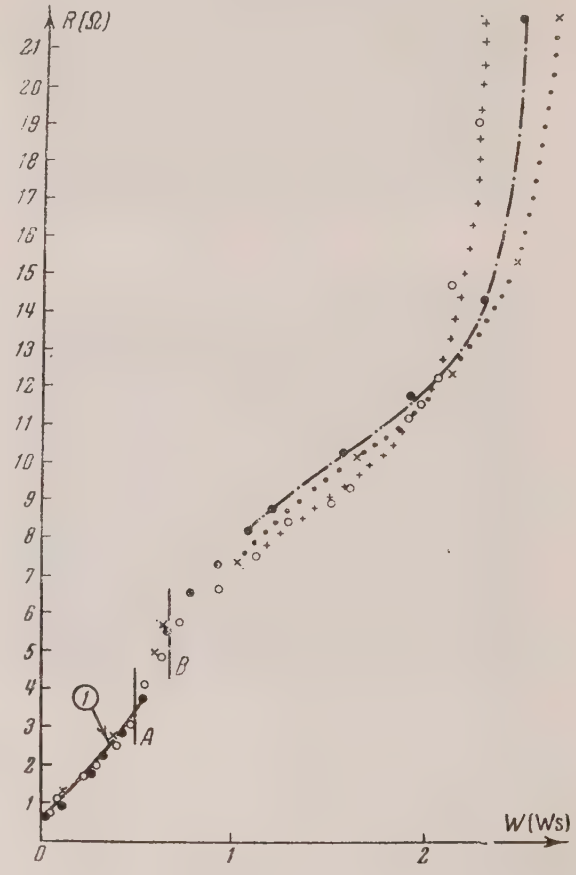

Fig. 3. Resistance curve for copper wire

3. RESULTS OF MEASUREMENTS AND THEIR DISCUSSION

Shown in Figs. 3,4,5 and 6 are curves picturing the dependence of resistance of the wire in ohms on the introduction of energy in watt-seconds. They were obtained from oscillograms of current and voltage, taken with maximum allowable speed of the sweep.

Figures 3 and 4 show the curves for copper and silver wires, having 6 cm length and 0.05 mm diameter.

Experimental points for copper correspond to initial voltages 3 KV, 4 KV and 5 KV and for silver 3.5 KV and 4KV with a capacity of 8.4 microfarads. Curves are given in Figures 5 and 6 for platinum and tungsten wires of 6 cm length and 0.1 and 0.2 mm diameter. The experimental points refer to 3,

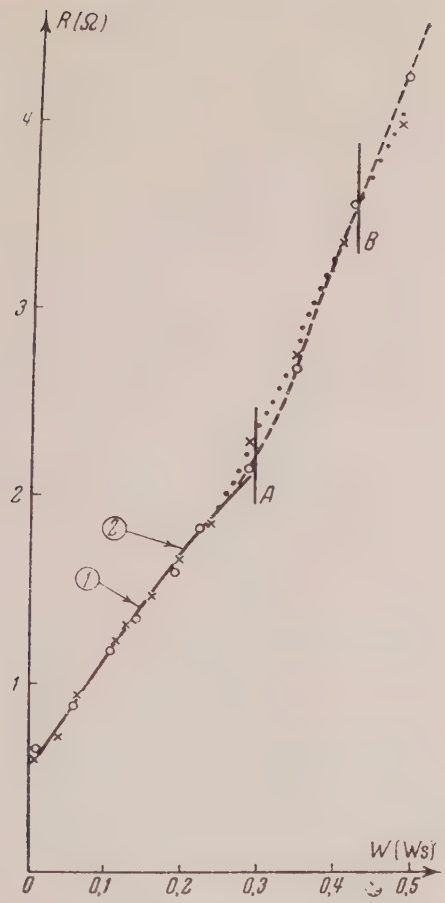

Fig. 4. Resistance curve for silver wire.

4, 5 and 7 KV for platinum, and 4,5,6 and 7 KV for tungsten. The parameters of the circuit for platinum are unchanged. In the case of tungsten, C_1 is 10 microfarads. The inductance of the circuit for all curves is a minimum.

The energy value $W = 0$ corresponds to room temperature. The initial value of the wire resistance (points of intersection of the curve with the ordinate axis) coincides well with the values of resistance of these wires measured in a bridge circuit at room temperature using weak currents. Points corresponding to the initiation of fusion (point A Fig. 5) and the end of melting of the wire (point B Fig. 5) are located in the interval shown by straight lines drawn parallel to the ordinate axis. These points are obtained by calculation from tabulated data. The circled numbers designate maximum and near maximum values of current density for a given wire. In Fig. 3, No. 1 indicates a current density of 6.5×10^7 A/cm^2 for copper. In Fig. 4, No. 1 indicates a current density of 5.9×10^7 A/cm^2 for silver and No. 2 to 6×10^7 A/cm^2. In Fig. 6 for tungsten, the points are 1.3×10^7 A/cm^2 and 1.5×10^7 A/cm^2. In Fig. 5 for platinum, both points indicate a current density of 2.5×10^7 A/cm^2. Analogous curves and the same order of current densities are obtained for gold, iron and aluminum.

It should be noted that at points with maximum current density, the temperature of the wire does not exceed a few hundred degrees. With a lowering of the current density the temperature of the wire becomes lower. With temperatures of a few tens of degrees we still have current densities of about 10^7 A/cm^2 for copper and silver. In addition the trace of the curve $R = R(W)$ for platinum and tungsten is not changed even if the explosion of the wire takes place at the temperature of liquid air.

The continuous curves in the figures (from the origin to point A) are calculated curves. They are computed for each wire on the basis of tabulated data and picture the dependence of resistance on the energy for small current densities. As is evident, in the limits of accuracy of our measurements (5 to 7%) the experimental points for all metals investigated agree well with these curves. From this can be drawn a basic inference, that the resistance of metals: copper, silver, gold, aluminum, platinum, tungsten and iron, in the solid phase below the temperature of fusion, does not depend on the current density up to the value of 10^7 A/cm^2.

It is hard to say anything definite with reference to the dependence of resistance on the introduction of energy into the region from the beginning of fusion and higher. At the beginning of this region there is a rapid rise of resistance, increasing with the introduction of energy for nearly all metals. Experimental points for various voltages have a noticeable scatter. However it is possible to draw the conclusion that, at points of fusion, platinum, tungsten and iron show a region in which their resistance is almost independent of temperature. This shows that, in the liquid phase, these metals are characterized by a very small value of the temperature coefficient of resistance. As concerns copper, silver and gold, the rise rate of their resistance at the completion of fusion is in the direction given above, either decreasing not at all, or decreasing insignificantly (Figs. 3 and 4). However, with longer wires (12 cm and longer) the oscillograms for these metals show clearly the presence of discrete steps, sloping more or less than for platinum, tungsten and iron. In the qualitative example in Fig. 2 the oscillogram is given for silver 0.15 mm diameter and 24 cm length, with $C_1 = 10$ microfarads and 6 KV. The presence of

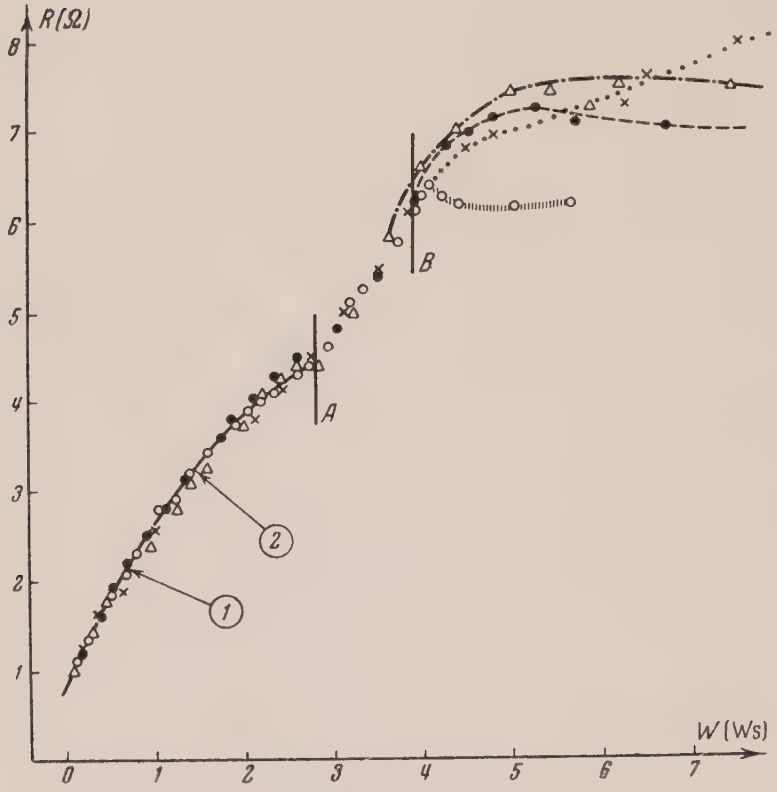

Fig. 5. Resistance curve for platinum wire.
○ — $V_0 = 3$ kV; ● — 4 kV; △ — 5 kV; × — 7 kV

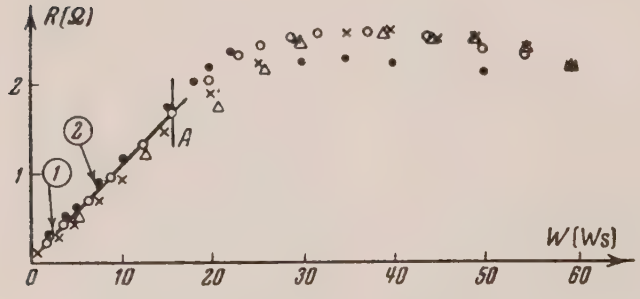

Fig. 6. Resistance curve for tungsten wire.
○ — $V_0 = 4$ kV; △ — 5 kV; × — 6 kV;
● — 7 kV

these little steps leads to the conclusion that in these metals in the liquid phase also, the temperature coefficient of resistance is smaller than in the region of the fusion process.

It should be noted that from the curves $R = R(W)$ in the transitional region from the solid to the liquid phase (at point A) and further in the liquid phase, for different conditions of explosion (different initial voltage, current density along the curve, etc.) the conclusion can be drawn that the resistance of metals in these regions does not depend on current density or other factors, and is defined, within the limits of accuracy of the experiment, as soon as energy is introduced. Hence Ohm's law is valid in the transitional region and in the liquid phase.

Translated by H. W. Parker
28

The Quantum Theory of the Radiating Electron, IV

A. A. SOKOLOV AND I. M. TERNOV
Moscow State University

(Submitted to JETP editor March 23, 1954)
J. Exper. Theoret. Phys. USSR **28**, 431-436 (April, 1955)

An expression is derived for the quantum corrections to the trajectory of a relativistic electron moving in an axially symmetric magnetic field.

IN a series of papers[1-3] on the theory of the radiating electron, it was shown that the electromagnetic radiation emitted by an electron moving in a magnetic field becomes extremely intense at high velocities. The radiative energy loss produces a significant contraction of the orbit radius.

A quantum mechanical treatment shows that in addition to the contraction of the orbit the radiation causes radial oscillations of the electron (radiation recoil effect) which leads to a broadening of the trajectory. In our earlier papers[4-6] on the quantum theory of the radiating electron, we investigated these effects for an electron in a constant magnetic field (H = const).

In the present paper we use the methods of our papers[4-6] and generalize the results to the case of of an inhomogeneous magnetic field with axial symmetry, assuming the field in the neighborhood of the stable orbit to be given by

$$H_x = H_y = 0, \quad H_z = H_0 r^{-q}, \tag{1}$$

$$0 < q < 1, \quad z = 0.$$

Our old results will be obtained by putting $q = 0$.

It is convenient to take the components of the vector potential A in the form

$$A_x = -yH_0/r^q(2-q), \tag{2}*$$

$$A_y = xH_0/r^q(2-q), \quad A_z = 0.$$

Neglecting quantities of order $\hbar^2$, we need not consider spin effects, i.e., we may use the scalar relativistic wave equation

$$\left\{E^2 + c^2\hbar^2\nabla^2 - e^2A^2 - \frac{2ec\hbar}{i}(\mathbf{A}\overrightarrow{\nabla}) - m^2c^4\right\}\psi = 0, \tag{3}$$

where E is the energy and m the rest mass of the electron. In what follows we investigate only the motion of the electron in the orbital plane, so that we look for solutions of Eq. (3) of the form

$$\psi = \frac{e^{il\varphi}}{\sqrt{2\pi}}\sqrt{\frac{mc^2}{E}\frac{1}{r}}\,u(r). \tag{4}$$

The radial function u is normalized to unity,

$$\int_0^\infty u^2(r)\,dr = 1. \tag{5}$$

The azimuthal quantum number l takes large integer values ($l \gg 1$) in all cases of interest

The wave equation for the radial function is

$$u'' + f(r)\,u = 0, \tag{6}$$

* It is well known that the external currents which maintain the magnetic field must not lie near to the orbital plane $z = 0$, i.e., the condition curl H = 0 must be fulfilled. This is achieved by letting the vector-potential A depend on z:

$$A_x = -\frac{yH_0}{r^q(2-q)}\left(1 + \frac{q(2-q)}{2r^2}z^2\right), \tag{2a}$$

$$A_y = \frac{xH_0}{r^q(2-q)}\left(1 + \frac{q(2-q)}{2r^2}z^2\right), \quad A_z = 0.$$

Then it is easy to see that

$$\text{curl } \mathbf{H}\,|_{z=0} = 0.$$

When $z = 0$, Eq. (2a) reduces to Eq. (2).

[1] D. D. Ivanenko and I. Ia. Pomeranchuk, Doklady Akad. Nauk SSSR **44**, 343 (1944)

[2] D. D. Ivanenko and A. A. Sokolov, Doklady Akad. Nauk SSSR **59**, 1551 (1948)

[3] D. D. Ivanenko and A. A. Sokolov, *Classical Field Theory*, Gostekhisdat, 1951. A detailed bibliography of the classical theory of the radiating electron will be found in this monograph.

[4] A. A. Sokolov, N. P. Klepikov and I. M. Ternov, J. Exper. Theoret. Phys. USSR **23**, 632 (1952)

[5] A. A. Sokolov, N. P. Klepikov and I. M. Ternov, J. Exper. Theoret. Phys. USSR **24**, 249 (1953); see also Doklady Akad. Nauk SSSR **89**, 665 (1953)

[6] A. A. Sokolov and I. M. Ternov, J. Exper. Theoret. Phys. USSR **25**, 698 (1953); see also Doklady Akad. Nauk SSSR **92**, 537 (1953)

with

$$f(r) = \frac{E^2 - m^2c^4}{c^2\hbar^2} - \gamma^2 r^{2(1-q)} - 2\gamma l r^{-q} - \frac{l^2 - 1/4}{r^2}, \quad (7)$$

$$\gamma = eH_0/c\hbar(2-q), \quad u' = du/dr.$$

We develop $f(r)$ in a Taylor series in the neighborhood of its maximum given by

$$f'(a) = 0. \quad (8)$$

The last equation fixes the value of the radius of the stable orbit

$$a = \left[\frac{l}{\gamma(1-q)}\right]^{1/(2-q)} \quad (9)$$

In deriving Eq. (9) we neglected the ¼ in Eq. (7) in comparison with l^2.

Keeping only terms to the order of $x^2 = (r - a)^2$ in the Taylor series, the function u satisfies

$$u'' + (\alpha - \lambda^2 x^2)u = 0, \quad (10)$$

where

$$\alpha = f(a) = \frac{E^2 - m^2c^4}{c^2\hbar^2} - \gamma^2(2-q)^2 a^{2(1-q)}, \quad (11)$$

$$\lambda^2 = -\frac{1}{2}f''(a) = \gamma^2(2-q)^2(1-q)a^{-2q}.$$

With good accuracy we may assume that x varies between the limits $-\infty$ and $+\infty$, so that Eq. (10) is identical with the equation of motion of a harmonic oscillator. The frequency Ω of radial oscillations of the electron about the stationary orbit is given by

$$\lambda^2 = \mu^2\Omega^2/\hbar^2, \quad (12)$$

where $\mu = E/c^2$ is the relativistic mass of the electron. From Eqs. (11) and (12) we find

$$\Omega = (v/a)\sqrt{1-q} \quad (13)$$

in agreement with the known result[7] obtained from classical theory.

2. From Eq. (9) it is easy to show that, in the absence of radiation, the radius a will remain constant (independent of the value of the magnetic field) only when Wideroe's condition is satisfied. In fact, by the adiabatic principle of Ehrenfest, the quantum number $(l - l_0)$ must remain constant when the magnetic field increases slowly with time. From Eq. (9) we find

$$= \frac{d(l-l_0)}{dt} = \frac{d}{dt}\frac{ea^2}{c\hbar}\left[H(a) - \frac{1}{2}\overline{H}(a)\right], \quad (14)$$

where $H(a)$ and $\overline{H}(a)$ are respectively the magnetic field and its mean value over the stable orbit,

$$a^2\overline{H}(a) = 2\int_0^a H(r)\,r\,dr + \frac{2c\hbar l_0}{e}, \quad (15)$$

and the constant term depnds on the law of variation of the magnetic field away from the region of the stationary orbit. From Eq. (14) it follows that the radius a can remain constant while H_0 is varied, only if $H(a) = \frac{1}{2}\overline{H}(a)$.

3. From the wave equation (10) we find the eigenvalues of the energy and the eigenfunctions describing radial oscillations [see also reference 4, Eq. (45)]:

$$\frac{\alpha}{\lambda} = 2s + 1, \quad (16)$$

$$E = c\hbar\left\{(2-q)\frac{\gamma}{a^q}\left[2l + a^{2-q}\,q\gamma + (2s+1)\sqrt{1-q}\right] + m^2c^2\hbar^{-2}\right\}^{1/2},$$

$$u_s = \sqrt[4]{\frac{\lambda}{\pi}}\frac{1}{\sqrt{2^s s!}}e^{-(\lambda/2)(r-a)^2}H_s(\sqrt{\lambda}(r-a)). \quad (17)$$

Here H_s is a Chebyshev-Hermite polynomial, and $s = 0, 1, 2,\cdots$ is the radial quantum number.

Using the wave-functions (17), it is easy to find the mean-square fluctuation of the radius which defines the breadth of the trajectory:

$$\xi^2 = \overline{x^2} = \int_0^\infty x^2 u_s^2 dr \approx \int_{-\infty}^{\infty} x^2 u_s^2 dx = s/2\gamma', \quad (18)$$

where

$$\gamma' = \frac{eH(a)}{2c\hbar}\sqrt{1-q}.$$

For a constant magnetic field ($q = 0$), the value of ξ^2 reduces to the expression $\xi^2 = s/2\gamma$ found by us previously[6].

4. We shall determine the angular frequency $\omega_{\nu\nu'}$, and the probability $w_{\nu\nu'}$ of the radiation associated with a transition of the electron from the state l,s to the state l', s', ($\nu = l - l'$, $\nu' = s - s'$), keeping terms only up to the order ν^2/l. These are

$$\omega_{\nu,\nu'} = \omega_0(\nu + \nu'\sqrt{1-q}), \quad (19)$$

$$w_{\nu,\nu'} = \frac{W_{\nu,\nu'}}{\hbar\nu\omega_0} = \frac{1}{\hbar\nu\omega_0}I^2_{s,s'}(x)\frac{3\sqrt{3}}{4\pi} \times \frac{e^2c}{a^2}\left(\frac{E}{mc^2}\right)^4 y\,dy\int_y^\infty K_{5/3}(z)\,dz. \quad (20)$$

Here $W_{\nu\nu'}$ is the radiation intensity,

---

[7] D. Kerst and R. Serber, Phys. Rev. **60**, 53 (1941); see also the Science-review volume *Betatron*, Moscow, 1948

$$y = \frac{2}{3}\nu\left(\frac{mc^2}{E}\right)^3, \tag{21}$$

$$x = \frac{\nu^2}{2(2-q)\sqrt{1-q}}\frac{1}{l}, \qquad \omega_0 = \frac{v}{a},$$

and the function $I_{ss'}(x)$ is connected with the Laguerre polynomial $Q_s^{\nu'}(x)$ by

$$I_{s,s'}(x) = (-1)^{\nu'}\frac{x^{\nu'/2}e^{-x/2}}{\sqrt{s!\,s'!}}Q_{s'}^{\nu'}(x). \tag{22}$$

It is easy to see that the intensity (20) differs from the corresponding classical expression (in this approximation) only by the factor $I_{ss'}^2$, which as we repeatedly showed (for example in reference 6) reduces to unity when summed over all final states s'. In this approximation therefore

$$W_\nu = \sum_{\nu'} W_{\nu,\nu'} = W_{\text{class}} \tag{23}$$

5. We shall use the quantum expressions to determine the change in orbit radius produced by the radiation. In a single transition the quantum number l changes by an amount $\Delta l_1 = l' - l = -\nu$. Multiplying this by $w_{\nu\nu'}\,dt$ and summing over all possible transitions, we obtain the change dl occurring in an interval of time dt:

$$dl = -\sum_{\nu,\nu'}\nu w_{\nu,\nu'}dt = -\frac{2}{3}\frac{e^2}{r}\left(\frac{E}{mc^2}\right)^4\frac{1}{\hbar}\,dt. \tag{24}$$

Hence, using the equation

$$e\left\{\frac{\overline{H}(r,t)}{2} - H(r,t)\right\} \tag{25}$$

$$= -\frac{e\Delta r}{a}\frac{\partial aH(a,t)}{\partial a} = -\frac{\Delta r}{a}\frac{\partial E}{\partial a}$$

(see reference 3) where $\Delta r = r - a$, and also using Eqs. (14) and (15), we find the well-known classical result for the radiative contraction of the orbit radius (see page 260 of refernce 3),

$$\Delta r = -\frac{2}{3}\left(\frac{e^2}{mc^2}\right)^3\frac{a^2B^3(a)}{mce(1-q)}\frac{1}{\omega'}F_1(\omega' t), \tag{26}$$

with

$$F_1(y) = \frac{1}{\sin y}\int_0^y \sin^4 z\,dz \tag{27}$$

$$= \frac{3}{8}\left\{\frac{y}{\sin y} - \cos y - \frac{2}{3}\sin^2 y\cos y\right\}.$$

In deriving Eq. (26) we assume that the magnetic field H is increasing slowly with time,

$$H = B\sin\omega' t, \quad E = E_0\sin\omega' t,$$

$$\omega' \ll \omega_0 = v/a,$$

so that the field remains practically constant during the period of one revolution of the electron.

6. We proved[6] in the case of a constant magnetic field ($q = 0$) that the quantum corrections to the intensity of radiation and to the contraction of the orbit are of order $(E/mc^2)^2$ $(\hbar/mca)$ relative to the classical values. Therefore the quantum corrections become an appreciable fraction of the whole effect only at an energy comparable with $E_{1/2} = mc^2(mca/\hbar)^{1/2}$. Considering quantum corrections in general, the most interesting effect to investigate is the broadening of the trajectory (fluctuation of the orbit radius) which is characterized by the radial quantum number s.

As we see from Eq. (18), the quantity s remains unchanged as the magnetic field $H(a)$ is increased adiabatically. Therefore the mean-square breadth of the trajectory ξ^2 must decrease[7] inversely to $H(a)$, since, by Eq. (18),

$$\xi^2 H(a) = sc\hbar/e\sqrt{1-q} = \text{const}.$$

However, as we showed in the case of a constant field, at an energy of the order of $E_{1/5} = mc^2(mca/\hbar)^{1/5}$ pure quantum transitions involving a change in the radial quantum number s begin to occur. These transitions, in contrast to the classical theory, must produce an increase in the trajectory breadth $\sqrt{\xi^2}$. The quantum broadening of the trajectory begins to outweigh the classical decrease in breadth at a comparatively low energy $E = aE_{1/5}$ with a about 3. This broadening of the trajectory is an increase in the amplitude of radial oscillations, arising from the recoil when photons are emitted.

The formula for the increase in ξ^2 were derived by us[6] for the case of a constant magnetic field. Here we generalize the results to the case of an axially symmetric field varying adiabatically with time.

By Eqs. (18) and (22) we have

$$ds = -\sum_{\nu,\nu'}\nu' w_{\nu,\nu'}\,dt \tag{28}$$

$$= \frac{55}{48\sqrt{3}}\frac{e^2}{mcr^2}\left(\frac{E}{mc^2}\right)^6\frac{dt}{(1-q)^{3/2}},$$

where $\nu' = s - s'$. In addition we had to take into account the expression for the change $\Delta\xi^2$ produced by the emission of a single photon with energy ΔE,

$$\Delta\xi^2 = \frac{1}{2\gamma'}\sum_{s'}(s'-s)I_{s,s'}^2(x) = \frac{2a^2}{(2-2q)^2}\left(\frac{\Delta E}{E}\right)^2, \tag{29}$$

which will evidently remain valid in the presence of forces acting on the electron parallel to its trajectory, or in the presence of other transient forces. Hence we find the law of variation of the breadth of the trajectory

$$\xi^2 = \xi_0^2 \frac{\beta_0 E_0 r}{E(t)\, a} \tag{30}$$

$$+ \frac{55}{48\sqrt{3}} \frac{e^2 \hbar r}{m(1-q)^2 E(t)} \int_0^t \left(\frac{E(t)}{mc^2}\right)^6 \frac{1}{r^2}\, dt,$$

where $c\beta_0$, E_0 and a represent the initial values of velocity, energy and radius. The last equation gives for $q = 0$ the variation of ξ^2 in a constant magnetic field, agreeing with our earlier result[6].

In particular, if the energy increases like $E = E_0 \sin \omega' t$, the quantum broadening becomes

$$\xi_{qv}^2 = \frac{55}{48\sqrt{3}} \frac{1}{(1-q)^2} \frac{e^2}{mc} \frac{\hbar}{mca} \left(\frac{E_0}{mc^2}\right)^5 \frac{1}{\omega'} F_2(\omega' t), \tag{31}$$

with
$$F_2(y) = \frac{1}{\sin y} \int_0^y \sin^6 z\, dz \tag{32}$$

$$= \frac{1}{\sin y}\left\{\frac{5}{16}\, y - \frac{15}{64} \sin 2y + \frac{3}{64} \sin 4y - \frac{1}{192} \sin 6y\right\}.$$

The maximum value of F_2 occurs when $\omega' t = \pi/2$ and is equal to $F_2^{MAX} = F_2(\pi/2) = (5/32)\pi$. From Eq. (30) we see that the first term, which comes from the classical theory, gives a mean-square breadth of trajectory decreasing inversely with energy; the second term, which is obtained only from a quantum treatment, gives a mean-square breadth increasing proportional to E^5.

Note added in proof. In a recently published paper [Phys. Rev. **97**, 470 (1955)], Sands investigated the effect of quantum fluctuations on the phase-oscillations of a synchroton. We considered, in our series of papers on the quantum theory of the radiating electron (see for example reference 6), a similar mechanism for the quantum excitation of macroscopic radial oscillations.

Sands' final result [Eq. (23)] can be derived from our Eq. (18) [Doklady Akad. Nauk SSSR **97**, 823 (1954)] or from Eq. (30) of this paper, if one restricts the action of the beatron oscillations, which produce the main part of the total effect, and which are correctly described by our theory, to operate only for a time equal to the decay-time of the synchroton oscillations. This decay-time is shorter than the acceleration time of the electrons.

Translated by F. J. Dyson
77

Dispersion Formulas of the Quantum Optics of Metals in the Many-electron Theory with Consideration of Electron Damping

A. V. Sokolov, V. I. Cherepanov and I. B. Shteinberg
Institute for the Physics of Metals, Ural Affiliate of the Academy of Sciences, USSR
(Submitted to JETP editor March 12, 1954)
J. Exper. Theoret. Phys. USSR **28**, 330-334 (March, 1955)

The general dispersion formulas of the quantum optics of metals with consideration of electron damping have been derived for the aggregate of interacting electrons which can be described by the general wave function.

In reference (1) there were obtained some dispersion formulas of the quantum optics of metals based on the many-electron theory. However, they are correct in the visible and ultra-violet regions of the spectrum only when the damping of electron motion is not taken into account. It is of interest to consider the general case, which includes electron damping.

In the general case the effect of the alternating field of a light wave on the electrons in a metal can be twofold. Correspondingly the quantum optics of metals differentiates between two types of processes — acceleration, and the transition of electrons into higher energy states. In the first case the electrons can lose the acquired acceleration by virtue of their interaction with the elastic vibrations of the lattice (phonons); in the second case the electron system in general does not remain in the excited state, but "jumps back", with the phonon-lattice interaction having an influence, among other causes, on the duration of the excited state. This interaction can be taken into account by introducing a damping factor of electron motion $\Gamma_{\vec{\xi}_1'\vec{\xi}_2'\cdots\vec{\xi}_N'}^{\rightarrow\rightarrow\quad\rightarrow} = \Gamma'$.

In considering the interaction of the electron system with the lattice vibrations, the principle of conservation of energy and the interference condition will assume the form:

$$E(\vec{\xi}_1', \ldots, \vec{\xi}_N') = E(\vec{\xi}_1, \ldots, \vec{\xi}_N) \pm \hbar\omega \mp \hbar\omega_{\mathbf{q}}, \quad (1)$$

$$\sum \mathbf{k}_i' = \sum \mathbf{k}_i + \mathbf{K} \mp \mathbf{q} + 2\pi\mathbf{g}, \quad (2)$$

where $\mathbf{q}$ is the wave vector and $\hbar\omega_{\mathbf{q}}$ is the energy of the phonon being absorbed or emmited.

If it were possible to neglect the interaction of the electron system with the lattice vibrations, then the electron system would be in the excited state for a long time (stationary state). However, if the interaction is large, then the electron system, being in an excited state, will give up its energy to the lattice vibrations (nonstationary states). During this process the energy of lattice vibrations will grow, and with time, become uniformly distributed among all frequencies, i.e., there will finally result a rise in the lattice temperature.

The effect of the lattice vibrations on the electron system can be expressed by a decrease in the duration of electron occurence in the excited state. Mathematically this is developed by replacing the energy of the electron system in the excited state $(\vec{\xi}_1', \ldots, \vec{\xi}_N', s')$ by the complex quantity

$$E(\xi_1', \xi_2', \ldots, \xi_N', s') \rightarrow E(\xi_1' \xi_2', \ldots, \xi_N', s') - i\hbar\Gamma_{\vec{\xi}_1', \ldots, \vec{\xi}_N'}^{\rightarrow},$$

where $\Gamma_{\vec{\xi}_1', \ldots, \vec{\xi}_N'}^{\rightarrow}$ is the damping factor of electron motion. To derive dispersion formulas which take into consideration the interaction of the electron system with the lattice vibrations it is necessary, therefore, to make the aforementioned substitution; the formulas (2.6), [1] expressing the law of conservation of energy and the interference condition, are to be replaced by formulas (1) and (2) of this paper. However, in as much as the wave vectors of the photon and the phonon can be neglected in comparison with the generalized vector of the entire electronic system, the interference condition will have the same expression as in reference (1). As in the one-electron theory, the lattice quantum energy can be neglected in comparison with the energy of the entire electron system, and therefore, instead of equation (1) we shall have the previous form of the law of conservation of energy (2.6) [1]. In taking into account the above

[1] A. V. Sokolov, J. Exper. Theoret. Phys. USSR **25**, 341 (1953)

considerations, the expression for the current density (3.17) in reference (1) takes the form:

$$\mathbf{j} = \frac{e^2}{m^2 c\hbar\,(Ga)^{3N}} \tag{3}$$

$$\times \sum_{s,\,s'} \int d\vec{\xi}_1 \ldots d\vec{\xi}_N \,[\rho_0(\vec{\xi}_1, \ldots, \vec{\xi}_N, s')$$

$$- \rho_0(\vec{\xi}_1, \ldots, \vec{\xi}_N, s)]$$

$$\times (\vec{\xi}_1, \ldots, \vec{\xi}_N, s' | \sum \hat{\mathbf{p}}_i | \vec{\xi}_1, \ldots, \vec{\xi}_N, s)$$

$$\times \Big\{ \mathbf{B}\, e^{i\omega t} \frac{1 - [\exp -(\omega' + \omega - i\Gamma')\, t]}{\omega' - \omega - i\Gamma'}$$

$$+ \mathbf{B}^* e^{-i\omega t} \frac{1 - \exp[-i(\omega' - \omega - i\Gamma')\, t]}{\omega' - \omega - i\Gamma'} \Big\}$$

$$\times (\vec{\xi}_1, \ldots, \vec{\xi}_N, s \,|\, \sum \hat{\mathbf{p}}_i \,|\, \xi_1, \ldots, \xi_N, s')$$

$$- \frac{e^2}{mc\,(Ga)^{3N}} \mathbf{A} \sum_s \int \rho_0(\vec{\xi}_1, \ldots, \vec{\xi}_N, s)$$

$$\times e^{-\Gamma' t}\, d\vec{\xi}_1, \ldots, d\vec{\xi}_N,$$

where $\omega' = \omega_{\vec{\xi}_1, \ldots, \vec{\xi}_N, s; \vec{\xi}'_1, \ldots, \vec{\xi}'_N, s'}$.

This expression has a simple physical meaning. Immediately after the application of the field at $t \approx 0$ this expression gives the displacement current, specified by the original distribution of the electrons among the states $\rho_0(\vec{\xi}_1, \vec{\xi}_2, \ldots, \vec{\xi}_N, s)$. Afterwards with $t > 0$, there appear two more types of terms as a result of the redistribution of electrons among the states by the action of the field: those harmonically dependent on t with the frequency ω of the external electro magnetic field and terms containing function of t with frequencies ω' and damping out with time. The first refer to the forced vibrations of the system, while the second describe its natural oscillations, set up at the starting time of field application and damped out exponentially with time. The current, determined by the initial electron distribution is also damped out with time. With strong damping, as in the case of large t one can completely neglect the natural vibrations of the system and the initial current. However, when damping is absent ($\Gamma' = 0$), or when it is weak ($\Gamma' \approx 0$), the natural oscillations of the system must also be taken into account.

For the convenience of subsequent calculations, Eq. (3) may be rearranged as

$$\mathbf{j} = \mathbf{j}_1 + i\,\mathbf{j}_2, \tag{4}$$

where

$$\mathbf{j}_1 = \frac{e^2}{m^2 c\hbar\,(Ga)^{3N}} \sum_{s,\,s'} \int d\vec{\xi}_1, \ldots, d\vec{\xi}_N \tag{4a}$$

$$[\rho_0(\vec{\xi}_1, \ldots, \vec{\xi}_N, s')$$

$$- \rho_0(\vec{\xi}_1, \ldots, \vec{\xi}_N, s)]$$

$$\times (\vec{\xi}_1, \ldots, \vec{\xi}_N, s' | \sum \mathbf{p}_i | \vec{\xi}_1, \ldots, \vec{\xi}_N, s)$$

$$\times \Big\{ \mathbf{B}\, e^{i\omega t} \frac{1}{\omega' + \omega - i\Gamma'} + \mathbf{B}^* e^{-i\omega t} \frac{1}{\omega' - \omega - i\Gamma'} \Big\}$$

$$\times (\vec{\xi}_1, \ldots, \vec{\xi}_N, s \,|\, \sum \hat{\mathbf{p}}_i \,|\, \vec{\xi}_1, \ldots, \vec{\xi}_N, s')$$

$$- \frac{e^2}{mc\,(Ga)^{3N}} \mathbf{A} \sum_s \int \rho_0(\vec{\xi}_1, \ldots, \vec{\xi}_N, s)$$

$$\times e^{-\Gamma' t}\, d\vec{\xi}_1, \ldots, d\vec{\xi}_N,$$

$$\mathbf{j}_2 = \frac{e^2}{m^2 c\hbar\,(Ga)^{3N}} \sum_{s,s'} \int d\vec{\xi}_1, \ldots, d\vec{\xi}_N \tag{4b}$$

$$\times [\rho_0(\vec{\xi}_1, \ldots, \vec{\xi}_N, s') - \rho_0(\vec{\xi}_1, \ldots, \xi_N, s)]$$

$$\times (\vec{\xi}_1, \ldots, \vec{\xi}_N, s' | \sum \hat{\mathbf{p}}_i | \vec{\xi}_1, \ldots, \vec{\xi}_N, s)$$

$$\times \Big\{ \mathbf{B}\, e^{i\omega t} \frac{\exp[-i(\omega' + \omega - i\Gamma')\, t]}{-i(\omega' + \omega - i\Gamma')}$$

$$+ \mathbf{B}^* e^{-i\omega t} \frac{\exp[-i(\omega' - \omega - i\Gamma')\, t]}{-i(\omega' - \omega - i\Gamma')} \Big\}$$

$$\times (\vec{\xi}_1, \ldots, \vec{\xi}_N, s | \sum \hat{\mathbf{p}} | \vec{\xi}_1, \ldots, \vec{\xi}_N, s').$$

In (4a) the sum over s, s' is broken up into two parts, corresponding to $\rho_0(\vec{\xi}_1, \ldots, \vec{\xi}_N, s')$ and $\rho_0(\vec{\xi}_1, \ldots, \vec{\xi}_N, s)$ and in the first of them the summation indices $s \rightleftarrows s'$ are interchanged so that

$$\omega_{\vec{\xi}_1, \ldots, \vec{\xi}_N, s; \vec{\xi}_1, \ldots, \vec{\xi}_N, s'} \to -\omega_{\vec{\xi}_1, \ldots, \vec{\xi}_N, s;} \tag{5}$$

$$\vec{\xi}_1, \ldots, \vec{\xi}_N, s' \quad \text{and} \quad \Gamma_{\vec{\xi}_1, \ldots, \vec{\xi}'_N} \to \Gamma_{\vec{\xi}'_1, \ldots, \vec{\xi}'_N}.$$

Collecting again all the terms into a single sum, instead of the expression in the braces of (4a), we shall have

$$\left\{\mathbf{B}\,e^{i\omega t}\,\frac{1}{-\omega'+\omega-i\Gamma'}+\mathbf{B}^{*}\,e^{-i\omega t}\,\frac{1}{-\omega'-\omega-i\Gamma'}\right.,$$

$$\left.-\mathbf{B}\,e^{i\omega t}\,\frac{1}{\omega'+\omega-i\Gamma'}-\mathbf{B}^{*}\,e^{-i\omega t}\,\frac{1}{\omega'-\omega-i\Gamma'}\right\}.$$

Grouping in pairs the terms of this parenthesis, the first with the fourth, and the second with the third, and taking into account that

$$\mathbf{B}\,e^{i\omega t}+\mathbf{B}^{*}e^{-i\omega t}=\mathbf{A},$$

$$\mathbf{B}\,e^{i\omega t}-\mathbf{B}^{*}\,e^{-i\omega t}=(1/i\omega)\,\dot{\mathbf{A}},$$

the parenthesis in question can be represented by

$$\left\{-\left[\frac{\omega'-\omega}{(\omega'-\omega)^2+\Gamma'^2}+\frac{\omega'+\omega}{(\omega'+\omega)^2+\Gamma'^2}\right]\mathbf{A}\right.$$

$$\left.+\frac{1}{\omega}\left[\frac{\Gamma'}{(\omega'-\omega)^2+\Gamma'^2}-\frac{\Gamma'}{(\omega'+\omega)^2+\Gamma'^2}\right]\dot{\mathbf{A}}\right\}.$$

Separating (4b) into two parts, and entering $\mathbf{B}$ into one, and $\mathbf{B}^*$ into the other, the following transformation can be made:

$$\frac{\exp\left[-i\,(\omega'+\omega-i\,\Gamma')\,t\right]}{-i\,(\omega'+\omega-i\Gamma')} \qquad (6)$$

$$=e^{-\Gamma' t}\,\frac{\exp\left[-i\,(\omega'+\omega)\,t\right]}{-i\,(\omega'+\omega)}\,\frac{1}{1+\left(\frac{\Gamma'}{i\,(\omega'+\omega)}\right)}$$

$$=e^{-\Gamma' t}\,\frac{\exp\left[-i\,(\omega'+\omega)\,t\right]}{-i\,(\omega'+\omega)}$$

$$\times\left(1-\frac{\Gamma'}{i\,(\omega'+\omega)}-\frac{\Gamma'^2}{(\omega'+\omega)^2}-\ldots\right).$$

Before making the analogous transformation for the expression

$$\exp\left[-i\,(\omega'-\omega-i\,\Gamma')\,t\right]/-i\,(\omega'-\omega-i\,\Gamma')$$

in that part of Eq. (4b) which contains $\mathbf{B}^*$, the indices $s \rightleftharpoons s'$ are interchanged and, taking into account (5), we obtain

$$\frac{\exp\left[-i\,(-\omega'-\omega-i\,\Gamma')\,t\right]}{-i\,(-\omega'-\omega-i\,\Gamma')} \qquad (7)$$

$$=e^{-\Gamma' t}\,\frac{\exp\left[-i\,(-\omega'-\omega)\,t\right]}{-i\,(-\omega'-\omega)}\,\frac{1}{1+\left[\Gamma'/i\,(-\omega'-\omega)\right]}$$

$$=e^{-\Gamma' t}\,\frac{\exp\left[-i\,(-\omega'-\omega)\right]t}{-i\,(-\omega'-\omega)}$$

$$\times\left(1+\frac{\Gamma'}{i\,(\omega'+\omega)}-\frac{\Gamma'^2}{(\omega'+\omega)^2}\ldots\right).$$

Making then a transition in the expression (4b) from the integration variables $\vec{\xi}_1\,(\xi_1\,\eta_1\zeta_1)\ldots.$ $\vec{\xi}_N\,(\xi_N\,\eta_N\zeta_N)$ to variables ω', $u_1,\ldots,u_{3N-1}$ in a manner analogous to that of reference 1, and neglecting in (6) and (7) the terms in $\Gamma'/(\omega'+\omega)$, i.e., considering the damping small*, we obtain in place of (4b) the following expression:

$$\frac{\pi e^2}{m^2 c\,\hbar\,\omega\,(Ga)^{3N}}\sum_{s,s'}\int du_1,\ldots,\ du_{3N-1}\,e^{-\Gamma' t}$$

$$\times\ \frac{\rho_0\,(\vec{\xi}_1,\ldots,\vec{\xi}_N,\ s')-\rho_0(\vec{\xi}_1,\ldots,\vec{\xi}_N,\ s)}{\left|\operatorname{grad}_{\vec{\xi}_1,\ldots,\vec{\xi}_N}\omega'\right|}$$

$$\times\ (\vec{\xi}_1,\ldots,\vec{\xi}_N,\ s'\,|\,\textstyle\sum\hat{\mathbf{p}}_i\,|\,\vec{\xi}_1,\ldots,\vec{\xi}_N,\ s)$$

$$\times\ (\vec{\xi}_1,\ldots,\vec{\xi}_{1N},\ s\,|\,\textstyle\sum\hat{\mathbf{p}}_i\,|\,\vec{\xi}_1,\ldots,\vec{\xi}_N,\ s').$$

The final expression for the total current density in the metal will have the form:

$$\mathbf{j}=-\frac{e^2}{mc\,(Ga)^{3N}}\sum_{s}\int d\vec{\xi}_1,\ldots,\ d\vec{\xi}_N,\rho_0$$

$$\times\ (\vec{\xi}_1,\ldots,\ \vec{\xi}_N,\ s)\ \times\left\{\mathbf{A}\,e^{-\Gamma' t}\right.$$

$$+\frac{1}{m\hbar}\sum_{s'}\left(\frac{\omega'-\omega}{(\omega'-\omega)^2+\Gamma'^2}+\frac{\omega'+\omega}{(\omega'+\omega)^2+\Gamma'^2}\right)$$

$$\left.\times\ \mathbf{D}_{\vec{\xi}_1,\ldots,\ \vec{\xi}_N,\ s\ \vec{\xi}_1,\ldots,\ \vec{\xi}_N,\ s'}\mathbf{A}\right\}-\frac{e^2}{m^2 c\hbar\ \omega\ (Ga)^{3N}}$$

$$\times\sum_{s,s'}\int d\vec{\xi}_1,\ldots,\ d\vec{\xi}_N,\ \ \rho_0\,(\vec{\xi}_1,\ldots,\ \vec{\xi}_N,\ s)$$

$$\times\left(\frac{\Gamma'}{(\omega'+\omega)^2+\Gamma'^2}-\frac{\Gamma'}{(\omega'-\omega)^2+\Gamma'^2}\right)$$

$$\times\mathbf{D}_{\vec{\xi}_1,\ldots,\ \vec{\xi}_N,\ s;\ \vec{\xi}_1,\ldots,\ \vec{\xi}_N\ s}\ \dot{\mathbf{A}}\ +\frac{\pi e^2}{m^2 c\hbar\omega(Ga)^{3N}}$$

$$\times\sum_{s,s'}\int du_1\ldots\ du_{3N-1}\,e^{-\Gamma' t}$$

$$\times\frac{\rho_0\,(\xi_1,\ldots,\ \xi_N,\ s')-\rho_0\,(\xi_1,\ldots,\ \xi_N,\ s)}{\operatorname{grad}_{\vec{\xi}_1,\ldots,\ \vec{\xi}_N}\omega'}$$

$$\times\ \mathbf{D}_{\vec{\xi}_1,\ldots,\ \vec{\xi}_N,\ s\ \vec{\xi}_1,\ldots,\ \vec{\xi}_N\ s'}\dot{\mathbf{A}}.$$

---

* This case is of particular interest to us since we wish to prove that with $\Gamma'=0$ our final formulas for ϵ and σ become the formulas of reference (1). In the presence of strong damping the entire expression (4b) vanishes because of the presence of $e^{-\Gamma' t}$.

A comparison of this expression with the current calculated from classical theory

$$\mathbf{j} = \frac{\varepsilon - 1}{4\pi}\frac{\omega^2}{c}\mathbf{A} - \frac{\sigma}{c}\dot{\mathbf{A}},$$

gives the following expressions for the dielectric constant ϵ and the electrical conductivity σ

$$\varepsilon = 1 - \frac{4\pi e^2}{m\omega^2 (Ga)^{3N}} \times \sum_s \int \Big[e^{-\Gamma' t} + \frac{1}{m\hbar}\sum_{s'} \Big(\frac{\omega' - \dot{\omega}}{(\omega'-\omega)^2+\Gamma'^2} + \frac{\omega' + \omega}{(\omega'+\omega)^2+\Gamma'^2}\Big) \mathbf{D}_{\vec{\xi}_1,\ldots,\vec{\xi}_N,\, s\; \vec{\xi}_1',\ldots\vec{\xi}_N',\, s;} \Big] \times \rho_0(\vec{\xi}_1, \ldots, \vec{\xi}_N,\, s)\, d\vec{\xi}_1, \ldots, d\vec{\xi}_N;$$

$$\sigma = -\frac{\pi e^2}{m^2\hbar\omega\,(Ga)^{3N}} \times \sum_{s,s'} \int e^{-\Gamma' t} \frac{\rho_0(\vec{\xi}_1, \ldots, \vec{\xi}_N, s') - \rho_0(\vec{\xi}_1, \ldots, \vec{\xi}_N, s)}{\operatorname{grad}_{\vec{\xi}_1 \ldots \vec{\xi}_N} \omega'} \times \mathbf{D}_{\vec{\xi}_1,\ldots,\vec{\xi}_N;\, \vec{\xi}_1',\ldots,\vec{\xi}_N'} du_1 \ldots du_{3N-1}$$

$$+ \frac{e^2}{m^2\hbar\omega\,(Ga)^{3N}} \sum_{s,s'} \int \Big(\frac{\Gamma'}{(\omega'+\omega)^2+\Gamma'^2} - \frac{\Gamma'}{(\omega'-\omega)^2+\Gamma'^2} \Big) \times \rho_0(\vec{\xi}_1, \ldots, \vec{\xi}_N,\, s)\, \mathbf{D}_{\vec{\xi}_1,\ldots,\vec{\xi}_N;\, \vec{\xi}_1',\vec{\xi}_N'} d\vec{\xi}_1, \ldots, d\vec{\xi}_N.$$

As we expected, with $\Gamma' = 0$ the expressions for ϵ and σ become Eqs. (3.23) and (3.24) of reference 1, whereas with $\Gamma' \neq 0$, the terms containing $\exp(-\Gamma' t)$ vanish and, finally, we obtain

$$\varepsilon = 1 - \frac{4\pi e^2}{m\omega^2 (Ga)^{3N}} \sum_s \int \Big[\frac{1}{m\hbar} \sum_{s'} \Big(\frac{\omega' - \omega}{(\omega'-\omega)^2+\Gamma'^2} + \frac{\omega' + \omega}{(\omega'+\omega)^2+\Gamma'^2} \mathbf{D}_{\vec{\xi}_1,\ldots,\vec{\xi}_N;\, \vec{\xi}_1',\ldots,\, \vec{\xi}_N'} \Big] \times \rho_0(\vec{\xi}_1, \ldots, \vec{\xi}_N, s)\, d\vec{\xi}_1, \ldots, d\vec{\xi}_N,$$

$$\sigma = + \frac{e^2}{m^2\hbar\omega\,(Ga)^{3N}} \sum_{s,s'} \int \Big(\frac{\Gamma'}{(\omega'+\omega)^2+\Gamma'^2} - \frac{\Gamma'}{(\omega'-\omega)^2+\Gamma'^2} \Big) \rho_0(\vec{\xi}_1, \ldots, \vec{\xi}_N,\, s) \times \mathbf{D}_{\vec{\xi}\ldots,\vec{\xi}_N;\, \vec{\xi}_1'\ldots,\, \xi_N'} d\vec{\xi}_1, \ldots, d\vec{\xi}_N.$$

Translated by H. Kruglak
56

The Effect of Concentration on the Optical Properties of Solutions of Acridine Compounds

L. V. LEVSHIN
Moscow State University

(Submitted to JETP editor March 2, 1954)
J. Exper. Theoret. Phys. USSR 28, 213-222 (1955)

The effect of concentration of nine acridine compounds on absorption spectra (in the range of 500 to 220 mμ), luminescence spectra, polarization spectra, yield of luminescence and average lifetime of the excited state was studied. It was shown that many effects produced by change in concentration are the results of association of molecules of the solute. Molecular association annihilates the luminescence power in some compounds and changes the spectral composition of the others.

IN previous work[1] the effect of concentration on optical properties of 3, 6 - diaminoacridine solutions was studied and significant action of molecular association on development of effects due to change in concentration was indicated.

The assumption was made that the significant change in the shape of the absorption spectrum of 3, 6 - diaminoacridine solutions is the result of a "pileshaped" aggregation of the molecules in process of association.

In this paper the effect of concentration on the optical properties of acridine and its eight derivatives is considered[2].

In Fig. 1 the names and structural formulas of investigated compounds are given. The experimental investigation was done by means of the same equipment as in the previous work[1].

The experiments showed that for most compounds the association of the molecules of the solute is of great importance for the development of the effects due to change in concentration. In some cases, particularly at not very high concentrations, the migration of excitation energy between neighboring molecules is an essential factor. Both kinds of interaction are coexistent.

No significant changes in shape of absorption spectra of the investigated compounds result upon increase in concentration. As the concentration increases, only uniform decrease or increase of absorption over the entire spectrum takes place. Apparently the aggregation of molecules here must be different from that of 3, 6 - diaminoacridine. One can assume that in this case the molecules aggregate in the form of a "chain". The possibility of bonds of this kind is indicated by the existence of two-ring acridine molecules, separated rings of which aggregate with each other in the form of a "chain"[3]. This assumption gets some confirmation when one compares the absorption spectrum of the concentrated acridine solution with the absorption spectrum of 9, 9′ - biacridyl. The biacridyl molecule consists of two acridine rings connected with each other by a single bond (Fig. 1). The absorption spectrum of pyridine solution of 9, 9′- biacridyl is shown in Fig. 2*a*, and the absorption spectrum of ethyl alcohol solution of acridine is shown in Fig. 2*b**.

The comparison of these spectra show that as we go from acridine to biacridyl the form of the absorption spectrum does not change much. However, some increase in absorption power of the molecules was observed in this case.

The increase in concentration from a dilute acridine solution to a concentrated one changes the shape of the spectrum even less. Increase of absorption due to change of concentration of acridine solution is somewhat smaller than the difference between absorption of acridine and 9, 9′- biacridyl (Fig. 2*b*)**.

[1] L. V. Levshin, J. Exper. Theoret. Phys. USSR 28, 201 (1955); Soviet Phys. 1, 244 (1955)

[2] L. V. Levshin, Doklady Akad. Nauk SSSR 96, 473 (1954)

[3] V. L. Levshin and T. M. Tarasova, Izv. Akad. Nauk SSSR, Ser. Fiz. 15, 573 (1951)

* In this Figure and in all further analogous figures the ordinate shows the absorption coefficients. The concentrations are given in gm/cm^3. The change of absorption coefficient upon concentration (measured in these units) defines the change in absorption power of coupled molecules, which takes place as a result of association. The absorption power of a single associated molecule is equal to the observed variation in absorption coefficient multiplied by the number of molecules of which it is composed.

** Comparison of only first absorption bands was made, since we could not obtain the second band of 9, 9′- biacridyl (because of the strong absorption of the pyridine in this part of the spectrum).

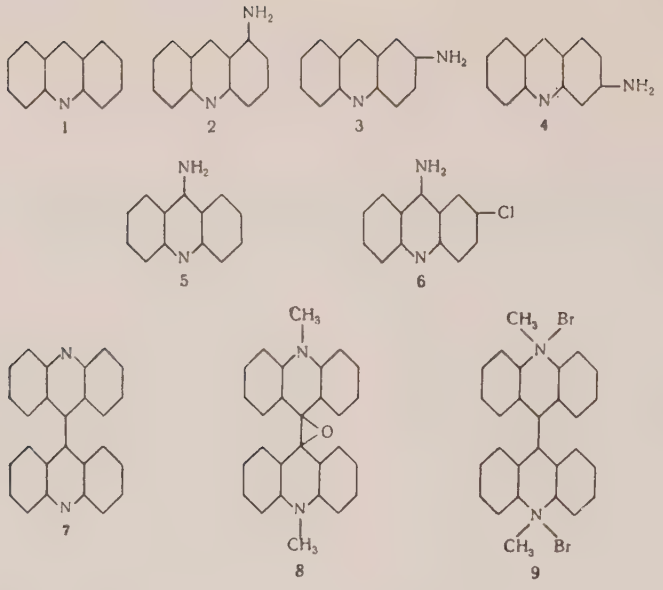

Fig. 1. Structural formulas of the acridine compounds:
1. acridine; *2.* 1-aminoacridine; *3.* 2-aminoacridine; *4.* 3-aminoacridine; *5.* 9-aminoacridine; *6.* 2-chloric-9-aminoacridine; *7.* 9, 9′-biacridyl; *8.* 10, 10′-dimethyl-9, 9′-biacridine-oxide; *9.* dibrommethylate of 9, 9′-biacridyl

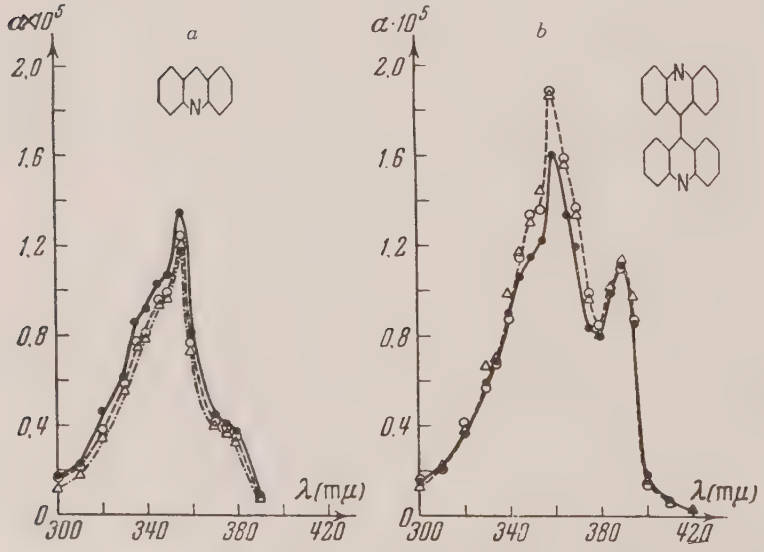

Fig. 2. Comparison of acridine and 9, 9′-biacridyl absorption spectra.
a. Absorption spectra of ethyl alcohol solution of acridine,
● $= 5 \times 10^{-4}$, ○ $= 1 \times 10^{-4}$, △ $= 1 \times 10^{-5}$ gm/cm^3.
b. Absorption spectra of pyridine solution of 9, 9′-biacridyl,
● $= 8 \times 10^{-4}$, ○ $= 1 \times 10^{-4}$, △ $= 1 \times 10^{-5}$ gm/cm^3.

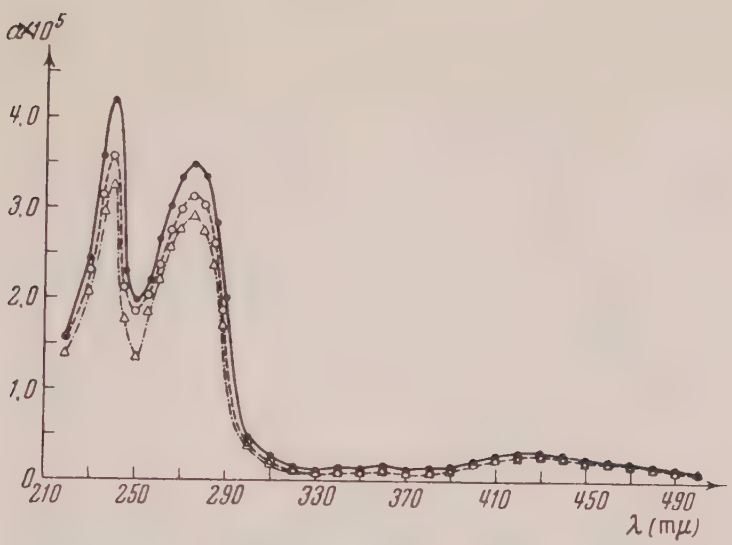

Fig. 3. Dependence of absorption spectrum of an ethyl alcohol solution of 1-aminoacridine on the concentration.
● = 1×10^{-3}, ○ = 1×10^{-4}, △ = 1×10^{-5} gm/cm^3

Hence, at least in an optical sense, there is no significant difference between the association of acridine molecules and the coupling of them by means of single chemical bonds. However, in the case of a chemical bond, the compound must be more stable. Apparently this explains the somewhat greater difference in absorption spectra observed in the transition from acridine to biacridyl in comparison with the spectra of the concentrated acridine solutions.

The increase in absorption power upon increase in concentration was found also in the case of alcohol solutions of 1-aminoacridine (Fig. 3). where the spectral form also remains without any significant changes. The luminescence spectra of acridine as well as of 1 - aminoacridine do not depend on concentration.

The absorption and luminescence spectra of alcohol solutions of 2 - aminoacridines and 3 - aminoacridines remain practically unchanged in a wide interval of concentrations (Fig. 4*a*). At the same time one observes a significant extinction of luminescence and a decrease in the average lifetime of the excited state τ of the molecules (Fig. 4*b*). The decrease in yield of luminescence is more rapid than the decrease in τ. Hence, for these compounds, the extinction due to change in concentration is apparently caused mainly by migration of the excitation energy. This conclusion is confirmed by the noticeable decrease of τ upon an increase of concentration of the solution.

The polarization spectrum of glycerin solution of 2 - aminoacridine was obtained and its dependence on concentration was studied (Fig. 5). The abscissa represents the wavelength of the exciting light, and the ordinate shows the percent values of degree of polarization. From Fig. 5 one can see that the polarization caused by 2 - aminoacridine molecules is positive over the whole polarization spectrum.

The increase in the concentration of the solution up to $c = 1 \times 10^{-3}$ gm/cm^3 does not change the polarization spectrum of 2-aminoacridine*. The explanation of this phenomenon will be given below.

In ethyl alcohol solutions of 9 - and 2 - chloric-9 - aminoacridines, increase in concentration results in a significant decrease of the absorption power of the molecules (Fig. 6). The main changes are observed here in the ultraviolet absorption band where the spectral form does not change very much.

The effect of concentration on molecular absorption of a solute was studied previously for the visible part of the spectrum**[4,5].

* The effect of reabsorption must be insignificant because of very little superposition of the luminescence and absorption spectra of 2 - aminoacridine.

** The only exception known to us is the work done by Kravetz and his coworkers, in which the ultraviolet absorption band of crystallic violet was studied as a function of concentration of the solution[6].

[4] V. L. Levshin, Zh. Fiz. Khim. **6**, 1 (1935)

[5] E. Rabinowitch and L. Epstein, J. Amer. Chem. Soc. **63**, 69 (1941)

[6] G. P. Kravetz, A. L. Pes'kina and Z. V. Zhidkova, Izv. Akad. Nauk SSSR, Ser. Fiz. **14**, 493 (1950)

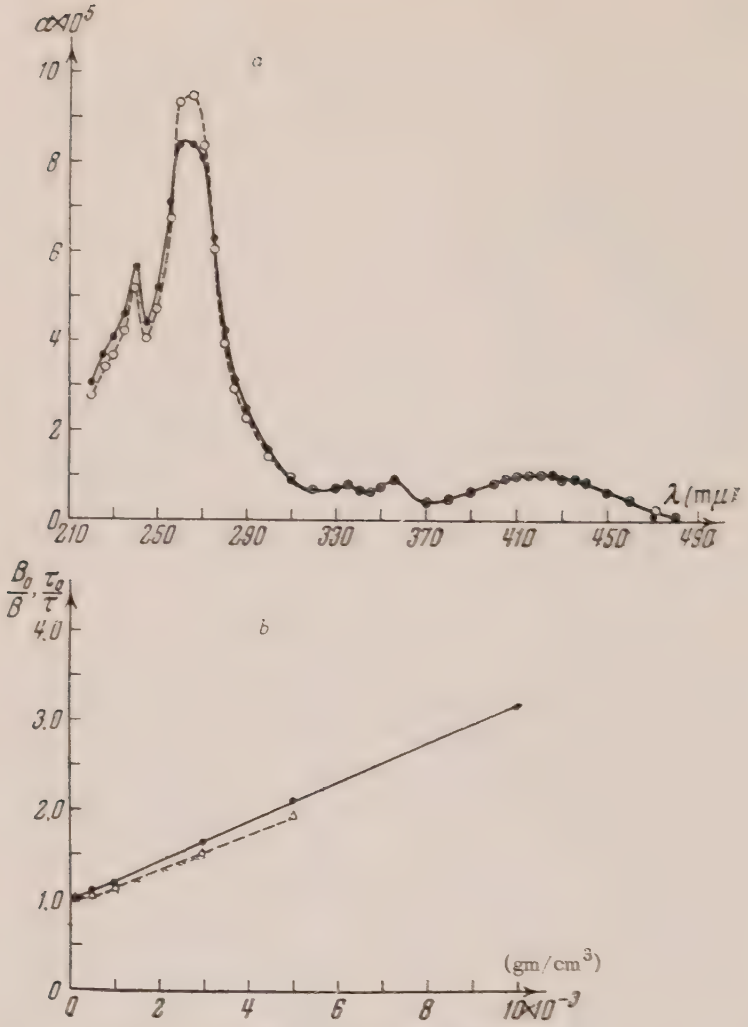

Fig. 4. Ethyl alcohol solution of 2-aminoacridine.

a. Dependence of absorption spectrum on the concentration of the solution, ● $= 1 \times 10^{-3}$, ○ $= 1 \times 10^{-5}$ gm/cm^3.

b. The extinction of luminescence and variation of τ. ● $= B_0/B$, △ $= \tau_0/\tau$.

In this work, as also in the work described in reference 1, the study of the effects due to change in concentration also was extended to the ultraviolet part of the absorption spectrum. In the case of 9 - aminoacridine one can see that the ultraviolet band is often more sensitive to the increase in concentration than the absorption in the long wave part of the spectrum.

The associated molecules can either retain their luminescence power[7] or lose it completely. For many acridine compounds, such as acridine, 1 - aminoacridine, 2 - and 3 - aminoacridine and others, the luminescence spectrum remains unchanged over a wide range of concentrations. However, in the case of some of them (9 - and 2 chloric - 9 - aminoacridine, 3, 6 - aminoacridine) the emission spectrum changes significantly in a concentrated solution. In case of 9 - aminoacridine, the luminescence spectrum changes markedly in form, and shifts in the long wave direction upon the increase in concentration (Fig. 7)*.

Apparently, in the diluted solution ($c = 2 \times 10^{-5}$ gm/cm^3) the emission is entirely caused by the

[7] V. L. Levshin, Z. Physik **43**, 230 (1927)

* In the luminescence spectra of all investigated materials reabsorption corrections were made.

molecules in monomeric state. The change of luminescence spectrum observed upon increase in concentration indicates the formation of the associated molecules, which have luminescence power. Their luminescence spectrum differs in form and location from that of monomers. At $c = 1 \times 10^{-3}$ gm/cm^3 the association is completed and the spectrum remains stable with respect to increase in concentration. At this concentration of the solution the luminescence spectrum belongs completely to the associated molecules.

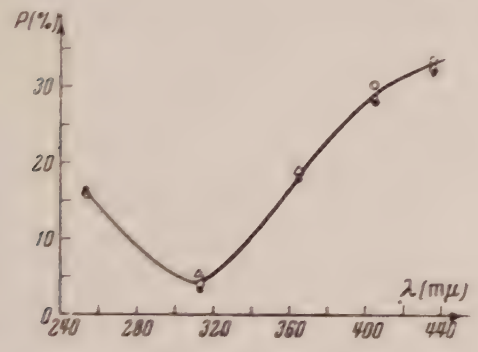

Fig. 5. Dependence of the polarization spectrum of glycerin solution of 2-aminoacridine upon the concentration.
● = 1×10^{-3}, ○ = 1×10^{-4}, △ = 1×10^{-5} gm/cm^3

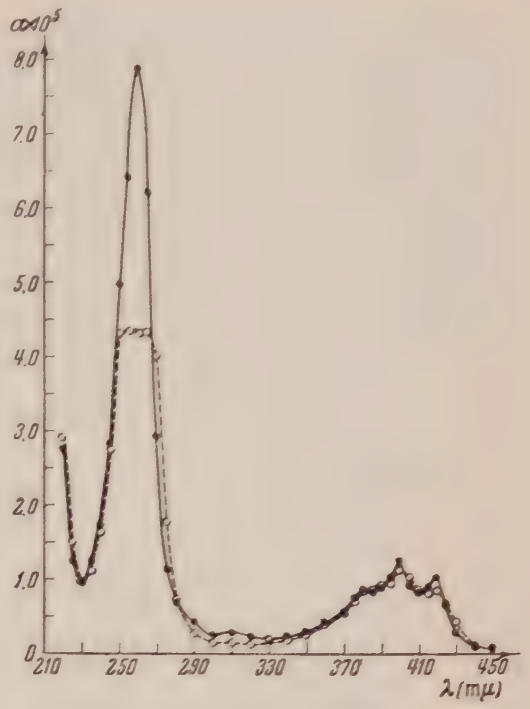

Fig. 6. Dependence of absorption spectrum of ethyl alcohol solution of 9-aminoacridine upon the concentration of the solution.
● = 2×10^{-5}, ○ = 1×10^{-3} gm/cm^3

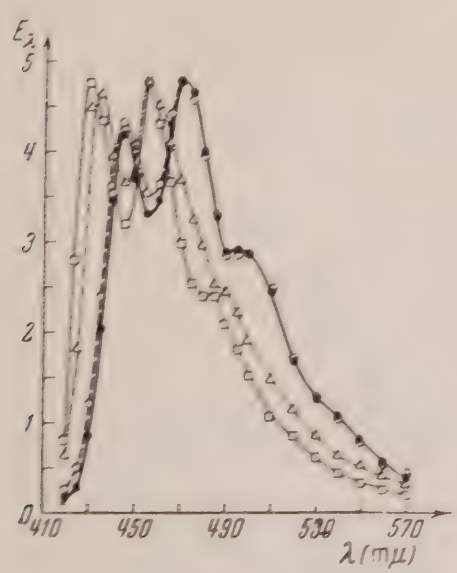

Fig. 7. Dependence of luminescence spectrum of ethyl alcohol solution of 9-aminoacridine on concentration of the solution. ● = 1×10^{-2}, ○ = 1×10^{-3}, △ = 1×10^{-4}, □ = 2×10^{-5} gm/cm^3

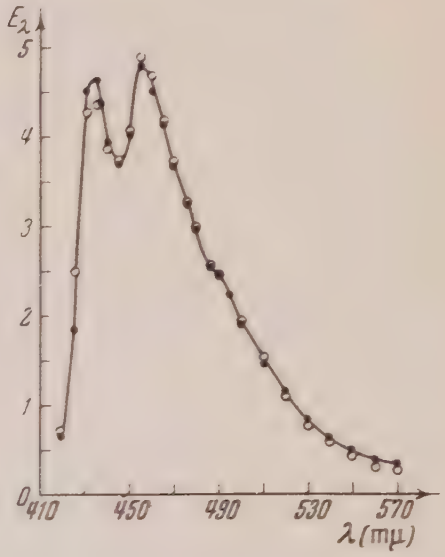

Fig. 8. The comparison of experimental and computed luminescence spectra of 9-aminoacridine.
● = experimental
○ = computed

If the above reasonings are correct, then, by superposition of a dimeric and a monomeric spectra, and taking into account the degree of participation of monomers and dimers in emission, one can obtain the spectrum of the solution with the intermediate concentration ($c = 1 \times 10^{-4}$ gm/cm^3).

Figure 8 shows the comparison of experimental and computed curves for luminescence spectrum of 9 - aminoacridine ($c = 1 \times 10^{-4}$ gm/cm^3). The computations are made by considering that 80% of the emission was caused by monomers and 20% by dimers. One can see that the experimental and computed curves are in good agreement. Analogous changes in luminescence spectrum were also discovered for alcohol solutions of 2 chloric - 9 - aminoacridine.

The increase in concentration results in significant extinction of luminescence and the decrease of the average lifetime of the excited state of the 9 - aminoacridine molecules (Fig. 9*a*). At the same time the polarization spectrum of 9 - aminoacridine does not depend on concentration, within the limits of experimental errors (Fig. 9*b*).

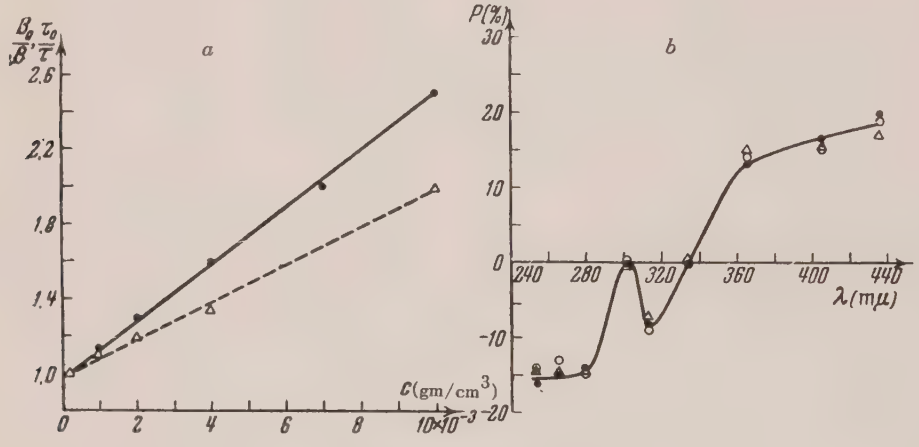

Fig. 9. 9-aminoacridine. *a*. ethyl alcohol solution. *b*. glycerin solution
a. extinction of luminescence and variation of τ.
● $= B_0/B$, △ $= \tau_0/\tau$;
b. dependence of polarization spectrum on the concentration of the solution.
● $= 5 \times 10^{-4}$, ○ $= 1 \times 10^{-4}$, △ $= 1 \times 10^{-5}$ gm/cm^3.

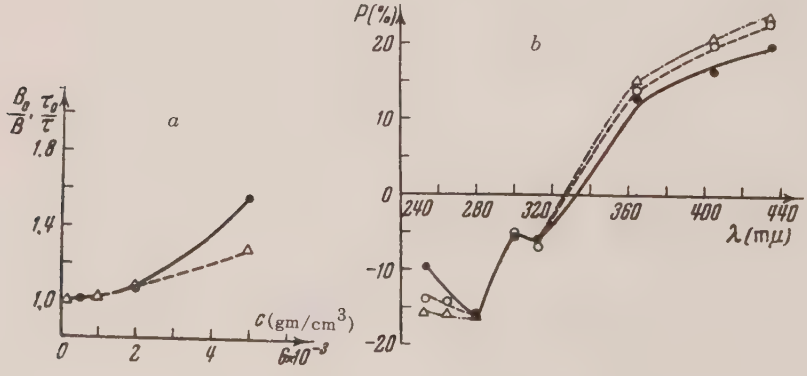

Fig. 10. 2-chloro-9-aminoacridine: *a*. in ethyl alcohol; *b*. in glycerine.
a. extinction of luminescence and variation of τ, ● $= B_0/B$, △ $= \tau_0/\tau$;
b. dependence of polarization spectrum in the concentration of the solution:
● $= 5 \times 10^{-4}$, ○ $= 1 \times 10^{-4}$, △ $= 1 \times 10^{-5}$ gm/cm^3

Meanwhile, it is known that the changes in degree of polarization usually occur much more rapidly than the extinction of the luminescence can develop and increase of τ can take place[8].

Lack of depolarization due to change in concentration apparently can be explained by competition of two counteracting processes. On one hand the degree of polarization decreases upon increase in concentration because of migration of the excitation energy between the neighboring molecules. On the other hand the migration of energy results in development of extinction of luminescence and decrease of τ (Fig. 9*a*). The decrease of τ leads to increase of polarization of luminescence. In our case both effects apparently cancel each other, and the polarization spectrum remains unchanged*. There is no cancellation in case of 2 chloric - 9 - aminoacridine, and the polarization spectrum changes markedly upon increase in concentration (Fig. 10*b*). This is in agreement with insignificant extinction and small variation of τ, observed in case of solutions of this compound (Fig. 10*a*).

The association must result in an increase of molecular volumes, which can be determined from experiments with polarization. The theory of polarized luminescence gives the relationship as follows[8]:

$$\frac{1}{P} = \frac{1}{P_0} + \left(\frac{1}{P_0} - \frac{1}{3}\right)\frac{TR\tau}{\eta V},$$

Here P is degree of polarization, P_0 = limit polarization, T = temperature, η = viscosity of the solution, R = universal gas constant, τ = average lifetime of the excited state of molecules, V = their volume. If ordinate represents $1/P$ and abscissa = T/η, then $1/P$ as a function of T/η will be a straight line. Intersection of this line with the ordinate gives us $1/P_0$, and its slope determines the value of $\left(\frac{1}{P_0} - \frac{1}{3}\right)\frac{R\tau}{V}$. The value of τ can be measured with a fluorometer. Then, from the last relationship, one can determine the average molecular volume and study its variation upon increase of concentration.

By this method the gram molecular volumes of two glycerin solutions of 9 - aminoacridine ($c_1 = 1 \times 10^{-5}$ gm/cm^3 and $c_2 = 5 \times 10^{-4}$ gm/cm^3) were determined. It turns out that an increase of concentration in this range approximately doubles the average volume of 9 - aminoacridine molecules. The results are not identical to the true volumes of luminescent molecules since the presence of a solvation envelope complicates the real situation. However, it is important that the volume increases, which is a direct proof of association of the 9 - aminoacridine molecules[7].

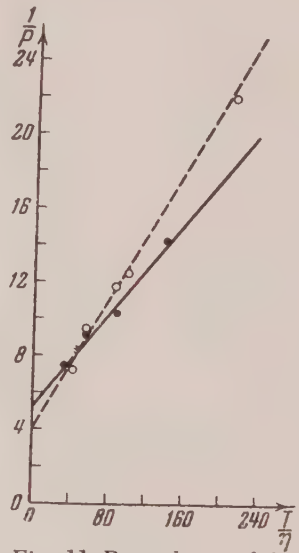

Fig. 11. Dependence of the limiting polarization of 9-aminoacridine in glycerine on the concentration of the solution.
● = 5×10^{-4}, ○ = 1×10^{-5} gm/cm^3.

In Fig. 11 the experimental results are shown. Here one can see that the increase in concentration markedly changes the slope of the straight line and considerably decreases the value of the limit polarization (at $c_1 = 1 \times 10^{-5}$ gm/cm^3, $P_0 = 25\%$; at $c_2 = 5 \times 10^{-4}$ gm/cm^3, $P_0 = 19\%$). The value of the limit polarization of the diluted 9 - aminoacridine solution is close to that obtained by Feofilov[9].

An increase in concentration changes the optical properties of the solution of two-ring acridine compounds significantly. In Fig. 12*a* the dependence of absorption spectra of alcohol solutions of dibromethylate - 9, 9′- biacridyl on the concentration is shown. From Fig. 12 one can see that the shape of absorption spectrum does not change significantly. The absorption power in-

[8] V. L. Levshin, *Photoluminescence in Liquids and Solids*, State Publishing House of the Technical Literature, Moscow - Leningrad, 1951

* An analogous explanation can be suggested for the above described stability of polarization spectrum of 2 - aminoacridine (Fig. 5).

[9] P. P. Feofilov, Izv. Akad. Nauk SSSR, Ser. Fiz. 13, 254 (1949)

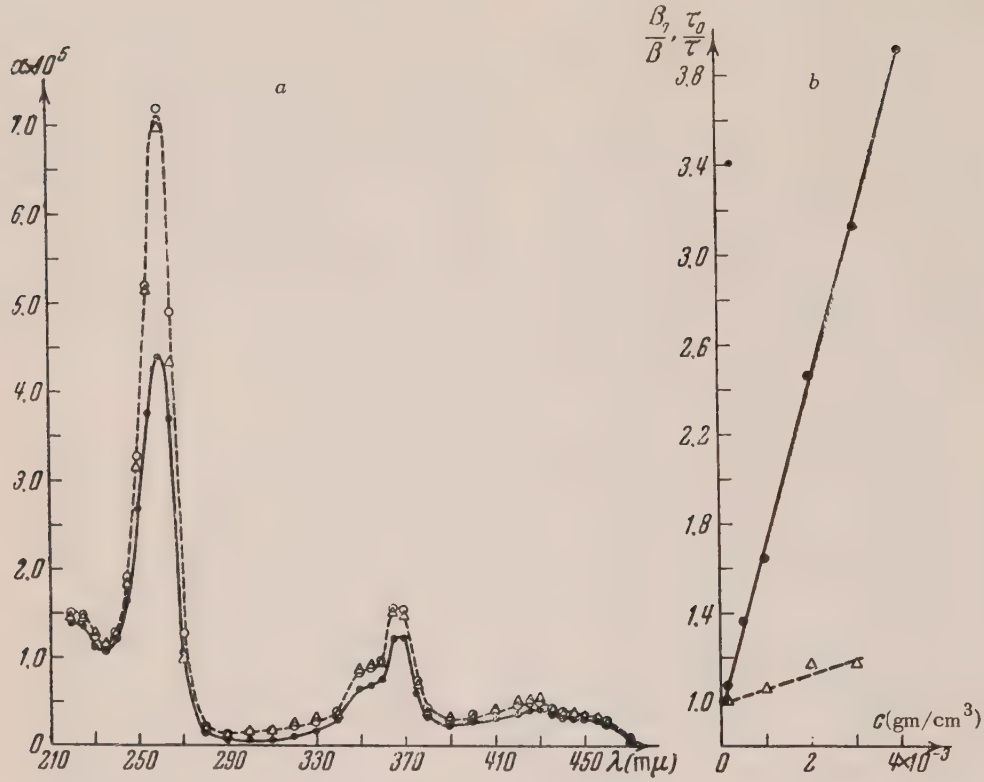

Fig. 12. Ethyl alcohol solution of dibromethylate-9, 9′-biacridyl.
a. dependence of absorption spectrum on concentration,
● = 2×10^{-3}, ○ = 2×10^{-4}, Δ = 2×10^{-5};
b. extinction of luminescence and variation of τ,
● = B_0 / B, Δ = τ_0 / τ.

creases uniformly along the whole absorption spectrum. The increase in concentration causes extremely strong extinction of luminescence, which is accompanied by small change of τ (Fig. 12*b*). Luminescence spectrum remains unchanged. The changes of the absorption spectrum support the assumption that association takes place in this compound also. Moreover, the changes of τ indicate the migration of excitation energy, which apparently is the reason for some fraction of observed extinction of luminescence. However, apparently, the non-luminescent associated molecules that are formed are largely responsible for the development of intensive extinction of luminescence since the changes of τ are small (Fig. 12*b*).

The association of molecules is also probably of chief importance in the case of other two-ring compounds (Fig. 1), since τ for them is completely independent of concentration in investigated range. The majority of acridine compounds have luminescent power in the crystalline state as well as in

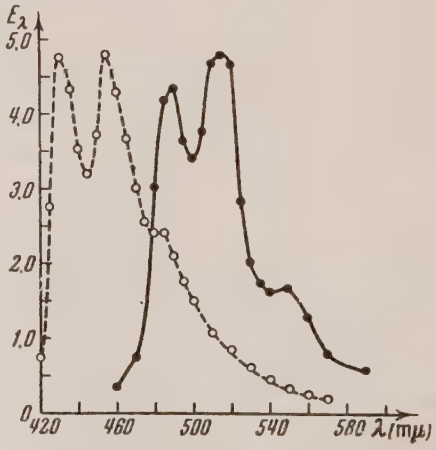

Fig. 13. The comparison of luminescence spectra of ethyl solution of 9-aminoacridine with that of its crystalline state.
● = spectrum of crystals, ○ = spectrum of the solution ($c = 2 \times 10^{-5}$ gm/cm³).

their solutions. Only in case of few materials (2 - aminoacridine, dibromethylate ; 9, 9′- biacridyl) does the transition from a solution to a crystal lead to the disappearance of luminescence.

In this work the luminescence spectra of crystals of many acridine compounds were studied. In Fig. 13 the luminescence spectra of a diluted solution of 9 - aminoacridine and its crystals are shown as an example. The common rule which holds for the majority of acridine compounds, and also for the great majority of other luminescent compounds in crystalline state (see, for instance, reference 10) is the bathochromic shift of luminescence spectra of the crystal with respect to luminescence spectra of the solutions (Fig. 13). The only exception is 1 - aminoacridine, where the reversed phenomenon is observed.

CONCLUSIONS

1. An increase in concentration of the solutions of the acridine compounds (Fig. 1) results in the development of molecular association. It is possible to assume that a joining of many molecules takes place in the shape of a "chain" during the association. This explains the small changes in the shape of the absorption spectra. The 9, 9′- biacridyl molecule can apparently be regarded as an analogue of an associated acridine molecule.

2. Processes of inductive migration of the excitation energy are also important for explanation of the effects of concentration in the solutions of acridine compounds.

3. The associated molecules that are formed through an increase of concentration either lose their luminescence power or have their own emission different from the emission of molecules in monomeric state.

4. The increase of volume of the 9 - aminoacridine molecules in a concentrated solution is a direct proof of their association.

5. For most acridine compounds the transition from the solution to a crystal causes the shift of luminescence spectrum in the long wave direction. This is also a characteristic property of the majority of known luminescent crystals of other compounds.

In conclusion I express deep appreciation to Prof. P. A. Bazhulin for his attention in guidance of this work, to Prof. A. M. Grigorovskii for kindly providing me with chemical supplies and for his consultations, M. D. Galanin for giving me the opportunity to use his fluorometer, N. D. Zhevandrov for great help during measurements of polarization and his advice during discussion of this work.

Translated by G. Filipovich
31

SOVIET PHYSICS - JETP VOLUME 1, NUMBER 2 SEPTEMBER, 1955

The Effect of Concentration on the Optical Properties of Solutions of 3, 6 - Diaminoacridine

L. V. Levshin
Moscow State University

(Submitted to JETP editor March 2, 1954)
J. Exper. Theoret. Phys. USSR 28, 201-212 (February, 1955)

The effect of concentration of 3, 6 - diaminoacridine solution on absorption spectra, luminescence spectra, intensity of glow, average lifetime of excited state and polarization spectra was studied. It was shown that the changes in the optical properties due to increase of concentration of a solution are the result of dimerization of molecules in the solution. Optical properties of dimers were established, and the degrees of association of the solutes at various concentrations were determined. Study of the effect of solvent and temperature on the association of 3, 6 - diaminoacridine molecules were carried out.

An increase in the concentration of solutions of complicated organic compounds usually causes essential changes in the optical properties of the solute. These changes are: depolarization of luminescence, increase of extinction, and decrease in average lifetime of excited state τ of luminescent material. In cases of large increases in concentration one often observes significant changes in absorption spectra and sometimes also in luminescence spectra.

The above-mentioned effects of concentration were known long ago and different hypotheses were offered as explanations. Most of them were abandoned for one reason or another. At present only two basic concepts remain in favor. One of them associates the concentration changes with the inductive transfer of excitation energy from an excited molecule to a non-excited one[1]. Another considers the association of molecules of solute as the main reason for concentration effects[2].

The theory of inductive migration of energy is well developed at present. It has been proved many times experimentally. The theory of molecular association is in fact not yet created. Only some computations were made, which later were confirmed by experiment. It should be mentioned that none of these notions can explain all known experimental facts without making some special assumptions. Hence the theory of inductive migration of excitation energy generally omits consideration and explanation of the significant changes in absorption spectra, and sometimes also in luminescence spectra, which occur in concentrated solutions. On the other hand, starting from the notion of molecular association, one cannot explain, without making some special assumptions, the parallel decrease in emission of light and in τ when the concentration of the solution increases.

The change in optical properties due to the increase in concentration is different for different materials. Some cases can be better explained by migration of energy, others by association. Thus, apparently, both notions are based on correct assumptions, but each of them has its own domain of application. In some cases operation of both mentioned kinds of interaction between the molecules seems to be probable.

In this work the effect of concentration of solution on optical properties of acridine and of nine of its derivatives was studied[3]. The data obtained lead us to the conclusion that the concentration effects of acridine solutions are the results of the association of the molecules of these materials. Formation of associated molecules was explained by some authors as a result of the action of dispersion forces[4]. Association is a reversible process. The molecules return to the monomeric state as a result of dilution of the solution.

The increase of concentration has different effects on solutions of different compounds. Apparently association can occur in different ways depending on the structure of the molecules in question. With respect to the type of effect of concentration on ab-

[1] F. E. Vavilov, *Microstructure of Light*, Publishing House of Academy of Sciences of USSR (1950)

[2] V. L. Levshin, *Photoluminescence of Liquid and Solids*, State Publishing House of Technical Literature Moscow-Leningrad (1952)

[3] V. L. Levshin, Doklady Akad. Nauk SSSR 96, 473 (1954)

[4] E. Rabinowitch and L. Epstein, J. Amer. Chem. Soc. 63, 69 (1941)

sorption spectra the investigated compounds can be grouped in the following manner. To the first group belongs 3, 6 - diaminoacridine. This article is devoted to the effect of concentration on its optical properties. The changes in optical characteristics due to changes in concentration of 3, 6 - diaminoacridine are strong and unique. The data on the effects of concentration on the optical properties of other acridine compounds we have investigated, which belong to the second group, and also considerations concerning the character of their association, will be described in the next article. The measurements were made by photoelectric methods. The absorption spectra were obtained by means of spectrophotometer SF - 4. The luminescence spectra were measured with photoelectric apparatus, arranged on the principle of the monochromator UM - 2 connected to the photoamplifier FEU - 19. The average lifetime of the excited state of the molecules was measured with phase fluorometer designed by Galanin[5]. The polarization spectra were obtained by means of the photoelectric arrangement of N. D. Zhevandrov which was wired according to Spektorov's circuit diagram[6].

1. THE EFFECT OF CONCENTRATION ON THE ABSORPTION SPECTRUM OF 3, 6 - DIAMINOACRIDINE

The absorption spectrum of 3, 6 - diaminoacridine consists of two wide bands, located in the visible and the ultraviolet ranges of the spectrum. Fig. 1 shows the results of measurements on 3, 6 - diaminoacridine solutions in ethyl alcohol*. In the long wave band the increase in concentration causes a sharp decrease of the absorption maximum at $\lambda = 460$ mμ. At the same time a new absorption maximum appears at $\lambda = 405$ mμ. At a concentration of 2×10^{-3} gm/cm^3 the 460 mμ band absorption maximum decreases almost by a factor of three and becomes equal in absolute value to the absorption in the new maximum at 405 mμ. Analogous changes are observed in the ultraviolet absorption band. At a concentration $c = 2 \times 10^{-5}$ gm/cm^3, in addition to the maximum at $\lambda = 260$ mμ, a shoulder absorption (secondary maximum) appears at $\lambda = 285$ mμ. As concentration increases the main absorption maximum becomes lower, and the shoulder absorption increases markedly.

The above-described changes in absorption spectra of 3, 6 - diaminoacridine have previously been found in the long wave absorption bands of some compounds in water solutions. Thus Levshin discovered similar changes in the spectrum of rhodomine 6 G[7,8], and Rabinowitch and Epstein observed them in thionine and methylene blue[4], etc.[9-12]. Significant changes in the absorption spectrum, such as the appearance of new maxima and disappearance of the old ones, can be explained at high concentrations by formation of associated groups of 3, 6 - diaminoacridine molecules having absorption spectra which are different from the spectrum of molecules in the monomer state. Also the absorption spectra of associated molecules consist of two bands which are located closer to each other than the corresponding bands of the monomers.

From the fact that the spectral curves obtained at different concentrations cross at one point ($\lambda = 417$ mμ) one can consider the concentrated solutions as binary mixtures consisting of molecules in monomer and associated conditions[7,1]. From the absorption spectrum of 3, 6 - diaminoacridine one can see that at increased concentration all associated groups of molecules must have a common spectrum. Hence it is natural to consider that in a concentrated solution of 3, 6 - diaminoacridine only monomers and dimers are present. If, however, some groups of higher aggregation are formed, their spectrum must coincide with the absorption spectrum of the dimer. The absorption spectrum of 3, 6 - diaminoacridine changes markedly with increase of concentration, which can be explained by a strong interaction of molecules in the process of dimerization. Assuming that the molecules of 3, 6 - diaminoacridine aggregate in a "pile", the distance between the components of associated molecules in this case will be very small and interaction between them large. A similar conclusion is drawn by the previous workers[4] whose computations for

[5] M. D. Galanin, Doklady Akad. Nauk SSSR 73, 925 (1950)

[6] L. A. Spektorov, Doklady Akad. Nauk SSSR 65, 485 (1949)

* Ordinate shows absorption coefficients. Concentrations are computed in grams per cm^3.

[7] V. L. Levshin, Zh. Fiz. Khim. 6, 1 (1935)

[8] V. L. Levshin and T. M. Tarasova, Izv. Acad. Nauk SSSR, Ser. Fiz. 15, 573 (1951)

[9] V. Söderberg, Ann. Physik. 41, 381 (1913)

[10] B. Van der Plaats, Ann. Physik 47, 424 (1915)

[11] T. P. Kravets, A. L. Peshkina and Z. V. Zhidkova, Izv. Acad. Nauk SSSR, Ser. Fiz. 14, 493 (1950)

[12] V. Zauker, Z. Phys. Chem. 199, 225 (1952)

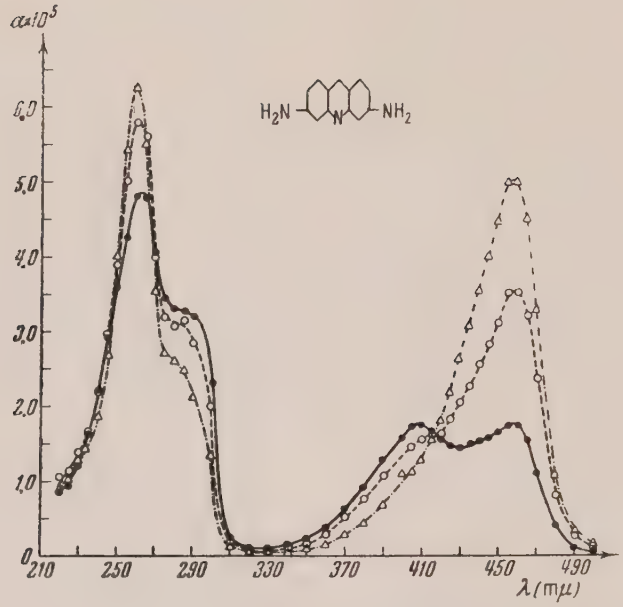

Fig. 1. Dependence of absorption spectrum of 3, 6 - diaminoacridine in ethyl alcohol on concentration of the solution.

● - 2×10^{-3}, ○ - 2×10^{-4}, △ - 2×10^{-5} gm/cm^3.

thionine solutions show that the distance is only 3.12 Å.

The comparison of structural formulas of materials for which changes in absorption spectra similar to that of 3, 6 - diaminoacridine were observed, shows that all of them, in spite of different composition have substituents symmetrically located on both sides of the molecular skeleton. The compound 3, 6 - diaminoacridine has this type of structure (Fig. 1). It is possible that the aggregation of associated molecules may take place by means of these groups.

The determination of areas of absorption spectra of 3, 6 - diaminoacridine shows that with an increase of concentration the absorption ability of the molecules decreases markedly. This decrease takes place because of an absorption drop in long wave band. In the ultraviolet range of the spectrum the increase in concentration causes the redistribution of absorption inside the band only. The total value of absorption in the ultraviolet region remains unchanged.

Physical-chemical properties of the solvent must have a significant effect on the association of molecules of the solute. In this work the effect of concentration on absorption spectra of 3, 6 - diaminoacridine in various solvents was investigated. Identical spectra were observed in both glycerin and ethyl alcohol (Fig. 1), which is natural, since the two solvents are related to each other. However, this shows that the viscosity of a medium has an insignificant effect on the association of 3, 6 - diaminoacridine molecules. In acetone (Fig. 2*a*), even at $c = 5 \times 10^{-6}$ gm/cm^3, most of the 3, 6 - diaminoacridine molecules are in an associated state. At $c = 2 \times 10^{-3}$ gm/cm^3, the process of dimerization is completed, which is expressed by the complete disappearance of a monomeric maximum. In a pyridine solution the most active association of 3, 6 - diaminoacridine molecules takes place. At $c = 2 \times 10^{-5}$ gm/cm^3, practically all the molecules are in an associated state. With a further increase of concentration, the absorption spectrum remains unchanged (Fig. 2*b*). Similar phenomena can be observed in water solutions of hydrochloric 3, 6 - diaminoacridine.

Hence, from experiments with various solvents, one observes that the 3, 6 - diaminoacridine molecules associate most actively in media (such as pyridine, acetone, glycerin, alcohol) which hinder the development of association of dyestuffs. Herewith one cannot relate the association phenomena either to dielectric constant or to dipole moment of the investigated solvent.

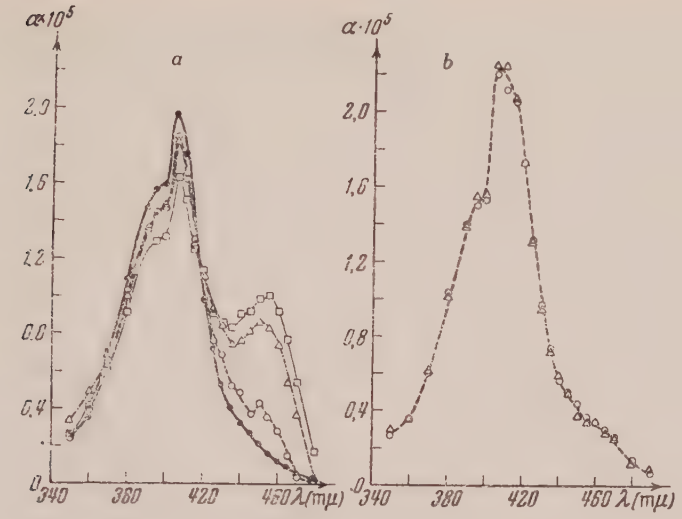

Fig. 2. The effect of solvent on the absorption spectrum of 3, 6 - diaminoacridine, *a* - solution in acetone, *b* - solution in pyridine, ● - 2×10^{-3}, ○ - 2×10^{-4}, △ - 2×10^{-5}, □ - 5×10^{-6} gm/cm^3

To compute a degree of association of solvents with different concentration one can separate the dimer bands from monomeric bands in their absorption spectra. From Fig. 1 ($c = 2 \times 10^{-5}$ gm/cm^3) it follows that the monomeric absorption maximum corresponds to $\lambda = 460$ mμ and the absorption band is more or less symmetrical. Assuming that the long wave band edge is caused purely by a monomeric absorption, one can draw the short wave part of the monomeric band according to it. By subtraction of the monomeric part from the total band, one can determine the absorption which is characteristic for the dimeric state of molecules. This enables one to determine how the absorption strength is distributed between monomers and dimers as the concentration of the solution increases. Performed computation has shown that during a transition from the monomeric state to a dimeric state the absorption strength of the molecules decreases by a factor of approximately 2.3. Knowing this and also the absorption strength of monomers and dimers at different concentrations of the solution, one can calculate the percentage of the monomers and dimers for each of the concentrations investigated. This calculation can also be made by some other methods.

It was mentioned above that, in concentrated acetone or pyridine solutions of 3, 6 - diaminoacridine, the dimeric band appears in its pure form. By comparing these bands with the monomeric band obtained for low concentration solutions in alcohol, one can determine the content of monomers and dimers in alcohol solutions of different concentrations. The result of computations by three methods are shown in Table I*.

It is evident that in spite of the approximations made in the computations all three methods give results which are in good agreement.

As one can see from Fig. 1, the maximum at $\lambda = 285$ mμ in the ultraviolet absorption band does not vanish completely even at considerable dilution of the solution. From this it follows that dimers as well as monomers show absorption in this region. By use of the results shown in Table I, the true absorption bands of molecules in monomeric and dimeric conditions were calculated.

Monomeric bands $\lambda_{max} = 260, 285; 460$ mμ

Dimeric bands $\lambda_{max} = 270, 290; 405$ mμ

Hence the dimers of 3, 6 - diaminoacridine molecules have two absorption bands which are located somewhat closer to each other as compared with the absorption bands of the monomers.

---

* First method - direct analysis of absorption bands of the alcohol solutions.

Second method - analysis by use of the band from acetone solutions.

Third method - analysis by use of the band from pyridine solutions.

TABLE I

Concentration of the alcohol solution of gm/cm^3	First Method		Second Method		Third Method		Average Value	
	Monomers	Dimers	Monomers	Dimers	Monomers	Dimers	Monomers	Dimers
2×10^{-5}	0.88	0.12	0.89	0.11	0.86	0.14	0.88	0.12
2×10^{-4}	0.63	0.37	0.64	0.36	0.59	0.41	0.62	0.38
2×10^{-3}	0.31	0.69	0.32	0.68	0.28	0.72	0.30	0.70

2. THE EFFECT OF CONCENTRATION ON LUMINESCENCE SPECTRA OF 3, 6 - DIAMINOACRIDINE SOLUTIONS

The dimers which are formed due to the increase of concentration can either retain some luminescence intensity[13] or lose it completely.

In the case of 3, 6 - diaminoacridine the dimers retain the luminescence intensity. The luminescence spectra of 3, 6 - diaminoacridine are shown in Fig. 3 *a* and 3 *b* as functions of concentrations of the solutions for two different wavelengths of exciting light. These wavelengths were chosen in such a way that in one case mainly the monomers and in the other case mainly the dimers were excited*.

From the graphs on Fig. 3 one can see that the transition form a dilute solution to a concentrated one results in a small shift of the luminescence spectrum toward longer wavelengths and makes the emission band wider on account of development of the long wave part of the spectra. Decrease in the wavelength of the exciting light also causes some shift of the spectrum toward longer wavelengths and widens the emission band. This is clearly seen in Fig. 3*c* where the dependence of the luminescence spectrum of the concentrated 3, 6 - diaminoacridine solution on the wavelength of exciting light is shown. Thus either an increase in concentration or a change of excitation wavelength in the region of a dimeric maximum yields approximately the same results with respect to the luminescence spectra. The noticeable change in the shape and location of the emission band, which takes place either upon increase in concentration of the solution or upon a decrease of wavelength of the exciting light gives additional confirmation of the association of 3, 6 - diaminoacridine molecules. The changes in luminescence spectra can be explained in the following way: the dimers, formed as concentration increases, have their own luminescence intensity, and their spectrum is shifted somewhat in the long wave direction and differs in shape from the monomeric spectrum. With the increase in concentration, the dimers take a larger and larger part in the emission, which results in the observed change in the luminescence spectrum.

We mentioned above that different absorption bands correspond to monomers and dimers. Decreasing the wavelength of the exciting light and going over from $\lambda_{\text{excitation}} = 436\ \text{m}\mu$ to $\lambda_{\text{excitation}} = 365\ \text{m}\mu$ we change the relative degree of excitation of the monomeric and dimeric fractions of the molecules. In the first case (Fig. 1), mainly the monomers and in the second case mainly the dimers will be excited. Correspondingly, the luminescence spectra will belong either to the monomers or to dimers, or to the mixture of both in certain proportion. By proper choice of the excitation and the concentration of the solution, one can get the monomeric and dimeric spectra in pure form. Thus, in Fig. 3*a* there is shown a monomeric luminescence spectrum ($c = 5 \times 10^{-6}$ gm/cm^3) and in Fig. 3*b*, a dimeric spectrum ($c = 2.2 \times 10^{-3}$ gm/cm^3).

If the above-mentioned line of reasoning is correct, one can represent any of the experimentally obtained spectra by superposition of a monomeric and a dimeric luminescence spectrum taken in the proper proportions. In the Figs. 4*a* and 4*b* is shown a comparison of experimental data with the computed data for two of the luminescence spectra obtained. In the first case one has to assume that 0.7 of the emission is by dimers and only 0.3 by the monomers (Fig. 4*a*): in the second case the dimeric emission is 0.2 and the monomeric emission is 0.8 (Fig. 4*b*). As one can see from the plotted curves, agreement between experiment and computation is

[13] V. L. Levshin, Z. Physik 43, 230 (1927)

* The necessary corrections with respect to secondary absorption were introduced according to the formula suggested in reference 2, page 51. However, because of the small superposition of the absorption spectra and the luminescence spectra of 3, 6 - diaminoacridine, these corrections were small.

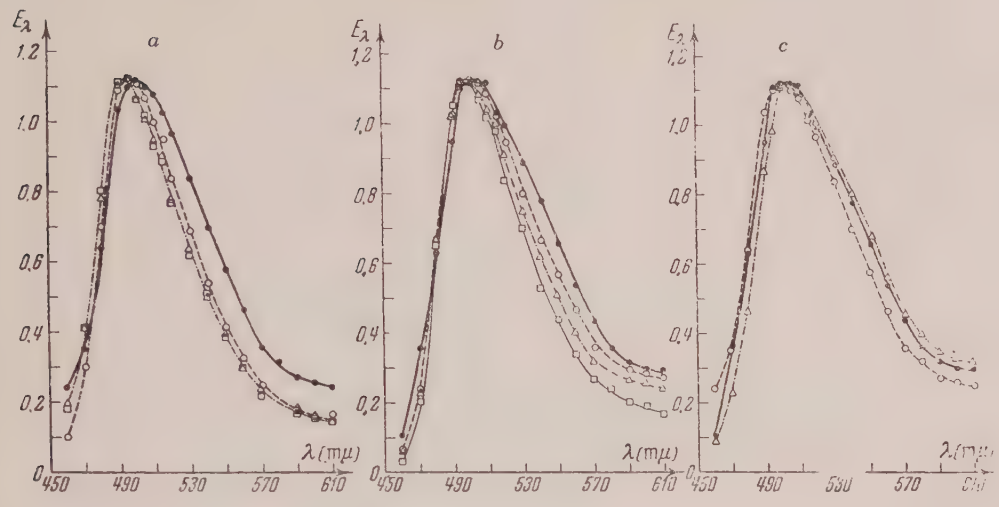

Fig. 3. Dependence of the luminescence spectra of alcohol solutions of 3, 6 - diaminoacridine on concentration and wavelength of exciting light. *a* - $\lambda_{excitation} = 436$ mμ; *b* - $\lambda_{excitation} = 365$ mμ, ● - 2.2×10^{-3}, ○ - 2×10^{-5}, △ - 2×10^{-5}, □ - 5×10^{-6} gm/cm^3, *c* - $c = 2.2 \times 10^{-3}$ gm/cm^3, ○ - $\lambda_{excitation} = 436$, ● - $\lambda_{excitation} = 365$, △ - $\lambda_{exc} = 303 + 313$ mμ

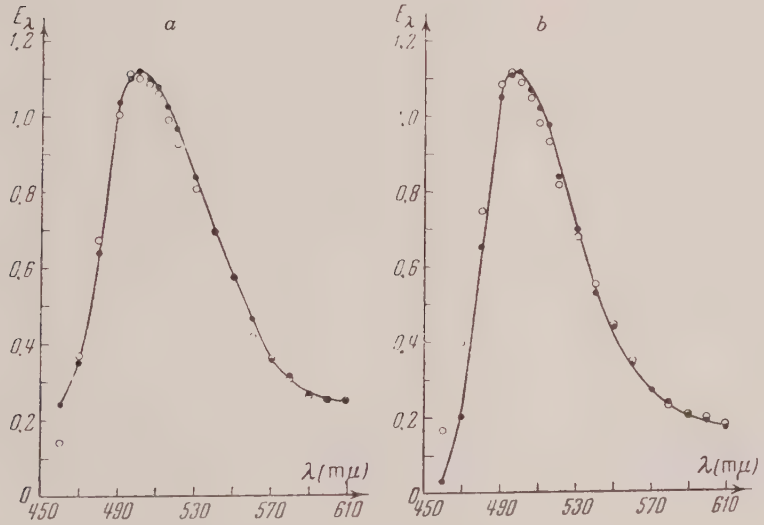

Fig. 4. Comparison of the shape of luminescence spectra for 3, 6 - diaminoacridine, obtained by calculation and by experiment:
a - $\lambda_{excitation} = 436$ mμ, $c = 2.2 \times 10^{-3}$ gm/cm^3;
b - $\lambda_{excitation} = 365$ mμ $c = 5 \times 10^{-6}$ gm/cm^3;
● — experiment; ○ — calculation

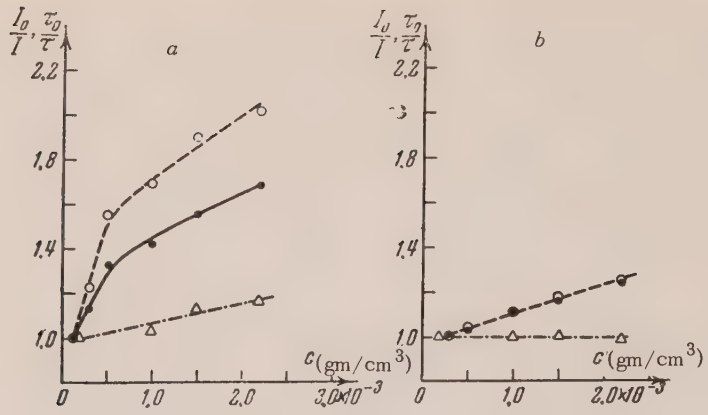

Fig. 5. The change of intensity of luminescence and of τ at increase of concentration of the 3, 6 - diaminoacridine solution in alcohol: *a* - $\lambda_{exc} = 436$ mμ; *b* - $\lambda_{exc} = 365$ mμ; ● I_0/I ($\lambda_{obs} = 530$ mμ), ○ - I_0/I ($\lambda_{obs} = 490$ mμ), △ - τ_0/τ

fairly good.

Marked divergence between the experimental and computed curves in the short wave part of the spectrum (Fig. 4*b*) apparently can be explained by the errors in measurements, which are to be expected at such small concentrations and (correspondingly) very low intensity of luminescence.

3. EXTINCTION OF LUMINESCENCE DUE TO CHANGE IN CONCENTRATION AND VARIATION OF τ

The increase in concentration results in extinction of luminescence and in variation of the average lifetime of the excited state of the 3, 6 - diaminoacridine molecules. The experiments have shown that the process of extinction depends on the wavelength of the exciting light and on the wavelength of the emission. In Fig. 5 the curves which describe the change of luminescence intensity due to increase of concentration of the solution are shown.

Strong extinction is observed at $\lambda_{excitation} = 436$ mμ (Fig. 5). In this connection its observed behavior is different in regions of $\lambda_{observation} = 490$ and 530 mμ. The extinction is markedly weaker at $\lambda_{excitation} = 365$ mμ. In this case the extinction curve is linear, and its concentration dependence is the same for both of the observation wavelengths chosen (Fig. 5*b*).

The changes of τ due to changes in concentration also depend on the wavelength of the exciting light. At the $\lambda_{excitation} = 436$ mμ, τ markedly decreases as the concentration increases (Fig. 5*a*). As we go over to $\lambda_{exc} = 365$ mμ, τ remains unchanged in the entire interval of concentrations investigated (Fig. 5*b*).

The above-described extinction due to change in concentration and variation of τ can be explained with the help of the notion of dimerization of the molecules of 3, 6 - diaminoacridine. In the case of excitation of luminescence by the mercury line 436 mμ (Fig. 5*a*), the majority of the excited molecules are monomers. With increase of concentration the intensity of luminescence of the monomers becomes weaker, partly because of extinction due to change in concentration and partly because of the transition of the molecules from the monomeric state to a dimeric one. Although the dimers also have luminescence intensity, the chosen excitation conditions are not favorable for the appearance of their luminescence. For this reason only a small fraction of the dimers will take part in emission. The majority of them will not become excited, thus contributing to the extinction. The difference in the shape of the extinction curves resulting from observation of luminescence at different wavelengths is explained by the fact that $\lambda_{obs} = 490$ mμ lies in the region of the monomeric maximum and $\lambda_{obs} = 530$ mμ is located closer to the dimeric maximum. In the first case the extinction curve represents mainly the decrease in luminescence of the monomeric part of the molecules, while in the second case the participation of the monomer in the emission decreases and the extinction is less in-

tense. Upon excitation of luminescence by the line 365 mμ (Fig. 5*b*) the participation of the monomer in the emission is not large. Therefore the drop in intensity of luminescence with increase in concentration does not depend on the choice of the wavelength of observation.

There was mentioned above the difference in variation of τ due to concentration upon excitation of luminescence by mercury lines 436 and 365 mμ. On that basis, apparently, one can consider that with increase in concentration, the τ of the monomers decreases, and the τ of the dimers remains unchanged. The absolute values for τ of the monomers and dimers obtained at low concentrations of the solution at which the extinction does not occur are similar within the limits of the errors of the experiment ($\tau_{\text{monomers}} = \tau_{\text{dimers}} \approx 5.3 \times 10^{-9}$ sec).

Since τ of the monomers decreases upon increase in concentration, the extinction of the monomers, apparently, must be ascribed to migration of the excitation energy from an excited monomer to the neighboring non-excited monomers. Migration of energy from a monomer to a dimer is improbable, since the luminescence spectrum of the monomers practically never superimposes on the absorption spectrum of the dimers.

A weak extinction, which one observes when excitation of the dimeric fraction of the molecules prevails (Fig. 5*b*), cannot be explained by migration of energy from the excited dimers to the non-excited dimers or to the monomers. Indeed, one cannot expect a transfer of energy from one dimer to another dimer, since their luminescence and absorption spectra never superimpose. The transfer of energy from a dimer to a monomer is also improbable since τ remains unchanged upon increase of concentration. Most likely this weak extinction can be explained by the smaller emission of dimers compared to the emission of monomers.

4. THE EFFECT OF CONCENTRATION ON THE POLARIZATION SPECTRA OF 3, 6 - DIAMINOACRIDINE SOLUTIONS

Dimerization of 3, 6 - diaminoacridine molecules, which causes considerable changes in the absorption spectrum, can affect the mutual arrangement of the absorbing oscillators of these molecules. These changes can be detected by changes in the polarization spectrum of 3, 6 - diaminoacridine upon increase of concentration of the solution*.

On Fig. 6 are shown the results of the measurements. From this Figure it follows that the 3, 6 - diaminoacridine molecules have positive polarization throughout the entire polarization spectrum. The increase in concentration markedly decreases the polarization maximum and leaves the polarization almost unchanged between the maximums. At $c = 1 \times 10^{-3}$ gm/cm^3 the polarization spectrum degenerates into an almost straight line.

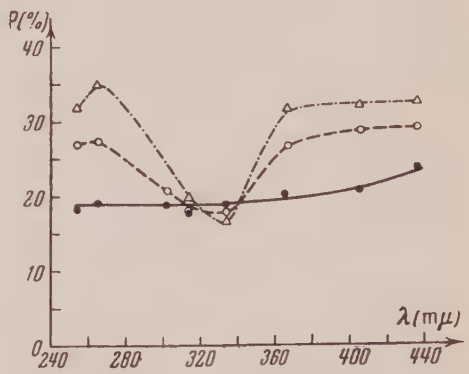

Fig. 6. The dependence of the polarization spectrum of 3, 6 - diaminoacridine in glycerin on concentration of the solution.
●-1×10^{-3}; ○ - 2×10^{-4}; △ - 2×10^{-5} gm/cm^3.

Significant changes of the polarization spectrum cannot be explained by depolarization due to change in concentration alone, since this depolarization only results in the decrease in absolute value of the degree of polarization throughout the spectrum[14].

The changes indicate the formation of new bonds between molecules. Therefore it is their aggregation which yields the changes in mutual arrangement of the absorbing oscillators.

Apparently the curve for $c = 2 \times 10^{-5}$ gm/cm^3 characterizes the polarization spectrum of the monomers and the curve $c = 1 \times 10^{-3}$ gm/cm^3 characterizes the polarization spectrum of the dimers. It is probable that upon increase of concen-

---

[14] P. P. Feofilov, Izv. Akad. Nauk SSSR, Ser. Fiz. 9, 317 (1945)

* The superposition of the absorption and luminescence spectrum of 3, 6 - diaminoacridine was small. Because of this, the effect of reabsorption on the degree of polarization was insignificant.

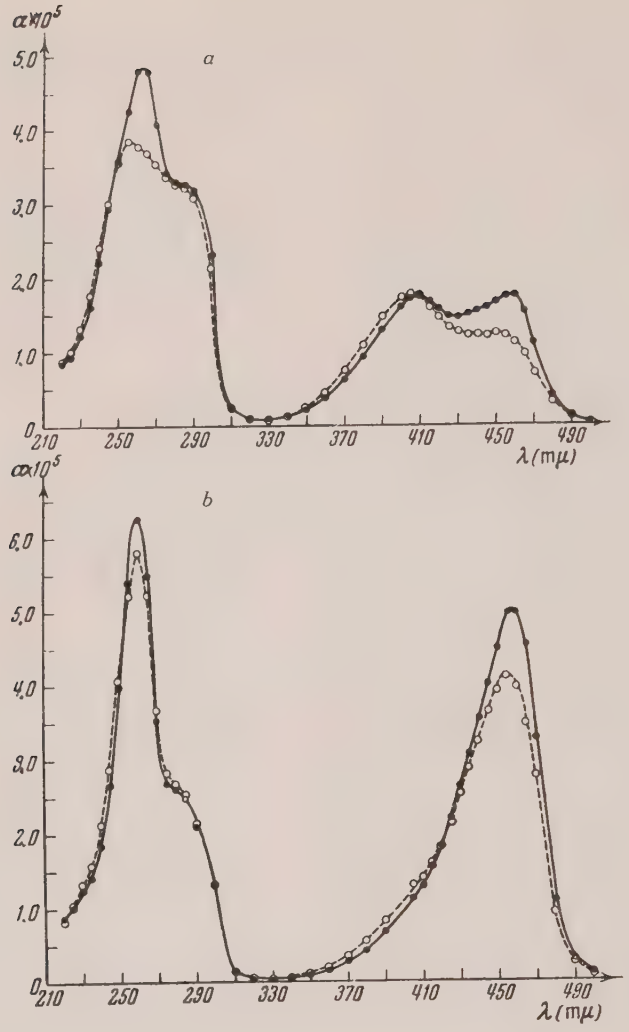

Fig. 7. Temperature dependence of the absorption spectra of 3, 6 - diaminoacridine:
a - $c = 2 \times 10^{-3}$ gm/cm^3; *b* - $c = 2 \times 10^{-5}$ gm/cm^3;
● — 20°C, ○ — 73°C

tration in regions of spectral maxima, the depolarization due to change of concentration, as well as the process of passing over to the polarization spectrum of the dimers, are acting in the same direction. This results in the decrease of degree of polarization. In the region between the maxima, these two processes are acting in opposite directions, which results in the approximate stability of the degree of polarization in this part of the spectrum.

5. THE EFFECT OF THE TEMPERATURE ON THE ABSORPTIVE POWER OF THE MOLECULES OF 3, 6 - DIAMINOACRIDINE

Absorption and emission spectra as a rule depend strongly on temperature[15]. Upon increase of temperature the absorption spectrum of the concentrated solution of a dye usually changes in the direction of the restoration of the spectrum of the diluted solution[4,12]. A different picture is observed in the case of 3, 6 - diaminoacridine. In Fig. 7*a* is shown the dependence of the absorption spectrum of the concentrated solution of 3, 6 - diaminoacridine upon temperature. From this Figure one can see that in this case the warming from 20°C to 73° C does not restore the original form of the spectrum (Fig. 1). On the

[15] T. M. Tarasova, J. Exper. Theoret. Phys. USSR 21, 189 (1951)

contrary, the long wave absorption maximum markedly decreases, while there is almost complete stability in the shortwave maximum. The warming also results in the decrease in absorption in the ultraviolet band. It is particularly noticeable in the region of the monomeric maximum. The warming of the diluted solution ($c = 2 \times 10^{-5}$ gm/cm^3) also results in some decrease of both absorption bands (Fig. 7*b*). Thus a decrease of the long wave maximum of a concentrated solution can be explained by considering the experimentally observed decrease in absorption power of the monomers upon increase of temperature.

The degree of association of 3, 6 - diaminoacridine solutions at various concentrations (at room temperature) was established above, and monomeric and dimeric absorption bands were obtained. Similarly, analysis of the bands observed for a heated solution resulted in the separation of the absorption due to the monomers from that of the dimers. Computation showed that the increase in temperature results in some decrease of absorption power of the dimers as well as of the monomers. Decrease of dimeric absorption can take place on account of decreasing number of dimers, due to their destruction. However, possible destruction of dimers is small and proceeds much more slowly than in the case of dye solutions. Analogous results are obtained from experiments with glycerin solutions of 3, 6 - diaminoacridine upon warming to 97° C.

It should be mentioned that even in the case of dyes a complete restoration of the absorption spectrum (of the dilute solution) was not achieved by warming the concentrated solutions[7]. The unusual stability of 3, 6 - diaminoacridine dimers is probably explained by the fact that for their formation the coupling monomers must be given some energy. In this case the increase in temperature will not only cause the dissociation of dimers but also simultaneously will increase the probability of coupling of monomers into dimers. Since the absorption spectrum does not change much upon the increase of temperature, one can assume that these two processes counterbalance each other. The necessity of an activation energy for the dimerization of molecules has been brought out by other authors[4].

The effect of temperature on the association is very important; therefore the further experiments carried out in a wider range of temperatures are very interesting.

6. CONCLUSIONS

1. An increase in concentration of 3, 6 - diaminoacridine solution results in significant changes in the absorption spectrum, which can be explained by formation of dimers of molecules of this compound with a different absorption spectrum than the monomers.

2. Association of 3, 6 - diaminoacridine molecules proceeds differently in different solutions. It is most extreme in pyridine, acetone, alcohol, glycerin. These are media which usually counteract association in dye solutions. In addition the association can be related neither to viscosity, nor to dielectric constant, nor to the value of the dipole moment of the solvent.

3. The dimers are luminescent. Their spectrum differs somewhat in shape from the spectrum of monomers. It is also shifted in the long wave direction, as compared to the monomeric spectrum.

4. The extinction due to change in concentration is considerable. It can be explained by migration of excitation energy from an excited monomer to a non-excited one. The observed weak extinction when excitation of dimers prevails is explained by the smaller yield of luminescence of dimers as compared to the luminescence yield of monomers.

5. The average life time of the excited state of the monomer decreases upon increase of concentration. At the same time τ of the dimers remains insensitive to changes of concentration. At low concentrations, at which extinction does not yet occur, τ of monomers and dimers are equal within the limits of the error of the experiment.

6. The increase in concentration results in substantial changes in the form of the polarization spectrum, which indicates the aggregation of 3, 6 - diaminoacridine molecules, and with this a resulting change in the mutual orientation of absorbing dipoles.

7. The 3, 6 - diaminoacridine dimers are stable with respect to increase of temperature and apparently require a certain activation energy for their formation.

In conclusion I express deep appreciation to Prof. P. A. Bazhulin for his attention in guidance of this work, to Prof. A. M. Grigorovskii for kindly providing me with chemical supplies and for his consultations, M. D. Galanin for giving me the opportunity to use his fluorometer, N. D. Zhevandrov for great help during measurements of polarization and his advice during discussion of this work.

Translated by G. Filipovich
30

The Entropy of Systems with a Random Number of Particles

R. L. STRATONOVICH
Moscow State University

(Submitted to JETP editor January 19, 1954)
J. Exper. Theoret. Phys. USSR **28**, 409-421 (April, 1955)

The amount of entropy in a volume which contains a random number of particles is found on the basis of entropy and indeterminacy considerations.

THE entropy of a system consisting of a fixed number of particles N (neglecting internal degrees of freedom) is defined by the well-known formula*

$$S = -\int p_N \ln p_N d\Omega + \text{const}, \qquad (1)$$

where p_N is the probability density for a point representing the state of the system in the $6N$-dimensional phase space Ω, However, to the best of my knowledge, the problem of finding the entropy in a volume V which is a part of the whole space accessible to the particles has not yet been solved. A formula like (1) cannot be applied in this case, since the number n of particles in the volume V is itself indeterminate (random). If we set n equal to its mathematical expectation $\overline{n}$ we can evaluate an entropy S_V' in the volume V by a formula analogous to (1). However, S_V' will not be the entropy of the original system, but the entropy of the volume V for some other system, namely a system in which the volume V is surrounded by an impenetrable barrier. To determine correctly the entropy in a volume V of the original system, we need a new formulation, suggested by regarding the entropy as a random quantity.

The subject of the present paper can be approached in another way. The use of a probability density in a $6N$-dimensional space is justified by a consideration of states in thermodynamic equilibrium, because then p_N can be expressed directly by Gibbs' formula. The use of p_N for non-equilibrium states appears purely formal, in view of the impossibility of expressing analytically how p_N changes with time. The solution of a differential equation with a number of independent variables of the order of Avogadro's number is obviously not feasible. To be in a position to carry out calculations (which are perharps tedious, but possible) of non-equilibrium processes, we must return to a consideration of distribution functions. The latter are used, in particular, by Bogoliubov[1]. It is most convenient to deal with distribution functions which characterize local statistical properties as, for example, the functions defined in reference 2. Instead of distribution functions, we can also use a system of correlation functions, which, in their turn, adequately describe the statistical system. The latter functions have the following advantages over distribution functions: In the absence of correlation between the particles, the distribution function becomes a product of lower order distribution functions. In this case the correlation functions become zero. In ordinary physical systems the correlation function is different from zero only when its arguments are sufficiently near one another. The lower order distribution functions and correlation functions are the most important. If a certain accuracy is specified, we can neglect higher order correlations beginning with an order k, depending on the accuracy desired. However, neglecting higher correlations means that the higher order distribution functions factor into products of lower order distribution functions, since the higher the order correlations are set equal to zero. Of course, this considerably simplifies the problem. In the light of what has just been said, there is much more basis for terminating a series made up of correlation functions than of distribution functions. One might say that the transition from distribution functions to correlation functions makes the series converge more rapidly.

Thus, in treating non-equilibrium states it is expedient to consider correlation functions (instead of p_N) and to find out how they change with time. Inasmuch as they completely describe the physical system, we can calculate, in terms of them, all the physical parameters of the system which interest us (density, fluctuations, energy, pressure, entropy, etc.). Accordingly, in view of the application in statistical physics (of non-equilibrium processes)

* We shall write the entropy in dimensionless units, omitting Boltzmann's constant.

[1] N. N. Bogoliubov, *Problems of Dynamical Theory in Statistical Physics*, Moscow, 1946

[2] P. I. Kuznetsov, R. L. Stratonovich, and V. I. Tikhonov, Zh. Tekh. Fiz. **24**, 103 (1954)

of a new apparatus, viz. distribution functions and correlation functions, the question arises of how to express the entropy in terms of these functions. This question will be investigated in this paper.

Following Shannon[3] we shall understand entropy to be a measure of the indeterminacy ("neginformation") contained in the given physical process, or, in other words, an index of the amount of its statistical disorder.

We define the entropy of a finite complete set of mutually exclusive events $A_1, \ldots, A_n$ by the formula

$$S = -\sum_{i=1}^{n} P(A_i) \ln \frac{P(A_i)}{Q(A_i)}, \tag{2a}$$

where $P(A_i)$ is the probability of the event A_i and $Q(A_i)$ is its "volume".

The introduction of the "volumes" of events allows us to regard the entropy as a characteristic of an object which can be given a probabilistic description, i.e., as a characteristic of a statistical aggregate. For according to the usual formula

$$S = -\sum_{i=1}^{n} P(A_i) \ln P(A_i)$$

(see reference 3), the entropy depends on which set of mutually exclusive events is chosen, and changes if another complete set of mutually exclusive events is used, even though the object itself and its statistical characteristics have not changed.

The size of the "volumes" of events is derived from the nature of the physical object considered. For example, if a true die is being considered, then the volume of the event consisting of the even throws is three times as large as the volume consisting of a throw of the number one. The reader will become acquainted with another example below, which is not so trivial.

In the general case, including continuous distributions, the entropy is defined by the formula

$$S = -\lim_{Q(A_i)\to \min} \sum_i P(A_i) \ln \frac{P(A_i)}{Q(A_i)}. \tag{2}$$

Here the summation is over mutually exclusive events, the sum of which is an event which is certain to occur; the passage to the limit corresponds to the maximally fine subdivision of events.

If we apply Eq. (2) to a system of particles, the state of which is represented by the random point M in the phase space Ω, we have

$$S = -\int p_N(M) \ln \frac{p_N(M)}{q_N(M)} d\Omega_M. \tag{3}$$

Here ρ_N is the probability density function for the point M in Ω, q_N is the density of "volume" in the space Ω. Consequently, recalling the third law of thermodynamics and the indeterminacy principle of quantum mechanics, we can conclude (as shown in other work) that in a space of canonically conjugate variables

$$S = -\int p_N \ln (h^{3N} p_N)\, d\Omega. \tag{4}$$

In the same way, the additive constant in Eq. (1) is determined by Planck's constant.

We shall be interested in how the entropy changes if the number N is increased or decreased without changing the local statistical structure (i.e., with a proportional change in the volume V). For these considerations it is expedient to decompose the entropy (neginformation) into two components, configuration neginformation and exchange neginformation.

$$S = S_c + S_e \tag{5}$$

The exchange neginformation S_e corresponds to the indeterminacy entering the result because of the possibility of exchange between particles at all sets of N points at which particles may be located. Which distribution of the particles on the points (of the $N!$ possible permutations) is actually realized is indeterminate. To each distribution we must ascribe a unique probability and a unique "volume". The probability of each distribution is $1/N!$. Designating the "volume" of each distribution by Q_1, we have, according to Eq. (2),

$$S_e = \ln N! + \ln Q_1.$$

The exchange neginformation must vanish when there is only one particle. From this condition we find

$$Q_1 = 1,$$

whence

$$S_e = \ln N! \tag{6}$$

Corresponding to this fact, the configuration entropy is

$$S_c = -\int p_N \ln (N!\, h^{3N} p_N)\, d\Omega. \tag{7}$$

Let us consider the so-called Gibbs' paradox, consisting in the fact that if we divide a volume (albeit hypothetically) into several parts, the sum of the entropies of the separate volumes does not equal the entropy of the original volume. For example, if we divide the volume V_1 into two volumes $V_2 = V_1/2$, the entropy of the original volume exceeds the sum of the entropies of the

[3] *The Theory of Transmission of Electrical Signals in the Presence of Noise*, collection of translations under the editorship of N. A. Zheleznoff, Moscow, 1953

subvolumes by $N_1 \ln 2$, i.e.,

$$S(V_1) - 2S(V_2) = (R/k)\, n_1 \ln 2, \qquad (8)$$

where n_1 is the number of gram-molecules of matter in the volume V_1 ; $N_1 = (R/k)\, n_1$ is the number of molecules in the same volume.

The solution of this paradox is easily achieved, if we bear in mind that the entropy occurring in Eq. (8) is the sum of an exchange entropy and a configuration entropy. Indeed, using Eq. (6) and applying Stirling's formula, we have

$$S_e(V_1) = \ln N_1! \approx N_1(\ln N_1 - 1);$$
$$S_e(V_2) = \ln \left(\frac{N_1}{2}\right)! \approx \frac{N_1}{2}\left(\ln \frac{N_1}{2} - 1\right),$$

whence

$$S_e(V_1) - 2S_e(V_2) \approx N_1 \ln 2.$$

Consequently, for the configuration entropy, which describes the statistical structure without individualizing the particles, the Gibbs' paradox does not take place, and

$$S_c(V_1) \approx 2S_c(V_2).$$

According to the quantum mechanical principles the indistinguishability of particles it is impossible to acquire knowledge of the individuality of the particles occupying the given positions (states). Therefore the indeterminacy of the distribution of the particles in different states is actually not a real indeterminacy. The real indeterminacy is the indeterminacy in the position (state) of the non-individualized particles, i.e, the configuration neginformation.

Thus the principle of indistinguishability of particles requires us to restrict our attention to configuration neginformation, which removes Gibbs' paradox. In what follows we shall consider only configuration entropy, but omitting for simplicity the index c. The configuration entropy is in its turn not completely additive, but this non-additivity, which enters because of statistical correlation, is of a completely different nature from the non-additivity of exchange entropy.

Let us return to Eq. (7). We designate by B the event consisting of the Nth particle occupying the element $d\omega_1$ of the six-dimensional canonical variable space, located near the point L_1, at the same time that the second particle lies in the element $d\omega_2$, the third in $d\omega_3$, etc. The probability of the event B is

$$dP_N = p_N(L_1, \ldots, L_N)\, d\omega_1 \ldots d\omega_N. \qquad (9)$$

Since Eqs. (2), (3) have universal validity, the event B has a configuration "volume" equal to

$$dQ_N = q_c d\omega_1 \ldots d\omega_N. \qquad (10)$$

Here, as follows from a comparison of Eqs. (3) and (7)

$$q_c = \frac{1}{N!} h^{-3N} \qquad (11)$$

is the density of configuration "volume".

Summing elementary events of the indicated type, we can calculate the configuration "volume" of the event consisting of just N particles lying in the region W of the space ω. It equals**

$$Q_W(N) = \int_W \ldots \int_W q_c d\omega_1 \ldots d\omega_N = \frac{1}{N!}\left(\frac{W}{h^3}\right)^N \qquad (12)$$

We note that the "volume" of the event consisting of any number of particles lying in the region W is given by the equation

$$Q_W = \sum_{N=0}^{\infty} Q_W(N) = \exp\{W/h^3\}, \qquad (13)$$

whence it follows that when the geometric volumes are added, the abstract "volumes" of the corresponding events are multiplied.

Let us pass from p_N to a consideration of the functions $e_N(L_1, \ldots, L_N)$ $(N = 1,2,\ldots)$, which determine the probability

$$dP_N = e_N(L_1, \ldots, L_N)\, d\omega_1, \ldots, d\omega_N \qquad (14)$$

of the event (we designate it by C) consisting of any arbitrary particle lying in the element $d\omega_1$, while at the same time any other particle lies in the element $d\omega_2$, etc., given that, in all, just N particles lie in W. It is easy to convince oneself that the indicated functions can be expressed in terms of the functions appearing in Eq. (9) in the following way:

$$e_N(L_1, \ldots, L_N) = \sum p_N(L_{\alpha_1}, \ldots, L_{\alpha_N}), \qquad (15)$$

where the summation is over all possible $(N!)$ permutations of the arguments of the function p_N. When p_N is symmetric, Eq. (15) becomes

$$e_N = N!\, p_N. \qquad (15a)$$

In an analogous fashion we find that the "volume" of the event C is

$$dQ_N = h^{-3N}\, d\omega_1, \ldots, d\omega_N. \qquad (16)$$

Let us examine how we must sum events of the type C in order to obtain the event A_N, consisting of just N particles lying in W. If we index the particles by the magnitude of any coordinate x (of the six coordinates designated by L), then to obtain

** The volume of a region is designated by the same letter as the region.

the event A_N, we must sum events of the type C, subject to the condition $x_1 \leqslant x_2 \leqslant \ldots \leqslant x_N$ (in order to avoid duplication of elementary events). Accordingly

$$P_W(N) = \int_{x_1 \leqslant \ldots \leqslant x_N} \ldots \int e_N(L_1, \ldots, L_N)\, d\omega_1 \ldots d\omega_N.$$

If we remove the ordering in the coordinate x, then, because of the symmetry of the function e_N, we obtain a quantity $N!$ larger. From this it follows that

$$P_W(N) = \frac{1}{N!} \int_W \ldots \int_W e_N(L_1, \ldots, L_N)\, d\omega_1 \ldots d\omega_N, \quad (17)$$

The equations we have written are valid in the general case when the number of particles in the volume W is random. The events A_N can be represented as a sum of events of the type B or of the type C. In both cases we finally get unique meanings for the probability $P_W(N)$, the "volume" $Q_W(N)$, and the entropy.

According to Eq. (2), to go from the preliminary formula for the entropy

$$S_W = -\sum_N P_W(N) \ln \frac{P_W(N)}{Q_W(N)}$$

to the exact formula, we must pass to the limit in the elementary events (of type B or type C), i.e.,

$$S_W = -\sum_N \int dP_N \ln \frac{dP_N}{dQ_N}.$$

Substituting Eqs. (9), (10), (11) or (14), (16), we obtain

$$S_W = -\sum_{N=0}^{\infty} \int_W \ldots \int_W p_N \times \ln (N! h^{3N} p_N)\, d\omega_1 \ldots d\omega_N \quad (18)$$

or

$$S_W = -\sum_{N=0}^{\infty} \frac{1}{N!} \int_W \ldots \int_W e_N \times \ln (h^{3N} e_N)\, d\omega_1 \ldots d\omega_N. \quad (18')$$

The expression just obtained reduces to Eq. (7) when the number N is determinate. In this case only one function p_N or e_N is different from zero.

One is usually interested in the entropy included in a definite region (with volume V) of three-dimensional configuration space (which we designate by ω^*) with coordinates q_1, q_2, q_3. Corresponding to this, the region W will have a projection V on the space ω^* and will extend to infinity in momentum space:

$$-\infty < p_1,\ p_2,\ p_3 < \infty.$$

Let us consider the special case in which the distribution in momenta is statistically independent of the distribution in coordinates, so that

$$e_N = e_N^*(q_1^1, \ldots, q_3^N)\, \varphi(p_1^1, p_2^1, p_3^1) \ldots \varphi(p_1^N, p_2^N, p_3^N), \quad (19)$$

where $\phi(p_1, p_2, p_3)$ is the momentum distribution function for one particle; e_N^* is a function having the same meaning as e_N, only pertaining to the three-dimensional space ω^*. So that there may be a complete identity of formulas for the two functions, in particular, so that the probability that just N particles lie in V may be given by the equation

$$P_V^*(N) = \frac{1}{N!} \int_V \ldots \int_V e_N^* d\omega_1^* \ldots d\omega_N^*, = P_W(N), \quad (20)$$

analogous to Eq. (17), we must normalize $\phi(p_1, \ldots, p_3)$ to unity.

Substituting Eq. (19) in Eq. (18), and using Eq. (20) and the normalization condition, we obtain

$$S_W = S_q + \bar{N} S_1, \quad (21)$$

where $\bar{N}$ is the mean value of the number N;

$$S_1 = \iiint \varphi(p_1, p_2, p_3) \times \ln [h^3 \varphi(p_1, p_2, p_3)]\, dp_1\, dp_2\, dp_3, \quad (22)$$

$$S_q = -\sum_{N=0}^{\infty} \frac{1}{N!} \int_V \ldots \int_V e_N^* \ln e_N^*\, d\omega_1^* \ldots d\omega_N^*. \quad (23)$$

The expression (23) has the same appearance as Eq. (18) (if we disregard an additive constant). We proceed to investigate it, omitting for simplicity the asterisk, and noting that analogous calculations can be carried out immediately for Eq. (18).

The functions e_N are not local characteristics of the particle distribution, since they depend on the choice of the volume V. However, they can be expressed in terms of distribution functions or correlation functions, which express just such local statistical properties. Each distribution function $f_N(M_1, \ldots, M_N)$ (M is a point in the space ω) is defined analogously to Eq. (14) with only this difference, that the condition that just N particles lie in V is abandoned. Following methods applied in reference 2, we can obtain

$$e_N(M_1, \ldots, M_N) = \sum_{s=0}^{\infty} \frac{(-1)^s}{s!} \int_V \ldots \int_V f_{N+s} \times (M_1, \ldots, M_{N+s})\, d\omega_{N+1} \ldots d\omega_{N+s}. \quad (24)$$

Thus, knowing the distribution functions, which completely describe the statistics of the system of particles, we can calculate from Eqs. (23), (24) the entropy of any region V. As was shown in the introduction, instead of distribution functions it is more convenient to consider correlation functions g_N ($N = 1,2,..$), defined by the equations

$$\sum_{n=0}^{\infty} \frac{1}{n!} \sum_{\alpha_i} f_n(M_{\alpha_1}, \ldots, M_{\alpha_n}) z_{\alpha_1} \ldots z_{\alpha_n} \quad (25)$$

$$= \exp\left\{\sum_{n=1}^{\infty} \frac{1}{n!} \sum_{\alpha_i} g_n(M_{\alpha_1}, \ldots, M_{\alpha_n}) z_{\alpha_1} \ldots z_{\alpha_n}\right\},$$

where z_α are arbitrary numbers; $f_0 = 1$. From this, assigning the proper values to z_α, we can obtain

$$\sum_{k=0}^{\infty} \frac{1}{k!} \sum_{\alpha_i} e_k(M_{\alpha_1}, \ldots, M_{\alpha_k}) z_{\alpha_1} \ldots z_{\alpha_k} \quad (26)$$

$$= \exp\left\{\sum_{k=0}^{\infty} \frac{1}{k!} \sum_{\alpha_i} h_k(M_{\alpha_1}, \ldots, M_{\alpha_k}) z_{\alpha_1} \ldots z_{\alpha_k}\right\}.$$

Here

$$h_k(M_1, \ldots, M_k) = \sum_{s=0}^{\infty} \frac{(-1)^s}{s!} \quad (27)$$

$$\times \int_V \ldots \int_V g_{k+s}(M_1, \ldots, M_{k+s})\, d\omega_{k+1} \ldots d\omega_{k+s};$$

the $e_k(M_1, \ldots, M_k)$ are expressed by Eq. (24).

Equation (26) differs in form from (25) only by the presence of the term h_0 in the exponent. Therefore, setting

$$e_k = e_k^0 e^{h_0}, \quad (28)$$

we obtain for the functions e_k^0 and h_k an equation completely analogous to Eq. (25). Such an equation (which is encountered also in the theory of random functions and relates the moment functions with the correlations) always gives the unique relations:

$$e_1^0(M_1) = h_1(M_1);$$

$$e_2^0(M_1, M_2) = h_2(M_1, M_2) + h_1(M_1) h_1(M_2);$$

$$\ldots\ldots\ldots\ldots\ldots\ldots\ldots\ldots\ldots\ldots:$$

$$e_k^0(M_1, \ldots, M_k) \quad (29)$$

$$= \sum_{n_1+2n_2+\ldots=k} \underset{\left(\frac{k!}{n_1!\, n_2!\, (2!)^{n_2}\ldots}\right)}{\mathrm{S}} h_1^{(n_1)} h_2^{(n_2)} \ldots,$$

where

$$h_i^{(n)} = \overbrace{h_i h_i \ldots h_i}^{n \text{ times}}.$$

By the symbol S is meant summation over all possible permutations of the arguments (M) of the functions h_i, which do not give identical results The number of such permutations is indicated below in brackets. (To calculate them it is necessary to consider the symmetry of the functions h_i).

If the correlation functions are known, then, by using Eqs. (27), (29) and substituting the latter in the expression

$$S = -h_0 - e^{h_0} \sum_{N=0}^{\infty} \frac{1}{N!} \quad (30)$$

$$\times \int_V \ldots \int_V e_N^0 \ln e_N^0\, d\omega_1 \ldots d\omega_N,$$

which is a consequence of Eqs. (23), (28), we can calculate the entropy of a volume V.

Let us pass to a consideration of the important special case in which there are correlations between the particles only for sufficiently small distances. If the distance between the points considered is much larger than r, a certain correlation distance, then we can assume statistical independence for the occurence of particles at these points. Obviously, just such a state of affairs occurs in physical systems (e.g., in gases), where r is of the order of a radius of action of the intermolecular forces.

We shall make yet another assumption: we shall assume that our system is homogeneous. This assumption is less basic since, if it were not made, the formulas would be only slightly more complicated (provided the inhomogeneities change only slightly over distances r). For the indicated system of particles, the $g_n(M_1, \ldots M_n)$ are appreciably different from zero only when all the points $M_1, \ldots, M_n$ are within distances of the order r of each other, i.e., when

$$|M_1 - M_i| \lesssim r \quad (i = 2, \ldots, n).$$

From this it follows that (if g_n vanishes sufficiently rapidly as $|M_i - M_j|$ increases the integral

$$\int_V \ldots \int_V g_n(M_1, \ldots, M_n)\, d\omega_1 \ldots d\omega_n$$

over a volume V, the linear dimensions of which are much larger than r, is approximately proportional to the volume V, i.e.,

$$\int_V \dots \int_V g_n(M_1, \dots, M_n)\, d\omega_1 \dots d\omega_n \qquad (31)$$
$$= G_n V\left[1 + O\left(\frac{r}{D}\right)\right],$$

where

$$G_n = \int_V \dots \int_V g_n(M_1, M_2, \dots, M_n)\, d\omega_2 \dots d\omega_n$$

(The point M_1 is fixed, but lies inside V).

At the same time, because of Eqs. (27), (31), we have

$$\int_V \dots \int_V h_n(M_1, \dots, M_n)\, d\omega_1 \dots d\omega_n \approx H_n V. \qquad (32)$$

Here

$$H_n = \sum_{s=0}^{\infty} \frac{(-1)^s}{s!} G_{n+s}. \qquad (33)$$

Let us examine in turn the terms of the summation with respect to N in the right hand side of Eq. (30). The term corresponding to $N = 0$ equals zero. The second term, which corresponds to $N = 1$, is proportional to V:

$$\int_V e_1^0 \ln e_1^0\, d\omega = R_1 V, \qquad (34)$$

where, because of Eq. (29),

$$R_1 = h_1 \ln h_1.$$

Consider the next term. According to Eq. (29) the following equations hold everywhere except in the hyperlayer for which $|M_1 - M_2| \leqslant r$:

$$e_2^0(M_1, M_2) = h_1(M_1)\, h_1(M_2) = h_1^{(2)};$$
$$\ln e_2^0(M_1, M_2) = \ln h_1(M_1) \qquad (35)$$
$$+ \ln h_1(M_2) = (2) \ln h_1;$$
$$e_2^0 \ln e_2^0 = (2)\, h_1^{(2)} \ln h_1 \quad (|M_1 - M_2| \gg r).$$

(Abbreviations like those used here will be used in what follows). Because of the failure of Eqs. (35) in the layer $|M_1 - M_2| \leqslant r$, the integration of $e_2^0 \ln e_2^0$ leads to the appearance of an additional term [as compared with the integral from Eq. (2) $h_1^{(2)} \ln h_1$] which is proportional to V. Therefore

$$\int_V \int_V e_2^0 \ln e_2^0\, d\omega_1\, d\omega_2 = 2h_1 R_1 V^2 + R_2 V, \qquad (36)$$

where by R_2 we designate the corresponding coefficient of proportionality.

Let us consider the term corresponding to $N = 3$. If all three points M_1, M_2, M_3 are far from one another (the number of isolated points $n_1 = 3$), then

$$e_3^0 = e_1^{0\,(3)};$$
$$e_3^0 \ln e_3^0 = (3)\, e_1^{0\,(3)} \ln e_1^0. \qquad (37)$$

Accordingly, the integral from $e_3^0 \ln e_3^0$ will contain a term equal to

$$3h_1^2 R_1 V^3.$$

There are the following three hyperlayers: 1) points M_1 and M_2 are near each other and point M_3 is distant from them; 2) M_1 and M_3 near, M_2 distant; 3) M_2 and M_3 near, M_1 distant. These layers are characterized by a number of isolated points $n_1 = 1$, and a number of pairs $n_2 = 1$. For them

$$\epsilon_3^0 = \epsilon_{1\ 2}^{0\ 0};$$
$$\epsilon_3^0 \ln e_3^0 = e_1^0 \epsilon_2^0 \ln e_1^0 + e_1^0 \epsilon_2^0 \ln e_2^0. \qquad (38)$$

In the indicated layers Eq. (38) exceeds (37) by an amount

$$e_1^0 e_2^0 \ln e_1^0 + e_1^0 e_2^0 \ln e_2^0 - (3)\, e_1^{0\,(3)} \ln e_1^0 \qquad (39)$$
$$= e_1^0 [e_2^0 - e_1^{0\,(2)}] \ln e_1^0 + e_1^0 [e_2^0 \ln e_2^0 - e_1^{0\,(2)} \ln e_1^{0\,(2)}].$$

But, by Eq. (29),

$$e_2^0 - e_1^{0\,(2)} = h_2;$$

so the excess

$$e_2^0 \ln e_2^0 - e_1^{0\,(2)} \ln e_1^{0\,(2)}$$

is just the excess which gave the increment $R_2 V$ in Eq. (36). Because of this fact and Eq. (32), we find that the integral from Eq. (39) equals

$$(H_2 V)(R_1 V) + (h_1 V)(R_2 V).$$

The expression just found must be multiplied by three, since there are three hyperlayers of the specified type.

Finally, since Eq. (38) is not valid in the hyperlayer in which all three points are near one another ($n_1 = 0$, $n_2 = 0$, and the number of groups of three points, $n_3 = 1$), we must introduce an additional term, proportional to V, with a coefficient which we designate by R_3. In all, we have

$$\iiint e_3^0 \ln e_3^0\, d\omega_1\, d\omega_2\, d\omega_3 \qquad (40)$$
$$= 3h_1^2 R_1 V^3 + 3H_2 R_1 V^2 + 3h_1 R_2 V^2 + R_3 V.$$

An analogous method can be applied to the examination of the integral from $e_4^0 \ln e_4^0$ (and higher integrals). If the region in which all points are far from one another introduces a term $4h_1^3 R_1 V^4$ into the integral, then the layers corresponding to

points near one another bring contributions proportional to V^3 and V^2. These contributions, being of the same nature as the contributions $R_2 V$, $R_3 V$, can be expressed in terms of the latter. Finally, there remains an additional term $R_4 V$, proportional to the first power of the volume, which cannot be expressed in terms of $R_1, R_2, R_3, h_1, H_2, H_3$.

Let us make a similar examination of the general integral of the indicated type, i.e., the integral from $e_k^0 \ln e_k^0$. We introduce a hyperlayer defined by a set of numbers $n_1, n_2, \ldots$. The latter have the same meaning as above (n_i is the number of groups of i nearby points); therefore $\Sigma i n_i = k$. For this layer

$$e_k^0 = e_1^{0\,(n_1)} e_2^{0\,(n_2)} \ldots e_k^{0(n_k)};$$

$$e_k^0 \ln e_k^0 = (n_1)\, e_1^{0\,(n_1)} e_2^{0\,(n_2)}$$

$$\ldots \ln e_1^0 + (n_2)\, e_1^{0\,(n_1)} e_2^{0\,(n_2)} \ldots \ln e_2^0 + \ldots$$

On evaluating the integral, the following term corresponds to this layer:

$$[n_1 h_1^{n_1 - 1} H_2^{n_2} \ldots R_1 + n_2 h_1^{n_1} H_2^{n_2 - 1} \ldots R_2 + \ldots]\; V^{n_1 + n_2 + \ldots}$$

The number of such layers having the same structure (the same set of numbers $n_1, n_2, \ldots$) equals

$$\frac{k!}{n_1!\, n_2!\, (2!)^{n_2} \ldots n_k!\, (k!)^{n_k}}.$$

Consequently, summing over the different layers, we have

$$\int_V \ldots \int_V e_k^0 \ln e_k^0\, d\omega_1 \ldots d\omega_k \qquad (41)$$

$$= \sum_{n_1 + 2n_2 + \ldots = k} \frac{k!\, V^{n_1 + n_2 + \ldots}}{n_1!\, n_2!\, (2!)^{n_2} \ldots} \sum_j n_j R_j H_j^{n_j - 1} \prod_{i \neq j} H_i^{n_i},$$

where $H_1 = h_1$.

If we carry out the summation (41) over $k = 0, 1, 2, \ldots$, then the restriction $n_1 + 2n_2 + \ldots = k$ disappears. Writing

$$\nu_i = \begin{cases} n_i, & i \neq j; \\ n_j - 1, & i = j, \end{cases}$$

we have, changing the order of summation

$$\sum_{k=0}^{\infty} \frac{1}{k!} \int \ldots \int e_k^0 \ln e_k^0\, d\omega_1 \ldots d\omega_k \qquad (42)$$

$$= V \sum_{j=1}^{\infty} \frac{1}{j!} R_j \prod_{i=1}^{\infty} \sum_{\nu_i = 0}^{\infty} \frac{1}{\nu_i!} \left(\frac{H_i V}{i!} \right)^{\nu_i}$$

$$= V \left(\sum_{j=1}^{\infty} \frac{1}{j!} R_j \right) \exp \left\{ \sum_{i=1}^{\infty} \frac{1}{i!} H_i V \right\}.$$

Substituting this expression in Eq. (30) and bearing in mind that the sum in the exponent vanishes, we find

$$h_0 + V \sum_{i=1}^{\infty} \frac{1}{i!} H_i = V \sum_{i=0}^{\infty} \sum_{s=0}^{\infty} \frac{(-1)^s}{i!\, s!} G_{i+s} = 0.$$

Because of Eq. (27), (33), and the fact that

$$\sum_{i+s=r} \frac{(-1)^s}{i!\, s!} = \frac{1}{(i+s)!} (1-1)^{i+s} = 0,$$

we obtain the result

$$S = -h_0 - V \sum_{j=1}^{\infty} \frac{1}{j!} R_j \qquad (43)$$

$$= -V \sum_{j=1}^{\infty} \frac{1}{j!} [R_j + (-1)^j G_j] \quad (G_1 = g_1).$$

This formula, in deriving which, equalities of the type (32) were used, which contains errors of the order r/D, is valid for sufficiently large regions V, when $D \gg r$. Thus, for large volumes, additivity of the entropy holds. If the dimensions of the region are comparable with the correlation distance, then additivity does not hold. Analogously, the energy of a system of mutually interacting particles can be considered additive only for regions, the linear dimensions of which are quite large compared with the radius of action of the intermolecular forces, for, otherwise, the interaction energy between the regions will be significant. The non-additivity of the entropy derives from the presence of correlations between the particles in different regions. When the volumes are large ($D \gg r$), then the correlation, which occurs mainly at the boundaries of the regions, is negligible compared with the general lack of correlation, and to the extent that correlation can be neglected, the entropy is additive and becomes proportional to the volume. The entropy density (which has meaning for sufficiently large volumes) is, according to Eq. (43)

$$s = \frac{S}{V} = -\sum_{j=1}^{\infty} \frac{1}{j!} [R_j + (-1)^j G_j]. \qquad (44)$$

The entropy is strictly additive only in the case of the Poisson distribution, corresponding to the absence of all correlations. In this case, if β is the particle density,

$$G_1 = \beta; \quad G_2 = G_3 = \ldots = 0;$$

$$R_1 = \beta \ln \beta; \quad R_2 = R_3 = \ldots = 0;$$

whence, because of Eq. (44)

$$s = \beta (1 - \ln \beta). \qquad (45)$$

This formula can be obtained by other means, e.g., by using the expression (23).

The Poisson law corresponds to a complete lack of correlation between the particles and is therefore an extreme case. It gives the maximum entropy density for a given particle density g_1. If the class of admissible distributions is restricted to those with the same energy density, then, of course, the Poisson distribution will not be the maximizing distribution. For non-Poisson distributions the most important correlations are those between pairs, described by the functions $g_2(M_1, M_2)$. As an example, we shall find the expression for the entropy for the case where third-order and higher correlations vanish, i.e., $g_3 = g_4 = \ldots = 0$. In this case, according to Eq. (27)

$$h_1 = g_1 - G_2; \quad h_2 = g_2; \tag{46}$$

$$h_3 = h_4 = \ldots = 0; \quad H_2 = G_2;$$

$$H_3 = \ldots = 0; \quad G_2 = \int_{\omega_2} g_2(M_1, M_2)\, d\omega_2,$$

where the point M_1 is fixed.

The method of calculating the quantities R_1, R_2, R_3,... follows from their definitions. From Eq. (36), we obtain

$$R_2 = \frac{1}{V}\int_V\int_V \left[g_2 \ln (h_1^2 + g_2) + h_1^2 \ln\left(1 + \frac{g_2}{h_1^2}\right)\right] d\omega_1 d\omega_2.$$

Having fixed the point M_1, we can decrease the the number of integrations needed to determine R_2;

$$R_2 = \int_{\omega_2} \left[g_2 \ln (h_1^2 + g_2) + h_1^2 \ln\left(1 + \frac{g_2}{h_1^2}\right)\right] d\omega_2, \tag{47}$$

where $g_2 = g_2(M_1, M_2)$. Corresponding considerations for R_3 lead to the integral

$$R_3 = h_1 \int_{\omega_2}\int_{\omega_3} \left\{g_2^{12} \ln \frac{A}{h_1^2 + g_2^{12}} + g_2^{23} \ln \frac{A}{h_1^2 + g_2^{23}} + g_2^{31} \ln \frac{A}{h_1^2 + g_2^{31}} + h_1^2 \ln \frac{h_1^4 A}{(h_1^2 + g_2^{12})(h_1^2 + g_2^{23})(h_1^2 + g_2^{31})}\right\} d\omega_2 d\omega_3, \tag{48}$$

where

$$A = h_1^2 + g_2^{12} + g_2^{23} + g_2^{31};$$

$$g_2^{12} = g_2(M_1, M_2); \quad g_2^{23} = g_2(M_2, M_3);$$

$$g_2^{31} = g_2(M_3, M_1).$$

It is easily seen that the integrand vanishes if the condition that all three points be near each other be violated. Indeed, in this case, two of the distances $|M_1 - M_2|$, $|M_2 - M_3|$, $|M_3 - M_1|$ become large (compared with r), so that two of the quantities $g_2^{12}, g_2^{23}, g_2^{31}$ vanish, which leads to the vanishing of the entire integrand and, consequently, to the convergence of the integral. Analogous behavior occurs for $R_4, R_5, \ldots$.

The entropy density is equal to

$$s = g_1 - \frac{1}{2}G_2 - h_1 \ln h_1 - \frac{1}{2}R_2 - \frac{1}{6}R_3 - \ldots,$$

where the corresponding quantities are defined by Eqs. (46), (47), (48). In special cases there can be relations of smallness between g_1, g_2, and G_2, which can be used to simplify calculations with the indicated formulas.

The results of the present investigation can be extended to cases in which the particles (molecules) have internal degrees of freedom.

Translated by R. Silverman
75

Multiple Scattering in a Coulomb Field in Very Thin Layers of Material

A. S. KOMPANEETS
Moscow Institute of Engineering Physics
(Submitted to JETP editor March 17, 1954)
J. Exper. Theoret. Phys. USSR **28**, 308-311 (March, 1955)

Data about multiple Coulomb scattering in foils of optical thickness 1 and 3 are given. The relative role of single and triple scattering for different angles of deflection is clarified. In the Appendix a model of Coulomb scattering through small angles is considered.

IN many nuclear experiments it is essential to take into account multiple scattering of charged particles traversing layers of material which are so thin that the entire number of collisions is comparable with unity. The usual approximate theory of multiple scattering, in which it is assumed that the number of collisions is very large, is not applicable here, so that a more exact theory must be employed[1,2] The distribution function for small angles, obtained in this theory, was studied by Biberman[3], but the results of his work cannot be extended to angles, which are large in comparison with the minimum diffraction angle of deflection (see below). Even if the thickness of the scattering foil constitutes one mean free path for elastic scattering, a considerable number of particles undergo more than one collision in traversing it. It is very easy to determine the fraction of such particles in the total scattering effect. With the help of the exact theory of multiple scattering it is also possible to determine the fraction of particles which, after having suffered multiple scattering, leave the material at a definite angle with the original direction of incidence.

The general formula for the distribution function of particles which have passed through some thickness of material and have been deflected through a small angle, was given in references 1 and 2. This function can be written thus:

$$f(\theta) = \frac{1}{2\pi}\int_0^\infty J_0(u\theta)\exp\left\{-N\int d\sigma'\right. \times \left.(1 - J_0(u\theta'))\right\} u\,du, \tag{1}$$

where N is the number of scattering atoms per square centimeter, J_0 the Bessel function of zero order and $d\sigma'$ the differential cross section.

For light elements it is necessary to substitute the differential cross section for Coulomb scattering into Eq. (1), taking into account the screening:

$$d\sigma = \frac{8\pi Z^2 e^4}{m^2 v^4}\,\frac{\theta\,d\theta}{[\theta^2 + (\hbar\alpha/mv)^2]^2}; \tag{2}$$

here Z is the atomic number, v the velocity of the particle, α the screening parameter. A potential field of the form $V = (Ze/r)\,e^{-\alpha r}$ corresponds to Eq. (2).

We introduce the optical thickness of the scatterer (d being the geometrical thickness)

$$\tau \equiv 8\pi N Z^2 e^4 d/\hbar^2\alpha^2 v^2 \tag{3}$$

and the dimensionless screening parameter

$$\nu = \hbar\alpha/2mv. \tag{4}$$

Substituting Eqs. (2), (3) and (4) in the general formula Eq. (1) we obtain the formula for multiple Coulomb scattering in light elements:

$$f(\theta) = \frac{e^{-\tau}}{8\pi\nu^2\tau}\int_0^\infty J_0\left(\xi\frac{\theta}{2\nu\sqrt{\tau}}\right) \times \exp\{\xi\sqrt{\tau}\,K_1(\xi/\sqrt{\tau})\}\,\xi\,d\xi; \tag{5}$$

here K_1 is the Macdonald function. For large optical thicknesses this function can be written in the form

$$K_1\left(\frac{\xi}{\sqrt{\tau}}\right) \approx \frac{\sqrt{\tau}}{\xi} - \frac{\xi}{2\sqrt{\tau}}\ln\frac{0.89\xi}{\sqrt{\tau}}, \tag{6}$$

since then the main contributions to the integral in Eq. (5) are given by values of ξ much smaller than $\sqrt{\tau}$

Substitution of Eq. (6) in Eq. (5) yields a formula, valid for large τ (of the order of several tens):

[1] A. S. Kompaneets, J. Exper. Theoret. Phys. USSR **15**, 236 (1945)

[2] A. S. Kompaneets, J. Exper. Theoret. Phys. USSR **17**, 1059 (1947)

[3] L. M. Biberman, Izv. Akad. Nauk SSSR, Ser. Fiz. **15**, 424 (1951)

$$f(\vartheta) = \frac{1}{8\pi\nu^2\tau} \int_0^{\xi<2\sqrt{\tau}} \exp\left\{\frac{\xi^2}{2} \ln\frac{0{,}89\xi}{\sqrt{\tau}}\right\} \times J_0\left(\xi\frac{\theta}{2\nu\sqrt{\tau}}\right)\xi\, d\xi. \quad (7)$$

A similar expression was obtained in reference 1, where the scattering in heavy elements was investigated, and it turned out that $f(\theta)$ is very reminiscent of the Gaussian distribution. Equation (5) was tabulated by Snyder and Scott[5] for $\tau = 100$ without transition to the asymptotic form (7).

If $\tau = 1$ or 3, Eq. (7) is, of course, entirely inapplicable. To find the distribution formula in this case it is necessary to integrate the Eq. (5) numerically . As was already mentioned, a calculation of $f(\theta)$ for small τ was carried out by Biberman. He replaced the elementary scattering law by a sum of Gaussian functions. Such a sum can give a good of Gaussian functions. Such a sum can give a good approximation to $f(\theta)$ for the smallest deflection angles ($\theta \sim 2\nu$), but it is known not to be applicable in the range $\theta \gg 2\nu$, because the mean square of the deflection angle, as calculated according to Eq. (2), diverges logarithmically, whereas it converges, if Gaussian functions are used instead of Eq. (2). But as the characteristic peculiarity of the Coulomb scattering consists just in the fact that the mean square of the deflection angle diverges on the side of large angles, it follows that in order to investigate $f(\theta)$ for as large θ as possible, one must not use the Gaussian approximation.

In the first place, we note that a direct numerical integration according to Eq. (5) is not feasible, because the integral converges very slowly at the upper limit. Therefore it is necessary to separate out of the integrand the part due to unscattered and singly scattered particles. The remaining distribution function has the form

$$f_{>1}(\vartheta) = \frac{1}{8\pi\nu^2\tau} e^{-\tau} \int_0^\infty J_0\left(\xi\frac{\theta}{2\nu\sqrt{\tau}}\right) \times \left(\exp\left\{\xi\sqrt{\tau}K_1\left(\frac{\xi}{\sqrt{\tau}}\right)\right\} - 1 - \xi\sqrt{\tau}K_1\left(\frac{\xi}{\sqrt{\tau}}\right)\right)\xi\, d\xi. \quad (8)$$

The subscript >1 indicates that only multiple scattering has been taken into account. It is easy to verify that the third term in the bracket under the integral sign gives single scattering, because (see Watson[4])

$$\int_0^\infty K_1(ax) J_0(bx)\, x^2 dx = \frac{2a}{(a^2+b^2)^2}.$$

In the case $\tau = 3$ it was also convenient to separate out the double scattering, since the integral (8) does not converge sufficiently well for them. The distribution of doubly scattered particles, written separately, has the form

$$f_2(\vartheta) = \frac{\tau^2 e^{-\tau}\vartheta^2}{2\pi(\vartheta^4+4\vartheta^2)^2}\left[\frac{2(\vartheta^2+1)}{(\vartheta^4+4\vartheta^2)^{1/2}} \times \ln\frac{\vartheta^2+2+\sqrt{\vartheta^4+4\vartheta^2}}{\vartheta^2+2-\sqrt{\vartheta^4+4\vartheta^2}} + \vartheta^2 - 2\right], \quad (9)$$

where

$$\vartheta = \theta/2\nu\sqrt{\tau}. \quad (10)$$

It can be seen that

$$2\pi\int_0^\infty f_2(\vartheta)\,\vartheta\, d\vartheta = \frac{\tau^2 e^{-\tau}}{2},$$

as it should be.

We give the results of numerical computations for $\tau = 1$ and $\tau = 3$ (the calculations were carried out by T. N. Shatalova):

TABLE I

Distribution function for particles which have traversed a foil of thickness of one mean free path ($\tau = 1$)

$\vartheta = \frac{\theta}{2\nu\sqrt{\tau}}$	0	0.5	1	1.5	2	2.5
$2\pi f_{>1}$	0.149	0.130	0.091	0.057	0.0342	0.0204
$2\pi f_1$	0.735		0.184		0.0394	

3	3.5	4	4.5	5
0.0136	0.00735	0.00515	0.00386	0.0026
0.00735		0.00254		0.0011

Here $f > 1\ (\theta)$ denotes the distribution function of particles which have suffered more than one col-

[5] H. S. Snyder and V. T. Scott, Phys. Rev. 76, 220 (1949)

[4] T. Watson, *Bessel Functions*

lision, f_1 the distribution function of particles which have suffered one collision. It turns out that the number of the former and the number of the latter become comparable to $\theta = 2$, and for larger angles the particles which have suffered multiple scattering prevail.

The distribution given in Table 1 is normalized to unity:

$$e^{-1} + 2\pi \int_0^\infty (f_{>1} + f_1)\, \vartheta d\vartheta = 1.$$

Here e^{-1} is the fraction of particles which have passed without a single scattering event. Actually Table 1 comprises 97.5% of all particles which have passed; the remaining particles are scattered through angles θ larger than 5.

TABLE II

Distribution function for particles which have traversed a foil of thickness of three mean free paths ($\tau = 3$)

ϑ $\frac{\theta}{2\nu\sqrt{\tau}}$	0	0.5	1.0	1.5	2.5	4	6	8
$2\pi f_{>1}(\vartheta)$	0.295	0.268	0.205	0.143	0.0645	0.0201	0.0043	0.0023
$2\pi f_1(\vartheta)$	0.298	0.191	0.746	0.028	0.0118	0.00103	0.0002	0.00007
$2\pi f_2(\vartheta)$	0.149	0.133	0.088	0.056	0.0162	0.030	0.0075	0.00024

This table comprises 92% of all particles which have passed. We note that now multiple scattering becomes larger than single scattering already for very small values of θ.

APPENDIX

The distribution function for multiple Coulomb scattering can also be studied experimentally with the help of a simple optical model.

Consider an emulsion compounded of two transparent media of very close refractive indices. We will assume that one of the substances constitutes the medium proper, into which the other has been injected in the form of small spheres of equal radius R, distributed at random. This radius will be assumed to be large in comparison with the wave length of the transmitted light, so that the laws of geometrical optics can be applied. Thus the scattering under consideration is, in a certain sense, opposite to the Rayleigh scattering, where the wave length is large as compared with the dimensions of the obstacle.

We will first determine the deflection of a light ray in an elementary scattering event. According to assumption, the relative refractive index ν of the two media is a small number. We draw the polar axis from the center of the sphere in the direction of incidence of the ray. The polar angle of the point of incidence of the ray on the sphere will be called β. Then, as is seen from an elementary construction, the deflection angle of the ray in the sphere is

$$\theta = 2\nu \tan\beta.$$

The angle θ is regarded as small, since $\nu \ll 1$, and the contribution from larger angles is insignificant. From this it is easy to obtain the differential scattering cross section. According to general formulas of the classical scattering theory it is equal to *

$$d\sigma = 2\pi R^2 \frac{4\nu^2 \theta d\theta}{(4\nu^2 + \theta^2)^2}.$$

This formula is quite similar to Eq. (2), with the designation ν corresponding to the previous one, and

$$R = 2Ze^2/\hbar v.$$

The formula for $d\sigma$ can also be obtained from the diffraction theory by a transition to the limit.

Translated by Z. V. Chraplyvy
52

* We notice that Eq. (2) is obtained in the Born approximation from the wave equation, and the present formula in the approximation of geometrical optics. The wave aspect for particles appears to be analogous to the ray aspect for light. Consequently the analogy found here is by no means a special case of the optical-mechanical analogy. We were unable to find out the physical reason for this analogy.

The Phenomenological Relations of Onsager

KHRISTO KARANIKOLOV
Sofia, Bulgaria

(Submitted to JETP editor January 8, 1954)
J. Exper. Theoret. Phys. USSR 28, 283-286 (March, 1955)

IN Ref. 1, Popov established the fact that the phenomenological relations (in the thermodynamics of irreversible processes)

$$x_i' = \sum_{k=1}^{n} L_{ik} X_k,$$

$$i = 1, 2, \ldots, n \quad (x_i' = dx_i/dt)$$

are obtained directly as the first integrals of the set of differential equations

$$d^2x_i/dt^2 = X_i \quad (i = 1, 2, \ldots, n), \tag{1}$$

which satisfy the conditions $\chi_i = \chi_i^0$ for $t = t_0$ and $\chi_i = 0$ for $t = +\infty$ ($i = 1, 2, \ldots, n$), where

$$X_i = \partial(-\Delta S)/\partial x_i \tag{2}$$

and

$$\Delta S = -\tfrac{1}{2} \sum g_{ik} x_i x_k \quad (g_{ik} = g_{ki})$$

are positive definite quadratic forms.

The integrals of this system, which satisfy the above mentioned conditions, have the form

$$x_i'(t) = C_1 \eta_{i1} e^{r_1 t} + C_2 \eta_{i2} e^{r_2 t} + \ldots + C_n \eta_{in} e^{r_n t}$$

(C_k, η_{ik} — are constants),

where the r_i^2 are the positive roots of the algebraic equation of $2n$ th degree

$$\gamma(r) = \begin{vmatrix} g_{11} - r^2 & g_{12} & \ldots & g_{1n} \\ g_{21} & g_{22} - r^2 & \ldots & g_{2n} \\ \ldots & \ldots & \ldots & \ldots \\ g_{n1} & g_{n2} & \ldots & g_{nn} - r^2 \end{vmatrix} = 0. \tag{3}$$

Eliminating $C_1 e^{r_1 t}$, $C_2 e^{r_2 t}$, . . . , $C_n e^{r_n t}$ from the expressions for $\chi_i'(t)$ and $X_1, X_2, \ldots, X_n$, Popov* obtained

$$\begin{vmatrix} x_i' & \eta_{i1} & \eta_{i2} & \ldots & \eta_{in} \\ X_1 & \eta_{11} r_1 & \eta_{12} r_2 & \ldots & \eta_{1n} r_n \\ X_2 & \eta_{21} r_1 & \eta_{22} r_2 & \ldots & \eta_{2n} r_n \\ \ldots & \ldots & \ldots & \ldots & \ldots \\ X_n & \eta_{n1} r_1 & \eta_{n2} r_2 & \ldots & \eta_{nn} r_n \end{vmatrix} = 0$$

$$(i = 1, 2, \ldots, n),$$

which can be written in the form

$$x_i' = \sum_{k=1}^{n} L_{ik} X_k \quad (i = 1, 2, \ldots, n),$$

where $L_{i1}, L_{i2}, \ldots, L_{in}$ ($i = 1, 2, \ldots, n$) are functions of g_{ik} which do not depend on the constants of integration of $C_1, C_2, \ldots, C_n$.

With the help of an iteration process, which leads to the necessity of analyzing infinite series, Popov established the symmetry of the matrix

$$\begin{Vmatrix} L_{11} & L_{12} & \ldots & L_{1n} \\ L_{21} & L_{22} & \ldots & L_{2n} \\ \ldots & \ldots & \ldots & \ldots \\ L_{n1} & L_{n2} & \ldots & L_{nn} \end{Vmatrix}$$

For the particular case $n = 2$, he established this property by an algebraic method also.

Since the case $n = 3$ is very important for the application of the theory to specific problems, we demonstrate below the symmetry of the matrix in this case also.

For $n = 3$ the equation

$$\gamma(r) = \begin{vmatrix} g_{11} - r^2 & g_{12} & g_{13} \\ g_{21} & g_{22} - r^2 & g_{23} \\ g_{31} & g_{32} & g_{33} - r^2 \end{vmatrix} = 0$$

has three positive roots: r_1^2, r_2^2, r_3^2.

We assume that these roots are single and that*

[1] K. A. Popov, J. Exper. Theoret. Phys. USSR 28, 257 (1955); Soviet Phys. 1, 336 (1955)

* $X_i = \dfrac{d^2x_i}{dt^2} = \sum_{k=1}^{n} C_k \eta_{ik} r_k e^{r_k t} \quad (i = 1, 2, \ldots, n).$

* By means of a suitable transition to the limit, it is possible to show that these conditions are not restricting. Here $\gamma_{31}(0) = \begin{vmatrix} g_{12} & g_{12} \\ g_{22} & g_{23} \end{vmatrix}$, $\gamma_{32}(0) = -\begin{vmatrix} g_{11} & g \\ g_{21} & g \end{vmatrix}$

$$g_{32}\gamma_{31}(0) - g_{31}\gamma_{32}(0) \neq 0.$$

The integrals of the system (1) for stated conditions which characterize the physical processes, have the form

$$x_i = \sum_{\lambda=1}^{3} C_\lambda \gamma_{3i}(r_\lambda) e^{r_\lambda t}, \tag{4}$$

where $\gamma_{3i}(r)$ is the algebraic complement of the corresponding element of the determinant $\gamma(r)$.

From this we obtain

$$X_i = \sum_{\lambda=1}^{3} C_\lambda \gamma_{3i}(r_\lambda) r_\lambda^2 e^{r_\lambda t} \quad (i = 1, 2, 3), \tag{5}$$

$$\frac{dx_1}{dt} = \sum_{\lambda=1}^{3} C_\lambda \gamma_{31}(r_\lambda) r_\lambda e^{r_\lambda t};$$

$$X_i = \sum_{\lambda=1}^{3} C_\lambda \gamma_{3i}(r_\lambda) r_\lambda^2 e^{r_\lambda t} \quad (i = 1, 2, 3), \tag{6}$$

$$\frac{dx_2}{dt} = \sum_{\lambda=1}^{3} C_\lambda \gamma_{32}(r_\lambda) r_\lambda e^{r_\lambda t}.$$

Eliminating $C_1 e^{r_1 t}$, $C_2 e^{r_2 t}$, $C_3 e^{r_3 t}$ from Eqs. (5) and (6), we obtain

$$\begin{vmatrix} X_1 & \gamma_{31}(r_1) & \gamma_{31}(r_2) & \gamma_{31}(r_3) \\ X_2 & \gamma_{32}(r_1) & \gamma_{32}(r_2) & \gamma_{32}(r_3) \\ X_3 & \gamma_{33}(r_1) & \gamma_{33}(r_2) & \gamma_{33}(r_3) \\ x_1' & \frac{1}{r_1}\gamma_{31}(r_1) & \frac{1}{r_2}\gamma_{31}(r_2) & \frac{1}{r_3}\gamma_{31}(r_3) \end{vmatrix} = 0;$$

$$\begin{vmatrix} X_1 & \gamma_{31}(r_1) & \gamma_{31}(r_2) & \gamma_{31}(r_3) \\ X_2 & \gamma_{32}(r_1) & \gamma_{32}(r_2) & \gamma_{32}(r_3) \\ X_3 & \gamma_{33}(r_1) & \gamma_{33}(r_2) & \gamma_{33}(r_3) \\ x_2' & \frac{1}{r_1}\gamma_{32}(r_1) & \frac{1}{r_2}\gamma_{32}(r_2) & \frac{1}{r_3}\gamma_{32}(r_3) \end{vmatrix} = 0;$$

so that

$$\Delta L_{12} = -\begin{vmatrix} \gamma_{31}(r_1) & \gamma_{31}(r_2) & \gamma_{31}(r_3) \\ \gamma_{33}(r_1) & \gamma_{33}(r_2) & \gamma_{33}(r_3) \\ \frac{1}{r_1}\gamma_{31}(r_1) & \frac{1}{r_2}\gamma_{31}(r_2) & \frac{1}{r_3}\gamma_{33}(r_3) \end{vmatrix}; \tag{7}$$

$$\Delta L_{21} = \begin{vmatrix} \gamma_{32}(r_1) & \gamma_{32}(r_2) & \gamma_{32}(r_3) \\ \gamma_{33}(r_1) & \gamma_{33}(r_2) & \gamma_{33}(r_3) \\ \frac{1}{r_1}\gamma_{32}(r_1) & \frac{1}{r_2}\gamma_{32}(r_2) & \frac{1}{r_3}\gamma_{32}(r_3) \end{vmatrix};$$

$$\Delta = \begin{vmatrix} \gamma_{31}(r_1) & \gamma_{31}(r_2) & \gamma_{31}(r_3) \\ \gamma_{32}(r_1) & \gamma_{32}(r_2) & \gamma_{32}(r_3) \\ \gamma_{33}(r_1) & \gamma_{33}(r_2) & \gamma_{33}(r_3) \end{vmatrix},$$

where the determinant Δ, under our assumptions of single roots, is different from zero.

Consequently

$$\Delta(L_{21} - L_{12}) \tag{8}$$

$$= \begin{vmatrix} 1 & 1 & 1 \\ F(r_1, r_2, r_3) & F(r_2, r_3, r_1) & F(r_3, r_1, r_2) \\ \frac{1}{r_1} & \frac{1}{r_2} & \frac{1}{r_3} \end{vmatrix},$$

where

$$F(u, v, w) = \gamma_{33}(u)[\gamma_{31}(v)\gamma_{31}(w) + \gamma_{32}(v)\gamma_{32}(w)].$$

The determinant on the right side of Eq. (8) is equal to zero. Consequently it is easy to show that

$$F(r_1, r_2, r_3) = [G_{33} - (g_{11} + g_{22})\rho_1 + \rho_1^2][(G_{31} + g_{31}\rho_2)(G_{31} + \rho_3 g_{31}) + (G_{32} + g_{32}\rho_2)(G_{32} + \rho_3 g_{32})]$$

is a symmetric function of the roots $\rho_1 (= r_1^2)$, $\rho_2 (= r_2^2)$, $\rho_3 (= r_3^2)$. Here G_{ik} denotes the algebraic complement of the element g_{ik} in the determinant obtained from $\gamma(r)$ for $r = 0$.

Making use of the elementary dependence of the roots on the coefficients of the characteristic equation $\gamma(r) = 0$, we have

$$[\gamma(r) \equiv \rho^3 - (g_{11} + g_{22} + g_{33})\rho^2 + (G_{11} + G_{22} + G_{33})\rho - g = 0],$$

$$\rho_1 + \rho_2 + \rho_3 = g_{11} + g_{22} + g_{33},$$

$$\rho_1(\rho_2 + \rho_3) + \rho_2\rho_3 = G_{11} + G_{22} + G_{33};$$

$$\rho_1\rho_2\rho_3 = g = \begin{vmatrix} g_{11} & g_{12} & g_{13} \\ g_{21} & g_{22} & g_{23} \\ g_{31} & g_{32} & g_{33} \end{vmatrix},$$

after some arrangements we obtain

$$F(r_1, r_2, r_3) = A + [G_{33}(g_{31}^2 + g_{32}^2) + (g_{11} + g_{22})(g_{31}G_{31} + g_{32}G_{32}) + G_{31}^2 + G_{32}^2]\rho_2\rho_3 - [(g_{31}G_{31} + g_{32}G_{32})(b + G_{33}) - g_{33}(G_{31}^2 + G_{32}^2) - g(g_{31}^2 + g_{32}^2)]\rho_1,$$

where A does not depend on ρ_1, ρ_2, ρ_3 and $b = G_{11} + G_{22} + G_{33}$.

Direct evaluation of the coefficients ρ_2, ρ_3 and ρ_1 in the expression $F(r_1, r_2, r_3)$ shows that they are equal to zero and that

$$F(r_1, r_2, r_3) = F(r_2, r_3, r_1) = F(r_3, r_1, r_2) = A.$$

Consequently, the determinant on the right side of Eq. (8) is equal to zero, and since $\Delta \neq 0$, $L_{12} = L_{21}$. In a similar fashion it can be shown that $L_{13} = L_{31}$.

Translated by R. T. Beyer
48

SOVIET PHYSICS-JETP VOLUME 1, NUMBER 2 SEPTEMBER, 1955

On the Theory of the Hall and Nernst-Ettinghausen Effects in Semiconductors with Mixed Conductivities

F. G. Bass and I. M. Tzidilkovski
Dagestan Section, Academy of Sciences, USSR, Makhachkala

(Submitted to JETP editor March 4, 1954)
J. Exper. Theoret. Phys. USSR 28, 312-320 (March, 1955)

The Hall and the Nernst-Ettinghausen voltages and the distribution of current carrier concentrations are calculated for a semiconductor with mixed conductivities located in a non-homogeneous magnetic field. Recombination of current carriers and energy levels due to impurities are taken into account.

1. INTRODUCTION

SOME papers[1-3] have recently been published in which the effect of body and surface recombinations on the Hall effect in semiconductors has been investigated. The basic assumption in all these works has been Ohm's law in a form valid only for semiconductors without impurities, a form in which the mean free path of the current carriers does not depend on their velocity.

This work investigates both the Hall effect and the thermomagnetic Nernst-Ettinghausen effect under the assumption of a more general dependence of the length l of the mean free path of the current carriers on the velocity v :

$$l = \Phi(T)\, v^n, \tag{1}$$

where $\Phi(T)$ is some function of the temperature T, and n is any given number. It will be shown that such a more general dependence of l on v leads to substantial quantitative changes in both the current carrier concentrations and the voltages in both effects, as well as to qualitative changes in the case of the Nernst-Ettinghausen effect. By analyzing the general case of a non-homogeneous magnetic field it is possible to determine how the non-uniformity of the magnetic field near the edges of pole-pieces affect the phenomena under consideration.

The following assumptions are made:

1. The magnitude of the exponent n in Eq. (1) has the same value for both electrons and holes. This is equivalent to assuming an identical scattering process for both electrons and holes by the phonons.

2. The primary current (either electric or thermal) is directed along the x axis, and the magnetic field, which is a function of y, is directed along the z axis ($H = H_z$). Therefore the electric fields of both the Hall and the Nernst-Ettinghausen effects are functions of y only.

2. BASIC EQUATIONS

The generalized differential equation of Ohm's law for electrons and holes, as derived by Tolpygo[4], can be written:

$$\mathbf{j}_+ = -eu_+N_+\Big\{-\mathbf{E} + \frac{kT}{e} \times \Big[\nabla \ln N_+ + \frac{n+1}{2}\nabla \ln T\Big] + \frac{c_n u_+}{c} \times \Big[-\mathbf{E} + \frac{kT}{e}\Big(\nabla \ln N_+ + \frac{n+1}{2}\nabla \ln T\Big)\Big] \times \mathbf{H}\Big\}; \tag{2a}$$

$$\mathbf{j}_- = -eu_-N_-\Big\{-\mathbf{E} - \frac{kT}{e}\Big[\nabla \ln N_- + \frac{n+1}{2}\nabla \ln T\Big] \tag{2b}$$

[1] H. Welker, Z. Naturforsch, 6a, 184 (1951)

[2] A. I. Ansel'm, Zh. Tekhn. Fiz. 22, 1146(1952)

[3] R. Landauer and J. Swanson, Phys. Rev. 91, 207 (1953)

[4] K. B. Tolpygo, Trans. of Inst. of Phys, Acad. Sci. USSR 3, 52 (1952)

$$-\frac{a_n u_-}{c}\left[-\mathbf{E}-\frac{kT}{e}\left(\nabla \ln N_- + n\nabla \ln T\right)\right]\times \mathbf{H}\Big\}.$$

The total current density is:

$$\mathbf{j}=\mathbf{j}_+ + \mathbf{j}_- = -e\Big\{-A_1\mathbf{E} + \frac{kT}{e}\left(\nabla A_2 + A_3\nabla \ln T\right) + \left[-A_4\mathbf{E}+\frac{kT}{e}\left(\nabla A_5 + A_6\nabla \ln T\right)\right]\times\frac{\mathbf{H}}{c}\Big\}. \tag{2c}$$

where $\mathbf{j}_+$, $\mathbf{j}_-$ are current densities (the plus and minus subscripts designating holes and electrons respectively), N_+, N_- the concentrations, $m_\pm$ the effective masses, e the absolute value of charge on the electron, $\mathbf{H}$ the strength of the magnetic field, $u_\pm$ the mobilities, which are

$$u_\pm = \frac{4}{3\sqrt{\pi}}\frac{e}{m_\pm}\Phi(T)\left(\frac{2kT}{m_\pm}\right)^{(n-1)/2}\times\Gamma\left(\frac{n}{2}+2\right)$$

where

$$\Gamma(n)=\int_0^\infty x^{n-1}e^{-x}dx,$$

and

$$a_n = \frac{3\sqrt{\pi}}{4}\frac{\Gamma(n+(3/2))}{\Gamma^2((n/2)+2)}; \tag{3}$$

$$A_1 = u_+N_+ + u_-N_-, \quad A_2 = u_+N_+ - u_-N_-,$$

$$A_3 = \frac{n+1}{2}A_2, \quad A_4 = a_n(u_+^2N_+ - u_-^2N_-),$$

$$A_5 = a_n(u_+^2N_+ + u_-^2N_-), \quad A_6 = nA_5.$$

The equations of continuity for hole and electron currents in a semiconductor having energy levels due to impurities (see diagram) can be written:

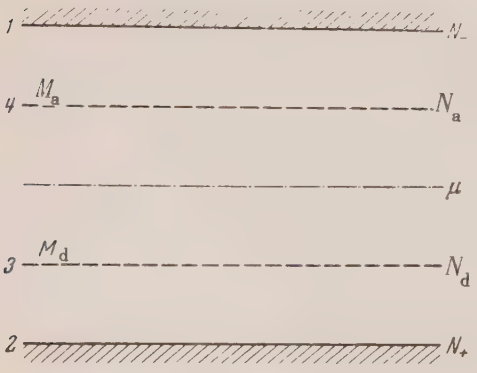

Energy level diagram in a semiconductor. μ is Fermi level.

$$\frac{1}{e}\operatorname{div}\mathbf{j}_+ = \frac{1}{e}\operatorname{div}\mathbf{j}_- = k_{21} - k_{12}N_+N_- + M_b\frac{k_{31}k_{23}-k_{13}k_{32}N_+N_-}{k_{31}+k_{23}+k_{13}N_- + k_{32}N_+} + M_a\frac{k_{41}k_{24}-k_{14}k_{42}N_+N_-}{k_{41}+k_{24}+k_{14}N_- + k_{42}N_+}, \tag{4}$$

where M_a, M_d are densities of acceptors and donors respectively, and k_{ij} are kinetic coefficients with indices i and j denoting the type of transition. The kinetic coefficients have the following correlations[5]:

$$\frac{k_{21}}{k_{12}} = N_+^0N_-^0; \quad \frac{k_{31}}{k_{13}} = \frac{N_-^0(M_b - N_b^0)}{N_b^0}; \tag{5}$$

$$\frac{k_{41}}{k_{14}} = \frac{N_-^0N_a^0}{M_a - N_a^0}; \quad \frac{k_{23}}{k_{32}} = \frac{N_+^0N_b^0}{M_b - N_b^0},$$

$$\frac{k_{21}}{k_{12}} = \frac{N_+^0(M_a - N_a^0)}{N_a^0}; \quad \frac{k_{34}}{k_{43}} = \frac{(M_b - N_b^0)(M_a - N_a^0)}{N_b^0N_a^0}$$

where N_+^0 and N_-^0 are the equilibrium densities of holes and electrons in the upper and lower zones, and N_a^0, N_d^0 the equillibrium densities of holes and electrons at the acceptor and donor levels.

It will now be assumed that extraneous magnetic fields cause small divergences from equillibrium in the concentrations of holes and electrons, and that these divergences are equal for both holes and electrons:

$$N_+ - N_+^0 = N_- - N_-^0 = \nu; \quad \nu/N_\pm^0 \ll 1. \tag{6}$$

Applying Eq. (5), Eq. (4) becomes

$$\operatorname{div}\mathbf{j}_+ = \operatorname{div}\mathbf{j}_- = -e\alpha\nu(N_+^0 + N_-^0), \tag{4a}$$

where

$$\alpha = k_{12} + \frac{k_{13}k_{32}M_b}{k_{31}+k_{23}+k_{13}N_-^0 + k_{32}N_+^0} + \frac{k_{14}k_{42}M_a}{k_{41}+k_{24}+k_{14}N_-^0 + k_{42}N_+^0}. \tag{7}$$

The first component of Eq. (7), representing the recombination of holes and electrons in the upper and lower zones, predominates over the other components at high temperatures where intrinsic conductivity plays the main role. This value of $\alpha = k_{12}$ was used by Ansel'm in his investigations of semiconductors without impurities. At low

[5] A. I. Gubanov, J. Exper. Theoret. Phys. USSR **21**, 79 (1951)

temperatures, where conductivity is determined by thermal transitions between the impurity energy levels and the upper and lower zones, the other two components are dominant in determining the value of a. This case, apparently, rarely occurs in practice.

Isothermal Hall Effect

As is well known, the isothermal Hall effect (for $\nabla T = 0$ in the specimen) consists of the fact that a so-called Hall voltage (V^x) appears in a semiconductor along the y axis when the semiconductor with current flowing along its x axis is placed in a transverse magnetic field directed along the z axis. For no current flowing along the y axis ($j_y = 0$), the value of the Hall electric field (E^x) is :

$$E^{\mathrm{X}} = \frac{kT}{e}\frac{u_+ - u_-}{N_+^0 u_+ + N_-^0 u_-}\frac{d\nu}{dy} + \frac{a_n}{ec}\frac{N_+^0 u_+^2 + N_-^0 u_-^2}{(N_+^0 u_+ + N_-^0 u_-)^2} j_{\mathrm{X}} H. \tag{8a}$$

The Hall voltage is then:

$$V^{\mathrm{X}} = \int_0^a E^{\mathrm{X}} dy = \frac{kT}{e}\frac{u_+ - u_-}{N_+^0 u_+ + N_-^0 u_-}[\nu(a) - \nu(0)] + \frac{a_n}{ec}\frac{N_+^0 u_+^2 - N_-^0 u_-^2}{(N_+^0 u_+ + N_-^0 u_-)^2} \times j_{\mathrm{X}} \int_0^a H dy, \tag{8b}$$

where a is the length of the specimen along the y axis.

The Hall coefficient in the case of an arbitrary n is:

$$R = \frac{a_n}{ec}\frac{N_+ u_+^2 - N_- u_-^2}{(N_+ u_+ + N_- u_-)^2}. \tag{9}$$

As can be seen from Table 1, the choice of a_n can cause the value of the Hall coefficient to change by as much as 1.5 to 2 times. Combining Eqs. (2), (5), (8a) and (4a) we can state the equation for charge distribution with accuracy to the order of $\nu H/c$ by :

$$\frac{d^2\nu}{dy^2} - \frac{1}{\lambda_0^2}\nu = -f^{\mathrm{X}}\frac{dH}{dy}. \tag{10}$$

where

$$f^{\mathrm{X}} = \frac{a_n}{c}\frac{e}{kT}\frac{N_+^0 N_-^0 (u_+ + u_-)}{N_+^0 + N_-^0} E_0,$$

E_0 is the strength of the electric field along the x axis, and $\lambda_0 = \sqrt{\frac{kT}{e}\frac{u_+ u_-}{\alpha (N_+^0 u_+ + N_-^0 u_-)}}$ is the current carrier's average diffusion length.

Table I

Values of coefficients a_n for various n[4]

n	a_n	n	a_n
−0.5	1.5740	2.0	1.1043
0	1.1781	2.5	1.2276
0.5	1.0356	3.0	1.4003
1.0	1.0000	3.5	1.6308
1.5	1.0277	4.0	1.9328

When surface energy levels and surface recombination are present in a semiconductor it is possible to obtain the boundary conditions of the problem by applying Eq. (10) to a case of an infinitely thin layer of thickness δ:

$$\frac{d\nu}{dy} - \frac{\nu}{\lambda_s} = -f^{\mathrm{X}} H \qquad \text{for } y = 0 \tag{11}$$

$$\frac{d\nu}{dy} + \frac{\nu}{\lambda_s} = -f^{\mathrm{X}} H \qquad \text{for } y = a$$

Here a new characteristic length is introduced: $\lambda_s = \lim_{\delta \to 0} (\lambda_0^2 / \delta)$

Isothermal Nernst-Ettinghausen Effect

The isothermal Nernst-Ettinghausen effect ($\partial T/\partial y = 0$) consists of the appearance of a potential difference in a semiconductor along the y axis when its x axis, along which exists a temperature gradient, is placed in a transverse magnetic field along the z axis.

For $j_x = j_y = 0$, the Nernst-Ettinghausen field E_{H} is:

$$E^{\mathrm{H}} = \frac{kT}{e}\left\{\frac{u_+ - u_-}{N_+^0 u_+ + N_-^0 u_-}\frac{d\nu}{dy} + \frac{a_n}{c}\left[\frac{1-n}{2}\frac{N_+^{02} u_+^3 + N_-^{02} u_-^3}{(N_+^0 u_+ + N_-^0 u_-)^2} - \frac{3n+7}{2}\frac{N_+^0 N_-^0 u_+ u_- (u_+ + u_-)}{(N_+^0 u_+ + N_-^0 u_-)^2} \times \left(1 + \frac{2}{3n+7}\frac{\Delta E}{kT}\right)\right] H \frac{d \ln T}{dx}\right\}. \tag{12a}$$

and the Nernst-Ettinghausen voltage V^{H} is:

$$V^{\mathrm{H}} = \int_0^a E^{\mathrm{H}} dy = \frac{kT}{e}\left\{\frac{u_+ - u_-}{N_+^0 u_+ + N_-^0 u_-} \times [\nu(a) - \nu(0)] + \frac{a_n}{c}\left[\frac{1-n}{2} \times \frac{N_+^{0^2} u_+^3 + N_-^{0^2} u_-^3}{(N_+^0 u_+ + N_-^0 u_-)^2}\right.\right. \tag{12b}$$

$$-\frac{3n+7}{2}\frac{N_+^0 N_-^0 u_+u_-(u_+ + u_-)}{(N_+^0 u_+ + N_-^0 u_-)^2}\left(1+\frac{2}{3n+7}\frac{\Delta E}{kT}\right)\Big]$$
$$\times \frac{d\ln T}{dx}\int_0^a H\,dy\Big\}.$$

In expressions (12a) and (12b) ΔE denotes the width of the forbidden zone. The Nernst-Ettinghausen coefficient, in the case of an arbitrary n, is:

$$Q=\frac{k}{e}\frac{a_n}{c}\left[\frac{1-n}{2}\frac{N_+^2u_+^3+N_-^2u_-^3}{(N_+u_+ + N_-u_-)^2}\right. \tag{13}$$
$$\left.-\frac{3n+7}{2}\frac{N_+N_-u_+u_-(u_+ + u_-)}{(N_+u_+ + N_-u_-)^2}\times\left(1+\frac{2}{3n+7}\frac{\Delta E}{kT}\right)\right].$$

The charge distribution is given by

$$\frac{d^2\nu}{dy^2}-\frac{1}{\lambda_0^2}\nu=-f^H\frac{dH}{dy}, \tag{14}$$

where

$$f^H=\frac{a_n}{c}\frac{d\ln T}{dx} \tag{15}$$
$$\times\Big(N_+^0N_-^0\Big[\frac{1-n}{2}\left(N_+^0u_+^2-N_-^0u_-^2\right)+\frac{3n+7}{2}$$
$$\times u_+u_-\left(N_+^0-N_-^0\right)\left(1+\frac{2}{3n+7}\frac{\Delta E}{kT}\right)\Big]\Big)$$
$$\times\frac{1}{(N_+^0+N_-^0)(N_+^0u_+ + N_-^0u_-)},$$

$$\frac{d\nu}{dy}-\frac{\nu}{\lambda_s}=-f^HH \quad \text{for } y=0$$

$$\frac{d\nu}{dy}+\frac{\nu}{\lambda_s}=-f^HH \quad \text{for } y=a$$

Thus the investigation of both effects is reduced to solving equations of the type (10) and (14) with boundary conditions of the type (11) and (15).

3. SOLUTION OF EQUATIONS AND ANALYSIS OF RESULTS

The solution of Eqs. (10) and (14) with boundary conditions (11) and (15) has the form:

$$\nu^X=f^XF(y),\quad \nu^H=f^HF(y), \tag{16}$$

where

$$F(y)=\frac{\lambda_0}{\left(1+\frac{\lambda_0^2}{\lambda_s^2}\right)\operatorname{sh}\frac{a}{\lambda_0}+2\frac{\lambda_0}{\lambda_s}\operatorname{ch}\frac{a}{\lambda_0}} \tag{17}$$
$$\times\Big[H(0)\Big(\operatorname{ch}\frac{y-a}{\lambda_0}-\frac{\lambda_0}{\lambda_s}\operatorname{sh}\frac{y-a}{\lambda_0}\Big)$$
$$+\Big(\int_0^a\operatorname{ch}\frac{a-y_1}{\lambda_0}\frac{dH}{dy_1}dy_1$$
$$+\frac{\lambda_0}{\lambda_s}\int_0^a\operatorname{sh}\frac{a-y_1}{\lambda_0}\frac{dH}{dy_1}dy_1-H(a)\Big)$$
$$\times\Big(\operatorname{ch}\frac{y}{\lambda_0}+\frac{\lambda_0}{\lambda_s}\operatorname{sh}\frac{y}{\lambda_0}\Big)\Big]-\lambda_0\int_0^y\operatorname{sh}\frac{y-y_1}{\lambda_0}\frac{dH}{dy_1}dy_1.$$

It is now possible to determine in the equations for the Hall and the Nernst-Ettinghausen voltages the components that are dependent on the charge distribution.

These components, V_1^X (for Hall effect) and V_1^H (for Nernst-Ettinghausen effect) are:

$$V_1^X=\frac{kT}{e}\frac{u_+-u_-}{N_+^0u_+ + N_-^0u_-}f^X[F(a)-F(0)], \tag{18a}$$

$$V_1^H=\frac{kT}{e}\frac{u_+-u_-}{N_+^0u_+ + N_-^0u_-}f^H[F(a)-F(0)]. \tag{18b}$$

where, from Eq. (17)

$$F(a)-F(0)=\frac{\lambda_0}{\left(1+\frac{\lambda_0^2}{\lambda_s^2}\right)\operatorname{sh}\frac{a}{\lambda_0}+2\frac{\lambda_0}{\lambda_s}\operatorname{ch}\frac{a}{\lambda_0}} \tag{19}$$
$$\times\Big[H(0)\Big(1-\operatorname{ch}\frac{a}{\lambda_0}-\frac{\lambda_0}{\lambda_s}\operatorname{sh}\frac{a}{\lambda_0}\Big)+\Big(\int_0^a\operatorname{ch}\frac{a-y_1}{\lambda_0}\frac{dH}{dy_1}dy_1$$
$$+\frac{\lambda_0}{\lambda_s}\int_0^a\operatorname{sh}\frac{a-y_1}{\lambda_0}\frac{dH}{dy_1}dy_1-H(a)\Big)$$
$$\times\Big(\operatorname{ch}\frac{a}{\lambda_0}+\frac{\lambda_0}{\lambda_s}\operatorname{sh}\frac{a}{\lambda_0}-1\Big)\Big]-\lambda_0\int_0^a\operatorname{sh}\frac{a-y_1}{\lambda_0}\frac{dH}{dy_1}dy_1.$$

It is apparent from Eq. (16) that ν^X is always positive; that is, that the current carrier concentration can only increase in the case of the Hall effect. On the other hand, ν^H in the case of the Nernst-Ettinghausen effect, can have either sign. In the case of semiconductors having holes and electrons of equal mobilities the potential differences V_1^X and V_1^H are equal to zero at the same time that ν^X and ν^H differ from zero.

In the Nernst-Ettinghausen effect, the change in concentration becomes zero when either of the following two conditions is fulfilled:

1) $N_+^0=N_-^0$, $u_+=u_-$, for n = any number;

2) $N_+^0=N_-^0$, for $n=1$

It is interesting to consider the limiting case when the diffusion length $\lambda_0\to\infty$ ($a\to 0$), and

$N_+ = N_- = N$. Eq. (4a) can then be solved uniquely. The equations and boundary conditions now become:

$$\frac{d^2N}{dy^2} + b\frac{dHN}{dy} = 0; \tag{20}$$

$$\frac{dN}{dy} + bHN = \frac{N - N^0}{\lambda_s} \quad \text{for } y = 0 \tag{21}$$

$$\frac{dN}{dy} + bHN = -\frac{N - N^0}{\lambda_s} \quad \text{for } y = a$$

For the Hall effect

$$b = b^X = \frac{a_n e (u_+ + u_-)}{2ckT} E_0.$$

For the Nernst-Ettinghausen effect

$$b = b^H = \frac{1 - n}{2} \frac{u_+ - u_-}{c} \frac{d \ln T}{dx}$$

Solving (20) with boundary conditions (21), we get

$$N(y) = \frac{N^0}{1 + w^{-1}(a) + \lambda_s^{-1} w^{-1}(a) \int_0^a w(y) dy} \tag{22}$$

$$\times \left(\left[2 + \lambda_s^{-1} w^{-1}(a) \int_0^a w(y)\, dy \right] w^{-1}(a) \right.$$

$$\left. + [1 - w^{-1}(a)]\, \lambda_s^{-1} w^{-1}(y) \int_0^y w(y)\, dy \right)$$

where $$w(y) = \exp\left(b \int_0^y H dy\right).$$

The voltages V_1 (V_1^X or V_1^H) dependent on the change in the concentration of current carriers are:

$$V_1 = \frac{kT}{e} \frac{u_+ - u_-}{u_+ + u_-} \tag{23}$$

$$\times \ln \frac{\left[2 + \lambda_s^{-1} \int_0^a w(y)\, dy \right] w^{-1}(a)}{2 + \lambda_s^{-1} w^{-1}(a) \int_0^a w(y)\, dy}.$$

The extent to which the proposed theory is applicable will now be determined. To simplify matters, we will assume $N_\pm^0 = N_-^0 = N$; and will let u stand for the greater of the magnitudes u_+ and u_-. Using as a criterion of validity the magnitude of the discarded components in (10) and (14) we can say: for the Hall effect

$$\frac{\lambda_0 e F_0}{2kT} \frac{uH}{c} \ll 1; \tag{24a}$$

for the Nernst-Ettinghausen effect

$$\frac{\lambda_0}{4} \frac{d \ln T}{dx} \frac{uH}{c} \ll 1. \tag{24b}$$

Let us consider the case of a high conducting semiconductor of the germanium type. Let us assume $u = 10^6$ cgs units, $\lambda_0 = 0.1$ cm, $T = 300$ °K, and say the Hall effect is to be investigated at $E_0 = 1$ V/cm and $H = 10^3$ oersteds. Then

$$\frac{\lambda_0 e E_0}{2kT} \frac{uH}{c} \approx 0.07 \ll 1.$$

For the Nernst-Ettinghausen effect, let us assume H to be 10^4 oersteds, and $d \ln T/dx = 1$ cm^{-1} Then $\frac{\lambda_0}{4} \frac{uH}{c} \frac{d \ln T}{dx} \approx 0.008 \ll 1$.

These estimates show that in the case of high conducting semiconductors with current carriers of high mobility, the Hall effect theory is valid for a temperature range not lower than room temperatures if at the same time the magnetic fields do not exceed 10^3 oersteds. The Nernst- Ettinghausen effect theory, on the other hand, holds good for a greater range of temperatures (in the direction of lower temperatures) and magnetic fields (in the direction of stronger fields). In the case of semiconductors with current carriers of low mobility (of Cu_2O type) the range of applicability of both theories considerably increases.

We will now examine how the diffusion of the current carriers affects both their concentration and the strength of the Hall and the Nernst-Ettinghausen fields. For simplicity, we will assume that the magnetic field is uniform and that surface effects are absent ($\lambda_s \to \infty$). Then

$$F(a) - F(0) \approx -2\lambda_0 H,$$

and the relative change of concentration in the Hall effect is

$$\left| \frac{\nu^X}{N^0} \right| \approx \frac{\lambda_0 e E_0}{kT} \frac{uH}{c}.$$

For semiconductors of the germanium type having the above parameters, the relative change in concentration in the Hall effect will be about 13%, while the relative change in the Hall voltage due to diffusion (if we assume the length a along the y axis of the specimen to be 0.5 cm) must reach 20%. In the Nernst-Ettinghausen effect, the relative change in concentration as determined by the expression

$$\left| \frac{\nu^H}{N^0} \right| \approx \frac{\lambda_0 d \ln T}{2dx} \frac{uH}{c},$$

should be, under the same conditions, about 2%, while the relative change in voltage should reach about 20%

Numerical calculations show that the non-uniformity of the magnetic field at the edges of pole-pieces can not cause any significant changes in the magnitude of the effects under consideration.

CONCLUSION

Analysis of Eqs. (8b), (12b), (18a) and (18b) shows that for both phenomena, when surface effects are missing, $|(V - V_0)/V_0| \approx \lambda_0/a$, , where V is the actual voltage determined experimentally, and V_0 is the intrinsic Hall or Nernst-Ettinghausen voltage before inclusion of voltage effects due to changes in current carrier concentrations. From this it follows that the magnitudes of the Hall and the Nernst-Ettinghausen voltages will be determined with the same degree of exactness with which the inequality $\lambda_0/a \ll 1$ is attained. When the condition that $\lambda_0/a \ll 1$ is fulfilled experimentally, V will not differ from V_0

If the length of the specimen a_1 is far greater than its width a_2 , and the latter is equal to several current carrier diffusion lengths λ_0, then λ_0 can be evaluated by:

$$\lambda_0 \approx \frac{V(a_2)}{V(a_1)} a_1 - a_2, \tag{26}$$

where $V(a_1)$ and $V(a_2)$ are the Hall or the Nernst-Ettinghausen voltages measured along the length and along the width respectively. Thus to evaluate λ_0 it is sufficient to measure the voltage V across the specimen at two mutually perpendicular orientations of it. It follows from the statement at the conclusion of the preceeding section that equation (26) will hold true as well in the case of a specimen which is located in a field that is non-uniform at the edges.

The authors wish to express their gratitude to Kh. I. Amirkhanov and V. P. Zhuze for their interest in the work and discussion of results.

Translated by V. Kibort
53

On the Stability of a Homogeneous Phase. II Determination of the Limit of Stability

I. Z. FISHER
Byelorussian State University

(Submitted to JETP editor March 20, 1954)
J. Exper. Theoret. Phys. USSR 28, 437-446 (April, 1955)

On the basis of the general theory developed in reference 1, a criterion is given for the stability of a homogeneous phase. An analysis of the basic properties of a system in the vicinity of the limiting points of equilibrium is inquired into. Two examples of the application of the criterion for stability are considered.

1. THE CRITERION FOR STABILITY

THE determination of the limits of stability of a homogeneous phase, in particular, of the liquid state, is one of the most important problems of the statistical thermodynamics of molecular systems. This question was considered in connection with the theory of crystallization in the works of Tiablikov[2] and Vlasov[3]. However, the criteria of crystallization given in these works are in error. We will not delay here to consider this matter in detail. It is sufficient to note that Vlasov's theory leads to a positive value of dv/dT along the crystallization curve (see Fig. 4, p. 198[3]), which is manifestly contradictory to experiment[4]. A similar difficulty arises in Tiablikov's theory.

It will be shown in the present paper that the problem of the limit of the stability of a homogeneous phase can be solved in a general manner, one starting from the theory of the liquid state and based on a study of the radial distribution function. In what follows below we shall use the results and the symbols of the preceding communication[1].

We shall start from the basic result of our earlier work[1], according to which the absolute limit of stability of a homogeneous phase for a given temperature T is determined as the edge of a continuous band spectrum of eigenvalues of the volume parameter λ in Bogoliubov's equation for the radial distribution function under the "boundary condition" $r(g(r)-1)\to 0$ for $r\to\infty$. This leads to the following criterion for the stability of a homogeneous phase: the boundary value $\lambda=\lambda_0$ is a value of the parameter λ such that it makes the root of the equation

$$\lambda L(\gamma)=1 \quad (\lambda>0) \tag{1}$$

real with the imaginary part vanishing, that is,

$$\operatorname{Im}\{\gamma_1(\lambda_0)\}=0, \tag{2}$$

but such that there exists a neighborhood $\delta\lambda$ of the point λ_0 in which

$$|\operatorname{Im}\{\gamma_1(\lambda_0+\delta\lambda)\}|>0. \tag{3}$$

The phase will accordingly be stable in a neighborhood $\delta\lambda$ where (3) is fulfilled. There are two possible cases:

1. Condition (3) is fulfilled only on one side of λ_0, that is, only for $\delta\lambda>0$ or for $\delta\lambda<0$. Then we have a "normal" boundary point of the type of crystallization, vaporization or condensation of a gas, where a homogeneous phase is possible only for smaller (greater) densities and impossible for greater (smaller) densities.

2. Condition (3) is fulfilled on both sides of λ_0. The point λ_0 is an isolated unstable point on the isotherm. This is an instability of the type of the critical point.

In. Eq. (1) we have used the designations (see reference 1):

$$L(\gamma)=\int_{-\sigma}^{\sigma}K(z)\,e^{i\gamma z}\,dz; \quad \lambda=2\pi a^3/v; \tag{4}$$

$$K(z)=\tfrac{1}{2}\int_{|z|}^{\sigma}(e^{-\Phi(t)/kT})'\,u(t)\,(z^2-t^2)\,dt. \tag{5}$$

Since T is contained as a parameter in $L(\gamma)$, then conditions (2) and (3) determine $\lambda_0=\lambda_0(T)$ or, by

[1] I. Z. Fisher, J. Exper. Theoret. Phys. USSR 28, 171 (1955)

[2] S. V. Tiablikov, J. Exper. Theoret. Phys. USSR 17, 386 (1947)

[3] A. A. Vlasov, *Many Particle Theory*, Moscow, 1950

[4] P. Bridgman, *Physics of High Pressures*, 1935

means of Eq. (4), determine the limiting line of stability of the system on its $v - T$ surface: $v = v_{\lim}(T)$. Then with the help of the known expression for the pressure[5], which, in our notation, has the form

$$\frac{pv}{kT} = 1 + \frac{\lambda}{3}\int_0^\sigma (e^{-\Phi(r)/kT})' u(r) r^3 dr, \quad (6)$$

we can also find the limiting line of stability of the system on its $p - T$ surface: $p = p_{\lim}(T)$. These lines on the $v - T$ and $p - T$ surfaces of the system determine the absolute limit of the stability of a homogeneous phase (that is, gas or liquid), in other words, determine the limit of its possible existence, including metastable (superheated and supercooled) states. The lines of equilibrium phase transitions, that is, the limits of relative stability, are determined, as always, by the equality of the chemical potentials of the different phases. We wish to remark, however, that for the simplest systems of the type of argon, the only ones to which the theory of liquids in its developed form applies, a knowledge of the absolute limits of the stability of the system gives simultaneously, and with sufficient exactness, a knowledge of the lines of the phase transitions, inasmuch as for these systems the regions of metastable states are comparatively narrow.

It is evident that conditions (2) and (3) lead to the existence of limiting points of two types which are distinguished by whether for $\mathrm{Im}\{\gamma_1(\lambda_0)\} = 0$ there appears simultaneously either $\mathrm{Re}\{\gamma_1(\lambda_0)\} = 0$, or $\mathrm{Re}\{\gamma_1(\lambda_0)\} \neq 0$. The analysis of these cases is carried out separately below. As in reference 1, the analysis is limited to that which is possible without an actual solution of Bogoliubov's equation for $g(r)$, proceeding only from a knowledge of the behavior of $g(r)$ for $r \to \infty$.

2. BOUNDARY POINTS OF THE FIRST TYPE

If $L(\gamma)$ is such that $L(0) > 0$, then it may be shown that $\gamma_1(\lambda_0) = 0$; whence, according to Eq. (1), λ_0 itself is given by

$$\lambda_0 = [L(0)]^{-1}. \quad (7)$$

This determines $\lambda_0(T)$ or $v_{\lim}(T)$. From this one can readily obtain a general expression for $p = p_{\lim}(T)$. Integrating Eq. (4) by parts and taking Eq. (5) into account, we readily obtain the expression

$$L(0) = -\tfrac{2}{3}\int_0^\sigma (e^{-\Phi/kT})' u(r) r^3 dr. \quad (8)$$

Hence we have from Eq. (6)

$$pv/kT = 1 - \tfrac{1}{2}\lambda L(0) \quad (9)$$

and by comparison with (7) we find

$$(pv)_{\lim} = \tfrac{1}{2} kT. \quad (10)$$

Let us consider now a small neighborhood $\delta\lambda$ of the point λ_0. In virtue of the eveness of $K(z)$ we have $L'(0) = 0$, and Eq. (1) can be written

$$(\lambda_0 + \delta\lambda)\{L(0) + \tfrac{1}{2} L''(0)\gamma_1^2 + \ldots\} = 1. \quad (11)$$

We suppose that $L''(0) \neq 0$, but this last term we take into account, and we neglect the dependence of $L(0)$ on λ, which occurs on account of the presence of $u(t)$ in $K(z)$, according to Eq. (5). It will be shown below that for small γ this dependence is unimportant and Eq. (11) is exact. Taking account of Eq. (7), we find for small $\delta\lambda$ and γ_1

$$\gamma_1(\lambda) = \frac{1}{\lambda_0}\sqrt{\frac{2}{L''(0)}(\lambda_0 - \lambda)}. \quad (12)$$

As in reference 1, we use the notation $\gamma_1 \equiv \beta_1 + i\alpha_1$. There are then two possible cases:

1. $L''(0) < 0$. From Eq. (12) we have

$$\beta_1 \equiv 0;\ \alpha_1 = \frac{1}{\lambda_0}\sqrt{\frac{2}{L''(0)}(\lambda - \lambda_0)}, \quad \text{if} \quad \lambda < \lambda_0,$$
$$\alpha_1 \equiv 0;\ \beta_1 = \frac{1}{\lambda_0}\sqrt{\frac{2}{L''(0)}(\lambda_0 - \lambda)}, \quad \text{if} \quad \lambda > \lambda_0. \quad (13)$$

In agreement with the remark made in connection with Eq. (3), in accordance with the general theory[1], we have in Eq. (13) a boundary point of the type of the limit for a supercooled vapor: the phase exists for $\lambda < \lambda_0$ and the phase is impossible for $\lambda > \lambda_0$.

2. $L''(0) > 0$. In this case α_1 and β_1 exchange places in Eqs. (13) and we have a boundary point of the type of the limit for a superheated liquid: the phase exists for $\lambda > \lambda_0$ and the phase is impossible for $\lambda < \lambda_0$.

Thus boundary points of the type under consideration are such that on one side of them[1]

$$g(r) = 1 + \frac{A_1}{r} e^{-|\alpha_1| r} \quad (r \gg \sigma) \quad (14)$$

(stables states), and on the other side

$$g(r) = 1 + \frac{A_1}{r}\cos(\beta_1 r + \delta_1) \quad (r \gg \sigma) \quad (15)$$

[5] N. N. Bogoliubov, *Problems of Dynamical Theory in Statistical Mechanics*, Moscow, 1946

(absolutely unstable states). At the exact boundary point $\varkappa_1 = \beta_1 = 0$. The function $g(r)$ in the form (14) is postulated in the theory of critical opalescence[7-9]. To it corresponds the deviation in the density of free energy from the equilibrium value for fluctuations in the number of particles, the deviation being

$$f - f_0 = B\{(\vec{\nabla}\phi)^2 + \alpha_1^2\phi^2\} \qquad (16)$$

(see references 1, 9, where ϕ is the relative density, while $\varkappa_1^2 B$ is proportional to $(-\partial p/\partial v)_T$. Since for $\lambda \to \lambda_0$ we have $\varkappa_1 \to 0$, then at the exact boundary point we have $(-\partial p/\partial v)_T = 0$, in conformity with the general thermodynamic theory of boundary points (see reference 10).

Thus the limit of stability of a homogeneous phase, determined by Eqs. (2) and (3), coincides with the general thermodynamic definition of the limit of stability, since $(-\partial p/\partial v)_T = 0$ along the line $p = p_{\lim}(T)$.

We shall now show that $(\partial L/\partial\lambda)_{\lambda_0} = 0$ and, consequently, that Eq. (11) is exact. From Eqs. (4) and (5) we have

$$\left(\frac{\partial L}{\partial\lambda}\right)_{\gamma=0} = 2\int_0^\sigma \left(\frac{\partial K}{\partial\lambda}\right)_{\lambda_0} dz \qquad (17)$$

$$= \int_0^\sigma dz \int_{|z|}^\sigma (e^{-\Phi(t)/kT})' \left(\frac{\partial u(t)}{\partial\lambda}\right)_{\lambda_0} (z^2 - t^2)\, dt$$

and, integrating by parts, we find [analogous to Eq. (8)]

$$\left(\frac{\partial L}{\partial\lambda}\right)_{\gamma=0} = -\frac{2}{3}\int_0^\sigma (e^{-\Phi/kT})' \left(\frac{\partial u(r)}{\partial\lambda}\right)_{\lambda_0} r^3 dr. \qquad (18)$$

The right side here is equivalent, by Eq. (6), to the expression

$$-2\left[\frac{\partial}{\partial\lambda}\left\{\frac{1}{\lambda}\left(\frac{pv}{kT} - 1\right)\right\}\right]_{\lambda=\lambda_0} \qquad (19)$$

$$= \frac{2}{\lambda_0^2}\left[\frac{\partial}{\partial v}\left(\frac{pv^2}{kT} - v\right)\right]_{\lim},$$

which on calculation turns out to be zero, if we take account of Eq. (10) and the fact that $(-\partial p/\partial v)_{\lim} = 0$. Here it is essential that $(-\partial p/\partial v)_{\lim}$ be zero as a result of Eqs. (14) and (16), independently of whether the member containing $(\partial L/\partial\gamma)$ is considered in Eq. (11) or not.

Finally, let us consider the special case which occurs for $L''(0) = 0$. In this case it is necessary to consider further terms in the expansion in (11), and this gives

$$(\lambda_0 + \delta\lambda)\{L(0) + {}^1/_{24}\, L^{(IV)}(0)\,\gamma_1^2 + \ldots\} = 1. \qquad (20)$$

Taking Eq. (7) into account, we find that

$$\gamma_1(\lambda) = \sqrt[4]{\frac{24}{\lambda_0^2 L^{(IV)}(0)}(\lambda_0 - \lambda)}. \qquad (21)$$

Let us suppose for definiteness that $L^{(IV)}(0) < 0$. Then for $\lambda < \lambda_0$ all four values of the root in Eq. (21) will be complex, so that $\varkappa_1(\lambda) \neq 0$ and these states are stable. For $\lambda > \lambda_0$ there are among the roots of Eq. (21) two which are purely real, for which $\varkappa_1 \equiv 0$, and two purely imaginary, for which $\varkappa_1(\lambda) \neq 0$. Consequently the root with imaginary part of smallest absolute value will be the $\gamma_1(\lambda)$ with $\varkappa_1 \equiv 0$, and this state is unstable. It is easy to see that an analogous situation arises if $L^{IV}(0) = 0$ but $L^{(VI)}(0) \neq 0$, and so forth.

Thus the boundary points of the first type considered, that is, determined by Eq. (7), are such that they are always boundaries separating two regions of states of a system --- stable and unstable. Isolated points of instability cannot occur here, and consequently a thermodynamic singularity of the type of the critical point (see, above, the end of Section 1) cannot be a boundary point of the first type. The special significane of this circumstance will be considered separately later.

3. EXAMPLE OF A SYSTEM WITH BOUNDARY POINTS OF THE FIRST TYPE. SUBLIMATION

As an example of a system leading to boundary points of the type considered, we take a system of mutually attracting point particles, the intermolecular potential of which may be expressed as a rectangular potential well, so that

$$\Phi(r) = -\varepsilon \quad \text{for} \quad r < 1; \qquad (22)$$

$$\Phi(r) = 0 \quad \text{for} \quad r > 1.$$

The units of length here are dimensionless; a in Eq. (4) is thus the width of the potential well and

---

[6] J. Kirkwood, V. Levinson and B. Mann, J. Chem. Phys. 20, 929 (1952)

[7] L. Ornstein and F. Zernicke, Physik. Z. 19, 134 (1918)

[8] L. Ornstein and F. Zernicke, Physik. Z. 27, 761 (1926)

[9] M. A. Leontovich, *Statistical Mechanics*, Moscow, 1944

[10] L. D. Landau and E. M. Lifshitz, *Statistical Mechanics*, Moscow, 1951

$\sigma = 1$ (more precisely, $\sigma = 1 + 0$). Here also

$$(e^{-\Phi(r)/kT})' = -(e^{\varepsilon/kT} - 1)\,\delta(r-1). \quad (23)$$

The kernel $K(z)$ and its Fourier transform $L(\gamma)$ are equal, respectively, to

$$K(z) = {}^1/_2 Eu(1)(1-z^2), \quad (24)$$

$$L(\gamma) = 2Eu(1)\gamma^{-3}(\sin\gamma - \gamma\cos\gamma), \quad (25)$$

where $E \equiv e^{\epsilon/kT} - 1 > 0$. By means of a separation into a series in powers of γ we find that

$$L(0) = {}^2/_3 Eu(1) > 0; \quad (26)$$
$$L''(0) = -{}^2/_{15} Eu(1) < 0.$$

From this it is clear that Eq. (1) has the solution $\gamma = 0$ of the gaseous condensation point type for

$${}^2/_3 \lambda_0 Eu(1) = 1. \quad (27)$$

It will be shown below that all the remaining solutions of Eq. (1) with $\alpha(\lambda) = 0$ for our system lead to greater magnitudes of the density than Eq. (27) (see Section 5, below). If, therefore, we move along the λ axis from $\lambda = 0$ in the direction of increasing λ, then the solution $\gamma(\lambda)$ of Eq. (1), which, according to Eq. (27), goes to zero at the point λ_0, actually possesses its imaginary part of smallest absolute value for $\lambda < \lambda_0$, that is, $\gamma_1(\lambda)$. Hence λ_0 from Eq. (27) actually determines the limit of stability of our system and, taking Eq. (4) into consideration, we have

$$v_{\lim}(T) = \frac{4\pi a^3}{3}(e^{\varepsilon/kT} - 1)\,u(1). \quad (28)$$

The limiting pressure according to Eq. (10) is

$$p_{\lim}(T) = 3kT/8\pi a^3 u(1)(e^{\varepsilon/kT} - 1). \quad (29)$$

In order to find out the exact form of $v_{\lim}(T)$ and $p_{\lim}(T)$, it is necessary to know how $u(1)$ depends on λ and T, that is, $u(1; \lambda; T)$, and for this a knowledge of the exact solution of Bogoliubov's equation for $g(r)$ or $u(r)$ is required. But since it has been shown that $u(r) \sim 1$ always, then in Eqs. (28) and (29) we may discard the factor $u(1)$. This is the more accurate for low temperatures, where $(\epsilon/kT) \gg 1$. Then $v_{\lim}(T)$ is large (highly rarefied gas) and the equality $u(1) \approx 1$ is fulfilled with very great exactness, since for an ideal gas $u(r) \equiv 1$. Thus for $(\epsilon/kT) \gg 1$ we may write

$$v_{\lim}(T) \approx \frac{4\pi a^3}{3} e^{\varepsilon/kT}; \quad p_{\lim}(T) \approx \frac{3kT}{8\pi a^3} e^{-\varepsilon/kT}. \quad (30)$$

The system under consideration, apart from its extreme schematization, can serve as a model of a real system if the density of the latter is sufficiently small. Actually the neglect of the forces of repulsion between the particles, which forces act only at short range, is allowed if the average distance between the particles is large. A simultaneous neglect of the forces of attraction is not allowed, since then there would be no reason for the loss of stablity, and this would contradict the properties of real systems. Since, according to Eq. (28), the case of small densities corresponds to low temperatures, we may then suppose that the relation (30) represents with sufficient accuracy the limiting line of the stability of a real gaseous phase at low temperatures, for example, below the triple point; $p_{\lim}(T)$ is then the sublimation pressure.

That Eq. (30) is fully admissable quantitatively is evident from the following example. For argon the temperature and pressure at the triple point are, respectivley, 83°K and 0.68 atm = 66.7×10^3 abs. units. If we then take 1.43 as the magnitude of ϵ/kT at the triple point, as follows from the magnitude of the Lennard-Jones potential[11], then from Eq. (30) the radius of action of the intermolecular forces is found to have the magnitude $a = 7.7 \times 10^{-8}$ cm, which is more than twice the diameter of an atom of argon and is a fully acceptable result, although perhaps somewhat high. However, we must take into account that the actual pressure at a limiting point on the isotherm $T = T_{tr}$ is notably greater than p_{tr}, and hence a more exact estimate for a would be less than the indicated magnitude of 7.7×10^{-8} cm.

We note in conclusion that the pressure $p_{\lim}$ and volume $v_{\lim}$ which we have obtained agree well with the corresponding magnitudes calculated for the sublimation equilibrium[12]

$$p_{\text{subl}}(T) = \frac{(2\pi\tilde{\nu}^2)^{3/2}}{\sqrt{kT}} e^{-\varepsilon/kT}; \quad (pv)_{\text{subl}} \approx kT, \quad (31)$$

where $\tilde{\nu}$ is the geometrical mean frequency of the natural oscillations of the crystalline lattice.

---

[11] Zh. de-Bur, Usp. fiz. nauk 51, 41 (1953)

[12] M. Born and M. Goeppert-Mayer, *Theory of the Rigid Body*, 1933

4. BOUNDARY POINTS OF THE SECOND TYPE

We will call the boundary point $\lambda = \lambda_0$ determined by (2) and (3) a boundary point of the second type if $\mathrm{Re}\{\gamma_1(\lambda_0)\} \neq 0$.

Let us consider a certain magnitude λ near λ_0 and satisfying condition (3). We use the notation $\gamma_1 \equiv \beta + i\alpha$ (omitting the index 1). For λ near λ_0, α is small and we may write

$$L(\gamma) = \left\{L(\beta) - \frac{\alpha^2}{2}L''(\beta) + \ldots\right\} + i\alpha\left\{L'(\beta) - \frac{\alpha^2}{6}L'''(\beta) + \ldots\right\}. \quad (32)$$

As a consequence of the eveness of the function $K(z)$, it turns out, according to Eq. (4), that $L(\beta)$, $L'(\beta)$, etc., are purely real. Substituting Eq. (32) into Eq. (1) and separating the real and imaginary parts, we obtain

$$\lambda\left\{L(\beta) - \frac{\alpha^2}{2}L''(\beta) + \ldots\right\} = 1, \quad (33)$$

$$L'(\beta) - \frac{\alpha^2}{6}L'''(\beta) + \ldots = 0.$$

At the very boundary point $\alpha = 0$, and consequently

$$\lambda_0 L(\beta_0) = 1;\ L'(\beta_0) = 0. \quad (34)$$

These equations can be regarded as a definition of a boundary point of the second type. Since $L(\beta)$ contains the temperature T as parameter, then we find the limiting line of stability of the system on its $\lambda - T$ or $v - T$ surfaces: $\lambda = \lambda_0(T)$ or $v = v_{\lim}(T)$, and with the aid of Eq. (6) we also find the limiting line of stability of the system on its $p - T$ surface: $p = p_{\lim}(T)$.

Let us now consider the behavior of $\alpha(\lambda)$ and $\beta(\lambda)$ near a boundary point. Putting $\lambda = \lambda_0 + \delta\lambda$ and $\beta = \beta_0 + \delta\beta$ into Eq. (33), we obtain

$$(\lambda_0 + \delta\lambda)\{L(\beta_0) + (\partial L/\partial\lambda)_0\,\delta\lambda + {}^1/_2 L''(\beta_0)((\delta\beta)^2 - \alpha^2) + \ldots\} = 1, \quad (35)$$

$$(\partial L'(\beta)/\partial\lambda)_0\,\delta\lambda + L''(\beta_0)\,\delta\beta - (\alpha^2/6)L'''(\beta_0) + \ldots = 0.$$

We will suppose that $L''(\beta_0) \neq 0$. Then solving the resulting system of equations for α and $\delta\beta$, we obtain for small $\delta\lambda$

$$\alpha(\lambda) = \sqrt{\frac{2[1 + \lambda_0^2(\partial L/\partial\lambda)_0]}{\lambda_0^2 L''(\beta_0)}(\lambda - \lambda_0)}; \quad (36)$$

$$\delta\beta = \frac{1}{3\lambda_0^2[L''(\beta_0)]^2}\left\{L'''(\beta_0) + \lambda_0^2\left[L'''(\beta_0)\left(\frac{\partial L}{\partial\lambda}\right)_0 - 3L''(\beta_0)\left(\frac{\partial L'}{\partial\lambda}\right)_0\right]\right\}(\lambda - \lambda_0). \quad (37)$$

Thus in the neighborhood of a boundary point λ_0 (on the side of the stable states) we always have

$$\beta(\lambda) = \beta_0 + C(\lambda - \lambda_0). \quad (38)$$

With respect to $\alpha(\lambda)$ there are two possible cases:

1. $L''(\beta_0)$ and $1 + \lambda_0^2(\partial L/\partial\lambda)_0$ of opposite sign. Then a homogeneous phase is stable for $\lambda < \lambda_0$ ($\alpha_1 \neq 0$) and a homogeneous phase is impossible for $\lambda > \lambda_0$ ($\alpha_1 \equiv 0$). We have a boundary point of the type of a gaseous condensation or of crystallization.

2. $L''(\beta_0)$ and $1 + \lambda_0^2(\partial L/\partial\lambda)_0$ of the same sign. Then a homogeneous phase is stable for $\lambda > \lambda_0$ and a homogeneous phase is impossible for $\lambda < \lambda_0$. We have a boundary point of the vaporization type.

Special cases arise when $L''(\beta_0) = 0$ or $1 + \lambda_0^2(\partial L/\partial\lambda)_0 = 0$. They are connected with the critical point. In view of the importance and special physical interest of these cases, they will be specially studied in a separate communication, and we shall not consider them at present.

Thus boundary points of the second type are such that on one side of them,

$$g(r) = 1 + \frac{A_1}{r}e^{-|\alpha_1|r}\cos(\beta_1 r + \delta_1) \quad (r \gg \sigma) \quad (39)$$

(stable states), and on the other,

$$g(r) = 1 + \frac{A_1}{r}\cos(\beta_1 r + \delta) \quad (r \gg \sigma) \quad (40)$$

(absolutely unstable states). At the very boundary point $\alpha_1(\lambda_0) = 0$, but $\beta_1(\lambda_0) \neq 0$. Equally possible are the special cases noted above, when the point λ_0 is an isolated unstable point and Eq. (39) is correct on both sides.

The question of the thermodynamic properties of a system in the vicinity of a boundary point is very important. But now, unfortunately, in contrast to the case taken up in Sec. 2, our method, which is based only on a study of the behavior of $g(r)$ for $r \to \infty$, yields almost nothing. If, as is usually done, we make use of the relation

$$\frac{4\pi}{v}\int_0^\infty (g(r) - 1)\,r^2\,dr = \frac{kT}{v^2(-\partial p\ \partial v)_T} - 1, \quad (41)$$

it will then turn out that $(-\partial p/\partial v)_T = 0$ at the boundary point, in conformity with thermodynamic theory[10]. But, as we have seen in reference 1, Eq. (41) cannot be considered proved in the neighborhood of a boundary point. It is very important that this relation in the form (41), or with slight modifications, actually be correct. However, its proof represents a very difficult problem.

In conclusion we consider the distribution of boundary points on the λ axis. For $\lambda \to 0$, as we have seen, all the $|\alpha_n| \to \infty$. For increasing λ the first boundary point will always be of the type of a gaseous condensation or a crystallization. If subsequently $\alpha_1(\lambda)$ nowhere ceases to be equal to zero, then we have the case shown in Fig. 1*a*. A

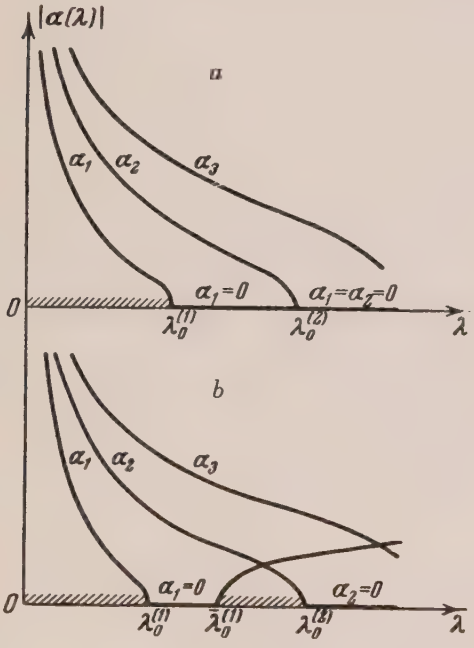

Fig. 1

homogeneous phase is possible only in the interval $0 \leq \lambda < \lambda_0^{(1)}$ (shown hatched in the figure). This corresponds to the behavior of a real system for $T > T_{cr}$ or $T < T_{tr}$. However, it is possible that $\alpha_1(\lambda)$, equal to zero in a certain interval $\lambda_0^{(1)} \leq \lambda \leq \bar{\lambda}_0^{(1)}$, may subsequently be different from zero, and in this case $\lambda_0^{(1)}$ lies on the left side of the first zero of $\alpha_2(\lambda)$. This case is shown in Fig. 1*b*. The spectrum of eigenvalues of the parameter λ now consists of two continuous bands: $0 \leq \lambda < \lambda_0^{(1)}$ and $\bar{\lambda}_0^{(1)} < \lambda < \lambda_0^{(2)}$, where a homogeneous phase is possible. This corresponds to the behavior of a real system for $T_{tr} < T < T_{cr}$. The left band corresponds to a gas, the right to a liquid. Note that in Fig. 1*b* we have for clarity introduced a notation not in full agreement with the general theory, since for those values of λ where $|\alpha_1| > |\alpha_2|$ (see the Figure) a larger $|\alpha_n|$ corresponds to a smaller number γ_n. Strictly speaking, it follows that we should rename α_2 as α_1, and vice versa.

The positions of the points $\lambda_0^{(1)}$, $\bar{\lambda}_0^{(1)}$ and $\lambda_0^{(2)}$ on the λ axis depend on the temperature. On variation of the latter it can happen that the points $\lambda_0^{(1)}$ and $\bar{\lambda}_0^{(1)}$ will coincide. This clearly corresponds to the critical temperature and the density $\lambda = \lambda_0^{(1)} = \bar{\lambda}_0^{(1)}$ is the density of the liquid at the critical point. It may happen also that on variation of the temperature the points $\bar{\lambda}_0^{(1)}$ and $\lambda_0^{(2)}$ will coincide, and this clearly corresponds to the triple point (more truly to its analogy on the limiting line of stability, since literally the triple point lies on an equilibrium phase transition line).

5. EXAMPLE OF A SYSTEM WITH BOUNDARY POINTS OF THE SECOND TYPE

Let us consider the problem of the determination of the minimum volume for which a system of a great number of hard noninteracting spheres of diameter a in "thermal agitation" can be homogeneous (that is, disordered). This problem has been solved earlier by another method[13-15] and is introduced here for the purpose of illustrating the theory developed above. But it must be noted that the correct result was obtained in these researches by a method that was not rigorous: the boundary value λ_0 signifying the maximum possible density of the system was obtained from an analysis of an approximate equation which was true only for small densities, and hence one cannot be sure that this λ_0 will be conserved at large densities in the more rigorous theory.

In dimensionless units of length we have for $\Phi(r)$

$$\Phi(r) = +\infty, \quad \text{if} \quad r < 1; \qquad (42)$$

$$\Phi(r) = 0, \quad \text{if} \quad r > 1,$$

---

[13] J. Kirkwood, J. Chem. Phys. **7**, 919 (1939)

[14] J. Kirkwood and E. Monroe, J. Chem. Phys. **10**, 394 (1942)

[15] J. Kirkwood, B. Mann and B. Alder, J. Chem. Phys. **18**, 1040 (1950)

so that

$$(e^{-\Phi(r)/kT})' = \delta(r-1), \tag{43}$$

and the number σ is equal to $1+0$. By means of Eqs. (4) amd (5) we find further

$$K(z) = {}^1/_2\, u(1)(z^2-1), \tag{44}$$

$$L(\gamma) = 2u(1)\gamma^{-3}(\gamma\cos\gamma - \sin\gamma). \tag{45}$$

since $L(0) = -2/3\, u(1) < 0$, then there are no boundary points of the first type, and $\gamma \neq 0$. Equations (34), basic for finding λ_0, can be written in the form

$$2\lambda u(1)\beta^{-3}(\beta\cos\beta - \sin\beta) = 1, \tag{46}$$
$$\beta^{-4}((3-\beta^2)\sin\beta - 3\beta\cos\beta) = 0.$$

The problem comes down to a solution of the transcendental equation

$$\operatorname{tg}\beta = 3\beta/(3-\beta^2). \tag{47}$$

Its solution is

$$\beta_n = n\pi\left\{1 - \frac{3}{(n\pi)^2} - \frac{9}{(n\pi)^4} - \frac{81}{5(n\pi)^6} - \frac{1701}{16(n\pi)^8} - \cdots\right\}, \tag{48}$$

with $n = 2, 3, 4, \ldots$. This leads, according to the first of the Eqs. (46), to the result

$$(2\lambda u(1))_n = (-1)^n\left\{(n\pi)^2 - \frac{9}{2} - \frac{43}{8(n\pi)^2} - \frac{4991}{112(n\pi)^4} - \cdots\right\}. \tag{49}$$

In order to determine the necessary value of n, we note that all odd n disappear as negative densities are approached. Among the even n the one which gives the smallest λ_0 must be chosen (Fig. 1*a*). This determines the choice $n = 2$, so that

$$(2\lambda u(1))_{\lim} = 4\pi^2 - \frac{9}{2} - \frac{43}{32\pi^2} - \frac{4991}{1792\pi^4} - \cdots = 34.812. \tag{50}$$

If the results of the direct numerical integration of Bogoliubov's equation for $g(r)$ for the problem under consideration[15] are used, then it is found that, for $2\lambda u(1) = 34.8$, the value of $u(1)$ is 2.90, which leads, according to Eq. (4), to the following value for the limiting volume:

$$v_{\lim} = (\pi a^3/3) = 2v_0, \tag{51}$$

where v_0 is the volume of a single spherical particle. The limiting volume does not depend on the temperature. By. Eqs. (6), (33) and (51) we find the limiting pressure to be

$$p_{\lim}(T) = \frac{3.4}{v_0}kT \tag{52}$$

("fusion curve" of a system of hard noninteracting spheres).

In conclusion we note that if we formally set $E = -1$ in the equations considered in Sec. 3 of the problem, they go over into the equations just considered. In connection with this the statement made without proof in Sec. 3, namely, that Eq. (27) gives the smallest value of λ_0 for which $\alpha_n = 0$, becomes evident. If we actually substitute $n = 3, 5, 7, \ldots$ into Eqs. (49), we arrive at values of the density λ_0 greater than we obtain from Eq. (27).

Translated by Brother Simon Peter, F.S.C.
78

The Stability of Homogeneous Phase. III
THEORY OF THE CRYSTALLIZATION CURVE

I. Z. FISHER
Byelorussian State University

(Submitted to JETP editor March 26, 1954)
J. Exper. Theoret. Phys. 28, 447-451 (April, 1955)

A theoretical justification of an empirical law by Simon for pressure along the melting curve of ordinary materials is given. Theory is compared with experimental results.

1. INTRODUCTION

THE most significant and physically interesting problem of the theory of the stability of the liquid state is the study of the loss of stability of a liquid due to its crystallization. This is the problem of the "theory of crystallization" or the "theory of melting". For simple systems like argon the empirical relation of Simon gives the equation of the melting curve in the p- T plane as follows[1]:

$$p_{\text{melt}}(T) = -A + BT^m, \tag{1}$$

which is correct with sufficient accuracy in a very broad range of temperatures and pressures. Here A, B, and m are constants. For argon, for example,

$$A = 3000 \text{ kg/cm}^2; \tag{2}$$

$$B = 2.73 \text{ kg/cm}^2 \text{ (degree)}^m; \quad m = 1.288.$$

The recent experimental results verified the correctness of Simon's relation[2,3].

The major task of the "theory of crystallization" should be the theoretical derivation of Eq. (1). Domb[4] has given a physical interpretation of Eq. (1) in terms of the known melting theory[5,6], which considers melting as an order-disorder transition of binary alloy of atoms and vacant cells. Since the physical foundations of this latter theory are doubtful, Eq. (1) still remains theoretically unexplained.

In the present work it will be shown that the problem of the theoretical derivation of the empirical relation (1) can be solved using the theory of the limit of stability of a homogeneous phase, developed in references 7,8.

2. THE LIMIT OF STABILITY OF HOMOGENEOUS PHASE FOR THE INVERSE POWER LAW MODEL

We consider a system of particles with intermolecular potential of the form

$$\Phi(r) = 4\varepsilon (a_0/r)^n \tag{3}$$

("inverse law model"). Here ϵ is a constant with the dimensions of energy, a_0 is a constant of the dimension of length, and n is some number which we shall consider large. We shall introduce dimensionless length using as a unit of length the quantity $a = a_0 (4\epsilon/kT)^{1/n}$ so that

$$r \to \rho = \frac{r}{a_0}\left(\frac{kT}{4\varepsilon}\right)^{1/n} \tag{4}$$

Then

$$e^{-\Phi(r)/kT} = e^{-1/\rho^n}, \tag{5}$$

and the parameter λ of the general theory[7,8] is equal to

$$\lambda = \frac{2\pi a^3}{v} = \frac{2\pi a_0^3}{v}\left(\frac{4\varepsilon}{kT}\right)^{3/n} \tag{6}$$

Furthermore, the solution $K(\zeta)$ of the integral equation which determines the behavior of the radial function as $g(\rho)$ approaches infinity, turns out to be (cf. reference 7)

$$K(\zeta) = {}^1/_2 \int_{|\zeta|}^{\infty} (e^{-1/\rho^n})' u(\tau)(\zeta^2 - \tau^2)\, d\tau. \tag{7}$$

If the number n is sufficiently large, then the function $(e^{-1/\rho^n})'$ has a sharp maximum in the neighborhood of the point $\rho = 1$ and vanishes very

[1] F. Simon, M. Ruhemann and A. Edwards, Z. Phys. Chem. B6, 331 (1930)

[2] P. Bridgman, *Physics of High Pressure*

[3] P. Bridgman, *New Research in the Region of High Pressures*

[4] C. Domb. Phil. Mag. 42, 1316 (1951)

[5] J. Lennard-Jones and A. Devonshire, Proc. Roy. Soc. 169 A, 317 (1939)

[6] J. Lennard-Jones and A. Devonshire, Proc. Roy. Soc. 170 A, 469 (1939)

[7] I. Z. Fisher, J. Exper. Theoret. Phys. USSR 28, 171 (1955); Soviet Phys. 1, 154 (1955)

[8] I. Z. Fisher, J. Exper. Theoret. Phys. USSR 28,437 (1955); Soviet Phys. 1, 273 (1955)

rapidly for all other ρ. Furthermore, the integral of this function from $\rho = 0$ to $\rho = \infty$ is equal to unity and the following relation holds

$$(e^{-1/\rho^n})' \to \delta(\rho - 1), \quad \text{if} \quad n \to \infty. \tag{8}$$

If n is finite, but sufficiently large, then in the first approximation we can substitute a δ-function instead of $(e^{-1/\rho^n})'$ in Eq. (7). Finally we obtain

$$K(\zeta) \approx {}^1/_2\, u(1)(\zeta^2 - 1), \quad \text{if} \quad \zeta \ll 1, \tag{9}$$

$$K(\zeta) \approx 0, \quad \text{if} \quad \zeta > 1.$$

In this approximation the solution $K(\zeta)$ is identical with the solution $K(z)$ of the problem of hard non-interacting spheres which was considered in detail in reference 8. We can write then

$$(2\lambda u(1))_{\lim} = 34.81; \quad (u(1))_{\lim} = 2{,}90 \tag{10}$$

(cf. reference 8). Using Eq. (6) we find then that

$$v_{\lim}(T) \approx \frac{\pi a_0^3}{3}\left(\frac{4\varepsilon}{kT}\right)^{3/n}. \tag{11}$$

Furthermore, we have from the general theory the following relation for pressure

$$\frac{pv}{kT} = 1 + \frac{\lambda}{3}\int_0^\infty (e^{-1/\rho^n})'\, u(\rho)\, \rho^3 d\rho \tag{12}$$

$$\approx 1 + \frac{\lambda}{3}u(1),$$

so that according to Eq. (10), $(pv/kT)_{\lim} = 6.80$ and, using Eq. (11), we obtain

$$p_{\lim}(T) \approx \frac{20.4}{\pi a_0^3}\,\frac{(kT)^{1+3/n}}{(4\varepsilon)^{3/n}}. \tag{13}$$

The Eqs. (11) and (13) describe in an exhaustive manner the limit of stability of homogeneous phase for the inverse law model for large values of n. As $n \to \infty$, the derived equations become exact expressions for the problem of hard spheres, as should be expected. The result allows an elementary physical interpretation[9]. The particles, according to Eq. (3), possess a property of natural compressibility and their effective diameter, i.e., the smallest separation to which two particles can come, depends on the energy of the colliding particles. It is evident that we can write for the effective diameter

$$\Phi(a_{\text{eff}}) \sim kT, \tag{14}$$

so that Eq. (3) yields

$$a_{\text{eff}} \sim a_0(4\varepsilon/kT)^{1/n}; \quad (v_0)_{\text{eff}} \sim v_0(4\varepsilon/kT)^{3n}. \tag{15}$$

Since for spheres of constant natural volume v_0 we have, according to Eq. (8) $v_{\lim} = 2v_0$, so that we obtain from Eq. (15)

$$v_{\lim}(T) \sim 2(v_0)_{\text{eff}} \sim 2v_0(4\varepsilon/kT)^{3n}, \tag{16}$$

which is the previous result. An elementary proof of the relation (13) follows from this expression and the equation of melting curve of a system of hard spheres[8] $p_{\text{melt}} = (3.4/v_0)\,kT$.

3. TRANSITION TO REAL SYSTEMS AND COMPARISON WITH EXPERIMENTAL DATA

The model discussed so far differs from real systems mainly because it neglects intermolecular forces of attraction. These forces can be included by considering, instead of the potential (3), the potential usually employed.

$$\Phi(r) = 4\varepsilon\{(a_0/r)^n - (a_0/r)^6\}, \tag{17}$$

where the term r^{-6} has been added to the potential (3). However, a rigorous solution of the problem for such potential encounters serious mathematical difficulties. The problem can be solved approximately if we take into account in the main term of Eq. (17) only repulsive forces, and then introduce a correction for forces of attraction. This is entirely correct at high temperatures when the crystallization (and even more, the absolute loss of stability of the liquid) takes place at very high pressures, so that the density of the particles is very large. Under such conditions the repulsive force of particles strongly compressed by the external pressure are the most important, and the forces of attraction play only a secondary role.

In this case the main member determining the pressure at the limit of stability of liquid appears to be Eq. (13). To this pressure it is necessary to add a correction which accounts for the attractive forces between particles. Such correction is, evidently, the "internal pressure" of a liquid which is opposite in sign, so that

$$p_{\lim}(T) \approx -|p^{(\text{int})}| + \frac{20.4}{\pi a_0^3}\,\frac{(kT)^{1+3/n}}{(4\varepsilon)^{3/n}}. \tag{18}$$

The internal pressure turns out to be only slightly dependent on temperature at the very high densities which are present during crystallization and at the limit of stability of the liquid. As a first approximation we can consider this internal pressure to be a constant quantity, and then dimensional

[9] I. Fisher Usp. Fiz. Nauk **51**, 71 (1953)

considerations lead to $p_{int.} \sim (\epsilon/a_0^3)$. In such a way we finally obtain

$$p_{lim}(T) \approx -\gamma \frac{\varepsilon}{a_0^3} + \frac{20.4}{\pi a_0^3} \frac{(kT)^{1+3/n}}{(4\varepsilon)^{3/n}}, \qquad (19)$$

where γ is some dimensionless coefficient of the order of unity.

A direct comparison of the theory with experimental results is not possible because of the lack of quantitative data on the behavior of the curve of the limiting stability of supercooled liquids. However, it is possible to assume that the difference in behavior of this curve from the curve of equilibrium phase transition from liquid to crystal is not important for liquids similar to argon. Then a possibility appears to interpret the relations (11) and (19) as referring to the crystallization curve, and compare them with the experimental data. It is well known that the potential (17) corresponds to the experimental results for compressed gases most accurately when $n \sim 10 - 12$. The investigation of the second virial coefficient results in the following values for a_0 and ϵ for argon [10]:

$$a_0 = 3.50 \cdot 10^{-8} \text{ cm}; \quad \varepsilon = 13.9 \cdot 10^{-15} \text{ erg}, \qquad (20)$$

$$\text{if} \quad n = 10,$$

$$a_0 = 3.41 \cdot 10^{-8} \text{ cm}; \quad \varepsilon = 16.5 \cdot 10^{-15} \text{ erg},$$

$$\text{if} \quad n = 12$$

We shall use these data to verify the theory, assuming that Eq. (11) and (19) apply to the melting curve.

The data for pressure: It is immediately evident that the temperature dependence of p_{melt} of the theoretical expression (19) is the same as for the experimental law (1). The constant m in Eq. (1) is

$$m = 1 + \frac{3}{n} = \begin{cases} 1.30, & \text{if} \quad n = 10, \\ 1.25, & \text{if} \quad n = 12, \end{cases} \qquad (21)$$

which agrees very well with the experimental data (2). For the coefficients A and B in Eq. (1) we have

$$A = \frac{\gamma\varepsilon}{a_0^3}; \quad B = \frac{20.4 \cdot k^{1+3/n}}{\pi a_0^3 (4\varepsilon)^{3/n}} \qquad (22)$$

The substitution of the values (20) results in evaluation of the quantity $\gamma \sim 7 - 9$ which is quite satisfactory. Finally the numerical evaluation of B results in

$$B = \begin{cases} 3.47 \text{ kg/cm}^2 \text{ (degree)}^{1.30}, & \text{if} \quad n = 10, \\ 4.54 \text{ kg/cm}^2 \text{ (degree)}^{1.25}, & \text{if} \quad n = 12. \end{cases} \qquad (23)$$

The agreement with the experimental data (2) within an order of magnitude is good, but the theoretical values are somewhat too high. This can be partially explained by the fact that Eq. (19), strictly speaking, applies only to the limiting pressure of the supercooled liquid which should be somewhat larger than the pressure of the equilibrium crystallization.

THE DATA FOR VOLUME: A comparison of the theoretical result (11) with the experimental data for volume of liquid undergoing equilibrium crystallization is given in Table 1. The second column of the table is computed from the data of reference 11. The third and fourth columns are computed from Eq. (11), using Eq. (20).

In this manner we find that the theory describes well the general behavior of the change of the limiting volume of the liquid and leads to values of the correct order of magnitude for the limiting volume of the liquid. Numerically the volume computed from the theoretical expressions is somewhat too large.

TABLE 1

T°K	$(v_{liq})_{melt} \times 10^{23}$ cm³ Experimental	$(v_{liq})_{lim} \times 10^{23}$ cm³ Theoretical	
		$n = 10$	$n = 12$
83.9	4.63	7.20	6.41
126.3	4.33	6.39	5.82
162.0	4.20	5.94	5.49
193.1	4.14	5.53	5.24

THE DATA FOR (pv): The experimental data for the melting curve result in a linear temperature dependence of the quantity $[(p + A)\, v]_{melt}$, where A is the internal pressure from Eq. (1):

$$[(p + A)\, v]_{melt} = CT. \qquad (24)$$

This relation is easily derived from the numerical data of reference (11). The theory results in the same conclusion. From Eqs. (11) and (19) we find that theoretically the following relationship holds:

$$\left[\left(p + \gamma \frac{\varepsilon}{a_0^3}\right) v\right]_{lim} = 6.8\, kT. \qquad (25)$$

[10] P. Fowler and E. Guggenheim, *Statistical Thermodynamics*

[11] O. Rice, J. Chem. Phys. 7, 136 (1939)

A comparison of the coefficients of T on the right hand side of Eqs. (23) and (24) shows that they are of the same order of magnitude. This fact should be evident from the data for p and v already discussed.

4. DISCUSSION OF RESULTS

The results of comparison of the theory with the experimental data show that the inverse law model can be used as a first approximation to describe the properties of the melting curve or real liquids. It was already pointed out at the beginning of Part 3 that the inverse law model is not appropiate at low temperatures and should become more accurate with higher temperatures. This expectation is verified by the data in Table 1. The remaining disagreement in numerical values of the volume v_{melt} and v_{lim} can be partly explained in the following manner. A correction of the same origin as the correction for internal pressure in p_{lim} (T) should have been introduced in v_{lim} (T). It is physically evident that this correction would diminish the numerical values of v_{lim} (T) and so improve the agreement with experimental results.

Another source of inaccuracy in the numerical evaluations of the theoretical results enters in a_0 and ϵ which is derived by us from the data for only moderately compressed gases. Generally speaking, using such data for liquids is not correct since the collective interaction of particles causes the interaction potential of two particles in the liquid to be different from that of an isolated pair of particles.

It can be concluded that the general theory of the limit of stability of a homogeneous phase developed in references 7,8 describes correctly the basic behavior of the melting curve (crystallization curve) of real systems.

Translated by M. J. Stevenson
79

The Decay Laws of the Afterglow of Zinc Sulfide Phosphors in the Temperature Extinction Region

F. I. VERGUNAS AND N. L. GASTING
Siberian Physico-Technical Institute,
Tomsk State University

(Submitted to JETP editor March 30, 1953)
J. Exper. Theoret. Phys. USSR **28**, 352-360 (March, 1955)

Results are presented of an investigation of the effect of temperature and intensity as well as the length of excitation on the decay law of the afterglow of some zinc sulfide phosphors near and in the extinction region.

1. PRESENTATION OF THE PROBLEM

THE laws of the afterglow of zinc-sulfide phosphors in the low temperature region, where the length of the afterglow is considerable, have been studied sufficiently fully. In spite of this, there is no uniform point of view on the fundamental decay law of the afterglow. Three laws: the exponential[1], the square law[2] and Adirovich's law[3] figure in the literature as fundamental decay laws. This state of the question is explained by the absence of experimental data which confirms beyond dispute the use of any one of these laws.

The ability to explain the behavior with temperature may be taken as a criterion of the correctness of a theory. Investigations of the laws of the afterglow in the temperature extinction region can serve as a test of the theory. It is worth noting that these investigations have value not only as control experiments, but have an independent interest, inasmuch as the decay laws in the extinction region have been comparatively little studied.

The present work contains a description of some investigations carried out by us on the afterglow of some zinc sulfide phosphors in the extinction region.

2. LAWS OF THE AFTERGLOW OF ZnS-Cu PHOSPHORS

Two ZnS-Cu phosphors with a copper concentration of 10^{-4} gm/gm were studied. In the process of preparation, one was heated to 900 °C, the other to 1100 °C. For both samples, qualitatively identical laws were obtained. The curves given below are for only one sample, namely the one heated to 1100 °C.

The sample was studied in the form of a thin (3 mg/cm^2) layer of powder. The phosphor was heated and cooled in vacuum. It was excited with light from a mercury lamp (the 365 mμ triplet). Decay curves were taken visually with the aid of a Pulfrich photometer. Measurements in all cases were begun within 0.7 second after turning off the exciting light.

Temperature extinction of the green zone of the ZnS-Cu phosphor began at 444 °K. The afterglow, however, was studied in the interval 398-506 °K, i.e., near and in the extinction region. The investigations were carried out with both continuous (strong and weak) and instantaneous excitation. Sample and arrangement remained unchanged throughout the measurements. For all conditions of excitation, the temperature behavior of the total light was determined.

Three series of measurements were made in all. The first series was from strong excitation to equilibrium (excitation time 30 sec). The second series was from weak excitation to equilibrium (excitation time 1 min), with the intensity of the exciting light 10 times less than in the first series. The third series was with instantaneous excitation. The intensity of the exciting light was the same as in the first series, but the time of excitation was 0.01 sec.

The decay curves corresponding with strong continuous excitation are presented in log-log and semi-log coordinates in Fig. 1, *a* and *b*. It can be seen that near extinction (397-431 °K) they approximate to a 1.72 power law, with the exponent independent of the temperature. In the extinction region, the exponent increases. At the temperatures 476 and 488 °K, the initial part of the curve approximates an exponential while the remainder of the curve is a power law. The exponentials in Fig. 1*b* are continued dotted. At temperatures 499 °K and higher the curves are exponentials from beginning to end.

[1] G. F. Garlik and A. F. Gibson, Nature **158**, 704 (1946); Proc. Phys. Soc.(London) **60**, 574 (1948); G. F. Garlik and M. H. Wilkins, Proc. Roy. Soc. (London) **184A**, 408 (1945); J. T. Randall, Proc. Roy. Soc. (London) **184**, 365,374 (1945); J. T. Randall and M. H.F.Wilkins, Proc. Roy. Soc. (London) **184**, 390(1945)

[2] V. V. Antonov-Romanovskii, Trudy Fiz. Inst. Akad. Nauk SSSR **1**, 35 (1937); **2**, 157 (1942)

[3] E. I. Adirovich, *Some Questions on the Theory of the Luminescence of Crystals*, Gostekhizdat, (1951)

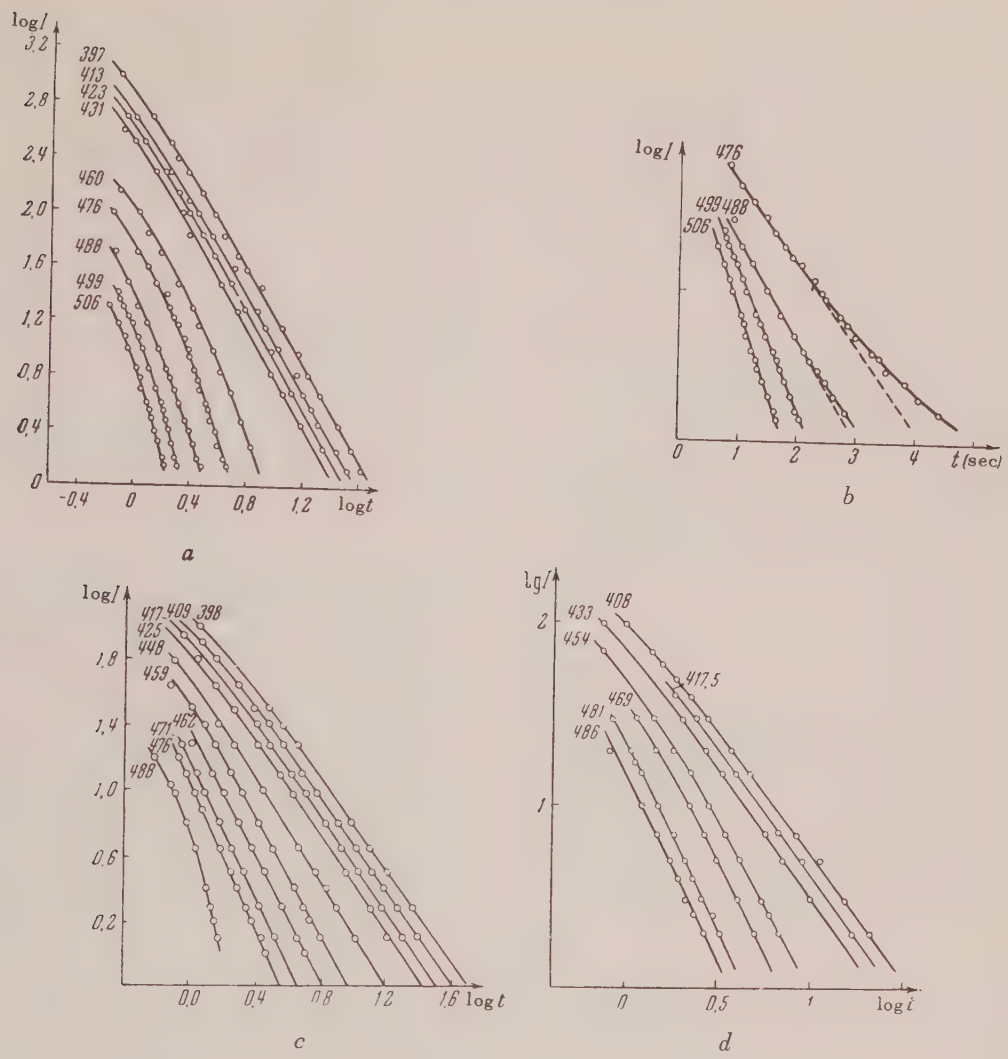

Fig. 1. Decay curves of the afterglow of a ZnS-Cu phosphor. *a* and *b* - Continuous strong excitation; *c*-continuous weak excitation; *d*-instantaneous exitation.

From the slopes of the exponentials the time constants p were determined. They varied with temperature according to the law $p = p_0 e^{-\epsilon/KT}$

With weak continuous excitation, the decay curves, both in and near the extinction region were power law (Fig. 1 *c*). Near the extinction (398-425 °K), the exponent α did not change with temperature, and was equal to 1.44. In the extinction region (448-476 °), it increased with temperature. An analogous behavior of α for ZnS-Cu phosphors was found in reference 4. The last curve ($T = 488$°K) in Fig. 1*c* was an exponential.

The results of the measurements for instantaneous excitation are given in Fig. 1*d*. Near extinction (408-433 °K) the decay curves follow a 1.37 power law. In the extinction region, beginning at 469 °K, they are square law. In the interval 433-469 °K, the exponent varies from 1.37 to 2.

Comparing Figs. 1 *a*, *b*, *c* and *d*, it is seen that under all conditions of excitation, the decay is power law near extinction, with only a change in the value of the exponent from one condition to another. In the further stages of temperature extinction, i.e., at the highest temperatures studied, the decay curves approximate exponentials for both strong and weak excitation. In the transition region the decay law is more complicated. By transition region we mean the temperature interval in which , with strong continuous excitation, the initial exponential decay goes over into a power law. This region corresponds to the initial stages of tempera-

4 V. A. Iastrebov, Trudy Fiz. Inst. Akad. Nauk SSSR 3, 123 (1946)

ture extinction. In a given region, the decay law depends upon the intensity of the excitation, and whether it is continuous or instantaneous. Thus, for example, in the temperature interval 469-481 °K with strong continuous excitation the decay curves are exponentials in the initial stages (Fig. 1b) and go over into power laws later on. With weak continuous excitation, they are power laws (Fig. 1c). With instantaneous excitation, they are square law (Fig. 1d).

Some quantitative characteristics were determined from the curves. Thus, from the temperature variation of the time constants of the exponentials (Fig. 1b), the energy ϵ_1 was determined. From the displacements Δ, parallel to the axis of log t, of the square law curves in the extinction region and the power law curves near extinction (Fig. 1d), using the method of Antonov-Romanovskii[5] the depth of the localized levels ϵ_1 was determined from the formula:

$$\Delta = \frac{\varepsilon_1}{4{,}6\,k}\left(\frac{1}{T_1} - \frac{1}{T_2}\right). \qquad (1)$$

The values of the activation energy are given in Table 1. From the table it is obvious that the energies, determined from the displacements Δ, have different values depending upon whether they are in or near the extinction region. In the extinction region greater values of the activation energy were obtained than near extinction. An analogous result was found in reference 5.

For all conditions of excitation, the total light radiation was determined planimetrically from the curves of intensity against time. We corrected the temperature variation of the total radiation to temperature extinction, although other authors do not do this[4]. In Fig. 2, to coordinates of log L against $1/T$, is plotted the temperature dependence, corrected to extinction, of the total light for a series of curves, taken with continuous weak excitation. From the Figure it is obvious that this dependence is described by two intersecting straight lines, with the slope of the line in the extinction region greater than near extinction.

From the temperature variation of the total light near extinction the depth of the localized levels ϵ[4] was determined from the formula:

$$L = L_0 e^{\varepsilon/2kT} \qquad (2)$$

From the same formula, the activation energy in the extinction region was determined. The results are given in Table 1. Values of the activation energy obtained for other conditions of excitation are given in the same Table.

From the Table it is obvious that, independent of the condition of excitation, practically identical values are obtained for the activation energy from the temperature variation of the total light. We are the first to have noticed this result.

The values of the activation energy obtained for a ZnS-Cu phosphor heated to 900 °C are likewise given in Table 1.

In order to test whether or not the laws which we

TABLE 1

Activation energy ev			Phosphors			
			ZnS-Cu	ZnS-Cu Heated to 1100 °C	ZnS-Cu Heated to 900 °C	ZnS-Cu,Co
From the temperature variation of the Time Constant of the Exponential			0.23	0.67	0.17	1.57
From the displacement Δ	Near Extinction			0.62	0.22	
	In the Extinction region			1.38	0.63	2.12
From the temperature variation of the total light radiation	near extinction	strong excitation		0.64		
		weak excitation		0.63	0.2	
		instantaneous excitation		0.6		
	in the extinction region	strong excitation				2.38
		weak excitation		1.33	0.68	
		instantaneous excitation		1.35		2.10

[5] V. V. Antonov-Romanovskii, Doklady Akad. Nauk SSSR 17, 95 (1937)

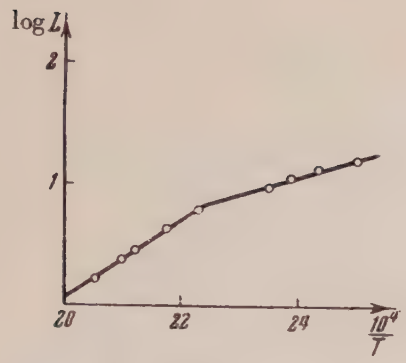

Fig. 2. Temperature variation of the light sum for a ZnS-Cu phosphor with continuous weak exitation.

observed for a ZnS-Cu phosphor are general for all zinc sulfide phosphors and likewise to study the decay law over a large interval of intensity, we investigated two more phosphors: ZnS-Cu,Co and ZnS-Zn.

3. THE DECAY LAWS OF THE PHOSPHOR ZnS-Cu,Co

A characteristic peculiarity of the temperature extinction curve of the green zone of this phosphor (Cu concentration 10^{-5} gm/gm, Co concentration 10^{-5} gm/gm) is that there are two temperature drop offs[6]. In the interval 170-270 °K, the first drop off is observed, then there is an increase in intensity, and beginning with 390 °K, the second drop off is observed. We studied the decay law only in the region of the second drop off. Three series of measurements were carried out. The first series: continuous strong excitation, excitation time 1 min. The second series: continuous weak excitation, excitation time 1 min , the intensity of the exciting light 20 times weaker than in the first series. Third series: instantaneous (0.2 sec) excitation, the intensity of the exciting light the same as in the first series.

The decay curves obtained with continuous strong excitation are given in log-log and semi-log coordinates in Fig. 3a,b, and c. From Fig. 3b it is obvious that at the beginning of extinction (444-470 °K) the decay curves are exponentials, going over in the further stages of decay to power laws, the transition being later, the higher the temperature. At temperatures 484-501 °K, the last points do not fit an exponential either (Fig. 3c). Beginning with 507 °K, the decay curves approximate exponentials from beginning to end of the measurement.

The results obtained for continuous weak excitation are given in Fig. 3d. It is obvious that at temperatures 473-494 °K, the decay law approximates a power law; at higher temeperatures (496-504 °K) it approximates an exponential.

Comparing Figs. 3b,c and d shows that in the case of a ZnS-Cu,Co phosphor, as well as in the case of a ZnS-Cu phosphor, the decay curves in the transition region essentially approximate exponentials with strong excitation, and approximate power laws with weak excitation.

For the temperature interval 481-508 °K, decay curves were taken for instantaneous (0.2 sec) excitation, Fig. 3e. From the Figure it is obvious that they approximate square laws. The last curve (T=508 °) is an exponential.

Thus for ZnS-Cu,Co phosphor in the transition region, depending upon the intensity and the continuity of excitation, the decay curves approximate exponentials, power or square laws.

From the extinction curves of this phosphor, the activation energies were determined 1) from the temperature variation of the time constant (Fig. 3c), 2) from the displacements of the square law curves (Fig. 3e) and 3) from the temperature variation of the light sums. The results are given in Table 1.

4. THE DECAY LAWS OF THE BLUE ZONE OF A ZnS-Zn PHOSPHOR

Investigations of a ZnS-Zn phosphor were carried out with a blue filter. The phosphorescence was measured near 203-264 °K and in the extinction region (264-323 °K).

The decay curves, obtained with continuous strong excitation, are given in log-log and semi-log coordinates in Fig. 4, the low temperature curves in Fig. 4a, the high temperature curves in Fig. 4b. It is obvious from Fig. 4a that at low temperatures the decay curves approximate power laws, the exponent of which depends on T (Fig. 5).

The curves corresponding to 283 °K are given in both log-log and semi-log coordinates (Figs. 4a and b). It is obvious that at this temperature the power law applies only to the latter part of the curve, while the initial part is described by an exponential.

Beginning at room temperature and higher, the decay curves are described by two intersecting exponentials. Obviously the decay laws of a ZnS-Zn phosphor are more complicated than for a ZnS-Cu phosphor, for which a single exponential was observed.

In Fig. 6 are given the exponentials obtained from analysis of complicated decay curves taken at

[6] F. I. Vergunas and Iu. M. Sainchenko, J. Exper. Theoret. Phys. USSR 14, 470 (1953)

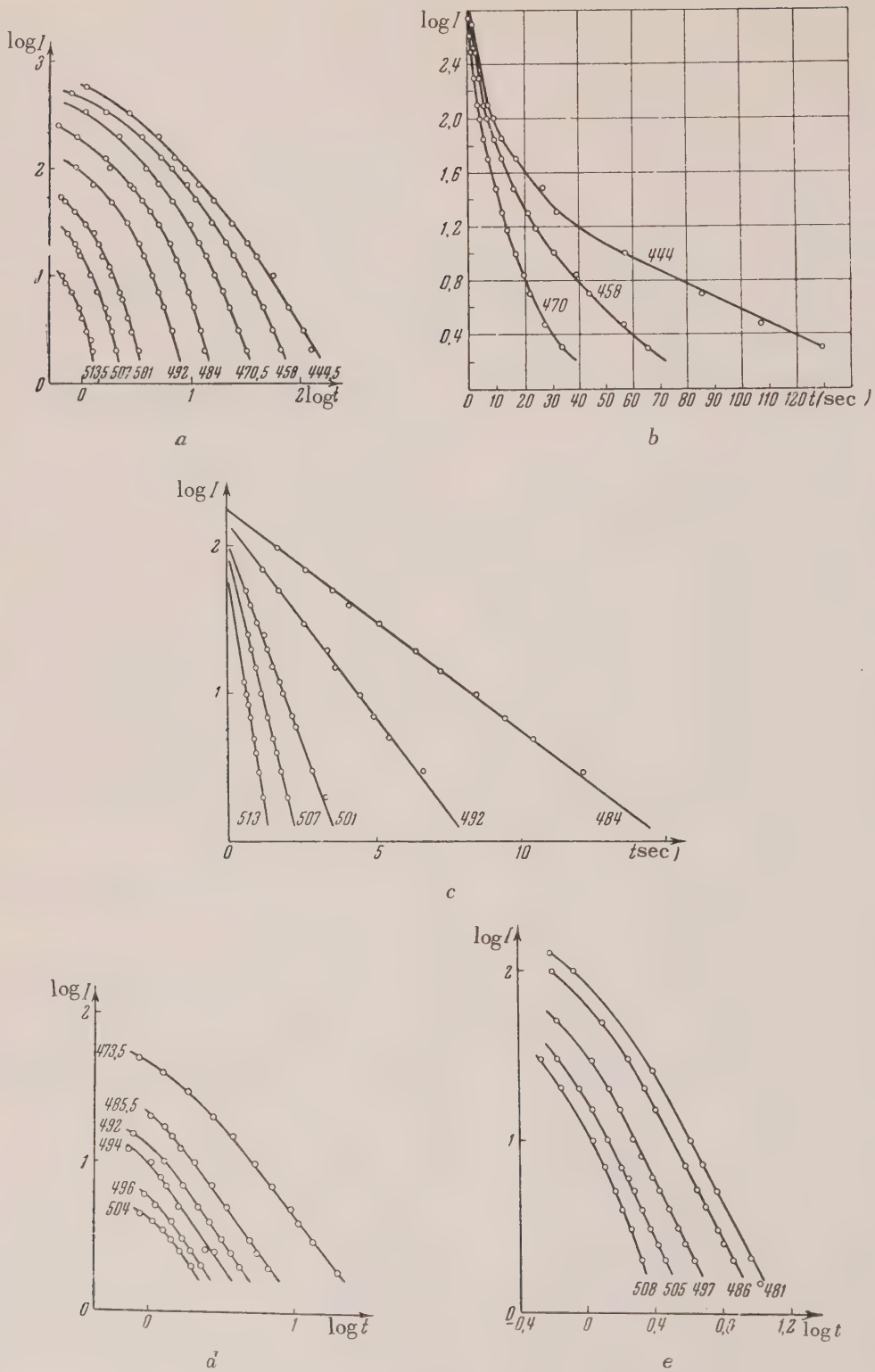

Fig. 3. Decay curves of the afterglow of a ZnS-Cu,Co phosphor. *a*, *b*, *c*,- continuous strong excitation; *d*- continuos weak excitation; *e*-instantaneous excitation.

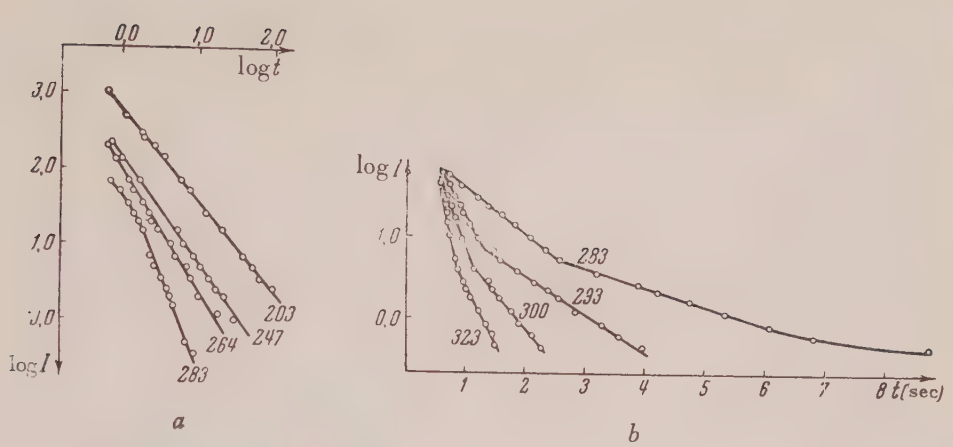

Fig. 4. Decay curves of a ZnS-Zn phosphor. *a*- at low temperatures, *b*- at high temperatures.

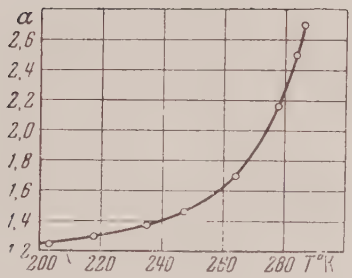

Fig 5. Dependence of the exponent α on temperature for a ZnS-Zn phosphor.

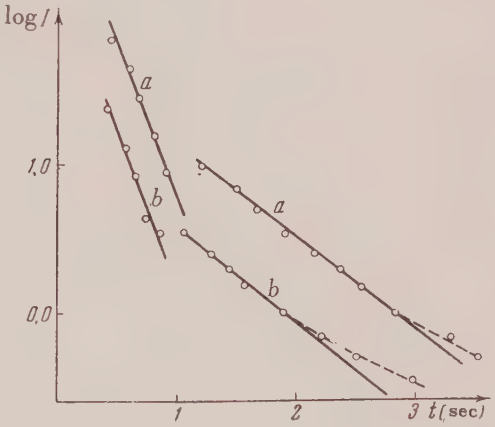

Fig. 6. Decay curves of a ZnS-Zn phosphor, obtained from the analysis of complex curves. $T = 292\,^{\circ}$K. *a*-intensity of the exciting light $E = 1$; *b*- $E = 0.14$.

292 °K with two different intensities E of the exciting light. From the Figure it is clear that the slope of the straight lines does not change appreciably with a sevenfold diminution in E. However the last points fit a power law, shown dotted. The less the intensity of the exciting light, the earlier the transition from exponential to power law. The exponentials in the figure are continued as solid lines.

The effect of the intensity of the exciting light on the decay law in the transition region was investigated at one temperature, 283 °K. In Fig. 7, curves are given in log-log and semi-log coordinates, taken at different intensitis E. From the Figure it is clear that for $E = 1$ the luminescence goes exponentially at the start, then the curve goes over into a power law. For $E = 0.14$ and 0.02 the exponential part is missing; the decay goes as a power law, its slope decreasing with decreasing E. Accordingly, in the transition region, with decreasing intensity of the exciting light, the exponential decay law goes over into a power law. Thus in the blue zone of the ZnS-Zn phosphor the same laws were found as for the ZnS-Cu and ZnS-Cu,Co phosphors

From the slopes of the exponentials corresponding with long afterglow times (Fig. 4b) the time constants were determined, and from their variation with temperature the activation energy ϵ_1 was determined.

5. CONCLUSIONS

The character of the afetrglow of all the phosphors investigated was the same; the decay law changed with temperature, and with the intensity of the exciting light. The effect of temperature was as follows: near extinction the decay curves

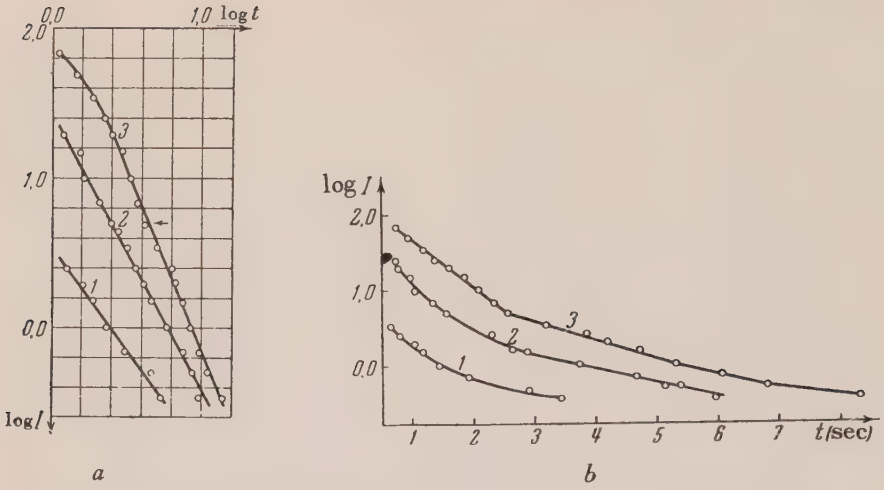

a *b*

Fig. 7. Decay curves of a ZnS-Zn phosphor taken for different values of intensity of the exciting light E. *a*-log-log plot; *b*- semi-log plot. *1* - $E = 0.02$, $\alpha = 1.36$; *2* - $E = 0.14$ $\alpha = 1.83$; *3*- $E = 1$, $\alpha = 2.5$.

were approximate power laws, the exponent of which did not depend appreciably on the temperature. In the extinction region the exponent increased with temperature, then the initial part of the curve went over into an exponential, while the last part remained as before an approximate power law. The higher the temperature, the later the transition from exponential to power law. At sufficiently high temperatures, the power law part disappeared, and the curves were approximately exponential from beginning to end.

The intensity and length of excitation showed the following effects: Near extinction the exponent of the power law decreased with decreasing intensity of the exciting light, but the form of the decay law did not change. Nor did the decay law change in the later stages of temperature extinction. Even at the highest temperatures the curves remained exponentials for strong and weak excitation. However in the transition region the decay law changed with change in intensity and length of excitation. For large intensities of the exciting light the exponential in the initial stages of the decay went over into a power law in the later stages, while for small intensities the exponential part disappeared, and the curves approximated power laws. For instantaneous excitation in the transition region square laws were obeserved.

In all the zinc sulfide phosphors a transition region exists in which, for the same sample, at the same temperature, one finds, depending upon the conditions of excitation, an exponential, a power law or a square law. From this condition it follows that neither the exponential nor the square law is the fundamental decay law for these phosphors.

The long argument between the adherents of the exponential vs. the square law as the fundamental law of decay, is explained, in our opinion, by the fact that comprehensive experiments on the laws of the afterglow had never been carried out on the same samples over a wide temperature interval, and with different conditions of excitation.

Conclusions on the afterglow laws were made on the basis of limited experiments.

The explanation of the laws obtained by us, as well as our opinion on the form of the fundamental decay law will be given in a following paper.

Translated by C. V. Larrick
59

The Absence of Stable Isotopes of Tc and Pm and Other Anomalies in the Distribution of β-stable Nuclei

A. V. SAVICH
Moscow

(Submitted to JETP editor Oct. 12, 1953; resubmitted Oct. 25, 1954)
J. Exper. Theoret. Phys. USSR **28**, 361-368(April, 1955)

Rules are established for the distribution of atomic nuclei on the nuclear diagram; these rules are based on a criterion of the maximum binding energy of the isobar. All violations of these rules are linked to the filling of the nuclear shells. The absence of stable isotopes of the Tc and Pm is one of the particular cases of a violation of this type.

TO formulate the distribution rules for atomic nuclei, we use the criterion of maximum binding energy of an isobar: nuclei with the most densely packed neutrons and protons for a given mass number A are considered "bound" nuclei in the diagram of atomic nuclei given below. The possibility of using such a criterion was uncovered only recently, in connection with the accumulation of experimental data on the decay energies and masses of nuclei. Although the experimental data are incomplete (at present 38 isobars with maximum binding energy cannot be accurately established), they permit the formulation of certain rules.

The mass of the bound nucleus ${}_zM^A_{\text{bound}}$ should satisfy the following inequalities:

for odd A

$$ {}_{z+1}M^A - {}_zM^A_{\text{bound}} > -0.78 \text{ MeV}, \quad \text{(Ia)} $$

$$ {}_{z-1}M^A - {}_zM^A_{\text{bound}} > +0.78 \text{ MeV}, \quad \text{(Ib)} $$

for even A (even Z)*

$$ {}_{z+2}M^A - {}_zM^A_{\text{bound}} > -1.56 \text{ MeV}, \quad \text{(IIa)} $$

$$ {}_{z-1}M^A - {}_zM^A_{\text{bound}} > +1.56 \text{ MeV}. \quad \text{(IIb)} $$

The corresponding differences in mass are given in the table of bound nuclei, compiled from data given in references 1-7**. From the list of bound nuclei it is seen that they contain β-active nuclei (with a decay energy < 0.78 MeV, equal to the difference in mass between neutron and proton). The diagram of atomic nuclei (see illustration) shows all known β-stable nuclei and all known β-active nuclei with decay energy < 0.78 MeV, and also certain β^-, β^+, and K-active nuclei of interest. The bound nuclei are marked by different symbols.

The diagram makes evident the following rules♀:

1) The differences $N - Z = I_{\text{bound}}$ between the number of neutrons and protons increases with A in the bound nuclei; in this case, because of the absence of odd-odd bound nuclei, I_{bound} assumes alternately two values for nuclei with even A; these values differ by two.

2) Nuclei with $N - Z$ constant (arranged on the diagram in one horizontal row) change their properties as A increases, in accordance with the following sequence: (a) non-bound β-active nuclei (as a rule not shown); (b) bound nuclei that are not minimum-mass isobars (frequently β^--active nuclei with decay energy less than 0.78 MeV); (c) β-stable bound nuclei, which are at the same time minimum-mass isobars; (d) non-bound β-stable nuclei; (e) β^+ and K-active nuclei (as a rule not shown). For nuclei with A even this sequence applies only to even-even nuclei.

These rules reflect the universally known fact that the increasing coulomb-repulsion energy of the protons in the nucleus is balanced by the ex-

[1] I. P. Selinov, *Atomic Nuclei and Nuclear Transmutations*, Moscow, 1951

[2] V. A. Kravtsov, Usp. Fiz. Nauk **54**, 3 (1954)

[3] N. S. Dzhelepov and L. N. Zyrianova **48**, 465 (1952)

[4] J. M. Cork, J. M. Le Blanc, W. H. Nester, and F. B. Stumpf, Phys. Rev. **88**, 685 (1952)

* Odd-odd nuclei are not considered, since as a rule they do not have the maximum binding energy. There exist only two very bound odd-odd isobars, namely H^2 and Li^6.

** See the remark in the table concerning the reliability of determination of the bound nucleus.

[5] J. M. Hollander, T. Perlman, and G. T. Seaborg, Revs. Mod. Phys. **25**, 469 (1953)

[6] A. B. Smith, C. G. Mitchell, and R. C. Caird, Phys. Rev. **87**, 454 (1952)

[7] V. A. Kravtsov, Usp. Fiz. Nauk **47**, 341 (1952)

[8] J. D. Knight, M. E. Bunker, B. Warren, and J. W. Starner, Phys. Rev. **91**, 889 (1953)

♀ The same symbol is used in the diagram to denote both bound nuclei, established with certainty, and nuclei that are assumed bound from their position on the diagram.

Table of Bound Nuclei

A (mass number)	Element	Percentage of isotope content or half life	log ft or type of decay	$Z+1M^A-ZM^A$ bound or $Z+2M^A-ZM^A$ bound in MeV	$Z-1M^A-ZM^A$ bound or $Z-2M^A-ZM^A$ bound in MeV	Reliability of determination	Reference
1	2	3	4	5	6	7	8
1	H	99.98	—	—	0.78	+	1
2	H	0.016	—	—		(+)	
3	H	12.46 years	3.06	0.018		(+)	1
4	He	100	—	—		(+)	
5	He	$<10^{-8}$ sec	$\alpha+n$	−0.02		(+)	3
6	Li	7.3	—	—	3.2	+	1
7	Li	92.7	—	—			
8	Be	<1 sec	$\alpha+\alpha$	—	(>12.8)	+	1
9	Be	100	—	—	14.0	+	1
10	Be	$2.7\cdot10^6$ years	13.7	−0.56		(+)	1
11	B	81.2	—	—			
12	C	98.9	—	—	(>13.4)	+	1
13	C	1.1	—	—			
14	C	5720 years	9.0	−0.156		(+)	1
15	N	0.38	—	—	8.8	+	5
16	O	99.76	—	—	(>10.5)	+	1
17	O	0.04	—	—	3.7	+	1
18	O	0.2	—	—		(+)	
19	F	100	—	—	4,5	+	1
20	Ne	90.5	—	—	(>5.3)	+	1
21	Ne	0.3	—	—	>2.1	+	1
22	Ne	9.2	—	—		(+)	
23	Na	100	—	—	4.1	+	1
24	Mg	78.6	—	—	(>2.7)	+	1
25	Mg	10.1	—	—	3.4	+	1
26	Mg	11.3	—	—			
27	Al	100	—	—	2.64	+	1
28	Si	92.2	—	—	(>4.65)	+	5
29	Si	4.7	—	—	3.7	+	1
30	Si	3.1	—	—		(+)	
31	P	100	—	—	1.8	+	1
32	S	95.1	—	—	(>1.7)	+	1
33	P	25 days	5.2	−0.26		(+)	5
34	S	4.2	—	—	(>5.7)	+	1
35	S	87.1 days	5.0	−0.167		(+)	1
36	S	0.01	—	+0.37		(+)	3
37	Cl	24.6	—	—	4.3	+	1
38	A	0.06			(>4.8)	+	1
39	A	15 years	~10	−0.565	3.31	+	5
40	A	99.6	—	+0.21		(+)	3
41	K	6.9	—	—	2.55	+	1
42	Ca	0.64	—	—	(>3.5)	+	1
43	Ca	0.13	—	—	0.81	+	1
44	Ca	2.13	—	—		(+)	
45	Ca	152 days	5.98	−0.254		(+)	1
46	Ca	0.003	—	−0.028 interpolated		(+)	2
47	Sc	5.4 days	5.65	0.62	2.06	+	2
48	Ti	73.4	—	—	4.3	+	6
49	Ti	5.5	—	—	1.8	+	1
50	Ti	5.3	—	+1.05		(+)	6
51	V	99.8	—	—	2.2	+	2
52	Cr	83.8	—	—	(>4.12)	+	2
53	Cr	9.6	—	—	2.0 interpolated	+	2
54	Cr	2.4	—	0.65		(+)	2
55	Mn	100	—	—	2.85	+	2
56	Fe	91.6	—	—	(>3.69)	+	2
57	Fe	2.2	—	—	1.0	+	2
58	Fe	0.3	—	+1.7		(+)	2
59	Co	100	—	—	1.56	+	2
60	Ni	26.1	—	—	4.3	+	2

A (mass number)	Element	Percentage of isotope content or half life	log ft or type of decay	$Z+1M^A - ZM^A$ bound or $Z+2M^A - ZM^A$ bound in MeV	$Z-1M^A - ZM^A$ bound or $Z-2M^A - ZM^A$ bound in MeV	Reliability of determination	Reference
1	2	3	4	5	6	7	8
61	Ni	1.25	-	—	1.42	+	2
62	Ni	3.7	—	—	(>3.6)	+	2
63	Ni	300 years	7.06	—0.063		(+)	1
64	Ni	1.16	—	+1.1		(+)	2
65	Cu	30.9	—	—	2.1	+	1
66	Zn	27.8	—	—	(>2.6)	+	1
67	Cu	58.8 hours	5.5	—0.577		(+)	2
68	Zn	18.6	—	—	(>3.0)	(+)	2
69	Ga	60.2	—	—	0.897	+	2
70	Zn	0.62	—	-1.18 ± 0.2		?	2
71	Ga	39.8	—	—	2.1	+	2
72	Ge	27.4	—	—	6.52	+	2
73	Ge	7.9	—	—	1.5	+	2
74	Ge	36.3	—	+1.2		(+)	2
75	As	100	—	—	1.1	+	1
76	Se	9.0	—	—	2.2	+	2
77	As	40 hours	5.75	—0.7	2.46	+	5
78	Se	23.5	—	+3.1	5	+	2
79	Se	$0.5 \cdot 10^4$ years	~9	—0.150	2.1	+	5
80	Se	49.8	—	—0.16		(+)	2
81	Br	49.5	—	—	1.38	+	
82	Kr	11.5	—	—	3.5	+	2
83	Kr	11.48	—	—	0,98	+	2
84	Kr	57.0	—	0.7 interpolated	4.68	+	2
85	Kr	9.4 years	9.22	—0.695	2.5	+	1
86	Kr	17.4	—	—1.18		(+)	2
87	Rb	$16 \cdot 10^{10}$ years	16.5	—0.27	3.6	+	2
88	Sr	82.7	—	—	7.0	+	2
89	Y	100	—	—	1.463	+	1
90	Zr	51.4	—	—	2.83	+	2
91	Zr	11.2	—	—	1.55	+	2
92	Zr	17.1	—	+1.25	(>4.7)	+	2
93	Zr	$15 \cdot 10^6$ years	11.5	—0.060	3.1	+	1
94	Zr	17.4	—	—1.14	(>6.8)	+	2
95	Mo	15.7	—	—	0.91	+	5
96	Mo	16.6	—	+2.8	3.6	+	2
97	Mo	9.5	—	—	1.93	+	2
98	Mo	23.8	—	+0.04 interpolated		(+)	2
99	Tc	$5 \cdot 10^5$ years	12.7	—0.29	1.37	+	5
100	Ru	12.7	—	—	2.4 interpolated	+	2
101	Ru	17.0	—	—	1.5	+	1
102	Ru	31.3	—	+1.1		(+)	2
103	Ru	43. days	8.25	—0.75		(+)	5
104	Ru	18.3	—	—1.2 interpolated		(+)	2
105	Rh	3.6 hours	5.5	—0.57	2.01	+	5
106	Pd	27.2	—	+2.7	3.57	+	2
107	Pd	$7 \cdot 10^6$ years	11	—0,035	1.2	+	1
108	Pd	26.8	—	+0,18		(+)	2
109	Ag	48.6	—	—	1.1	+	1
110	Cd	12.4	—	—	$1.23 \pm 0,24$	?	2
111	Cd	12.7	—	—	1.0	+	1
112	Cd	24.1	—	+1.9	4.32	+	2
113	Cd	12.2	8	—0.18	2.1	+	5
114	Cd	28.9		—0.31		(+)	2
115	In	$6 \cdot 10^{14}$ years	23.2	—0.63	1.45	+	1
116	Sn	14.4	—	—	2.5	+	2
117	Sn	7.54	—	—	1.73	+	2
118	Sn	24.0	—	—	(>1.5)	+	5
119	Sn	8.6	—	—	2.7	+	1
120	Sn	33.0	—	+2,15		(+)	2

A (mass number)	Element	Percentage of isotope content or half life	log ft or type of decay	$Z+1M^A-ZM^A$ bound or $Z+2M^A-ZM^A$ bound in MeV	$Z-1M^A-ZM^A$ bound or $Z-2M^A-ZM^A$ bound in MeV	Reliability of determination	Reference
1	2	3	4	5	6	7	8
121	Sn	400 days	9,4	—0.38		(+)	2
122	Sn	4.8	—	—0.49		(+)	2
123	Sb	42.7	—	+0.09	1.41	+	2
124	Te	4.63	—	—	2.1	+	2
125	Sb	2.7 hours	9,4	—0.76	2.4	+	5
126	Te	18.7	—	+0.84	(>2)	+	2
127	Te	9.3 hours	5.6	—0.9	1.9	+	2
128	Te	31.7	—	—1,56+0,2		?	2
129	I	$1.7 \cdot 10^7$ years	13,4	—0,17	2.6	+	2
130	Xe	4.05	—	+2.53	3.4	+	2,6
131	Xe	21.2	—	—	0.97	+	2
132	Xe	26.9	—		3.1		2
133	Xe	5.7 days	5.7	—0.43	1.93	+	5
134	Xe	10.5	—		(>3.9)		2
135	Cs	$2 \cdot 10^6$ years	13.9	—0.21	1.15	+	5
136	Ba	7.8	—		0.27	—*	2
137	Ba	11.3	—	—	1.2	+	5
138	Ba	71.7	—	—	5.1		1
139	La	99,9	—	—	2.27	+	1
140	Ce	88.5	—	—	4.91	+	5
141	Ce	33.1 days	7.72	—0.56	2.9	+	1
142	Ce	11.1	—				
143	Nd	12.2	—	—	0.93	+	5
144	Nd	23.9	—		(>3.5)		1
145	Nd	8.3	—	—	3.2	+	1
146	Nd	17.2	—	—	(>3)	+	1
147	Pm	3.5 hours	7.6	—0.227	0.91	+	1
148	Sm	11.3	—	—			
149	Sm	13.9	—	—	1.1	+	1
150	Sm	7.5	—	—	>3.0	+	5
151	Sm	500 years	8.3	—0.076	1.1	+	5
152	Sm	26.6	—				
153	Eu	52.2	—	—	>0.80	+	5
154	Gd	2.15	—	—			
155	Eu	1.72 years	7.1	—0.3	1.9	+	1
156	Gd	20.8	—		>3.3		1
157	Gd	15.7	—	—	1.8	+	1
158	Gd	24.8	—		(>2.5)		1
159	Tb	100	—	—	>0.95	+	1
160	Dy	2.3	—	—			
161	Tb	240 days	6.7	—0.52	>1.5	+	4
162	Dy	25.5	—				
163	Dy	25.0	—	—			
164	Dy	28.1	—				
165	Ho	100	—	—	1.3	+	1
166	Er	32.9	—	—	(>1.9)	+	5
167	Er	24.4	—	—			
168	Er	26.9	—				
169	Er	9.4 days	6.10	—0.33		(+)	1
170	Er	14.2	—				
171	Tu	500 days	6.3	—0.10	⩾1.49	+	5
172	Yb	11,9	—	—		(+)	
173	Yb	16.2	—	—			

* *Note added in proof.* Certain mass differences in the table are based on reference 2, published after this article was submitted. According to that reference, another violation of rule 2 is observed: the $_{54}Xe^{136}_{82}$ nucleus has a greater binding energy than the $_{56}Ba^{136}_{80}$ nucleus, designated as bound on the diagram and in the table. This is apparently due to presence of a closed shell $N = 82$ in Xe 136

A (mass number)	Element	Percentage of isotope content or half life	log ft or type of decay	$Z+1M^A-ZM^A$ bound or $Z+2M^A-ZM^A$ bound in MeV	$Z-1M^A-ZM^A$ bound or $Z-2M^A-ZM^A$ bound in MeV	Reliability of determination	Reference
1	2	3	4	5	6	7	8
174	Yb	31.8	—				
175	Yb	99 hours	6.4	—0.5		(+)	1
176	Yb	12.0	—				
177	Lu	6.9 days	6.8	—0.49	1.3	+	5
178	Hf	27.1	—	—			
179	Hf	13.8	—	—			
180	Hf	35.1	—				
181	Ta	100	—	—	1.02	+	5
182	W	26.3	—	—			
183	W	14.3	—	—			
184	W	30.6	—				
185	W	73 days	7.5	—0.57	$\geqslant$1.7	+	5
186	W	28.6	—	—			
187	Re	$4\cdot10^{12}$ years	17.7	—0.043	1.32	+	1
188	Os	13.3	—	—	>2.07	+	1
189	Os	16.1	—	—	>1.2	+	5
190	Os	26.4	—				
191	Os	15 days	5.34	—0.27		(+)	
192	Os	41.0	—				
193	Ir	61.5	—	—	1.16	+	
194	Pt	32.8	—	—	(>2.5)	+	
195	Pt	33.7	—	—	>1.8	+	5
196	Pt	25.4	—	+1.02		(+)	7
197	Pt	18 hours	6.3	—0.73	>1.65	+	7
198	Pt	7.2	—	—1.02	(>3.6)	+	7
199	Au	33 days	7.8	—0.46	1.8	+	7
200	Hg	23.2	—	—	(>2.4)	+	7
201	Hg	13.5	—	—	>1.5	+	5
202	Hg	29.6	—	+1.4 interpolated		(+)	7
203	Hg	43.5 days	—	—0.487	>1.9	+	7
204	Hg	6.69	—	—0.56		(+)	7
205	Tl	70.5	—	—	1.75	+	7
206	Pb	25.1	—	+9.4 interpol.	2.9 interpol.	+	7
207	Pb	21.1	—	+1.8 interpol.	1.44	+	7
208	Pb	53.4	—	+3.9	(>4.9)	+	7
209	Pb	3.24 hours	5.64	—0.68	1.8	+	1
210	Pb	22 years	6.02	—1.24	(>1.8)	+	1
211	Bi	2.16 min		—0.25	1.39	+	7
212	Po	$3.4\cdot10^{-7}$ sec	α	+1.41	2.83	+	7
213	Po	$4.4\cdot10^{-5}$ sec		—0.6	1.25	+	7
214	Po	$1.4\cdot10^{-4}$ sec	α	—1.0	4.55	+	7
215	At	10^{-4} sec	α	+0.37 interpolated	1.1	+	7
216	Em	10^{-5} sec	α		1.6	+	7
217	At	0.021 sec		—0.56	1.78 interpol.	+	7
218	Em	0.019 sec	α	(>1.77)	3.63	+	7
219	Em	3.92 sec		—0.62		(+)	7
220	Em	54.4 sec	α	—0.41		(+)	7
221	Fr	4.8 min		—0.046	1.58 interpolated	+	7
222	Ra	38 sec	α	(2.2)	12.33	+	7
223	Ra	11.2 days	α	+3.2	1.2	+	7
224	Ra	3.64 days	α	+0.13		(+)	7
225	Ra	14.8 days	6.08	—0.2		(+)	7
226	Ra	1622 years	α	—0.84		(+)	7
227	Ac	21.7 years	$\sim$5	—0.37	1.21 interpolated	+	7
228	Th	1.9 years	α	+2.32	(>2.58)	+	7
229	Th	$7\cdot10^3$ years	α	—	1.0	+	7
230	Th	$8\cdot10^4$ years	α	+0.37	3.35	+	7
231	Th	25.5 hours	5.07	—0.32		(+)	7
232	Th	$1.5\cdot10^{10}$ years	α	—0.96		(+)	7
233	Po	27.9 days	6.63	—0.62	1.23	+	7
234	U	$2.5\cdot10^5$ years	α	+3.0	4.1	+	7

Diagram of the nuclei. The mass number A is plotted horizontally, and the difference between the number of protons and neutrons is plotted vertically.

A (mass number)	Element	Percentage of isotope content or half life	log ft or type of decay	$Z+1M^A-ZM^A$ or $Z+2M^A-ZM^A$ bound in MeV	$Z-1M^A-ZM^A$ or $Z-2M^A-ZM^A$ bound in MeV	Reliability of determination	Reference
1	2	3	4	5	6	7	
235	U	$7.7\cdot10^8$ years	α	+0.18	1.4	+	5,7
236	U	10^8 years	α	+0.046		(+)	7
237	U	6.63 days	6,04	—0.511		(+)	5
238	U	$5\cdot10^9$ years	α	$-1.56\pm0,60$		?	7
239	Np	2.31 days		—0.715	>1,2	+	7
240	Pu	6000 years	α	+1.17	2,516	+	7,5
241	Pu	10 years		—0.18	>0.89	+	7,8

Notes on Table:

a) A line is drawn through column 5 if the nuclei $_{Z+1}M^A$ and $_{Z+2}M^A$ are β^+ or K-active [in this case equations (Ia) and (IIa) are always satisfied];

b) the figure in column 6 is placed in parentheses in the case of bound nuclei with even A, when the nucleus $_{Z-2}M^A$ is β-active and the determination is based on the decay energy of the odd-odd nucleus $_{Z-1}M^A$;

c) A + is placed in column 7 when the nodal nucleus is definitely established, and a (+) is placed when equations (Ib) and (IIb) cannot be verified for β^- active bound nuclei and for individual β-stable even-even isobars; a negative result of such a verification is not very likely. The doubtful cases $A = 70, 110, 128$, and 238 are marked?; here the data in the literature are contradictory and insufficiently accurate, and the average of two measurement data, cited in reference 2 cannot be considered fully reliable;

d) if interpolated data from survey articles [2,7] are used, the abbreviation (int) is placed next to the figures in columns 5 and 6.

cess neutrons. Of interest are the cases of violation of these rules. As can be seen from the diagram, violations occur in those regions, where the nuclei with filled proton and neutron shells (doubly-magic nuclei) are located to the side of the basic line of bound nuclei. Near the doubly-magic nuclei $_{20}Ca_{20}^{40}$, $_{20}Ca_{28}^{48}$, the sequence is disrupted in the variation of the property of the nuclei (rule 2) for $N - Z = 3$ and 8 respectively: the β^- active nucleus A^{39} is located between the β-stable nuclei Cl^{37} and K^{41}, as a result of the anomalously high binding energy of the K^{39} nucleus. The β^--stable nucleus Ca^{48} is located among β^--active nuclei; it is followed by three β^--active nuclei: Ti^{52}, Cr^{56}, and Fe^{60}, and only then by the β-stable nucleus Ni^{64}. In the vicinity of the "peripherally" located doubly-magic nuclei $_{28}Ni_{40}^{68}$, $_{40}Zr_{50}^{90}$ [9], and $_{58}Ce_{82}^{140}$ [10,11] rule 2 is violated for $N - Z$ equal to 7,9,10,11,12,13,14 and 20, 23, 25, and 28, respectively (see diagram). Also Also violated is rule for the bound nuclei Cu^{67} Y^{89}, Zr^{90}, Zr^{91}, Mo^{95}, and Nd^{143}, respectively. The character of these violations points to an anomalously large binding energy of Ni^{68}, Zr^{90}, and Ce^{140}. In those cases when the doubly-magic nuclei $_2He_2^4$, $_8O_8^{16}$, $_{50}Sn_{70}^{120}$ [9] and $_{82}Pb_{125}^{208}$ follow rigorously the curve of bound nuclei, no violation of rules 1 and 2 is observed.

The dotted lines on the diagram denote the absence of bound nuclei with $N = 17, 39, 43, 73, 91$, 95, and 131, and with $Z = 41$ (Nb) and 59 (Pr). As is well known, there are no β-stable nuclei with $N = 19, 21, 35, 39, 45, 61, 84, 115$, and 123, and with $Z = 43$ (Tc) and 61 (Pm). These two series of numbers have only $N = 39$ in common. The absence of bound nuclei for seven values of N (and it is possible that there may be more values for the experimental data are incomplete) cannot be considered an anomaly. In fact, in bound nuclei with A odd, I_{bound} increases, as a rule by two for certain values of Z, because N also increases by two. If these transient isotopes have an odd Z, there will be two bound isotopes with odd Z, and there will be no bound nucleus with odd N (for example, the sequence of bound nuclei $_{14}Si^{19}$, $_{15}P_{16}^{31}$, $_{15}P_{18}^{33}$, $_{16}S_{19}^{35}$ contains no bound nucleus with $N = 17$, but contains instead two bound phosphorus isotopes with $Z = 15$). If the transient isotopes have an

[9] H. E. Duckworth and S. Preston, Phys. Rev. **82**, 468(1952)

[10] H. E. Duckworth, C. L. Kegley, J. M. Olson, and G. S. Stanford, Phys. Rev. **83**, 1114(1951)

[11] G. P. Dube and S. Jha. Phys. Rev. **85**, 1042(1952)

□ - bound β-stable nucleus
⊠ - bound β⁻-active nucleus with decay energy less than 0.78 MeV
⊠→ - β⁻-active non-bound nucleus with decay energy less than 0.78 MeV
□→ - β⁻ - stable non-bound nucleus
○ - β-active nucleus, located in the region of bound nuclei
○→○ - other β⁻, β⁺, and K-active nuclei
◐ - doubly-magic nuclei.

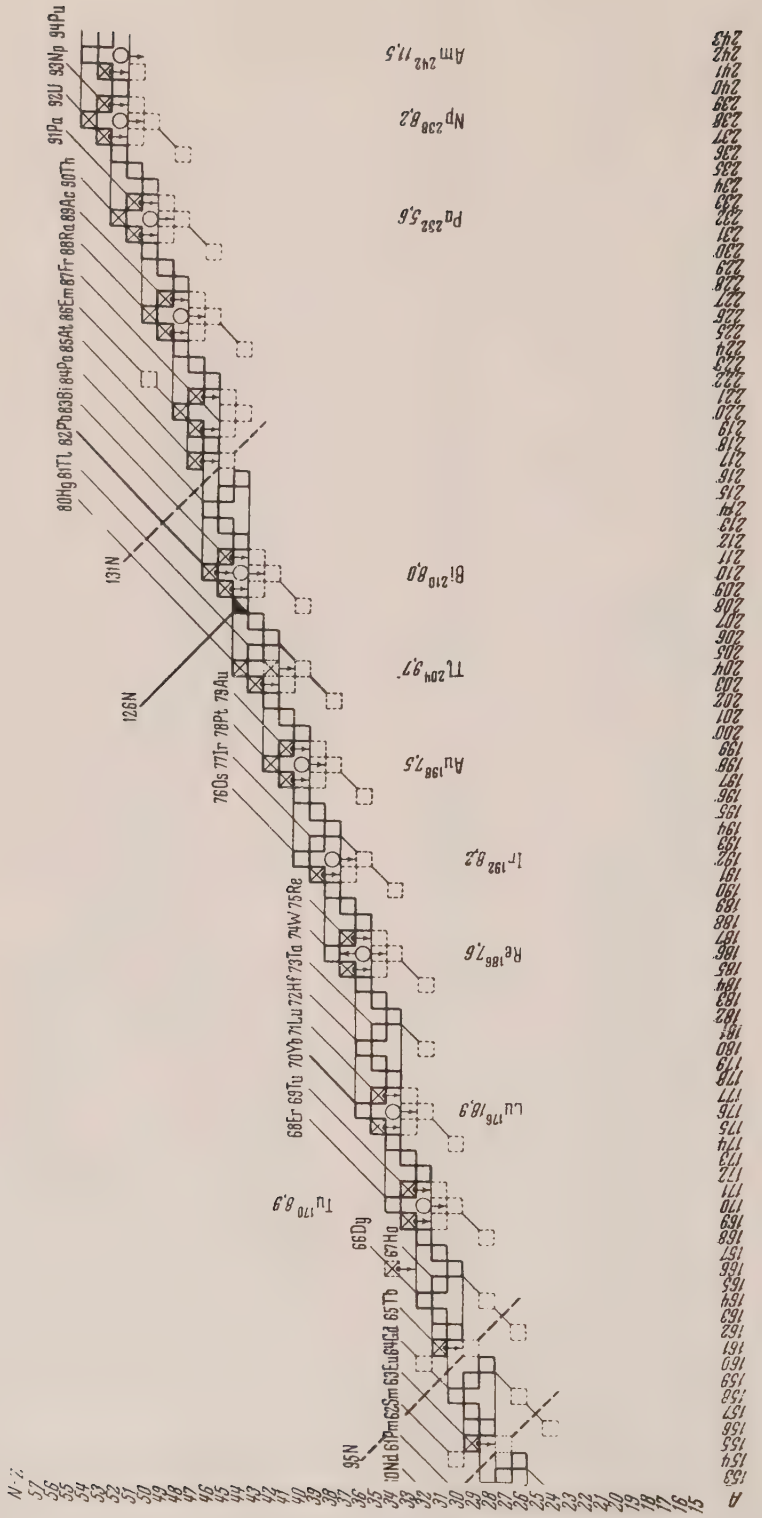
80Hg 81Tl 82Pb 83Bi 84Po 85At 86Em 87Fr 88Ra 89Ac 90Th 91Pa 92U 93Np 94Pu
131N
126N
95N
76Os 77Ir 78Pt 79Au
Tl 204 9,7'
Bi 210 8,0
Au 198 7,5
Ir 192 8,2
Re 186 7,6
Lu 176 18,9
Tu 170 8,9
Np 238 8,2
Pu 232 5,6
Am 242 11,5

even Z, no absence of bound nuclei with some odd N will be observed; consequently there will be no two bound isotopes with identical odd Z (for example, the sequence $_{37}Co^{59}_{32}$, $_{28}Ni^{61}_{33}$, $_{28}Ni^{63}_{35}$, and $_{29}Cu^{65}_{36}$). Both possibilities have equal probability, and it can therefore be expected that, in approximately half the cases, the absence of nodal nuclei with an odd number of neutrons will be observed. At the present time this is known to occur for 7 out of 27 possible cases (I_{bound} changes 27 times). Analogous considerations should apply also to β-stable nuclei with odd A (minimum-mass criterion approximating the maximum-binding-energy criterion). In fact, it is because the absence of β-stable nuclei with odd N is always accompanied by the presence of a pair of β-stable isotopes with odd Z.

From our point of view the only things that can be considered anomalies in the distribution are the absence of bound nuclei with $Z = 41$ and 50, and the absence of both bound and β-stable nuclei for $N = 39$. All these anomalies are simultaneous violations of rules 1 and 2 in the vicinity of the peripheral doubly-magic nuclei $_{28}Ni^{68}_{40}$, $_{40}Zr^{90}_{50}$, and $_{58}Ce^{140}_{82}$. The numbers 41 and 59 each exceed by one the magic numbers 40 and 58, while 39 is one less than the magic number 40. In the same region anomalies are also observed in the distribution of the β-stable isotopes -- the absence of stable isotopes of Tc ($Z = 43$) and Pm ($Z = 61$), but the connection of these anomalies with the filling of the nuclear shell is not as pronounced as the anomalies in the distribution of the bound nuclei.

The table lists the values of log ft for β-active bound nuclei[5,12,13]. Similar data are also given on the margin of the diagram for certain β-active nuclei for which the ratio between the number of neutrons and protons should be particularly convenient, starting with the normal course of the bound-nuclei curve. These are odd-odd nuclei, located in the transition regions, where $N - Z$ increases by four for the bound even-even nuclei, and also such β-active nuclei as Sr^{89} and others, which would have been bound were it not for the anomalously excessive binding energy of the doubly-magic nucleus Zr^{90} and of the neighboring nuclei.

All these β-transitions are in most cases rigorously forbidden, and among them are most transitions in the forbidden form of the β-spectrum (except one). This circumstance indicates the dependence of the degree of forbidenness of the beta transition, in addition to all other factors, on the position of the nucleus in the atomic-nuclei diagram.

Thus, attempts to explain the anomalies in the distribution of the β-stable nuclei by the presence of some other special nuclear configurations, other than the known nuclear shells, must be considered to be in error; all the anomalies are due to the filling of the nuclear shells, although this cannot be always established off hand.

---

[12] M. G. Mayer and S. A. Moszkowsky, Revs. Mod. Phys. **23**, 315 (1951)

[13] A. M. Feingold, Revs. Mod. Phys. **23**, 10(1951)

Translated by G. J. Adashko

60

The Problem of the Position of the Copper Activator in Zinc-Sulfide Scintillators

A. A. CHEREPNEV
P. N. Lebedev Institute of Physics, Academy of Sciences, USSR
(Submitted to JETP editor March 24, 1954)
J. Exper. Theoret. Phys. USSR **28**, 458-462 (April, 1955)

An outline of the implanting process of an activator is presented, based upon investigation of the luminescent properties of ZnSCu-scintillators, obtained by thermal treatment at low temperatures (up to 600 °C) and by repeated firing. This outline is in agreement with the assumption of the dispersed position of copper in the scintillator system.

1. Two ways were used to obtain the characteristics of the behavior of the copper activator in ZnS-scintillators: a) preparation of the ZnSCu-scintillators according to the typical technological method, but applying low temperatures (below 600 °C), and b) investigation of the penetration of copper into an already formed crystalline ZnS structure that was obtained by heat treatment.

The scintillators were prepared from dry amorphous zinc sulfide powder, obtained by precipitating the sulfate in warm weak acid solution with hydrogen sulfide. The aqueous solution of the activator was introduced to the sulfide. After drying, addition of the crystalline flux, and careful mixing, the mixture was put in a quartz crucible, the cover of which was coated with kaolin paste. Crucibles and contents were heated up to 300-320 °C, then placed in the furnace that was heated up to the required temperature, and maintained at temperature. The luminescence was investigated at room temperature, with the exciting light $\lambda = 365 m\mu$ of the mercury lamp at the distance of 25cm (lamp PRK4 with filter UFS); the brightness was measured with the Pulfrich photometer, spectra were studied with the visual spectrophotometer.

2. In thermal treatment of the amorphous sulfide[1], the formation of crystals and the incorporation of the activator can take place at comparatively low temperature (in range of 400 °C), however, the indicated processes, under these conditions, are slow and require many hours. When ZnS is heated, with NaCl flux at 400 °C during 1 hour period without addition of copper, the mixture is obtained without notable luminescence, but at 450 °C a yellow fluorescence shows up (possibly, from ZnO[2]). At 500 °C a bluish luminescence occurs, which develops to a bright one at 600 °C when, the sample heated for 1 hour.

When ZnS is heated with Cu (10^{-4} g/g) and with NaCl flux (5%) at 350 °C for a long time (up to 30 hrs.) specimens are obtained with a rather weak orange-yellow luminescence, the intensity of which increases constantly with time of heating. The rise in temperature of the thermal treatment up to 400 °C produces remarkable intensities of the orange luminescence which is apparently connected with the formation of Cu_2S[3] or double sulfides of zinc and copper. The intensity of the luminescence increases with the increasing heating time (Table 1); the color changes from dark orange to yellow and even to yellow-green (Fig. 1). The after-glow also increases. When the firing temperature is raised, the increase of brightness and occurrence of yellow-green fluorescence are observed: after 4-hour heating at 450 °C, specimens with yellow-green luminescence with after-glowing are obtained. At 600 °C this event develops to full scale and upon further rise in temperature, typical ZnSCu-scintillators are formed, Table 1.

In case of H_3BO_3 flux the occurrence of luminescent properties is much weaker and slower. In the absence of copper, pale luminescence is first observed at 600 °C, and blue light-at 700 °C. In the presence of copper (10^{-4} g/g) at 400 °C, dark orange luminescence takes place, while a constant increase of brightness with the heating time is observed. At 600 °C the yellow-green luminescence does not appear at once, and remarkable intensities are obtained after prolongued period of time (Table 2 and Fig. 2). Samples obtained at 700 °C firing temperature (in 30 min. period) exhibit a pale-yellow luminescence, the after-glowing being faint; at the firing temperature of 800 °C (30 min) blue luminescence shows up and the after-glowing almost disappears.

In order to explain the nature of the orange

[1] F. Tiede and F. Weiss, Chem. Ber. **65**, 364 (1932)

[2] N. F. Zhirov, *Luminophors*, Defense J., 1941, p. 307; F. A. Kroeger and J. A. M. Dikhoff, Electrochem. Soc., **99**, 144 (1952)

[3] Ia. I. Gerasimov and A. N. Krestovnikov, *The Chemical Themodynamics in Color Metallurgy*, ONTI, 1933, Vol. 1, p. 163; Vol.2, p. 40

luminescence of ZnSCu, two series of samples were prepared at various temperatures with one-and two-valent chlorides of copper and with a great excess of the activator (calculated as 5% Cu). In case of Cu^{++}, where, in the first place, CuS being already dissociated[3] is formed; the process takes place more slowly than with Cu^{+}, where Cu_2S appears at once, and therefore the sample, obtained

TABLE I

Dependence of the Brightness of the Luminescent Light of ZnSCu-system on Heating Time at 400 °C

Time in hrs.	1	2	4	6	8	10	14	18	22
$I_{relative}$	2.4	6	22	42	57	71	83	90	100

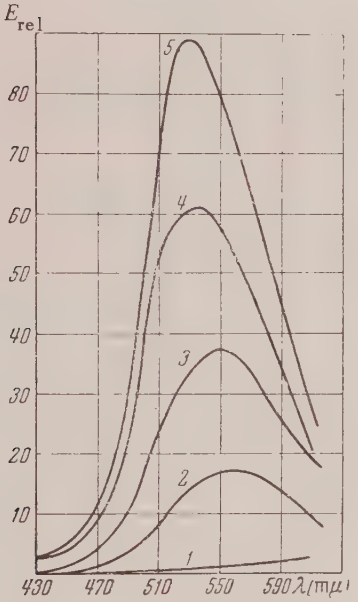

Fig. 1. Spectra of luminescent light of ZnSCu-NaCl scintillators for various heating periods at 400 °C; *1*=1, *2*=4, *3*=8, *4*=18, *5*=22 hours.

by firing at 400 °C, in 30 minutes, shows, in case of univalent copper, more intensive luminosity (red color). At 500 °C the mixture with univalent copper exhibits yellow-green luminescence, whereas the mixture with bivalent copper--the yellow one. In Fig. 3, spectral characteristics of the luminescence of the two samples prepared at 600 °C (firing time 30 min) are presented. At still higher firing temperature luminescence almost disappears.

A similar picture is observed by heating with the addition of separately prepared CuS and Cu_2S.

3. For the purpose of investigating the processes taking place in the crystalline ZnS, three series of experiments were carried out.

a) In the first experiment a typical ZnSCu-scintillator with the green luminescence was used, prepared with 10^{-4} g/g Cu and chloride flux washed out after firing; it was heated for the second time with H_3BO_3 flux. After a half an hour firing at 1100 °C, blue fluorescence shows up while the phosphorescence remains still green. By prolonging the second firing time, the after-glowing disappears and blue fluorescence stays.

TABLE II

The relative intensities of the luminescent light of ZnSCu-systems, fired for various periods of time at 450 ° and 600 °C with NaCl and H_3BO_3 fluxes

Firing Time	450 °C		600 °C	
	NaCl	H_3BO_3	NaCl	H_3BO_3
30 min	—	—	84	0.36
1 hr	11	0.15	100	0.48
2 hrs	21	0.18	106	0.60
4 hrs	31	0.20	—	0.72
8 hrs	—	—	—	1.02
12 hrs	—	—	—	1.64
16 hrs	—	—	—	2.34

b) A ZnSCu mixture was used as the initial sample, and was prepared with an excess of activator (10^{-4} g/g Cu) and H_3BO_3 flux, i.e., with a blue fluorescence[4]. When heated with NH_4Cl (10%) for 1 hour at 500 °C it shows green luminescence. In case of NaCl flux (10%) at 500 °C, even 4 hour heating does not produce mixture with the green luminescence; however, heated at 600 °C for 1 hour, the mixture shows green luminescence.

[4] A. A. Cherepnev and T. S. Dobroliubskaia, Doklady Akad. Nauk SSSR 66, 621 (1949)

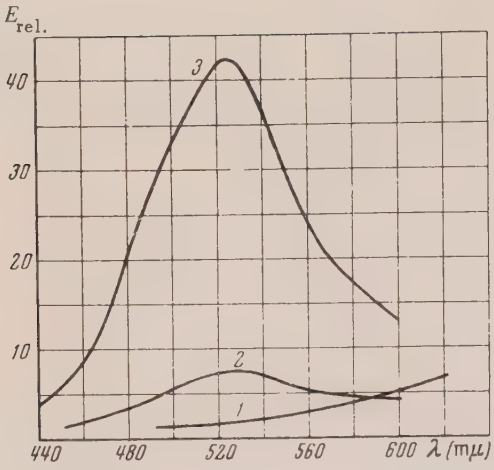

Fig. 2. Luminescence spectra of ZnSCu - H_3BO_3 -scintillators with various firing time at 600 °C: *1*=30 min, *2*=4, *3*=16 hours.

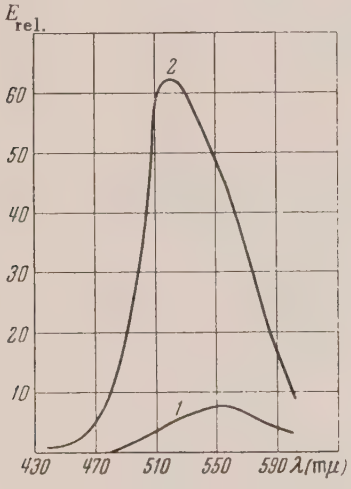

Fig. 3. Luminescence spectra of ZnS-scintillators, fired at 600 °C with the additions: *1*=$CuCl_2$, *2*=CuCl.

c) The method of references 5,6 of activating, by subsequent heating, pure ZnS which was already fired was applied. ZnSZn-specimens were prepared by firing amorphous ZnS at 900 ° and 1100 °C for 30 min period: two of them were with NaCl flux, the other two with high H_3BO_3, 5% each. Mixtures fired at 900 °C had bright-blue luminescence, whereas mixtures fired at 1100 °C showed faint bluish luminescence with a green phosphorescence not greater than that of residual, hardly removable copper. These mixtures were heated secondarily for 30 minutes with the copper activator added (10^{-4} and 10^{-5} g/g) and with the same flux (5%) which was used during the first firing operation. A series of new luminescent specimens were obtained, which are illustrated in Table 3 with the characteristics of color of their luminescence.

As it is seen from the table, the fluxes have an effect upon the final result. With the increased time of secondary heating, the NaCl flux produces the yellow-green luminescence, of characteristic copper, and after glowing, and the H_3BO_3 flux shows the same luminescence only with small amounts of activator. With its larger concentration, the flux produces a blue fluorescence without after glowing.

4. To explain the reported experimental data, the following suppositions are made [4,7,8]. During the formation of ZnS-scintillators in the system being subjected to the thermal treatment, a series of chemical reactions of separation of metals is possible through the mutual action of the sulfides and the oxidized compounds [3,8]. The sources of oxygen are oxygen compounds decomposing in the technological process (ZnO, $ZnSO_4$), fluxes containing oxygen, moisture, atmospheric oxygen, absorbed or penetrated into the system from the outside (explanation of experiments of Grillot [9]). The fluxes facilitate the course of the reactions and the formation of metals in the dispersed phase (the molten chlorides help in dispersion of metals [10]). The experimental fact of activation by copper at low temperatures can be explained by the electrolytic displacement by the diffusing copper of zinc that is stoichiometrically in excess, the formation of which can be explained by the indicated reactions (mainly between the oxide and sulfide [11]), or by the removal of sulfur as a result of dissociation [12]. It is natural to assume that copper can

[5] N. Riehl and H. Ortman, Doklady Akad. Nauk SSSR **66**, 613, 841 (1949); N. Riehl and H. Ortman Z. Phys. Chem.(A), **188**, 109(1941).

[6] F. A. Kroeger, J. E. Hellingman and N. W. Smith, Physica **15**, 990 (1949); F. N. Garlick, *Luminescent Materials*, Oxford 1949, p. 65

[7] A. A. Cherepnev, J. Exper. Theoret. Phys. USSR **21**, 322 (1951)

[8] A. A. Cherepnev, Izv. Akad. Nauk SSSR, Ser. Fiz. **15**, 742 (1951)

[9] E. Grillot and M. Bancie-Grillot, C. R., **231**, 966 (1950)

[10] R. Lorenz and W. Eitel, *Pyrosole*, Leipzig, 1926

[11] B. M. Gugel, Zh. Ob. Khim. **20**, 1376 (1950)

[12] A. A. Bundel' and A. I. Russanova, Izv. Akad. Nauk SSSR, Ser. Fiz. **13**, 173 (1949)

TABLE III

Color of the luminescence of the ZnS-Scintillators with NaCl and H_3BO_3 fluxes, activated twice by copper and heated twice

Temperature of the first firing		900 °C								1100 °C							
Concentration of the activator g/g		10^{-5}				10^{-4}				10^{-5}				10^{-4}			
Flux		NaCl		H_3BO_3		NaCl		H_3BO_3		NaCl		H_3BO_3		NaCl		H_3BO_3	
Temperature of the second heating	300 °	lb	ph	lb	ph	plb	ph	lb	-	plb	ph	plb	ph	gr-lb	ph	gr-lb	ph
	350 °	lb	ph	lb	ph	pl	ph	lb	-	plb	ph	plb	ph	lb	ph	lb	ph
	400 °	pl	ph	pl	strong ph	pl	ph	plb	strong ph	plb	ph	plb	ph	lb	ph	plb	ph
	500 °	pl-ye	ph	ye	strong ph	ye	ph	w	n-ag	lb-ye	ph	plb	ph	lb	ph	pl	ph
	600 °	ye	ph	ye	bright ph	ye-grn	ph	b	n-ag	ye	ph	y-grn	ph	ye-grn	strong ph	b	n-ag

CODE: ph-phpsphorescence, n-ag- no after glowing, lb-light blue, b-blue, gr-gray, pl-pale, w-white, ye-yellow, grn-green.

show up in various dispersed conditions; fine, almost atomic, dispersion, is the cause of green luminescence and also of after glowing, because of the creation of structures connected with the occurrence of the "trap sites" of electrons. When particle of copper grows up to the colloidal size, the luminescent properties of copper disappear. The degree of dispersion of copper metal can change under influence of the secondary action of the chlorides. Thus, the fluxes can play a great but auxiliary role.

I express my gratitude to M. A. Konstantinova-Shlezinger for many valuable comments and M. V. Danilova for the help in measurements.

Translated by A. Cybriwsky
81

SOVIET PHYSICS - JETP VOLUME 1, NUMBER 2 SEPTEMBER, 1955

The Theory of Scattering in the Semi-Classical Approximation

I. I. Gol'dman and A. B. Migdal

(Submitted to JETP editor April 26, 1954)
J. Exper. Theoret. Phys. USSR **28**, 394-400 (April, 1954)

A method is given for finding the wave function and the Green's function for a three-dimensional problem in the semi-classical approximation. The idea of the method is illustrated by the problem of reflection from a barrier.

1. INTRODUCTION

In scattering problems the semi-classical approximation is usually applied to the calculation of the phase shifts corresponding to the different angular momenta of the particle. This method is applied only in the case of a central field.

In the present work it is shown that the wave function can be found without the assumption of the central character of the potential field, if the trajectories of the classical problem are known.

As is well known, the semi-classical approximation, which has been thoroughly studied in the one-dimensional case, does not give the exact solution, but an asymptotic series in the semi-classical parameter ξ ($\xi = \lambda\!\!\!^{-} / l$ where $\lambda\!\!\!^{-}$ is the wave-length of the particle, l, is a length characterizing the variation of the potential). Quantum effects, which decrease exponentially with diminishing ξ, cannot be determined in any approximation of this asymptotic series, because the error of the asymptotic representation exceeds the effect sought.

Let us consider, for example, the problem of the calculation of the reflection coefficient from a potential barrier V, when the conditions of the semi-classical approximation are fulfilled in the entire space (i.e., the kinetic energy is nowhere reduced to zero). It is not difficult to see that neither the first nor the succeeding approximations in ξ contain terms corresponding to the reflected wave. Analogous questions arise in the three-dimensional problem also. For example, in the case in which the deflection into large angles is forbidden in classical mechanics, the scattering into these angles decreases exponentially with diminishing ξ, and cannot be found with the aid of an asymptotic expansion in ξ.

In the present work a method is given for improving the semi-classical approximation, which enables us to find the solution of the above-mentioned problems. This method consists of the following: the wave function of the problem is written in the form $\psi = \psi_0 + \psi_1$, whereby ψ_0 is the ordinary semi-classical solution; for ψ_1 an inhomogeneous equation is obtained, the solution of which is found by the use of the Green's function. In this work it is shown how one can obtain an approximate Green's function, if the trajectories of the classical problem is known.

2. ONE-DIMENSIONAL PROBLEM

1. It is required to find the solution of the Schrödinger equation

$$\psi'' + k^2(x)\psi = 0, \qquad k^2 = 2[E - V(x)], \quad m = \hbar = 1, \tag{1}$$

describing the reflection from a potential barrier $V(x)$ under conditions such that the condition for

the application of the semi-classical approximation is satisfied at all points ($d\lambda/dx \ll 1$).

The solution of the problem can be sought in the form

$$\psi_0 = Ae^{iS}. \tag{2}$$

The function S satisfies the equation

$$S'^2 - (A''/A) = k^2; \quad A = \sqrt{k_0/S'}. \tag{3}$$

Equation(3) is an exact consequence of Eqs. (1) and (2). Considering A''/A a small quantity and finding S by the method of successive approximations, we find (for particles incident from the left)

$$\varphi_0 = \sqrt{k_0/k}\,\exp\left\{i\int^x k\,dx\right\} \tag{4}$$

$$\times \quad \{1 + \xi F_1(x) + \xi^2 F_2(x) + \ldots\},$$

where $\xi = \lambda/l$ is the semi-classical parameter.

The solution (4) as $x \to -\infty$ does not contain terms of the form e^{-ik_0x} in any approximation in ξ, which corresponds to the absence of the reflected wave. In order to determine the coefficient of reflection we put $\psi = \psi_0 + \psi_1$, where

$$\psi_0 = Ae^{iS}, \quad A = \sqrt{k_0/S'}, \; S = \int^x k\,dx.$$

Substituting these expressions in Eq. (1), we obtain

$$\psi_1 + k^2(x)\psi_1 = -A''e^{iS} = -f(x). \tag{5}$$

If we know two linearly independent solutions ϕ_1 and ϕ_2 of Eq. (5) without the right-hand side, then

$$\psi_1(x) = \frac{1}{\Delta}\left\{\varphi_1(x)\int_{-\infty}^{x}\varphi_2(x')f(x')\,dx' + \varphi_2(x)\int_{x}^{\infty}\varphi_1(x')f(x')\,dx'\right\}, \tag{6}$$

where Δ is the Wronskian determinant: $\Delta = \phi_1\phi_2' - \phi_1'\phi_2$. We assume that $\phi_1 \to e^{ik_0x}$ as $x \to +\infty$, $\phi_2 \to e^{-ik_0x}$ as $x \to -\infty$; then the wave function possesses the required asymptotic form:

$$\psi = \psi_0 + \psi_1 = e^{ik_0x} + \frac{e^{-ikx}}{\Delta}\int_{-\infty}^{+\infty}\varphi_1 f\,dx' \quad (x\to-\infty),$$

$$\psi \to e^{ik_0x}\left[1 + \frac{1}{\Delta}\int_{-\infty}^{+\infty}\varphi_2 f\,dx\right] \quad (x\to+\infty).$$

The coefficient of reflection is given by the formula:

$$R = \left|\frac{1}{\Delta}\int_{-\infty}^{+\infty}\varphi_1 f\,dx\right|^2 \tag{7}$$

Since Δ = const, we shall calculate Δ as $x \to \infty$. As $x \to \infty$ the function ϕ_1 takes the form e^{ik_0x}, while the function ϕ_2, on account of the smallness of the coefficient of reflection, is approximately given by

$$\varphi_2 \to e^{-ik_0x + i\alpha}.$$

From this it follows that $|\Delta| = 2k_0$.

For calculation of the integral in Eq. (7) one can use for ϕ_1 the semi-classical expression in first approximation. It is easy to see that an improvement in the precision of ϕ_1 leads to small corrections in R (of the order of ξ). Therefore the expression for R has the form

$$R = \frac{1}{4k_0^2}\left|\int_{-\infty}^{\infty}A''Ae^{2iS}\,dx\right|^2. \tag{8}$$

2. For calculation of the integral in Eq. (8) it is convenient to transform to integration in the complex plane. First of all we make the following transformation:

$$I = \int_{-\infty}^{\infty}A''Ae^{2iS}\,dx = A'Ae^{2iS}\Big|_{-\infty}^{\infty} - \int_{-\infty}^{\infty}(A'A\,2iS' + A'^2)e^{2iS}\,dx.$$

The first term reduces to zero, since $V' \to 0$ as $x \to \pm\infty$. The second term under the integral sign is small in comparison with the first, on account of the semi-classical conditions of the problem. Expressing A in terms of S', we get:

$$I \approx ik_0 \int_{-\infty}^{+\infty} \frac{S''}{S'} e^{2iS}\, dx = \frac{ik_0}{2} \int_{-\infty}^{+\infty} \frac{V'}{E-V} e^{2iS}\, dx. \quad (9)$$

It is convenient to carry out the integration of Eq. (9) in the complex plane. The integral along the infinite semicircle in the upper half-plane is equal to zero, since as $x \to \infty$, $S(x) \to +kx$. In this way the problem is reduced to the investigation of the singular points of the integrand of Eq. (9).

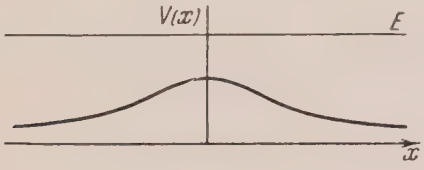

Fig. 1

3. THE THREE-DIMENSIONAL PROBLEM

1. Let us find an expression for the wave-function in the semi-classical approximation in the three-dimensional case. In the wave equation

$$\Delta\psi + 2(E - V(\mathbf{r}))\psi = 0$$

let us make the substitution $\psi = e^{iS}$, where A and S are real functions. From the requirement of the vanishing of the imaginary part, we obtain $\operatorname{div}(A^2 \nabla S) = 0$, or

$$\int A^2 \frac{\partial S}{\partial n} d\sigma = 0, \quad (10)$$

where the integration is carried out over a closed surface. Setting the real part equal to zero, we find

$$(\Delta A/A) - (\nabla S)^2 + k^2 = 0, \quad k^2 = 2(E - V).$$

The condition for the application of the semi-classical approximation implies the smallness of the first term $\Delta A/A$. Neglecting this term, we obtain for S the Hamilton-Jacobi equation of classical mechanics

$$(\nabla S)^2 = 2(E - V).$$

If the trajectories are known for this classical problem, then

$$S(\mathbf{r}) = \int_{\mathbf{r}} k\, dl, \quad (11)$$

where $k = \sqrt{2(E-V)}$ and the integration is carried out along the classical trajectory.

At the end of this work we shall need the semi classical expression for the Green's function $G(\mathbf{r}, \mathbf{r}')$. The semi-classical expression for G can be found if one knows the classical trajectories starting at the point $\mathbf{r}$ and passing into the neighborhood of the point $\mathbf{r}$. Then $G = Ae^{iS}$, where S is determined by the Eq. (11). The meaning of A can be found if one makes use of Eq. (10). The surface of integration must be chosen so that it forms the boundary of a bundle of trajectories passing within a vanishingly small solid angle from point $\mathbf{r}$ and arriving in the neighborhood of the point $\mathbf{r}'$. Along such a surface $\partial S/\partial n$ reduces to zero, since $\partial S/\partial n$ is the component of the momentum normal to the trajectory. From this we find that $A^2(\mathbf{r}, \mathbf{r}')\, k(\mathbf{r}')\, df(\mathbf{r}')$ does not depend on $\mathbf{r}'$ (df is the transverse cross-section of the bundle of trajectories), and consequently, as $\mathbf{r} \to \mathbf{r}'$ (the length of the trajectory tends to zero) A^2 behaves like $a/|\mathbf{r} - \mathbf{r}'|^2$. The constant a must be chosen equal to unity, so that, as $\mathbf{r} \to \mathbf{r}'$,

$$G \to e^{ik|\mathbf{r}-\mathbf{r}'|}/|\mathbf{r} - \mathbf{r}'|.$$

With this normalization, $A = \sqrt{[k(\mathbf{r})/k(\mathbf{r}')]\, d\omega/df(\mathbf{r})}$ ($d\omega$ is the element of solid angle of the bundle of trajectories at the point $\mathbf{r}$).

If there are two or more trajectories connecting the points $\mathbf{r}$ and $\mathbf{r}'$, then, as follows from the principle of superposition, the Green's function is equal to

$$G = \sum A_\lambda e^{iS\lambda}; \quad A_\lambda = \sqrt{[k(\mathbf{r})/k(\mathbf{r}')]\,(d\omega/df)} \quad (12)$$

where the index λ designates the number of the trajectory.

2. Let us now go over to the finding of the semi-classical wave-functions for the scattering problem; these have the asymptotic form $e^{i\mathbf{k}_0\mathbf{r}} + \frac{F}{r} e^{ik_0 r}$. In order to find such wave functions in the semi-classical approximation, it is necessary to know the classical trajectories coming from infinity in the direction of the vector $\mathbf{k}_0$. The corresponding wave functions have the form $\psi_{\mathbf{k}_0} = \sum A'_\lambda e^{iS\lambda}$, where the sum is taken over the various trajectories leading to the given point from infinity.

Let us examine the asymptotic behavior $\psi_{\mathbf{k}_0}(\mathbf{r})$.

As $\mathbf{r} \to \infty$ along a certain direction characterized by the unit vector $\mathbf{n}$, A'_λ falls off as $1/r$. An exception to this is the one term ($\lambda = \lambda_0$) corresponding to particles far from the scattering center, for which the cross-section of the tube of trajectories and the magnitude of the momentum are constant (Fig. 2). In this case we have $A'_{\lambda_0} = 1$ for the indicated normalization of $\psi_{\mathbf{k}_0}$. In agreement with Eq. (10), for the remaining λ, $A'_\lambda = \sqrt{df_0/df_\lambda}$ as $\mathbf{r} \to \infty$, where df_0 is the cross-section of the bundle of trajectories as $\mathbf{k}_0\mathbf{r} \to -\infty$ and $df_\lambda = r^2 d\Omega$, with $d\Omega$ the solid angle of the scattered bundle. It is obvious that $df_0/d\Omega = \sigma_\lambda$ is the classical differential cross-section. Thus, for $\lambda \neq \lambda_0$, A'_λ is given by $A'_\lambda = (1/r)\sqrt{\sigma_\lambda}$. The wave function, as $\mathbf{r} \to \infty$, consists of the sum of two terms: a plane wave (trajectory λ_0) and a diverging wave:

$$\psi \to e^{ik_0\mathbf{r}} + \sum_{\lambda \neq \lambda_0} A'_\lambda e^{iS_\lambda} = e^{ik_0\mathbf{r}} + \frac{e^{ikr}}{r} \sum_\lambda \sqrt{\sigma_\lambda}\, e^{i\varphi_\lambda}, \tag{13}$$

where σ_λ is the classical differential cross section calculated for a trajectory of type λ, while φ_λ, as follows from Eq. (11), is given by

$$\varphi_\lambda = \int k\, dl_\lambda - k_0 \int dl^* + \nu_\lambda \frac{\pi}{2} \tag{14}$$

The second integral is taken along two rays: from $-\infty$ along $\mathbf{k}_0$ to the origin, and from the origin to ∞ along $\mathbf{n}$; the infinities in each of the integrals mutually cancel each other. The integral $k_0 \int dl^*$ along the ray parallel to $\mathbf{n}$ arose from separating out the multiplier e^{ikr}, while on the other hand the integration along $\mathbf{k}_0$ originated in the multiplication of the ψ-function by that multiplying factor which reduces the phase of the plane wave to zero at $r = 0$. The last term of Eq. (14) is determined by the following circumstance: in the three-dimensional problem the semi-classical approximation turns out to be inapplicable near those points of the bundle of trajectories where the cross-sectional area of the bundle vanishes ($A \to \infty$) ‡.

One can become convinced that in crossing such a point there appears an additional phase shift equal to $\pi/2$. In Eq. (14) ν_λ is the number of such points on the trajectory of type λ.

According to Eq. (13) the scattering cross section reduces to zero for scattering angles which are not attained in the classical mechanical solution. The scattering amplitude for these angles can be found by a method analogous to that used in the problem of the reflection from a barrier.

3. We shall seek a wave function in the form

$$\psi = \psi_0 + \psi_1,$$

where $\psi_0 = \sum_\lambda A'_\lambda e^{iS_\lambda}$. For ψ_1 we obtain

$$\Delta\psi_1 + k^2(\mathbf{r})\,\psi_1 = -\sum_\lambda \Delta A_\lambda' e^{iS_\lambda}.$$

If a Green's function satisfying the radiative condition is known, then the solution of the wave equation is

$$\psi = \psi_0 + \frac{1}{4\pi}\int G(\mathbf{r}'\mathbf{r}) \sum_\lambda \Delta A'_\lambda(\mathbf{r}')\, e^{iS_\lambda(\mathbf{r}')}\, d\mathbf{r}'. \tag{15}$$

The expression for the wave function can also be obtained in another way. Let us seek a wave function of the form

$$\psi = e^{ik_0\mathbf{r}} + \psi_1.$$

Then for ψ_1 we obtain the equation

$$\Delta\psi_1 + k^2(\mathbf{r})\,\psi_1 = 2\,Ve^{ik_0\mathbf{r}};$$

by use of the Green's function we obtain a wave function having the required asymptotic form

$$\psi = e^{ik_0\mathbf{r}} - \frac{1}{2\pi}\int G(\mathbf{r}'\mathbf{r})\, V(\mathbf{r}')\, e^{ik_0\mathbf{r}'}\, d\mathbf{r}'. \tag{16}$$

For the Green's function it is sufficient to apply the semi-classical expression (12). Choosing as an initial expression not ψ_0 but ψ, one can obtain the following approximation with respect to the parameter ξ.

4. Let us examine in more detail the case in which the potential is small compared with the energy of the particle ($|V| \ll E = k^2/2$). This condition, as is well known, does not indicate the application of the perturbation theory. As a criterion for the applicability of the perturbation theory, we have the requirement:

$$\frac{|V|}{E}\,\frac{l}{\lambda} \ll 1,$$

‡ For this remark I am indebted to V. S. Kudryavtsev.

where l is a length characterizing the variation of the potential, and $\lambda\!\!\!^{-}$ is the wave-length of the particle.

In the case $V \ll E$ the trajectories are nearly rectilinear , and the computation is considerably simplified. It is easy to show that in order to obtain the terms linear with respect to the potential in the function S one need carry out the integration only along rectillinear trajectories. Indeed, let K_0 be the momentum of the particle moving in a potential V_0, dl_0 an element of length of the trajectory. The change in S upon changing the potential by the amount δV will be

$$\delta S = \int \delta k dl_0 + \int k_0 \delta dl.$$

The second term consists of the change in S due to variation of the trajectory with the potential left unchanged. On account of the stationary character of S this term is quadratic in δl,and consequently, in δV. Therefore, to within terms of second order in δV,

$$\delta S = \int \frac{\delta V}{k_0} dl_0.$$

In this way δS is determined by an integral along the unperturbed trajectory.

Since in the case under study there is only one rectilinear trajectory connecting the points $\mathbf{r}$ and $\mathbf{r}'$ for the unperturbed problem (free motion), the Green's function takes the form

$$G = \frac{e^{ik_0|\mathbf{r}-\mathbf{r}'|}}{|\mathbf{r}-\mathbf{r}'|} \exp\left\{i\int_{\mathbf{r}'}^{\mathbf{r}} (k-k_0)\,dl\right\}. \quad (17)$$

The integration is carried out along a straight line connecting points $\mathbf{r}'$ and $\mathbf{r}$.

With the use of the Green's function (17) we find from Eq. (16)

$$\psi = e^{ik_0\mathbf{r}} - \frac{1}{2\pi}\int \frac{e^{ik_0|\mathbf{r}-\mathbf{r}'|}}{|\mathbf{r}-\mathbf{r}'|} \quad (18)$$

$$\times\, V(\mathbf{r}') \exp\left\{i\mathbf{k}_0\mathbf{r}' - \frac{i}{k_0}\int_{\mathbf{r}}^{\mathbf{r}'} V\,dl_1\right\} d\mathbf{r}',$$

where dl_1 is an element of the rectilinear trajectory connecting points $\mathbf{r}'$ and $\mathbf{r}$. The wave function can be written in the form

$$\psi = e^{ik_0\mathbf{r}}\left(1 - \frac{1}{2\pi}\int \frac{e^{ik_0\rho}}{\rho} V(\mathbf{r}+\vec{\rho})\right.$$

$$\left.\times \exp\left\{i\mathbf{k}_0\vec{\rho} - \frac{i}{k_0}\int_0^{\rho} V\left(\mathbf{r} + l_1\frac{\vec{\rho}}{\rho}\right) dl_1\right\} d\vec{\rho}\right).$$

Here the vector $\vec{\rho} = \mathbf{r}' - \mathbf{r}$.

Let us carry out the integration over the angles of the vector $\vec{\rho}$, using the fact that in varying the angle between $\vec{\rho}$ and $\mathbf{k}_0$, the factor $e^{i\mathbf{k}_0\vec{\rho}}$ oscillates extremely rapidly. Integrating by parts and keeping the first term of order $\xi = 1/k_0 l$, we obtain

$$\psi = e^{ik_0\mathbf{r}}\left(1 + \frac{i}{k_0}\int_0^{\infty} \exp\left\{ik_0\rho - \frac{i}{k_0}\int V dl_1\right\}\right.$$

$$\left.\times\left\{V\left(\mathbf{r} + \rho\frac{\mathbf{k}_0}{k_0}\right)e^{ik_0\rho} - V\left(\mathbf{r} - \rho\frac{\mathbf{k}_0}{k_0}\right)e^{-ik_0\rho}\right\} d\rho\right).$$

Within a precision of the order of the quantity ξ it is permissible to discard the term under the integral sign containing the rapidly oscillating factor $e^{2ik_0\rho}$. Therefore we obtain

$$\psi = e^{ik_0\mathbf{r}}\left(1 - \frac{i}{k_0}\int_0^{\infty} d\rho V\left(\mathbf{r} - \rho\frac{\mathbf{k}_0}{k_0}\right)\right.$$

$$\left.\times \exp\left\{-\frac{i}{k_0}\int_0^{\rho} V\left(\mathbf{r} - \rho_1\frac{\mathbf{k}_0}{k_0}\right) d\rho_1\right\}\right)$$

$$= e^{ik_0\mathbf{r}} \quad (19)$$

$$\times\left(1 - 1 + \exp\left\{-\frac{i}{k_0}\int_0^{\infty} V\left(\mathbf{r} - \rho_1\frac{\mathbf{k}_0}{k_0}\right) d\rho_1\right\}\right)$$

$$= \exp\left\{i\mathbf{k}_0\mathbf{r} - \frac{i}{k_0}\int_{-\infty}^{k} V\,dl_0\right\}.$$

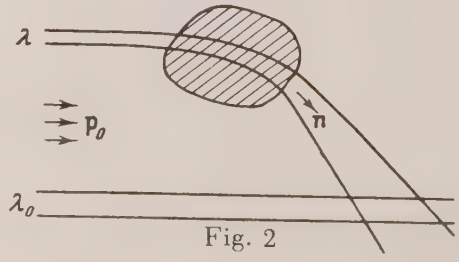

Fig. 2

Equation (19) is the well-known expression for the semi-classical wave function at finite distances from the scattering center[1].

Let us find the asymptotic form of the wave function as $r \to \infty$. From Eq. (19) we find

$$\psi = e^{i\mathbf{k}_0\mathbf{r}} - \frac{e^{ik_0 r}}{r}\left[\frac{1}{2\pi}\int \exp\left\{i\mathbf{q}\mathbf{r}' + \frac{i}{k_0}\int_{\mathbf{r}'}^{\infty} V dl_1\right\} V(\mathbf{r}')\, d\mathbf{r}'\right]$$

$$(\mathbf{q} = \mathbf{k}_0 - k_0\mathbf{n}),$$

where $\mathbf{n}$ is a unit vector in the direction $\mathbf{r}$, dl_1 is an element of the rectilinear trajectory parallel to $\mathbf{n}$. The integral in the exponent of the exponential function can be also written in the form

$$\int_{\mathbf{r}'}^{\infty} V\, dl_1 = \int_0^{\infty} V(\mathbf{r}' + r_1\mathbf{n})\, dr_1.$$

Thus the scattering amplitude is given by the expression

$$f = -\frac{1}{2\pi}\int \exp\left\{i\mathbf{q}\mathbf{r}'' + \frac{i}{k_0}\int_0^{\infty} V(\mathbf{r}' + r_1\mathbf{n})\, dr_1\right\} V(\mathbf{r}')\, d\mathbf{r}', \tag{20}$$

which reduces to the result of perturbation theory for sufficiently small V.

The scattering at large angles, for $V \ll E$, which is not contained in the classical solution of the problem, can be found from Eq. (20). For this we introduce integration by parts with respect to the cosine of the angle between the vectors $\mathbf{r}'$ and $\mathbf{q}$, considering that the expression $e^{i\mathbf{q}\mathbf{r}}$ oscillates rapidly, and we shall keep only the term of the series of order $\xi = 1/k_0 l$:

$$f = -\int \exp\left\{iqr'x + \frac{i}{k_0}\int_{r_1}^{\infty} V dl_1\right\} V(\mathbf{r}')\, dx\, r'^2 dr'$$

$$\approx -\int_0^{\infty} \frac{r'^2\, dr'}{iqr'}\left[V\left(r'\frac{\mathbf{q}}{q}\right)e^{iqr'}\right.$$

$$\exp\left\{\frac{i}{k_0}\int_0^{\infty} V\left(r\frac{\mathbf{q}}{q} + r_1\mathbf{n}\right)dr_1\right\}$$

$$\left. - V\left(-r'\frac{\mathbf{q}}{q}\right)e^{-iqr'}\right.$$

$$\left.\exp\left\{\frac{i}{k_0}\int_0^{\infty} V\left(-r\frac{\mathbf{q}}{q} + r_1 n\right)dr_1\right\}\right].$$

Two terms of the square bracket can be combined, so that

$$f = \frac{i}{q}\int_{-\infty}^{+\infty} r'\, dr' V\left(r'\frac{\mathbf{q}}{q}\right)\exp\left\{iqr' + \frac{i}{k_0}\int_0^{\infty} V\left(r'\frac{\mathbf{q}}{q} + r_1\mathbf{n}\right)dr_1\right\}. \tag{21}$$

Equation (21) recalls the formula for the reflection coefficient in the one-dimensional problem, and it is extremely convenient for integration in the complex plane.

---

[1] L. D. Landau and E. M. Lifshitz, *Quantum Mechanics*, part I, p. 184, 1948

Translated by C. W. Helstrom
73

Hyperfine Structure of the Spectral Lines and Nuclear Spins of U^{233} and Pu^{239}

L. A. KOROSTYLEVA, A. R. STRIGANOV AND N. M. IASHIN

(Submitted to JETP editor July, 1954)
J. Exper. Theoret. Phys. USSR 28, 471-479 (April, 1955)

The hyperfine structure in 12 lines of the U^{233} was investigated. In four cases the maximum total of six components was observed. It was determined that the spin $I_{233} = 5/2$. A deviation from the interval rule was detected, which is explained by the presence of a nuclear quadrupole moment in U^{233}.

Approximately 70 lines with doublet hyperfine structure were discovered in the Pu^{239} spectra. The spin $I_{239} = 1/2$. The width of the hyperfine splitting varied from 0.04 to 0.2 cm^{-1}. In certain spectral lines the stronger component was located on the long wavelength side and in other lines, on the contrary, on the short wavelength side. For principal sublevels this corresponds to a transition from an upper non-split level to a lower split level, and conversely.

1. INTRODUCTION

THE study of the hyperfine structure of the spectral lines of the actinide elements presents great interest. It is known that in many cases the hyperfine structure of the lines suffices provide a reliable determination of the nuclear moments, which are requisites for further development of nuclear shell structure, theory of isomers and beta disintegration, and a series of other questions of nuclear physics. It ought to be noted, however, that up to now researches on the hyperfine structure and nuclear moments of isotopes of the actinide elements are far from complete. According to publications in foreign literature, the nuclear spins of Pa^{231} [1], U^{235} [2], Np^{237} [3], and Am^{241} [4] were determined at the beginning of the present year. In addition, at the end of 1952 and the beginning of 1953 the nuclear spins of U^{233} and Pu^{239} were measured by us and, independently, by S. E. Frisch, N. I. Kalitievskii, and M. P. Chaika. Later in the year our results were confirmed by references 5,6. In reference 5 data are also published concerning the magnetic quadrupole moments of U^{235}. In the present paper results are reported on the determination of the spins of U^{233} and Pu^{239} and, also on our investigations of the hyperfine structure of the lines of the mentioned isotopes.

2. EXPERIMENTAL PART

A discharge tube with a hollow cathode was utilized for the excitation of the spectra of uranium and plutonium. A schematic representation of this tube is given in Fig. 1. The essential part of the tube is the all-metal aluminum cylinder *M*, having in the bottom part a cylindrical cavity *K*, of 5 mm diameter and 10 mm depth, in which the experimental sample is placed. The cylinder *M* is the cathode, in the cavity of which the electric discharge is concentrated. The anode *A* is also made of aluminum. It is a small cylindrical cup with a hole in the bottom for the passage of a light beam. Such construction of the anode permits a more complete recovery of the sample, since, in the main, the sample settles out on the bottom. The anode is connected through the outlet *L* to a high voltage rectifier. The glass tube *N* is incased within cylinder *M* and is bonded to it by the use of picein. This tube *N* has two branches, *F* and *E* (pure gas enters at the opening *F*, impure gas leaves the tube through opening *E*). A circulating inert gas on one side promotes the excitation of luminescence of the test sample and on the other side (at the right time), cleans the discharge tube of contamination. For cooling, the discharge tube was placed in a vessel of water. Such a light source gives sufficiently sharp and intense lines and permits one to work with a small amount of material.

The discharge tube was connected to the vacuum system in the manner shown in Fig. 2. A high vacuum (10^{-4}-10^{-5} mm Hg) was obtained by use of mercury vapor pump *I* in steps. The circulation of

[1] H. Schuler and H. Gollnow, Naturwiss 22, 511 (1934)

[2] O. E. Anderson and H. E. White, Phys. Rev. 71, 911 (1947); G. L. Stukenbrocker and J. R. McNally, Opt. Soc. Am. 40, 336 (1950)

[3] F. S. Tomkins, Phys. Rev. 73, 1214 (1948)

[4] M. Fred and F. S. Tomkins, Phys. Rev. 89, 318 (1953)

[5] K. L. V. Sluis and J. R. McNally, Opt. Soc. Am. 44, 87 (1954)

[6] M. van den Berg, P. F. A. Klinkenberg and P. Regnaut, Physica 20, 37 (1954)

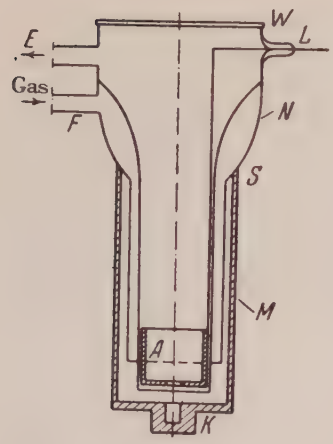

Fig. 1. Discharge Tube

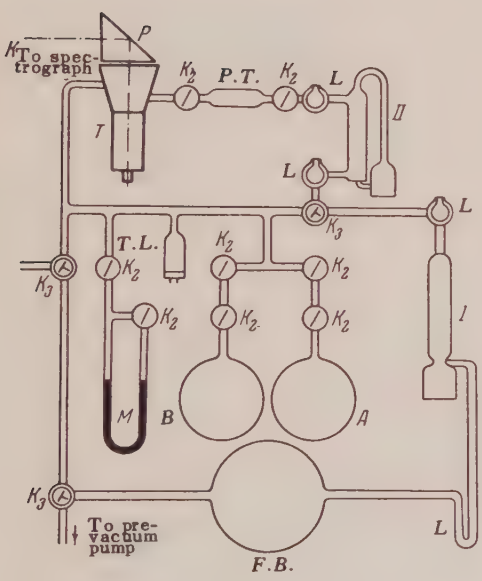

Fig. 2. Scheme of the vacuum arrangement. *T*-discharge tube, *I*-mercury vapor pump, *II*-circulating mercury vapor pump, *P.T.*- potassium trap, *L*-trap for mercury, *T.L.*- thermocouple lamp, *M*-oil manometer, *A* and *B*-balloons filled with gas, *F.B.*-pre-vacuum balloon, K_2-two way stopcock, K_3- three way stopcock, *P*-prism of complete internal reflection

an inert gas through the tube was accomplished by using another mercury vapor pump, *II*. The construction of the circulating pump is such that it can function in pressures of a few millimeters of mercury. The circulating current of such inert gases as argon and krypton was cleaned in a potassium trap. The potassium trap was a glass balloon, on the internal surface of which was applied a fine layer of metallic potassium. For work with helium it is necessary to provide a carbon trap. For measuring the pressure in the discharge tube in the interval from 0.1 to 5 x 10^{-4} mm Hg, a thermocouple manometer (UTV-49 with lamp LT-2) was used. An oil manometer was used for measuring higher pressures.

In our experiments a Fabry-Perot interferometer (IZS-9), prepared in GOI, with half-silvered glass plates was employed as the high resolving power instrument. For preliminary dispersion, a three prism glass Shteinkhel spectrograph was used with a camera having an objective of focal length $F = 640$ mm. The Fabry-Perot interferometer was placed between the light source and the slit of the spectrograph. The interference pattern was projected onto the widened slit of the spectrograph by using a high quality Tessar objective ($F = 600$ mm).

Pure isotopes in the combined oxide forms, U_3O_8 and PuO_2, were used for the investigations of the hyperfine structure of the spectral lines of U^{233} and Pu^{239}. Samples of weight from 3.5 to 8 mg were inserted into the discharge tube. It appeared that uranous oxide and the plutonium oxide in the discharge tube were not immediately excited, even though different inert gases, He, A, Kr, and mixtures of them, were used for the final filling. In order to excite the spectra of uranium and plutonium, we had to reduce initially the uranous oxide and the plutonium oxide to the metallic forms. This reduction was carried out in the discharge tube with atomic hydrogen, under conditions of an electric discharge with current strength near 0.3 amp in the presence of a hydrogen pressure of the order of 2 mm Hg. A time of 1-5 hours was required for reduction to the metal. The tube was fed with a constant current from a high voltage rectifier. Optimum conditions for the excitation of uranium and plutonium are: argon pressure, 2 mm Hg; current strength, 0.2 amp. Hyperfine structure in the spectra of uranium was photographed with interferometer plate separations of 6,10 and 15 mm, with exposures of 20 min. Hyperfine structure in the spectra of plutonium was obtained with separation of 10 and 15 mm and exposures of 30 min.

Hyperfine structure of the lines of uranium and plutonium was measured with an ABBE comparator Central rings located on one side of the interference pattern were used for the measurement of the hyperfine structure of the lines of uranium. The method of Ritschel-Schrammen[7,8] was used for

[7] R. Ritschel, Z. Physik. 79, 1 (1932)

[8] S. Tolansky, *High Resolution Spectroscopy*, London, 1947, Ch. 9

finding the diameters of the circles in this case. Treatment of the measured results proceeded by the method of "right-angled tables" [8] Non-central rings were utilized for measurement of the hyperfine structure of the lines of plutonium. The approximate method of Mc Nair[8] was used for treatment of the measured results.

3. RESULTS

A) Hyperfine structure of the lines of U^{233}

Careful analysis of the U^{233} spectrogram permitted us to observe marked hyperfine structure in 12 lines. Among them a complete resolution of the six-component hyperfine structure was found on five lines: 6826.93; 5976.34; 5915.40; 4515.28 and 4171.59 A. In the remaining lines there was observed either a partial resolution, or strong broadening of the contours of the lines. Combined data on the hyperfine structure of these lines are presented in Table I. Our measurements for the complete range of the splitting are presented in the fourth column of this table; the type of splitting is shown in the fifth column. "Complete" splitting means that six distinct components are observed in the spectrogram; "partial" splitting shows that the structure of the lines, under our conditions, is not fully obtained. The direction of the component of decreasing intensity is recorded in the sixth column. "Red" decrease means that the intensity of the components is diminished on the side of the decreasing wave numbers; "violet" decrease means that the intensity of the components decreases on the side of increasing wave numbers. It is seen from the table that the splitting in spark lines is larger than in arc lines. Among the arc lines the largest width of splitting ($0.32\ cm^{-1}$) is observed for line 5915.40 A; among the spark lines the line 4515.28 A experiences the largest splitting (nearly $0.7\ cm^{-1}$).

Table I

Hyperfine structure in the spectra of U^{233}

Wave length in A	Type of atom	Classification[9]	Total width of the splitting (cm^{-1})	Type of splitting	Direction of decreasing intensity
6826.93	I	$f_3ds^3\ {}^5L_6^0 - 146_6$	~0.15	Complete	Violet
6449.16	I	${}^5K_5^0 - 161_4$	~0.18	Partial	"
6077.29	I	${}^5K_5^0 - 170_6$	—	"	—
5976.34	I	$A_7^0 - 205_8$	~0.25	Complete	Red
5915.40	I	${}^5L_6^0 - 169_7$	0.323	"	"
5564.17	I	$A_7^0 - 218_6$	~0.2	Partial	Violet
4543.63	II	$f_3ds\ \ K^9/_2 - 229^{11}/_2$	~0.5	"	Red
4515.28	II	$L^{11}/_2 - 224^9/_2$	~0.7	Complete	"
4472.33	II	$L^{11}/_2 - 226^{11}/_2$	—	Partial	"
4341.69	II	$L^{11}/_2 - 233^9/_2$	—	"	"
4171.59	II	$L^{13}/_2 - 257^{13}/_2$	~0.6	Complete	Violet
4090.13	II	$L^{13}/_2 - 261^{13}/_2$	~0.5	Partial	—

It is not difficult to make a deduction based on the six-component hyperfine structure of the four completely resolved lines concerning the value of the nuclear spin of U^{233} If it is assumed that $J < I$, the terms ought to split into $2J + 1$ sublevels. This means that each of the investigated lines of uranium should split, not into six components, but into a considerably larger, and moreover, variable, number of components. It is easy to see that arc lines should split into an odd number of components and spark lines into an even number of components. Insofar as this contradicts experiment, the assumption $J < I$ must be considered untrue. Another possibility remains, namely that $I < J$. In this case each term will split into $2I + 1$ sublevels of hyperfine structure. If one assumes that for each observed transition either the upper or the lower level experiences splitting, then the split lines ought to be composed of $2I + 1$ components. On the basis of our experiment, it follows that $2I + 1 = 6$, hence the nuclear spin of U^{233} equals 5/2.

The hyperfine structure of U^{233} in the arc line

[9] C. C. Kiess, C. J. Humphreys and D. D. Laun, J. Nat. Bureau Stand. 37, 57 (1946); J. C. Van den Bosch, Physica 15. 503 (1949)

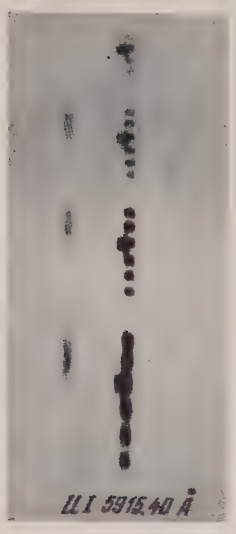

Fig. 3. Hyperfine structure of the line UI 5915.40 A

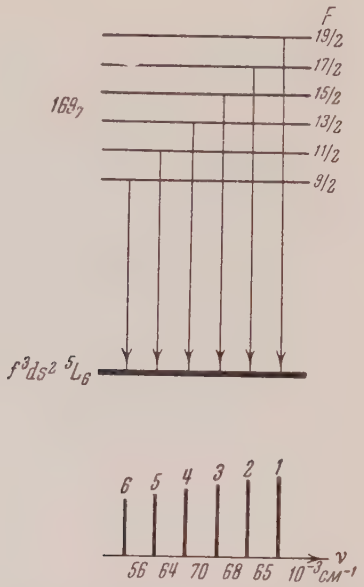

Fig. 5. Transition scheme and hyperfine structure of the line UI 5915.40 A

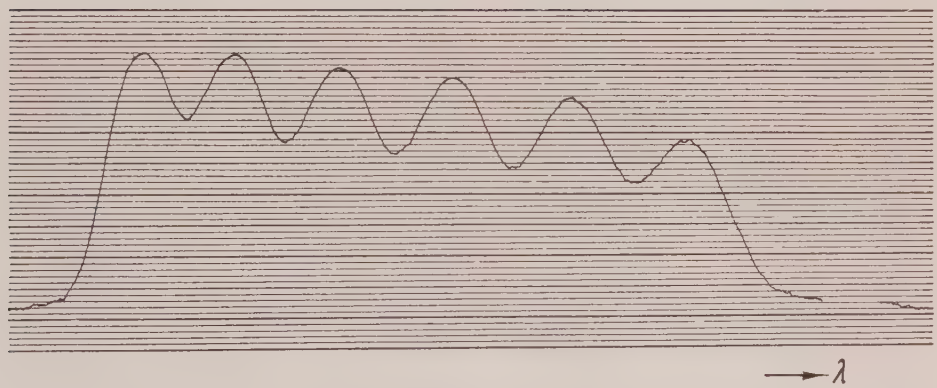

Fig. 4. Microphotograph of the line UI 5915.40 A

5915.40 A was studied by us in the most detail. In Fig. 3 there is shown a spectrogram of this line, obtained with an interval of 10 mm between plates of the interferometer. Fig. 4 shows a microphotograph of the hyperfine structure of this line, recorded by using a registering microphotometer. The six components structure, with the components gradually decreasing in intensity on the side of decreasing wave numbers, is clearly seen in the photographs. At the top of Fig. 5 there is a scheme of transitions, and below, a diagrammatic structure of the line 5915.40 A. The scheme of the transitions is based on the experimental determination of the direction of decrease of intensity of the components of the hyperfine structure, in view of the intensity rule, and on the assumption that only the upper term experiences splitting. From this scheme we see that the term 169_7 appears normal Our assumption concerning the splitting of the upper term in the case of line 5915.40 A is confirmed by the fact that line 6826.93 A, with the same lower term, has half the width of splitting and an inverted decrease of intensity in the components of the hyperfine structure.

By use of the blackening of the marks, we found a relation for the intensities of the components of the hyperfine structure for line 5915.40 A which was shown equal to : $i_1 : i_2 : i_3 : i_4 : i_5 : i_6 = 34 : 30 : 28 : 25 : 21 : 19$. Inasmuch as the times of exposure for production of the darkened marks and plotting of the structure were different, this was assumed to be a Shwartzchild constant. Moreover, the variation of intensities in the interference pattern from order to order was calculated; and a correction was made for the superposition, one on the other, of the edges of the hyperfine structure components. The distribution of intensities along the contour of the interference maxima was found, for the non-splitting argon lines, to be located near the investigated uranium lines. The discovered relation for intensity shows that within the limits of error of the measurements, the intensity rule is obeyed.

The intervals between components of the hyperfine structure, beginning with the long wavelength components, were shown equal to : 0.056; 0.064; 0.070; 0.068; 0.065 cm^{-1} (Fig. 5). The complete width of the structure comprises 0.323 cm^{-1}. If one proceeds from the splitting of the upper term, then according to the interval rule, the relation for the spacing between components ought to be equal to: 56 : 66.2 : 76.4; 86.5 : 96.7. From a comparison of the experimental and theoretical data it is seen that the discovered intervals between components are not contained in the interval rule. This can be explained by the presence of a quadrupole moment in the U^{233} nucleus. If one neglects the excitations of lower terms of the hyperfine structure, the discovered intervals for the line 5915.40 A are contained in the Eq.[10]:

$$\Delta T = \frac{A}{2} C + B \frac{{}^{3}/_{8} C(C+1) + {}^{1}/_{2} IJ(J+1)(I+1)}{IJ(2I-1)(2J-1)}$$

where $A = +0.009$ and $B = -3.8 \times 10^{-2}$. In this formula ΔT is the displacement of the lower term, expressed in cm^{-1} ; $C = F(F+1) - I(I+1) - J(J+1)$; A is a constant, characteristic of the magnetic interaction of the nucleus with the electron shells; B is a constant electric quadrupole interaction.

Comparing data from reference 2 on the hyperfine structure of line 5915.40 A for U^{235} with our data for U^{233}, it is possible to draw the conclusion that the magnetic moments of these isotopes have opposite signs. According to reference 5 the magnetic moment of the U^{235} nucleus has a negative sign; consequently, for the magnetic moment of U^{233} it is necessary to write a positive sign. Judging from the overall width of splitting of the line 5915.40 A for U^{233} and U^{235} [2], it is possible to show that the magnetic moment of U^{233} is approximately 1.5 times larger than the magnetic moment of U^{235}

[10] H. Casimir, Physica 2, 719 (1935)

b) Hyperfine Structure of the Lines of Pu^{239}

Careful analysis of the spectrogram obtained for the study of the hyperfine structure of plutonium showed that approximately 70 lines are split into two components. Of these the following lines were the clearest: 4196.16; 4206.37; 4289.10; 4393.87; 4396.31; 4406.73; 4441.57; 4456.61; 4468.48; 4472.70; 4504.80; 4535.95; 4630.82; 4664.10 A. As an example we reproduce (Fig. 6) one of the sections of plutonium spectra with lines possessing the characteristic doublet hyperfine structure.

Proceeding from the doublet hyperfine structure of the spectral lines of plutonium, it is easy to determine the mechanical nuclear moment. Let us assume that $J < I$; then the terms ought to split into $2J + 1$ sublevels. If one assumes that for each observed transition either the upper or the lower level experiences splitting, the lines ought to be split into $2J + 1$ components. Inasmuch as both arc and spark lines, having different integral and half integral values J, are present in the spectra of plutonium, the different lines ought to split into different numbers of components (arc lines into an odd number of components; spark lines into an even number of components). In our case, however, all split lines have only two components. Consequently, the assumption $J < 1$ falls away and there remains the other possibility, that $J \geq I$. In this case each term will split into $2I + 1$ sublevels of hyperfine structure. Hence, the mechanical nuclear moment of Pu^{239} equals 1/2.

We measured the intervals between components for all lines with this structure. Results of the measurements are presented in Table 2. It was shown that the overall width of the hyperfine structure ranges from 0.04 to 0.2 cm^{-1}. The greatest splitting is found in the lines 4097.51; 4468.48; 4472.70; 4504.80 A, and the least in lines 4753.47; 5549.49; 5562.06; 6091.92; 6119.25; 6488.84 A. Under the conditions of our experiment approximately one hundred lines of plutonium do not give hyperfine splitting. Of these the most intense are: 4101.91; 4167.57; 4189.97; 4335.91; 4385.37; 4419.34; 4627.39; 4689.40; 4731.02 A.

The majority of the split lines of plutonium have components with nearly similar intensities. However, the order of the component lines of the

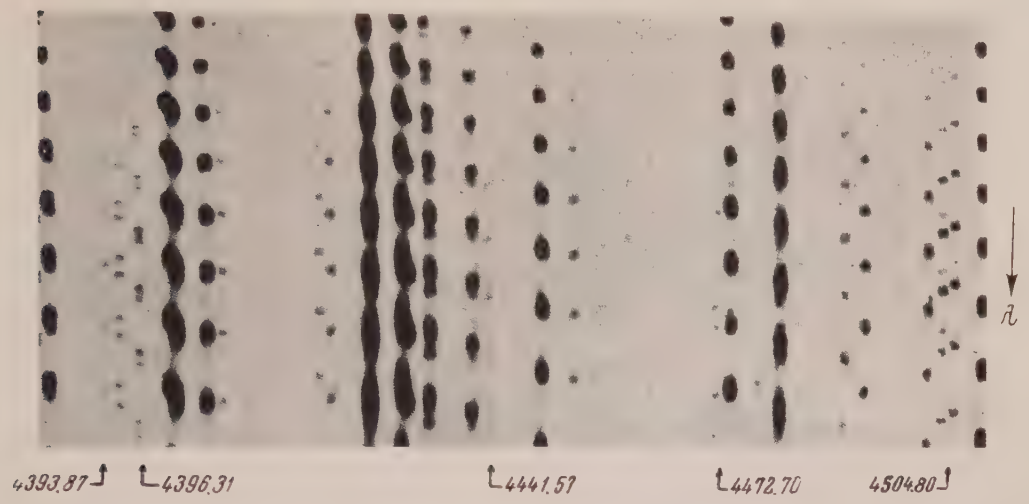

Fig. 6. Hyperfine structure of the lines of plutonium

TABLE II

Lines of plutonium possessing hyperfine structure

Wave length in A	Intensity in Arc	Width of hyperfine structure		Wave length in A	Intensity in Arc	Width of hyperfine structure	
		in cm^{-1}	in A			in cm^{-1}	in A
4064.65	4	0.098	0.016	4691.96	2	0.154	0.034
4097.51	4	0.198	0.033	4698.63		0.101	0.022
4141.22	4	0.158	0.027	4701.04	5	0.121	0.027
4196.16	7	0.111	0.019	4715.64	2	0.08	0.018
4206.37	7	0.128	0.023	4720.62	2	0.06	0.013
4211.96	3	0.119	0.021	4735.31	2	0.097	0.022
4224.02	2	0.116	0.021	4741.82	1	0.089	0.020
4229.63	5	0.130	0.023	4753.47	1	0.048	0.011
4249.63	3	0.118	0.021	4808.89	3	0.116	0.027
4269.64	2	0.073	0.013	4810.54	3	0.061	0.014
4289.10	2	0.115	0.021	4823.04	7	0.133	0.031
4316.61	3	0.143	0.027	4842.40		0.167	0.039
4326.23	2	0.136	0.025	4957.4		0.161	0.040
4358.00	6	0.139	0.026	5014.15		0.136	0.034
4392.73	4	0.089	0.017	5023.28	5	0.089	0.022
4393.87	8	0.134	0.026	5270.01		0.114	0.032
4396.31	8	0.09	0.017	5328.35		0.149	0.042
4406.73	8	0.066	0.013	5341.98		0.149	0.042
4441.57	7	0.101	0.020	5358.44	1	0.074	0.021
4456.61	5	0.127	0.025	5498.42		0.081	0.024
4468.48	4	0.161	0.032	5549.49	2	0.038	0.012
4472.70	10	0.167	0.033	5562.06	4	0.052	0.016
4491.61	3	0.091	0.018	5570.43	3	0.121	0.037
4496.73	2	0.154	0.031	5667.29	1	0.100	0.032
4504.80	10	0.165	0.033	5733.19		0.059	0.019
4507.63		0.078	0.016	5838.92	2	0.054	0.018
4512.75		0.094	0.019	5864.83	1	0.062	0.021
4527.57	2	0.097	0.020	6091.92	4	0.050	0.018
4606.81	4	0.236	0.050	6100.32	5	0.060	0.022
4625.62	2	0.142	0.030	6119.25	4	0.044	0.016
4630.82	4	0.163	0.035	6176.21	4	0.071	0.027
4639.28	3	0.142	0.031	6192.63	7	0.039	0.015
4664.10	6	0.139	0.030	6449.6		0.064	0.027
4676.18	1	0.092	0.020	6488.84	5	0.048	0.020
4689.40	2	0.067	0.015	6542.1		0.051	0.022

hyperfine structure is strongly dependent on the intensity. In some of these the long wavelength component is brighter, in others, on the contrary, the short wavelength component is brighter. As an example we have reproduced in Fig. 7 a microphotograph of the hyperfine structure of the lines 4206.37 and 4393.87 A in two orders, obtained by using a recording Zeiss microphotometer. Such microphotographs were utilized by us for determining the difference of blackening and comparative intensities of the components of the hyperfine structure.

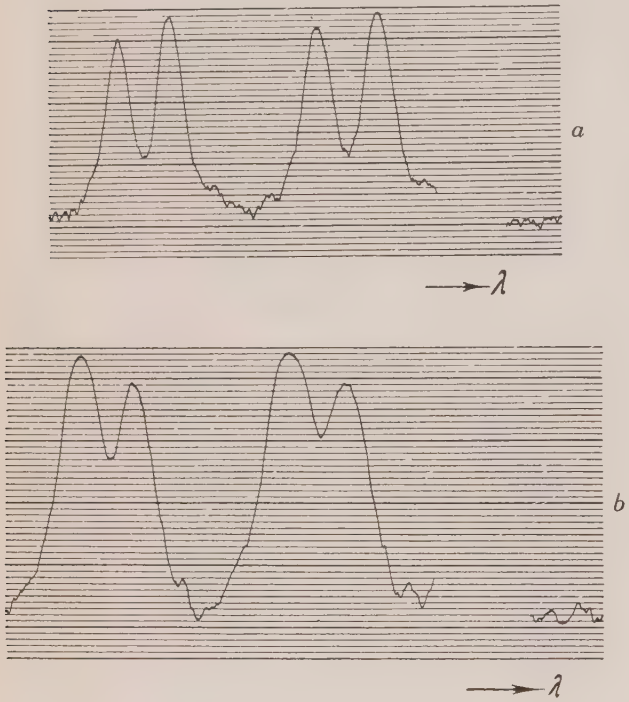

Fig. 7. Microphotographs of the lines of plutonium: $a - \lambda = 4393.87$ A; $b - \lambda = 4206.37$ A

The results of the measurements for five lines of plutonium are presented in Table 3. In the second column are given the differences of blackening between the long wavelength and short wavelength components of the hyperfine structure ($S_g - S_k$). The sign (+) means that the long wavelength component appears more intense in comparison to the short wavelength component; the sign (-) means the inverse relation of intensities. Knowing the degree of darkening of the components of the hyperfine structure, we estimated the comparative intensities of these components, I_g/I_k (see the third column of Table 3), by using characteristic curves, plotted according to the blackened marks of iron spectra, obtained by a nine-fold reduction.

TABLE III

Wave length in A	Difference of darkening $S_g - S_k$	Comparative intensity	
		I_g/I_k	I_B/I_A
4206.37	−0·33	0.49	2.04
4393.87	+0·08	1.25	1.25
4396.31	−0·14	0.75	1.33
4468.48	+0·12	1.37	1.37
4504.80	+0·29	1.87	1.87

It is necessary to explain that in the splitting of the levels (upper or lower) the long wavelength component is brighter in some cases and weaker in others. For the principal sub-levels of the hyperfine structure, the brighter long wavelength component results in transitions from an upper non-split level to a lower split level (Figure 8 A); and on the contrary, the brighter short wavelength component corresponds to transitions from an upper split level to a lower non-split one (Figure 8 b).

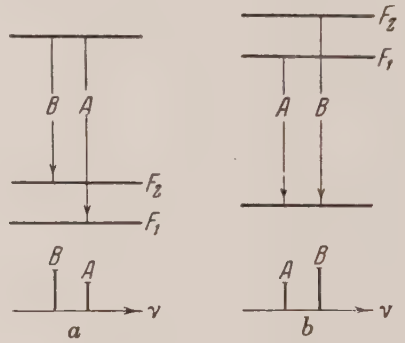

Fig. 8

In the first case $I_g/I_k > 1$; in the second, on the contrary, $I_g/I_k < 1$.

If the hyperfine structure of the lines is determined by the splitting of only one level, the intensities of the hyperfine components will be proportional to the statistical weights of the hyperfine sub-levels. In this case one can write (Fig. 8)

$$\frac{I_B}{I_A} = \frac{2F_2 + 1}{2F_1 + 1}.$$

Since for the plutonium nucleus, $I = 1/2$, then $F_1 = J - 1/2$, $F_2 = J + 1/2$. Hence we obtain :

$$\frac{I_B}{I_A} = \frac{J+1}{J}.$$

In this fashion, knowing the exact relation for the

intensities of two components of the hyperfine structure, one can find the numerical value of the quantum number J for split levels, and on the basis of this number determine the quantum numbers F_1, F_2, characterizing the total angular momentum of the whole atom. From the derived formulas it follows that if $I_B / I_A \approx 1$ (approximately equal intensity components), then the split level of the given lines will be characterized by a large value of the quantum number J; and, on the contrary, if $I_B / I_A > 1$ and attains a value in the interval $(1.5 - 3.0)$ (component intensities strongly differing), then the split level will not have a large value for the size of the quantity J.

It follows from our data that if the terms are principal ones in the case of transitions corresponding to the lines 4206.37 and 4396.31 A, there is a split upper term; and on the contrary, in the case of lines 4393.87; 4468.48; 4504.80 A, there is a split lower term. It is possible, apparently, to consider that for the upper term of the line 4206.37 A and the lower term of the line 4504.80 A. the quantum numbers are $J = 1$, $F_1 = 1/2$ and $F_2 = 3/2$. It ought, nevertheless, to be noted that insofar as the majority of the split lines of plutonium have components of similar intensity, a large part of the terms are characterized by large values for the size of the numbers J.

Very simple deductions show, that for doublet structure of the levels, transitions between split levels in some cases can give three and four-component structure lines. Carefully scanning our spectrograms, we found only one line with four components (4521.04 A) and one with three (4535.95 A). Nevertheless, the structure of these lines ought to be investigated more thoroughly, since it is necessary to keep in mind that it is possible in each of these cases to have a superposition of two different lines, close in wavelength.

If one proceeds from the size of the spin of Pu^{239}, that has been determined, then, in correspondence with theory, the quadrupole moment of this nucleus equals zero.

Translated by D. J. Barth
83

SOVIET PHYSICS - JETP VOLUME 1, NUMBER 2 SEPTEMBER, 1955

The Problem of the Effect of Concentration on the Luminescence of Solutions

M. D. GALANIN
P. N. Lebedev Institute of Physics, Academy of Sciences, USSR
(Submitted to JETP editor April 23, 1954)
J. Exper. Theoret. Phys. USSR **28**, 485-495 (April, 1955)

Improved experimental data are obtained on the effect of concentration on the luminescence of solutions of fluorescent dyes, in connection with their optical properties. It is shown that the theory of resonance excitation energy, correlating the transfer probability with the optical properties of molecular interactions, permits an approximate calculation of the depolarization constants which were previously introduced as empirical data, and also shows the relation between extinction and decrease of the duration of fluorescence.

I. INTRODUCTION

THE influence of the concentration of solutions on fluorescence is already noticeable at relatively small concentrations as concentration depolarization of fluorescence, concentration quenching and decrease of the duration of fluorescence, and is being explained as a resonance transfer of excitation energy between the molecules of the solutes. Vavilov[1-6] developed the general semiphenomenological theory of these effects, in which

[1] S. I. Vavilov, J. Exper. Theoret. Phys. USSR **13**, 13 (1943)

[2] S. I. Vavilov, *Structure of the World*, Moscow, 1950

[3] Th. Förster, Ann. Physik 2, 55 (1948)

[4] Th. Forster, Z. Naturforsch, **4a**, 321 (1949)

[5] M. D. Galanin, J. Exper. Theoret. Phys. USSR 21, 126 (1951)

[6] D. L. Dexter, J. Chem. Phys. 21, 836 (1953)

the transfer probability constants were introduced as empirical data. Further development of the theory of resonance transfer of excitation energy allows us to connect the transfer probability between the molecules with the electron transition probabilities in each of the molecules, and thus with their optical properties[3-6]. However, until now there has been made no quantitative comparison between the experimental data on concentration effects and theoretically calculated data. The significance of this question arose lately from the use of the idea of resonance energy transfer; for instance, in the explanation of fluorescence by fast particles, and of the sensitized luminescence of crystal phosphors.

The experimental data on concentration effects available in the literature are insufficient for a comparison with the theory for their lack of exact spectral measurements. It is also desirable to work out more accurately the details of the method of measurement of the data on the duration of fluorescence.

This work is an attempt to obtain needed experimental data and to compare them with the theory.

2. THE THEORY ON THE INFLUENCE OF EXCITATION ENERGY TRANSFER ON THE LAW OF FLUORESCENCE DECAY

The calculation of the probability of excitation energy transfer between two molecules with known emission and absorption spectra was first developed in the publications of Forster[3,4], and in a more general way by Dexter[6]. The classical interpretation was given in references 5 and 7. If the transitions in both molecules are of the dipole type --- as is the case in the dye molecules discussed later --- then the transfer probability per unit time from molecule M_1 to molecule M_2, at a distance R from M_1 equals

$$W(R, \vartheta_1, \vartheta_2, \phi) = \frac{9}{8\pi}\left(\frac{\overline{\lambda}}{2\pi n}\right)^4 \frac{\overline{\alpha}}{\tau_e}\frac{1}{R^6} \qquad (1)$$

$$\times (2\cos\vartheta_1\cos\vartheta_2 - \sin\vartheta_1\sin\vartheta_2\cos\phi)^2,$$

in which $\overline{\alpha}$ = "average" absorption coefficient of the M_2 molecules (calculated for one molecule) in the region of the emission spectrum of M_1; $\overline{\lambda}$ = average wavelength of the region of overlap of these spectra*; n = index of refraction; τ_e = average natural lifetime of the excited molecule M_1; ϑ_1 and ϑ_2 = angles of the axes of the dipoles with the direction of $\mathbf{R}$; ϕ = azimuth angular difference of the dipoles. Applying Eq. (1) for the calculation of the energy transfer in the luminescence process, it is necessary to sum over all the molecules M_2 surrounding the excited molecule M_1, and to average the integrated average for the molecules M_1. There are possible different physical conditions. In the case of a sufficiently viscous solution, the average separation of the molecules in the mixture is small during the lifetime of the excited state, and the molecules may be considered immobile. In this case the sum of the transfer probabilities will not be constant over the lifetime of the excited state because the distance R between the various M_1 and M_2 will be different, and a strong dependence of the transfer probability on R will call for a larger summed transfer probability during the first part of the excited state than during the later parts of the excited state. Consequently, the decrease of the numbers of M_1--- and therefore the law of decay of the luminescence of M_1 --- will not be exponential[4].

For solutions with relatively low viscosity, with the average diffusion distance comparable or larger than the average distance between the interacting molecules, the assumption can be made that during the lifetime of the excited state of M_1, a continuous mixing with M_2 is taking place, and that the summed transfer probability will remain constant. Such a case was discussed in reference 5 to explain the extinction of fluorescence by absorbing matter.

Both cases must be limiting cases of the precise theory accounting for the influence of diffusion of molecules on the kinetics of the transfer. However, when a very viscous solvent is used in the experiments on the polarization of the luminescence, then the experimental conditions come very close

---

* A more accurate expression [3,6] must include $\int \frac{\alpha(\nu) F(\nu)}{\nu^4} d\nu$, in which $\alpha(\nu)$ = absorption coefficient of M_2; $F(\nu)$ = the normalized spectrum of M_1. As the region of overlap of the absorption spectrum $\alpha(\nu)$ and $F(\nu)$ is usually small, the $\int$ may be replaced by $\frac{\overline{\lambda^4}}{c^4}\int \alpha(\lambda) F(\lambda)\, d\lambda = \frac{\overline{\lambda^4}}{c^4}\overline{\alpha}$.

[7] M. D. Galanin and I. M. Frank, J. Exper. Theoret. Phys. USSR 21, 114 (1951)

to the first case. Indeed the mean square free path length of the diffusional motion during the lifetime of the excited state ($\tau \sim 5 \times 10^{-9}$ sec) equals

$$\overline{\Delta x^2} = \frac{kT}{3\pi\eta}\frac{\tau}{r}, \qquad (2)$$

in which η = viscosity, r = effective radius of the molecule. For viscosities of approximately 5 Poise (glycerine) $\sqrt{\overline{\Delta x^2}} \sim 1$ Å, which is considerably less than the average distance of transfer. Assuming the molecules to be immobile during the lifetime of the excited state, and further assuming a chaotic distribution in the solution, we can find the law of the decrease of the number $n(t)$ of the excited molecules M_1 with time:

$$n(t) = n_0 \exp\left\{-\frac{t}{\tau_0} - N\int (1 - e^{-W(R,\vartheta_1,\vartheta_2,\phi)t})\, dv\right\}, \qquad (3)$$

in which the $\int$ is taken over the entire volume. N = number of molecules M_2 in a unit volume, τ_0 = average duration of the excited state for $N = 0$, whereby τ_0 may be smaller than τ_e because of other processes of extinction of the second kind.

This expression can be obtained by the method indicated by Antonov-Romanovskii for a somewhat different case (bimolecular process)[8]. We carry out the deduction here since only the result is given in reference 8.

If $n(t)$ is the concentration of the excited molecules M_1^* at time and $n(r,t)$ is the concentration of the excited molecules at a distance r from the molecules M_2, $N(r, t)$ the concentration of molecules M_2 at a distance r from M_1^*, $W(r)$ = transfer probability from M_1^* to M_2 in unit time, at a distance r, N = concentration of M_2, $1/\tau$ the probability of emission from M_1, then

$$\frac{dn(t)}{dt} = -\left\{\frac{1}{\tau} + \int_0^\infty N(r,t)\, W(r)\, dv\right\} n(t). \qquad (4)$$

If M_1 and M_2 are initially distributed statistically with respect to each other, then an expression can be written down for the decrease of the pairs of M_1 and M_2 which are separated by a distance r:

$$\frac{dn(r,t)}{dt} = -\left\{\frac{1}{\tau} + \int_0^\infty N(r,t)\, W(r)\, dv + W(r)\right\} n(r,t). \qquad (5)$$

Taking into account that

$$n(t)\, N(r,t) = N n(r,t), \qquad (6)$$

we obtain Eq. (3) from Eq. (4) and Eq. (5). Introducing Eq. (1), the exponent can be written out*:

$$\int_0^\infty (1 - e^{-W(R,\vartheta_1,\vartheta_2,\phi)t})\, dv \qquad (7)$$

$$= \iiint \sin\vartheta_1 \sin\vartheta_2\, d\vartheta_1\, d\vartheta_2\, d\phi \times \int_0^\infty (1 - e^{-\Phi^2(\vartheta_1,\vartheta_2,\phi)t/R^3})\, R^2\, dR$$

$$= \iiint \frac{\sqrt{\Phi^2(\vartheta_1\vartheta_2\phi)}\, t}{3} \sin\vartheta_1 \sin\vartheta_2\, d\vartheta_1\, d\vartheta_2\, d\phi \int_0^\infty \times (1 - e^{-1/x^3})\, dx;\ \int_0^\infty (1 - e^{-1/x^3})\, dx \approx 1{,}8.$$

To integrate over the angles, one must take the absolute value of the angle-dependent factor $\Phi(\vartheta_1, \vartheta_2, \phi)$. In averaging over ϑ_2 one must, holding ϑ_1 fixed, direct the polar axis along the electrical field of the first dipole and to measure ϑ_2 from this direction, then to integrate over ϑ_1 taking into account the angular dependence of the absolute value of the electrical dipole field. Thus we obtain:

$$\iiint |\Phi(\vartheta_1, \vartheta_2, \phi)| \sin\vartheta_1 \sin\vartheta_2\, d\vartheta_1\, d\vartheta_2\, d\phi \qquad (8)$$

$$= 2\int_0^{\pi/2} \sqrt{3\cos^2\vartheta_1 + 1}\, \sin\vartheta_1\, d\vartheta_1 \int_0^{\pi/2}\int_0^{2\pi} \cos\vartheta_2 \sin\vartheta_2 \times d\vartheta_2\, d\phi \approx 4\pi \cdot 0{,}69.$$

[8] V. V. Antonov-Romanovskii, Doklady Akad. Nauk SSSR 2, 93 (1936)

* At the integration over R the lower limit must equal the sum of the radii $2r_0$ of the interacting molecules. Taking zero for it does not introduce any considerable error because $(2r_0)^3 \ll a^3$ (see Sec. 3).

Substituting Eqs. (7) and (8) into Eq. (3) we obtain the law of extinction:

$$n(t) = n_0 \exp\left\{-\frac{t}{\tau_0} - 2q\sqrt{\frac{t}{\tau_0}}\right\}, \quad (9)$$

$$q \approx 1{,}55\left(\frac{\bar{\lambda}}{2\pi n}\right)^2 \sqrt{\frac{\tau_0}{\tau_e}\bar{\alpha}N}. \quad (9')$$

An analogical law of extinction was obtained in a somewhat different way by Förster[4].

3. THE EFFECT OF EXCITATION ENERGY TRANSFER ON THE LUMINESCENCE OF SOLUTIONS

The dependence of the luminescence yield of the molecules M_1 on the concentration of M_2 can be obtained from Eq. (9). Introducing $t/\tau_0 = x$, we obtain:

$$B = B_0 \int_0^\infty e^{-x-2q\sqrt{x}}\,dx \quad (10)$$

$$= B_0\left(1 - 2qe^{q^2}\int_q^\infty e^{-x^2}\,dx\right)$$

$$\approx B_0\left(1 - \sqrt{\pi}\,q + 2q^2 + \cdots\right).$$

The average lifetime τ of the excited molecules is determined by

$$\tau = \int_0^\infty tn(t)\,dt \Big/ \int_0^\infty n(t)\,dt = \tau_0 \quad (11)$$

$$\times\left(\int_0^\infty xe^{-x-2q\sqrt{x}}\,dx \Big/ \int_0^\infty e^{-x-2q\sqrt{x}}\,dx\right)$$

$$= \tau_0\left[\left(1 + q^2 - (3+2q^2)\,qe^{q^2}\int_q^\infty e^{-x^2}\,dx\right)\right.$$

$$\left.\times\left(1 - 2qe^{q^2}\int_q^\infty e^{-x^2}\,dx\right)\right]$$

$$\approx \tau_0\left(1 - \frac{\sqrt{\pi}}{2}\,q + \cdots\right).$$

These results apply to the case of M_1 and M_2 being different (extinction or sensibilized luminescence), as well as to the case when M_1 and M_2 are equal (concentration effects). In the latter case the reverse transfer from M_2 to M_1 is possible, but this transfer can be regarded as independent of the previous one, as the molecule returns very quickly to its normal excited state after the transfer.

In the case of equal molecules the extinction of molecules M_1 [by Eq. (10)] does not determine the decrease of the luminescence yield of the solution, as the larger part of the energy transfers does not lead to extinction, but causes only a depolarization of the luminescence.

For the determination of the relative number of transfers which do not lead to extinction, one must use the following: it is natural to assume that the decrease in luminescence yield in the anti-Stokes part of the spectrum is justified, not only at excitation by radiation from the outside, but also for excitation energy transfer, inasmuch as in both cases the same molecular energy states are participating*. Therefore, to determine the number of energy transfers with and without extinction, the average value of the yield must be found for the region of the overlap of the spectra:

$$\bar{\rho} = \int \rho(\lambda)\alpha(\lambda)F(\lambda)\,d\lambda \Big/ \int \alpha(\lambda)F(\lambda)\,d\lambda$$

in which $\rho(\lambda)$ = quantum yield of luminescence, depending on the wavelength of the exciting light**. The ratio of the numbers of transfers with extinction to the number of transfers without extinction is $(1-\bar{\rho})/\bar{\rho}$. Evidently the transfers without extinction do not reduce the lifetime of the excited state of the molecules. The reduction in lifetime, as well as the decrease in yield, is determined by the transfers with extinction. The depolarization of the luminescence depends on the relative number of molecules emitting before a transfer, and after one or several transfers. Assuming a complete depolarization of the emission after one transfer[2,9], we obtain for the degree of depolarization:

$$P = \frac{\left(\sum \frac{2P_k}{3-P_k} I_k\right)}{\left(\sum \frac{2}{3-P_k} I_k\right) \approx P_0 I_0} \Big/ \left(\sum I_k\right), \quad (12)$$

[9] M. D. Galanin, Trudy Fiz. Akad. Nauk SSSR 5, (1950)

* The shifting and broadening of the levels as a consequence of interaction for complex molecules is small compared to the width of the spectra.

** For the evaluation of the absolute value of ρ, it is necessary to consider only the "extinction of the first kind" since the "extinctions of the second kind", competing with the transfer, is calculated by the introduction of τ_0 instead of τ_e.

where P_k and I_k are the polarization and intensity after k transfers [taking $P_1 = P_2 \ldots = 0$; $2/(3 - P_k) \approx 2/3$]. It appears that I_0 is proportional to the yield of emission of molecules which were not subject to an energy transfer, but ΣI_k proportional to the yield of luminescence of all molecules.

On the basis of Eqs. (10), (11) and (12), we obtain the following expressions for the yield, duration and degree of polarization of the fluorescence as a function of the concentration, at small concentrations:

$$B/B_0 = 1 - \sqrt{\pi}\, q\,(1 - \bar{\rho}), \qquad (13)$$
$$\tau/\tau_0 = 1 - {}^1/_2 \sqrt{\pi}\, q\,(1 - \bar{\rho}),$$
$$P/P_0 = 1 - \sqrt{\pi}\, q,$$

in which q is determined by Eq. (9′). By a comparison of these expressions with the corresponding formulas in Vavilov's theory[1,2], it is possible to connect the empirical constants with factors determining the transfer probability. Vavilov's theory introduces the ratio of the transfer probability without extinction to the probability of emission τ_0/k_2, corresponding to the expression for the transfer with extinction τ_0/k_1. Vavilov's theory further postulates that there exists a "momentary" extinction within the sphere of action ω. The latter is required to explain the observation of the unproportional change of yield and τ. From Eq. (13) we obtain for the empirical constants

$$\frac{\tau_0}{k_2} = 2{,}74\left(\frac{\bar{\lambda}}{2\pi n}\right)^2 \sqrt{\frac{\tau_0}{\tau_e}\,\bar{\alpha}}; \quad \frac{\tau_0}{k_1} \qquad (14)$$
$$= \omega = \frac{1}{2}\,\frac{\tau_0}{k_2}\,(1 - \bar{\rho}).$$

In accordance with Eq. (13), the change of the yield is not proportional to τ: at small concentrations the yield decreases twice as fast as τ. Thus the concentration extinction in itself does not represent a pure "extinction of the second kind"[2,4,9]. This result is obtained from the theory without the use of a "sphere of action of momentary extinction". From this standpoint the concept of the sphere of action gives an approximation to the decay law (9) (with the transfer probability changing during the duration of the excited state) for the momentary extinction, with the consequent exponential law of decay corresponding to the constant transfer probability. Figure 1 demonstrates the law of extinction (9) with $q = 0.5$, and the exponential law of decay with preceding instantaneous drop (the areas under the curves are equal), showing the degree of such an approximation. The radius of the sphere of action of Vavilov's theory can be compared (see also reference 4) with the characteristic distance $a = (3/4 \times q/N)^{1/3}$. At such a concentration, with the average distance between the molecules of the order of magnitude of a, the transfer probability becomes comparable to the emission probability.

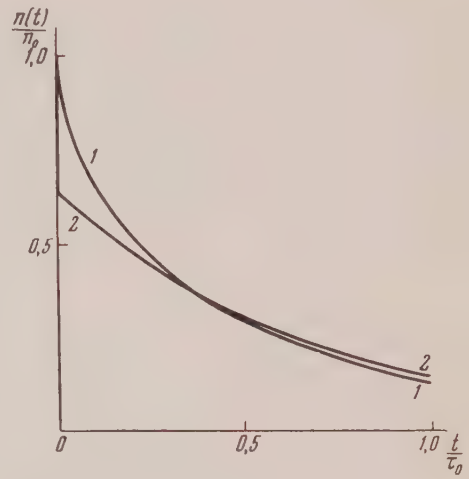

Fig. 1. Law of luminescence decay:
1. according to Eq. (9) with $q = 0.5$
2. exponential law with instantaneous extinction at the beginning.

4. METHOD OF MEASUREMENT

In empirical studies of the influence of the concentration of solutions on the luminescence, it is necessary to consider reabsorption and secondary emission[2,10]. Reabsorption can be avoided by the use of sufficiently thin layers. Vavilov[11] gives the method to account for the influence of secondary emission on the depolarization of the luminescence. In similar fashion, reabsorption can be avoided or accounted for by the measurement of the relative yield and the duration of the fluorescence. Up to now all measurements of the dependence of the duration of the fluorescence on the concentration have been made in thick layers. It was first mentioned in reference 9 that the duration of the fluorescence of a fluorescein solution is considerably increased by reabsorption and secondary emis-

[10] S. I. Vavilov, M. D. Galanin and F. M. Pekerman, Izv. Akad. Nauk SSSR, Ser. Fiz. 13, 18 (1949)

[11] S. I. Vavilov, Doklady Akad. Nauk SSSR 16, 263 (1953)

sion. This effect was recently studied in detail by Bailey and Rolefson[12], and by Schmillen[13]. The following is a brief account of the method of measurement of this investigation.

a) POLARIZATION OF LUMINESCENCE

Polarization of luminescence was measured visually with the aid of Savard's plate and compensating glass wedge. The exciting light from a Hg-lamp with light filters for 436 mμ and 546 mμ was polarized with a polarizing prism. Thin layers were used to avoid secondary emission; they were obtained by squeezing a drop of the solution between two glass plates. From 5 to 10% of the exciting light was absorbed by these layers. For high concentrations it was difficult to obtain such layers, and corrections according to Vavilov's method[11] were applied.

b) RELATIVE YIELD

The relative yield was measured by the intensity of the long wavelength part of the fluorescence spectrum of thin layers. A monochromator UM-2 was used with a photomultiplier behind the exit slit. The absorption of the exciting light in the layer was measured simultaneously by means of a selenium cell. The thickness of the layers was such that 10 to 20% of the exciting light was absorbed.

c) ABSORPTION AND LUMINESCENCE SPECTRA

The absorption spectra in the visible part of the spectrum were measured with a recording spectrophotometer. The luminescence spectra were obtained with the monochromator UM-2 and a photomultiplier. The spectral sensitivity was established with an incandescent lamp of known color temperature. Thin layers of low concentration solutions were used to avoid distortion of the spectra by reabsorption. Within the region of concentrations used, the absorption and emission spectra do not change with concentration.

d) THE DEPENDENCE OF THE YIELD ON THE WAVELENGTH OF THE EXCITING LIGHT

The dependence of the yield on the wavelength of the exciting light in the long wavelength part was measured by excitation with light of different wavelength from the monochromator UM-2 (source: incandescent lamp).

The relative brightness of the solutions was measured with a photomultiplier through a filter transmitting the long wavelength part of the luminescence spectrum. Thick layers of considerable concentration were used to establish complete absorption of all wavelengths of the exciting light. The relative energy in the various spectral sections was measured with a thermopile.

e) FLUORESCENCE DURATION τ

The fluorescence duration τ was measured with a "phase-fluorometer"[14]. The time τ depends strongly on the thickness of the layer of the solution for reabsorption and secondary fluorescence. Table I shows the measured τ for solutions of fluorescein in glycerine at 10^{-4} g/ml and 10^{-3} g/ml under excitation with 436 mμ.

TABLE I

Dependence of τ of fluorescein solution on the thickness of the layer

Layer thickness mm	$\tau \times 10^9$ sec	
	$c = 10^{-4}$ g/ml	$c = 10^{-3}$ g/ml
8	5.5	6.1
1	5.0	5.9
0.2	4.0	5.2
0.04	—	4.2

The dependence of τ on concentration can be strongly distorted at measurements of thick layers as shown in Fig. 2 for Rhodamine 5G (compare references 12,13).

The dependence of τ on concentration was measured on thin layers similar to those used for the measurement of the relative yield. In measurements of the duration of luminescence by the phase method with sinusoidal modulation it is well to keep in mind that the result depends on the law of extinction and can be compared with an average τ as determined by Eq. (11) if this law is known. To arrive at τ from the phase shift it is useful in our

[12] E. A. Bailey and G. K. Rolefson, J. Chem. Phys. 21, 1315 (1953)

[13] A. Schmillen, Z. Physik 135, 294 (1953)

[14] L. A. Tumerman, J. Exper. Theoret. Phys. USSR 11, 515 (1941); M. D. Galanin, Doklady Akad. Nauk SSSR 73, 925 (1950)

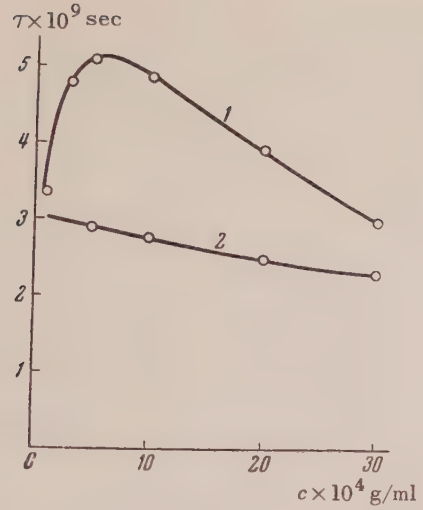

Fig. 2. Dependence of τ on concentration of Rhodamine 5G in glycerine:
1. thick layer
2. thin layer.

case to apply the formula established for the exponential decay and to apply a correction for the law of extinction (9) for small q. Exciting the luminescence with sinusoidally modulated light of frequency Ω, the phase shift x between excitation and luminescence with a decay law (9) can be found, with the phase determined in reference 9:

$$\int_0^\infty e^{-x-2q\sqrt{x}} \cos(\Omega\tau_0 x)\, dx. \qquad (15)$$

The solution gives:

$$\operatorname{tg}\psi = \Omega\tau_{fl} = \Omega\tau_0 [1 - {}^1/_2 \sqrt{\pi}\, q f(\Omega\tau_0)]. \qquad (16)$$

The correction to Eq. (11):

$$f(\Omega\tau_0) = \sqrt[4]{1 + (\Omega\tau_0)^2} \,/\, \sqrt{1 + {}^9/_4 (\Omega\tau_0)^2}$$

is, in our case (with $1/\Omega = 6.8 \times 10^{-9}$ sec), between 0.8 and 0.9.

f) DETERMINATION OF "NATURAL" LIFETIME OF THE EXCITED MOLECULE IN THE ABSENCE OF ANY OTHER EXTINCTION PROCESSES

This lifetime was determined from the first absorption band under the supposition that the probabilities are equal for transitions from the ground state to the excited electronic state, and reverse. For such a case it is known that

$$\frac{1}{\tau_e} = \frac{8\pi c}{\bar{\lambda}_1^4} \int \alpha(\lambda)\, d\lambda, \qquad (17)$$

in which $\bar{\lambda}_1$ = average wavelength of the absorption band and $\alpha(\lambda)$ = absorption coefficient reduced for one molecule.

5. RESULTS OF MEASUREMENTS AND COMPARISON WITH THEORY

Measurements were made on three dyes in solution in glycerine: Fluorescein (alkaline solution); Rhodamine 5G and acridine orange. Figures 3, 4 and 5 show the dependence on concentration of the degree of polarization P, duration of fluorescence τ, and relative yield B. The general appearance of the curves corresponds qualitatively with Eqs. (10) and (11). For a quantitative comparison it is more appropriate to use the experimental data for low concentrations, since at higher concentrations complications occur that are unaccounted for by the theory. In Table II are listed the coefficients determined from the initial slope of the curves; these coefficients correspond to the empirical constants (14) of the phenomenological theory, and the values calculated from the transfer theory (13).

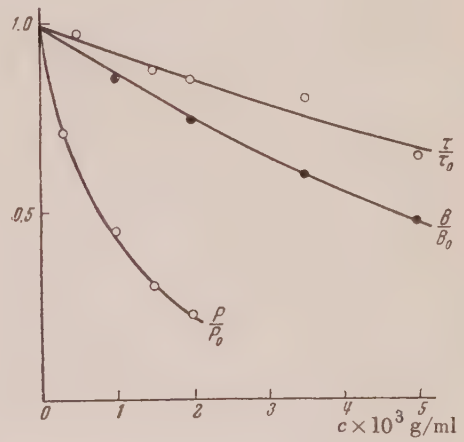

Fig. 3. Dependence of P, τ, and B on concentration of fluorescein solution.
(10^{-3} g/ml = 1.6×10^{18} molecules/cm^3)

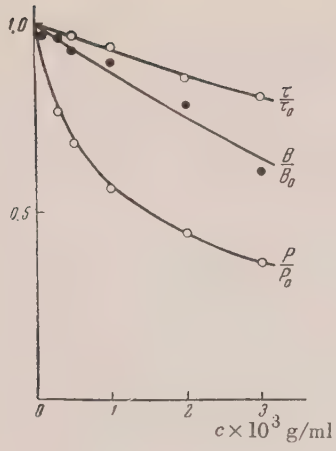

Fig. 4. Dependence of P, τ, and B on concentration of Rhodamine 5G solution. (10^{-3} g/ml = 1.3×10^{18} molecules/cm^3)

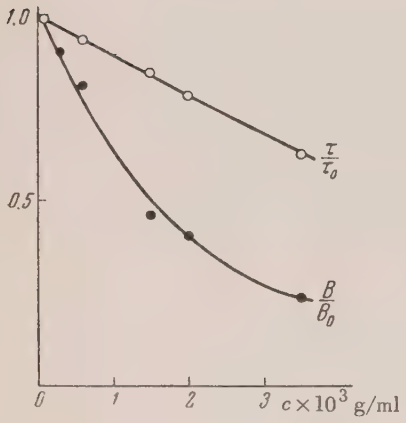

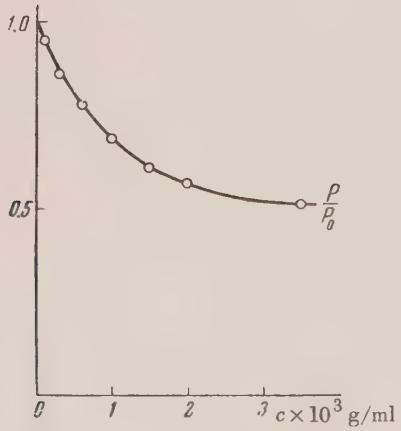

Fig. 5. Dependence of P, τ, and B on concentration of acridine orange solution. (10^{-3} g/ml = 1.8×10^{18} molecules/cm^3)

Comparison of the experimental and theoretical data allows the following conclusions:

1. The probabilities (τ_0 / k_2) calculated from the transfer theory agree satisfactorily with the τ_0 / k_2 determined from the depolarization of the luminescence.

2. The ratio of the relative yield to τ (twice the slope of the yield as compared with τ, or in terms of the theory which includes the sphere of action, the equality $\tau_0 / k_1 = \omega$) is noted approximately*. Deviations from this relation [see $k_1 (\tau_0 / k_1 + \omega) \tau_0$ in Table II] are within the experimental error.

3. The ratio between transfer probabilities with and without extinction, for fluorescein, agree to the order of magnitude with the decrease of the yield for the "anti-Stokes transfer". In the other two cases the transfer probability with extinction is considerably greater than would result from the dependence of the yield on the wavelength of the exciting light. This is apparently due to the quantum yield being close to unity for fluorescein in the Stokes region[15] while it is smaller than unity for the other two dyes, and it is possible that there exist extinctions of the first kind in addition to those of the second kind. Therefore, it is incorrect in these cases to normalize the yield to unity in the Stokes region, as it is being done for the calculation of $\bar{\rho}$ in the region of overlap of the spectra.

Thus the theory of excitation energy transfer satisfactorily agrees with the experimental data on fluorescent solutions of fluorescent solutions of dyes. Several observed discrepancies can be attributed to the inaccuracy of experimental data (possible error in the entity of the measurements which are necessary for a comparison with the theory should be estimated at not less than 20-30%), as well as to the fact that some complicating conditions have not been taken into account. It is, for instance, possible in some cases that a Coulomb repulsion has an effect on the statistical distribution of the molecules if they are ionized. As mentioned in reference 4, this influence is small at distances of transfer, all the more as the dielectric constant of the solvent

* In the Table the values of (τ_0 / k_1) (exp) were determined from the curve for τ, corrections introduced according to Eq. (16).

[15] M. D. Galanin and S. A. Chishikova, J. Exper. Theoret. Phys. USSR 26, 624 (1954)

TABLE II

Material	$\tau_e \times 10^8$ sec	$\tau_0 \times 10^8$ sec	$\bar{\lambda}$ mμ	$\bar{\alpha} \times 10^{-8} \left(\frac{\text{mol}}{\text{e}} \text{ cm}\right)^{-1}$	$\frac{\tau_0}{k_2}$ (exp)	$\frac{\tau_0}{k_2}$ (theor)	$\frac{\tau_0}{k_1}$ (exp)	$\frac{\tau_0}{k_1} + \omega$ (exp)	$\frac{\tau_0}{k_1} + \omega$ / τ_0/k_2 (exp)	$1-\bar{\rho}$	$\frac{\tau_0}{k_2} + \omega$ / τ_0/k_1 (exp)	a Å
					$10^{20} \left(\frac{\text{molecules}}{\text{cm}^3}\right)^{-1}$							
Fluorescein	4.2	4.2	509	0.20	59	48	5.5	8.8	0.15	0.08	1.6	43
Rhodamine 5G	6.2	3.0	544	0.24	54	42	6.2	10	0.18	0.06	1.6	42
Acridine Orange	7.25	3.8	514	0.10	25	25	8.2	18	0.72	0.16	2.2	32

is very large ($\epsilon = 74$), but it may be significant for doubly charged ions. Also, density fluctuations need further precision for the energy transfer at concentrations when it is necessary to account for both, the first and subsequent transfers. As a consequence of the very strong dependence of the transfer probability on the distance after the first transfer, there is a relative increase of the number of excited molecules near unexcited molecules from which the excitation energy was obtained. Evidently this condition will have as a consequence a faster decay but a slower depolarization. The theory also does not account for the influence of the larger transfer probability of molecules whose dipole axes form a small angle; but it was assumed that already the first transfer leads to a complete depolarization.

Corrections to increase the mentioned accuracy apparently should not be large, but will have no influence on the qualitative explanation by the theory of resonance energy transfer, of the effects of concentration in the region of sufficiently small concentrations.

I take this opportunity to express my sincere appreciation to V. V. Antonov-Romanovskii and M. W. Fok for their discussion of this work.

Translated by W. Jaskowsky
85

Investigation of High Frequency Discharges by the Probe Method

Kh. A. Dzherpetov and G. M. Pateiuk
Moscow State University

(Submitted to JETP editor March 6, 1954)
J. Exper. Theoret. Phys. USSR **28**, 343-351 (March, 1955)

A comparison is made of existing probe methods for the investigation of high-frequency discharges in He, Ne, Ar and H_2. We consider changes in a discharge which arise when additional electrodes---counterprobes---are inserted in a high frequency discharge. An investigation is carried out of the distribution of temperature, electron concentration and space potential along the axis of the discharge tube, and also of the dependence of these parameters upon the gas pressure and the voltage of the high-frequency field at the exterior electrodes of the discharge tube.

1. INTRODUCTION

THE method of probes is a very widespread one for measuring the electrical parameters of the positive column of a gas discharge. Probe methods, adequately proven for the investigation of direct current gas discharges, have not been sufficiently examined for their application to high-frequency discharges.

As is well known, in probe measurements in a direct current discharge, the potential of the probe is referred to the potential of one of the electrodes. In high-frequency discharges, in view of the fact that there is a high-frequency varying potential on the electrodes, they cannot be used as reference points, or counterprobes.

In the researches in references 1,2 on investigation of high-frequency gas discharges by the method of probes, a third electrode at ground potential is used as a counterprobe. The potential of the probe can be referred to that of the counterprobe only under the condition that the potential of the region about the counterprobe does not depend upon the probe current. This is possible only if many more electrons and ions from the discharge fall on the counterprobe than on the probe. This condition requires a counterprobe of large surface area. However it is not known how a counterprobe of large dimensions will influence the regime of a high-frequency discharge. Taking these circumstances into account, Biberman and Panin [3] advanced a method of two probes, and used it to determine the electron temperature and the concentration of charged particles, under the hypothesis that there was a Maxwellian distribution of electrons and ions in velocity. However the method of counterprobes has been used to determine not only the electron temperature and the concentration of charged particles but also the space potential. In addition, it gives criteria for a Maxwellian distribution of the electrons in velocity. Therefore the study of this method of investigating high-frequency discharges presents some interest.

The aims of the present work are:

a) The comparison of data obtained by the experimental method of two probes with data obtained by the application of counterprobes.

b) The experimental study of possible disturbances caused by introducing counterprobes in the discharge.

c) The investigation of the distribution along the axis of the discharge tube of the electron temperature and concentration and the space potential for various gas pressures.

2. EXPERIMENTAL ARRANGEMENT

A gas discharge tube of length 70 cm and diameter 3.2 cm (Fig. 1a) was employed in carrying out the proposed undertaking. Inside the tube are placed two counterprobes: one, *f*, is fixed in the center of the tube near the probe, and the other, *m*, is movable. Both counterprobes are made of nickel foil with equal surface areas (30 cm^2).

In the middle of the tube (at its axis) are located two identical platinum probes *P*, 4 mm apart, with diameters of 0.1 mm and lengths of 4 mm. The ratio of the area of the probes to the area of the counterprobe is approximately 1:2500. The probes

[1] Banerji and A. Ganguli, Phil. Mag. 11, 410 (1931); 13, 494 (1932); 15, 676 (1933)

[2] H. Beek, Z. Physik 97, 355 (1935)

[3] B. Biberman and L. Panin, Zh. Tekhn. Fiz. 21, 12 (1951)

are situated strictly on the tube axis, in order that a possible gradient in the density of charged particles in the discharge should not affect the conditions under which particles strike the probe.

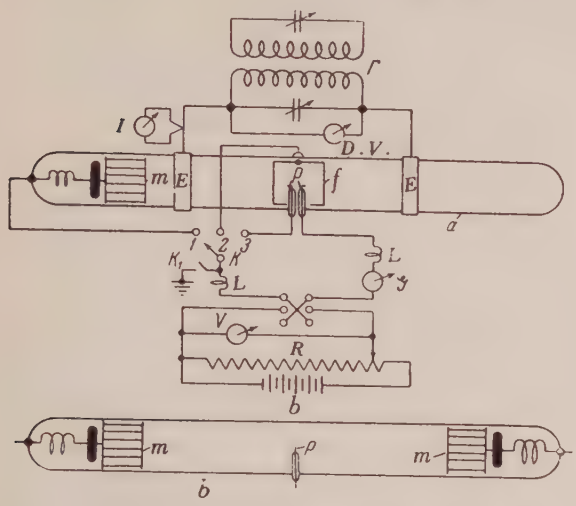

Fig. 1. Scheme for taking probe characteristics and types of discharge tubes.

In this manner we succeeded in getting a symmetric probe characteristic by means of the two probes method.

In investigating the distribution of electron temperature T_e, electron concentration n_e and space potential V_s, two movable counterprobes of identical form and dimensions are used (Fig. 1b). A cylindrical probe P is located in the center of the tube (perpendicular to the axis). Most of the discharge tubes for work with inert gases were unsoldered from the vacuum system. Absorbers were used to maintain the purity of the gas.

The scheme for probe measurements is presented in Fig. 1. Two external electrodes E in the form of rings surround the tube on the outside. Using the switch K it is possible to take the probe characteristics with the movable counterprobe (position 1), with the inmovable counterprobe (position 2), and with two probes (position 3). While taking the probe characteristics the counterprobe is grounded separately, but in working with the two probes the ground is opened by means of the switch K_1. The chokes L are inserted in the probe circuit to suppress the high-frequency oscillations. In taking the probe characteristics for a field of frequency 5 mc, the discharge current in the tube is taken as a parameter. The current is measured by means of a milliammeter I. For higher frequencies (100 mc and above) the high-frequency voltage between the external electrodes serves as parameter. The voltage is measured by means of a diode voltmeter D.V. assembled in the laboratory.

Linear extrapolation of the ion current is used to determine the electron current from the probe characteristic. The electron temperature is determined from the slope of a semi-logarithmic plot of the characteristic in the case of one-probe measurements, or computed from the formula of Biberman-Panin[3] in the case of two-probe measurements. The point on the semilogarithmic plot at which the graph of the characteristic begins to depart from a straight line is taken as the space potential.

3. COMPARISON OF ELECTRON TEMPERATURES FOUND BY ONE-AND TWO-PROBE METHODS

Measurements were performed in neon and helium to compare the values of the electron temperature gotten by means of the methods of one or two probes.

In Fig. 2 is shown the probe characteristic obtained by means of the probes (a), and also the volt-ampere and the semilogarithmic characteristics obtained by means of a movable counterprobe (b) and a central (immovable) counterprobe (c) respectively, with helium in the tube given in Fig. 1a.

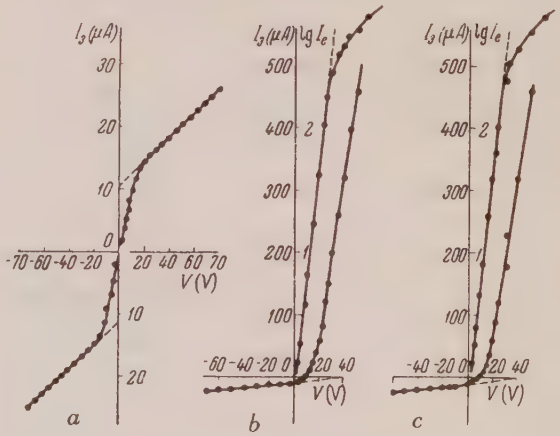

Fig. 2. Probe characteristics in He, obtained:(a) by the two-probe method, (b) by the one-probe method with the use of a fixed counterprobe f, (c) by the one-probe method with a movable counterprobe m.

The frequency of the field was 5 mc. These semilogarithmic plots, the same for one counterprobe as the other, point in the direction of a Maxwellian

distribution of the electrons in velocity, which makes possible the use of the semilogarithmic characteristic as a general method of determining the electron temperature. However it must be pointed out that at low gas pressures cases were observed that depart from a straight-line semilogarithmic curve, indicating the absence of a Maxwellian distribution in electron velocity in a high-frequency discharge. The comparison of the two methods refers to those cases where there is a Maxwellian distribution of the electrons in velocity.

The results of the measurement of electron temperature by the various methods in helium and neon are given in Table 1.

From the data given in Table 1 the conclusion can be drawn that all three methods give the same value of the electron temperature. Some differences, evidently, can be put down to the account of experimental error. Thus it can be said that in the determination of the electron temperature by the the method of probes in a high-frequency discharge, counterprobes produce no essential modification.

4. MODIFICATIONS PRODUCED BY COUNTERPROBES

In the work with the tube illustrated in Fig. 1a it was noticed that for low gas pressures the discharge in the vicinity of the central counterprobe was restricted to the axis of the tube. This circumstance, naturally, shows some distortion of the discharge by the movable counterprobe, which can be verified by the measurement of other parameters. To study these modifications by means of a movable counterprobe inserted in the discharge, a tube was used of the type presented in Fig. 1b.

Argon was selected for this work since the semilogarithmic characteristic in argon has a sharp break that permits a high precision determination of space potential and the electron concentration along with the electron temperature. Measurements were taken for a field of frequency of 5 mc with a pressure of 0.23 mm Hg and a discharge current of 100 ma. In the discharge under the indicated conditions were observed three luminous parts separated by dark spaces.

The study of the effect of the counterprobe was carried out in the following manner. The external electrodes are stationed at a distance of 18 cm from each other, and the counterprobe at distances of 3 cm from the external electrodes, i.e., 24 cm from each other. Keeping the distance between the external electrode and counterprobe constant, the electrode and counterprobe are displaced along the tube axis so that the probe falls at successively different positions along the tube axis. Thus at each position along the axis of the discharge tube a probe characteristic is taken with either the left counterprobe, the right counterprobe, or finally both, connected as reference electrodes.

From the probe characteristics obtained for various points along the axis of the discharge tube, the electron temperature, the space potential, and the electron concentration are determined. These measurements are taken within the luminous parts of the discharge. The distribution obtained for the space potential is shown in Fig. 3. In the lower part of Fig. 3 is presented the external form of the working part of the discharge in which measurements were carried out (Fig. 1b). Curve 1 gives the distribution of space potential along the axis of the tube found in measurements with the right-

TABLE 1

Gas	Pressure (mm Hg)	Field Frequency mc	Electron Temperature (°K)		
			Two probes	Movable probe	Inmovable probe
Helium	0.23	5	52000	57500	58000
	—	—	50000	58000	57500
	—	—	48000	53000	53000
	—	—	55000	53000	54000
	0.4	5	50000	55000	55000
	—	—	47000	54000	53000
	—	—	48000	50000	50000
	—	—	49000	50000	50000
Neon	0.56	130	50000	46000	–
	—	—	49000	46000	—
	—	—	50000	45500	—

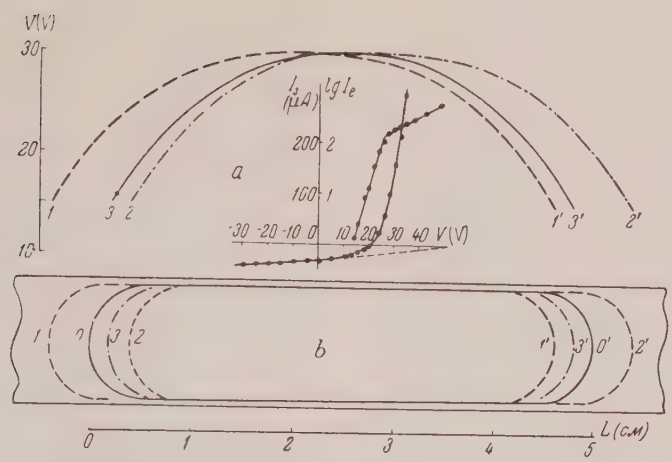

Fig. 3. Distribution of potential along the tube axis in A. The reference electrodes with which the distributions are gotten are: (1) right-hand counterprobe, (2) left-hand counterprobe, (3) both counterprobes connected simultaneously.

hand probe; curve 2, the left-hand probe; curve 3, both on simultaneously.

As is evident from the graphs shown, the space potential distribution is found to be symmetric with respect to the center of the discharge for the measurements taken with both probes on simultaneously, and somewhat assymetric when the left or right-hand counterprobe was on separately. This phenomenon is connected with the change in form of the discharge depending on the location of the counterprobes. The change exhibited consists in the fact that when the right counterprobe is on, the working domain of the discharge shifts to the left, as shown by Fig. 1b, Nos. 1-1′. When the left counterprobe is on, the working part of the discharge shifts to the right, as shown by Nos. 2-2′. Finally, when both counterprobes are on, the working part (the luminous part) of the discharge is compressed at both sides, as shown by Nos. 3-3′. Nos. 0-0′ show the form of this part of the discharge when the counterprobes are disconnected. The volt-ampere and semilogarithmic characteristics in argon, obtained for both counterprobes on simultaneously, are shown in the center of Fig. 3a.

It follows from the graphs that the presence of a counterprobe introduces a certain modification in the structure of a discharge. This modification is expressed in a change in position along the axis of the discharge tube of the luminous and dark domains of the discharge. The deformation of the discharge exhibited in our case was comparatively minor, not more than 3-4 mm at the two ends. Further it must be concluded that the use of two counterprobes as reference electrodes, located symmetrically with respect to the interior electrode, is more convenient than the use of one counterprobe. In this case the internal structure of the discharge is kept symmetric with respect to the electrode.

5. INVESTIGATION OF THE INTERNAL ELECTRICAL PARAMETERS IN A HIGH-FREQUENCY DISCHARGE IN ARGON, NEON AND HYDROGEN

An investigation of the distribution of electron temperature T_e, electron concentration n_e, and space potential V_g along the axis of the discharge tube was carried out in a tube of type b(Fig. 1) filled with argon, neon, and hydrogen.

In Fig. 4 graphs of the distribution of T_e, n_e and V_g along the axis of the discharge tube are presented for argon at a pressure $p = 0.07$ mm Hg and an external field of frequency 130 mc (with a voltage amplitude of 180 V at the external electrodes). Under these conditions the discharge was homogeneous.

From the graphs of Fig. 4 follow:

a) The distribution of the electron temperature is symmetric about the electrode with its maximum value at the center of the discharge interval (Fig. 4a).

b) The electron concentration (Fig. 4b) and the space potential (Fig. 4c) along the tube axis also are distributed symmetrically about the electrodes and achieve their maximum values at the center between them. A particularly strong variation of

space potential along the axis of the discharge tube was found by us in argon for a pressure of .07 mm Hg.

The configuration of the distribution curves of electron temperature and concentration and of space potential along the axis of the tube in general depends on the pressure and nature of the gas, on the diameter of the tube, and on the discharge current, but the curves are always symmetric about the electrodes.

Generally, in a homogeneous high-frequency discharge with not too great a distance between the electrodes, the distribution curve of electron temperature along the tube has its maximum value in the center between the electrodes. With increasing separation between the electrodes but constant high-frequency voltage amplitude, there is finally a change in the course of this curve.

The dependence of the distribution of electron temperature and concentration, and space potential, upon gas pressure was investigated with hydrogen in the discharge tube Fig. 1b (length 80 cm, diameter 35 mm, separation between external electrodes 13 cm, field frequency 130 mc). Measurements were carried out in the range of pressure from 0.1 to 1.1 mm Hg for a discharge current of 150 ma. Under these conditions the discharge in the tube is homogeneous. During the measurements the probe was on the axis of the tube centrally between the electrodes. The results are shown in Fig. 5.

From the graphs of Fig. 5 it is evident that:

a) The electron temperature decreases with increasing pressure just as for DC discharges (curve a).

b) With rising pressure (approximately from 0.1 to 0.3 mm Hg) the electron concentration rises to some maximum value but then with a further increase in pressure the electron concentration begins to decrease monotonically (curve b).

c) With fixed discharge current and rising pressure, the space potential in the center of the region between the electrodes falls (curve c).

Fig. 6 gives the graphs of the dependence of temperature (a), concentration of electrons (b) and space potential (c) on the amplitude of the high-frequency voltage at the external electrodes for

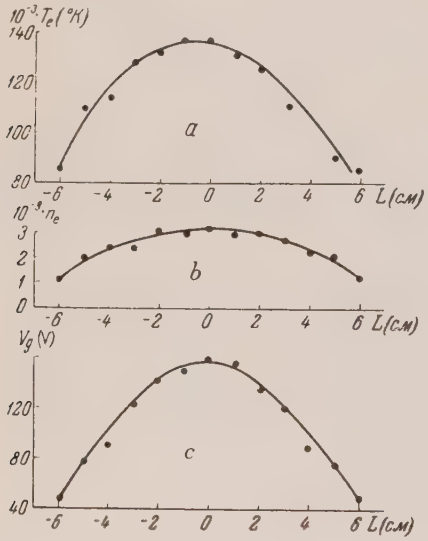

Fig. 4

Fig. 4. Distribution of (a) electron temperature, (b) electron concentration, (c) space potential along the tube axis in Ar at a frequency of 130 mc; $p = 0.07$ mm Hg; amplitude of voltage between the external electrodes 180 V.

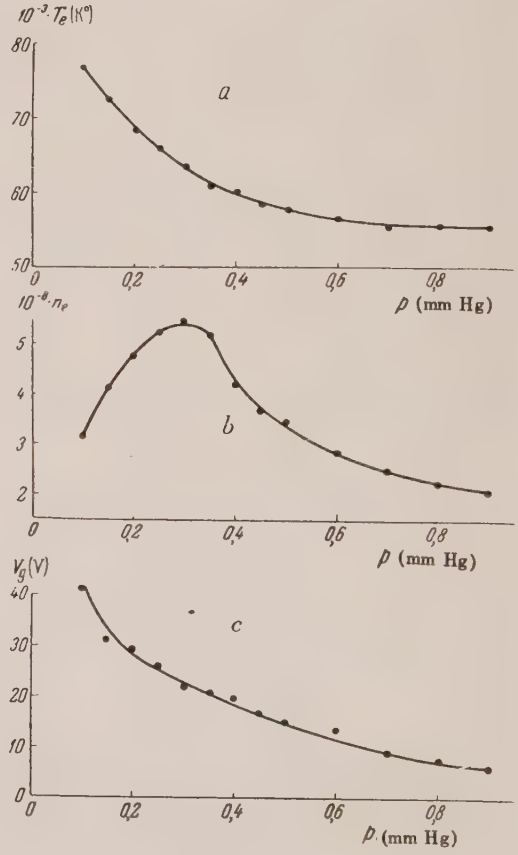

Fig. 5

Fig. 5. Dependence of T_e, n_e and V_g upon pressure in H_2, at a frequency of 100 mc and a discharge current of 100 ma.

neon at pressures of 0.07 mm Hg (curve 1) and 0.56 mm Hg (curve 2), and with a field of frequency 130 mc. The measurements were taken in a discharge tube of the type shown in Fig. 1b, of length 80 cm and diameter 27 mm. From the graphs in Fig. 6 it follows that the electron temperature rises with increasing high-frequency voltage on the electrodes. The value of the electron concentration midway between the electrodes finally rises with increasing voltage, but the magnitude of the space potential, on the contrary, decreases with increasing voltage.

6. DISCUSSION OF RESULTS

In an investigation of high-frequency discharges by means of the method of probes, it was established that the electron temperatures determined both by the method of two probes and by the method of one probe with the use of a counterprobe, have the same value within the limits of experimental error. The use of a counterprobe as reference point leads to an insignificant redistribution of the electrical parameters of the discharge along the discharge tube. This gave us reason to carry out an investigation of high-frequency voltages in a tube of the type shown in Fig. 1b.

From Fig. 4, 5 and 6 for argon, hydrogen and neon it is evident that the temperature of the electrons in a high-frequency discharge decreases with rising gas pressure. Apparently this is explained basically by the same circumstances as in a DC discharge. However one should bear in mind that in a high-frequency discharge the frequency of the applied field also can have an influence upon the value of T_e . In a high-frequency discharge at comparatively high pressures, where the frequency of the field is significantly less than the collision frequency of the electrons with the gas molecules, the character of the behavior of T_e with varying pressure does not differ essentially from that in a DC discharge. For higher field frequencies or comparatively low gas pressure, i.e., when the collision frequency is of the same order as or smaller than the field frequency, one can expect some difference between the behaviors of T_e in a high-frequency discharge and a DC discharge.

Table 2 compares the value of the electron temperature in a high-frequency discharge obtained by us with the value of the electron temperature in a DC discharge gotten by other authors[4] . As is evident from Table 2, in the case of A the value of T_e in a high-frequency discharge is significantly greater than in a DC discharge at the same pressure.

In all our measurements in the range of pressures from 0.07 to 1 mm Hg, for homogeneous discharges in hydrogen, argon and neon, with field frequencies from 5 to 130 mc. a Maxwellian distribution of electrons in velocity was obtained.

The intensity of the high-frequency field increases with increasing voltage amplitude at the electrodes. The energy which the electron acquires from the field on the average in a mean free path increases with increasing field intensity. Therefore the value of T_e in a high-frequency field increases with increasing voltage amplitude at the electrodes, other things being equal (Fig. 6). The very same result was obtained by Brasefield[5] in an investigation of high-frequency discharges by an optical method.

TABLE 2

Gas	Pressure (mm Hg)	$T_e \times 10^{-3}$ (°K)			
		DC discharge current		H.F. discharge current	
		50 ma	300 ma	50 ma	300 ma
Neon	0.07	57	53	60	—
	0.29	40.2	35	51	—
	0.56	35	37	48	—
Argon	0.07	26	22	—	100
	0.24	22	18	—	43.5
	0.96	16	12	—	40

The value of the electron concentration is a complicated function of the gas pressure (Fig. 5,6). The nature of the dependence of electron concentration on gas pressure can be explained in the

[4] R. Seeliger and R. Hirchert, Ann. Physik. 11, 817 (1931)

[5] C. Brasefield, Phys. Rev. 35, 92 (1930)

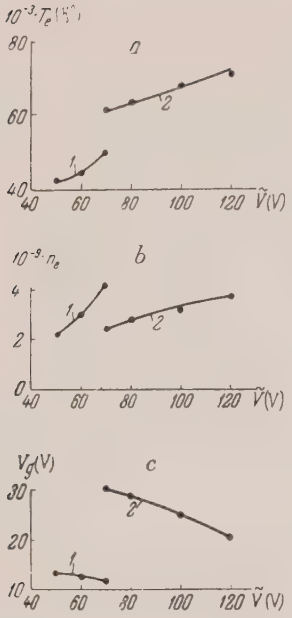

Fig. 6. Dependence of T_e, n_e and V_g upon the amplitude V of the high-frequency voltage in Ne: (1) $p = 0.07$ mm Hg, (2) $p = 0.56$ mm Hg; frequency = 130 mc.

following manner. In going from high pressure to less, the basic cause of the rise in electron concentration is the increase in energy of the electrons over a mean free path; this increase in energy increases the probability of ionization of a molecule by electron collisions. In going to the low pressures, there is a decrease in electron concentration as a result of a large loss of electrons, on account of diffusion and also on account of the decreased probability of encounters between electrons and gas molecules.

The experimental curve we obtain for the dependence of electron concentration on gas pressure for hydrogen recalls in its shape the curve obtained theoretically[6] for the dependence of the conductivity of an ionized gas on pressure at ultra-high frequencies. It likewise follows from the curves for the distribution of electron concentration in its dependence on pressure in hydrogen, that at pressures at which the electron concentration has its maximum value, the frequency of collisions of electrons with gas molecules is of the same order as the frequency of the applied field. This is also in accord with the theoretical results of some authors[6,7] who have investigated the conductivity of high-frequency discharges. The electron concentration increases with increasing high-frequency field intensity.

Investigating the distribution of space potential along the axis of the discharge tube, we verified the result of Banerji and Ganguli[1] on the existence, in some cases, of a large steady field in a high-frequency discharge. It was shown the magnitude of the steady field strongly depends on the gas pressure, the intensity of the high-frequency field and the diameter of the discharge tube. With a rise in gas pressure and high-frequency field intensity, there is a decrease in the steady field on account of the decrease in the volume of positive charge on the axis of the discharge tube between the electrodes. The increase of the steady field in a high-frequency field with decreasing gas pressure also occurs as a result of more intensive flow of electrons from the discharge region because of increased processes of diffusion to the wall of the discharged tube, both on account of the greater mean free path of the electrons and on account of the greater mean energy of the electrons.

The flow of positive ions from the discharge region as a result of diffusion processes is significantly less. Therefore there will result an accumulation of positive space charge at the axis of the discharge tube as long as the increase of positive charge is not stopped as a result of the establishment of ambipolar diffusion of electrons and ions to the walls of the discharge tube.

RESULTS

1. A comparison is made of existing probe methods for investigating high-frequency discharges. Measurements are made by the two-probe method, and by a one-probe method with the use of a counterprobe.

The results of the measurement show that both methods give the same result for the electron temperature within the limits of experimental error. The use of a counterprobe as a reference point leads to an insignificant redistribution of the electrical parameters of the high-frequency discharge along the axis of the tube. This resolves the contradiction between references 1 and 2.

2. An investigation is made of the dependence of temperature, electron concentration and space potential at the axis of the discharge tube upon the pressure of the gas.

3. The distribution of temperature, electron concentration and space potential along the axis of the tube are obtained. In a homogeneous high-frequency discharge these parameters are symmetric with respect to the electrodes and have their maximum values between the electrodes. The distributions of temperature, electron concentration

[6] F. Adler, J. Appl. Phys. **20**, 1125 (1940)

[7] H. Margenau, Phys. Rev. **69**, 508 (1946)

and space potential along the tube depend essentially on the gas pressure, diameter of the discharge tube and high-frequency field intensity.

L. A. Rosnovskaia took part in carrying out some of the measurements.

We express our gratitude to Prof. N. A. Kaptsov and A. A. Zaitsev for their interest in this work.

Translated by D. Finkelstein
58

SOVIET PHYSICS - JETP VOLUME 1, NUMBER 2 SEPTEMBER, 1955

The Absorption and Emission of X-Rays in Ferromagnetic Metals

A. V. SOKOLOV
Institute of the Physics of Metals, Ural Affiliate, Academy of Sciences, USSR

(Submitted to JETP editor March 12, 1954)
J. Exper. Theoret. Phys. USSR 28, 326-329 (March, 1955)

The problem of absorption and emission of x-rays by a ferromagnetic is examined in the framework of interaction of the inner and outer electrons.

1. There has been to date no theoretical examination of the absorption and emission of x-rays by ferromagnetic substances. In view of the importance of a study of the subject, we shall attempt to solve the problem in a very rough, qualitative approximation.

In the absorption of x-rays by inner shell electrons it is essential that the frequency of the x-ray be sufficient to excite the electron into an unoccupied level above the conduction levels. By examining the fine structure of the absorption band edge, one can hope to obtain some detailed information about the highest electron energy levels in the metal.

Since the initial electron level is part of an inner shell, it can be taken as infinitely narrow. Let ψ_0 be the normalized wave function of the initial state, $\hbar\omega_{\xi' 0}$ --- the energy difference between this state and a state of conductivity k. The optical conductivity, which determines absorption, is given by the equation [1]

$$nk\nu = \sigma = -\frac{\pi e^2}{m^2\hbar\omega G^3 a^3}\sum_{ss'}\int\frac{\rho_0(\xi, s') - \rho_0(\xi, s)}{|\mathrm{grad}_\xi \omega_{\xi\xi'}|} \times |p_x(\xi, \xi')|^2\, du\, dv. \quad (1)$$

Here s is the sum index over initial states, and s' the sum index over final states of the metal electrons in the first Brillouin zone. Since, in the present case, the initial levels are essentially the discrete levels of isolated atoms, the corresponding wave function is different from zero only in a small region. This makes the summation over s easy. If there are N_0 atoms per unit volume, then we have for the optical conductivity:

$$(\rho_0(\xi, s') = 0, \quad \text{and} \quad \rho_0(\xi, s) = G^3/8\pi^3)$$

$$\sigma = nk\nu = \frac{\pi e^2\hbar N_0 G^3}{8\pi^3 m^2\hbar\omega a^3}\Omega\int\{[\nabla_\xi E(\xi)]^{-1} \times |p_x(\xi, 0)|^2\}_{\omega_{\xi 0}=\omega}\, du\, dv, \quad (2)$$

where we take into account the relation

$$\omega_{\xi 0} = [E(\xi) - E(0)]/\hbar, \quad (3)$$

$E(0) = \mathrm{const}$, is the energy of the K electron in the atom; the summation over s' in the first zone is replaced by multiplication by the number of states in unit volume of k-space.

2. With the removal of an electron from an inner shell, a conduction electron may make the transition to the vacant lower level, simultaneously emitting an x-ray quantum. Because of this, a study of the emission spectra of a metal serves as a source of information about the energy levels occupied by conduction electrons [2]. The intensity of x-rays emitted in the frequency interval ω to $\omega + d\omega$ is

$$I(\omega)\, d\omega = \frac{4N_0\omega^2\hbar^2 e^2}{3c^3 m^2} d\omega \sum_{s'}\left|\int\psi_k^*\nabla\psi_0\, d\tau\right|^2, \quad (4)$$

where the summation is carried over all occupied states of the conduction electrons with energy corresponding to a frequency ω_0 such that $\omega \le \omega_0 \le \omega + d\omega$, i.e., $\hbar\, d\omega = dE$.

Instead of a summation over all possible values of k, it is possible to write an integral over $(G/2\pi)^3\,\Omega_0 dk_1\, dk_2\, dk_3$; we then obtain

$$I(\omega)\, d\omega = \frac{N_0\hbar^2\omega^2 e^2 G^3\Omega_0}{6\pi^3 m^2 c^3} dE\int\left(\frac{\partial E}{\partial k_1}\right)^{-1} \quad (5)$$

[1] A. V. Sokolov, J. Exper. Theoret. Phys. USSR 25, 9 (1953)

[2] A. Wilson, *Quantum Theory of Metals*, pp. 42-44

$$\times \left| \int \psi_k^* \nabla \psi_0 \, d\tau \right|^2 dk_2 \, dk_3.$$

Multiplying and dividing the right side of Eq. (5) by $\hbar$, we obtain

$$I(\omega)\, d\omega = \frac{N_0 \hbar^3 \omega^2 e^2 G^3 \Omega_0}{6\pi^3 m^2 c^3} \frac{dE}{\hbar} \int \left(\frac{\partial E}{\partial k_1} \right)^{-1} \times \left| \int \psi_k^* \nabla \psi_0 \, d\tau \right|^2 dk_2 \, dk_3, \quad (6)$$

But $dE/\hbar = d\omega$, and, therefore, the final expression for the emitted radiation is

$$I(\omega) = \frac{N_0 \hbar^3 \omega^2 e^2 G^3 \Omega_0}{6\pi^3 m^2 c^3} \int \left\{ \left(\frac{\partial E}{\partial k_1} \right)^{-1} \times \left| \int \psi_k^* \nabla \psi_0 \, d\tau \right|^2 \right\}_{\omega_{k0} = \omega} dk_2 \, dk_3. \quad (7)$$

Examining Eqs. (2) and (7), we see that both absorption and emission of x-rays is determined by the quantity

$$F = F_1 + F_2 + F_3 = \int \left\{ \left(\frac{\partial E}{\partial k_1} \right)^{-1} \times \left| \int \psi_k^* \nabla \psi_0 d\tau \right|^2 \right\} dk_2 \, dk_3. \quad (8)$$

This quantity is determined both by the density of conduction electron states, and by the transition probability.

3. For the generalization of the calculation of absorption and emission of x-rays by ferromagnetic metals, using band theory, we shall use a model (originally proposed by Vonsovskii) of exchange interaction between outer s and inner d electrons. In the following we shall use the same notation as in the calculation of conduction electron state density in a ferromagnetic, that is κ_1 --- the component of the wave vector perpendicular to the boundary plane, and κ_2 and κ_3 --- components parallel to this plane.

For the wave function of the s electron we shall use a Brillouin function. All the coefficients of a Fourier expansion of the potential are real and negative for a simple lattice; then for small values of κ_1 the unnormalized wave function for conduction electrons has the form:

$$\psi_k^{(B)} = e^{i\vec{\varkappa}\mathbf{r}} \sin \pi |\mathbf{g}| x \quad \text{(upper band)}$$
$$\psi_k^{(H)} = e^{i\vec{\varkappa}\mathbf{r}} \cos \pi |\mathbf{g}| x \quad \text{(lower band)}$$

If the x-ray level is in the K-shell, then ψ_0 has spherical symmetry, and the corresponding transition probability is determined by the expression

$$\int \psi_0^* \frac{\partial \psi_k^{(B)}}{\partial x} d\tau = \int \exp[-\lambda r + i\vec{\varkappa}\mathbf{r}] \times (i\varkappa_1 \sin \pi |\mathbf{g}| x + \pi |\mathbf{g}| \cos \pi |\mathbf{g}| x)\, d\tau = M, \quad (9)$$

$$\int \psi_0^* \frac{\partial \psi_k^{(H)}}{\partial x} d\tau = \int \exp[-\lambda r + i\vec{\varkappa}\mathbf{r}] \times (i\varkappa_1 \cos \pi |\mathbf{g}| x - \pi |\mathbf{g}| \times \sin \pi |\mathbf{g}| x)\, d\tau = \varkappa_1 M',$$

where M and M' are quantities independent of κ_1 in the first approximation; λ for the K-shell is approximately Z/a_0 --- the atomic number divided by the radius of the first atomic orbit.

We shall carry out the calculation as in reference 5. Calculation of F for a state in the lower band proceeds as follows in ordinary band theory. We use Eq. (8), and need to find the density of states and the transition probability. The first is

$$\left(\frac{\partial E}{\partial \varkappa_1} \right)^{-1} = \frac{m}{\pi \hbar^2 g} \frac{\Gamma}{(\Gamma^2 - |V_g|^2)^{1/2}},$$

The second, using Eq. (10), is

$$\left| \int \psi_k^* \nabla_x \psi_0 \, d\tau \right|^2 = \varkappa_1^2 M'^2.$$

Taking into account that

$$\varkappa_1^2 = \frac{m^2}{\pi^2 \hbar^4 g^2} (\Gamma^2 - |V_g|^2) \quad \text{and that}$$

$$d\varkappa_2 \, d\varkappa_3 = -\frac{m}{\hbar^2} d\Gamma \, d\varphi,$$

we have

$$F_1 = \int \frac{m}{\pi \hbar^2 g} \frac{\Gamma}{(\Gamma^2 - |V_g|^2)^{1/2}} \varkappa_1^2 M'^2 \frac{m}{\hbar^2} d\Gamma \, d\varphi = \frac{2m^4 M'^2}{\pi^2 \hbar^8 g^3} \int \sqrt{\Gamma^2 - |V_g|^2}\, \Gamma \, d\Gamma. \quad (11)$$

To obtain the analogous quantity in the case of a ferromagnetic metal, we consider the electrons as a mixture of two gasses with respective spins s^+ and s^-. In this case we can write

$$m_\pm = m_1 / (1 \pm (\beta'/\beta)\, y); \quad (12)$$

$$\sqrt{\Gamma_\pm^2 - |V_g|^2} = (1 \pm (\beta'/\beta)\, y) \sqrt{\Gamma^2 - |V_g|^2},$$

$$\Gamma_\pm \, d\Gamma'_\pm = (1 \pm (\beta'/\beta)\, y)^2 \, \Gamma \, d\Gamma.$$

Substituting Eq. (12) into Eq. (11), we obtain

$$F_1^\pm = \frac{2m_1^4 M'^2}{\pi^2 \hbar^8 g^3} \frac{1}{(1 \pm (\beta'/\beta)\, y)} \int \sqrt{\Gamma^2 - |V_g|^2}\, \Gamma \, d\Gamma. \quad (13)$$

Adding F_1^+ and F_1^-, we obtain

$$F_1(E,y)=\frac{4m_1^4M'^2}{\pi^2\hbar^8g^3}(1+A^2y^2)\int\sqrt{\Gamma^2-|V_g|^2}\,\Gamma\,d\Gamma \tag{14}$$

Carrying out a similar calculation for the upper band, we have

$$F_1(E,y)=\frac{4m_1^2M^2}{\hbar^4g}(1+A^2y^2)\int\frac{\Gamma\,d\Gamma}{\sqrt{\Gamma^2-|V_g|^2}} \tag{15}$$

The changes of F are therefore determined by the following three quantities:

I) $E<V_{000}+E_g-|V_g|$: (16)

$$F_1(E,y)\sim\frac{4}{3}\frac{m_1^4M'^2}{\pi^2\hbar^8g^3}(1+A^2y^2)\,[(E_g^2-|V_g|^2)^{3/2}-\{(V_{000}+E_g-E)^2-|V_g|^2\}^{3/2}];$$

II) $V_{000}+E_g-|V_g|<E<V_{000}+E_g+|V_g|$: (17)

$$F_1(E,y)\sim\frac{4}{3}\frac{m_1^4M'^2}{\pi^2\hbar^8g^3}(1+A^2y^2)\,(E_g^2-|V_g|^2)^{3/2};$$

III) $V_{000}+E_g+V_g<E$; (18)

$$F_1(E,y)\sim\frac{4}{3}\frac{m_1^4M'^2}{\pi^2\hbar^8g^3}(1+A^2y^2)\,(E_g^2-|V_g|^2)^{3/2}+\frac{4m_1^2M^2}{\hbar^4g}(1+A^2y^2)\,\{(E-E_g-V_{000})^2-|V_g|^2\}^{1/2}.$$

In this calculation we have taken into account only the **g** and **– g** planes. Therefore the deviation of of the $F_1(E,y)$ curve from the corresponding curve for free electrons must be multiplied by the number of pairs of equivalent planes which bound the first zone. The quantities $F_2(E,y)$ and $F_3(E,y)$, corresponding to radiation with electric vector parallel to the discontinuity (boundary) plane, can also be easily calculated. It turns out that they have the same general form as $F_1(E,y)$, with the exception that their derivatives are everywhere continuous. Thus the form of $F(E,y)$ is primarily determined by $F_1(E,y)$ (see Figure).

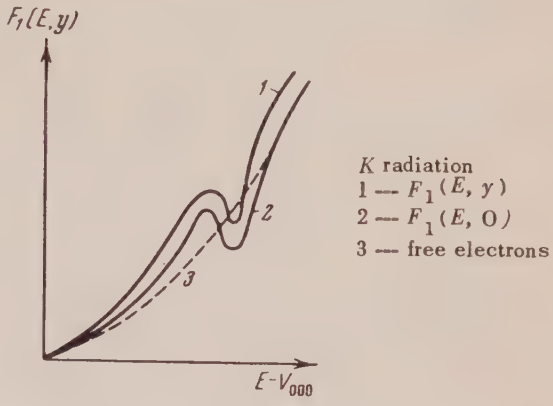

The curve $F_1(E,y)$ for K radiation is somewhat higher than $F_1(E,0)$ in the absence of magnetization. To observe this effect one should examine the emission spectra of ferromagnetic metals (which are experimentally convenient) above and below the ferromagnetic Curie point. From Eqs. (14) and (15) it follows that the difference of ordinates of the $F_1(E,y)$ and $F_1(E,0)$ curves can be several percent of the value for the unmagnetized state.

4. Thus, in the framework of an s – d exchange model it is shown that the emission and absorption of x-rays by ferromagnetic metals must depend on the spontaneous magnetization. In the vicinity of the ferromagnetic Curie point this dependence is quadratic [Eqs. (14) - (18)].

Additional Footnotes:

[3] S. V. Vonsovskii, J. Exper. Theoret. Phys. USSR **16**, 981 (1946)

[4] S. V. Vonsovskii and E. A. Turov, J. Exper. Theoret. Phys. USSR **24**, 419 (1953)

[5] A. V. Sokolov and S. M. Tsipis, J. Exper. Theoret. Phys. USSR **28**, 321 (1955); Sov. Phys. **1**, 218 (1955)

Translated by G. L. Gerstein
55

The Mathematical Foundations of the Theory of Irreversible Thermodynamical Processes

KIRIL POPOV
Bulgarian Academy of Sciences, Sofia
(Submitted to JETP editor January 8, 1954)
J. Exper. Theoret. Phys. USSR 28, 257-282 (March, 1955)

It is shown that the Onsager relations

$$\dot{x}_i = \sum_{k=1}^{n} L_{ik} X_k \quad (i = 1, 2, \ldots, n), L_{ik} = L_{ki},$$

when limited to terms of second order in x, are first integrals of a more general set of differential equations

$$d^2x_i / dt^2 = X_i \quad (i = 1, 2, \ldots, n).$$

In the most general case, in which all terms in the expansion of ΔS are kept, we obtain $L_{ik} = L_{ki}$ with accuracy to terms of second order. The theory so developed is applied to the phenomenon of thermal conduction and to the theory of phases in adiabatically isolated systems.

INTRODUCTION

We consider an adiabatically isolated system, whose state is completely determined by the variables $\xi_1, \xi_2, \xi_3, \ldots, \xi_n$. Let $\xi_1^0, \xi_2^0, \ldots, \xi_n^0$ be the values of these variables when the system is in thermal equilibrium. Denoting by $S(\xi_1, \xi_2, \ldots, \xi_n)$ the entropy of the system, we have

$$\Delta S = S(\xi_1, \xi_2, \ldots, \xi_n) - S(\xi_1^0, \xi_2^0, \ldots, \xi_n^0) = \frac{1}{2}\left(\frac{\partial^2 S}{\partial x_1^2} x_1^2 + 2\frac{\partial^2 S}{\partial x_1 \partial x_2} x_1 x_2 + \cdots + \frac{\partial^2 S}{\partial x_n^2} x_n^2\right) + \cdots = -\frac{1}{2}\sum_{k=1}^{n} g_{ik} x_i x_k + \cdots \quad (i = 1,2, \ldots, n), \tag{1}$$

where $g_{ik} = g_{ki}$, $\chi_i = \xi_i - \xi_i^0$, and where the derivatives are taken at $\chi_1 = \chi_2 = \ldots = \chi_n = 0$. Here $\Sigma g_{ik}\chi_i\chi_k$ is a positive definite quadratic form.

We now set ourselves the problem of determining the differential equations for irreversible thermodynamic adiabatic processes.

Lord Kelvin, studying thermoelectric phenomena, came to the conclusion that it was possible to write down differential equations which give the interaction between electric currents and thermal currents $\dot{\chi}_1, \dot{\chi}_2$ in the form

$$\dot{x}_1 = L_{11}X_1 + L_{12}X_2, \quad \dot{x}_2 = L_{21}X_1 + L_{22}X_2,$$

where X_1 and X_2 are "forces" which depend on the electrical and thermal phenomena in the system. Later, Rayleigh, formulating a "principle of minimum energy dissipation" pointed out the possibility of considering ΔS as a potential function.

Onsager, studying hypothetical unimolecular chemical processes in a substance which can exist in a given homogeneous phase in three forms A, B, C, which undergo spontaneous transition from one to another ("triangular processes"), and also phenomena of thermal conduction in anisotropic crystals, concluded that the tensor L_{ik} was symmetric. Following Boltzman's example and starting from the assumptions of statistical mechanics on the "microscopic reversibility" of elementary processes and from the theory of fluctuation, Onsager[1] established the phenomenological relations

$$\dot{x}_i = \sum_{k=1}^{n} L_{ik} X_k \quad (i = 1,2, \ldots, n), \tag{2}$$

where $L_{ik} = L_{ki}$, χ_i is the flow of χ_i, X_k are the "forces", which are partial derivatives of the potential function $(-\Delta S)$ with respect to the χ_k, i.e.,

[1] L. Onsager, Phys. Rev. 37, 405 (1931); 38, 2265 (1931)

$$X_k = \partial(-\Delta S)/\partial x_k. \tag{3}$$

Later Casimir[2] pointed out gaps in Onsager's argument, showing that Onsager assumed that the fluctuations on the average follow the usual phenomenological macroscopic laws. Landau and Lifshitz[3] proved that L_{ik} must be coefficients of essentially positive quadratic form. However, as we have shown[4], this is still not sufficient to establish the Onsager relation. De Groot[5] suggested that the Onsager relations (in those cases where only their applications are concerned) be taken as a new thermodynamic principle.

We consider below the problem of irreversible thermodynamic processes from the mathematical point of view and obtain several consequences from the second law of thermodynamics in conjunction with irreversible processes in adiabatically isolated systems. Following established custom, we keep only quadratic terms in the expansion of ΔS in powers of $\chi_1, \chi_2, \ldots, \chi_n$. Then, following the method of integration developed by Poincaré, we show that consideration of all terms in the expansion of ΔS does not lead to any essential changes in the results.

1. ANALYSIS OF THE PHENOMENOLOGICAL RELATIONS OF ONSAGER

First of all, we note that for each set of initial values $\chi_1^0, \chi_2^0, \ldots, \chi_n^0$ it is necessary, in adiabatically isolated systems, that $\lim \chi_i(t) = 0$ for $t \to +\infty$. Thus the point $\chi_1 = \chi_2 = \ldots = \chi_n = 0$ is a critical point of the integral of the system of differential equations

$$dx_i/dt = L_{i1}X_1 + L_{i2}X_2 + \cdots + L_{in}X_n \qquad (i = 1, 2, 3, \ldots, n), \tag{4}$$

where $L_{ik} = L_{ki}$. Since

$$X_i = g_{i1}x_1 + g_{i2}x_2 + \cdots + g_{in}x_n,$$

the integral of the system of linear differential equations of nth order[4] possesses n constants of integration. This characteristic permits us to make an arbitrary choice of the initial values $\chi_1^0, \chi_2^0, \ldots, \chi_n^0$ of the independent variables $\chi_1, \chi_2, \ldots, \chi_n$. However, this is not sufficient to guarantee that the integrals of the given system have physical significance. It is also necessary that $\lim \chi_i(t) = 0$ for $t \to +\infty$ or, in other words, that the point $\chi_1 = \chi_2 = \ldots = \chi_n = 0$ be a common point of the family of integral curves, i.e., that all the integral curves which satisfy the arbitrary set of initial conditions $\chi_1^0, \chi_2^0, \ldots, \chi_n^0$ of the independent variables meet at this point. In order that the integrals

$$x_i(t) = C_1\gamma_{i1}e^{r_1 t} + C_2\gamma_{i2}e^{r_2 t} + \cdots + C_n\gamma_{in}e^{r_n t} \qquad (i = 1,2, \ldots, n) \tag{5}$$

of this system satisfy the condition $\lim \chi_i(t) = 0$ for $t \to +\infty$, it is necessary that all r_i be negative. But, since the r_i are functions of the L_{ik}, which thus determine the state of the system, this requirement contradicts the basic hypothesis that $\xi_1, \xi_2, \ldots, \xi_n$ are the only variables that define the state of the system.

As an example, for $n = 2$, we have

$$dx_1/dt = L_{11}(g_{11}x_1 + g_{12}x_2) + L_{12}(g_{21}x_1 + g_{22}x_2), \tag{6}$$

$$dx_2/dt = L_{21}(g_{11}x_1 + g_{12}x_2) + L_{22}(g_{21}x_1 + g_{22}x_2).$$

Setting $\chi_1 = \alpha e^{rt}$, $\chi_2 = \beta e^{rt}$, we get the quadratic equation

$$\begin{vmatrix} L_{11}g_{11} + L_{12}g_{21} - r & L_{11}g_{12} + L_{12}g_{22} \\ L_{21}g_{11} + L_{22}g_{21} & L_{21}g_{12} + L_{22}g_{22} - r \end{vmatrix} = 0, \tag{7}$$

for determining r. The roots of this equation are

$$r_{1,2} = \tfrac{1}{2}(L_{11}g_{11} + 2L_{12}g_{12} + L_{22}g_{22}) \pm \tfrac{1}{2}\Big((L_{11}g_{11} + 2L_{12}g_{12} + L_{22}g_{22})^2 - 4(L_{11}L_{22} - L_{12}^2)(g_{11}g_{22} - g_{12}^2)\Big)^{1/2}. \tag{8}$$

[2] H. B. C. Casimir, Rev. Mod. Phys. **17**, 343 (1945); Philips Res. Rep. **1**, 185 (1946)

[3] L. Landau and E. Lifshitz, *Statistical Physics*, 1951

[4] Kyrille Popoff, Compt. rend. **238**, 648 (1952); J. de Math. Phys. Appl. **3**, 42, 440 (1952); **5**, 67 (1954); Compt. rend. **236**, 785, 1640 (1953); Ann. Phys. **9**, 261 (1954)

[5] S. R. de Groot, *Thermodynamics of Irreversible Processes* (North Holland Publ. Co., Amsterdam, 1951)

In order that the differential equations have physical meaning, r_1, r_2 must be negative, i.e.,

$$0<(L_{11}g_{11}+2L_{12}g_{12}+L_{22}g_{22})^2 \qquad (9)$$
$$-4(L_{11}L_{22}-L_{12}^2)(g_{11}g_{22}-g_{12}^2)$$
$$<(L_{11}g_{11}+2L_{12}g_{12}+L_{22}g_{22})^2,$$
$$(L_{11}g_{11}+2L_{12}g_{12}+L_{22}g_{22})<0.$$

We now show that the set of differential equations

$$d^2x_i/dt^2=X_i \qquad (i=1,2,\ldots,n), \qquad (10)$$
$$X_i=g_{i1}x_1+g_{i2}x_2+\cdots+g_{in}x_n,$$

satisfies the physical requirements and has the phenomenological relations (2) as first integrals.

We rewrite the set (10) in the form

$$d^2x_1/dt^2=g_{11}x_1+g_{12}x_2+\cdots+g_{1n}x_n, \qquad (10')$$
$$\cdots\cdots\cdots\cdots\cdots\cdots,$$
$$d^2x_n/dt^2=g_{n1}x_1+g_{n2}x_2+\cdots+g_{nn}x_n.$$

Setting

$$x_1=\alpha e^{rt},\ x_2=\beta e^{rt},\ \ldots,\ x_n=\nu e^{rt},$$

we obtain

$$(g_{11}-r^2)\alpha+g_{12}\beta+g_{13}\gamma+\cdots+g_{1n}\nu=0, \qquad (11)$$
$$\cdots\cdots\cdots\cdots\cdots\cdots,$$
$$g_{n1}\alpha+g_{n2}\beta+g_{n3}\gamma+\cdots+(g_{nn}-r^2)\nu=0.$$

In order that this homogeneous system of algebraic equations in $\alpha, \beta, \ldots, \nu$ possess near zero solutions we must have

$$\begin{vmatrix} g_{11}-r^2 & g_{12} & \cdots & g_{1n} \\ g_{21} & g_{22}-r^2 & \cdots & g_{2n} \\ \vdots & \vdots & & \vdots \\ g_{n1} & g_{n2} & \cdots & g_{nn}-r^2 \end{vmatrix}=0.$$

Since $\Sigma g_{ik}\chi_i\chi_k$ is a positive definite quadratic form, all the roots of the equation of nth degree in

$$\Delta(r^2)=0$$

are real and positive. Thus n roots ($r_1, r_2, \ldots, r_n$) of this system are negative and n roots ($r_{n+1}=-r_1, r_{n+2}=-r_2, \ldots, r_{n+p}=-r_p, \ldots, r_{2n}=-r_n$) are positive.

In the set of equations (11) it is always possible to set $\alpha=1$. Since r appears only as a squared term, the roots r_i and $r_{n+i}=-r_i$ correspond to one and the same set of values $\alpha_i=1, \beta_i, \gamma_i, \ldots, \nu_i$. Then the general integral of the set of differential equations has the form

$$x_1(t)=C_1e^{r_1t}+C_2e^{r_2t}+\cdots+C_ne^{r_nt}$$
$$+C_{n+1}e^{r_{n+1}t}+\cdots+C_{2n}e^{r_{2n}t},$$
$$x_2(t)=C_1\beta_1e^{r_1t}+C_2\beta_2e^{r_2t}+\cdots+C_n\beta_ne^{r_nt}$$
$$+C_{n+1}\beta_{n+1}e^{r_{n+1}t}+\cdots+C_{2n}\beta_{2n}e^{r_{2n}t},$$
$$x_n(t)=C_1\nu_1e^{r_1t}+C_2\nu_2e^{r_2t}+\cdots+C_n\nu_ne^{r_nt}$$
$$+C_{n+1}\nu_{n+1}e^{r_{n+1}t}+\cdots+C_{2n}\nu_{2n}e^{r_{2n}t},$$

where $r, \alpha, \beta, \ldots, \nu$ depend only on the g_{ik}. For $\lim_{t\to+\infty}\chi_i(t)=0$, we must have

$$C_{n+1}=C_{n+2}=\cdots=C_{2n}=0.$$

Then we obtain

$$x_1(t)=C_1e^{r_1t}+C_2e^{r_2t}+\cdots+C_ne^{r_nt}, \qquad (12)$$
$$x_2(t)=C_1\beta_1e^{r_1t}+C_2\beta_2e^{r_2t}+\cdots+C_n\beta_ne^{r_nt},$$
$$\cdots\cdots\cdots\cdots\cdots\cdots,$$
$$x_n(t)=C_1\nu_1e^{r_1t}+C_2\nu_2e^{r_2t}+\cdots+C_n\nu_ne^{r_nt}$$

In determining $C_1, C_2, \ldots, C_n$, we obtain the relations for $t=0$:

$$x_1^0=C_1+C_2+\cdots+C_n,$$
$$x_2^0=C_1\beta_1+C_2\beta_2+\cdots+C_n\beta_n,$$
$$\cdots\cdots\cdots\cdots\cdots,$$
$$x_n^0=C_1\nu_1+C_2\nu_2+\cdots+C_n\nu_n,$$

where $\chi_1^0, \chi_2^0, \ldots, \chi_n^0$ are the arbitrarily chosen initial values of $\chi_1, \chi_2, \ldots, \chi_n$.

Substituting $\chi_1(t), \chi_2(t), \ldots, \chi_n(t)$ from Eq. (12) in the expressions (10) for $X_1, X_2, \ldots, X_n$, we get

$$X_1=C_1e^{r_1t}A_1+\cdots+C_ne^{r_nt}A_n, \qquad (13)$$
$$X_2=C_1e^{r_1t}B_1+\cdots+C_ne^{r_nt}B_n,$$
$$\cdots\cdots\cdots\cdots\cdots\cdots,$$
$$X_n=C_1e^{r_1t}N_1+\cdots+C_ne^{r_nt}N_n.$$

Here $A, B, \ldots, N$ are functions of g_{ik} only and do not depend on $C_1, C_2, \ldots, C_n$. Further, we have

$$\dot{x}_i(t)=C_1\eta_{i1}r_1e^{r_1t}+C_2\eta_{i2}r_2e^{r_2t} \qquad (14)$$
$$+\cdots+C_n\eta_{in}r_ne^{r_nt}\quad (i=1,2,\ldots,n).$$

Eliminating $C_1e^{r_1t}, C_2e^{r_2t}, \ldots, C_ne^{r_nt}$ from Eqs. (13) and (14), we get

$$\begin{vmatrix} x_i & \gamma_{i1}r_1 & \gamma_{i2}r_2 & \dots & \gamma_{in}r_n \\ X_1 & A_1 & A_2 & \dots & A_n \\ X_2 & B_1 & B_2 & \dots & B_n \\ \dots & \dots & \dots & \dots & \dots \\ X_n & N_1 & N_2 & \dots & N_n \end{vmatrix} = 0,$$

i.e.,

$$x_i' = L_{i1}X_1 + L_{i2}X_2 + \dots + L_{in}X_n \qquad (15)$$
$$(i = 1, 2, \dots, n).$$

Thus the phenomenological relations are first integrals of the system (10). Here the L_{ik} are constant quantities, determined by the coefficients g_{ik} alone.

For $n = 2$, when

$$X_1 = g_{11}x_1 + g_{12}x_2, \quad X_2 = g_{21}x_1 + g_{22}x_2,$$

we have

$$d^2x_1/dt^2 = g_{11}x_1 + g_{12}x_2, \qquad (16)$$
$$d^2x_2/dt^2 = g_{21}x_1 + g_{22}x_2.$$

Setting $x_1 = e^{rt}$, $x_2 = \beta e^{rt}$, we obtain

$$g_{11} - r^2 + g_{12}\beta = 0, \qquad (17)$$
$$g_{21} + (g_{22} - r^2)\beta = 0.$$

The determinant of the coefficients now has the form

$$\Delta(r^2) = \begin{vmatrix} g_{11} - r^2 & g_{12} \\ g_{21} & g_{22} - r^2 \end{vmatrix} = 0$$

and, consequently,

$$r^2_{1,2} = \frac{g_{11} + g_{22}}{2} \qquad (18)$$
$$\pm\sqrt{\left(\frac{g_{11} + g_{22}}{2}\right)^2 - (g_{11}g_{22} - g_{12}^2)}.$$

Since $\Sigma g_{ik}\chi_i\chi_k (i = 1, 2)$ is a positive definite quadratic form, we have

$$g_{11} > 0, \; g_{22} > 0, \; g_{11}g_{22} - g_{12}^2 > 0$$

and consequently

$$\left(\frac{g_{11} + g_{22}}{2}\right)^2 - (g_{11}g_{22} - g_{12}^2) < \left(\frac{g_{11} + g_{22}}{2}\right)^2.$$

On the other hand,

$$\left(\frac{g_{11} + g_{22}}{2}\right)^2 - (g_{11}g_{22} - g_{12}^2)$$
$$= \left(\frac{g_{11} - g_{22}}{2}\right)^2 + g_{12}^2 > 0,$$

so that

$$r_1^2 > 0, \; r_2^2 > 0.$$

Consequently, all the roots of the equation $\Delta(r^2) = 0$ are real and

$$r_1 = -\sqrt{\left(\frac{g_{11} + g_{22}}{2}\right)^2 + \sqrt{\left(\frac{g_{11} + g_{22}}{2}\right)^2 - (g_{11}g_{22} - g_{12}^2)}} < 0, \; r_3 = -r_1 > 0,$$

$$r_2 = -\sqrt{\left(\frac{g_{11} + g_{22}}{2}\right)^2 - \sqrt{\left(\frac{g_{11} + g_{22}}{2}\right)^2 - (g_{11}g_{22} - g_{12}^2)}} < 0, \; r_4 = -r_2 > 0.$$

Setting $C_3 = C_4 = 0$, we have

$$x_1 = C_1e^{r_1t} + C_2e^{r_2t}, \quad x_2 = C_1\beta_1e^{r_1t} + C_2\beta_2e^{r_2t},$$

where β_1 and β_2 correspond to the roots r_1 and r_2 and are determined by Eq. (17)

Making use of the above values of χ_1, χ_2, and keeping in mind Eq. (17) we obtain

$$X_1 = C_1e^{r_1t}r_1^2 + C_2e^{r_2t}r_2^2,$$
$$X_2 = C_1e^{r_1t}\beta_1r_1^2 + C_2e^{r_2t}\beta_2r_2^2.$$

On the other hand,

$$x_1' = C_1e^{r_1t}r_1 + C_2e^{r_2t}r_2,$$
$$x_2' = C_1e^{r_1t}\beta_1r_1 + C_2e^{r_2t}\beta_2r_2.$$

Eliminating $C_1e^{r_1t}$ and $C_2e^{r_2t}$ from these four equations we get

$$x_1' = L_{11}X_1 + L_{12}X_2, \quad x_2' = L_{21}X_1 + L_{22}X_2,$$

where

$$L_{12} = -\frac{r_2 - r_1}{r_1r_2(\beta_2 - \beta_1)}, \quad L_{21} = \frac{\beta_1\beta_2(r_2 - r_1)}{r_1r_2(\beta_2 - \beta_1)}.$$

From Eq. (17) we have

$$\beta_1 = -\frac{g_{11} - r_1^2}{g_{12}}, \quad \beta_2 = -\frac{g_{21}}{g_{22} - r_2^2};$$

Consequently,

$$\beta_1\beta_2 = \frac{g_{11} - r_1^2}{g_{22} - r_2^2}.$$

However, keeping (18) in mind, we get

$$g_{11} - r_1^2 = \frac{g_{11} - g_{22}}{2} - \sqrt{\left(\frac{g_{11} + g_{22}}{2}\right)^2 - (g_{11}g_{22} - g_{12}^2)},$$

$$g_{22} - r_2^2 = -\frac{g_{11} - g_{22}}{2} - \sqrt{\left(\frac{g_{11} + g_{22}}{2}\right)^2 - (g_{11}g_{22} - g_{12}^2)}.$$

As a consequence,

$$\beta_1\beta_2 = -1,$$

$$L_{12} = L_{21}.$$

We now consider a numerical example for $n = 3$, setting

$$g_{11} = 5, \quad g_{12} = 1, \quad g_{13} = 3,$$
$$g_{21} = 1, \quad g_{22} = 4, \quad g_{23} = 2,$$
$$g_{31} = 3, \quad g_{32} = 2, \quad g_{33} = 6.$$

The corresponding quadratic form is positive definite, since

$$g_{11} > 0, \; g_{22} > 0, \; g_{33} > 0, \; \begin{vmatrix} g_{11} & g_{12} \\ g_{21} & g_{22} \end{vmatrix} > 0,$$

$$\begin{vmatrix} g_{11} & g_{13} \\ g_{31} & g_{33} \end{vmatrix} > 0, \; \begin{vmatrix} g_{22} & g_{23} \\ g_{32} & g_{33} \end{vmatrix} > 0, \; \begin{vmatrix} g_{11} & g_{12} & g_{13} \\ g_{21} & g_{22} & g_{23} \\ g_{31} & g_{32} & g_{33} \end{vmatrix} > 0.$$

The roots of the algebraic equation

$$\begin{vmatrix} g_{11} - r^2 & g_{12} & g_{13} \\ g_{21} & g_{22} - r^2 & g_{23} \\ g_{31} & g_{32} & g_{33} - r^2 \end{vmatrix} = 0,$$

are

$$r_1^2 = 9.4189, \; r_2^2 = 2.1944, \; r_3^2 = 3.3868,$$

as can be easily verified, so that

$$r_1 = -\sqrt{9.4189}, \quad r_2 = -\sqrt{2.1944}, \quad r_3 = -\sqrt{3.3868}.$$

Setting $\alpha_1 = \alpha_2 = \alpha_3 = 1$, we get

$$\lg \beta_1 = \bar{1}.81185; \qquad \lg \gamma_1 = 0.09931;$$
$$\lg \beta_2 = \bar{1}.98156; \qquad \lg \gamma_2 = 0.07554\, n;$$
$$\lg \beta_3 = 0.14968\, n; \qquad \lg \gamma_3 = \bar{2}.82822\, n;$$

and

$$L_{12} = -\frac{r_1^2 r_2^2 r_3^2}{\Delta} 0{,}070; \qquad L_{21} = -\frac{r_1^2 r_2^2 r_3^2}{\Delta} 0.071;$$

$$L_{13} = -\frac{r_1^2 r_2^2 r_3^2}{\Delta} 0.744; \qquad L_{31} = -\frac{r_1^2 r_2^2 r_3^2}{\Delta} 0.741;$$

$$L_{23} = -\frac{r_1^2 r_2^2 r_3^2}{\Delta} 0.515; \qquad L_{32} = -\frac{r_1^2 r_2^2 r_3^2}{\Delta} 0{,}520;$$

where

$$\Delta = \begin{vmatrix} r_1^2 & r_2^2 & r_3^2 \\ r_1^2\beta_1 & r_2^2\beta_2 & r_3^2\beta_3 \\ r_1^2\gamma_1 & r_2^2\gamma_2 & r_3^2\gamma_3 \end{vmatrix}.$$

THE SYMMETRY OF THE TERMS L_{ik} ITERATION METHOD.

The terms L_{ik} in the integrals of the system of differential equations that we have just considered are symmetric under less restrictive conditions than those given above. This fact makes it possible to explain the results obtained by several investigators who started out from the phenomenological relations of Onsager, in which it was not required that $\lim_{t \to +\infty} \chi_i(t) = 0$.

Pierre Curie[6], taking as his point of observation the symmetry in the structure of crystals, had already come to the conclusion that "when certain causes produce a given effect, then elements of symmetry in the cause also appear in the effect produced by these causes", and that "when certain effects display a known asymmetry, then one must find a similar asymmetry in the causes which produce these effects".

In the case in point the symmetry of the matrix g_{ik} requires the symmetry of the matrix L_{ik}.

Considering the system (18), we have established the existence of a set of integrals which satisfies the conditions $\lim \chi_i(t) = 0$, $\lim \chi_i'(t) = 0$ for $t = +\infty$. This is sufficient to establish the phenomenological relations and the symmetry of the matrix L_{ik}, independent of algebraic considerations.

For simplicity we consider the system

$$d^2x/dt^2 = ax + by = X, \quad d^2y/dt^2 = bx + cy = Y, \tag{19}$$

where a, b, c are arbitrary constants. We find the integrals of this system, which satisfy the condi-

6 P. Curie, J. Phys. , 393 (1894)

tions $t = 0$, $\chi' = 0$, $y' = 0$.

The method of iteration which we have followed is general: we apply it for each n.

Integrating both sides of the first of these equations from 0 to t, and setting $\chi'(0) = 0$, $y'(0) = 0$, we get

$$x'(t) = \int_0^t X dt = Xt - \int_0^t t\dot{X} dt$$

$$= Xt - \tfrac{1}{2}\dot{X}t^2 + \tfrac{1}{2}\int_0^t t^2 \ddot{X} dt.$$

But

$$\ddot{X} = a\ddot{x} + b\ddot{y} = aX + bY, \tag{20}$$

$$\ddot{Y} = b\ddot{x} + c\ddot{y} = bX + cY,$$

so that

$$x'(t) = Xt - \frac{t^2}{2!}\dot{X} + \frac{1}{3!}\int_0^t (aX + bY)\, dt^3$$

$$= Xt - \frac{t^2}{2!}\dot{X} + \frac{t^3}{3!}(aX + bY)$$

$$- \frac{1}{3!}\int_0^t (a\dot{X} + b\dot{Y})\, t^3 dt$$

$$= Xt - \frac{t^2}{2!}\dot{X} + \frac{t^3}{3!}(aX + bY)$$

$$- \frac{t^4}{4!}(a\dot{X} + b\dot{Y}) + \frac{1}{4!}\int_0^t t^4 (a\ddot{X} + b\ddot{Y})\, dt.$$

Substituting the values of $\ddot{X}$ and $\ddot{Y}$ from Eq. (20) in the last integral and integrating by parts we get, after some simplification (recalling that $\dot{X} = a\dot{x} + b\dot{y}$, $\dot{Y} = b\dot{x} + c\dot{y}$),

$$\left(1 + \frac{a}{2!}t^2 + \frac{a^2 + b^2}{4!}t^4\right)\frac{dx}{dt} + \left(\frac{b}{2!}t^2 + \frac{b(a+c)}{4!}t^4\right)\frac{dy}{dt}$$

$$= \left(t + \frac{a}{3!}t^3 + \frac{a^2 + b^2}{5!}t^5\right)X + \left(\frac{b}{3!}t^3 + \frac{b(a+c)}{5!}t^5\right)Y \tag{21a}$$

$$- \frac{a^2 + b^2}{5!}\int_0^t t^5 \dot{X} dt - \frac{b(a+c)}{5!}\int_0^t t^5 \dot{Y} dt.$$

It is necessary to extend the iteration process to infinity.

In the same fashion we get from the second equation,

$$\left(\frac{b}{2!}t^2 + \frac{b(a+c)}{4!}t^4\right)\frac{dx}{dt} + \left(1 + \frac{c}{2!}t^2 + \frac{b^2 + c^2}{4!}t^4\right)\frac{dy}{dt}$$

$$= \left(\frac{b}{3!}t^3 + \frac{b(a+c)}{5!}t^5\right)X + \left(t + \frac{c}{3!}t^3 + \frac{b^2 + c^2}{5!}t^5\right)Y \tag{21b}$$

$$- \frac{b(a+c)}{5!}\int_0^t t^5 \dot{X} dt - \frac{b^2 + c^2}{5!}\int_0^t t^5 \dot{Y} dt.$$

INVESTIGATION OF THE CONVERGENCE OF THE SERIES

To establish the convergence of the series we consider the dominating system of differential equations

$$d^2x/dt^2 = p(x + y) = X, \tag{A}$$

$$d^2y/dt^2 = p(x + y) = Y,$$

where p is the largest of the numbers $|a|$, $|b|$, $|c|$.

Proceeding with the system (A) as we did for the system (19) we get

$$\left(1 + \frac{p}{2!}t^2 + \frac{2p^2}{4!}t^4 + \frac{2^2p^3}{6!}t^6 + \cdots + \frac{2^{n-1}p^n}{(2n)!}t^{2n}\right)\frac{dx}{dt}$$

$$+ \left(\frac{p}{2!}t^2 + \frac{2p^2}{4!}t^4 + \frac{2^2p^3}{6!}t^6 + \cdots + \frac{2^{n-1}p^n}{(2n)!}t^{2n}\right)\frac{dy}{dt}$$

$$= \left(t + \frac{p}{3!}t^3 + \frac{2p^2}{5!}t^5 + \cdots + \frac{2^{n-2}}{(2n-1)!}p^{n-1}t^{2n-1}\right)X \tag{22}$$

$$+ \left(\frac{p}{3!}t^3 + \frac{2p^2}{5!}t^5 + \cdots + \frac{2^{n-2}}{(2n-1)!}p^{n-1}t^{2n-1}\right)Y$$

$$+ \frac{2^{n-1}}{(2n)!}p^n \int_0^t t^{2n}(X + Y)\, dt.$$

Here for each finite value of t

$$\lim_{n\to\infty} \frac{2^{n+1}p^n}{(2n)!}\int_0^t t^{2n}(X + Y)\, dt = 0.$$

Since the relation of the $(n+1)$st to the

nth term in each series tends to zero as $1/n$, then the series which occur in the coefficients of our equations quickly converge for each value of t; consequently, the coefficients in Eqs. (21) also converge. We write these formulas in the form

$$A\frac{dx}{dt}+B\frac{dy}{dt} \tag{23}$$
$$=\alpha X+\beta Y,\ B\frac{dx}{dt}+C\frac{dy}{dt}=\beta X+\gamma Y,$$

where

$$A=1+\frac{a}{2!}t^2+\frac{a^2+b^2}{4!}t^4+\cdots,$$
$$\alpha=t+\frac{a}{3!}t^3+\frac{a^2+b^2}{5!}t^5+\cdots,$$
$$B=\frac{b}{2!}t^2+\frac{b(a+c)}{4!}t^4+\cdots, \tag{24}$$
$$\beta=\frac{b}{3!}t^3+\frac{b(a+c)}{5!}t^5+\cdots,$$
$$C=1+\frac{c}{2!}t^2+\frac{b^2+c^2}{4!}t^4+\cdots,$$
$$\gamma=t+\frac{c}{3!}t^3+\frac{b^2+c^2}{5!}t^5+\cdots$$

Here

$$AC-B^2=1+\frac{a+c}{2!}t^2+\cdots\neq 0$$

and, consequently,

$$dx/dt=L_{11}X+L_{12}Y, \tag{25}$$
$$dy/dt=L_{21}X+L_{22}Y,$$

where

$$L_{11}=\frac{C\alpha+B\beta}{AC-B^2},\ L_{12}=\frac{C\beta-B\gamma}{AC-B^2}, \tag{26}$$
$$L_{21}=\frac{A\beta-B\alpha}{AC-B^2},\ L_{22}=\frac{A\gamma-B\beta}{AC-B^2}.$$

Simple calculations show that

$$C\beta-B\gamma=A\beta-B\alpha \tag{27}$$

and thus

$$L_{12}=L_{21}.$$

We have seen that $\chi=0$, $y=0$ is a critical point of the system of differential equations and that all integral curves which correspond to a certain physical problem pass through this point.

If we take the moment of thermodynamic equilibrium at $t_0=0$, then $t<0$ will correspond to thermodynamic processes. For $t_1<t_2<0$, we have

$$x'(t_2)=L_{11}(t_2)X(t_2)+L_{12}(t_2)Y(t_2),$$
$$y'(t_2)=L_{21}(t_2)X(t_2) \tag{28}$$
$$+L_{22}(t_2)Y(t_2),\ L_{12}=L_{21},$$

where $t_2=t_1+\tau$. If we assume that t_1 is known, and set $t_2=t_1+\tau$, where the positive quantity τ runs from 0 to $-t_1$, all the quantities appearing in Eq. (28) will be functions of τ, so that we can write

$$x'(\tau)=L_{11}(\tau)X(\tau)+L_{12}(\tau)Y(\tau),$$
$$y'(\tau)=L_{21}(\tau)X(\tau)+L_{22}(\tau)Y(\tau),$$
$$L_{12}(\tau)=L_{21}(\tau).$$

If f is any of these quantities, we can write

$$f(t_2)=f(t_1)+\tau f'(t_1)+\frac{\tau^2}{2}f''(t_1)+\cdots$$

For convenience we write $f(\tau)$ in place of $f(t_1+\tau)$. Thus we have again obtained the phenomenological relations of Onsager and $L_{12}=L_{21}$. The application of the general method of iteration which we have used does not present any difficulties for $n>2$, so that in the general case, $L_{ik}=L_{ki}$. Here, however, it is not evident that the coefficients L_{ik} are independent of τ, as was shown in Eq. (15).

2. ANALYSIS OF THE GENERAL CASE IN WHICH ΔS CONTAINS ALL THE TERMS OF THE EXPANSION IN POWERS OF THE VARIABLES

We now examine the most general case. Keeping all the terms in the expansion of ΔS in powers of $\chi_1, \chi_2, \ldots, \chi_n$, we have

$$\Delta S=-\frac{1}{2}\sum_{i,k}g_{ik}x_ix_k+\cdots \tag{2.1}$$

The dots here indicate terms of third and higher order in the variables χ. The corresponding system of differential equations has the form

$$d^2x_1/dt^2 = g_{11}x_1 + g_{12}x_2 + \ldots + g_{1n}x_n + \ldots, \tag{2.2}$$
$$\ldots\ldots\ldots\ldots\ldots\ldots\ldots\ldots$$
$$d^2x_n/dt^2 = g_{n1}x_1 + g_{n2}x_2 + \ldots + g_{nn}x_n + \ldots,$$

with the dots indicating terms of second and higher order. Setting $\xi = dx/dt$, we rewrite this system of $2n$ th order in the form

$$\frac{dx_1}{\xi_1} = \frac{dx_2}{\xi_2} = \ldots \tag{2.3}$$
$$= \frac{dx_n}{\xi_n} = \frac{d\xi_1}{g_{11}x_1 + \ldots + g_{1n}x_n + \ldots} = \ldots$$
$$\ldots = \frac{d\xi_n}{g_{n1}x_1 + \ldots + g_{nn}x_n + \ldots} = dt.$$

With the help of a linear transformation we can rewrite this system in the form

$$\frac{du_1}{r_1u_1 + \ldots} = \frac{du_2}{r_2u_2 + \ldots} = \ldots \tag{2.4}$$
$$= \frac{dv_n}{r_nu_n + \ldots} = \ldots = \frac{du_{2n}}{r_{2n}u_{2n} + \ldots} = dt,$$

with the dots again indicating the terms of second and higher order in u_i. The values $r_1, r_2, \ldots, r_n, r_{n+1}, \ldots, r_{2n}$ are the roots of the algebraic equation of $2n$ th degree previously considered:

$$\begin{vmatrix} g_{11} - r^2 & g_{12} \cdots & g_{1n} \\ \cdots\cdots\cdots\cdots & & \\ g_{n1} & g_{n2} \cdots g_{nn} - r^2 \end{vmatrix} = 0. \tag{2.5}$$

As we have already seen, n roots ($r_1, r_2, \ldots, r_n$) of this equation are negative, and n roots ($r_{n+1}, r_{n+2}, \ldots, r_{2n}$) are positive.

Poincare'[7] showed that such a system of differential equations possesses a system of holomorphic integrals of $e^{r_1 t}, e^{r_2 t}, \ldots, e^{r_n t}$

$$u_i(t) = \psi_i(e^{r_1 t}, e^{r_2 t}, \ldots, e^{r_n t}) \tag{2.6}$$
$$(i = 1, 2, \ldots, 2n),$$

which approach zero as $t \to +\infty$ and which possess n constants of integration. Consequently these correspond to this set of integrals of the form

$$x_1(t) = \psi_i(e^{r_1 t}, e^{r_2 t}, \ldots, e^{r_n t}), \tag{2.7}$$
$$\xi_i(t) = \omega_i(e^{r_1 t}, e^{r_2 t}, \ldots, e^{r_n t})$$
$$(i = 1, 2, \ldots, n),$$

where $\omega_i = d\psi_i/dt$ and ψ_i and ω_i are holomorphic functions of $e^{r_1 t}, e^{r_2 t}, \ldots, e^{r_n t}$ which approach zero as $t \to +\infty$ and which possess no constants of integration, thus allowing the choice of arbitrary initial values $\chi_1^0, \chi_2^0, \ldots, \chi_n^0$.

All the necessary conditions for this rule are satisfied in this case.

For simplicity we consider the case for $n = 2$. Setting $\chi_1 = \chi$, $\chi_2 = y$, $g_{11} = a$, $g_{21} = g_{12} = b$, $g_{22} = c$, and recalling that $F^2_{xy} = F^2_{yx}$ we get

$$d^2x/dt^2 = ax + by + ex^2 \tag{2.8}$$
$$+ 2fxy + gy^2 + \ldots = X,$$
$$d^2y/dt^2 = bx + cy + fx^2$$
$$+ 2gxy + hy^2 + \ldots = Y.$$

Since $a\chi^2 + 2b\chi y + cy^2$ is a positive definite quadratic form,

$$a > 0, \quad c > 0, \quad ac - b^2 > 0.$$

Corresponding to this system we have the system

$$\frac{dx}{dt} = \xi = \Xi; \quad \frac{dy}{dt} = \eta = \mathrm{H}; \quad \frac{d\xi}{dt} = X; \quad \frac{d\eta}{dt} = Y, \tag{2.8'}$$

and the equivalent differential equation in partial derivatives

$$\frac{\partial F}{\partial x}\Xi + \frac{\partial F}{\partial \xi}X + \frac{\partial F}{\partial y}\mathrm{H} + \frac{\partial F}{\partial \eta}Y = 0. \tag{2.9}$$

The linear substitution

$$u = \alpha_{11}\xi + \alpha_{12}x + \alpha_{13}\eta + \alpha_{14}y; \tag{2.10}$$
$$w = \alpha_{31}\xi + \alpha_{32}x + \alpha_{33}\eta + \alpha_{34}y,$$
$$v = \alpha_{21}\xi + \alpha_{22}x + \alpha_{23}\eta + \alpha_{24}y;$$
$$z = \alpha_{41}\xi + \alpha_{42}x + \alpha_{43}\eta + \alpha_{44}y$$

yields the system

$$\frac{\partial F}{\partial \xi} = \frac{\partial F}{\partial u}\alpha_{11} + \frac{\partial F}{\partial v}\alpha_{21} + \frac{\partial F}{\partial w}\alpha_{31} + \frac{\partial F}{\partial z}\alpha_{41},$$
$$\frac{\partial F}{\partial x} = \frac{\partial F}{\partial u}\alpha_{12} + \frac{\partial F}{\partial v}\alpha_{22} + \frac{\partial F}{\partial w}\alpha_{32} + \frac{\partial F}{\partial z}\alpha_{42},$$

[7] H. Poincare', *Sur les propriétés des functions définies par les equations aux différences particlles*, Thèse de doctorat, Paris, 1879

$$\frac{\partial F}{\partial \eta} = \frac{\partial F}{\partial u}\alpha_{13} + \frac{\partial F}{\partial v}\alpha_{23} + \frac{\partial F}{\partial w}\alpha_{33} + \frac{\partial F}{\partial z}\alpha_{43},$$
$$\frac{\partial F}{\partial y} = \frac{\partial F}{\partial u}\alpha_{14} + \frac{\partial F}{\partial v}\alpha_{24} + \frac{\partial F}{\partial w}\alpha_{34} + \frac{\partial F}{\partial z}\alpha_{44},$$

and the equation

$$\begin{aligned}&\frac{\partial F}{\partial u}(\alpha_{11}X + \alpha_{12}\Xi + \alpha_{13}Y + \alpha_{14}\mathrm{H}) + \\ &+ \frac{\partial F}{\partial v}(\alpha_{21}X + \alpha_{22}\Xi + \alpha_{23}Y + \alpha_{24}\mathrm{H}) + \\ &+ \frac{\partial F}{\partial w}(\alpha_{31}X + \alpha_{32}\Xi + \alpha_{33}Y + \alpha_{34}\mathrm{H}) + \\ &+ \frac{\partial F}{\partial z}(\alpha_{41}X + \alpha_{42}\Xi + \alpha_{43}Y + \alpha_{44}\mathrm{H}) = 0.\end{aligned} \tag{2.11}$$

We choose α_{ik} so that, after some reduction, we get

$$\frac{F}{\partial u}(r_1u_1 + \cdots) + \frac{\partial F}{\partial v}(r_2v + \ldots) \tag{2.12}$$
$$+ \frac{\partial F}{\partial w}(r_3w + \ldots) + \frac{\partial F}{\partial z}(r_4z + \ldots) = 0,$$

where the dots indicate terms of higher order of smallness; in this case we must have

$$\begin{aligned}\alpha_{11}X_1 + \alpha_{12}\Xi + \alpha_{13}Y_1 + \alpha_{14}\mathrm{H} &= r_1u \\ &= r_1(\alpha_{11}\xi + \alpha_{12}x + \alpha_{13}\eta + \alpha_{14}y),\end{aligned} \tag{2.13}$$
$$\begin{aligned}\alpha_{21}X_1 + \alpha_{22}\Xi + \alpha_{23}Y_1 + \alpha_{24}\mathrm{H} &= r_2v \\ &= r_2(\alpha_{21}\xi + \alpha_{22}x + \alpha_{23}\eta + \alpha_{24}y),\end{aligned}$$
$$\begin{aligned}\alpha_{31}X_1 + \alpha_{32}\Xi + \alpha_{33}Y_1 + \alpha_{34}\mathrm{H} &= r_3w \\ &= r_3(\alpha_{31}\xi + \alpha_{32}x + \alpha_{33}\eta + \alpha_{34}y),\end{aligned}$$
$$\begin{aligned}\alpha_{41}X_1 + \alpha_{42}\Xi + \alpha_{43}Y_1 + \alpha_{44}\mathrm{H} &= r_4z \\ &= r_4(\alpha_{41}\xi + \alpha_{42}x + \alpha_{43}\eta + \alpha_{44}y),\end{aligned}$$

where X_1 and Y_1 are the quantities X and Y in which only terms of first order are kept. We then obtain

$$\begin{aligned}\alpha_{i1}a - \alpha_{i2}r_i + \alpha_{i3}b + \alpha_{i4}0 &= 0, \\ -\alpha_{i1}r_i + \alpha_{i2}1 + \alpha_{i3}0 + \alpha_{i4}0 &= 0, \\ \alpha_{i1}b + \alpha_{i2}0 + \alpha_{i3}c - \alpha_{i4}r_i &= 0, \\ \alpha_{i1}0 + \alpha_{i2}0 - \alpha_{i3}r_i + \alpha_{i4}1 &= 0.\end{aligned} \tag{2.14}$$

For the homogeneous system in α_{ik} to have non-zero solutions, we require

$$\begin{vmatrix} a & -r_i & b & 0 \\ -r_i & 1 & 0 & 0 \\ b & 0 & c & -r_i \\ 0 & 0 & -r_i & 1 \end{vmatrix} = \begin{vmatrix} a - r_i^2 & b \\ b & c - r_i^2 \end{vmatrix} = 0. \tag{2.15}$$

We saw in Eq. (18) that the roots of this equation of fourth degree are real, whereupon

$$r_1 < r_2 < 0,\ r_3 = -r_1,\ r_4 = -r_2. \tag{2.16}$$

To these roots there correspond the coefficients α_{ik} which, after we set $\alpha_{i1} = 1$, have the values

$$\alpha_{i2} = r_i = \beta_i, \tag{2.17}$$
$$\alpha_{i3} = (r_i^2 - a)/b = \alpha_i, \quad \alpha_{i4} = r_i\alpha_i = \gamma_i.$$

As we have already pointed out, the integrals of Eq. (2.11), which approach zero at $t \to +\infty$, are holomorphic functions of $k_1e^{r_1t}$ and $k_2e^{r_2t}$, where the constants k_1 and k_2 are sufficiently small. These integrals can be expanded in a series in powers of $k_1e^{r_1t}$ and $k_2e^{r_2t}$. The convergence of these series as $t \to \infty$ was investigated by Poincare'[7] and later by Picard[8].

We return to a consideration of Eq. (2.9) and the substitutions (2.10). Since the determinant of the coefficients χ, y, ξ, η in (2.10) differs from zero:

$$\begin{vmatrix} 1 & r_1 & \alpha_1 & \gamma_1 \\ 1 & r_2 & \alpha_2 & \gamma_2 \\ 1 & r_3 & \alpha_3 & \gamma_3 \\ 1 & r_4 & \alpha_4 & \gamma_4 \end{vmatrix} = -4r_1r_2(\alpha_1 - \alpha_2)^2 \neq 0, \tag{2.18}$$

the substitutions (2.10) determine χ, y, ξ, η as linear functions of u, v, w, z. All these quantities approach zero together. Consequently the integrals of χ, y, $\xi = \chi'$, $\eta = y'$ which go to zero for $t = +\infty$ can be represented by a series of powers of e^{r_1t}, e^{r_2t} which converge for $t = +\infty$. We then have

$$\begin{aligned}x(t) &= C_1k_1e^{r_1t} + C_2k_2e^{r_2t} + C_3k_1^2e^{2r_1t} \\ &\quad + C_4k_1k_2e^{(r_1+r_2)t} + C_5k_2^2e^{2r_2t} + \cdots,\end{aligned} \tag{2.19}$$
$$\begin{aligned}y(t) &= G_1k_1e^{r_1t} + G_2k_2e^{r_2t} + G_3k_1^2e^{2r_1t} \\ &\quad + G_4k_1k_2e^{(r_1+r_2)t} + G_5k_2^2e^{2r_2t} + \cdots,\end{aligned}$$
$$\frac{d^2x}{dt^2} = C_1k_1r_1^2e^{r_1t} + C_2k_2r_2^2e^{r_2t} + C_3k_1^24r_1^2e^{2r_1t}$$

[8] E. Picard, Traité d'Analyse, Paris, 1908

$$+ C_4 k_1 k_2 (r_1 + r_2)^2 e^{(r_1+r_2)t} + C_5 k_2^2 4 r_2^2 e^{2r_2 t} + \cdots,$$

and a similar expression for $y''(t)$, where the coefficients G replace the coefficients C.

The values of these coefficients can be found by the method of undetermined coefficients, substituting in X and Y the expressions for χ and y given above.

In this way we obtain

$$\begin{aligned} X &= ax + by + ex^2 + 2fxy + gy^2 + \cdots \\ &= k_1 (aC_1 + bG_1) e^{r_1 t} + k_2 (aC_2 + bG_2) e^{r_2 t} \\ &+ k_1^2 (aC_3 + bG_3 + eC_1^2 + 2fC_1G_1 + gG_1^2) e^{2r_1 t} \\ &+ k_1 k_2 [aC_4 + bG_4 + 2eC_1C_3 \\ &+ 2f (C_1G_2 + C_2G_1) + 2gG_1G_2] e^{(r_1+r_2)t} \\ &+ k_2^2 (aC_5 + bG_5 + eC_2^2 \\ &+ 2fC_2G_2 + gG_2^2) e^{2r_2 t} + \cdots; \\ Y &= k_1 (bC_1 + cG_1) e^{r_1 t} + k_2 (bC_2 + cG_2) e^{r_2 t} \\ &+ k_1^2 (bC_3 + cG_3 + fC_1^2 + 2gC_1G_1 + hG_1^2) e^{2r_1 t} \\ &+ k_1 k_2 [bC_4 + cG_4 + 2fC_1C_2 \\ &+ 2g (C_1G_2 + C_2G_1) + 2hG_1G_2] e^{(r_1+r_2)t} \\ &+ k_2^2 (bC_5 + cG_5 \\ &+ fC_2^2 + 2gC_2G_2 + hG_2^2) e^{2r_2 t} + \cdots \end{aligned} \tag{2.20}$$

Equating coefficients for corresponding powers of $e^{r_1 t}$ and $e^{r_2 t}$ in the expressions for X and d^2X/dt^2 and also in the expressions for Y and d^2Y/dy^2, we first obtain

$$\begin{aligned} C_1 (r_1^2 - a) - bG_1 &= 0, \\ -bC_1 + (r_1^2 - c) G_1 &= 0, \\ C_2 (r_2^2 - a) - bG_2 &= 0, \\ -bC_2 + (r_2^2 - c) G_2 &= 0. \end{aligned} \tag{2.21}$$

The first two of these equations give two values for G_1:

$$G_1 = C_1 \frac{r_1^2 - a}{b} \qquad G_1 = C_1 \frac{b}{r_1^2 - c}, \tag{2.22}$$

which are equal to each other, since $(r_1^2 - a)(r_1^2 - c) = b^2$. In other words,

$$(r_1^2 - a)/b = \alpha_1,$$

and, consequently, $G_1 = C_1 \alpha_1$. In the same way, we obtain

$$G_2 = C_2 \alpha_2.$$

from the last pair of the equations (2.21).

Comparison of the coefficients of $e^{2r_1 t}$, $e^{(r_1+r_2)t}$, $e^{2r_2 t}$ leads to the following equations for the determination of C_i, G_i:

$$\begin{aligned} C_3 (4r_1^2 - a) - G_3 b &= eC_1^2 + 2fC_1G_1 + gG_1^2, \\ -C_3 b + G_3 (4r_1^2 - c) &= fC_1^2 + 2gC_1G_1 + hG_1^2, \\ C_4 |(r_1 + r_2)^2 - a| - G_4 b &= 2eC_1C_2 + 2f (C_1G_2 + C_2G_1) + 2gG_1G_2, \\ -C_4 b + |(r_1 + r_2)^2 - c| G_4 &= 2fC_1C_2 + 2g (C_1G_2 + C_2G_1) + 2hG_1G_2, \\ C_5 (4r_2^2 - a) - G_5 b &= eC_2^2 + 2fC_2G_2 + gG_2^2, \\ -C_5 b + G_5 (4r_2^2 - c) &= fC_2^2 + 2gC_2G_2 + hG_2^2. \end{aligned} \tag{2.23}$$

The convergence of the series thus obtained is given by the method of Poincare[7]. The treatment is also set forth in Picard's work[8].

THE PHENOMENOLOGICAL RELATIONS IN THE GENERAL CASE

In order to show that the phenomenological relations follow from the equations

$$\frac{d^2x}{dt^2} = X = \frac{\partial(-\Delta S)}{\partial x}, \quad \frac{d^2y}{dt^2} = Y = \frac{\partial(-\Delta S)}{\partial y}, \tag{2.8''}$$

even in the general case, we rewrite Eqs. (2.19), keeping terms up to second order in k_1 and k_2:

$$\begin{aligned} x &= e^{r_1 t} k_1 C_1 \left(1 + C_3' k_1 e^{r_1 t} + \tfrac{1}{2} C_4' k_2 e^{r_2 t}\right) \\ &+ e^{r_2 t} k_2 C_2 \left(1 + \tfrac{1}{2} C_4'' k_1 e^{r_1 t} + C_5'' k_2 e^{r_2 t}\right), \\ y &= e^{r_1 t} k_1 G_1 \left(1 + G_3' k_1 e^{r_1 t} + \tfrac{1}{2} G_4' k_2 e^{r_2 t}\right) \\ &+ e^{r_2 t} k_2 G_2 \left(1 + \tfrac{1}{2} G_4'' k_1 e^{r_1 t} + G_5'' k_2 e^{r_2 t}\right), \end{aligned} \tag{2.24}$$

where

$$C_i' = \frac{C_i}{C_1}, \quad C_i'' = \frac{C_i}{C_2}, \quad G_i' = \frac{G_i}{G_1}, \quad G_i'' = \frac{G_i}{G_2}. \tag{2.25}$$

Since $G_1 = C_1\alpha_1, \quad G_2 = C_2\alpha_2,$

we can write

$$x = e^{r_1 t}k_1C_1(1+\lambda) + e^{r_2 t}k_2C_2(1+\mu), \tag{2.26}$$

$$y = e^{r_1 t}k_1C_1\alpha_1(1+\rho) + e^{r_2 t}k_2C_2\alpha_2(1+\pi);$$

$$x' = e^{r_1 t}k_1C_1r_1(1+\lambda_1) + e^{r_2 t}k_2C_2r_2(1+\mu_1), \tag{2.27}$$

$$y' = e^{r_1 t}k_1C_1r_1\alpha_1(1+\rho_1) + e^{r_2 t}k_2C_2r_2\alpha_2(1+\pi_1),$$

where $\lambda, \mu, \rho, \pi, \lambda_1, \mu_1, \rho_1, \pi_1$ contain k_1 and k_2 as factors of first power.

Substituting the values of $e^{r_1 t}$, $e^{r_2 t}$ from (2.26) in (2.27) we obtain

$$\begin{aligned} x'\delta &= x[r_1\alpha_2(1+\pi)(1+\lambda_1) \\ &\quad - r_2\alpha_1(1+\rho)(1+\mu_1)] \\ &+ y[r_2(1+\lambda)(1+\mu_1) - r_1(1+\mu)(1+\lambda_1)], \end{aligned} \tag{2.28}$$

$$\begin{aligned} y'\delta &= x[r_1\alpha_1\alpha_2(1+\pi)(1+\rho_1) \\ &\quad - r_2\alpha_1\alpha_2(1+\rho)(1+\pi_1)] \\ &+ y[r_2\alpha_2(1+\lambda)(1+\pi_1) - r_1\alpha_1(1+\mu)(1+\rho_1)], \end{aligned}$$

where

$$\delta = (1+\lambda)(1+\pi)\alpha_2 - (1+\mu)(1+\rho)\alpha_1. \tag{2.29}$$

We obtain the phenomenological relation directly from (2.28), substituting X and Y for χ and γ.

Since

$$X = xL + yM, \quad Y = xM + yN, \tag{2.30}$$

where

$$L = a + ex + fy, \quad M = b + fx + gy,$$
$$N = c + gx + hy,$$

we get

$$x\Delta = XN - YM, \quad y\Delta = -XM + YL; \tag{2.31}$$

here $\Delta = LN - M^2$

For these values of χ and γ we can rewrite the relations (2.28) in the form

$$\begin{aligned} x'\delta\Delta &= X\{N[r_1\alpha_2(1+\pi)(1+\lambda_1) \\ &\quad - r_2\alpha_1(1+\rho)(1+\mu_1)] \\ &- M[r_2(1+\lambda)(1+\mu_1) - r_1(1+\mu)(1+\lambda_1)]\} \\ &+ Y\{L[r_2(1+\lambda)(1+\mu_1) - r_1(1+\mu)(1+\lambda_1)] \\ &\quad - M[r_1\alpha_2(1+\pi)(1+\lambda_1) - r_2\alpha_1(1+\rho) \\ &\quad (1+\mu_1)]\} = AX + BY; \end{aligned} \tag{2.32}$$

$$\begin{aligned} y'\delta\Delta &= X\{N[r_1\alpha_1\alpha_2(1+\pi)(1+\rho_1) \\ &\quad - r_2\alpha_1\alpha_2(1+\rho)(1+\pi_1)] \\ &- M[r_2\alpha_2(1+\lambda)(1+\pi_1) \\ &\quad - r_1\alpha_1(1+\mu)(1+\rho_1)]\} \\ &+ Y\{L[r_2\alpha_2(1+\lambda)(1+\pi_1) \\ &\quad - r_1\alpha_1(1+\mu)(1+\rho_1)] \\ &- M[r_1\alpha_1\alpha_2(1+\pi)(1+\rho_1) \\ &\quad - r_2\alpha_1\alpha_2(1+\rho)(1+\pi_1)]\} = DX + CY. \end{aligned}$$

We now show that for the general case which we have considered, we have an almost symmetric tensor L_{ik}, i.e., that D and B differ only by terms which contain $k_1e^{r_1 t}$, $k_2e^{r_2 t}$ (i.e., by terms which go to zero as $t \to +\infty$) Actually, by keeping in the expressions for B and D only those terms which do not contain k_1 and k_2 explicitly, we would have

$$L = a, \quad M = b, \quad N = c$$

and consequently, recalling the values of a_1, a_2,

$$\begin{aligned} B &= a(r_2 - r_1) - b(r_1\alpha_2 - r_2\alpha_1) = a(r_2 - r_1) \\ &\quad - [r_1(r_2^2 - a) - r_2(r_1^2 - a)] = r_1r_2(r_1 - r_2) \end{aligned} \tag{2.33}$$

and

$$D = c(r_1\alpha_1\alpha_2 - r_2\alpha_1\alpha_2) - b(r_2\alpha_2 - r_1\alpha_1). \tag{2.34}$$

But $ca_1 = a_1r_1^2 - b$, $ca_2 = a_2r_2^2 - b$, so that

$$D = \alpha_1\alpha_2(r_2 - r_1)r_1r_2.$$

On the other hand

$$\begin{aligned} \alpha_1\alpha_2 &= \frac{(r_1^2 - a)(r_2^2 - a)}{b^2} \\ &= \frac{r_1^2r_2^2 - a(r_1^2 + r_2^2) + a^2}{b^2} - = -1 \end{aligned}$$

and consequently

$$D = r_1r_2(r_1 - r_2) = B, \tag{2.35}$$

i.e., $L_{12} = L_{21}$ with accuracy to terms which contain k_1 and k_2 as first powers which tend to zero with increasing t.

GENERAL PROPERTIES OF THE INTEGRALS OF THE SYSTEM OF EQUATIONS (2.2)

We consider the system

$$\frac{d^2x_i}{dt^2} = \frac{\partial(-\Delta S)}{\partial x_i} = X_i \quad (i = 1, 2, \ldots, n), \tag{2.2'}$$

where ΔS is taken in its most general form. Since

$$\delta(-\Delta S) = \sum_i \frac{\partial(-\Delta S)}{\partial x_i}\delta x_i = \sum_i X_i \delta x_i,$$

we have

$$\frac{d}{dt}(-\Delta S) = \sum_i X_i x_i'. \tag{2.36}$$

On the other hand, we get from (2.2′) and (2.36)

$$\sum_i x_i' \frac{d^2 x_i}{dt^2} = \frac{1}{2}\frac{d}{dt}\sum_i (x_i')^2 = \sum_i X_i x_i' = \frac{d}{dt}(-\Delta S);$$

consequently,

$$\frac{x_1'^2 + x_2'^2 \ldots + + x_n'^2}{2} + \Delta S = \text{const}. \tag{2.37}$$

In irreversible thermodynamic processes $\lim \chi_i'(t) \geq 0$ and $\lim \chi_i(t) = 0$ for $t \to +\infty$ and, consequently, in these processes

$$^1/_2 (x_1'^2 + x_2'^2 + \ldots + x_n'^2) + \Delta S = 0. \tag{2.38}$$

ADDITIONAL REMARKS

We pose the following problem: beginning with ΔS, can we obtain a much simpler set of differential equations whose integrals approach zero at $t = +\infty$ and which have n constants of integration, making it possible to choose arbitrarily the initial values $\chi_1^0, \chi_2^0, \ldots, \chi_n^0$ of the independent variables?

We consider the linear system of n th order

$$dx_i/dt = -X_i = -(g_{i1}x_1 + g_{i2}x_2 + \ldots + g_{in}x_n) \quad (i = 1, 2, \ldots, n), \tag{2.39}$$

(which is a partial case of the phenomenological relations of Onsager), in which $L_{ik} = 0$ for $i \neq k$ and $L_{ii} = -1$. Setting $\chi_1 = \alpha e^{-\lambda t}$, $\chi_2 = \beta e^{-\lambda t}, \ldots, \chi_n = \nu e^{-\lambda t}$, we get a system of homogeneous algebraic equations for X:

$$\begin{aligned}
&(g_{11} - \lambda)\alpha + g_{12}\beta + g_{13}\gamma + \ldots + g_{1n}\nu = 0;\\
&g_{21}\alpha + (g_{22} - \lambda)\beta + g_{23}\gamma + \ldots + g_{2n}\nu = 0,\\
&\ldots\ldots\ldots\ldots\ldots\ldots\ldots\ldots,\\
&g_{n1}\alpha + g_{n2}\beta + g_{n3}\gamma + \ldots + (g_{nn} - \lambda)\nu = 0.
\end{aligned} \tag{2.40}$$

For non-vanishing solutions of this system we must choose for X the roots of the algebraic equation

$$\begin{vmatrix} g_{11}-\lambda & g_{12} & g_{13}\ldots g_{1n} \\ g_{21} & g_{22}-\lambda & g_{23}\ldots g_{2n} \\ \ldots\ldots\ldots\ldots & & \\ g_{n1} & g_{n2} & g_{n3} \quad g_{nn}-\lambda \end{vmatrix} = 0. \tag{2.41}$$

which we already know.

As we have seen, all n roots of this equation are real and positive. It is evident from (2.40) that there corresponds to each root λ_i a set of solutions $\alpha_i = 1, \beta_i, \gamma_i, \ldots, \nu_i$ such that the general integral of the system (2.39) has the form:

$$\begin{aligned}
x_1 &= C_1\alpha_1 e^{-\lambda_1 t} + C_2\alpha_2 e^{-\lambda_2 t} + \ldots + C_n\alpha_n e^{-\lambda_n t},\\
x_2 &= C_1\beta_1 e^{-\lambda_1 t} + C_2\beta_2 e^{-\lambda_2 t} + \ldots + C_n\beta_n e^{-\lambda_n t},\\
&\ldots\ldots\ldots\ldots\ldots\ldots\ldots\ldots\\
x_n &= C_1\nu_1 e^{-\lambda_1 t} + C_2\nu_2 e^{-\lambda_2 t} + \ldots + C_n\nu_n e^{-\lambda_n t},
\end{aligned} \tag{2.42}$$

These tend to zero as $t \to +\infty$. The values of $C_1, C_2, C_3, \ldots, C_n$ are determined by the system

$$\begin{aligned}
x_1^0 &= C_1\alpha_1 + C_2\alpha_2 + \ldots + C_n\alpha_n,\\
x_2^0 &= C_1\beta_1 + C_2\beta_2 + \ldots + C_n\beta_n,\\
&\ldots\ldots\ldots\ldots\ldots\ldots\\
x_n^0 &= C_1\nu_1 + C_2\nu_2 + \ldots + C_n\nu_n.
\end{aligned}$$

If we compare the set of integrals (2.42) with the set (12) we see that $r_i = -\sqrt{\lambda_i}$ and that both $\alpha_i, \beta_i, \gamma_i, \ldots, \nu_i$ and $C_1, C_2, C_3, \ldots C_n$ have identical values in the two systems.

We now assume that

$$0 < \lambda_1 < \lambda_2 < \lambda_3 < \ldots < \lambda_n.$$

Since $|r_i| = +\sqrt{\lambda_i}$ we get

$$0 < |r_1| < |r_2| < \ldots < |r_n|.$$

Consequently we can write the integrals of the system (12) in the form:

$$x_i = C_1\eta_1 e^{r_1 t}\left[1 + \frac{C_2\eta_2}{C_1\eta_1}e^{(r_2 - r_1)t} + \ldots + \frac{C_n\eta_n}{C_1\eta_1}e^{(r_n - r_1)t}\right] \quad (i = 1, 2, \ldots, n),$$

and the integrals of the system (2.42) in the form

$$x_i = C_1\eta_1 e^{-\lambda_1 t}\left[1 + \frac{C_2\eta_2}{C_1\eta_1}e^{-(\lambda_2 - \lambda_1)t} + \ldots + \frac{C_n\eta_n}{C_1\eta_1}e^{-(\lambda_n - \lambda_1)}\right].$$

But since $r_j - r_1 < 0$ and $-(\lambda_j - \lambda_1) < 0$ for $j = 2, 3, \ldots, n$, then $\exp[(r_j - r_i)t]$ and $\exp[-(\lambda_j - \lambda_i)t]$ are very small for $t > 0$ and approach zero with increasing t. Therefore, the principle values of the integrals of the first set are $\chi_i(t) = C_1\eta_1 e^{r_1 t}$ and of the second set are $\chi_i(t) = C_1\eta_1 e^{-\lambda_1 t}$, i.e., the integral curves of both systems almost coincide, but motion of the particle $(\chi_1, \chi_2, \ldots, \chi_n)$ along these curves proceeds with different velocity. In the first case we have approximately $\chi_i' = C_1\eta_1 r_1 e^{r_1 t}$, and in the second case $\chi_i' = -C_1\eta_1\lambda_1 e^{-\lambda_1 t}$.

3. APPLICATION OF THE GENERAL THEORY TO SPECIFIC PROBLEMS

The Transfer of Heat from One System to Another

We now show that the Fourier hypothesis, which applies to the transfer of heat from one system to another, follows from our general theory of irreversible thermodynamic processes.

We consider a system consisting of two plates, i.e., two thin plane round disks, in thermal contact through their bases, and adiabatically isolated from their surroundings. In this case we shall neglect any work of thermal expansion. We denote by m_1 the mass per unit area of contact, T_1 the absolute temperature, c_1, the specific heat, all of the first plate; m_2, T_2, c_2 are the corresponding quantities for the second plate, T_0 is the overall temperature of the system after thermal equilibrium has been established. We have assumed that these plates were not thick, in order that it would be possible to consider the temperature at any moment to be uniform at all points on either of the two plates.

Let Q_1 be the amount of heat per unit area of contact that the first plate must receive from the second in order that the system come to thermal equilibrium ($T_1 = T_0$), and let Q_2 be the corresponding amount of heat which the second plate must receive from the first.

Here

$$Q_1 = m_1c_1(T_1 - T_0) = m_1c_1\Delta T_1, \qquad (3.1)$$

$$Q_2' = m_2c_2(T_2 - T_0) = m_2c_2\Delta T_2,$$

$$Q_1 + Q_2 = 0. \qquad (3.2)$$

Consequently,

$$m_1c_1T_1 + m_2c_2T_2 = T_0(m_1c_1 + m_2c_2), \qquad (3.3)$$

$$Q_1 = \frac{m_1c_1\, m_2c_2}{m_1c_1 + m_2c_2}(T_1 - T_2). \qquad (3.4)$$

Thus at a given moment t, we get for the entropy ΔS per unit area of thermal contact (keeping only terms of second order),

$$\Delta S = \frac{Q_1}{T_1} + \frac{Q_2}{T_2} = -\frac{T_1 - T_2}{T_0^2}Q_1 \qquad (3.5)$$

$$= -\frac{m_1c_1 + m_2c_2}{m_1c_1\, m_2c_2}\frac{Q_1^2}{T_0^2}.$$

Here

$$\frac{\partial(-\Delta S)}{\partial Q_1} = \frac{2}{T_0^2}\frac{m_1c_1 + m_2c_2}{m_1c_1\, m_2c_2}Q_1 = aQ_1, \qquad (3.6)$$

where $a \geq 0$.

We then have only the one equation

$$d^2Q_1/dt^2 = aQ_1, \qquad (3.7)$$

the integral of which is $Q_1 = Ce^{rt}$.

Substituting this value of Q_1 in Eq. (3.7), and recalling that $a \geq 0$, we get

$$r^2 = a, \quad r_{1,2} = \pm\sqrt{a}.$$

Here only $-\sqrt{a}$ is of importance in physical problems, since $\lim Q_1 = 0$ for $t = +\infty$. Consequently,

$$Q_1 = ce^{-\sqrt{a}t},$$
$$\dot{Q}_1 = -\sqrt{a}Ce^{-\sqrt{a}t} = -\sqrt{a}Q_1, \qquad (3.8)$$

where $C = Q_1^0$ is the value of Q_1 at the initial time $t = 0$. Recalling the value of Q_1 from Eq. (3.4) and the value of a, we get the Fourier formula for the "heat flow" $\dot{Q}_1$:

$$\dot{Q}_1 = -\frac{1}{T_0}\sqrt{\frac{2m_1c_1m_2c_2}{m_1c_1 + m_2c_2}}(T_1 - T_2) \qquad (3.9)$$

Up to this point we have assumed that at each moment the temperature of each of the two plates is uniform. But even for very small thickness the temperature of each plate, which is a continuous function of position along the axis, must have different values on the opposite faces of each plate, hence different values are obtained for the entropy when one or the other temperature value is inserted

in Eq. (3.5). However, this difference is very small, since the temperature difference between the faces of the disks is slight. The entropy of each plate will correspond to a mean temperature which depends on the thermal conductivity of the plate. Denoting by T_1 and T_2 the extreme temperature for each plate at a given moment and by T_0 the temperature at thermal equilibrium, we get

$$\Delta T_1 = T_1 - T_0, \qquad \Delta T_2 = T_2 - T_0;$$

Here we must assume for the average temperature at time t in each of the two plates

$$T_0 + \lambda_1 \Delta T_1, \qquad T_0 + \lambda_2 \Delta T_2,$$

where λ_1 and λ_2 depend on the thermal conductivity of the plates and differ very slightly from unity. We then have

$$Q_1 = m_1 c_1 \lambda_1 \Delta T_1, Q_2 = m_2 c_2 \lambda_2 \Delta T_2, Q_1 + Q_2 = 0, \tag{3.10}$$

which gives

$$Q_1 = \frac{m_1 c_1 \lambda_1 m_2 c_2 \lambda_2}{m_1 c_1 \lambda_1 + m_2 c_2 \lambda_2} (T_1 - T_2), \tag{3.11}$$

$$\frac{Q_1}{m_1 c_1} = \lambda_1 \Delta T_1, \qquad \frac{Q_2}{m_2 c_2} = \frac{-Q_1}{m_2 c_2} = \lambda_2 \Delta T_2,$$

$$\lambda_2 \Delta T_2 - \lambda_1 \Delta T_1 = -Q_1 \frac{m_1 c_1 + m_2 c_2}{m_1 c_1 m_2 c_2}, \tag{3.12}$$

$$\Delta S = \frac{Q_1}{T_0 + \lambda_1 \Delta T_1} + \frac{Q_2}{T_0 + \lambda_2 \Delta T_2}.$$

Limiting ourselves to terms of second order, we get

$$\Delta S = \frac{\lambda_2 \Delta T_2 - \lambda_1 \Delta T_1}{T_0^2} Q_1 = -\frac{m_1 c_1 + m_2 c_2}{m_1 c_1 m_2 c_2} \frac{Q_1^2}{T_0^2},$$

$$\frac{d(-\Delta S)}{dQ_1} = 2 \frac{(m_1 c_1 + m_2 c_2)}{m_1 c_1 m_2 c_2} \frac{Q_1}{T_0^2} = a Q_1.$$

Following the method of calculation given above, we get, finally,

$$\dot{Q}_1 = -\sqrt{\frac{2(m_1 c_1 + m_2 c_2)}{m_1 c_1 m_2 c_2} \frac{m_1 c_1 \lambda_1 m_2 c_2 \lambda_2}{m_1 c_1 \lambda_1 + m_2 c_2 \lambda_2} \frac{T_1 - T_2}{T_0}}.$$

HEAT PROPAGATION IN A HOMOGENEOUS ROD

We now consider heat propagation in a cylindrical rod with density ρ and specific heat c. The lateral surfaces of the rod are covered with a thermally insulating jacket. We assume that the temperature of the rod is a continuous function which has derivatives along the axis of the rod, taken as the abscissa. We take three cross-sections of the rod, corresponding to $\chi - d\chi$, χ, and $\chi + d\chi$, and designate the area of each of these cross sections by f. In this way we obtain two adjacent cells of volume $f\,d\chi$ and mass $\rho f\,d\chi$.

We now turn our attention to the system which consists of these two cells. We denote by $Q(\chi - d\chi)$ the heat flow per unit area into the system from the side at $\chi - d\chi$ and by $\dot{Q}(\chi + d\chi)$ the flow of heat entering from the side at $\chi + d\chi$.

Let dS be the increase in entropy per unit mass of the system of the two cells in the time interval dt. The entropy increase of the system per unit time will then be $2\rho f d\chi \frac{dS}{dt}$. We denote by du the increase of internal energy of the system per unit mass in the time interval dt. The internal energy increase per unit time will then be

$$2\rho f dx \frac{du}{dt} = f[\dot{Q}(x - dx) - \dot{Q}(x + dx)]$$

$$= -2f dx \frac{d\dot{Q}}{dx}.$$

Thus, neglecting the work of thermal expansion, we have

$$T \rho \frac{dS}{dt} = -\frac{d\dot{Q}}{dx}$$

or

$$\rho \frac{dS}{dt} = -\frac{1}{T} \frac{d\dot{Q}}{dx} = -\frac{d(\dot{Q}/T)}{dx} - \frac{\dot{Q}}{T^2} \frac{dT(x)}{dx}. \tag{3.13}$$

On the other hand,

$$T(x + dx) - T(x - dx) = 2 \frac{dT(x)}{dx} dx. \tag{3.14}$$

But this quantity is, from Eq. (3.4), proportional to the quantity of heat Q in an adiabatic process. Setting

$$dT/dx = \mu Q, \tag{3.15}$$

where μ is a proportionality constant, we get from Eq. (3.13)

$$\rho \frac{dS}{dt} = -\frac{d(\dot{Q}/T)}{dx} - \frac{\mu}{T^2} Q \dot{Q}. \tag{3.16}$$

The increase of entropy can be divided into two parts (superposition principle): the first, the divergence of the entropy

$$\left[-\frac{d(\dot{Q}/T)}{dx}\right]$$

and second, the quantity

$$\Delta\dot{\sigma} = -\frac{\mu}{T^2} Q\dot{Q}$$

or entropy flow which, by Eq. (3.5), corresponds to the entropy

$$\Delta\sigma = -\frac{1}{2}\frac{\mu}{T^2} Q^2, \qquad (3.17)$$

which appears in the irreversible adiabatic process considered in the previous section. As a consequence we can write

$$d^2Q/dt^2 = bQ, \qquad b>0, \qquad (3.18)$$

which leads to the relation

$$\dot{Q} = -\sqrt{b}Q = -\sqrt{1/b}\,dT/dx, \qquad (3.19)$$

which appears in the formula for heat flow in Fourier's theory.

Similar results obtained by Prigogine with the help of direct application of the phenomenological relations of Onsager are reproduced in de Groot's work[5]. In this case the coefficients L_{ik}, as we have shown, must satisfy certain conditions in order that $\lim Q = 0$ for $t = +\infty$.

APPLICATION TO THE THEORY OF PHASES

Let a liquid (I) and its vapor (II) at temperatures T_1 and T_2 be contained in a given closed reservoir with heat proof walls. Let M, V, U be, respectively, the total mass, volume and energy of this system, M_i $(i = 1, 2)$ the masses of the components, p_i the pressure and $\bar{v}_i$, u_i, s_i the volume, energy and entropy per unit mass, so that

$$\begin{aligned} &M_1 + M_2 = M, \qquad M_1v_1 + M_2v_2 = V,\\ &M_1u_1 + M_2u_2 = U,\\ &S = M_1s_1 + M_2s_2. \end{aligned} \qquad (3.20)$$

Taking the mass M_1, the energy u_1 and the volume v_1 as the independent variables that define the state of the components, we find that Eqs. (3.20) define M_2, v_2, u_2 as functions of M_1, v_1, u_1. Inasmuch as s_i, T_i appear as functions of u_i, v_i, they are also functions of M_1, v_1, u_1. Therefore the total entropy S of the system is also a function of these three variables.

Denoting by M_1^0, v_1^0, u_1^0 the values of the variables M_1, v_1, u_1 for the equilibrium state, we have, limiting ourselves to terms of the first and second order,

$$\begin{aligned} \Delta S &= S(v_1, u_1, M_1) - S(v_1^0, u_1^0, M_1^0)\\ &= \left(\frac{\partial S}{\partial v_1}\right)_0 v + \left(\frac{\partial S}{\partial u_1}\right)_0 u + \left(\frac{\partial S}{\partial M_1}\right)_0 m\\ &+ \frac{1}{2}\left[\left(\frac{\partial^2 S}{\partial v_1^2}\right)_0 v^2 + 2\left(\frac{\partial^2 S}{\partial v_1 \partial u_1}\right)_0 vu\right.\\ &+ 2\left(\frac{\partial^2 S}{\partial v_1 \partial M_1}\right)_0 vm + \left(\frac{\partial^2 S}{\partial u_1^2}\right)_0 u^2\\ &\left. + 2\left(\frac{\partial^2 S}{\partial u_1 \partial M_1}\right) um + \left(\frac{\partial^2 S}{\partial M_1^2}\right) m^2\right], \end{aligned}$$

where

$$v_1 - v_1^0 = v, \qquad u_1 - u_1^0 = u, \qquad M_1 - M_1^2 = m$$

Since the derivatives are taken at v_1^0, u_1^0, M_1^0, which correspond to the maximum of the entropy S,

$$\left(\frac{\partial S}{\partial u_1}\right)_0 = \left(\frac{\partial S}{\partial v_1}\right)_0 = \left(\frac{\partial S}{\partial M_1}\right)_0 = 0 \qquad (3.21)$$

and, consequently,

$$\begin{aligned} \Delta S = \frac{1}{2}&\left[\left(\frac{\partial^2 S}{\partial v_1^2}\right)_0 v^2\right.\\ &+ 2\left(\frac{\partial^2 S}{\partial v_1 \partial u_1}\right)_0 vu + 2\left(\frac{\partial^2 S}{\partial v_1 \partial M_1}\right)_0 vm\\ &\left. + \left(\frac{\partial^2 S}{\partial u_1^2}\right)_0 u^2 + 2\left(\frac{\partial^2 S}{\partial u_1 \partial M_1}\right)_0 um + \left(\frac{\partial^2 S}{\partial M_1^2}\right)_0 m^2\right]. \end{aligned}$$

To calculate the second derivatives of S, we make use of the formula for the second total differential:

$$\begin{aligned} d^2S = &\frac{\partial^2 S}{\partial v^2} dv^2 + 2\frac{\partial^2 S}{\partial v \partial u} dvdu + 2\frac{\partial^2 S}{\partial v \partial m} dvdm\\ &+ \frac{\partial^2 S}{\partial u^2} du^2 + 2\frac{\partial^2 S}{\partial u \partial m} dudm + \frac{\partial^2 S}{\partial m^2} dm^2. \end{aligned}$$

The differential equations of the process under consideration have the form

$$\frac{d^2v}{dt^2} = -\left(\frac{\partial^2 S}{\partial v_1^2}\right)_0 v - \left(\frac{\partial^2 S}{\partial v_1 \partial u_1}\right)_0 u - \left(\frac{\partial^2 S}{\partial v_1 \partial M_1}\right)_0 m,$$

$$\frac{d^2u}{dt^2} = -\left(\frac{\partial^2 S}{\partial u_1 \partial v_1}\right)_0 v - \left(\frac{\partial^2 S}{\partial u_1^2}\right)_0 u - \left(\frac{\partial^2 S}{\partial u_1 \partial M_1}\right)_0 m, \tag{3.22}$$

$$\frac{d^2m}{dt^2} = -\left(\frac{\partial^2 S}{\partial M_1 \partial v_1}\right)_0 v - \left(\frac{\partial^2 S}{\partial M_1 \partial u_1}\right)_0 u - \left(\frac{\partial^2 S}{\partial M_1^2}\right)_0 m.$$

The interesting integrals of this system depend on the negative root of the algebraic equation

$$\begin{vmatrix} -\left(\frac{\partial^2 S}{\partial v_1^2}\right)_0 - r^2 & -\left(\frac{\partial^2 S}{\partial v_1 \partial u_1}\right)_0 & -\left(\frac{\partial^2 S}{\partial v_1 \partial M_1}\right)_0 \\ -\left(\frac{\partial^2 S}{\partial u_1 \partial v_1}\right)_0 & -\left(\frac{\partial^2 S}{\partial u_1^2}\right)_0 - r^2 & -\left(\frac{\partial^2 S}{\partial u_1 \partial M_1}\right)_0 \\ -\left(\frac{\partial^2 S}{\partial M_1 \partial v_1}\right)_0 & -\left(\frac{\partial^2 S}{\partial M_1 \partial u_1}\right)_0 & -\left(\frac{\partial^2 S}{\partial M_1^2}\right)_0 - r^2 \end{vmatrix} = 0.$$

Since $(-\Delta S)$ is a positive definite quadratic form, three of the roots of this equation are negative and the other three are positive. The results which are obtained are of physical interest only if both masses are positive for the case of thermal equilibrium.

To determine the values of the independent variables which apply to the case of stable equilibrium, we follow the Gibbs method as it is stated in the thermodynamics text of Planck[9].

From Eq. (3.20) we get

$$dM_2 = -dM_1, \tag{3.24}$$

$$M_2 dv_2 = -M_1 dv_1 - (v_1 - v_2)\, dM_1,$$

$$M_2 du_2 = -M_1 du_1 - (u_1 - u_2)\, dM_1$$

$$dS = M_1 ds_1 + M_2 ds_2 + s_1 dM_1 + s_2 dM_2 \tag{3.25}$$

$$= M_1 \frac{du_1 + p_1 dv_1}{T_1} + M_2 \frac{du_2 + p_2 dv_2}{T_2} + (s_1 - s_2)\, dM_1$$

$$= M_1 \left(\frac{1}{T_1} - \frac{1}{T_2}\right) du_1 + M_1 \left(\frac{p_1}{T_1} - \frac{p_2}{T_2}\right) dv_1$$

$$+ \left[s_1 - s_2 - \frac{(u_1 - u_2) + p_2 (v_1 - v_2)}{T_2}\right] dM_1.$$

Thus Eqs. (3.4), which determine the state of thermodynamic equilibrium, and which in our case, have the form

$$\frac{\partial S}{\partial u_1} = M_1 \left(\frac{1}{T_1} - \frac{1}{T_2}\right) = 0,$$

$$\frac{\partial S}{\partial v_1} = M_1 \left(\frac{p_1}{T_1} - \frac{p_2}{T_2}\right) = 0, \tag{3.26}$$

$$\frac{\partial S}{\partial M_1} = \left[s_1 - s_2 - \frac{(u_1 - u_2) + p_2 (v_1 - v_2)}{T_2}\right] = 0$$

lead to Gibb's conditions

$$T_1 = T_2 = T_0, \qquad p_1 = p_2 = p_0. \tag{3.27}$$

Choosing M_1, ν_1, u_1 as independent variables, we have

$$T_1 = f_1(u_1, v_1).\ T_2 = f_2(u_2,\ v_2) = f(u_1,\ v_1,\ M_1),$$

$$s_1 = \psi_1(u_1,\ v_1),\ s_2 = \psi_2(u_2,\ v_2) = \psi(u_1,\ v_1,\ M_1),$$

$$p_1 = \varphi_1(u_1,\ v_1),\ p_2 = \varphi_2(u_2,\ v_2) = \varphi(u_1,\ v_1,\ M_1).$$

Substituting these values of T_1, T_2, s_1, s_2, p_1, p_2 in Eqs. (3.26), we get from them v_1^0, u_1^0, M_1^0, which define the state of thermodynamic equilibrium. We note here that Eqs. (3.26) contain s and u in the form $s_1 - s_2$ and $u_1 - u_2$.

Following Planck, we can give another form to the last of Eqs. (3.26). Since the difference $(s_1 - s_2)$ depends, in thermodynamic equilibrium, only on state I and state II and not on the path from I to II, we can find this difference in the transition from I to II along the isotherm T_0. But, since s_1 and s_2 pertain to a unit mass of one and the same material at the temperature T_0, we have

$$s_1 - s_2 = \int_{(2)}^{(1)} ds$$

$$= \frac{1}{T_0} \int_{(2)}^{(1)} (du + pdv) = \frac{u_1 - u_2}{T_0} + \frac{1}{T_0} \int_{(2)}^{(1)} pdv.$$

Now, assuming $T_2 = T_0$, we find, from Eq. (3.26)

$$\frac{1}{T_0} \int_{(2)}^{(1)} pdv - \frac{p_2 (v_1 - v_2)}{T_0} = 0,$$

$$\int_{(2)}^{(1)} pdv = p_2 (v_1 - v_2).$$

It now remains to find, with the help of d^2S, the second derivatives which enter into Eq. (3.22) and which pertain to the equilibrium state, introducing

[9] M. Planck, *Thermodynamics*, 1930

only such quantities which can be obtained by laboratory measurement.

Recalling Eqs. (3.26) we get, from (3.25),

$$d^2S = \frac{M_1}{T_0^2}(-dT_1 + dT_2)\,du_1 \tag{3.28}$$

$$+ \frac{M_1 p_0}{T_0^2}(-dT_1 + dT_2)\,dv_1$$

$$+ \frac{M_1}{T_0}(dp_1 - dp_2)\,dv_1$$

$$+ \left[ds_1 - ds_2 - \frac{du_1 - du_2 + p_0(dv_1 - dv_2)}{T_0}\right.$$

$$\left. - \frac{(v_1 - v_2)\,dp_2}{T_0} + \frac{(u_1 - u_2) + p_0(v_1 - v_2)}{T_0^2}\,dT_2\right] dM_1$$

$$= \frac{M_1}{T_0^2}(-dT_1 + dT_2)\,du_1$$

$$+ \frac{M_1 p_0}{T_0^2}(-dT_1 + dT_2)\,dv_1 + \frac{M_1}{T_0}(dp_1 - dp_2)\,dv_1$$

$$+ \left[\frac{u_1 - u_2 + p_0(v_1 - v_2)}{T_0^2}\,dT_2 - \frac{v_1 - v_2}{T_0}\,dp_2\right] dM_1.$$

The quantities u_1, v_1, u_2, v_2 and M_1, which appear here, relate to the equilibrium state. The differentials dT_1, dT_2, du_2, dv_2, dp_1, dp_2 must be taken as functions of du_1, dv_1 and $dM_1 = dm$. For this purpose we first use

$$M_2 dv_2 = -M_1 dv_1 - (v_1 - v_2)\,dm,$$

$$M_2 = M - M_1.$$

But, inasmuch as we chose M_1, u_1, v_1 as the independent variables, then $T = T(u, v)$; conversely, $u = u(v, T)$ as a function of v and T satisfy the identity relation

$$T \equiv T[u(v, T), v].$$

From this identity we get, by differentiating with respect to T,

$$\frac{\partial T(u, v)}{\partial u}\,\frac{\partial u(v, T)}{\partial T} = 1,$$

$$\frac{\partial T(u, v)}{\partial u} = \frac{1}{\partial u(v, T)/\partial T} = \frac{1}{c_v},$$

and by differentiating with respect to v,

$$\frac{\partial T(u, v)}{\partial v} =$$

$$-\frac{\partial T(u, v)}{\partial u}\,\frac{\partial u(v, T)}{\partial v} = -\frac{1}{c_v}\,\frac{\partial u(v, T)}{\partial v}.$$

From the first law of thermodynamics

$$dq = du(v, T) + p(v, T)\,dv = \frac{du(v, T)}{\partial T}\,dT$$

$$+ \left[\frac{\partial u(v, T)}{\partial v} + p(v, T)\right] dv = c_v dT + a dv,$$

so that

$$\partial u(v, T)/\partial v = a - p,$$

and therefore

$$\frac{\partial T(u, v)}{\partial v} = -\frac{1}{c_v}(a - p).$$

We finally obtain

$$dT = \frac{\partial T(u, v)}{\partial u}\,du$$

$$+ \frac{\partial T(u, v)}{dv}\,dv = -\frac{a - p}{c_v}\,dv + \frac{1}{c_v}\,du.$$

Consequently,

$$dT_1 = -\frac{a_1 - p_0}{c_{v1}}\,dv_1 + \frac{1}{c_{v1}}\,du_1,$$

$$dT_2 = -\frac{a_2 - p_0}{c''_{v2}}\,dv_2 + \frac{1}{c''_{v2}}\,du_2$$

$$= \frac{a_2 - p_0}{c''_{v2}}\,\frac{M_1}{M_2}\,du_1 - \frac{1}{c''_{v2}}\,\frac{M_1}{M_2}\,du_1$$

$$+ [(a_2 - p_0)(v_1 - v_2) - (u_1 - u_2)]\,\frac{dm}{c_{v2} M_2}$$

We now express dp as a function of du, dv. We have

$$dp(u, v) = \frac{\partial p(u, v)}{\partial u}\,du + \frac{\partial p(u, v)}{\partial v}\,dv.$$

From the First Law we get

$$dq = du(p, T) + p\,dv(p, T)$$

$$= \left[\frac{\partial u(p, T)}{\partial p} + p\,\frac{\partial v(p, T)}{\partial p}\right] dp$$

$$+ \left[\frac{\partial u(p, T)}{\partial T} + p\,\frac{\partial v(p, T)}{\partial T}\right] dT = k\,dp + c_p\,dT.$$

On the other hand, assuming u, v in the expression for p as functions of p and t, we get the identity

$$p = p(u,\ v) = p[u(p,\ T),\ v(p,\ T)],$$

and differentiating with respect to p and T, we find

$$\frac{\partial p(u,\ v)}{\partial u}\frac{\partial u(p,\ T)}{\partial p} + \frac{\partial p(u,\ v)}{\partial v}\frac{\partial v(p,\ T)}{\partial p} = 1,$$

$$\frac{\partial p(u,\ v)}{\partial u}\frac{\partial u(p,\ T)}{\partial T} + \frac{\partial p(u,\ v)}{\partial v}\frac{\partial v(p,\ T)}{\partial T} = 0.$$

Recalling the expressions for k and c_p introduced above and assuming

$$\Delta = k\frac{\partial v(p,\ T)}{\partial T} - c_p\frac{\partial v(p,\ T)}{\partial p},$$

we obtain

$$\Delta\frac{\partial p(u,\ v)}{\partial v} = -\frac{\partial u(p,\ T)}{\partial T} = -c_p + p\frac{\partial v(p,\ T)}{\partial T},$$

$$\Delta\frac{\partial p(u,\ v)}{\partial u} = \frac{\partial v(p,\ T)}{\partial T}$$

and, consequently,

$$dp = \frac{\partial p(u,\ v)}{\partial u}du + \frac{\partial p(u,\ v)}{\partial v}dv$$

$$= \frac{\partial v(p,\ T)/\partial T}{\Delta}du - \frac{c_p - p[\partial v(p,\ T)/\partial T]}{\Delta}dv.$$

We then have

$$dp_1 = \left[\frac{\partial v(p,\ T)/\partial T}{\Delta}\right]_1 du_1$$

$$- \left[\frac{c_p - p[\partial v(p,\ T)/\partial T]}{\Delta}\right]_1 dv_1,$$

$$dp_2 = -\frac{M_1}{M_2}\left[\frac{\partial v(p,\ T)/\partial T}{\Delta}\right]_2 du_1$$

$$+ \frac{M_1}{M_2}\left[\frac{c_p - p[\partial v(p,\ T)/\partial T]}{\Delta}\right]_2 dv_1$$

$$- \frac{1}{\Delta_2 M_2}\Big[[u_1 - u_2 + p_0(v_1 - v_2)]\left(\frac{\partial v(p,\ T)}{\partial T}\right)_2$$

$$- c_{p_2}(v_1 - v_2)\Big]dm,$$

where the expressions in square brackets pertain to phase I and II in thermodynamic equilibrium.

From $dq = du + pdv$ we get the following expression for the quantity of heat necessary to vaporize a unit mass at the temperature T_0 and pressure p_0.

$$q_1 - q_2 = (u_1 - u_2) + p_0(v_1 - v_2).$$

Making use of this expression and those for dT and dp obtained earlier, we get from (3.28), after some simplification

$$d^2S = Adu_1^2 + 2Bdu_1dv_1$$

$$+ 2Cdu_1dm + Ddv_1^2 + 2Edv_1dm + Fdm^2,$$

where the coefficients $A, B, \ldots, F$ are identical with the second derivatives which enter into the set of equations (3.20).

In this fashion we get the system of differential equations

$$\begin{aligned} d^2m/dt^2 &= -Cu - Ev - Fm, \\ d^2u/dt^2 &= -Au - Bv - Cm, \\ d^2v/dt^2 &= -Bu - Dv - Em, \end{aligned} \qquad (3.22')$$

which describe the time development of the process.

The author extends his cordial gratitude to K. Shaposhnikov for his great assistance in the preparation of the manuscript for publication in the Russian language.

Translated by R. T. Beyer
47

The Isotopic Shift in the Spectrum of Plutonium

A. R. STRIGANOV, L. A. KOROSTYLEVA AND IU. P. DONTSOV

(Submitted to JETP editor July 27, 1954)
J. Exper. Theoret. Phys. USSR 28, 480-484 (March, 1955)

The isotopic shift of 19 lines of plutonium has been found in the region of 4100-6500 Å. It appears that 13 of these lines possess a purely isotopic structure while 6 lines display an isotopic and hyperfine structure. All the lines, with the exception of 6192.63 Å, experience a negative shift. The magnitude of the isotopic shift for the lines measured varies from 0.08 to 0.29 cm^{-1}. On the basis of the data on the isotopic shift and on the hyperfine splitting of the lines, transition schemes for the lines are determined which are based on the hyperfine structure, on the isotopic structure, or on both together. In addition the electronic configurations are predicted for several of the levels, with varying certainty.

I. INTRODUCTION

AT this time much attention is being paid to the investigations of the isotopic shift in the spectrum of elements in the actinium series. The most thoroughly studied isotopic shift is in the spectrum of uranium. Initially this effect was found in the spectrum of uranium by Anderson and White[1] It was then thoroughly investigated in several other researches[2]. Recently the isotopic shift in the spectrum of thorium has been found and studied[3].

While our work was in progress, there appeared a paper on the isotopic shift in the spectrum of plutonium[4]. The authors photographed the spectrum of two-isotope samples of plutonium (Pu^{238} + Pu^{242} and Pu^{239} + Pu^{240}) on a large 9-meter diffraction spectrograph (dispersion = 0.92 Å/mm) and they studied the ultraviolet region of the spectra in the interval 3350-4050 Å. Twenty lines were found with a noticeable isotope shift between the Pu^{238} and Pu^{240} components. Of these only four lines were found to have a measurable shift between the Pu^{239} and Pu^{240} components. The resolving power of the set-up above was approximately six times less than the resolving power of our equipment. For this reason the authors[4] were unable to find the hyperfine structure of the lines of the isotope Pu^{239}, which, of course, affected the accuracy of the measurement of the magnitude of the isotopic shift in several cases.

This work, performed in the middle of 1953, is concerned with the investigation of the isotopic shift in the spectrum of plutonium. The problem included the measurement of the intervals between the components of the isotopic structure and the determination of the relation of the intensities of the components of the isotopic structure.

II. EXPERIMENTAL PART

The same kind of discharge tube with hollow cathode and the same kind of vacuum system was used for the excitation of the spectrum of plutonium as had been used by us for the investigation of the hyperfine structure of the lines of U^{233} and Pu^{239} [5]. For an arrangement of high resolving power, a Fabry-Perot etalon was used together with a three-glass prism Steinheil spectrograph. The Fabry-Perot etalon was placed between the source of the light and the spectrograph aperture. The interference picture was projected on the spectrograph slit by means of a Tessar objective (f = 600 mm).

For the investigation of the isotopic structure of the spectrum of plutonium a mixture of two isotopes Pu^{239} + Pu^{240}, in the form of an oxide, was used. A sample of approximately 8 mg was placed in the (discharge) tube. The plutonium oxide reduced to the metal hydride under electric discharge[5]. The excitation took place under an

[1] O. E. Anderson, H. K. White, Phys. Rev. 71, 911 (1947)

[2] L. E. Burchart, G. L. Stukenbrocker and S. Adams, Phys. Rev. 75, 83 (1949); J. R. McNally, J. Opt. Soc. Am. 39, 271 (1949); D. D. Smith, G. L. Stukenbrocker and J. R. McNally, Phys. Rev. 84, 383 (1951)

[3] G. L. Stukenbroker and J. R. McNally, J. Opt. Soc. Am. 43, 36 (1953)

[4] J. G. Conway and M. Fred, J. Opt. Soc. Am. 43, 216 (1953)

[5] L. A. Korostyleva, A. R. Striganov and N. M. Iashin, J. Exper. Theoret. Phys. USSR 28, 471 (1955), Soviet Phys. 1, 310 (1955)

argon pressure of 1-2 mm of mercury and a discharge current of 0.2 amp. Two spectra were photographed in the region 4100-6500 Å with an exposure time of 60 minutes and with intervals of 10 and 15 mm between the plates of the etalon.

III. RESULTS

Having looked carefully at the obtained spectrograms, we have found about twenty lines showing evidence of isotopic structure. Some of the lines found by us were composed of two components, others of three components. Visually comparing the structure of these lines on the spectrograms from the two-isotope sample $Pu^{239} + Pu^{240}$ with the structure of the same lines on the spectrograms from the one-isotope sample Pu^{239}, we have determined that one of the components in the structure of these lines is due to the isotope Pu^{240}. Figure 1 shows

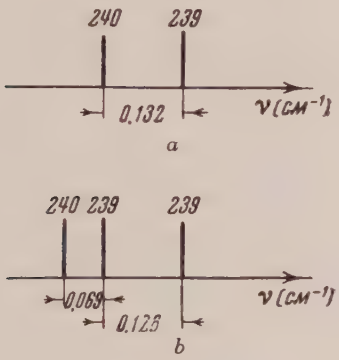

Fig. 1. The structure of the plutonium lines: a. λ = 4493.67 Å; b. λ = 4206.37 Å.

as an example the schematic structure of two lines 4493.67 and 4206.37 Å, one of which consists of two components, while the other consists of three (on this and on the following drawings the isotopic components are identified by the mass number). We measured the intensities of the components of a series of spectral lines having isotopic structure. This confirmed the existence of isotopic shift in the spectrum of plutonium.

We found 13 lines of plutonium exhibiting a purely isotopic structure and 6 lines with isotopic and hyperfine structure in the region of the spectrum investigated. All lines, with the exception of line 6192.63 Å, were found to have a negative shift (i.e., the component of Pu^{240} is displaced in the direction of lower wave numbers).

Off-center approximations were used to determine the magnitudes of the shifts. The method of Mac Nair[6] was employed in processing the results of the measurements. The final results are shown in Table I. Columns 3 and 4 show the magnitude of the splitting between the Pu^{239} components, column 5 gives the interval between the Pu^{240} component and the neighboring Pu^{239} component. Columns 6 and 7 show the magnitude of the isotopic shift between the Pu^{239} and Pu^{240} components, where for those lines with isotopic and hyperfine structure it was calculated by adding to the interval between the Pu^{239} component and the neighboring Pu^{240} component half the width of the hyperfine structure (columns 3 and 4), without center of mass calculation. The results obtained show that the magnitude of the isotopic shift in the spectrum of plutonium varies between 0.08 and 0.29 cm^{-1} for a mass number difference, ΔA, between two isotopes equal to 1. The largest shifts are observed for the lines 4159.87; 4396.31; 4468.48; 4484.20; and 4986.72 Å; the smallest for lines 4567.45; 5590.51; and 6192.63 Å. It is possible to say with certainty that the lines 4393.87, 4441.57, 4491.61 and 4504.80 Å do not exhibit isotopic structure because these lines are not reduced in their intensities in our spectra by comparison with other lines where the Pu^{240} component is found.

The isotopic shift in the spectrum of plutonium is nearly the magnitude of the shifts in the spectra of uranium[2] and thorium[3]. If the isotopic shift in the spectra of the elements of the actinium shell is compared with the isotopic shift of the heavy elements of the preceding shell (Hg, Tl, Pb) it is easily seen that in the region of the actinium shell nuclei there is a "jump" in the value of the isotopic shift. Such "jumps" have already been observed in the cases of cerium, neodymium, samarium and europium, and also in the case of lead. It has been shown over the past few years that these jumps are related to a large deformation of the shape of the nucleus. It is apparently possible in this way to explain the large negative isotopic shift in the spectra of the elements of the actinium series.

IV. ON THE QUESTION OF THE ELECTRONIC CONFIGURATIONS IN THE PLUTONIUM ATOM

All the plutonium lines whose structure we have

[6] W. A. McNair, Phil. Mag. 2, 613 (1926); S. Tolansky, *High Resolution Spectroscopy*, London, 1947

TABLE I

Spectral lines of plutonium exhibiting isotopic structure.

Wavelength in Å	Intensity	Width of the Hyperfine Structure		Interval between Pu^{240} and neighboring Pu^{239} component in cm	Isotopic shift Pu^{239} - Pu^{240}	
		in cm^{-1}	in Å		in cm^{-1}	in Å
4140.10	3	—	—		—0.197	—0.034
4151.38	4	—	—		—0.167	—0.029
4159.87	4	—	—		—0.261	—0.045
4206.37	7	0.128	0.023	0.069	—0.133	—0.023
4396.31	8	0.09	0.017	0.244	—0.289	—0.058
4468.48	4	0.161	0.032	0.172	—0.252	—0.050
4472.70	10	0.167	0.033	0.075	—0.158	—0.032
4478.63	1	—	—	—	—0.093	—0.019
4484.20	1	—	—	—	—0.239	—0.048
4493.67	10	—	—	—	—0.132	—0.027
4506.56	—	—	—	—	—0.195	—0.040
4567.28	1	—	—	—	—0.111	—0.023
4676.18	1	0.092	0.020	0.177	—0.223	—0.049
4798.93	1	—	—	—	—0.169	—0.039
4986.72	3	—	—	—	—0.235	—0.058
5044.53	2	—	—	—	—0.215	—0.055
5590.51	4	—	—	—	—0.122	—0.038
5630.48	6	—	—	—	—0.123	—0.039
6192.63	7	0.039	0.015	0.058	+0.077	+0.029

investigated can be sorted into four groups.

1. Lines which exhibit only hyperfine structure (in all 65 lines)[5].

2. Lines which undergo a purely isotopic shift (13 lines).

3. Lines which exhibit both hyperfine and isotopic structure (6 lines).

4. Lines which do not undergo either hyperfine splitting or an isotopic shift.

Comparing PuI with SmI, by analogy with UI and NdI, it is thought that the ground state of the neutral atom of plutonium is related to the ground-state configuration $5f^56d7s^2$. In comparison with the classification of the uranium spectra, it is supposed that higher excited states belong to the configurations $5f^56d^27s$, $5f^56d7s7p$, $5f^57s^27p$, $5f^26d^27p$, $5f^56d^3$. In the case of a singly ionized plutonium atom there appear to be two systems of energy levels. Levels of the configurations $5f^57s^2$, $5f^56d7s$, $5f^56d^2$, $5f^57s7p$, $5f^56d7p$ belong to one of these, while $5f^67s$, $5f^66d$, $5f^67p$ belong to the other.

On the basis of our experimental data it is not difficult to present certain considerations on the electronic configurations to which the levels from several transitions apparently belong. As is known, the energy levels of atoms, having closed shell electronic configurations s^2 and p^6, do not exhibit hyperfine splitting. The largest splitting is experienced by levels related to configurations with one unbalanced s-electron. As far as isotopic shift is concerned, it is strongest for those levels which belong to configurations having a group of penetrating s^2-electrons.

From this it is thought that lines of the first group, which exhibit only hyperfine structure, belong to transitions between levels of the excited configurations of the type $5f^56d^27p$ - $5f^56d^27s$ (PuI) or $5f^56d7p$ - $5f^56d7s$ (PuII). One of these levels undergoes doublet splitting. Lines of this group cannot be related to transitions to the ground state with non-excited configurations $5f^56d7s^2$ or $5f^57s^2$, since they would then exhibit an isotopic shift.

Lines of the second group, which undergo only an isotopic shift, appear to belong to transitions of the type $5f^56d^27p$ - $5f^56d7s^2$ (PuI) or $5f^56d7p$ - $5f^57s^2$ (PuII), which either end or start with mixed levels. The scheme of such a type of transition is shown by us as Fig. 2*a*. This scheme explains the shift of the Pu^{240} component in the structure of the lines on the red side. Fig. 2*b*

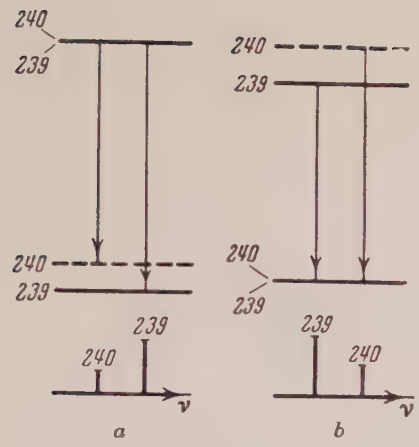

Fig. 2. Transition schemes explaining the isotopic shift:
a. red shift; *b*. violet shift of the component Pu^{240}.

shows a scheme of transitions from upper mixed levels to lower unmixed ones, which corresponds to the shift of the Pu^{240} component in the structure of the lines on the violet side, a type of shift observed on several lines (by Conway and Fred)[4]

Lines of the third group, exhibiting both hyperfine and isotopic structure, seem to be related to transitions of the type $5f^5 6d7s7p - 5f^5 6d7s^2$ (PuI) or $5f^5 7s7p - 5f^5 7s^2$ (PuII). Levels of these transitions experience at the same time both hyperfine splitting and an isotopic shift. Fig. 3 shows four schemes which permit an explanation of the origin of the observed structure of all six lines belonging to this group. Apparently these lines are related to the transitions between levels of low-excited configurations and levels of non-excited configuration.

Lines of the fourth group are apparently related to transitions between levels of configurations with non-penetrating *f*, *d*, and *p* electrons, and also to highly excited levels of configurations with *s* and s^2-electrons which do not undergo observable hyperfine splitting and isotopic shift.

We see, using the results of the investigations of the hyperfine structure and the isotopic shift in the spectrum of uranium, it is possible to get fairly important information concerning its classification.

However the complete interpretation of the spectrum of plutonium is only possible on the basis of an investigation of the Zeeman effect. The data on the hyperfine structure and isotopic shift can be used only as an auxiliary aid in the assignment of levels to a particular electronic configuration. In conclusion, we note that the transition schemes discussed are related to the case of normal order of the isotope terms in accordance with the general

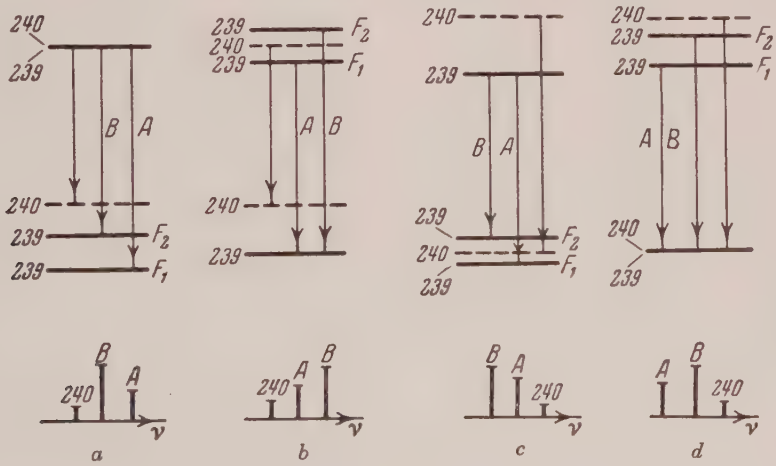

Fig. 3. Schemes of transitions explaining lines of mixed structure.
a and *b*: red shift of the Pu^{240} component with alternate intensities of the components *A* and *B* of the hyperfine structure of isotope Pu^{239}; *c* and *d*: violet shift with alternate intensities of the components *A* and *B* of the hyperfine structure.

theory of the isotopic effect (the terms of the lighter isotopes are placed deeper). One should keep in mind the fact that in complicated atoms non-normal positions of the isotope terms are sometimes found as the results of perturbation.

Translated by F. Ajzenberg
84

SOVIET PHYSICS - JETP VOLUME 1, NUMBER 2 SEPTEMBER, 1955

The Double Configuration Approximation to the Two Lowest Configurations of the Boron Atom

G. K. TSIUNAITIS AND A. P. IUTSIS
Vilna State University
Physico-technical Institute, Academy of Science, Lithuanian SSSR

(Submitted to JETP editor March 24, 1954)
J. Exper. Theoret. Phys. USSR 28, 452-457 (April, 1955)

The solutions of the equations of the self-consistent field without exchange are presented for the configurations $1s^2 2s^2 2p$ and $1s^2 2s^2 3s$ of boron. The values of the total energy, both in single configuration as well as in the double configuration approximation $1s^2 2s^2 2p^k 3s^{1-k} - 1s^2 2p^{k+2} 3s^{1-k}$ $(k = 1, 0)$ are computed with the help of these solutions. With the aid of the solutions of the equation of the self-consistent field without exchange, there are also computed the mass effect, the total dipole strength and the transition probability for the transition $1s^2 2s^2 3s - 1s^2 2s^2 2p$, both in the single configuration and the double configuration approximations.

1. INTRODUCTION

THE present work is devoted to the application of a multiple configuration approximation to the two lowest configurations $1s^2 2s^2 2p$ and $1s^2 2s^2 3s$ of the boron atom with the help of the solution of the equation of the self-consistent field without exchange. The method of analysis carried out in reference 1 shows that while we use single electron wave functions, which are determined in the single configuration approximation, the multiple configuration approximation, in practice, reduces to the double configuration approximation : $1s^2 2s^2 2p^k 3s^{1-k} - 1s^2 2p^{k+2} 3s^{1-k}$, where $k = 1$ or 0.

The approximate solutions for the lowest configuration, which were obtained in reference 2, were used as the initial functions for the solution of the self-consistent field equation without exchange. In both configurations, the solution was carried out to the degree of self-consistency 0.0015 [cf. Eq. (2.8) in reference 3]. The orthonormalized solutions are presented in Table I. The orthonormalization was obtained by means of Eqs. (2.2) and (2.3) of reference 4, and the values of the constants c_{ik} are also given in Table I.

2. NUMERICAL CALCULATION OF THE ENERGY

The non-diagonal matrix element of the energy, which combines the investigated configurations $1s^2 2s^2 2p^k 3s^{1-k}$ with a consideration of the configuration $1s^2 2p^{k+2} 3s^{1-k}$, can be put in the following form:

$$E_{12} = (-1)^{k+1} \frac{\sqrt{3-k}}{3} G_1(2s, 2p)_{12} N^2(1s, 1s)_{12} N^k \times (2p, 2p)_{12} N^{1-k}(3s, 3s)_{12}, k = 1, 0. \quad (1)$$

[1] A. P. Iutsis and V. I. Kavertskis, J. Exper. Theoret. Phys. USSR 21, 1139 (1951)

[2] F. W. Brown, J. H. Bartlett and C. G. Dunn, Phys. Rev. 44, 296 (1933)

[3] A. P. Iutsis and G. K. Tsiunaitis, J. Exper. Theoret. Phys. USSR 23, 512 (1952)

[4] G. K. Tsiunaitis and A. P. Iutsis, J. Exper. Theoret. Phys. USSR 25, 679 (1953)

TABLE I

Orthonormalized solutions of the equation of the self-consistent field without exchange for the two lowest configurations of the boron atom.

r	$P(1s\|r)$	$1s^2 2s^2 2p$		$1s^2 2s^2 3s$	
		$P'(2s\|r)$	$P'(2p\|r)$	$P(2s\|r)$	$P'(3s\|r)$
0.00	0.0000	0.0000	0.0000	0.0000	0.0000
0.01	0.1976	0.0339	0.0002_6	0.0371	0.0061
0.02	0.3761	0.0645	0.0010_2	0.0706	0.0117
0.03	0.5367	0.0921	0.0022_5	0.1006	0.0167
0.04	0.6810	0.1167	0.0039	0.1275	0.0211
0.06	0.9255	0.1579	0.0084	0.1728	0.0289
0.08	1.1187	0.1899	0.0142	0.2079	0.0350
0.10	1.2684	0.2139	0.0213	0.2340	0.0394
0.12	1.3815	0.2309	0.0294	0.2525	0 0424
0.14	1.4637	0.2417	0.0383	0.2643	0.0442
0.16	1.5197	0.2472	0.0479	0.2702	0.0451
0.18	1.5539	0.2481	0.0582	0.2711	0.0453
0.20	1.5700	0.2450	0.0691	0.2678	0.0447
0.22	1.5711	0.2385	0.0804	0.2607	0.0434
0.24	1.5599	0.2290	0.0922	0.2502	0.0416
0.26	1.5387	0.2169	0.1043	0.2368	0.0393
0.28	1.5093	0.2025	0.1166	0.2209	0.0367
0.30	1.4733	0.1861	0.1292	0.2028	0.0337
0.32	1.4323	0.1681	0.1419	0.1830	0.0304
0.34	1.3875	0.1486	0.1547	0.1617	0.0269
0.36	1.3398	0.1279	0.1675	0.1389	0.0231
0.38	1.2901	0.1062	0.1804	0.1150	0.0191
0.40	1.2391	0.0837	0.1934	0.0903	0.0149
0.42	1.1874	0.0606	0.2063	0.0648	0.0106
0.44	1.1355	0.0370	0.2191	0.0388	0.0062
0.46	1.0838	0.0129	0.2319	0.0123	0.0018
0.48	1.0326	—0.0115	0.2446	—0.0144	—0.0027
0.50	0.9824	—0.0361	0.2572	—0.0413	—0.0073
0.52	0.9333	—0.0607	0.2697	—0.0682	—0.0119
0.54	0.8855	—0.0853	0.2820	—0.0952	—0.0164
0.56	0.8390	—0.1098	0.2941	—0.1221	—0.0209
0.58	0.7941	—0.1341	0.3060	—0.1488	—0.0254
0.60	0.7510	—0.1582	0.3177	—0.1752	—0.0299
0.65	0.6499	—0.2172	0.3461	—0.2396	—0.0411
0.70	0.5598	—0.2737	0.3729	—0.3011	—0.0516
0.75	0.4800	—0.3273	0.3981	—0.2593	—0.0613
0.80	0.4099	—0.3775	0.4216	—0.4138	—0.0704
0.85	0.3488	—0.4241	0.4434	—0.4641	—0.0788
0.90	0.2959	—0.4670	0.4635	—0.5101	—0.0864
0.95	0.2505	—0.5061	0.4819	—0.5518	—0.0932
1.00	0.2115	—0.5414	0.4985	—0.5892	—0.0992
1.05	0.1781	—0.5730	0.5135	—0.6224	—0.1044
1.10	0.1497	—0.6011	0.5270	—0.6514	—0.1089
1.15	0.1256	—0.6255	0.5390	—0.6764	—0.1126
1.20	0.1053	—0.6466	0.5496	—0.6978	—0.1154
1.25	0.0882	—0.6646	0.5588	—0.7155	—0.1175
1.30	0.0737	—0.6796	0.5667	—0.7297	—0.1189
1.35	0.0615	—0.6918	0.5734	—0.7407	—0.1197
1.40	0.0514	—0.7014	0.5790	—0.7488	—0.1198
1.45	0.0429	—0.7086	0.5836	—0.7542	—0.1192
1.50	0.0358	—0.7135	0.5872	—0.7570	—0.1180
1.55	0.0299	—0.7164	0.5898	—0.7575	—0.1162
1.6	0.0250	—0.7173	0.5916	—0.7560	—0.1139
1.7	0.0174	—0.7142	0.5929	—0.7472	—0.1079
1.8	0.0121	—0.7054	0.5915	—0.7321	—0.1001
1.9	0.0084	—0.6920	0.5878	—0.7120	—0.0906
2.0	0.0058	—0.6749	0.5822	—0.6880	—0.0797
2.1	0.0040	—0.6549	0.5750	—0.6610	—0.0675

TABLE I (continued)

		$1s^22s^22p$		$1s^22s^23s$	
	$P(1s\|r)$	$P'(2s\|r)$	$P(2p\|r)$	$P'(2s\|r)$	$P'(3s\|r)$
2.2	0.0023	—0.6327	0.5664	—0.6320	—0.0543
2.3	0.0019	—0.6090	0.5566	—0.6017	—0.0402
2.4	0.0013	—0.5841	0.5459	—0.5705	—0.0253
2.5	0.0009	—0.5587	0.5344	—0.5390	—0.0099
2.6	0.0007	—0.5330	0.5223	—0.5076	0.0059
2.7	0.0005	—0.5073	0.5097	—0.4767	0.0222
2.8	0.0003	—0.4818	0.4967	—0.4465	0.0389
2.9	0.0002	—0.4566	0.4835	—0.4172	0.0558
3.0	0.0001	—0.4319	0.4701	—0.3889	0.0729
3.2		—0.3851	0.4430	—0.3360	0.1070
3.4		—0.3414	0.4159	—0.2882	0.1404
3.6		—0.3012	0.3891	—0.2456	0.1728
3.8		—0.2648	0.3630	—0.2082	0.2037
4.0		—0.2320	0.3377	—0.1758	0.2330
4.2		—0.2026	0.3134	—0.1478	0.2603
4.4		—0.1764	0.2902	—0.1237	0.2853
4.6		—0.1533	0.2682	—0.1032	0.3081
4.8		—0.1330	0.2473	—0.0859	0.3285
5.0		—0.1152	0.2277	—0.0713	0.3464
5.2		—0.0996	0.2092	—0.0591	0.3620
5.4		—0.0859	0.1919	—0.0488	0.3752
5.6		—0.0740	0.1758	—0.0402	0.3860
5.8		—0.0636	0.1609	—0.0331	0.3947
6.0		—0.0546	0.1470	—0.0273	0.4013
6.5		—0.0371	0.1167	—0.0169	0.4097
7.0		—0.0252	0.0919	—0.0104	0.4076
7.5		—0.0170	0.0720	—0.0064	0.3974
8.0		—0.0115	0.0561	—0.0039	0.3810
8.5		—0.0078	0.0435	—0.0024	0.3600
9.0		—0.0052	0.0336	—0.0015	0.3361
9.5		—0.0035	0.0259	—0.0010	0.3105
10.0		—0.0024	0.0198	—0.0006	0.2842
10.5		—0.0016	0.0151	—0.0004	0.2581
11		—0.0011	0.0115	—0.0002	0.2327
12		—0.0005	0.0067	—0.0001	0.1857
13		—0.0002	0.0039		0.1452
14		—0.0001	0.0023		0.1116
15		-0.0000_5	0.0013		0.0845
16			0.0008		0.0632
17			0.0005		0.0469
18			0.0003		0.0346
19			0.0001_5		0.0254
20			0.0000_8		0.0187
22			0.0000_3		0.0102
24					0.0055
26		$c_{12} = 0.0431$		$c_{12} = 0.0472$	0.0029
28				$c_{13} = 0.0151$	0.0015
30				$c_{23} = 0.119$	0.0008
32					0.0004
34					0.0002

Here the radial integral G_1 has the same definition as in Eq. (3.7) of reference 1, and $N(nl, nl)_{ij}$ coincides with C_{nlij} defined in Eq. (3.4) of reference 1. The diagonal matrix elements of the energy are expressed in the usual fashion by the radial integrals I, F and G, the definitions of which are also given in reference 1.

For the single electron wave functions of the configuration under examination, we use the corresponding functions of the configuration already investigated. Under such conditions,

$$N(nl, nl)_{ij} = 1. \qquad (2)$$

Furthermore, for the function $P(2p\,|\,r)$ of the configuration $1s^2 2p^2 3s$ we use the values of the corresponding function of the configuration $1s^2 2s^2 2p$. Such a procedure is based on the fact that the configuration under consideration is responsible only for a correction to the energy, which is small in comparison with the value of the total energy. Therefore, a variation in the correction of several percent involves a correspondingly smaller change in the value of the total energy of the desired configuration which was determined in the double configurational approximation.

The results of the numerical determination of the energy are given in Table II, where the experimental values of the energy, taken from references 5 and 6, are also listed.

3. DETERMINATION OF THE MASS EFFECT

The mass effect for the transition $1s^2 2s^2 3s - 1s^2 2s^2 2p$ of the boron atom in the single configuration approximation was calculated by Opechowski and de Vries[7] with the aid of the approximate functions of the self-consistent field

TABLE II

Values of the Lagrange multipliers, radial integrals and the energies for the configurations $1s^2 2s^2 2p$ and $1s^2 2s^2 3s$ of the boron atom (in atomic units).

	$1s^2 2s^2 2p$	$1s^2 2s^2 3s$		$1s^2 2s^2 2p$	$1s^2 2s^2 3s$
$\varepsilon_{1s,\ 1s}$	15.494	16.025	$G_0(1s,\ 2s)$	0.0299	0.0354
$\varepsilon_{2s,\ 2s}$	0.8897	1.3428	$G_0(1s,\ 3s)$		0.0010
$\varepsilon_{2p,\ 2p}$	0.4533		$G_0(2s,\ 3s)$		0.0039
$\varepsilon_{3s,\ 3s}$		0.2021	$G_1(1s,\ 2p)$	0.0327	
$I(1s)$	—12.437	—12.437	$G_1(2s,\ 2p)$	0.2459	
$I(2s)$	—2.5121	—2.6262	$G_1(2p,\ 3s)$*	0.0128	
$I(2p)$	—2.1098		E_{11}	—24.526	—24.336
$I(3s)$		—0.7088	E_{22}	—24.022	—23.758
$F_0(1s,\ 1s)$	2.8838	2.8838	E_{12}	0.116	— 0.142
$F_0(2s,\ 2s)$	0.4386	0.4749	ΔE	—0.025	— 0.033
$F_0(2p,\ 2p)$	0.3670		a_{12}	—0.22	0.23
$F_2(2p,\ 2p)$	0.1629		E_{theor}	—24.551	—24.369
$F_0(1s,\ 2s)$	0.6093	0.6532	E_{exp}	—24.655	—24.472
$F_0(1s,\ 3s)$		0.1532			
$F_0(2s,\ 3s)$		0.1485			
$F_0(1s,\ 2p)$	0.5382				
$F_0(2s,\ 2p)$	0.3992				
$F_0(2p,\ 3s)$*	0.1460				

Note: The asterisk indicates that the first function refers to the configuration $1s^2 2s^2 2p$ and the second to $1s^2 2s^2 3s$. E_{11} denotes the energy in the single configuration approximation, E_{theor} in the double configuration approximation $1s^2 2s^2 2p^k 3s^{1-k} - 1s^2 2p^{k+2} 3s^{1-k}$ ($k = 1, 0$).

[7] M. Opechowski and D. A. de Vries, Physica 6, 913 (1939)

[5] M. Morse L. A. Young and E. S. Haurwitz, Phys. Rev. 48, 948 (1935)

[6] R. F. Bacher and S. Goudsmit, *Atomic Energy States*, New York, 1932

without exchange. Here we shall determine this effect in the double configuration approximation with the help of the radial wave functions listed in Table I.

We find the following expression for the specific shift in the energy of the investigated configuration in the double configuration approximation $1s^2 2s^2 2p^k 3s^{1-k} - 1s^2 2p^{k+2} 3s^{1-k}$ by the method developed in reference 8:

$$\Delta_c E = \frac{1}{M}\frac{1}{1+a_{12}^2}[kK(1s, 2p)_{11} \quad (3)$$

$$+ kK(2s, 2p)_{11}$$

$$+ 2(-1)^{k+1}\sqrt{3-k} \times a_{12} K(2s, 2p)_{12} N^2$$

$$\times (1s, 1s)_{12} N^k (2p, 2p)_{12} N^{1-k} (3s, 3s)_{12}$$

$$+ (k+2) a_{12}^2 K(1s, 2p)_{22}$$

$$+ (1-k) a_{12}^2 K(2p, 3s)],$$

where all the symbols are taken from reference 8. The numerical results are given in Table III. Equation (3.1) of reference 8 was used for the calculation of the shift in the spectral line.

4. DETERMINATION OF THE VALUES OF TRANSITION THEORY

We obtain the following expression for the total dipole strength (cf. Bolotin and Iutsis[10]) in the double configuration approximation:

$$S(1s^2 2s^2 3s\,^2S, 1s^2 2s^2 2p\,^2P) \quad (4)$$

$$= \frac{2}{(1+a_{12}^2)(1+a_{12}'^2)}[N(r2p, 3s)_{11'}$$

$$\times N^2(1s, 1s)_{11'} N^2(2s, 2s)_{11'}$$

$$- \sqrt{2/3}\, a_{12} a_{12}' N(r2p, 3s)_{22'}$$

$$\times N^2(1s, 1s)_{22'} N^2(2p, 2p)_{22'}]$$

Here the integral $N(rnl, n'l')_{ij}$ has the definition of Eq. (2.5) in reference 10. The numbers 1 and 2 refer to the configurations $1s^2 2s^2 2p$ and $1s^2 2p^3$, and $1'$ and $2'$ refer to $1s^2 2s^2 3s$ and $1s^2 2p^2 3s$, respectively; a_{12} pertains to the first two configurations, a_{12}' to the latter two.

It is convenient to use the method given by

TABLE III

The results of the determination of the mass effect for the configurations $1s^2 2s^2 2p$ and $1s^2 2s^2 3s$ of the boron atom (ν in cm^{-1}, the remaining quantities in atomic units).

		$1s^2 2s^2 2p$	$1s^2 2s^2 3s$			$1s^2 2s^2 3s - 1s^2 2s^2 2p$	
						$M_2=11$	$M_2=12$
$K(1s, 2p)$		−0.2587		$\Delta_c\nu(M_2,10)$	*a*	−0.357	−0.655
$K(2s, 2p)$		−0.0675			*b*	−0.372	−0.683
$K(2s, 2p)^*$		−0.0783					
$K(2p, 3s)^*$		−0.0075					
$M\Delta_c E$	*a*	−0.326	0	$\Delta_H\nu(M_2,10)$	*a*	0.208	0.382
	b	−0.307	0.033		*b*	0.199	0.365
$M\Delta_H E$	*a*	24.526	24.336	$\Delta\nu(M_2,10)$	*a*	−0.149	−0.273
	b	24.551	24.369		*b*	−0.173	−0.317
					c	−0.17	

Note: The asterisk indicates that the first function refers to the configuration $1s^2 2s^2 2p$ and the second to $1s^2 2s^2 3s$, *a* refers to the single configuration approximation, *b* to the double configuration approximation, *c* to experimental data[9]

[8] A. P. Iutsis, A. S. Nakonechnyi and G. K. Tsiunaitis, J. Exper. Theoret. Phys. USSR **25**, 683 (1953)

[9] S. Mrozowski, Z. Phys. **112**, 223 (1939)

[10] A. B. Bolotin and A. P. Iutsis, J. Exper. Theoret. Phys. USSR **24**, 537 (1953)

Racah[11] for obtaining Eq. (4), since the signs in front of the values of the matrix elements of the electrical dipole moment (in first degree) must be considered in the case of the single configuration approximation. It must be noted that the sign in front of the first term in Eq. (4) in the square brackets depends, through a_{12} and a'_{12}, on the signs of the non-diagonal matrix elements of the energy in Eq. (1).

Terms with a single a_{12} and a'_{12} do not appear in Eq. (4). Therefore, in the given case, the double configuration approximation has an insignificant effect on the values of the transition theory.

In our approximation,

$$N(r\,2p,3\,s)_{11'} = N(r\,2p,3s)_{22'} \quad \text{and} \quad N(nl,nl)_{ii'} = 1. \tag{5}$$

TABLE IV

Transition probability for $1s^2 2s^2 3s\,^2S - 1s^2 2s^2 2p\,^2P$ for the boron atom (probability in units of 10^8/sec, other quantities in atomic units).

$N(r2p,3s) = 1.676$			
	$S(^2S,\ ^2P)$	$E(^2S) - E(^2P)$	$W(^2S,\ ^2P)$
a	5.62	0.190	4.11
b	5.52	0.182	3.54

Note: *a* gives the single configuration approximation, *b* the double configuration approximation.

[11] G. Racah, Phys. Rev. 62, 438 (1942); 63, 367 (1943)

We determine the integral $N(r2p,\ 3s)$ with the aid of the wave functions of Table I. The numerical results are given in Table IV. In this case the transition probability is determined by Eq. (4.3) of reference 10.

5. CONCLUSIONS

It can be seen from Table II that the correction to the energy in the double configuration approximation amounts to 0.025 atomic units for the configuration $1s^2 2s^2 2p$, and 0.033 atomic units for the configuration $1s^2 2s^2 3s$.

The data in Table III show that the mass effect for the transition $1s^2 2s^2 3s - 1s^2 2s^2 2p$, determined in the double configuration approximation, amounts to the entire observed isotopic shift of the given line.

As seen from Table IV, the double configuration approximation decreases the transition probability by approximately 14% in comparison with its value determined in the single figure approximation. This decrease arises principally because of the decrease in the value of the difference between the energies of the combined terms, which enters in third degree in the expression for the transition probability.

Translated by R. T. Beyer
80

Zone Theory of the Three-Dimensional Model of a Liquid

A. I. GUBANOV
Leningrad Physico-Technical Institute, Academy of Sciences, USSR
(Submitted to JETP editor March 16, 1954)
J. Exper. Theoret. Phys. USSR **28**, 401-408 (April, 1955)

The zone theory of a one-dimensional liquid model[1] proposed earlier by the author is extended to a three-dimensional model. By solving the Schrödinger equation in a deformed coordinate system, it is shown that during melting of a crystal, the electron energy spectrum retains its zone structure, in accordance with the experimental facts.

1. INTRODUCTION

AS is well known, the energy spectrum of electrons in solids possesses a zone structure. On this basis we are able correctly to explain the electrical conductivity of metals and semiconductors and a whole series of other phenomena. Theoretically, the occurrence of a zone structure is demonstrated for motion of the electron in a strictly periodic field, i.e., for the case of long range order. On the other hand, the electrical conductivity of metals and semi-conductors does not change during melting, despite the disappearance of long range order. This leads one to the idea that the zone structure of the energy spectrum is related, not to the long range, but rather to the short range order of location of atoms in a body.

In paper 1* we showed theoretically, for the simplest model of a one-dimensional chain of atoms, that for small disturbance of short range order and complete disappearance of long range order, the energy spectrum retains the zone character. In the present paper, the theory is extended to the more realistic case of a three-dimensional model. All the assumptions and the method of calculation are the same as for the one-dimensional model, so we shall repeat the discussion only very briefly, noting special features of the three-dimensional case.

Let us suppose that initially we have a crystal with a regular arrangement of atoms, so that the potential energy of an electron in the self-consistent field of the crystal is a periodic function $V(x_1, x_2, x_3)$ of Cartesian coordinates x_1, x_2, x_3 fixed in the crystal. This periodicity is meant in the sense that the potential is periodic along certain crystallographic directions, which either coincide with the axes x_1, x_2, x_3, or, in the case of crystals of lower symmetry, are described by linear equations in the x_1, x_2, x_3 coordinate system.

X-ray and electron diffraction studies show that liquids possess short range order. Upon melting it may turn out that the short range order is practically kept unchanged, or it may change abruptly if, as in the case of water, the number of nearest neighbors changes. We shall suppose that short range order always changes very little during melting. If the real crystal has essentially different short range order than the liquid, then we shall consider the melting of a certain hypothetical crystal with the same short range order as the liquid. In this connection, we suppose that each unit cell of the crystal suffers only a small deformation during melting, leading to slight changes in the lengths of the cell edges and the angles between them. The percentage deformation of the cell is of the order of a small quantity ϵ, and is a random variable. For simplicity, we shall assume that during melting there occurs no macroscopic deformation of the crystal, in particular, no change in its volume. In this case all deformations can have either sign with equal probability.

As shown in reference 1, the result of the superposition of small deformations of cells, according to the law of addition of random variables with varying sign, is the disappearance of long range order at distances of the order of $1/\epsilon^2$ from unit cells. In the three-dimensional case, this means not only that the probability of location of a particular atom is smeared over a region larger than the unit cell, but also that distant cells are turned relative to one another through arbitrarily large angles.

During melting, as a result of the deformation of the lattice, the potential field $V(x_1, x_2, x_3)$ undergoes two types of changes. First, all the maxima and minima of V are shifted in space parallel to

[1] A. I. Gubanov, J. Exper. Theoret. Phys. USSR 26, 139 (1954)

* The formulas of paper 1 will be cited as Roman I.

the displacement of the atoms. Secondly, because of the small disturbance of the short range order, the value of V changes by a small amount ΔV. As in the one-dimensional case, changes of the second type do not destroy the periodicity of the potential, but lead only to small corrections to the periodic field which can easily be taken into account by ordinary perturbation theory. We shall therefore not consider these changes at all, and shall suppose that the entire change of the potential field during melting is just the result of a shift in space of points with given potential parallel to the displacement of the atoms. This assumption is equivalent to the hypothesis of deformable ions which gives a good approximation for the calculation of the interaction of lattice waves and electrons in the theory of metals.

We introduce a distorted coordinate system ξ^1, ξ^2, ξ^3 in such a way that the coordinate curves in the liquid pass through points with the same values of the potential as do the corresponding coordinate lines x_1, x_2 x_3 in the crystal. By suitably selecting the variable scale for the coordinates ξ, we can arrange for the potential to be periodic in the coordinate system ξ, in the sense that the potential will be periodic along certain crystallographic lines (curves) which either coincide with the coordinate curves ξ or are described in this system of coordinates by linear equations. The coordinates ξ are slightly non-orthogonal.

Since corresponding elements of the coordinate lines x_α and ξ^α ($\alpha = 1, 2, 3$) can be turned through large angles relative to one another, we cannot in the three-dimensional case introduce ratios of dx_α and $d\xi^\alpha$ of the type of equation I - (5). However, for what follows it is not necessary to know completely the transformation from the coordinates x to the coordinates ξ; it is sufficient to give the metric tensor in the ξ coordinate system. Since, during melting, each element of the crystal undergoes a small random deformation, the diagonal and nondiagonal elements of the metric tensor must have the form:

$$g_{\alpha\alpha} = 1 + \varepsilon\gamma_{\alpha\alpha}; \quad (g_{\alpha\beta})_{\alpha\neq\beta} = \varepsilon\gamma_{\alpha\beta}; \qquad (1)$$

$$\alpha, \beta = 1, 2, 3.$$

Here the $\gamma_{\alpha\beta}$ are random functions of the coordinates, of order of magnitude unity. (Some of them may be of lower order, or be equal to zero.) Unlike the one-dimensional case, we cannot here normalize the $\gamma_{\alpha\beta}$ exactly, since their ratios depend on the liquid structure.

We note that the functions $\gamma_{\alpha\beta}$ are defined somewhat differently from the function γ for the one-dimensional case; on the basis of Eq. (1) we would write in place of Eq. I - (5):

$$d\xi / dx = 1 / \sqrt{1 + \varepsilon\gamma}. \qquad (2)$$

Consequently, if we make the transition from the formulas derived in the present paper to the one-dimensional case, we obtain results differing from the corresponding formulas of reference 1 by the numerical factor ½ for the first approximation, and $^1/_3$ for the second approximation.

2. WAVE EQUATION IN THE DISTORTED COORDINATE SYSTEM

The method of calculation consists in solving the Schrödinger equation for the electron in the distorted coordinate system ξ, in which the potential energy of the electron is a periodic function. As in the one-dimensional case, the problem is solved in the adiabatic approximation -- for preassigned instantaneous positions of the atoms. We use the time-independent Schrödinger equation

$$-(\hbar^2 / 2m)\nabla^2\psi + V\psi = E\psi, \qquad (3)$$

with the usual symbols.

The Laplace operator in curvilinear nonorthogonal coordinates has the form

$$\nabla^2\psi = \frac{1}{\sqrt{g}} \sum_{\alpha,\beta} \frac{\partial}{\partial\xi^\alpha}\left(g^{\alpha\beta}\sqrt{g}\,\frac{\partial\psi}{\partial\xi^\beta}\right), \qquad (4)$$

where g is the determinant formed from the covariant components of the metric tensor, whose contravariant components are

$$g^{\alpha\beta} = G_{\beta\alpha} / g; \qquad (5)$$

$G_{\beta\alpha}$ is the algebraic complement of the element $g_{\beta\alpha}$ in the determinant, i.e., the corresponding minor multiplied by $(-1)^{\alpha+\beta}$.

Substitution of Eq. (5) in Eq. (4) and of Eq. (4) in Eq. (3), and expansion in powers of ϵ brings the Schrödinger equation to the form

$$\hat{H}\psi = E\psi; \quad \hat{H} = \hat{H}_0 + \varepsilon\hat{W} + \varepsilon^2\hat{w} + \ldots; \qquad (6)$$

$$\hat{H}_0 = -\frac{\hbar^2}{2m}\sum_{\alpha=1}^{3}\frac{\partial^2\psi}{\partial\xi^{\alpha^2}} + V(\xi^1, \xi^2, \xi^3); \qquad (7)$$

$$\hat{W} = \frac{\hbar^2}{2m}\sum_{\alpha=1}^{3}\left[\gamma_{\alpha\alpha}\frac{\partial^2}{\partial\xi^{\alpha^2}} - \frac{1}{2}\frac{\partial}{\partial\xi^\alpha}(\gamma_{\beta\beta} + \gamma_{\gamma\gamma}\right. \qquad (8)$$

$$-\gamma_{\alpha\alpha})\frac{\partial}{\partial\xi^{\alpha}}-(-1)^{\beta+\gamma}\left(\gamma_{\beta\gamma}\frac{\partial^2}{\partial\xi^{\beta}\partial\xi^{\gamma}}+\frac{\partial\gamma_{\beta\gamma}}{\partial\xi^{\beta}}\frac{\partial}{\partial\xi^{\gamma}}+\frac{\partial\gamma_{\beta\gamma}}{\partial\xi^{\gamma}}\frac{\partial}{\partial\xi^{\beta}}\right)\Big].$$

Here α, β, γ are a cyclic permutation of the indices 1, 2, 3. The operator $\hat{W}$ contains only terms variable in sign, of first order in the random functions $\gamma_{\alpha\beta}$.

The operator $\hat{w}$ can be separated into two parts

$$\hat{w}=\hat{w}'+\hat{w}''. \tag{9}$$

$\hat{w}'$ consists of terms of fixed sign, quadratic in the functions $\gamma_{\alpha\beta}$ and is equal to

$$\hat{w}'=-\frac{\hbar^2}{2m}\sum_{\alpha=1}^{3}(\gamma_{\alpha\alpha}^2+\gamma_{\alpha\beta}^2+\gamma_{\alpha\gamma}^2)\frac{\partial^2}{\partial\xi^{\alpha 2}}; \tag{10}$$

$\hat{w}''$ contains only terms variable in sign. The expression for it is rather complicated and has no practical value since $\hat{w}''$ is of the same order of magnitude as $\hat{W}$, is also variable in sign, and is multiplied by ϵ^2 rather than by ϵ.

The operators $\epsilon\hat{W}$ and $\epsilon^2\hat{w}$ or $\epsilon^2\hat{w}'$ are considered as perturbations. As in the one-dimensional case, they are not self-adjoint.

Since $V(\xi^1, \xi^2, \xi^3)$ is a periodic function, the solution of the unperturbed equation $\hat{H}_0\psi=E\psi$ is the familiar solution of the problem of an electron in a periodic field. Let the fundamental volume contain G^3 unit cells as is usually done in the theory of metals. In order to have a significant disturbance of the long-range order, we must impose the condition

$$G\gg 1/\varepsilon^2 \tag{11}$$

The energy spectrum of the unperturbed problem consists of a series of separated zones, in each of which the electron wave vector $\mathbf{k}$ can take on G^3 values. To each value there corresponds a Bloch wave function:

$$\psi^0_{n\mathbf{k}}=u_{n\mathbf{k}}\exp\left(i\sum_{\alpha=1}^{3}k_{\alpha}\xi^{\alpha}\right). \tag{12}$$

Here n gives the zone number, the k_α are coefficients giving the state within a zone, $u_{n\mathbf{k}}$ is a modulating function which has the period of the lattice.

We look for a solution of the perturbed problem in the form of a linear combination of Eq. (12)

$$\psi(\xi^1,\xi^2,\xi^3)=\sum_{n,\mathbf{k}}c_{n\mathbf{k}}\psi^0_{n\mathbf{k}}, \tag{13}$$

where the coefficients in the expansion are determined from the system of equations:

$$(E^0_{n\mathbf{k}}+\varepsilon W_{n\mathbf{k}n\mathbf{k}}+\varepsilon^2 w'_{n\mathbf{k}n\mathbf{k}}-E)c_{n\mathbf{k}}+\sum_{n',\mathbf{k}'\neq n,\mathbf{k}}(\varepsilon W_{n\mathbf{k}n'\mathbf{k}'}+\varepsilon^2 w'_{n\mathbf{k}n'\mathbf{k}'})c_{n'\mathbf{k}'}=0. \tag{14}$$

Summation over $\mathbf{k}$ means summation over all G^3 values of the three coefficients k_1, k_2, k_3.

The matrix elements $W_{n\mathbf{k}n'\mathbf{k}'}$ and $w_{n\mathbf{k}n'\mathbf{k}'}$ are calculated with weight functions equal to the factor of orthogonality of the zeroth order functions, i.e., to unity. The functions $\psi^0_{n\mathbf{k}}$ are normalized to unity, i.e.,

$$\int|\psi^0_{n\mathbf{k}}|^2\,d\xi^1\,d\xi^2\,d\xi^3=1, \tag{15}$$

where the integration extends over the whole fundamental domain, i.e., over G^3 elementary cells.

3. EVALUATION OF THE MATRIX ELEMENTS OF THE PERTURBATION

According to Eqs. (8) and (12), the matrix element of the operator $\hat{W}$ has the form

$$W_{n\mathbf{k}n'\mathbf{k}'}=\frac{\hbar^2}{2m}\int u^*_{n\mathbf{k}}B_{n'\mathbf{k}'}\times\exp\left[i\sum_{\alpha=1}^{3}(k'_\alpha-k_\alpha)\xi^{\alpha}\right]d\xi^1\,d\xi^2\,d\xi^3. \tag{16}$$

Explicit expressions for the functions $B_{n\mathbf{k}'}$ are rather complicated, but for determining the order of magnitude of the quantity $W_{n\mathbf{k}n\mathbf{k}'}$ it is sufficient to note that $B_{n\mathbf{k}'}$ consists of terms of the type

$$\gamma_{\alpha\beta}u_{n'\mathbf{k}'}k'_\alpha k'_\beta,\quad \gamma_{\alpha\beta}\frac{\partial u_{n'\mathbf{k}'}}{\partial\xi^{\alpha}}k'_\beta,\quad \gamma_{\alpha\beta}\frac{\partial^2 u_{n'\mathbf{k}'}}{\partial\xi^{\alpha}\partial\xi^{\beta}},$$

$$\frac{\partial\gamma_{\alpha\beta}}{\partial\xi^{\alpha}}\frac{\partial u_{n'\mathbf{k}'}}{\partial\xi^{\beta}}\quad\text{and}\quad\frac{\partial\gamma_{\alpha\beta}}{\partial\xi^{\alpha}}u_{n'\mathbf{k}'}k'_\beta.$$

The functions $u_{n\mathbf{k}'}$ have the periodicity of the lattice, while the functions $\gamma_{\alpha\beta}$ which are of order of magnitude unity, change substantially from cell to cell. Therefore, differentiating $u_{n\mathbf{k}'}$ and $\gamma_{\alpha\beta}$ with respect to ξ^{α} gives a factor of order $1/a$, where a is the lattice constant. The mean value of k'_α is also of order $1/a$. From the normalization condition of Eq. (15) we have $u_{n'\mathbf{k}'}\approx 1/G^{3/2}a^{3/2}$. Consequently, each of the terms which make up $B_{n'\mathbf{k}'}$ is of order of magnitude $(1/a^2)\,u_{n\mathbf{k}}\approx 1/G^{3/2}a^{7/2}$. The functions $B_{n'\mathbf{k}'}$, which consist of a finite number

of terms, are of this same order of magnitude.

To evaluate the integral in Eq. (16), we separate it into a sum of integrals over the G^3 elementary cells. Within the confines of a single unit cell, the functions $\gamma_{\alpha\beta}$ and their derivatives have more or less definite values. Therefore, if $u_{n\mathbf{k}}$ and $u_{n'\mathbf{k}'}$ are close to one another, and the factor $\exp\left[i\sum_{\alpha=1}^{3}(k'_\alpha - k_\alpha)\xi^\alpha\right]$ is close to unity, integration over the unit cell reduces to multiplication by a factor of order a^3, so that the integral I_l over the l'th unit cell is of order

$$|I_l| \approx \frac{1}{G^3 a^5} a^3 = \frac{1}{G^3 a^2}. \tag{17}$$

Actually, because of the factor

$$\exp\left[i\sum_{\alpha=1}^{3}(k'_\alpha - k_\alpha)\xi^\alpha\right]$$

and the non-equality of the functions $u_{n\mathbf{k}}$ and $u_{n'\mathbf{k}'}$, the quantity I_l will be somewhat smaller -- the smaller, the larger the difference $k_\alpha - k'_\alpha$. All the I_l are random quantities of variable sign. As discussed in detail in reference 1, on the basis of Liapounoff's theorem, the sum of random quantities of varying sign conforms to a Gaussian distribution, with average value zero and root mean square proportional to the square root of the number of terms. Therefore, carrying out the summation over the G^3 unit cells, we find that the root mean square of the matrix element $W_{n\mathbf{k}n'\mathbf{k}'}$ is of order

$$\sqrt{\overline{W^2_{n\mathbf{k}n'\mathbf{k}'}}} = \sqrt{G^3}\,\frac{\hbar^2}{2m}\frac{1}{G^3 a^2} = \frac{\hbar^2}{2mG^{3/2}a^2} \tag{18}$$

and decreases with increasing difference $k_\alpha - k'_\alpha$.

In precisely the same way one can evaluate the matrix elements of the operator $\hat{w}'$. Equation (17) is still valid for the order of magnitude of the integral over a unit cell. The integral over a unit cell, which enters into a non-diagonal matrix element $W'_{n\mathbf{k}\,n'\mathbf{k}'}$ is variable in sign because of the presence of the factor $\exp\left[i\sum_{\alpha=1}^{3}(k'_\alpha - k_\alpha)\xi^\alpha\right]$, which means that its mean square value is also given, in order of magnitude, by Eq. (18).

On the other hand, the integrals which enter into the diagonal matrix element $w'_{n\mathbf{k}\,n\mathbf{k}}$ are fixed in sign. Taking the quantities $\gamma^2_{\alpha\beta}$ out from under the integral sign for a given unit cell, and considering that

$$\int |u_{n\mathbf{k}}|^2\, d\xi^1\, d\xi^2\, d\xi^3 = \frac{1}{G^3}, \tag{19}$$

$$\int u^*_{n\mathbf{k}}\frac{\partial u_{n\mathbf{k}}}{\partial\xi^\alpha}\, d\xi^1\, d\xi^2\, d\xi^3 \approx 0,$$

$$\int u^*_{n\mathbf{k}}\frac{\partial^2 u_{n\mathbf{k}}}{\partial\xi^{\alpha^2}}\, d\xi^1\, d\xi^2\, d\xi^3 \approx -\frac{1}{G^3 a^2},$$

where the integrals go over a unit cell (cf the similar evaluations in reference 1), we obtain

$$w'_{n\mathbf{k}n\mathbf{k}} \tag{20}$$

$$\approx \frac{\hbar^2}{2m}\frac{1}{G^3}\sum_{\alpha=1}^{3}\sum_{l=1}^{G^3}(\gamma^2_{\alpha\alpha}+\gamma^2_{\alpha\beta}+\gamma^2_{\alpha\gamma})_l\left(\frac{1}{a^2}+k^2_\alpha\right),$$

where the values of the functions $\gamma_{\alpha\beta}$ are taken for the l'th cell. Carrying out the summation over l we have

$$w'_{n\mathbf{k}n\mathbf{k}} \approx \frac{\hbar^2}{2m}\sum_{\alpha=1}^{3}(\overline{\gamma^2_{\alpha\alpha}}+\overline{\gamma^2_{\alpha\beta}}+\overline{\gamma^2_{\alpha\gamma}})\left(\frac{1}{a^2}+k^2_\alpha\right). \tag{21}$$

The dash denotes and average over all cells. In the case of a cubic lattice, clearly $\overline{\gamma^2_{11}} = \overline{\gamma^2_{22}} = \overline{\gamma^2_{33}}$; $\overline{\gamma^2_{12}} = \overline{\gamma^2_{13}} = \overline{\gamma^2_{23}}$, consequently

$$w'_{n\mathbf{k}n\mathbf{k}} \approx \frac{\hbar^2}{2m}(\overline{\gamma^2_{\alpha\alpha}}+2\overline{\gamma^2_{\alpha\beta}})\left(\frac{3}{a^2}+k^2\right). \tag{22}$$

Finally, if we set $\overline{\gamma^2_{\alpha\alpha}} = \overline{\gamma^2_{\alpha\beta}} = 1$,

$$w'_{n\mathbf{k}n\mathbf{k}} \approx \frac{3\hbar^2}{2m}\left(\frac{3}{a^2}+k^2\right). \tag{23}$$

Comparing Eqs. (18) and (21) - (23), and noting the inequality (11), we see that in Eq. (14) we can neglect the diagonal element $\epsilon W_{n\mathbf{k}n\mathbf{k}}$ compared to $\epsilon^2 w'_{n\mathbf{k}\,n\mathbf{k}}$; on the other hand, the non-diagonal element $\epsilon^2 w'_{n\mathbf{k}n'\mathbf{k}'}$ is negligible compared to $\epsilon W_{n\mathbf{k}n'\mathbf{k}'}$.

4. SOLUTION BY THE METHOD OF RELATIVE DEGENERACY

If the unperturbed energy of the electron in a given zone, measured from the lower edge of the zone, is proportional to Σk^2_α (isotropic approximation), it is easy to show that the minimum distance between neighboring levels in the zone is

$$\Delta E_{\min} = 2\pi^2\hbar^2/a^2G^2. \tag{24}$$

In fact, if we fix k_1 and k_2, and give k_3 neighboring values -- zero and $\pm 2\pi/aG$, we get two energy values differing by the amount given in Eq. (24). The levels are highly degenerate, since their number does not exceed G^2 in order of magnitude, while the total number of electron states in the

zone is G^3. If we take account of the anisotropy, this degeneracy is partially removed, so that we get even closer spacing of energy levels.

Comparing Eqs. (18) and (24), and noting Eq. (11), we see that the non-diagonal matrix elements of the perturbation are larger than the distance between neighboring levels in zeroth approximation, so that we cannot use ordinary perturbation theory, but must, as in the one-dimensional case, carry out the calculation by the method of relative degeneracy. The system of equations for the zeroth approximation, completely analogous to I - (23) will have the form

$$(E'_{\mathbf{k}} - E)\, c_{\mathbf{k}} + \varepsilon \sum_{\mathbf{k}' \neq \mathbf{k}} W_{\mathbf{k}\mathbf{k}'} c_{\mathbf{k}'} = 0, \tag{25}$$

where we have dropped the index n and introduced the notation

$$E'_{\mathbf{k}} = E^0_{\mathbf{k}} + \varepsilon^2 w'_{\mathbf{k}\mathbf{k}}. \tag{26}$$

Setting the determinant of the system (25) equal to zero, and expanding according to the Laplace formula, we obtain an equation differing from I-(26) only in that the summation is taken over a vector index running through G^3 values:

$$1 - \varepsilon^2 \sum_{\mathbf{k}} \sum_{\mathbf{k}'} \frac{W_{\mathbf{k}\mathbf{k}'} W_{\mathbf{k}'\mathbf{k}}}{(E'_{\mathbf{k}} - E)(E'_{\mathbf{k}'} - E)} \tag{27}$$

$$+ \varepsilon^3 \sum_{\mathbf{k}} \sum_{\mathbf{k}'} \sum_{\mathbf{k}''} \frac{W_{\mathbf{k}\mathbf{k}'} W_{\mathbf{k}'\mathbf{k}''} W_{\mathbf{k}''\mathbf{k}}}{(E'_{\mathbf{k}} - E)(E'_{\mathbf{k}'} - E)(E'_{\mathbf{k}''} - E)} - \ldots$$

$$\ldots + (-1)^{r+1} \varepsilon^r \sum_{\mathbf{k}} \sum_{\mathbf{k}'} \ldots \sum_{\mathbf{k}^{(r)}} \frac{\prod_{j=1}^{r} W^j_{\mathbf{k}\mathbf{k}}}{\prod_{j=1}^{r} (E'_{\mathbf{k}^j} - E)} + \ldots = 0$$

So long as $r \ll G^3$, the number of terms in the sum appearing as a factor after ϵ^r is of order G^{3r}.

As in the one-dimensional case, we can show that $\overline{W_{\mathbf{k}\mathbf{k}'} W_{\mathbf{k}'\mathbf{k}}} > 0$. To do this, we separate the operator $\hat{W}$ into a Hermitian part $\hat{W}'$ and a skew-Hermitian part $\hat{W}''$

$$\hat{W}' = \frac{\hbar^2}{2m} \sum_{\alpha=1}^{3} \left[\gamma_{\alpha\alpha} \frac{\partial^2}{\partial \xi^{\alpha 2}} + \frac{\partial \gamma_{\alpha\alpha}}{\partial \xi^\alpha} \frac{\partial}{\partial \xi^\alpha} \right. \tag{28}$$

$$+ \frac{1}{4} \frac{\partial^2 (\gamma_{\alpha\alpha} + \gamma_{\beta\beta} + \gamma_{\gamma\gamma})}{\partial \xi^{\alpha 2}}$$

$$\left. - (-1)^{\beta+\gamma} \left(\gamma_{\beta\gamma} \frac{\partial^2}{\partial \xi^\beta \partial \xi^\gamma} - \frac{1}{2} \frac{\partial^2 \gamma_{\beta\gamma}}{\partial \xi^\beta \partial \xi^\gamma} \right) \right];$$

$$\hat{W}'' = \frac{\hbar^2}{2m} \sum_{\alpha=1}^{3} \left[-\frac{1}{2} \frac{\partial (\gamma_{\alpha\alpha} + \gamma_{\beta\beta} + \gamma_{\gamma\gamma})}{\partial \xi^\alpha} \frac{\partial}{\partial \xi^\alpha} \right. \tag{29}$$

$$- \frac{1}{4} \frac{\partial^2 (\gamma_{\alpha\alpha} + \gamma_{\beta\beta} + \gamma_{\gamma\gamma})}{\partial \xi^{\alpha 2}}$$

$$\left. - (-1)^{\beta+\gamma} \frac{1}{2} \left(\frac{\partial^2 \gamma_{\beta\gamma}}{\partial \xi^\beta \partial \xi^\gamma} + \frac{\partial \gamma_{\beta\gamma}}{\partial \xi^\beta} \frac{\partial}{\partial \xi^\gamma} + \frac{\partial \gamma_{\beta\gamma}}{\partial \xi^\gamma} \frac{\partial}{\partial \xi^\beta} \right) \right].$$

In summing random quantities, their squares accumulate. Therefore, since the terms in Eq. (29) are similar to those in Eq. (28), and some of them have the coefficient ½, we can conclude that

$$\overline{|W'_{\mathbf{k}\mathbf{k}'}|^2} > \overline{|W''_{\mathbf{k}\mathbf{k}'}|^2}, \tag{30}$$

which means that

$$\overline{W_{\mathbf{k}\mathbf{k}'} W_{\mathbf{k}'\mathbf{k}}} = \overline{|W'_{\mathbf{k}\mathbf{k}'}|^2} - \overline{|W''_{\mathbf{k}\mathbf{k}'}|^2} > 0. \tag{31}$$

Consequently we can repeat here the whole argument used in reference 1. If the energy E lies outside the band of values $E'_{\mathbf{k}}$, then, according to Eq. (18), each term in the sum for ϵ^r in Eq. (27) is of order $G^{-3r/2}$. For odd powers of ϵ, all these sums are variable in sign, and the root mean square value of the sum including the factor ϵ^r is of order $\epsilon^r (r>2)$; which means that these sums can be neglected. On the other hand, the sums for even values of ϵ have a number of terms of order G^{3r} and are fixed in sign; so these sums form a series of the type $1 - \epsilon^2 G^3 - \epsilon^4 G^6 - \ldots$ This means that Eq. (27) cannot be satisfied for a value of E lying outside the zone $E'_{\mathbf{k}}$.

Thus during melting of the crystal, the zone structure of the energy levels is retained, except that each level is shifted by an amount $\epsilon^2 w'_{n\mathbf{k}n\mathbf{k}}$.

The wave functions in zeroth approximation are linear combinations of all G^3 Bloch functions belonging to the given zone. However, it was shown in reference 1, on the basis of Eq. (25), that in each solution only a fraction ϵ^2 of all the functions have coefficients significantly different from zero. This estimate remains valid here. Consequently each wave function in zeroth approximation represents a packet of approximately $\epsilon^2 G^3$ Bloch functions, all corresponding to energy values $E'_{\mathbf{k}}$ close to E, but with various values of the coefficients k_α. However, as we pointed out earlier, the perturbation matrix element $W_{\mathbf{k}\mathbf{k}'}$ decreases with increase in the difference $k_\alpha - k'_\alpha$; thus in each wave packet, functions grouped around particular values of k_1, k_2, k_3 will predominate. Because of this the electrons in the liquid are not described by standing waves, but rather by wave packets moving

in definite directions, i.e., the medium is a conductor.

The uncertainty in the momentum component in the direction of the resultant motion of the packet is of order

$$\Delta p = (\hbar / a)\,\varepsilon^2, \tag{32}$$

if we note that the packet is built up from $\epsilon^2 G$ neighboring values of this momentum component; from the uncertainty relations it then follows that the packet is localized within a region of dimension

$$\Delta\xi = a / \varepsilon^2, \tag{33}$$

i.e., precisely the same interval within which the long range order shows a noticeable breakdown.

We could carry the calculation to the next approximation and take account of the interaction between zones, but nothing new would be gotten compared to the one-dimensional theory [formulas I - (32) - (34)].

In conclusion I take the opportunity to express my sincere thanks to A. I. Ansel'm and I. M. Shmushkevich for discussion of the work.

Translated by M. Hamermesh
74

Magnetostatics with Ferromagnetics

V. I. SKOBELKIN AND R. N. SOLOMKO
Moscow State University

(Submitted to JETP editor December 8, 1954)
J. Exper. Theoret. Phys. USSR 28, 385-393 (April, 1955)

The formulation and the foundation of a variational principle of magnetostatics with ferromagnetics in a field of currents is given. A direct method of analysis of magnetic fields in a general case of non-linear dependence on the magnetic permeability of a magnetic field is worked out.

THE present article is devoted to the general solution of the problem of magnetostatics with ferromagnetics.

Let us assume a closed magnetostatic system in space, containing n finite ferromagnetic domains $V_1, V_2, \ldots V_n$, limited by the surfaces $S_1, S_2, \ldots, S_n$, and having m finite domains of currents $\omega_1, \omega_2, \ldots \omega_m$, limited by the surfaces $\sigma_1, \sigma_2, \ldots \sigma_m$; in the domains ω_i, the magnetic permeabilities $\mu(H, x, y, z)$ are uniquely determined and the induction field $\mathbf{B}$ is given by the relation $\mathbf{B} = \mu\mathbf{H}$; also given in the domains ω_i is the current density distribution $\mathbf{j}_i$ (x, y, z) satisfying the condition $\operatorname{div} \mathbf{j}_i = 0$; outside the ferromagnetics $\mu = 1$ (using the absolute system of units).

To a system so defined correspond the following physical conditions: 1) The ferromagnetics are isotropic; 2) μ is determined by the magnetization curves; 3) The ferromagnetics may have inhomogeneously distributed magnetic properties.

The problem is to determine the induction field $\mathbf{B}$ of the system.

The Maxwell equations satisfying such a magnetostatic system have the form:

$$\operatorname{curl} \mathbf{H} = \frac{4\pi}{c}\mathbf{j}; \quad \operatorname{div} \mathbf{B} = 0; \quad \mathbf{B} = \mu\mathbf{H},$$

where the parameters μ and j on the surfaces of discontinuity s have to satisfy the boundary conditions*

$$[H_\tau]_s = 0; \quad [B_n]_s = 0,$$

where H_τ is the tangential component of the field $\mathbf{H}$, and B_n is the normal component of the field $\mathbf{B}$.

The integration of Maxwell's equations when the boundary conditions are given, represent insurmountable difficulties[1,2] because of non-linearity of the relationship between $\mathbf{B}$ and $\mathbf{H}$. Up to now, excluding the case of toroid and ellipsoid forms, the analysis of magnetostatic problems has been confined to idealized ferromagnetics[3], for which $\mu = \text{const}$ or $\mu = \infty$.

1. VARIATIONAL PRINCIPLE**

To solve the given problem it is expedient not to start from Maxwell's equations but to put as a base a variational principle, which can be stated as follows. Among all possible solenoidal induction fields for a real closed magnetostatic system the sum E of its magnetic energy W and the potential function U of the currents has a minimum.

The mathematical expression of this principle leads to the equation

$$\delta E = \delta(W + U) = 0, \tag{1}$$

under the condition

$$\operatorname{div} \mathbf{B} = 0. \tag{2}$$

Here

$$W = \int w\,dV = \int \Big(\frac{1}{4\pi} \int_{H=B=0}^{B} \mathbf{H}\cdot d\mathbf{B} \Big) dV, \tag{3}$$

where w is the magnetic energy density, dV - the volume element (the volume integration is performed over the whole field of the system);

$$U = -\frac{1}{c}\sum_{i=1}^{m} \int_0^{I_i} \Phi\, dI = -\frac{1}{c}\sum_{i=1}^{m} \int_{s_i} \Phi j_i ds, \tag{4}$$

where I_i is the total current ♀ in the domain ω_i, ds element of the surface normal to j, Φ is the flux of

[1] I. E. Tamm, *Foundations of the Theory of Electricity*, Moscow, 1949; pp. 327, 227

[2] S. V. Vonsovskii and Ia. S. Shur, *Ferromagnetism*, Moscow, 1948; p. 27

[3] G. A. Grinberg, *Selected Problems of the Mathematical Theory of Electrical and Magnetic Phenomena*, Akad. Nauk SSSR, 1948

* The symbol $[A]_s = 0$ represents the difference of the value of the parameter A on both sides of the discontinuity surfaces.

** The variational principle and its formulation giving the possibility of analysis of magnetic fields by the direct methods of variational calculus, were discribed by one of the authors (Skobelkin).

♀ If the current domain ω_i is of the form of a solenoid, then I_i means ampere-turns, and s is the cross-section of the solenoid.

$\mathbf{B}$ through the surface, limiting the current density j. The physical meaning of the function U is given[1] by the fact that the work done by the forces due to magnetic field for a virtual change of this field is equal to a decrease of the function U. From Eqs. (1) and (2) in particular, we obtain Maxwell's equation:

$$\text{curl } \mathbf{H} = \frac{4\pi}{c}\mathbf{j}. \tag{5}$$

The application of direct methods to obtain a solution of Eq. (1) under the condition (2), is most effective in conjunction with systems which have a plain-parallel or an axial symmetry. Therefore in the following we are going to investigate only such systems.

1. System with an Axial Symmetry

Let us take the x axis as symmetry axis of a magnetostatic system using cylindrical coordinates r,θ,x.

Let $\Phi(r,x)$ be the flux of B through a circle of radius $r = \sqrt{x^2 + y^2}$ in the plane $x = \text{const}$. Let

$$B_x = \frac{1}{2\pi r}\frac{\partial \Phi}{\partial r}; \quad B_r = -\frac{1}{2\pi r}\frac{\partial \Phi}{\partial x}; \tag{6}$$

$\mathbf{B}$, calculated from Eq. (6), satisfies Eq. (2) identically.

For a system with axial symmetry

$$E = \int\left(w - \frac{1}{2\pi c}\frac{j\Phi}{r}\right)2\pi r\, dr\, dx. \tag{7}$$

The integrand in Eq. (7),

$$L = 2\pi r\left(w - \frac{1}{2\pi c}\frac{j\Phi}{r}\right), \tag{8}$$

is the Lagrangian of the magnetostatic system with axial symmetry. Using the identity

$$HdB = dB^2 / 2\mu \tag{9}$$

and expressing μ through B^2 (e.g., using the magnetization curve), $\mu = B/H = \mu(B^2)$, we can write Eq. (8) as

$$L = 2\pi r\left(\frac{1}{4\pi}\int_0^{B^2}\frac{dB^2}{2\mu(B^2)} - \frac{1}{2\pi c}\frac{j\Phi}{r}\right) \tag{10}$$

$$= L\left(j, r, \Phi, \frac{\partial\Phi}{\partial x}, \frac{\partial\Phi}{\partial r}\right),$$

where, as follows from Eq. (6),

$$B^2 = \frac{1}{4\pi^2 r^2}\left[\left(\frac{\partial\Phi}{\partial x}\right)^2 + \left(\frac{\partial\Phi}{\partial r}\right)^2\right]. \tag{11}$$

The condition for a minimum gives the Euler's equations for each domain where the flux function Φ is twice differentiable:

$$\frac{\partial L}{\partial \Phi} - \frac{\partial}{\partial x}\left[\frac{\partial L}{\partial(\partial\Phi/\partial x)}\right] - \frac{\partial}{\partial r}\left[\frac{\partial L}{\partial(\partial\Phi/\partial r)}\right] \tag{12}$$

$$= -\frac{1}{c}j + \frac{1}{4\pi}\frac{\partial H_r}{\partial x} - \frac{1}{4\pi}\frac{\partial H_x}{\partial r} = 0.$$

From (12) we then obtain (5).

2. Plane Parallel Symmetry

In this case,

$$B_x = \frac{\partial\Phi}{\partial y}; \quad B_y = -\frac{\partial\Phi}{\partial x}; \tag{13}$$

$$B^2 = \left(\frac{\partial\Phi}{\partial x}\right)^2 + \left(\frac{\partial\Phi}{\partial r}\right)^2,$$

$$L = \frac{1}{4\pi}\int_0^{B^2}\frac{dB^2}{2\mu(B^2)} - \frac{1}{c}j\Phi = L\left(j, \Phi, \frac{\partial\Phi}{\partial x}, \frac{\partial\Phi}{\partial y}\right).$$

Euler's equation, corresponding to the minimum value of E, then has the form:

$$\frac{\partial L}{\partial\Phi} - \frac{\partial}{\partial x}\left[\frac{\partial L}{\partial(\partial\Phi/\partial x)}\right] - \frac{\partial}{\partial y}\left[\frac{\partial L}{\partial(\partial\Phi/\partial y)}\right]$$

$$= -\frac{1}{c}j + \frac{1}{4\pi}\frac{\partial H_y}{\partial x} - \frac{1}{4\pi}\frac{\partial H_x}{\partial y} = 0,$$

from which Eq. (5) follows.

For the Lagrangeian of type (10) and (13), a strong minimum of corresponding functionals exists and the uniqueness theorem can be applied which makes it possible to postulate a minimizing sequence $\Phi_1, \Phi_2 \ldots \Phi_n \ldots$ which, by Ritz's method, gives as limit Φ, when the complete set of functions of the given magnetostatic system is obtained.

One essential advantage of this direct method of solution of magnetostatic problems on the basis of a variational principle is the non-existence of complicated explicit non-linear boundary conditions:

$$\left[\frac{1}{\mu}B_\tau\right]_{S_i} = 0; \; [B_n]_{S_i} = 0, \tag{14}$$

which have to be taken into account when solving the same problem using Maxwell's equation. The equation div $\mathbf{B} = 0$ leads to the unique linear condition for the function Φ on the discontinuity surfaces S_i:

$$[\Phi]_{S_i} = 0. \tag{15}$$

The conditions $[B_n]_{S_i}$ indeed are consequences of Eq. (15). Considering the problem of determination of $\mathbf{B}$ from the variational principle (1) under the condition (2) as a discontinuity problem of second order variational calculus[4] and determining

[4] R. Courant and D. Hilbert, *Methods of Mathematical Physics*.

by known methods the conditions on the discontinuity surfaces, we obtain that, for the real field, the conditions $\left[\frac{1}{\mu} B_\tau\right] = 0$ on discontinuity surfaces are identically satisfied.

2. CONSTRUCTION OF THE COMPLETE SET OF FUNCTIONS

We divide the magnetostatic system into such regions δ, where μ and j do not possess discontinuities, in particular, the overlapping of V and ω represent such a region δ. We further assume that on some surface Γ, enclosing the magnetostatic system, the magnetic flux $\Phi = 0$. This boundary condition upon the closed magnetostatic system is always satisfied at infinity. When the systems are completely screened, and if it is possible to neglect the dispersion of flux outside, the condition $\Phi = 0$ is satisfied on the outer surface of the screen.

Let us construct the sequence of functions, satisfying the boundary condition (15), in which the first derivatives may be discontinuous on the limits of the region δ. This set of functions then defines the complete δ set.

Let

$$\varphi_1^{(\delta)}, \varphi_2^{(\delta)}, \ldots, \varphi_n^{(\delta)}, \ldots \tag{16}$$

be a complete set of functions, determined in regions δ, satisfying the conditions $\varphi_k^{(\delta)} = 0 (k = 1,2,\ldots)$ on the surfaces S_δ enclosing regions δ, and let

$$\psi_1, \psi_2, \ldots, \psi_n, \ldots \tag{17}$$

be a complete set of continuosuly differentiable functions, determined in the domain enclosed by surface Γ, on which they vanish.

It then is possible to show that the totality of functions $\{\varphi_k^{(\delta)}, \psi_k\}$ represents the complete δ-set.

For the sake of simplicity of analysis we shall limit our investigation to cases where δ regions are defined by two coordinates e.g., r,x (system with axial symmetry) or x,y (system with plane parallel symmetry). Let Φ be any arbitrary function satisfying following conditions:

1) Φ and its first derivatives are defined and are continuous inside each region δ;

2) On the limits of regions δ condition (15) is satisfied

3) $\Phi = 0$ on the Γ surface.

Let us represent Φ as a sum of two functions Φ_0 and Θ where Φ_0 and its first derivatives are continuous inside each region δ and vanish on the surfaces of δ, and θ and its first derivatives are continuos inside the domain limited by Γ and vanish on that surface. This representation is always possible when the limits of the regions δ are smooth. One of such possible representations leads to the following:

Let us construct a family of straight lines $x =$ const. and let $M_1(x)$, $M_2(x)$,..., $M_k(x)$, where $k = k(x)$, be points of intersection* of the boundaries of surfaces δ with the surface Γ. To each straight line we assign a corresponding polynomial $P(x,y)$ with respect to y, which coincides with the values of Φ at the points M_1, M_2,..., M_k. Then $\Theta = P(x,y)$ and $\Phi = \Phi_0 - P(x,y)$, where now $P(x,y)$ and its first derivatives are continuous in the domain limited by Γ, and vanish on that surface.

Since $\{\varphi_k^{(\delta)}\}$ is a complete set of functions in region δ, the function Φ_0 and its first derivatives are uniformly approximated by a linear combination of $\varphi_k^{(\delta)}$. The function Θ and its first derivatives on the other hand are approximated by a linear combination of ψ_k, so that $\Phi = \Phi_0 + \Theta$ and their first derivatives are given by a linear combination of $\varphi_k^{(\delta)}$ and ψ_k; therefore the totality of $\{\varphi_k^{(\delta)}, \psi_k\}$ represents a complete δ-set.

Thus the problem of setting up a complete δ-set is reduced to the writing of a complete set of functions $\varphi_k^{(\delta)}$ and ψ_k. The principle of construction of such complete sets is known[5,6].

Let us now reduce the δ-set to its normal form by introducing a new sequence of functions

$$\Psi_1, \Psi_2, \Psi_3, \ldots,$$

defined in the whole space Ω bounded by the surface Γ. Let us assume

Let us assume

$$\Psi_{(n-1)(p+k)+k} = \begin{cases} \varphi_n^{(\delta_k)} & \text{in region } \delta_k, \\ 0 & \text{outside } \delta_k, \end{cases} \tag{18}$$

$$\Psi_{n(p+1)} = \psi_n,$$

where p gives the number of regions δ of the magnetostatic system. The index $k = 1, 2,\ldots, p$ for each fixed n starting with $n = 1$. Thus the set of functions (18) represents a complete normalized set. An arbitrary function Φ and its first derivatives satisfying conditions 1. to 3. of the second section can be approximated by a linear combination of ψ_k, where derivatives of Φ may have discontinui-

[5] L. V. Kantorovich and V. I. Krylov, *Approximation Methods in Advanced Analysis*, Moscow, 1952

[6] I. Iu. Kharik Doklady, Akad. Nauk SSSR 80, 25 (1951)

* It is possible that in this case a part of the boundary of δ regions coincides with a straight line, but it is always possible to choose such lines which intersect δ at a finite number of points.

ties on the limits of regions δ.

It is possible to show in particular, using Weierstrass's theorem on uniform approximation of a continuous function by polynomials, that in a general case of magnetostatic problems, the complete system of functions (18) may be determined by following sequences of $\varphi_n^{(\delta_k)}$ and ψ_n:

$$\psi_1 = q,\ \psi_2 = qx,\ \psi_3 = qy,\ \psi_4 = qz,\ \psi_5 = qxy,$$
$$\psi_6 = qxz,\ \psi_7 = qyz,\ \psi_8 = qx^2, \ldots;$$

$$\varphi_1^{(\delta_k)} = q_{\delta_k},\ \varphi_2^{(\delta_k)} = q_{\delta_k}x,\ \varphi_3^{(\delta_k)} = q_{\delta_k}y,\ \varphi_4^{(\delta_k)} = q_{\delta_k}z,$$

$$\varphi_5^{(\delta_k)} = q_{\delta_k}xy,\ \varphi_6^{(\delta_k)} = q_{\delta_k}xz,\ \varphi_7^{(\delta_k)} = q_{\delta_k}yz, \ldots,$$

where $q_{\delta_k}(x,y,z) = 0$ is the surface equation of δ, and $q(x,y,z) = 0$ is the surface equation of Γ limiting the domain Ω.

Similarly, performing the transformation of variables x,y,z, it is possible to construct other complete sets of functions, e.g., trigonometric polynomials.

3. DETERMINATION OF MAGNETIC INDUCTION FLUX BY DIRECT METHOD

Let us represent the function Φ by the following form:

$$\Phi_n = \sum_{k=1}^{n} \alpha_k \Psi_k, \tag{19}$$

where ψ_k is the complete normalized set of functions and a_k constant coefficients, functions of n.

Φ_n satisfies identically the boundary conditions (15); therefore one can take Φ_n as the nth approximation of the variational problem using Ritz's method[5]. The problem of determination of the nth approximation of Φ reduces to integration of the Lagrangian L over the domain Ω. Substituting Φ_n and its partial derivatives into L and performing the integration, we obtain:

$$E = E\{\alpha_k\}.$$

The condition for a minimum of E leads to transcendental equations for solutions for a_k

$$\partial E / \partial \alpha_k = 0. \tag{20}$$

Let us introduce the components of current potential function U, defined by the following relation:

$$u_k = -\frac{1}{c} \sum_{i=1}^{m} \int_{s_i} \Psi_k(s) j_i ds. \tag{21}$$

Then the nth approximation of the current potential function U is represented as a linear combination of u_k:

$$U_n = \sum_{k=1}^{n} \alpha_k u_k. \tag{22}$$

The system of equations (20) with the condition (22) takes the form:

$$\partial W / \partial \alpha_k = -u_k \ (k = 1, 2, \ldots, n). \tag{23}$$

From Eq. (23) one can see that the unknown coefficients a_k are functions of $u_i (i = 1, 2, \ldots, n)$. This indicates that, for a given geometrical configuration of the magnetostatic system, the flux Φ is determined exclusively by components u_k of the current potential function U. Considering a_k as functions of u_i, and differentiating Eq. (23) with respect to u_k, we obtain

$$\sum_{i=1}^{n} \frac{\partial^2 W}{\partial \alpha_k \partial \alpha_i} \frac{\partial \alpha_i}{\partial u_k} = -1 \ (k = 1, 2, \ldots, n) \tag{24}$$

The set of equations (24) is a system of linear equations in $\frac{\delta \alpha_i}{\delta u_k}$ which can be integrated by the method of successive approximations, taking $\alpha_k = 0$ and $u_i = 0$ as initial conditions. The above conditions correspond to vanishing magnetic induction in the absence of the field of currents. In the particular, but practically important case when the current densities are everywhere the same, α_k can be taken as functions of j. Indeed from Eq. (21) it follows:

$$u_k = \left(-\frac{1}{c} \sum_{i=1}^{m} \int_{s_i} \Psi_k(s)\, ds \right) j = \bar{u}_k j,$$

where

$$\bar{u}_k = -\frac{1}{c} \sum_{i=1}^{m} \int_{s_i} \Psi_k(s)\, ds, \tag{25}$$

$$U_n = j \sum_{k=1}^{n} \alpha_k \bar{u}_k. \tag{26}$$

Let us introduce the specific potential function of currents relative to unit current density

$$\bar{U} = U / j. \tag{27}$$

Then

$$\bar{U}_n = \sum_{k=1}^{n} \alpha_k \bar{u}_k, \tag{28}$$

where u_k represents the components of the specific potential function of currents. In this case the system of equations (24) takes the form:

$$\sum_{i=1}^{n} \frac{\partial^2 W}{\partial \alpha_k \partial \alpha_i} \frac{d\alpha_i}{dj} = -\bar{u} \ (k = 1, 2, \ldots, n). \tag{29}$$

We normalize the system (29) by introducing the Jacobian of that system:

$$D = \frac{D\left(\frac{\partial W}{\partial \alpha_1}, \frac{\partial W}{\partial \alpha_2}, \ldots, \frac{\partial W}{\partial \alpha_n}\right)}{D(\alpha_1, \alpha_2, \ldots \alpha_n)}. \qquad (30)$$

The Jacobian (30) is not zero identically. Indeed, if the Jacobian (30) were zero, then $\alpha_1, \alpha_2 \ldots \alpha_n$ would be functionally dependent; this contradicts the definitions of $\Psi_1, \Psi_2, \ldots$ as a complete set of functions. Solving Eq. (29) for derivatives we obtain

$$\frac{d\alpha_i}{dj} = -\frac{D\left(\frac{\partial W}{\partial \alpha_1}, \frac{\partial W}{\partial \alpha_2}, \ldots, \frac{\partial W}{\partial \alpha_{i-1}}, U, \frac{\partial W}{\partial \alpha_{i+1}}, \ldots, \frac{\partial W}{\partial \alpha_n}\right) \Big/ D(\alpha_1, \alpha_2, \ldots, \alpha_n)}{D\left(\frac{\partial W}{\partial \alpha_1}, \frac{\partial W}{\partial \alpha_2}, \ldots, \frac{\partial W}{\partial \alpha_n}\right) \Big/ D(\alpha_1, \alpha_2, \ldots, \alpha_n)}. \qquad (31)$$

Writing

$$\overline{D_i} = D\left(\frac{\partial W}{\partial \alpha_1}, \frac{\partial W}{\partial \alpha_2}, \ldots, \frac{\partial W}{\partial \alpha_{i-1}}, \overline{U}, \frac{\partial W}{\partial \alpha_{i+1}}, \ldots, \frac{\partial W}{\partial \alpha_n}\right) \Big/ D(\alpha_1, \alpha_2, \ldots, \alpha_n), \qquad (32)$$

We get

$$d\alpha_i / dj = -\overline{D_i} / D. \qquad (33)$$

Let us now integrate Eqs. (33), taking $\alpha_i = 0$ and $j = 0$ as initial conditions. Using the successive approximation method and taking as zeroth approximation $\alpha_i^0 = 0 (i = 1,2,\ldots n)$, we get:

$$\alpha_i^{(1)} = -\int_0^j \left(\frac{\overline{D}_i}{D}\right)_0 dj; \qquad \alpha_i^{(2)} = -\int_0^j \left(\frac{\overline{D}_i}{D}\right)_1 dj;$$

$$\ldots; \ \alpha_i^{(m)} = -\int_0^j \left(\frac{\overline{D}_i}{D}\right)_{m-1} dj; \ \ldots;$$

where $(\overline{D}_i / D)_k = \overline{D}_i / D$ when $\alpha_i = \alpha_i^{(k)}$.
The exact value of α_i is obtained as the limit of sequence $\alpha_i^{(m)}$ when m tends to infinity.

It is possible to apply the same method when $j = j(x,y,z)$. Consider the system of equations:

$$\partial W / \partial \alpha_k = -\lambda u_k \quad (k = 1, 2, \ldots, n), \qquad (34)$$

where λ is an arbitrary variable parameter ranging from 0 to 1.

Differentiating Eq. (34) with respect to λ, we get

$$\sum_{i=1}^{n} \frac{\partial^2 W}{\partial \alpha_k \partial \alpha_i} \frac{\partial \alpha_i}{\partial \lambda} = -u_k, \qquad (35)$$

from which

$$\frac{\partial \alpha_i}{\partial \lambda} = \frac{D\left(\frac{\partial W}{\partial a_1}, \frac{\partial W}{\partial a_2}, \ldots, \frac{\partial W}{\partial a_{i-1}}, U, \frac{\partial W}{\partial a_{i+1}}, \ldots, \frac{\partial W}{\partial a_n}\right) \Big/ D(a_1, a_2, \ldots a_n)}{D\left(\frac{\partial W}{\partial a_1}, \frac{\partial W}{\partial a_2}, \ldots, \frac{\partial W}{\partial a_n}\right) \Big/ D(a_1, a_2, \ldots a_n)} \qquad (36)$$

Denoting the denominator of Eq. (36) by D_i, we have

$$\alpha_i = -\int_0^{\lambda} \left(\frac{D_i}{D}\right) d\lambda; \qquad (37)$$

when $\lambda = 0$, $\alpha_i = 0$, α_i depend on λ in (37). Again applying the method of successive approximations we obtain:

$$\alpha_i^{(1)}(\lambda) = -\int_0^{\lambda} \left(\frac{D_i}{D}\right)_0 d\lambda;$$

$$\alpha_i^{(2)}(\lambda) = -\int_0^{\lambda} \left(\frac{D_i}{D}\right)_1 d\lambda;$$

$$\ldots\ldots\ldots\ldots$$

$$\alpha_i^{(m)}(\lambda) = -\int_0^{\lambda} \left(\frac{D_i}{D}\right)_{m-1} d\lambda; \ \ldots$$

The limit of sequence α_i, when $m \to \infty$ gives the exact value of $\alpha_i(\lambda)$, satisfying system (34).

The complete set of α_i, satisfying system of equations (23) is obtained by setting $\lambda = 1$.

The roots α_i of the system of equations (20) then determine the nth approximation of the magnetic induction flux Φ_n, and the exact value of the flux Φ is given by the limit of sequence Φ_n when $n \to \infty$.

Translated by G. Cvijanovich
72

Letters to the Editor

Calculation of the Energy Distribution Function of Neutrons by Markov's Method

V. V. CHAVCHANIDZE AND O. D. CHEITVILI
Tbiliski State University
(Submitted to JETP editor July 28, 1954)
J. Exper. Theoret. Phys. USSR 28, 369-370
(March, 1955)

AN attempt is made to investigate by Markov's method some questions in the theory of slowing down of neutrons due to elastic collisions with the nuclei of the scatterer[1-6]. The results obtained are also applicable to slowing down by thin foils when the number of elastic collisions is not too large (between 25 and 30).

According to references 1 and 2, the normalized probability $f_0(u_j)\,du_j$, that the quantity $u_j = \ln(E_{j-1}/E_j)$ will lie in the interval $(u_j,\ u_j + du_j)$ can be written as:

$$f_0(u_j)\,du_j = \frac{(A+1)^2}{4A}\,e^{-u_j}du_j \text{ if } u_j \leqslant \ln\left(\frac{A+1}{A-1}\right)^2,$$
$$f_0(u_j)\,du_j = 0 \qquad \text{if } u_j > \ln\left(\frac{A+1}{A-1}\right)^2, \tag{1}$$

where E_{j-1} and E_j are, respectively, the neutron energy before and after the jth collision, and A is the atomic mass of the scattering nuclei (assuming that $A \neq 1$). We have the identity

$$\frac{E_0}{E_n} = \frac{E_0}{E_1}\frac{E_1}{E_2}\ldots\frac{E_{j-1}}{E_j}\ldots\frac{E_{n-1}}{E_n}, \tag{2}$$

where E_0 is the initial energy of the neutron and E_n the energy after n collisions. From Eq. (2):

$$\ln\frac{E_0}{E_n} = \ln\frac{E_0}{E_1} + \ln\frac{E_1}{E_2} + \ldots + \ln\frac{E_{j-1}}{E_j} + \ldots + \ln\frac{E_{n-1}}{E_n} \tag{3}$$

or

$$U = u_1 + u_2 + \ldots + u_n, \tag{3'}$$

where

$$U = \ln(E_0/E_n).$$

We can consider (3') as a stochastic equation. All the u_j's are stochastic variables, and we are confronted with the typical stochastic problem of summing n random variables. With the help of references 6 and 7, it is easy to write the function $A_n(\rho)$.

$$A_n(\rho) = \prod_{j=1}^{n}\int_0^{q_A} e^{i\rho\varphi_j} f_0(u_j)\,du_j, \tag{4}$$

where the function[7,8] ϕ_j can simply be defined as $\phi_j = u_j$; we denote $\ln[(A+1)/(A-1)]^2$ by q_A. Taking into account the fact that by definition $f_0(u_j)\,du_j$ does not depend on j, it is easily shown that

$$A_n(\rho) = \left[\frac{(A+1)^2}{4A}\right]^n \frac{(\exp\{(i\rho-1)\,q_A\}-1)^n}{(i\rho-1)^n}. \tag{4'}$$

Then the probability that, after n collisions, the quantity U lies in the previous given interval $(U,\ U+dU)$ is exactly

$$W_n(U)\,dU = \frac{dU}{2\pi}\int_{-\infty}^{+\infty} e^{-i\rho U} A_n(\rho)\,d\rho,$$

$$W_n(U) = \left[\frac{(A+1)^2}{4A}\right]^n \frac{e^{-U}}{(n-1)!} \times \sum_{m=0}^{n}(-1)^m C_n^m\,[(n-m)\,q_A - U]^{n-1}, \tag{5}$$

where the terms in the summation are different from zero when $(n-m)\,q_A - U > 0$.

In the case of scattering by hydrogen, we obtain for $A_n(\rho)$

$$A_n(\rho) = (-1)^n/(i\rho-1)^n \tag{6}$$

and the distribution function becomes

$$W_n(U) = U^{n-1}e^{-U}/(n-1)! \tag{7}$$

The distribution thus found is Poisson's distribution. In the case $n = 1$, we obtain Eq. (1). The results obtained here show that the method of Markov[4-7] permits a rather simple solution of some problems arising in the theory of the slowing down of neutrons.

Translated by M. A. Melkanoff
61

[1] A. I. Akhiezer and I. Ia. Pomeranchuk, *Certain Problems of Nuclear Theory*, Moscow, 1950

[2] R. E. Marshak, Revs. Mod. Phys. **19**, 185 (1947)

[3] S. Glasstone and M. Edlund, *The Elements of Nuclear Reactor Theory*, D. Van Nostrand Company, Inc., New York, 1954

[4] S. Chandrasekhar, Revs. Mod. Phys. **15**, 1 (1943)

[5] A. A. Markov, *Calculus of Probabilities*, 4th edition, Moscow, 1924

[6] V. V. Chavchanidze, J. Exper. Theoret. Phys. USSR **26**, 179, 185 (1954)

[7] V. V. Chavchanidze, Trudy Inst. Fiz. Akad. Nauk Gruz. SSR **2**, part II, Sec. 3, p. 119 (1954)

[8] V. V. Chavchanidze, Dissertation, Tbilisk State University (1953)

On the Angular Distribution of β-Radiation. II

G. R. Khutsishvili

(Submitted to JETP editor March 13, 1954)
J. Exper. Theoret. Phys. USSR **28**, 370-371
(March, 1955)

THE analysis of β-radiation from oriented nuclei is of considerable interest, as relative measurements of angular distribution of β-radiation, in conjunction with theory, can give valuable information about the spins, parities and magnetic moments of β-radioactive nuclei.

A theoretical analysis of angular distribution of β-radiation has been carried out in references 1 and 2. Reference 2 in particular gives the expression $W(E, \theta)$ for the distribution (as a function of energy and of angle) of β-particles emitted by oriented nuclei for the transition $\Delta I = \pm 2$, "yes" (I is the nuclear spin, "yes" denotes that the parity of the nucleus changes upon emission of a β-ray). However the introduction of this expression in reference 2 applies only in the Born approximation.

By comparing the expression for $W(E, \theta)$ obtained in the Born approximation with the expression for the β-spectrum of the corresponding transition (including Coulomb effects[3]), it becomes quite simple to include Coulomb effects in the formula for angular distribution: in order to carry this out it is sufficient to multiply by ϕ_1 the term proportional to p^2 in the square brackets of Eq. (2), reference 3, and to multiply by ϕ_0 the term proportional to q^2; according to reference 3 (using the notation and units of reference 2):

$$\varphi_0 = \frac{1 + s_0}{2} F_0(Z, E), \tag{1}$$

$$\varphi_1 = \frac{2 + s_1}{4} F_1(Z, E). \tag{2}$$

where

$$s_n = \sqrt{(n+1)^2 - (\alpha Z)^2}, \tag{3}$$

$$\xi = Z\alpha / \beta, \tag{4}$$

and the Coulomb factors F_0 and F_1 are given by the formula

$$F_n(Z, E) = \frac{[(2n+2)!]^2}{(n!)^2 [\Gamma(1 + 2s_n)]^2} \times (2pR)^{2(s_n - n - 1)} \exp(\pi\xi) |\Gamma(s_n + i\xi)|^2. \tag{5}$$

In Eqs. (1) - (5), α denotes the fine structure constant, R the nuclear radius, β the electron velocity, Z the nuclear charge (in the case of positron emission, ξ must be replaced by $-\xi$).

Finally we obtain for the distribution of β-radiation as a function of energy and angle, for the transition $\Delta I = \pm 2$, "yes":

$$W(E, \vartheta) = {}^1/_3 (2\pi)^{-5} \pi G^2 |B_{lk}|^2 pEq^2 \times \{q^2\varphi_0 + p^2\varphi_1 [1 - a(I) f_2 P_2(\cos\vartheta)]\}. \tag{6}$$

Note that Eq. (6) can be transformed into Eq. (2) of reference 2 by neglecting terms of the order of $(\alpha Z)^2$.

Translated by M. A. Melkanoff
62

[1] A. M. Cox and S. R. de Groot, Physica **19**, 683 (1953)

[2] G. R. Khutsishvili, J. Exper. Theoret. Phys. USSR **25**, 763 (1953)

[3] E. J. Konopinski and G. E. Uhlenbeck, Phys. Rev. **60**, 308 (1941)

The Absorption of Ultrasonic Waves in Armco Iron and Plexiglass

N. F. Otpushchennikov
Kursk Teachers' Institute

(Submitted to JETP editor September 27, 1954)
J. Exper. Theoret. Phys. USSR **28**, 371
(March, 1955)

THERE are a number of works devoted to the measurement of the ultrasonic absorption coefficient in solids, although the number is still comparatively small. In many metals and dielectrics, no measurements have as yet been made, and the existing theory of the mechanism of this

TABLE

Substance	Density ρ in gm/cm^3	Frequency ν in 10^6 cps	Absorption Coefficient in cm^{-1}	Ultrasonic Velocity v in m/sec	Measurements of Other Investigations	
					α in cm^{-1}	v in m/sec
Armco Iron	7.85	0.66	0.0024			
		6	0.024			
		10	0.038	5920		
Plexiglass	1.19	0.66	0.11		0.14 [5]	
		1.4	0.21		0.22 [5]	2660 [4]
		6	0.40			2640 [5]
		10	0.55	2680		2662 [6]

absorption has not been tested experimentally. Therefore the investigation of the propagation of ultrasonic waves in different solids over a wide range of frequencies and temperatures presents considerable scientific and practical interest.

In this letter we report the results of measurements by the pulse method of the absorption and propagation velocity of ultrasonic waves over a frequency range from 0.66 to 10 mc in two substances: Armco iron and plexiglass. The experimental arrangements and techniques of measurement will be reported separately.

The results of the measurement of the absorption coefficient of ultrasonic waves α, and the propagation velocity ν in the two materials are listed in the table.

From the values obtained in the frequency range 0.6 - 10 mc, it follows that the ultrasonic absorption coefficient in Armco iron is directly proportional to the ultrasonic frequency. Investigations [1] of ultrasonic absorption in magnesium over a wide frequency range also gave a linear frequency dependence.

The data for plexiglass indicate that the absorption increases proportional to $\sqrt{\nu}$, which is in agreement with the results of other authors [2,3]. The measured velocity of the ultrasonic waves in plexiglass at $\nu = 10$ mc is also in agreement with the values in the literature [4-6]. There were no available data on ultrasonic absorption in Armco iron.

Translated by R. T. Beyer
63

[1] W. Roth, J. Appl. Phys. 19, 901 (1948)

[2] I. G. Mikhailov, *The Propagation of Ultrasound in Liquids*, Moscow, 1949

[3] W. Mason, *Piezoelectric Crystals and Their Applications in Ultrasonics*

[4] N. F. Otpushchennikov, J. Exper. Theoret. Phys. USSR 22, 436 (1952)

[5] D. S. Hughes, W. L. Pandrom and R. L. Mims, Phys. Rev. 73, 1552 (1949)

[6] I. G. Mikhailov, Doklady Akad. Nauk SSSR 59, 1555 (1948)

On the Causal Development of a Coupled System in Relative Time

V. N. TSYTOVICH
Moscow State University

(Submitted to JETP editor August 21, 1954)
J. Exper. Theoret. Phys. USSR 28, 372-374
(March, 1955)

IN the relativistic covariant equation which describes the coupled motion of two interacting particles [1-3], one ascribes to each particle its own time: to the first particle t_1 and to the second t_2. The question in what manner are these times t_1 and t_2 related to each other is of interest. If the external fields are stationary, we can introduce a general time $T = (t_1 + t_2)/2$ and a relative time $t = t_1 - t_2$; for simplicity we assume that the masses of the particles are equal (this corresponds, for example, to the case of positronium). We are interested in how the wave function of different times ($t \neq 0$) can be found by means of the wave function of the same times ($t = 0$), in other words in the development of a coupled system in relative time.

We recall, for example, that the development of the wave function in time of a freely moving particle is described by the operator $e^{-(i/\hbar)Ht}$

$$\psi(t) = e^{-(i/\hbar)Ht}\psi(0), \qquad (1)$$

where H is the Hamiltonian, independent of time. If we know (for example by means of some measure-

ments performed on the system) the wave function at the initial moment of time, then Eq. (1) determines its value for all future moments of time. It is known that in the theory of a vacuum there occur causal functions of propagation which describe a causal development in time, different from (1). According to Feynman [4]

$$\psi(x_1, t_1) = \int G(x_1, t_1, x_1', 0)\,\psi(x_1', 0)\,d^3x_1', \qquad (2)$$

where G is the Green's function which satisfies the equation for the operator of the field with δ-function on the right side. If G can be computed by means of the theory of residues, under the assumption that the mass of the particle has an infinitesimally small negative imaginary part, we obtain

$$\psi(t_1) = \Lambda(t_1)\, e^{-(i/\hbar)Ht_1}\,\psi(0), \qquad (3)$$

where $\Lambda(t)$ is a generalization of the projection operators:

$$\Lambda_+ = \frac{|H| + H}{2|H|}, \quad \Lambda_- = \frac{|H| - H}{2|H|}; \qquad (4)$$

$$\Lambda(t_1) = \frac{H + (t_1/|t_1|)|H|}{2|H|} = \begin{cases} \Lambda_+; & t_1 > 0, \\ -\Lambda_-; & t_1 < 0, \end{cases}$$

with $|H| = \sqrt{H^2}$.

The effect of $\Lambda(t_1)$ on the wave function $\psi(0)$ with $t > 0$ is to cut off all negative energies and with $t_1 < 0$, all positive, and also to change the sign of the wave function:

$$\Lambda(t)|_{t>0}\,\psi(0) = \Lambda(t)|_{t>0} \sum_n c_n\psi_n = \sum_{E_n>0} c_n\psi_n;$$
$$\Lambda(t)|_{t<0}\,\psi(0) = \Lambda(t)|_{t<0} \sum_n c_n\psi_n = -\sum_{E_n<0} c_n\psi_n. \qquad (5)$$

Thus the positive frequencies are propagated in the future and the negative ones in the past [5].

In the theory of two bodies the operator of evolution in relative time $t = t_1 - t_2$ can be found in any case if the interaction is instantaneous, for in such a case the moment $t_2 = t_1$; $t = 0$ is singled out by the interaction. In this case an equation of the type used in references 1 - 3 has the form

$$\{F_1F_2 + i\hbar K(x_1, x_2)\,\delta(t)\}\,\psi_n(x_1, x_2, t, T) = 0, \qquad (6)$$

where $K(x_1, x_2)\delta(t)$ is the operator of the instantaneous interaction *

$$F_1 = \frac{E_n}{2} - \frac{\hbar}{i}\frac{\partial}{\partial t} - H_1; \quad F_2 = \frac{E_n}{2} + \frac{\hbar}{i}\frac{\partial}{\partial t} - H_2. \qquad (7)$$

Insofar as $\delta(t)$ enters the second term of (6) one can write

$$\psi(x_1, x_2, t, T) = \qquad (8)$$
$$-\frac{1}{F_1F_2}\,i\hbar K(x_1, x_2)\,\delta(t)\,\psi(x_1, x_2, 0, T),$$

or

$$\psi(x_1, x_2, t, T) = \int G(x_1, x_2, t_1, t_2, x_1', x_2', t_1', t_2') \qquad (9)$$
$$\times\, i\hbar\delta(t')\,\psi(x_1', x_2', 0, T)\,d^4x_1'\,d^4x_2'.$$

Further,

$$G(x_1, x_2, t_1, t_2, x_1', x_2', t_1', t_2') \approx$$
$$\frac{1}{\hbar^2}\,G^{(1)}(x_1, t_1, x_1', t_1')\,G^{(2)}(x_2, t_2, x_2', t_2'),$$

where

$$G^{(1)} = \Lambda^{(1)}(t_1 - t_1')\exp\left\{-\frac{i}{\hbar}H_1(t_1 - t_1')\right\}\delta(x_1 - x_1');$$
$$G^{(2)} = \Lambda^{(2)}(t_2 - t_2')\exp\left\{-\frac{i}{\hbar}H_2(t_2 - t_2')\right\}\delta(x_2 - x_2').$$

The indices (1) and (2) refer to the first and second particles respectively. Inserting these values into Eq. (9), integrating over t', and using $\delta(t')$, we obtain

$$\psi(x_1, x_2, t, T) = \frac{1}{(2\pi)^6\hbar^2}\int \Lambda^{(1)}(t_1 - T')\,\Lambda^{(2)}(t_2 - T') \times$$
$$\times \exp\left\{-\frac{i}{\hbar}H_1(t_1 - T')\right\}\exp\left\{-\frac{i}{\hbar}H_2(t_2 - T')\right\} \times$$
$$\times \exp\{k_1(x_1 - x_1') + ik_2(x_2 - x_2')\} \qquad (10)$$
$$\times\, i\hbar K(x_1', x_2')\,\psi(x_1', x_2', 0, T').$$

We give the integration of T' for the two cases: $t_1 > t_2$ and $t_1 < t_2$, by dividing the range of integration into the subintervals, for example, for $t_1 > t_2$ $[-\infty, t_2]$, $[t_2, t_1]$ and $[t_1, \infty]$. In this way we take it into account that the insertion of $T = \pm\infty$ in the resulting equation yields zero, due to the presence of the factors $\Lambda^{(1)}(T_1 - T)$ and $\Lambda^{(2)}(t_2 - T)$ and $m = m - i\delta$ for $\delta \to 0$. Then for the staionary state,

which corresponds to the total energy E_n, we obtain:

$$\psi_n(\mathbf{x}_1, \mathbf{x}_2, t) = \left\{\Lambda^{(1)}(t) \exp\left[-\frac{i}{\hbar}\left(H_1 - \frac{E_n}{2}\right)t\right] + \right.$$
$$\left. + \Lambda^{(2)}(-t) \exp\left[\frac{i}{\hbar}\left(H_2 - \frac{E_n}{2}\right)t\right]\right\} \chi_n(\mathbf{x}_1, \mathbf{x}_2), \quad (11)$$

where

$$\chi_n(\mathbf{x}_1, \mathbf{x}_2) = -\frac{1}{(2\pi)^6} \quad (12)$$
$$\times \int \frac{\exp\{i\mathbf{k}_1(\mathbf{x}_1 - \mathbf{x}_1') + i\mathbf{k}_2(\mathbf{x}_2 - \mathbf{x}_2')\}\, d^3k_1\, d^3k_2}{E_n - H_1 - H_2}$$
$$\times \varphi_n(\mathbf{x}_1', \mathbf{x}_2') \times K(\mathbf{x}_1', \mathbf{x}_2')\, d^3x_1'\, d^3x_2',$$

$$\varphi_n(\mathbf{x}_1, \mathbf{x}_2) = \psi_n(\mathbf{x}_1, \mathbf{x}_2, t)\,|_{t=0}.$$

Equations (11) and (12) establish the connection between $\psi_n(\mathbf{x}_1, \mathbf{x}_2, t)$ and $\phi_n(\mathbf{x}_1, \mathbf{x}_2)$, and they indicate the form of the unknown operator $\Theta_n(t)$, $\psi_n(\mathbf{x}_1, \mathbf{x}_2, t) = \Theta_n(t)\,\phi_n(\mathbf{x}_1, \mathbf{x}_2)$, which describes the causal development of the coupled system in relative time $t = t_1 - t_2$. If we multiply (12) by $\exp\{-\frac{i}{\hbar} E_n t\}$, then the general wave function can be written in the form:

$$\psi_n(t, T) = \exp\left\{-\frac{i}{\hbar} E_n T\right\} \psi_n(t)$$

$$= \begin{cases} \Lambda_+^{(1)} \exp\left\{-\frac{i}{\hbar} H_1 t_1\right\} \exp\left\{-\frac{i}{\hbar}(E_n - H_1) t_2\right\} \\ -\Lambda_-^{(2)} \exp\left\{-\frac{i}{\hbar} H_2 t_2\right\} \exp\left\{-\frac{i}{\hbar}(E_n - H_2) t_1\right\} \chi_n, \quad t > 0; \end{cases}$$

$$= \begin{cases} \Lambda_+^{(2)} \exp\left\{-\frac{i}{\hbar} H_2 t_2\right\} \exp\left\{-\frac{i}{\hbar}(E_n - H_2) t_1\right\} \\ -\Lambda_-^{(1)} \exp\left\{-\frac{i}{\hbar} H_1 t_1\right\} \exp\left\{-\frac{i}{\hbar}(E_n - H_1) t_2\right\} \chi_n, \quad t < 0. \end{cases}$$

We can say that the wave function corresponds either to the propagation of the first particle into the future in the form of a free wave with positive frequency $\Lambda_+^{(1)}$ (the frequency $H_1 = |H_1|$) and of the second particle into the past with a much more complicated sort of "coupling" (the frequency is $E_n - H_1$), or to the propagation of the second particle into the past in the form of a free wave with a negative frequency (the frequency : $-H_2 = |H_2|$) and of the first one into the future with a much more complicated sort of "coupling" (the frequency: $E_n - H_2$)**.

This result is a generalization of the result which was obtained by Salpeter and Bethe for the non-relativistic case, and it takes into account a new possibility which is connected with the propagation of particles with negative frequencies.

The operator of the causal development in time $\Theta(t)$ may be successfully applied to the integration over relative time of the matrix elements which occur in the theory of excitation and, in particular, for finding the effective excitation energy in the theory of two bodies (see reference 6).

---

* Instead of $K(\mathbf{x}_1, \mathbf{x}_2)$ one can also take the phenomenological potential.

**The future and the past of each particle is counted from the moment of interaction.

[1] E. E. Salpeter and H. A. Bethe, Phys. Rev. **84**, 1232 (1951)

[2] J. Schwinger, Proc. Natl. Acad. **7**, 432, 445 (1951)

[3] A. D. Galanin, J. Exper. Theoret. Phys. USSR **23**,488 (1952)

[4] R. P. Feynman, Phys. Rev. **76**, 749 (1949)

[5] E. Stuckelberg, Helv. Phys. Acta. **15**, 23 (1942)

[6] V. N. Tsytovich, J. Exper. Theoret. Phys. USSR **28**, 113 (1955)

Translated by S. I. Gaposchkin
64

The "Equilibrium" Energy Spectrum of Cascades of Photons

P. S. Isaev
P. N. Lebedev Institute of Physics, Academy of Sciences, USSR

(Submitted to JETP editor June 24, 1955)
J. Exper. Theoret. Phys. USSR **28**, 374-376 (March, 1955)

In the present work the "equilibrium" spectrum of photons generated in cascading electromagnetic processes is calculated, taking into account not only radiation damping and the creation of pairs, but also ionization losses and the Compton-effect.

The "equilibrium" spectrum of photons $\Theta(E)$ is determined by the following method:

$$\Theta(E) = \int_0^\infty \Theta(E, t)\, dt,$$

where $\Theta(E, t)dE$ is the average number of photons in the energy interval $(E, E + dE)$ at a depth t.

The approximate expression for $\Theta(E)$ occurs in Belenko's book [1] [Sec. 17, Eq. (17.8)]. For the calculation of this magnitude for the probability of the Compton-effect W_k, [reference 1, Eq. (2.20)]

the following approximation was used:

$$W_k(E', E)\,dE = g dE / EE'.$$

Here $W_k(E', E)$ is the probability that a photon of energy E', in its passage through a layer of unit thickness in the cascade, experiences Compton scattering by the electron, after which it will have the energy E; g is a certain constant, equal, for air, to 1.32 MeV; for carbon, 1.53 MeV; for aluminum, 0.839 MeV; for iron, 18.4 MeV; for copper, 0.404 MeV; and for lead 0.175 MeV.

In the work reported in reference 2, a more exact expression was obtained for the "equilibrium" spectrum of photons $\Theta(E)$. Precision in this case is connected with the fact, that for the probability of the Compton-effect the following more exact expression was taken:

$$W_q(E', E)\,dE = \frac{g dE}{EE'}\left[1 + \left(\frac{E}{E'}\right)^2\right] = \frac{g dE}{E'E}\,[1 + \delta(E'E)],$$

in which it was assumed that $\delta(E'E)$ is small compared to unity. The correction $\kappa(E)$ to the approximate "equilibrium" spectrum of photons $\Gamma(E)$, given in reference 1 [Sec. 17, Eq. (17.8)], was calculated only for air in reference 2.

In the Table there are presented the results of the calculation of the equilibrium photon spectrum $\Theta(E) = \Gamma(E) + \kappa(E)$ for hydrogen, aluminum, iron, copper and lead. The calculation was carried out according to formulas obtained in reference 2. From these data it is evident that, as was to be expected, the corrections are large for heavy elements in the energy region of the order of the critical energy or lower.

The following values of critical energy were used in the present work: for hydrogen 120, for aluminum 37.2, for iron 18.4, for copper 22.4, for lead 6.4 mev. The results of the calculations are given in the Table.

From a comparison of the spectra for a given energy for hydrogen, aluminum, iron, copper and lead, it is easy to see that $\Theta(E)$ increases with increasing Z. Copper is an "exception" (compare with Fe). However, this result is connected with the choice of an inaccurate value of the critical energy given in the review of Rossi and Greisen[3], which was made on the basis of calculations for copper.

It should be noted that the correction can be regarded as small up to energies $\sim 0.1\beta$ or up to $Z = 30$, where the corrections for $\Gamma(E)$ amount to less than 10%. However, for Pb, the correction at 0.5 β is already 10.7 / 14.4 or 74.5%, and it is impossible to speak of the complete applicability of the method used in reference 2.

Comparison of the spectrum obtained in the present work for Pb with the spectrum obtained by Richards and Nordheim[4] indicates that, in contrast to the spectrum for air (for the case $E_m = \infty$, see reference 2), where the discrepancy of the spectra has been observed only in the region $E = 1$ because of the doubtful approximation carried out in reference 4 at this point, for lead the divergence is obtained for all energies $E < 2$. This comparison shows that the method set forth by Rossi and Greisen cannot give the correct result in the calculation of the photon spectrum of heavy elements at energies $E \sim 1.5\beta$ and lower.

In conclusion I express my gratitude to S. Z. Belen'kii for supervision of this research, and also to L. Ia. Zhil'tsov who carried out the principal calculations.

Translated by D. G. Posin

65

[1] S. Z. Belen'kii, *Cascade Processes in Cosmic Rays*, Moscow, 1948

[2] P. S. Isaev, J. Exper. Theoret. Phys. USSR **24**, 78 (1953)

[3] B. Rossi and K. Greisen, *The Interaction of Cosmic Rays with Matter*, 1948

[4] A. Richards and W. Nordheim, Phys. Rev. **74**, 1106 (1948)

The Gravitational Self Energy of Particles in the Classical Field Theories

A. A. BORGARDT

Dneperpetrovsk State University

(Submitted to JETP editor September 17, 1954)

J. Exper. Theoret. Phys. USSR **28**, 377 (March, 1955)

IN several classical field theories[1,2] the electron is assigned an exclusively field self-energy. This energy can be calculated by a common formula[3], which allows the electron's own magnetism to be taken into account:

$$\mathcal{E}_0 = \int \varepsilon_0 (\mathbf{E}, \mathbf{H}) \sqrt{1/4 (\mathbf{H}^2 - \mathbf{E}^2)^2 + (\mathbf{E}, \mathbf{H})^2}\,(d\mathbf{x}), \qquad (1)$$

where $\mathbf{E}$, $\mathbf{H}$ are the vector field intensities, ϵ_0 is the dielectric permeability of the vacuum. The result (without considering the magnetic moment) turns out to be $\mathcal{E}_0 = (1.2361\ \ldots)\,(e/x_0)$ in the Born-Infeld theory[1] and $\mathcal{E}_0 = e/2x_0$ in the theory of Bopp-Podolsky[2] where x_0 is the classical radius of the electron.

The question of the form of the linear gravitational field of the electron with a field mass is usually not considered, although it is a matter of

considerable interest. We shall first calculate the gravitational potential of a point-electron with an infinite filled mass, making use of the relations

$$\Box^2 h_{\mu\nu} = -(2G/c^3)\, T_{\mu\nu}, \qquad (2)$$

where

$$T_{ik} = T_{i4} = 0, \qquad T_{44} = (e^2/2)\, x^{-4}. \qquad (3)$$

The potential h_{44} takes the form

$$h_{44} = (Ge^2/c^3)\,[(1/2x^2) - (1/x_0 x)], \qquad (4)$$

where x_0 is a constant small length, which it is necessary to introduce, in order to avoid the general divergence of h_{44}. At zero h_{44} now diverges as x^{-2}. The self-energy of the gravitational field is $\sim (\nabla h_{44})^2$ and diverges as x^{-6}. It is interesting, however, that by identifying h_{44} with the Newtonial potential, we obtain for x_0 the interpretation of classical radius $x_0 \doteq e^2/2\mathcal{E}_0$.

In the regulated theories we obtain the following results. In the theory of Born-Infeld*

$$\mathbf{D} = (e/x^2)\,\mathbf{x}^0, \quad \mathbf{E} = \mathbf{D}/\sqrt{1 + (x/x_0)^4}, \qquad (5)$$

and the gravitational potential is equal to

$$h_{44} = (Ge^2/c^3)\, F(\varphi, k)/2x_0 x$$
$$-(1/4x_0^2)\ln[(\sqrt{1 + (x/x_0)^4} - 1)/(\sqrt{1 + (x/x_0)^4} + 1)],$$

where $F(\phi, k)$ is the elliptic integral, $k = \sqrt{2}/2$,

$$\varphi = \arccos((1 - x^2/x_0^2)/(1 + x^2/x_0^2)).$$

For $x \gg x_0$, $h_{44} \sim 1/x$; for small distances $h_{44} \sim \ln x$ and diverges at zero. The gravitational self-energy converges and constitutes the portion of the self-energy of the electron required by the theory, as is easy to show,

$$m_{gr}/m_0 = aG^2 m_0^2/\hbar c,$$

where a is a number ~ 1.

In the theory of Bopp-Podolsky the result turns out to be divergent both for h_{44} and for m_{gr}. Thus only the non-linear electrodynamics allows a completely successful solution of the problem of the gravitational self energy. The result turns out to be favorable, notwithstanding the use of the linear theory of gravitation in calculation carried out above.

[1] M. Born and L. Infeld, Proc. Roy. Soc. (A) 143, 410 (1934)

[2] B. Podolsky and P. Schwed, Revs. Mod. Phys. 20, 40 (1948)

[3] A. A. Borgardt, J. Exper. Theoret. Phys. USSR 24, 248 (1953)

[4] I. Z. Fisher, J. Exper. Theoret. Phys. USSR 18, 668 (1948)

* The question of the gravitational field of the electron in the theory of Born and Infeld was investigated by Fisher[4], who found exact solutions of the Einstein equations for this case.

Translated by D. G. Posin
67

The Constriction and Curvature of an Arc in Rarified Gases at Large Currents

V. L. Granovskii and G. G. Timofeeva
All-Union Electrotechnical Institute

(Submitted to JETP editor November 30, 1954)
J. Exper. Theoret. Phys. USSR 28, 378
(March, 1955)

THE idea of the constriction of the column of an electric arc in rarefied gases at large currents under the influence of its own magnetic field (the "pinch-effect") was introduced by Tonks[1]. It was shown that this hypothetical effect could cause a rupture of the arc.

In attempts to observe this phenomenon experimentally in a DC arc (for a Hg-arc at i = 150 amp), Thoneman and Cowhig[2] detected only a weakening of the radial electric field, while Mamyrin[3] (for a H_2 arc at $i \sim 100$ amp) found a constriction of the current density distribution by only 30%.

We performed experiments with DC arcs in rarefied Hg-vapor and inert gases in straight cylindrical tubes without constriction. Measurements with a movable probe in a tube of 20 mm diameter in Hg-vapor at $p = 1\,\mu$Hg confirmed that with an increase in the current from 1 to 80 amp the half-width* of the column is diminished by $\sim 25\%$. For a further increase in current to 1-2 kamp, it was impossible to find the corresponding constriction of the arc with probes, as firstly the probe currents, then the tension of the arc, and finally the current of the arc show strong, ever increasing irregular variations with a predominant frequency of the order of $10^4 - 10^5$ cps. Experiments with two identical probes, placed symmetrically with respect to the axis, showed that the current variations in both probes are completely uncorrelated in time: not only the position of the peaks in current but their number and relative height are different. Therefore, there occur in the tube no overall changes of the current intensity in the entire cross section of the column simultaneously, but probably fast irregular motions of the constricted channel of the arc take place over the cross section of the tube. As the arc moves

in the tube in a time of the order of 10^{-5} sec, the determination of a possible constriction of the arc requires observation of the arc within times of the order of 10^{-6} sec. Therefore, the arc has been formed by a discharge of a condenser connected by short leads to the tube, the discharge occurring in $\tau = 1\text{-}2\,\mu$sec. Under these conditions one could observe the arc constricted to a narrow channel.

In Fig. 1 an arc is shown in argon with a tube diameter of 32 mm, $p = 1\,\mu$Hg and $i_{max} = 450$ amp. We see that, notwithstanding the low pressure, the channel of the arc is constricted as compared to the diameter of the tube. The constriction is stronger in Fig. 2, which shows an arc in Hg-vapor with a tube diameter at 9 mm at $\tau = 1.15\,\mu$sec, $i_{max} = 425$ amps. The arc is seen in the main part of the Figure to be a narrow channel, spirally curved and adjacent to the wall of the tube. A control experiment shown in Fig. 3 of an arc in the same tube at the same pressure but smaller current ($i_{max} = 225$ amp $\tau = 2\,\mu$sec) does not have any constriction.

The conditions and results of these and numerous analogous experiments in Hg-vapor and in argon compel us to reject for all of them the known explanations for the constrictions of the region of current conduction(contraction of a high-pressure column, the phase of a gas-focused electron beam[4]). One must therefore accept the observed phenomena as being caused by the electrodynamic effects of the magnetic field of the arc.

We did not find a rupture of the arc, caused by the "pinch-effect". An arc sustained continuously in a straight tube without constriction or other obstacles does not rupture, but moves rapidly across the cross section of the tube. A complete description of these experiments will follow.

V. I. Pugacheva participated in these experiments.

Translated by W. Philippoff
68

* The distance between points symmetric with respect to the axis, where the electron concentration is half that on the axis.

[1] L. Tonks, Trans. Electrochem. Soc. **72**, 167 (1937)

[2] P. C. Thoneman and W. T. Cowhig, Proc. Phys. Soc. **64**, 345 (1951)

[3] B. A. Mamyrin, Zh. Tekhn. Fiz. **23**, 1914 (1953)

[4] G. V. Spivak and E. L. Stoliarova, Zh. Tekhn. Fiz. **20**, 501 (1950)

[5] V. L. Granovskii, *Electrical Current in Gases*, Vol. 1, Moscow-Leningrad, 1952, Sec. 74

The Relation of the Oscillator Strengths for the Components of the Resonance-Doublet of Aluminum and Copper

G. F. Parchevskii and N. P. Penkin
Leningrad State University

(Submitted to JETP editor September 29, 1954)
J. Exper. Theoret. Phys. USSR **28**, 379 (1955)

THE experimental arrangement used in this paper has been described in detail in the papers of Rozhdestvenskii and Penkin[1] and Penkin[2]. It consists of a source of a continuous spectrum (an SVD tube with krypton), a large Rozhdestvenskii interferometer with a mirror separation of 30 cm, and a spectrometer (quartz-spectrograph E-1).

A column of vapor of the element to be investigated was obtained in a high temperature vacuum furnace with a graphite tube as a heater. The furnace was placed in one of the paths of the interferometer. When a compensation tube and a plane-parallel plate were simultaneously introduced in the other path of the interferometer, one could observe hooks in the spectrometer, coupled with the interferometer, near the absorption lines. The measurement of the distances between the summit of the hooks allows the determination of the oscillator strength of the corresponding transitions. With the help of this arrangement, spectrograms which consisted of photographs of the hooks at the absorption lines of aluminum and copper were obtained. These photographs are reproduced in Fig. 1.

The calculation of the relative values of the numbers f for the components were performed according to the formula of the method of hooks:

$$\frac{f_1}{f_2} = \frac{K_1}{K_2}\left(\frac{\Delta_1}{\Delta_2}\right)^2 \frac{N_2}{N_1}\left(\frac{\lambda_2}{\lambda_1}\right)^3.$$

The indices 1 and 2 relate to the short-wave and long-wave components of the doublet:

$$K = \left(\frac{n-1}{\lambda} - \frac{\partial n}{\partial \lambda}\right) d$$

Here d is a constant of the method, Δ the distance between the summits of the hooks, λ the wavelength of the absorption line, N the concentration of the atoms at the lower level.

For the resonance doublet of aluminum, the ratio

$$f_{3944}/f_{3962} = 3.44$$

Fig. 1 Fig. 2 Fig. 3

(Granovskii and Timofeeva, No. 68)

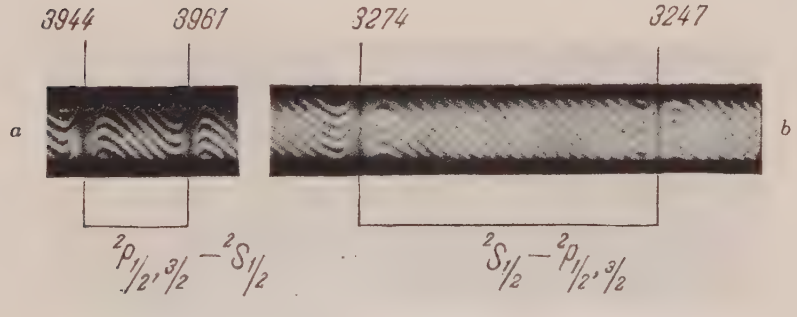

Fig. 1. Hooks near resonance doublets:
a. aluminum; *b.* copper
(Parchevskii and Penkin, No. 69)

with an error of 1.7% was obtained.

For the resonance doublet of copper we have

$$f_{3248}/f_{3274} = 1.98$$

with an error of the order of 1%.

The ratio of the *f*-numbers for the components of the doublet of copper was obtained also by King and Stockbarger[3]. Using the method of total absorption the authors of that paper obtained for this ratio

$$f_{3248}/f_{3274} = 1.94,$$

with estimated error of 10%.

In the error-limits of the experiments the results obtained by the methods of hooks and the method of absorption are identical.

[1] D. S. Rozhdestvenskii and N. P. Penkin, Izv. Akad. Nauk SSSR, Ser. Fiz. **5**, 635 (1941)

[2] N. P. Penkin, J. Exper. Theoret. Phys. USSR **17**, 355 (1947)

[3] R. King and D. Stockbarger, Astrophys. J. **91**, 488 (1940)

Translated by W. Philipoff
69

The Effect of a Uniform Compression Upon the Galvanomagnetic Effects in Bismuth and Its Alloys

N. E. Alexeevskii and N. B. Brandt
Institute for Physical Problems, Academy of Sciences, USSR

(Submitted to JETP editor June 14, 1954)
J. Exper. Theoret. Phys. USSR **28**, 379-383 (March, 1955)

A large number of studies have been devoted to the investigation of galvanomagnetic properties of metals. Recently, a broad and systematic investigation of the galvanomagnetic properties of pure metals was carried out by Borovik[1-4]. Utilizing the results of certain theoretical studies[5,6] Borovik obtained values for the density of conduction electrons, calculated on the basis of results of measurements of the Hall effect and the variation of the electrical resistance in the magnetic field.

In connection with our earlier considerations on the influence of the density of conduction electrons upon the nature of shift of the transition temperature of superconductors under elastic deformation[7,8], it was of interest to investigate the influence of uniform compression upon the electron concentration. For this purpose, measurements were undertaken of the Hall effect and of the variation of the electrical resistance in the magnetic field, for bismuth and for certain compounds of bismuth with other non-superconducting metals. We also investigated the temperature dependence of their electrical conductivity in a compressed as well as in a non-compressed state. The present communication presents the results obtained with bismuth.

The investigation of the influence of pressure upon galvanomagnetic properties in the region of low temperatures, as far as we know, has not been conducted by anyone and has therefore an intrinsic interest.

The study of galvanomagnetic phenomena was conducted on single crystal samples of bismuth having different purity and possessing in the most cases a spherical shape. This shape was convenient in that it assured a minimum of the irreversible processes connected with the possible deformation of the sample. Terminals were welded to the sample by the spark method.

For the investigation of samples under pressure we used a method which had been proposed by Lazarev and his collaborators[9], which we had already used sucessfully in our former studies. All temperature measurements were made in the broad range of temperatures from 1.5 to 300° K. The dependence of the electrical resistance upon temperature in zero magnetic field was measured during the heating-up of the apparatus, which had first been cooled down by liquid hydrogen or helium. The heating-up of the apparatus from 14 to 273° K lasted usually 5-6 hours, which permitted the measurement of the resistance with sufficient precision. The temperature was measured with the aid of a copper-constantan thermocouple, soldered to the external wall of the bomb opposite the center of the sample.

During the investigation of bismuth, 14 samples were investigated. The samples were prepared from Bi Hilger of a 99.9996% purity without preliminary recrystallization; and also from bismuth containing 0.02% of lead, some of the latter samples having been submitted to a purification process by recrystallization. Figure 1 shows the curves of the dependence of the ratio of the Hall field to the electrical field in the direction of the current, E_y/E_x, and the electrical resistance, r, upon the magnitude of the magnetic field, H, for a sample prepared from bismuth with 0.02 % lead, at a temperature of 20.4° K. Analogous results for the sample of bismuth No. 14, of the same purity, for a temperature of 4.2° K, and for two orientations in the field, are shown in Fig. 2. Uniform compression, as a rule, did not lead to a change in the

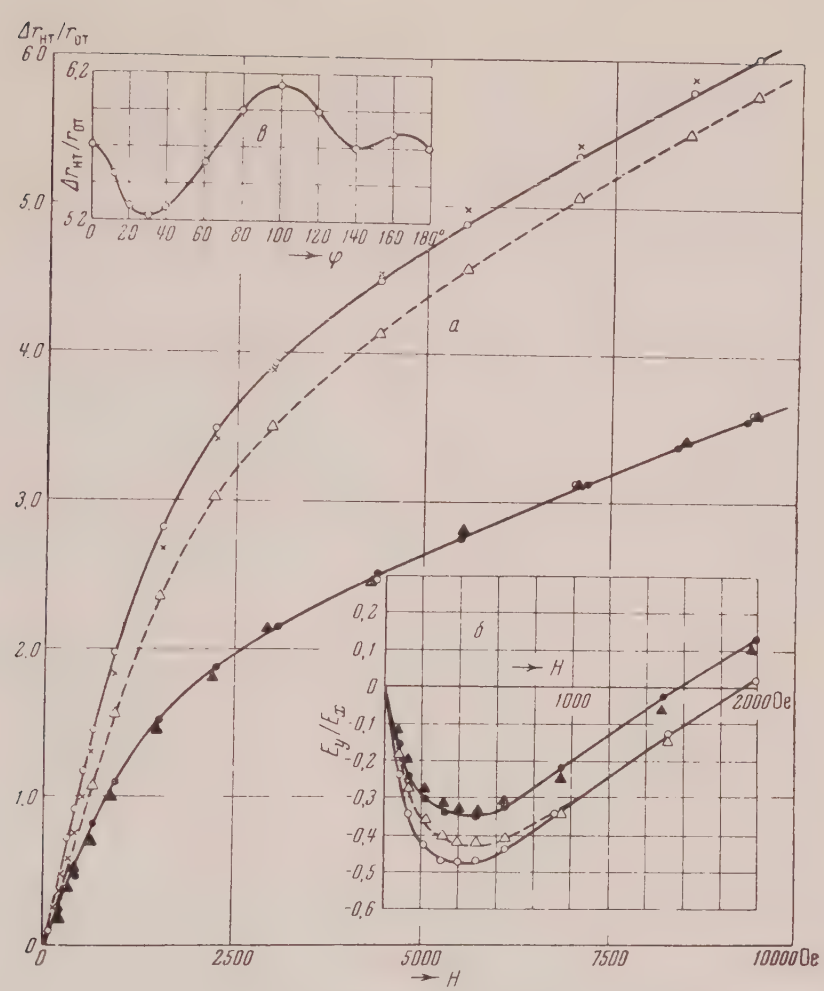

Fig. 1. Sample Bismuth No. 8_{II}, $T = 20.4°$ K, $\phi = 28°$.

a. dependence of resistance upon field,

b. dependence of E_y/E_x upon field,

c. diagram of rotation in the field H =7000 oersteds;

○ - points corresponding to the sample before pressure;

● - points with pressure of about 1500 atm. applied;

× - points for pressure removed;

▲ - repeated pressure of about 1500 atm.;

△ - after removal of the repeated pressure.

shape of the rotation diagram. In this, the sample anisotropy, characterized by the magnitude of the ratio of the minimum to the maximum resistance in a constant magnetic field, reversibly decreased 7 to 10% with the application of a uniform compression.

During measurement of the Hall effect in one of the samples of Hilger bismuth in the region of helium temperatures, a weak oscillation of the Hall electromotive force was discovered. An analogous phenomenon was noted in the work of references 10, 11 and 12. During uniform compression of this sample, the oscillation of the Hall electromotive force not only failed to subside but, to the contrary, increased somewhat and changed its period*.

During the investigation of temperature dependence of the electrical resistance of bismuth with a 0.02% lead content, it was found (on four samples) that a uniform compression to 1500 kg/cm^2 evokes the appearance of a maximum on the curve $r(T)$ at temperatures near 30-40° K, (Fig. 3). Of the above-mentioned four samples, Bi No. 7, No. 8 and No. 9

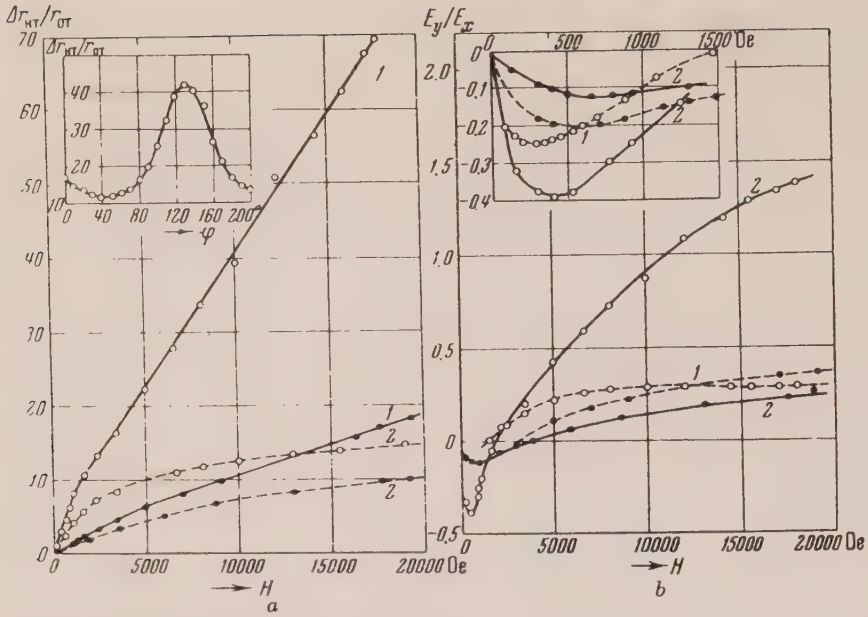

Fig. 2. Sample Bi No. 14, $T = 4.2°$ K

a. dependence of resistance upon the field and diagram of rotation in the field of H = 10,000 oersteds,

b. dependence of E_y/E_x upon the field;

1. for $\phi = 122°$, 2. for $\phi = 320°$,

○- sample without pressure,

●- sample under pressure of 1500 atm.

were spherical in shape, while the sample Bi No. 8_{II} was a cylinder of a diameter of 3 mm and a length of 12 mm. The direction of current in all these four samples was approximately perpendicular to the main axis. For other orientations, this phenomenon is apparently absent. The dotted curve in Fig. 3 represents the dependence of electrical resistance upon temperature for a sample under a pressure of the order of 1500 kg/cm^2; the direction of current in the sample is parallel to the main axis.

In comparing the results obtained with pure bismuth, in our experiments as well as in the experiments of other workers[13,14], the following can be noted. While pure bismuth gives an almost quadratic dependence of electrical resistance upon the magnitude of the magnetic field, the corresponding curve for bismuth with a small admixture of lead shows a tendency for saturation. In this case, the dependence of E_y/E_x upon H changes its sign in the same region of fields in which the dependence $r(H)$ shows a bend.

The appearance of a maximum in the curve $r(T)$ upon compression is not observed with the purer samples of bismuth. It is not impossible, however, that such a maximum can be discovered in these samples, also, at considerably higher pressures. The presence of a maximum on the curve $r(T)$ was noted in reference 15, where the temperature dependence of samples of bismuth with a different content of lead was investigated. In comparing our results on the magnitude of the maximum with the results of reference 15, we conclude that uniform compression of a sample up to a pressure of 1500 kg/cm^2 is equivalent to a variation in the concentration of lead from 0.02% to 0.15%. One must note, however, that a maximum of the same magnitude, caused by admixtures, is situated in a region of higher temperatures (about 80° K).

It is possible that the appearance of a maximum caused by pressure in the curve of the dependence of the electrical resistance upon temperature is a consequence of a change in the concentration of conduction electrons due to compression. The utilization of the bi-zonal theory for the evaluation of the concentration and mobility of electrons taking part in the conduction, appears to be difficult for bismuth, because the prior presence of small admixtures, for instance, lead, leads to substantial deviations of the dependences E_y/E_x upon H and

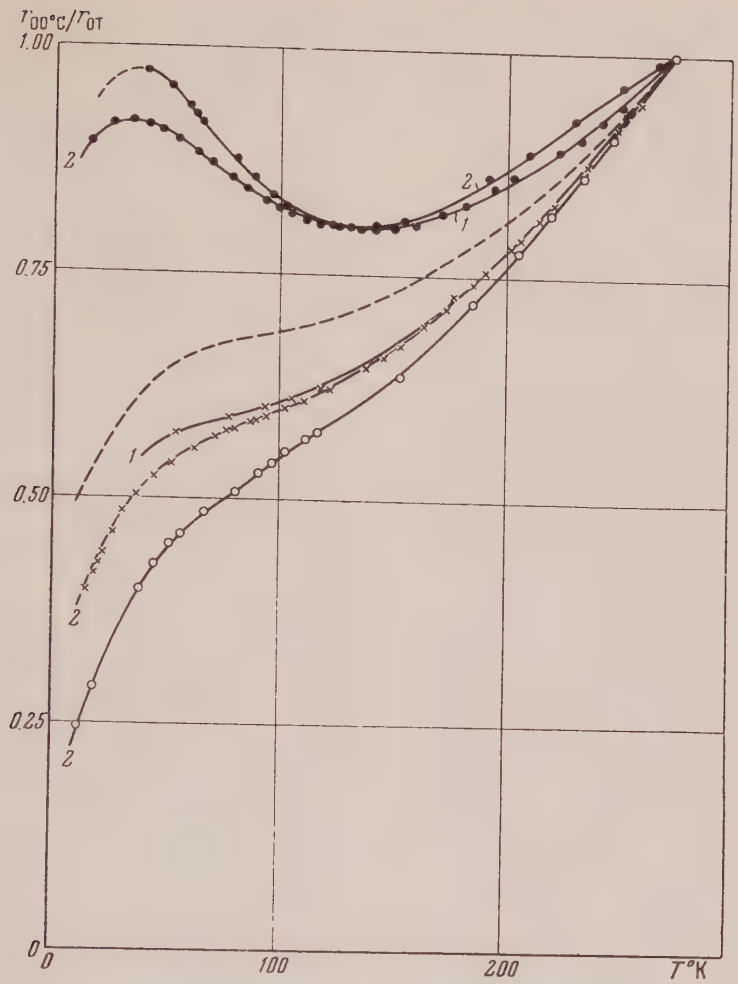

Fig. 3. Temperature dependence of electrical conductivity of bismuth with a 0.02% lead content.

1. Bi No. 14; *2.* Bi No. 8;

○- samples without pressure;

●- samples under pressure of 1500 atm.;

⊗ - after removal of pressure

$r(H)$ from those which are to to be expected from a model with an equal number of electrons and "holes", ($n_1 = n_2$). With the content of lead in bismuth reaching 0.02%, bismuth most likely corresponds to the case $n_1 \neq n_2$ and, although the variation of dependences of E_y/E_x upon H and $r(H)$ at uniform compression points toward a considerable change in the mobilities and in electronic concentration under the action of pressure, the determination of the magnitude of these changes requires experiments in considerably stronger magnetic fields. If, nevertheless, using the results with the purest bismuth, one evaluates the variation of electron concentration and mobility by regarding this as the case of a bi-zonal conductivity with an equal number of current carriers in each zone, it turns out that a uniform compression leads to a decrease in the concentration and mobility of current carriers. It is quite probable that one could thus explain the increase of electrical resistance of bismuth under a uniform compression at room temperatures, observed by Bridgman [16].

Mobility variations of conduction electrons and of their concentration under the influence of uniform compression, taking place evidently as a consequence of small variations of the lattice parameters, provides a basis for assuming that the

temperature variations of the lattice parameters may lead to analogous results. Thus, in addition to the previously noted change[17] in the concentration of current carriers in bismuth at temperatures higher than the degeneracy temperature of the electron gas, i.e., higher than 70-140° K, one can expect, for bismuth, a variation of the electron concentration related to the decrease of the lattice parameters upon cooling. The validity of this hypothesis could explain the lack of agreement in the curves of the dependence of the resistance of bismuth upon the magnitude of the effective magnetic field $H(r_{00°C}/r_{0T})$ (see references 3, 4) obtained at different temperatures, because the Köhler scheme[18] does not take into account the variation in the number of current carriers with temperature.

On the basis of these same considerations, a comparison of galvanometric properties of bismuth having different purities is not possible, because, in addition to the changes in the mean free path caused by the admixtures, a very strong variation in the electron concentration can take place. Therefore, the considerable discrepancy between the curves of the dependence of the Hall constant upon the magnitude of the magnetic field, discovered by Gerritsen and de Haas[10], and the curves of $\Delta r_{HT}/r_{0T}$ is $H(r_{00°C}/r_{0T})$, obtained by Borovik[3] for different samples of bismuth, is not surprising.

It is quite possible that the dependence of electron concentration upon pressure and the related dependence of electron concentration upon temperature may take place not only in bismuth, but also in a number of other metals and alloys.

It should be remarked that the oscillations of the Hall effect, preserved during the uniform compression, suggest the possibility of studying the influence of a uniform compression on the De Haas-van Alphen effect. This supposition becomes more probable if one evaluates the results of studies in references 10, 11, 12, which point out the correlation of the oscillation of the Hall e.m.f. with the magnetic susceptibility in bismuth.

A major part of the present work was conducted at the Cryogenic Laboratory of the Moscow State Institute of Measures and Measuring Apparatus, in connection with which we consider it our pleasant duty to express appreciation to the Director of the Laboratory, Prof. P. G. Strelkov and to A. S. Borovik-Romanov. We also express thanks to T. I. Kostina, N. M. Kreynes and V. V. Evdokimova for their assistance in conducting experiments.

Translated by D. E. Olshevsky
70

* A detailed communication about the results of the investigation of the influence of a uniform compression on pure bismuth will be published in the near future.

[1] E. S. Borovik, Doklady Akad. Nauk SSSR **70**, 601 (1950)

[2] E. S. Borovik, Doklady Akad. Nauk SSSR **75**, 693 (1950)

[3] E. S. Borovik, J. Exper. Theoret. Phys. USSR **23**, 91 (1952)

[4] E. S. Borovik, J. Exper. Theoret. Phys. USSR **23**, 83 (1952)

[5] D. Blokhintsev and L. Nordheim, Z. Physik **84**, 168 (1933)

[6] E. H. Sondheimer and A. H. Wilson, Proc. Roy. Soc. **190**, 435 (1947)

[7] N. E. Alexeevskii and N. B. Brandt, J. Exper. Theoret. Phys. USSR **22**, 200 (1952)

[8] N. E. Alexeevskii, N. B. Brandt and T. I. Kostina, Izv. Akad. Nauk SSSR, Ser. Fiz. **16**, 233 (1952)

[9] B. G. Lazarev and L. S. Kan, J. Exper. Theoret. Phys. USSR **14**, 470 (1944)

[10] A. N. Gerritsen and W. S. De Haas, Physica **7**, 802 (1940); **9**, 241 (1942)

[11] S. M. Reynolds, T. E. Leinhardt and H. M. Hemstreet, Phys. Rev. **93**, 247 (1954)

[12] T. G. Berlincourt and J. K. Logan, Phys. Rev. **93**, 348 (1954)

[13] E. S. Borovik and B. G. Lazarev, J. Exper. Theoret. Phys. USSR **21**, 857 (1951)

[14] W. S. De Haas and L. W. Schubnikov, Leid. Comm. Nos. 210a, 210b (1930)

[15] N. Thompson and H. H. Wills, Proc. Roy. Soc. **155**, 111 (1936)

[16] P. W. Bridgman, Proc. Am. Acad. Art and Sci. **72**, 157 (1938); **74**, 21 (1940)

[17] B. I. Davydov and I. Ia. Pomeranchuk, J. Exper. and Theoret. Phys. USSR **9**, 1294 (1939)

[18] M. Köhler, Ann. d. Physik **32**, 211 (1938)

On the Observation of Cerenkov Radiation Accompanying Broad Atmospheric Showers of Cosmic Rays

N. M. Nesterova and A. E. Chudakov
P. N. Lebedev Institute of Physics, Academy of Sciences, USSR

(Submitted to JETP editor November 30, 1954)
J. Exper. Theoret. Phys. USSR **28**, 384 (March, 1955)

CERENKOV radiation, generated during the passage of fast charged particles through matter, can take place not only in dense media, but also in air, under the condition of a sufficiently high velocity of the particles. The intensity of light emitted by each particle in this case is very small, but in the case of a passage through the atmosphere of broad showers of cosmic rays, when a large number of particles simultaneously create a directed radiation, this radiation can be registered above the background of the night sky light.

The first results on the observation of this phenomenon were published by Galbraith and Jelley[1,2]. Theoretically it was considered by Gol'danskii and Zhdanov[3].

We have conducted preliminary experiments on the investigation of flashes in the illumination of the night sky and on the determination of their connection with broad showers through the Cerenkov radiation which they generate. The work was conducted at a height of 3860 meters above sea level, on moonless nights. The intensity distribution of light flashes and their coincidence in time with the passage of broad showers was investigated. The apparatus consisted of a parabolic mirror with a diameter of 30 cm, a photomultiplier and an electronic network. The light which fell upon the mirror at an angle from 0° to 10° to the vertical, was focused upon the cathode of the photomultiplier. The amplitude of the electrical pulses of the photomultiplier was measured by means of a network with a resolution in time of 5×10^{-8} sec. The amplification ratio of the photomultiplier was regularly controlled during the experiments.

In measuring the distribution of the light impulses according to their magnitude, it was possible to register from 1.5 to 2 pulses a minute. Under these conditions, the background, determined by the current fluctuations in the photomultiplier, did not affect the results of the measurements. The measurement was being controlled by illuminating the photocathode by a constant source of light, creating the same current at the output of the photomultiplier.

Distribution of the pulse amplitudes, measured in a tenfold range, turned out to be close to a power law, with the exponent of the integral spectrum equal to -1.5. This form of the spectrum reminds one of the density spectrum of broad atmospheric showers.

Several experiments were also made during cloudy weather. At a height of the cloud layer of 2000 meters above the place of observations the number of pulses per minute decreased approximately to half its value. During the study of connection between light flashes and wide atmospheric showers, only those flashes were registered which coincided in time with the signal from the counter system. This system was situated at a distance of 70 meters from the mirror and represented a set of a large number of hodoscopic counters, directed by a scheme of multiple coincidences. With the aid of this arrangement showers were selected which had been created by primary particles with energies of about 10^{14} eV, the axes of which were located within the limits of a circle of a radius of 50 meters from the center of the counting system *.

It was found as the result of measurements that, in 5% of the cases, broad atmospheric showers were accompanied by light flashes, the intensity amplitude of which was above the level of our apparatus. Such a small percentage of coincidences is basically explainable by the fact that the light was being gathered within a space angle of 0.1 steradian, while the hodoscopic system registered showers passing at all possible angles to the vertical. The number of light flashes followed by registrations of showers in the hodoscopic system, turned out to be 25 times smaller than the total number of light flashes of the same amplitude. This should be explained by the fact that, in accordance with reference 3, the Cerenkov radiation of broad showers is distributed within the limits of a circle with the radius of about 250 meters and, consequently, the mirror system should register showers whose axes pass within a distance of 250 meters from the mirror system, while the counter system registered showers at distances up to only 50 meters.

Thus the experiments confirmed the possibility of observing the Cerenkov radiation engendered by wide atmospheric showers with an energy of 10^{14} eV.

Translated by D. E. Olshevsky
71

* Some 80% of the showers registered by the system passed within the limits of a circle of a 50 meter radius.

[1] W. Galbraith and J. V. Jelley, Nature 171, 349 (1953)

[2] J. V. Jelley and W. Galbraith, Phil. Mag. **44**, 619 (1953)

[3] V. I. Gol'danskii and G. B. Zhdanov, J. Exper. Theoret. Phys. USSR 26, 405 (1954)

In Connection with the Paper of Arifov, Aiuknanov and Starodubtsev[1]

M. A. Eremeev

(Submitted to JETP editor August 15, 1954)
J. Exper. Theoret. Phys. USSR 28, 376
(March, 1955)

IN the paper of Arifov, Aiukhanov and Starodubtsev[1], on the question of the decrease of the number of atoms adsorbed on a surface due to a rise in temperature, the following statement occurs: "As an example of such incorrect interpretations of the role of temperature we will cite one of the recent works of Eremeev[2], in which it is affirmed that the coefficient of secondary emission of electrons, due to ionic bombardment, diminishes with an increase in the temperature of the target". However, any reader can discover entirely different statements in my paper, namely, that at target temperatures which are not too high, the target becomes covered with ions adsorbed from the primary beam, so that, as the temperature of the target increases,the number of liberated electrons decreases at the same time that the number of particles adsorbed by the target also decreases. For some reason the authors of the paper in reference 1 remain silent on this point,even though they use these results immediately in their work.

During the last three years much has become known about the process of interactions of ions with surfaces and much has become precise as a result of the applications of the more recent methods of investigation, but the adsorption of ions from the primary beam and the dependence of electron emission (from the adsorbing layer) upon the target have not encountered further objection. It was possible to assume beforehand, that for hard targets this emission does not vanish completely with the increasing depth of the adsorbing layer, which in fact has been confirmed experimentally.

Translated by D. G. Posin
66

[1] U. A. Arifov, A. Kh. Aiukhanov and S. V. Starodubtsev, J. Exper. Theoret. Phys. USSR 26, 714 (1954)

[2] M. A. Eremeev, Doklady Akad. Nauk SSSR 79, 5 (1951)

The Degree of Orientation of Nuclei

G. R. Khutsishvili
Academy of Sciences, Georgian SSR

(Submitted to JETP editor October 11, 1954)
J. Exper. Theoret. Phys. USSR 28, 496-498
(April, 1955)

1. THE preparation of targets with oriented nuclei is of considerable interest to nuclear physics. Through experiments with oriented nuclei it is possible to obtain valuable information regarding spin dependence of nuclear forces, spins and magnetic moments of radioactive nuclei, etc. (see reference 1).

We shall limit ourselves to the examination of the most important case in which the quantization of the nuclear spin is axially symmetric. In this case the degree of orientation of the nuclear spins is usually described quantitatively by the values f_k, expressed as follows[2]:

$$f_k = \frac{(2I-k)!}{(2I)!}\sum_m a_m \times\left[\sum_{\nu=0}^{k}(-1)^\nu \frac{(I-m)!\,(I+m)!}{(I-m-\nu)!(I+m-k+\nu)!}\binom{k}{\nu}^2\right]. \quad (1)$$

where m = projection of the nuclear spin on the axis of quantization, I = maximum projection, a_m = relative population of states having spin projection equal to m, k takes on values 1, 2, . . . $2I$. The quantities f_k are normalized in such a way as to make the maxima of their absolute values equal to one. In particular, we have (the bar denoting the average over all the nuclei of a given type in the sample),

$$f_1 = \bar{m}\,/\,I, \quad (2)$$

$$f_2 = \frac{3}{I(2I-1)}\left[\overline{m^2} - \frac{1}{3}I(I+1)\right], \quad (3)$$

$$f_3 = \frac{5}{I(I-1)(2I-1)}\left[\overline{m^3} - \frac{1}{5}(3I^2+3I-1)\,\bar{m}\right], \quad (4)$$

$$f_4 = \frac{35}{2I(I-1)(2I-1)(2I-3)} \times\left[\overline{m^4} - \frac{1}{7}(6I^2+6I-5)\,\overline{m^2} + \frac{3}{35}I(I-1)(I+1)(I+2)\right]. \quad (5)$$

In the works of references 3, 4, f_1 and f_2 have been computed for different methods of production of oriented nuclei. However, in the above researches, a case is considered for which the differences in the energies of states corresponding to various m are much smaller than kT, i.e., a case

for which the degree of orientation of nuclei is small. Now it is important to have expressions for f_k for the case of a great degree of orientation. In reference 5 expressions for a_m are given; these expressions hold also in the case where the degree of orientation is great. Yet the final formulas rendering various oriented nuclei effects (angular distribution of radioactive radiation of oriented nuclei, e.g.) contain quantities f_k, and not a_m.

In the present article we shall give expressions for f_1, f_2, f_3 and f_4 for three methods of preparation of oriented nuclei.

2. In the first instance we shall obtain quantities f_k for polarization of nuclei by external fields. Energy levels of the nuclear spin in an external field H are given by

$$E_m = -m(\mu/I)H, \tag{6}$$

where μ = magnetic moment of the nucleus. A simple calculation yields

$$f_1 = B_I(\alpha I), \tag{7}$$

$$f_2 = \frac{2(I+1)}{2I-1} - \frac{3}{2I-1}\operatorname{cth}\frac{\alpha}{2}B_I(\alpha I), \tag{8}$$

$$f_3 = \frac{5}{(I-1)(2I-1)}\left\{\left[\frac{3}{2}\operatorname{cth}^2\frac{\alpha}{2}+\frac{1}{5}\right.\right. \tag{9}$$

$$\left.\left.\times\left(2I^2+2I-\frac{3}{2}\right)\right]B_I(\alpha I)-(I+1)\operatorname{cth}\frac{\alpha}{2}\right\}$$

$$f_4 = \frac{4(I+1)(I+2)}{(2I-1)(2I-3)} - \frac{5\operatorname{cth}(\alpha/2)}{2(I-1)(2I-1)(2I-3)} \tag{10}$$

$$\times\left\{\left[21\operatorname{cth}^2\frac{\alpha}{2}+8I^2+8I-9\right]\right.$$

$$\left.\times B_I(\alpha I)-14(I+1)\operatorname{cth}\frac{\alpha}{2}\right\}$$

In the above

$$\alpha = \mu H/IkT, \tag{11}$$

and B_I is the so-called Brillouin function:

$$B_I(y) = \frac{I+1/2}{I}\operatorname{cth}\left(\frac{I+1/2}{I}y\right) - \frac{1}{2I}\operatorname{cth}\left(\frac{y}{2I}\right). \tag{12}$$

3. Some years ago two methods for obtaining oriented nuclei in paramagnetic salts were proposed[1,6]. Those methods were based on the interaction of the nuclear spin with the spin of the electronic shell of the paramagnetic ion. The Hamiltonian describing a paramagnetic ion (nucleus possessing a spin) in an external magnetic field, can be written

$$V = \beta[g_\parallel H_z S_z + g_\perp(H_x S_x + H_y S_y)] + D \tag{13}$$

$$\times\left[S_z^2 - \frac{1}{3}S(S+1)\right]$$

$$+ [AS_z I_z + B(S_x I_x + S_y I_y)],$$

where I = nuclear spin, S = effective spin of the electron shell, β = magneton, A, B, and D are constants, obtainable from experimental data on the superfine structure of the paramagnetic resonance. Equation (13) is valid if the electric fields of the paramagnetic ion inside the crystal are axially symmetric, (usually the symmetry is rhombohedral or tetragonal, but close enough to axial); z is the symmetry axis of the internal crystal field. This axis is the direction of quantization for the spin of the nucleus and the spin of the electron shell of our paramagnetic ion. In the formula (13), $g_\parallel$ and $g_\perp$ are the g-factors of the electron shell of the paramagnetic ion, along and perpendicular to the z-axis, respectively.

In the case of paramagnetic salts of cobalt, copper and manganese, and also for some rare earths, the constants A and B are of the order 10^{-2} cm^{-1}. Now in most cases the effective spin of the electronic shell S is equal to one half, so that the D term of (13) vanishes. We shall limit ourselves to this case. Moreover, we shall deal with a monocrystal and assume that the z-direction is the same for all ions under consideration. In the case of Tutton's salts there are two non-equivalent groups of paramagnetic ions. Therefore, in this case, the quantities f_k, obtained below, must be averaged over these two groups.

4. If A is not equal to B, the nuclei will be oriented at very low temperatures, even in the absence of a magnetic field[6]. In this case the quantities f_k with odd k's vanish, (case of the so-called "lined-up" nuclei). In particular, for most paramagnetic salts of cobalt and copper, A is much greater than B. Let us first consider the case where $B = 0$, $S = \frac{1}{2}$, $H = 0$. Equation (13) gives $V = AS_z I_z$ and we get $2I + 1$ doubly degenerate levels:

$$E_m = \pm\tfrac{1}{2}Am.$$

A straightforward calculation shows that the quantities f_k with even indices are the same as in

the case of polarization by external fields, i.e., Equations (8) and (10) hold again, where, however,

$$\alpha = A / 2kT. \tag{14}$$

5. Again let $S = \frac{1}{2}$, $H = 0$. It has been shown in reference 6 that with a Hamiltonian

$$V = AS_z I_z + B(S_x I_x + S_y I_y) \tag{15}$$

mixing of states with different m takes place. In particular the state m, $M = \frac{1}{2}$ mixes with the state $m + 1$, $M = -\frac{1}{2}$ (M is the projection of the electronic shell spin on the z-axis). In the same reference the following corresponding energy levels were obtained

$$E_m = -\tfrac{1}{4}A \pm \tfrac{1}{2}\sqrt{A^2K^2 + B^2[(I+\tfrac{1}{2})^2 - K^2]} \tag{16}$$

where $K = M + m$.

Let B be much smaller than A and kT. We shall find f_2 up to terms quadratic in B, i.e., we shall keep terms of the order $(B/A)^2$, $(B/kT)^2$ and (B^2/AkT). We shall neglect terms of higher order. Calculation for $I = 3/2$ gives

$$f_2 = \operatorname{th}\frac{A}{2kT}\operatorname{th}\frac{A}{4kT} - \frac{3}{8\left(\operatorname{ch}\frac{3A}{4kT} + \operatorname{ch}\frac{A}{4kT}\right)^2} \times \left(\frac{B}{A}\right)^2 \phi\left(\frac{A}{kT}\right), \tag{17}$$

where

$$\phi(x) = (1 - x + 2/3\,x^2)e^{x} - (1 + x)e^{-x} \tag{18}$$

$$- 2xe^{\frac{1}{2}x} - (1 - 2/3\,x^2)e^{-\frac{1}{2}x} + e^{3/2\,x}$$

6. To produce polarized nuclei an external field of a few hundred oersteds must be imposed on the refrigerated salt[1,6]. At very low temperatures this induces a considerable polarization shell spins of paramagnetic ions, which in turn produces a considerable polarization of nuclei.

We shall examine quantitatively the following simple case: A monocrystal of paramagnetic salt, $S = \frac{1}{2}$, $A \gg B$ [we neglect the B term in Eq. (13)], with the external field in the z-direction. Here the energy levels are given by

$$E_m = \pm\tfrac{1}{2}(Am + \beta g_{\parallel} H). \tag{19}$$

A simple calculation shows that the quantities f_k, with k even, are the same as in the case of polarization by external fields [α given by Eq. (14)]. The odd-index f_k are obtained by multiplying Eqs. (7) and (9) by tank $\frac{g_{\parallel}\beta H}{2kT}$ [α given by Eq. (14)].

Translated by O. Bilaniuk
86

[1] R. J. Blin-Stoyle, M. A. Grace and H. Halban, Progr. in Nuclear Phys. 3, 63 (1953)

[2] S. R. de Groot, Physica 18, 1201 (1952)

[3] A. Simon, M. E. Rose and J. M. Jauch, Phys. Rev. 84, 1155 (1951)

[4] N. R. Steenberg, Phys. Rev. 93, 678 (1954)

[5] N. R. Steenberg, Proc. Phys. Soc. (London) 66A, 399 (1953)

[6] B. Bleaney, Phil. Mag. 42, 442 (1951)

The Spontaneous Fission of Thorium

A. V. Podgurskaia, V. I. Kalashnikova, G. A. Stoliarov, E. D. Vorob'ev and G. N. Flerov

(Submitted to JETP editor January 18, 1955)
J. Exper. Theoret. Phys. USSR 28, 503-505 (April, 1955)

In recent years there have been several references in the literature[1-5] to the spontaneous fission of thorium. According to the data of Segrè[5], the half life of the spontaneous process is 1.4×10^{18} years. We should like to point out that the probability of spontaneous fission indicated by these investigations is considerably too high.

In references 1,3, the spontaneous fission of thorium was observed by detecting the accompanying neutrons, the number of neutrons per spontaneous fission being presumably the same as the number per induced fission (i.e., 2-3). This method is suitable for the observation of spontaneous fission in uranium, but may be susceptible to error in the case of thorium, where the ex-

pected effect is very small. The chief sources of error involved in observing spontaneous fission by detecting the fission neutrons are the following: a) contamination of the thorium by traces of uranium, and b) contamination of the thorium by minute quantities of light elements. The first possibility can be easily controlled by carrying out special experiments to measure the amount of uranium in the thorium sample. Traces of light elements (Be, B, Si, etc.) in the material under investigation lead to neutrons through the (α, n) reaction in light nuclei. These processes are difficult to eliminate and are especially troublesome in thorium, where the energy of the α particles can be more than 8 Mev.

Segrè[5] detected spontaneous fission by directly observing the ionization due to fission fragments. Using this method, he conducted a long experiment in which 178 fission events were recorded in 6300 hours of operation with a chamber containing about 0.2 grams of effective thorium. Attributing these events to the spontaneous fission of thorium, the half life was calculated to be 1.4×10^{18} years, as noted above.

In 1940-41, attempts[6,7] to detect the spontaneous fission of thorium by using a large ionization chamber gave negative results. These investigations established a lower limit to the thorium half life of 10^{19} years.

In 1947, during a series of experiments on cosmic ray induced fission in heavy nuclei (uranium, thorium, bismuth) we found it necessary to know the half life of thorium more accurately. The spontaneous fission of thorium was observed by placing the substance to be investigated on plates in an ionization chamber and detecting the ionizing fission fragments. The sensitivity of the method was increased by using a multi-plate variant of the ionization chamber[6] which allowed us to increase the amount of effective thorium to 10-12 grams. Thorium oxide was used as the working substance on the plates. The amount of effective thorium was measured by comparing the fission rate in a thorium loaded chamber irradiated by fast neutrons from a Po + Be source, with the rate induced by the same source in the same geometry in a uranium loaded chamber. A measurement of the spontaneous fission rate in uranium gave the absolute amount of uranium present, while the ratio of the fast neutron fission cross section in uranium to that in thorium was taken to be 4.

The percent contamination of thorium by uranium was measured by comparing the fission rates in thorium and uranium loaded chambers irradiated by slow neutrons from a Raγ + Be source.

TABLE I

Chamber	Number of Fissions per Atom		Amount of Effective Substance in grams
	Po + Be Source	Without Source	
With thorium	98±6	—	11±1.5
With uranium	280±10	100±5	5±0.5

TABLE II

Chamber*	Number of fissions per hour (Raγ + Be source)		
	Surrounded by paraffin	Surrounded by paraffin and cadmium	Effect of thermal neutrons
With thorium	2.0±0.2	0.6±0.1	1.4
With uranium	24000	850	23150

* The amount of effective substance in the chambers was the same.

As can be seen from the tables, there were about 10 grams of effective thorium containing not more than 0.006% of uranium.

The smallness of the expected effect demanded special care in carrying out the measurements and the complete absence of any extraneous effects. Accordingly, the pulses at the amplifier output were registered in such a way that it was possible to record their size also. With this method of detecting spontaneous fission it was possible to monitor the apparatus continuously, which was very convenient, considering the long time of observation.

The results of experiments with the large thorium chamber (effective amount of thorium, 11 ± 1.5 grams) showed that the number of fission fragments counted per unit time depended appreciably on the external conditions of the experiment. These experimental results are shown in Table III.

TABLE III

Experimental Conditions	Time of observation, hours	Number of fission events	Number of fissions gram-hour	Half life
Laboratory attic	381	56	0.013	$1.5 \cdot 10^{19}$ yrs
Cellar (10 meters of soil above apparatus	392	8	0.002	10^{20} yrs

Both the dependence on external conditions (attic, cellar) and the absolute magnitude of the effect (0.002 - 0.013 fissions per gram-hour at sea level) agree well with the results of our experiments on cosmic ray induced fission in heavy nuclei at sea level and at high altitudes. As can be seen from Table III, the effect of fission in the chamber decreases by a factor of 6-7 when the apparatus is moved from attic to cellar. Hence the number of fission events in thorium which can be ascribed to the spontaneous mechanism is not more than 0.002 fission per gram-hour. It is well to note also that at least half of the effect in the cellar must be attributed to the spontaneous fission of uranium nuclei, which constituted 0.006% of the thorium sample investigated (see above).

In this way, our experiments with a big ionization chamber detecting fission fragments indicate that the probability of spontaneous fission in thorium is very small, the half life being more than 10^{20} years.

Our results on thorium fission at sea level differ from those of Segre, which were apparently carried out under the same conditions, by a factor of 10, approximately. If we discard the possibility of trivial mistakes in the work of Segrè, such as the contamination of his chamber by traces of artificial transuranium elements (for instance, Pu^{240}), or the improbable presence in his apparatus of vanishingly small quantities of natural transuranium elements, then considering our data it appears difficult to explain the fact that the rate of spontaneous fission in thorium observed by Segre was a whole order of magnitude larger than the rate induced in thorium by cosmic rays at sea level.

Translated by R. Krotkov
88

[1] H. Pose, Z. Physik 121, 293 (1943)

[2] N. A. Perfilov, J. Exper. Theoret. Phys. USSR 17, 476 (1947)

[3] F. R. Barclay, W. Galbraith and W. J. Whitehouse, Proc. Phys. Soc. (London) 65 A, 73 (1952)

[4] G. T. Seaborg, Phys. Rev. 85, 157 (1952)

[5] E. Segrè, Phys. Rev. 86, 21 (1952)

[6] K. A. Petrzhaki and G. N. Flerov, J. Exper. Theoret. Phys. USSR 10, 1013 (1940)

[7] E. S. Panasiuk and G. N. Flerov, Doklady Akad. Nauk SSSR 30, 699 (1941)

The Momentum Distribution in the Statistical Model of the Atom

S. I. LARIN
Moscow State University
(Submitted to JETP editor December 4, 1954)
J. Exper. Theoret. Phys. USSR 28, 498-501
(April, 1955)

1. In the statistical model of Thomas-Fermi, the distribution of the angular momentum over the particles can be determined. The number of particles with given angular momentum L is expressed by the equation[1]

$$n(L) = \frac{4L}{\pi} \int [r^2 P^2(r) \quad L^2]^{1/2} \frac{dr}{r}, \qquad (1)$$

where $P(r)$ is the maximum momentum for a given point. The mean value of the square of the orbital momentum, $\overline{L^2}$, has been determined by Jensen and Luttinger[2] from the momentum distribution (1). Taking the potential distribution of the atom to be that of the simple Thomas-Fermi model, the latter authors found $\overline{L^2}$, and compared it with the experimental data obtained for the electron level

scheme. Interest exists in a comparison of $\overline{L^2}$ from the Thomas-Fermi model, with exchange interaction of the electrons, with the $\overline{L^2}$ from the simple Thomas-Fermi model, and with experiment.

The mean square of the orbital momentum is given by

$$\overline{L^2} = \frac{1}{Z}\int L^2 n(L)\, dL = \frac{8}{15\pi Z}\int_0^\infty [rP(r)]^5 \frac{dr}{r}. \qquad (2)$$

The value of $\overline{L^2}$ can be determined here if the spatial distribution of particles, associated with $P(r)$, is known. In the case of the atom, $\rho(r)$ or $P(r)$ can be expressed by a self-consistent potential which is obtained as the solution of the Thomas-Fermi equation or of the Thomas-Fermi-Dirac equation. In the latter case, when[1]

$$\rho(r) = \frac{Z}{4\pi\mu^3}\left[\left(\frac{\psi}{x}\right)^{1/2} + \beta_0\right]^3; \quad r = \mu x; \qquad (3)$$

$$\mu = \left(\frac{9\pi^2}{128Z}\right)^{1/3} a_0; \quad \beta_0 = \left(\frac{3}{32\pi^2}\right)^{1/3} Z^{-1/3}$$

where $\psi(x)$ is the solution of the Thomas-Fermi-Dirac equation for the corresponding boundary conditions, we can get the following form for $\overline{L^2}$

$$\overline{L^2} = \frac{2}{5}\left(\frac{3\pi}{4}\right)^{2/3} Z^{2/3}\int_0^\infty x^4\left\{\left(\frac{\psi}{x}\right)^{1/2} + \beta_0\right\}^5 dx. \qquad (4)$$

For the simple Thomas-Fermi model, we get, for $\beta_0 = 0$ ($\psi \to \infty$),[2]

$$\overline{L^2}_{\text{T}-\Phi} = \frac{2}{5}\left(\frac{3\pi}{4}\right)^{2/3} Z^{2/3}\int_0^\infty (x\varphi)^{3/2}\frac{dx}{x} = 0{,}262\cdot Z^{2/3} \qquad (5)$$

(Here the integral is a constant, equal to 0.370.) It is easy to show that the integral in Eq. (4) will also be a function of Z. Making use of the numerical solution of the Thomas-Fermi-Dirac equation for inert gases[3], we found $\overline{L^2}$ for them. These results were plotted on a graph (see the Figure), where the empirical data, determined from the electron level scheme in the atom according to the formula

$$\overline{L^2}_{\text{опыт}} = \frac{1}{Z}\sum_i l_i(l_i+1) \quad (\hbar = 1). \qquad (6)$$

(summed over all Z electrons), are also plotted.

The values of $\overline{L^2}$ obtained from Eq. (4) are in better agreement with experiment at high values of Z than the values of $L^2_{\text{T-F}}$ from Eq. (5). The agreement is somewhat worse for the light atoms. We meet with a similar situation in the calculation of the total binding energy of the atoms, and also in the calculation of the value of Z at which the l state first appears (the "first appearance of the l state", see below). Nevertheless, inclusion of exchange improves the results of the calculations of a whole series of properties of the heavy atoms.

2. The distribution of angular momentum (1) was applied to the calculation of the first appearance in atoms of electrons with given orbital momentum by Fermi, and to the calculation of the limits of the l state of nucleons in nuclei by Ivanenko and Rodichev[4], and by other authors[5-7]*.

There are a number of unclear aspects to this problem. These are connected essentially with the continuous spectrum of the angular momentum in the Thomas-Fermi model. The first appearance of a state with given orbital momentum L is determined by the condition

$$n(L) = 0, \qquad (7)$$

where L is determined to be $l + \frac{1}{2}$ or** $[l(l+1)]^{1/2}$.

As was noted by Paneth[8], the total number of particles in the system for which $n(l) = 1$, is larger by one than the total number of particles for which $n(l) = 0$. The reason for this difference lies in the fact that the momentum is not quantized, so that, when a single particle is added to a given system, it does not receive a definite momentum, exceeding that corresponding to the maximum for the degree of filling. Rather, the particle is "distributed" continuously over the surface of the momentum sphere. Thus the $(N+1)$st particle will be distributed continuously over states with L ranging from zero to $rP_{N+1}(r)$. Therefore, for example, in the simple Thomas-Fermi model, the appearance of the d state in the atom will be found at $Z = 21.0$ from the relation

$$n(L) = 1, \qquad (8)$$

and at $Z = 19.4$ from Eq. (7). The location of the first appearance of the l state can also be determined from the condition that the number of particles with angular momentum greater than a given L,

$$n(L) = \int_L^\infty n(L)\, dL$$

will be zero:

$$N(L) = 0, \tag{9}$$

$$N(L) = 1. \tag{10}$$

or unity:

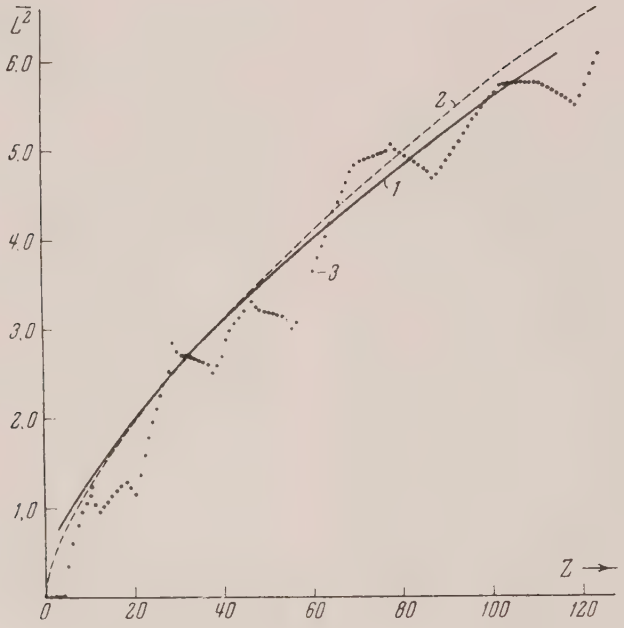

Mean value of the square of the orbital momentum of electrons in an atom. *1.* Thomas-Fermi-Dirac model [from Eq. (4)]; *2.* Thomas-Fermi model [from Eq.(5)]; *3.* empirical values from Eq. (6).

The next larger integer should be used for this first appearance in the results from Eq. (9) and also from Eq. (7). Jensen and Luttinger[2] suggested the determination of the first appearance of l from the relation

$$N\left\{\frac{[l(l+1)]^{1/2}+[l(l-1)]^{1/2}}{2}\right\} - N\left\{\frac{[l(l+1)]^{1/2}+[(l+1)(l+2)]^{1/2}}{2}\right\} = 1 \tag{11}$$

(Here $L = [l(l+1)]^{1/2}$.) We note that the latter relation, in view of the remark of Paneth[8] previously cited, reduces essentially to

$$N\left\{\frac{[l(l+1)]^{1/2}+[l(l-1)]^{1/2}}{2}\right\} = 1.$$

The question naturally arises: which of the determinations (7) - (11) of the first appearance is more accurate? We first note that the determinations from Eqs. (7) and (9) agree with each other. Following the remark of Paneth, we consider those determinations to be more accurate because the particle, as an entity, ought to receive a definite, higher angular momentum, in accordance with quantum mechanics. We should strictly apply the Thomas-Fermi method in this case only for systems with filled shells with spherically symmetric (5).

The determination of the limits of the l states from Eqs. (7) and (9) agrees, in the simple Thomas-Fermi model, with the determination of the first appearance from the condition of the tangency of the abscissa to the curve of "effective potential energy". In the calculation of the exchange interaction, it is impossible to express the entire

potential energy by a potential function and the determination becomes incorrect. The limits of the s, p, d, . . . , states can then be determined from Eq. (7) or Eq. (9), which reduce to the condition

$$[r^3\rho(r)]_{\text{макс}} = (1/24\pi^2)[4l(l+1)]^{3/2}.$$

Substituting $\rho(r)$ from the Thomas-Fermi-Dirac model (3), we get

$$Z_l = \gamma(Z)[4l(l+1)]^{3/2},\quad \gamma(Z) = \frac{1}{6\pi}[(x\psi)^{1/2} + \beta_0 x]^{-3}_{\text{макс}}. \tag{12}$$

By a numerical method, analogous to that of Ivanenko and Larin[9], we found for the limits of the s, p, d, and f states, $Z_l = 1$, 4, 19, 53, respectively, if $L = [l(l+1)]^{1/2}$, and $Z = 1$, 4, 20, 55 if $L = l + \frac{1}{2}$. Thus the Thomas-Fermi-Dirac model gives $\gamma(Z)$ with $\gamma = 0.155$ (which follows from the simple Thomas-Fermi model) only for sufficiently large Z.

In conclusion, gratitude is expressed to Prof. D. D. Ivanenko and N. N. Kolesnikov for their consideration of the problems examined here.

Translated by R. T. Beyer
87

* In Born and Yang[7] the parameters of the density distribution of nucleons in the nucleus are determined, in essence, by the number of the "first appearance". In this case there correspond to the numbers of the first appearance of the p, d and f states in reference 7, l of one integer less, i.e., l 0, 1 and 2, respectively. The numbers of the first appearance of the g, h and i states under the same conditions do not agree with experiment.

** The relative difference in the expressions $l + \frac{1}{2}$ and $[l(l+1)]^{1/2}$ is substantially greater for small l, since $l(l+1) = (l+\frac{1}{2})^2 - 1/4$.

[1] P. Gombas, *Statistical Theory of the Atom and Its Applications*, Moscow, 1951

[2] J. H. D. Jensen and J. M. Luttinger, Phys. Rev. **86**, 907 (1952)

[3] P. Gombas, and R. Gaspar, Acta Phys. Hung. **1**, 66 (1951)

[4] D. D. Ivanenko and V. Rodichev, Doklady Akad. Nauk SSSR **70**, 605 (1950)

[5] D. D. Ivanenko and A. Sokolov, Doklady Akad. Nauk SSSR **74**, 33 (1950)

[6] P. Gombas, Acta Phys. Hung. **2**, 247 (1952)

[7] M. Born and L. Yang, Nature **166**, 399 (1950); L. Yang, Proc. Phys. Soc. (London) **64 A**, 632 (1951)

[8] H. R. Paneth, Proc. Phys. Soc. (London) **64 A**, 937 (1951).

[9] D. D. Ivanenko and S. Larin, Doklady Akad. Nauk SSSR **88**, 45 (1953)

The Theory of the Dipole Lattice of Onsager

V. L. Pokrovskii
Novosibirsk Electrotechnical Institute of Communication

(Submitted to JETP editor November 3, 1954)
J. Exper. Theoret. Phys. USSR **28**, 501-503
(April, 1955)

In his paper[1] on phase transitions of the second kind in a plane dipole lattice, Onsager obtained the following expression for the logarithm of the partition function, per particle:

$$\ln\lambda^{(2)}(T) = \frac{1}{2\pi^2}\int_0^{\pi}\int_0^{\pi}\ln(\cosh 2\theta_1 \cosh 2\theta_2 - \sinh 2\theta_1 \cos\omega_1 - \sinh 2\theta_2 \cos\omega_2)\,d\omega_1\,d\omega_2. \tag{1}$$

Here $\theta_n = J_n/kT$ $(n = 1, 2)$; J_n is a constant characterizing the interaction between neighboring dipoles, and T is the temperature. Analysis[1,2] shows that Eq. (1) leads to a logarithmic divergence in the second derivative with respect to temperature, determined by the equation

$$\cosh 2\theta_1 \cosh 2\theta_2 - \sinh 2\theta_1 - \sinh 2\theta_2 = 0. \tag{2}$$

Taking one of the interaction constants to be zero, J_2, for example, Eq. (1) becomes a one dimensional integral:

$$\ln\lambda^{(1)}(T) = \frac{1}{2\pi}\int_0^{\pi}\ln(\cosh 2\theta - \sinh 2\theta\cos\omega)\,d\omega = \ln\cosh\theta, \tag{3}$$

which corresponds to a linear chain of dipoles.

It would seem natural[3] to conjecture that for a three dimensional dipole lattice, $\ln\lambda^{(3)}(T)$ would become a triple integral:

$$\ln \lambda^{(3)}(T) = \frac{1}{2\pi^3} \int_0^{\pi}\int_0^{\pi}\int_0^{\pi} \ln (\cosh 2\theta_1 \cosh 2\theta_2 \cosh 2\theta_3 - \sinh 2\theta_1 \cos \omega_1 - \sinh 2\theta_2 \cos \omega_2 - \sinh 2\theta_3 \cos \omega_3)\, d\omega_1\, d\omega_2\, d\omega_3. \quad (4)$$

However, Eq. (4) is incorrect, because for certain values of the temperature, it leads to complex values for the free energy. In particular, for the simple case of an isotropic lattice $\theta_1 = \theta_2 = \theta_3 = \theta$, it may be easily verified that the function $\cosh^3 2\theta - 3 \sinh 2\theta$ has a negative minimum at $\theta = 1/4$ Ar sinh 2.

It turns out that even the following more general form for $\ln \lambda^{(3)}(T)$ will not give the desired result. We shall show that taking $\ln \lambda^{(3)}(T)$ to be the following triple integral

$$\ln \lambda^{(3)}(T) = \int_0^{\pi}\int_0^{\pi}\int_0^{\pi} \ln F(\theta_1, \theta_2, \theta_3; \quad (5)$$

$$\omega_1, \omega_2, \omega_3)\, d\omega_1\, d\omega_2\, d\omega_3,$$

will not lead to a phase transition of the second kind if the function $F(\theta_k; \omega_k)$ $(k = 1, 2, 3)$ obeys the following conditions: 1) it is non-negative for all real values of its arguments; 2) $F(\theta_k; \omega_k)$ has no essential singularities.

The possible Curie points T_c are given by the zeros or poles of the function $F(\theta_k; \omega_k)$.* Let $F(\theta_k; \omega_k) = 0$ at $T = T_c$ and $\omega_k = \omega_k^0$. This point is at the same time a minimum of $F(\theta_k; \omega_k)$. In the neighborhood of this point F is a positive quadratic form in the variables $\tau = T - T_c$ and $x_k = \omega_k - \omega_k^0$, which by a rotation of the axes x_k, can be brought into the form:

$$F = a\tau^2 + \sum_{k=1}^{3} b_k x_k^2 + \tau \sum_{k=1}^{3} c_k x_k, \quad (6)$$

where a, b_k, c_k are functions of the structure constants.

The character of the singularity in $\ln \lambda(T)$ is determined from the integral of $\ln F$ over a small volume δ containing the point $x_k = 0$:

$$\mu(\tau) = \iiint_{\delta} \ln F(\tau, x_k)\, d^3x. \quad (7)$$

We transform variables according to the definition $y_k = \sqrt{b_k}\,(x_k + c_k/2b_k\,\tau)$. Considering τ to be sufficiently small, we integrate over a sphere of radius $r \gg (c_k/b_k)\,\tau$ with the center at the point $y_k = 0$. Changing to spherical coordinates, we obtain

$$\mu(\tau) = 4\pi \int_0^r \ln (a'\tau^2 + \rho^2)\, \rho^2\, d\rho \quad \left(a' = a - \sum_{k=1}^{3} \frac{c_k^2}{4b_k^2} > 0\right) \quad (8)$$

After some simple manipulations we find that

$$\mu(\tau) = P(\tau) + A\tau^3 \arctan \frac{1}{\sqrt{a'}} \frac{r}{\tau}, \quad (9)$$

where $P(\tau)$ is an analytic function of τ and A is a coefficient. Eq. (9) shows that $\ln \lambda^{(3)}(T)$ together with its first two derivatives are continuous, while the third derivative has a finite jump.

Similar calculations show that the following expression for $\ln \lambda^{(n)}(T)$

$$\ln \lambda^{(n)}(T) = \int\int \ldots \int \ln F(\theta_k; \omega_k)\, d\omega_1\, d\omega_2 \ldots d\omega_n \quad (10)$$

$$(k = 1, 2, \ldots, n).$$

where the function F obeys the same conditions as before, gives a logarithmic divergence in the n'th derivative if n is even and a finite jump for odd n.

So far we have assumed that not all the second derivatives of F are zero at the point where $F(\theta_k; \omega_k) = 0$. Suppose now that all derivatives up to order $2s$ are zero. Then in the neighborhood of its zero F is a positive, homogeneous form of $2s$'th degree. We shall show that no divergences can occur before the third derivative of $\ln \lambda^{(3)}(T)$. The second derivative of $\mu(\tau)$ at $\tau = 0$ is

$$\left.\frac{d^2\mu}{d\tau^2}\right|_{\tau=0} = \iiint_{\delta} \left.\frac{d^2}{d\tau^2} \ln F(\tau; x_k)\right|_{\tau=0} d^3x \quad (11)$$

$$= \iiint_{\delta} \left.\frac{\left(\frac{\partial F}{\partial \tau}\right)^2 - F\frac{\partial^2 F}{\partial \tau^2}}{F^2}\right|_{\tau=0} d^3x.$$

The numerator and denominator are homogeneous polynomials in the variables x_k of degree $4s - 2$ and $4s$ respectively. Let us change to spherical coordinates ρ, ϑ, ϕ. Then $F^2(0; \omega_k) = \rho^{4s} F_1(0, \vartheta, \phi)$, where F_1 is the value of F on the unit sphere in the space of the x_k. Since the function F is positive and continuous on the unit sphere, $1/F_1^2$

is bounded. The numerator can be written in the form $\rho^{4s-2} F_2(\vartheta, \phi)$. Hence the integral (11) does not diverge, as claimed. A similar proof shows that in a space of any dimension n, all derivatives up to the $(n-1)$th, inclusive, are continuous.

The above suggests that the presence of a phase transition of the second kind in Onsager's plane lattice is connected with the dimensionality of the space. In particular, we may expect that Onsager's model does not give a phase transition of the second kind in a real three dimensional lattice and hence cannot explain the properties of a ferromagnet. This might indicate that in the three dimensional case not only interactions between neighboring dipoles need to be considered.

In conclusion, I would like to express my thanks to Prof. Iu. B. Rumer for his valuable suggestions and discussions during the course of this work.

Translated by R. Krotkov
89

* In the case of a one dimensional lattice, the corresponding function $\cosh 2\theta - \sinh 2\theta \cos\omega$ has no zeros. Hence the theory does not give a phase transition in this case.

[1] L. Onsager, Phys. Rev. **65**, 117 (1944)
[2] Iu. B. Rumer, Usp. Fiz. Nauk. **53**, 245 (1945)
[3] Newell and Montroll, Revs. Mod. Phys. **25**, 353 (1953)

The Spatial Distribution of Nuclear-active Particles in Broad Atmospheric Showers of Cosmic Rays

Iu. N. Vavilov, S. I. Nikol'skii and V. P. Sarantsev
P. N. Lebedev Institute of Physics, Academy of Sciences, USSR

(Submitted to JETP editor September 12, 1954)
J. Exper. Theoret. Phys. USSR **28**, 505-506
(April, 1955)

In autumn of 1952 we measured the spatial distribution of nuclear-active particles in broad atmospheric showers of cosmic rays at 3860 m of altitude. For this work we used a special arrangement with a considerable number of coincidence counters. This enables us to locate the axis and the number of charged particles of broad atmospheric showers which were of interest to us. The flux of nuclear- active particles was determined by the number of nuclear electron showers, produced in lead by the penetrating particles during the passage of a broad atmospheric shower.

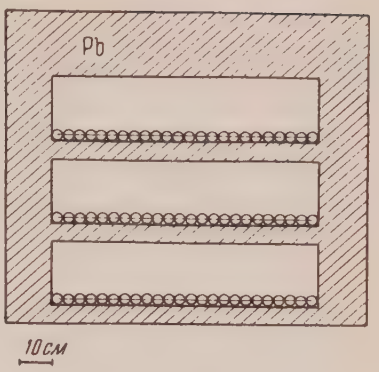

Fig. 1

The equipment for the observation of nuclear electron showers (Fig. 1) consisted of three groups of coincidence counters separated by shields of lead 6 cm thick. The presence of a 20 cm thick lead shield on the top of the counters allowed a reliable separation of penetrating particles belonging to the broad atmospheric shower from its photo-electronic component. The lead shielding on the bottom and the sides was 6 cm and 14 cm thick respectively.

The formation of the nuclear electron shower was characterized by the appearance of a discharge in two or more counters, placed in one row. The correction in lead due to μ mesons has been based on measurements of the number of δ showers produced in this apparatus by the hard component of the cosmic rays.

The relation between the observed number of nuclear electron showers produced by particles from broad atmospheric showers of a given energy at a given distance from the shower axis and the total number of broad atmospheric showers of same energy and same axis location can be expressed by the flux density of nuclear-active particles in the following way:

$$\frac{N_a}{N} = 1 - \exp\{-\rho\sigma(1 - e^{-x/\lambda})\}$$

Here ρ is the flux density of nuclear-active particles, σ is the counter surface recording the nuclear electron showers, x is the amount of matter in which the nuclear electron showers are produced, λ is the interaction path for nuclear-active particles ($\lambda = 160$ gm/cm^2 Pb). It is assumed that the probability of recording a nuclear electron shower originating in lead is unity, which may lower the flux density of nuclear-active particles*. The results of flux density measurements of nuclear-active particles obtained this way for different distances from the broad atmospheric shower axis

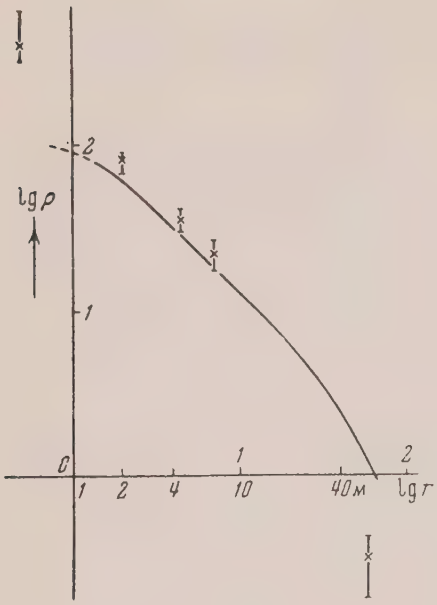

Fig. 2

are presented on Fig. 2. The log of the distance in meters is plotted on the abscissa and the log of flux densities on the ordinate (i.e., number of particles per m^2). The results are averaged around showers with 5×10^{13} to 1×10^{15} ev primary energy ($\overline{E}_0 = 1.5 \times 10^{14}$ ev). For the sake of comparison, the spatial distribution of all charged particles in broad atmospheric showers of same primary energy is given in the same Figure (solid curve). The particle flux density is given by the number of particles per square decimeter.

The concentration of nuclear-active particles around the shower axis as compared to the distribution of all charged particles is in accord with the assumption of balance of photo-electron component and the nuclear-active particles in a shower. Let us remark, that as shown by analysis of nuclear-electron showers with many particles, the energy flux carried by nuclear-active particles is even more strongly concentrated around the shower axis. The results obtained for the spatial distribution of nuclear-active particles allow us to determine the portion of nuclear-active particles in the whole shower. It is about 0.3 to 0.5% of the total number of charged particles.

In conclusion the authors express their gratitude to N. A. Dobrotin and G. T. Zatsepin for valuable advice during the design of experiments and the evaluation of results.

Translated by G. Cvijanovich
90

* The single parameter is the effective surface of the apparatus, apparently bigger than the effective surface of the counters, and of which the adopted value can increase the value of ρ.

[1] Iu. N. Vavilov, S. I. Nikol'skii and E. I. Tukish, Doklady Akad. Nauk SSSR 63, 233 (1953)

The Change in Dielectric Constant and Phosphors Under the Action of Infrared Light

E. E. Bukke
P. N. Lebedev Institute of Physics
Academy of Sciences, USSR
(Submitted to JETP editor December 2, 1954)
J. Exper. Theoret. Phys. USSR 28, 507-508
(April, 1955)

IN this paper results are presented of the investigation of the change of the dielectric constant and losses in unexcited, infrared light sensitive phosphors, irradiated in the wavelength region of $\lambda \approx 0.8\,\mu$ and $\lambda \approx 1.3\,\mu$. Radiation of these wavelengths falls, as it is known[1], in the maximum sensitivity range of these phosphors to the infrared radiation.

Phosphors with ZnS base were investigated. The test samples were prepared in the form of thin polystyrene films in which the phosphor under investigation was introduced (in 1:1 ratio by volume). The electrodes, an aluminum disk and a thin metallic grid, coated with polystyrene lacquer to prevent a direct contact between the grains of the scintillator and the electrodes, were pressed upon the film. The change in dielectric constant and the losses were measured during illumination of such a capacitor with infrared radiation through the grid electrode. The measurements were performed with an apparatus having a circuit similar to that of a Q-meter, at frequencies of about 50 kilocycles and field potential in the dielectric of 30-50 V/cm. The necessary wavelength ranges of infrared light were obtained by use of a monochromatic illuminator with wide slits (the width of the transmission range was approximately 100 mμ).

The infrared radiation acts upon the phosphors in the same way as the exciting radiation, causing an increase in dielectric constant and losses in unexcited phosphors (as it is known[2], the dielectric constant and the losses in excited phosphors decrease under influence of infrared radiation, approaching the "dark" values). The change which

we observed is approximately 20-50 times weaker than that induced by the action of exciting light. The establishing of a stationary condition of dielectric constant and losses under continuous action of infrared radiation proceeds relatively slowly. Thus, for instance, for Zn-Cu, Pb phosphor, the establishing of a stationary state requires 10-12 minutes under our conditions.

In all the phosphors tested, the change in dielectric constant and losses under irradiation with infrared light takes place only when the light of a certain wavelength causes a stimulation in the excited phosphor. However, in case the infrared radiation causes a quenching, there is either no change of dielectric constant and losses or the changes are very small. The basic results of investigation are given in the table below:

Phosphor	Optical effect of infrared radiation		Change of dielectric constant and losses under the action of infrared radiation	
	0.8 μ	1.3 μ	0.8 μ	1.3 μ
ZnS-Cu, Co	Quenching	Quenching	no	no
ZnS-Cu, Sm	Stimulation	Stimulation	yes	yes
ZnS-Cu, Tu	"	"	"	"
ZnS-Cu, Ni	"	Quenching	"	no
ZnS·CdS-Cu, Ni	"	"	"	"
ZnS-Cu, Pb	"	Stimulation	"	yes
ZnS·CdS-Mn, Ni	"	No effect	"	no

For the phosphors, ZnS·CdS-Cu, Ni and ZnS-Cu, Tu, which show the greatest change in dielectric constant and losses, the values of the dielectric constant and losses and the values of the stimulation brightness were measured as a function of wavelengths of infrared radiation. The results of these measurements are presented in the diagram. It is seen from the diagram that there is a rather good agreement between the position of the maxima of dielectric constant and the position of maxima of stimulation brightness. The shadowed area of this figure illustrates schematically the sensitivity range of phosphors to the infrared radiation (the reduction of the amount of light is independent of the type of action of the infrared radiation, regardless of whether this action is stimulating or quenching).

The influence of infrared radiation upon the unexcited phosphor has been noted previously[3]. It has been shown that the irradiation of phosphor with infrared radiation prior to the excitation changes the course of the curve of the growth of brightness. Experiments which we performed suggest that there is a connection between the excitation ability of the phosphor and the presence in it of centers which have a strong polarizability or even an ability to be ionized by infrared radiation, since the mechanism of excitation of these phosphors is related to the separation of charges. It should be noted that the results obtained indicate the difference in stimulation and quenching kinetics in phosphors tested.

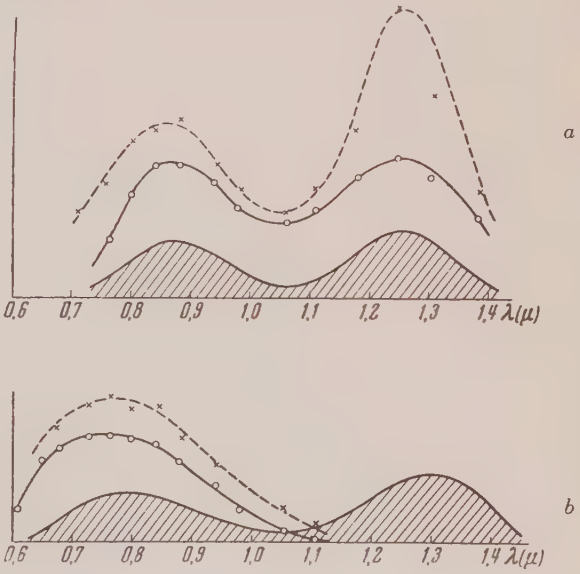

a. ZnS-Cu, Tu-phosphor, *b*. ZnS · CdS-Cu, Ni-phosphor. Continuous lines --- dielectric constant, dotted lines --- intensity of excitation.

In conclusion, I should like to take this opportunity to express my gratitude to V. V. Antonov-Romanovskii for his persistent interest in the work and his valued advice. Also, I express my gratitude to Z. A. Trapeznikova and V. V. Shchaenko for the preparation of phosphors with rare earth catalysts.

Translated by A. Cybriwsky
91

[1] N. T. Melamed, J. Electrochem. Soc. **97**, 33 (1950)

[2] H. Kallman, B. Kramer and A. Perlmutter, Phys. Rev. **89**, 700 (1953)

[3] S. A. Popok and F. D. Klement, J. Exper. Theoret. Phys. USSR **10**, 800 (1940); D. Klement, Izv. Akad. Nauk, Ser. Fiz. **13**, 141 (1949)

PARTIAL CONTENTS

DOKLADY AKADEMII NAUK SSSR VOLUME 100, NO. 1 JANUARY 1, 1955

HYDROMECHANICS

Kinetic Flow and Stability of Thin Fluid Layers on Solid Linings, Taking the Solvate Shell into Account as a Special Phase . . S. V. Nerpin and Assoc. Memb. B. V. Deriagin 17

ASTRONOMY

Possibility of Explaining the Nature of the Crab-shaped Nebula by Experimental Means . . . . . I. M. Gordon 21

MATHEMATICAL PHYSICS

On the Theory of the Multiplication of Causal Singular Functions . . . . . Acad. N. N. Bogoliubov and O. S. Parasiuk 25

PHYSICS

Seignette-ceramics with Sharply Expressed Nonlinear Properties . . . T. N. Verbitskaia 29

Secondary Electron Emission with (100) Boundaries of Single Crystal NaCl . . . . . L. N. Dobretsov and A. S. Titkov 33

Contribution to the Nuclear Model . . . . . D. Ivanenko, N. Kolesnikov and S. Larin 37

Generalization of Ward's Theorem in the Case of the Final Wavelength of Light for Particles with Spin 0 . . . . . Assoc. Memb. I. Pomeranchuk 41

Magneto-optic Properties of Excitons . . . . . A. G. Samoilovich and L. L. Korenblit 43

Computation and Interpretation of the Oscillatory Spectrum of Isobutylene . . . . . L. M. Sverdlov and O. N. Vinokhodova 45

GEOPHYSICS

Nutational Circumpolar Pressure Wave in the Earth's Atmosphere . . . . I. V. Maksimov 49

On Fundamental Types of Geomagnetic Activity . . . . . V. M. Mishin 53

BIOPHYSICS

On the Question of the Differential Diagnostics of Color Vision . . . . . A. B. Flekkel' 57

TECHNICAL PHYSICS

On the Effect of Tempering on the Graphitization of Iron Carbide Alloys . . . . . K. P. Bunin and E. N.Pogrebnoi 61

Effect of Chromium on the Self-diffusion of Iron . . . . . P. L. Gruzin 65

Coupling Forces and Static Distortion in Crystals of Alloyed Ferrites . . . . . V. A. Il'ina and V. K. Kritskaia 69

DOKLADY AKADEMII NAUK SSSR VOLUME 100, NO. 2 JANUARY 11, 1955

HYDROMECHANICS

Integral Similarity of Vortex and Temperature Fields . . . . . A. M. Fainzil'ber 225

PHYSICS

Use of Inhomogeneous Magnetic Fields in Order to Increase the Resolving Power of Mass Spectrometers . . . . . N. E. Alekseevskii, G. P. Prudkovskii, G. I. Kosourov and S. I. Filimonov 229

Infra-red Radiation Band and Kinetics of Semiconducting Processes in Cadmium Sulfide in the Luminescence-extinction Temperature Range . . . . . V. A. Arkhangel'skaia 233

On Possible Use of Correlation Functions to Study Nuclear Transformations . . . . . V. I. Gol'danskii and M. I. Podgoretskii 237

Luminescent Chamber . . . . . Assoc. Memb. E. K. Zavoiskii, G. E. Smolkin, A. G. Plakhov and M. M. Butslov 241

Effect of Mechanical Pressure on Dielectric Properties of Seignette-ceramics . . . . . E. V. Siniakov and I. A. Izhak 245

GEOPHYSICS

Three Dimensional Problem of Flow by an Air Stream over the Rough Surface of the Earth . . . . . Assoc. Memb. I. A. Kibel' 247

'Short' Method of Determining the Transparency Coefficient of the Earth's Atmosphere . . . . . G. Sh. Livshitz 251

TECHNICAL PHYSICS

On the Pore Form Emerging during Mutual Diffusion of Metals . . . . Ia. E. Gegugin 255

CRYSTALLOGRAPHY

Obtaining Equilibrium Dropping of a Crystal-solution System . . . . . M. O. Kliia 259

DOKLADY AKADEMII NAUK SSSR VOLUME 100, NO. 3 JANUARY 21, 1955

HYDROMECHANICS

On the Question of the Approximate Integration of the Equations of Plane Steady Supersonic Gas Motion . . . . . A. A. Grib and A. G. Riabinin 425

MATHEMATICAL PHYSICS

On Deductive Formalism in the Multiplication of Causal Singular Functions . . . . . Acad. N. N. Bogoliubov and O. S. Parasiuk 429

On the Question of the Unitariness of the S-matrix in Quantum Field Theory with Nonlocal Interaction . . . . . B. V. Medvedev 433

PHYSICS

On the Theory of Skin Effect in a Constant Magnetic Field . . . . . M. Ia. Azbel' 437

Experimental Confirmation of the Landau Formula to Determine the Fluid Viscosity Coefficient by the Method of Damping the Torsional Oscillations of a Disc . . . . . G. A. Gamtsemlidze 441

Kinetic Temperature of Electrons in Metals and Anomalous Electron Emission . . . . . Assoc. Memb. V. L. Ginzburg and V. P. Shabanskii 445

On the Theory of the Electron Spectra of Condensed Systems . . . . . A. E. Glauberman 449

Determination of the Mass of a Charged Particle in Terms of the Scattering Residual Path on Plates in a Wilson Chamber . . . . . M. I. Daion 453

On the Effect of Energy Migration on the Polarization of Fluorescent Single Crystals . . . . . N. D. Zhevandrov 455

Optical Properties of a Dielectric Mirror with Oblique Light Incidence . . . . . F. A. Korolev and A. Iu. Klement'eva 459

DOKLADY AKADEMII NAUK SSSR VOLUME 100, NO. 4 FEBRUARY 1, 1955

ASTRONOMY

Effect of Gallactic Configurations on the Dispersion of the Peculiar Velocities of Stars and Interstellar Clouds . . . . . G. M. Idlis 635

Identification of the Infra-red Spectra of Comets . . . . . S. M. Poloskov 639

MATHEMATICAL PHYSICS

On the Theory of Causal Singular Functions . . . . . O. S. Parasiuk 643

PHYSICS

On the Mechanism of Inhomogeneity Formation in the Ionesphere . . . . . B. N. Gershman and Assoc. Memb. V. L. Ginzburg 647

Gamma Ray Capture of Thermal Neutrons and the Structure of the Atomic Nucleus . . . . . L. V. Groshev 651

Exchange Scattering of Neutrons with 380 MeV Energy by Deutrons and the spin Dependence of the Exchange Forces . . . . . V. P. Dzhelepov, Iu. M. Kazarinov and V. B. Fliagin 655

Transition Effects and Angular Distribution for Single Cosmic Particles . . . . . A. P. Zhdanov and P. I. Fedotov 659

On the Study of Superspeed Light Processes . . . . . Assoc. Memb. E. K. Zavoiskii and S. D. Fanchenko 661

Dependence of the Charge of Lithium Ions on Their Speed . . . . . M. I. Kuznetsov, Acad. P. I. Lukirskii and N. A. Perfilov 665

On the Rotation of Liquid Helium . . . . . Acad. L. D. Landau and E. M. Lifshitz 669

$p + p \rightarrow d + \pi^+$ Reaction at 460 MeV . . . . .

Assoc. Memb. M. G. Meshcheriakov, B. S. Neganov, N. P. Bogachev and V. M. Sidorov 673
Formation of Mesons in the $p + p \rightarrow d + \pi^+$ Reaction in the 510-660 MeV Interval . . . . . Assoc. Memb. M. G. Meshcheriakov and B. S. Neganov 677
On Energy Losses of Charged Particles Moving in an Anisotropic Medium . . . . . A. G. Sitenko and M. I. Kaganov 681
On the Temperature Dependence of the Spectrum Intensity of Combination Scattering of a Gypsum Crystal . . . . . A. I. Stekhanov 685
Formation of π^0 Mesons by Protons with 670 MeV Energy in the Nuclei of Various Elements . . . . . A. A. Tiapkin, M. S. Kozodaev and Iu. D. Prokoshkin 689

ELECTROTECHNICS

Obtaining the Frequency Characteristics of an Automatic Regulation System Using Mikhailov Curves . . . . . O. P. Demchenko 693

+ Deceased

DOKLADY AKADEMII NAUK SSSR VOLUME 100, NO. 5 FEBRUARY 11, 1955

HYDROMECHANICS

Boundary Layer with a Shear Surface. Flow over a Plate with Fluid Escaping through Its Surface . . . . . G. G. Chernyi 867

MATHEMATICAL PHYSICS

On the Unsteady Flow of a Viscous Fluid with External Forces . . . . . A. A. Kiselev 871

PHYSICS

On Effect of Holes (Vacancies) in the Crystal Lattice on the Electron Resistance of Metals . . . . . Fellow B. G. Lazarev and O. N. Ovcharenko 875
Effect of Temperature on the Molecular Attracting Forces between Condensed Bodies . . . . . E. M. Lifshitz 879
Probable Ionization of μ-mesons in Gases in the 2×10^8 - 11.2×10^{11} eV/sec Pulse Band . . . . . V. A. Liubimov, G. P. Eliseev, V. K. Kosmachevskii and A. V. Kovda 883
Phase Transitions of the Second Kind in Bose Gases . . . . . Iu. V. Rumer 887
On the Question of the Introduction of Dynamic Variables in Quantum Field Theory . . . . . B. M. Stepanov 889
On the Rigid Dipole Moment of Colloid Particles in Water . . . . . N. A. Tolstoi 893
On the Problem of the Interaction of Two Quantum Fields . . . . . E. S. Fradkin 897

TECHNICAL PHYSICS

On the Diffusion of Antimony and Tin in the SbZn Semiconducting Compounds . . . . . B. I. Boltaks 901
Photometrization by the Flash Method in the Low Visibility Region . . . . . A. A. Vol'kenshtein and E. I. Dikan' 905

ELECTROTECHNICS

Mathematical Theory of the Synthesis of (1,k)-terminal Contacts . . . G. N. Povarov 909

CRYSTALLOGRAPHY

Electronographic Determination of the Structure of Cs_2CoCl_4 . . . . . G. N. Tishchenko and Z. G. Pinsker 913

DOKLADY AKADEMII NAUK SSSR VOLUME 100, NO. 6 FEBRUARY 21, 1955

MATHEMATICAL PHYSICS

Representation of Electromagnetic Fields by Retarded Potentials . . . I. S. Arzhanikh 1053

PHYSICS

Solution of the System of Equations for the Vacuum Functional . . . . . N. P. Klepikov 1057
On a New Derivation of the Equation for the Green's Function in Quantum Electrodynamics . . . . . M. K. Polivanov 1061

TECHNICAL PHYSICS

On the Correspondence of the Stability of Chemical Compounds and Electrical Durability . . . . . A. A. Vorob'ev, E. K. Zavadovskaia and A. M. Trubitsin 1065

Interference-polarized Light Filter for K Lines of Ionized Calcium . . . . . A. B. Gil'varg, G. I. Distler and E. A. Makarova 1067

Use of the Carbon Isotope C^{14} to Study Carbon Diffusion in Steel . . . . . P. L. Gruzin, V. G. Kostogonov and P. A. Platonov 1069

On the Question of Arsenic Diffusion in Steel . . . . . D. S. Kazarnovskii 1073

New Results on the Transformation of Perlite Carbon Steel into Austenite by Electrical Heating . . . . . Iu. A. Kocherzhinskii 1077

CRYSTALLOGRAPHY

Electronographic Investigation of the Bi-Se Alloy System . . . . . .

Electronographic Investigation of the Bi-Se Alloy System . . . . . S. A. Semiletov and Z. G. Pinsker 1079

CONTENTS

JOURNAL OF TECHNICAL PHYSICS, USSR VOLUME 25, NO. 6 JUNE, 1955

Bipolar Diffusion in Semiconductors with Considerable Currents . . . . . K. B. Tolpygo and I. G. Zaslavskaia 955

Electric Properties of Alloys of the NiTe-$NiTe_2$ System . . V. P. Zhuze and A. R. Regel' 978

Properties and Structure of Triple Semiconducting Systems. I. . . . . B. T. Kolomiets and N. A. Goriunova 984

Nernst Effect in Atomic Semiconductors Taking into Account Electron and Hole Scattering by Ionic Impurities . . . . . Iu. N. Obraztsov 995

Experimental Study of the Transverse Nernst-Ettinghausen Effect in Tellerium . . . . . N. V. Mochan 1003

New Method of Measuring Semiconductor Thermal Characteristics 1013

On the Theory of Good-conducting Semiconductors. I. . . . . L. L. Korenblit and T. Ya. Shraifel'd 1019

Photoelectron Emission from Alkali-halide Films Containing F-centers . . . I. M. Dykman 1026

Discharge Ignition Voltage in He, Ne, Ar, Kr and Xe at Low Pressures . . . . . A. N. Dikidzhi and B. N. Kliarfel'd 1038

Plastification of Polyvinylchloride Butadene Nitrile Copolymers. III . . . . . R. A. Reznikova, A. D. Zaionchkovskii and S. S. Voiutskii 1045

Thermal and Electric Properties of Hydrophobic Land . . . F. E. Koliasev and S. L. Levin 1053

Flow of a Viscous Gas in a Cylindrical Pipe with Heat Exchange and a Compression Shock . . . . . S. V. Romanenko 1058

On Thin Antenna Theory in Cavity Resonators . . . . . A. V. Gaponov 1069

Excitation of a Cavity Resonator by Thin Antennas . . . . . A. V. Gaponov 1085

Low Intensity Formations . . . . . A. A. Vol'kenshtein 1100

High Sensitivity Thermomagnetic Device to Study Phase Transformations in Steel . . . . . A. N. Alfimov 1105

Effect of Frequency on the Rectifying Property of Semiconducting Diodes for Low a.c. Volatge . . . . . S. C. Kalashnikov and N. A. Penin 1111

Theory of Electromagnetic Resonators Wich Approximate the Conical in Shape . . . . . A. S. Kompaneets and Iu. S. Saiasov 1124

Investigation of the Eddy Current Magnetic Fields in Planar Samples . . . T. M. Sycheva 1132

Radiation of Electric Oscillators Located Near a Perfectly Conducting Elliptic Cylinder . . . . . G. N. Kocherzhevskii 1140

Letters and Brief Communications

On the Criterion Establishing the Limits of Applicability of the Linear Law of Electron Damping in Solid Body on the High Energy Side . . . . . A. Ia. Viatskin 1155

On the Diffusion of Atom Impurities through the Contact Layer of Oxide Cathodes . . . . N. D. Morgulis and Yu. G. Ptushinskii 1157
On the Paper of N. N. Davidenkov, 'On the Nature of Collars in the Elongation of Samples' . . . . P. O. Pashkov 1160
Reply to P. O. Pashkov . . . . N. N. Davidenkov 1161

JOURNAL OF TECHNICAL PHYSICS, USSR VOLUME 25, NO. 7 JULY, 1955

Effect of Thermal Preparation on the Concentration and Mobility of Charge Carriers in Germanium . . . . V. V. Ostroborodova and S. G. Kalashnikov 1163
Recombination of Nonequilibrium Charge Carriers by Thermal Acceptors in Germanium . . . . V. V. Ostroborodova and S. G. Kalashnikov 1168
Bipolar Diffusion of Current Carriers in Semiconductors in the Case of Spherical Symmetry with an External Field (Linear Approximation) . . . . M. F. Deigen 1175
On the Theory of Good Conducting Semiconductors . . L. L. Korenblit and T. Ia. Shraifel'd 1182
Thermoelectric Properties of Antimony-Tellerium Alloy Systems . . . . . F. I. Vasenin 1190
Thermal Diffusion of Sodium Ions in Sodium Chloride Crystals . . . . T. I. Nikitinskaia and A. N. Murin 1198
Investigation of Relaxation Processes in Polyvinyl Acetate . . . . P. F. Veselovskii and A. I. Slutsker 1204
Investigation of Particle (High-frequency) Discharges in Paperoil Insulators . . . . G. S. Kuchinskii 1209
Measurement of the Heat Transfer Coefficient from a Gas Stream to a Furnace Charge under Nonadiabatic Heating Conditions .I. . . . . B. N. Vetrov and O. M. Todes 1217
Heating by Means of Longitudinal Heat Conduction of Granular Material in Pipes under Nonadiabatic Conditions, II. . . . . B. N. Vetrov and O. M. Todes 1232
Propagation of Thermal Waves when Heating a Furnace Charge by a Gas Stream, III. . . . . B. N. Vetrov and O. M. Todes 1242
Investigation of Light Phenomena Related to the Development of a Spark Discharge Channel . . . . M. P. Vaniukov, V. I. Isaenko and L. D. Khazov 1248
Certain Applications of Similarity and Dimensional Methods to the Theory of Coronal Discharge at Constant Voltage . . . . N. N. Tikhodeev 1257
Graphical Method of Studying Wavetrons . . . . V. M. Lopukhin and Iu. D. Samorodov 1265
Quantitative Radiography of Vegetables . . . . I. L. Finagina, A. L. Kartuzhanskii and B. P. Soltitskii 1276
On the Character of the Transition from Laminar to Turbulent Flow in the Boundary Layer . . . . L. M. Zysina-Molozhen 1280
Certain Quantitative Characteristics of the Transition from Laminar to Turbulent Flow in the Boundary Layer . . . . L. M. Zysina-Molozhen 1288
Two Simple Spectro-interference Methods of Studying Dispersion in the Visible and Ultraviolet Regions of the Spectrum . . . . I. S. Gorban' and A. A. Shishovskii 1297
On the Photoelectric Fluxmeter . . . . S. P. Kapitza 1307
New Hydrogen Lamp of Great Brightness . . . . . I. I. Kondilenko and M. P. Lisitsa 1316
On the Theory of Steam Jet Vacuum Pumps . . . I. M. Lifshitz and L. N. Rozensveitg 1323
On the Theory of the Optical Computation of Multi-layered Periodic Plates . . . . A. A. Vasil'kovskii 1326
Scientific Conference of the Siberian Physico-technical Institute . . . . S. S. Gutin and M. A. Krivov 1332

Letters and Brief Communications

Static Volt-ampere Characteristics of the Berrier Formed on the Boundaries of Electron and Hole Semiconductors in the Reverse Direction . . . . . E. I. Rashba and K. B. Tolpygo 1335

On the Question of the Isomorphism of Compounds of $A^{III}B^{V}$ Type . . . . . N. A. Goriunova and N. N. Fedorova 1339

On Increasing the Accuracy of Observations in Nuclear Photoplates . . . O. V. Lozhkin 1341

Dependence of the Lifetime of Excess Charge Carriers on the Concentration of Equilibrium Charge Carriers . . . . . R. Paramanova and A. Rzhanov 1342

Anelastic Scattering of Electrons in Single Crystals of NaCl and KCl . . . . . A. R. Shul'man and S. A. Fridrikovh 1344

CONTENTS — *continued*

Zone Theory of the Three-Dimensional Model of a Liquid . . . . . A. I. Gubanov 364
Magnetostatics with Ferromagnetics . . . . . V. I. Skobelkin and R. N. Solomko 370

Letters to the Editor:

Calculation of the Energy Distribution Function of Neutrons by Markov's Method . . . . . V. V. Chavchanidze and O. D. Cheitvili 375
On the Angular Distribution of β-Radiation. II . . . . . G. R. Khutsishvili 376
The Absorption of Ultrasonic Waves in Armco Iron and Plexiglass . . . . . N. F. Otpushchennikov 376
On the Causal Development of a Coupled System in Relative Time . . V. N. Tsytovich 377
The "Equilibrium" Energy Spectrum of Cascades of Photons . . . . . P. S. Isaev 379
The Gravitational Self Energy of Particles in the Classical Field Theories . . . . . A. A. Borgardt 380
The Constriction of an Arc in Rarefied Gases at Large Currents . . . . . V. L. Granovskii and G. G. Timofeeva 381
The Relation of the Oscillator Strengths for the Components of the Resonance-Doublet of Aluminum and Copper . . . . . G. F. Parchevskii and N. P. Penkin 382
The Effect of a Uniform Compression Upon the Galvanomagnetic Effects in Bismuth and Its Alloys . . . . . N. E. Alexeevskii and N. B. Brandt 384
On the Observation of Cerenkov Radiation Accompanying Broad Atmospheric Showers of Cosmic Rays . . . . . N. M. Nesterova and A. E. Chudakov 388
In Connection with the Paper of Arifov, Aiukhanov and Starodubtsev . . M. A. Eremeev 390
The Degree of Orientation of Nuclei . . . . . G. R. Khutsishvili 390
The Spontaneous Fission of Thorium . . . . . A. V. Podgurskaia, V. I. Kalashnikova, G. A. Stoliarov, E. D. Vorob'ev and G. N. Flerov 392
The Momentum Distribution in the Statistical Model of the Atom . . . S. I. Larin 394
The Theory of the Dipole Lattice of Onsager . . . . . V. L. Pokrovskii 397
The Spatial Distribution of Nuclear-Active Particles in Broad Atmospheric Showers of Cosmic Rays . . . . . Iu. N. Vavilov, S. I. Nikol'skii and V. P. Sarantsev 399
The Change in Dielectric Constant and Phosphors Under the Action of Infrared Light . . . . . E. E. Bukke 400

Tables of Contents, Doklady Akademii Nauk SSSR, Volume 100, Nos. 1 - 6 (1955) 403
Tables of Contents, Journal of Technical Physics USSR, Volume 25, Nos. 6, 7 (1955) . . 406

CONTENTS

The Kinetics of the Destruction of Superconductivity by a Magnetic Field . . . . . A. A. Galkin and P. A. Bezuglyi 197

The Velocity Distribution of Electrons in the Presence of a Varying Electric Field and a Constant Magnetic Field . . . . . V. M. Fain 205

Certain Properties of a Spark Counter for Counting α-Particles . . . . . E. Andreeschchev and B. M. Isaev 212

Density of States of Conduction Electrons in Ferromagnetic Materials . . . . . A. V. Sokolov and S. M. Tsipis 218

Resistance of Metals at High Current Densities . . . . . V. V. Bondarenko, I. F. Kvartskhava, A. A. Piutto and A. A. Chernov 221

The Quantum Theory of the Radiating Electron, IV . . . . A. A. Sokolov and I. M. Ternov 227

Dispersion Formulas of the Quantum Optics of Metals in the Many-Electron Theory with Consideration of Electron Damping . . . . . A. V. Sokolov, V. I. Cherepanov and I. B. Shteinberg 231

The Effect of Concentration on the Optical Properties of Solutions of Acridine Compounds . . . . . L. V. Levshin 235

The Effect of Concentration on the Optical Properties of Solutions of 3, 6 - Diaminoacridine . . . . . L. V. Levshin 244

The Entropy of Systems with a Random Number of Particles . . . . . R. L. Stratonovich 254

Multiple Scattering in a Coulomb Field in Very Thin Layers of Material . . . . . A. S. Kompaneets 262

The Phenomenological Relations of Onsager . . . . . Khristo Karanikolov 265

On the Theory of the Hall and Nernst-Ettinghausen Effects in Semiconductors with Mixed Conductivities . . . . . F. G. Bass and I. M. Tzidilkovski 267

On the Stability of a Homogeneous Phase II. Determination of the Limit of Stability . . . . . I. Z. Fisher 273

The Stability of a Homogeneous Phase III. Theory of the Crystallization Curve . . . . . I. Z. Fisher 280

The Decay Laws of the Afterglow of Zinc Sulfide Phosphors in the Temperature Extinction Region . . . . . F. I. Vergunas and N. L. Gasting 284

The Absence of Stable Isotopes of Tc and Pm and Other Anomalies in the Distribution of β-Stable Nuclei . . . . . A. V. Savich 291

The Problem of the Position of the Copper Activator in Zinc-Sulfide Scintillators . . . . . A. A. Cherepnev 300

The Theory of Scattering in the Semi-Classical Approximation . . . . . I. I. Gol'dman and A. B. Migdal 304

Hyperfine Structure of the Spectral Lines and Nuclear Spins of U^{233} and Pu^{239} . . . . . L. A. Korostyleva, A. R. Striganov and N. M. Iashin 310

The Problem of the Effect of Concentration on the Luminescence of Solutions . . . . . M. D. Galanin 317

Investigation of High Frequency Discharges by the Probe Method . . . . . Kh. A. Dzherpetov and G. M. Pateiuk 326

The Absorption and Emission of X-Rays in Ferromagnetic Metals . . . . . A. V. Sokolov 333

The Mathematical Foundations of the Theory of Irreversible Thermodynamical Processes . . . . . Kiril Popov 336

The Isotopic Shift in the Spectrum of Plutonium . . . . . A. R. Striganov, L. A. Korostyleva and Iu. P. Dontsov 354

The Double Configuration Approximation to the Two Lowest Configurations of the Boron Atom . . . . . G. K. Tsiunaitis and A. P. Iutsis 358

(Contents continued on inside back cover)